Lecture Notes in Civil Engineering

Ashish Dhamaniya
Sai Chand
Indrajit Ghosh *Editors*

Recent Advances in Traffic Engineering

Select Proceedings of RATE 2022

Springer

Lecture Notes in Civil Engineering

Volume 377

Lecture Notes in Civil Engineering (LNCE) publishes the latest developments in Civil Engineering—quickly, informally and in top quality. Though original research reported in proceedings and post-proceedings represents the core of LNCE, edited volumes of exceptionally high quality and interest may also be considered for publication. Volumes published in LNCE embrace all aspects and subfields of, as well as new challenges in, Civil Engineering. Topics in the series include:

- Construction and Structural Mechanics
- Building Materials
- Concrete, Steel and Timber Structures
- Geotechnical Engineering
- Earthquake Engineering
- Coastal Engineering
- Ocean and Offshore Engineering; Ships and Floating Structures
- Hydraulics, Hydrology and Water Resources Engineering
- Environmental Engineering and Sustainability
- Structural Health and Monitoring
- Surveying and Geographical Information Systems
- Indoor Environments
- Transportation and Traffic
- Risk Analysis
- Safety and Security

To submit a proposal or request further information, please contact the appropriate Springer Editor:

– Pierpaolo Riva at pierpaolo.riva@springer.com (Europe and Americas);
– Swati Meherishi at swati.meherishi@springer.com (Asia—except China, Australia, and New Zealand);
– Wayne Hu at wayne.hu@springer.com (China).

All books in the series now indexed by Scopus and EI Compendex database!

Ashish Dhamaniya · Sai Chand · Indrajit Ghosh
Editors

Recent Advances in Traffic Engineering

Select Proceedings of RATE 2022

Springer

Editors
Ashish Dhamaniya
Department of Civil Engineering
Sardar Vallabhbhai National Institute of Technology (SVNIT)
Surat, India

Sai Chand
Transportation Research and Injury Prevention (TRIP) Centre
Indian Institute of Technology Delhi
New Delhi, India

Indrajit Ghosh
Department of Civil Engineering
Indian Institute of Technology Roorkee
Roorkee, India

ISSN 2366-2557 ISSN 2366-2565 (electronic)
Lecture Notes in Civil Engineering
ISBN 978-981-99-4463-7 ISBN 978-981-99-4464-4 (eBook)
https://doi.org/10.1007/978-981-99-4464-4

Preface

Traffic flow in India and many other developing countries is characteristically mixed and observes weak lane discipline. Vehicles with diverse physical and operational characteristics interact, resulting in complex vehicle-to-vehicle and vehicle-to-infrastructure interactions. These complex interactions open multidimensional and multidisciplinary research opportunities for traffic engineers and researchers in the area of traffic operations and traffic safety. The key to understanding the traffic behaviour and safety aspects at a composite level is the availability of a detailed dataset that provides insight into varying macroscopic and microscopic traffic parameters of a traffic stream and its interactions based on the geometric, environmental and human conditions on the field. However, conventional methods for primary data collection are arduous and burdensome to meet the increasing need for strong research and effective measures. Transportation is on the cusp of a new technological revolution. With noteworthy technological advancements in vehicle technologies, such as connected and autonomous vehicles (CAVs), advanced driver assistance systems (ADAS), dedicated short-range communications (DSRC) and availability of detailed multisource trajectories datasets from videos captured using high-definition smart cameras. The unmanned aerial vehicles (UAVs), sensors, smartphones and instrumented vehicles also facilitated in developing robust and data-driven methodologies and theories for comprehending traffic behaviour and assessing traffic operations and safety for varying roadway and traffic flow conditions. Furthermore, emerging technologies, such as artificial intelligence, edge and cloud computing, machine learning and deep learning, have provided unprecedented opportunities to validate these theories and methodologies and enhance their application for real-time monitoring of traffic operations and safety.

The 4th National conference on Recent Advances in Traffic Engineering (RATE) held at SVNIT Surat during November 11–12, 2022 has received the overwhelming response from young researchers, academician and industry persons. The conference has received 114 full length papers in the area of traffic engineering, ITS management, Big data analytics, Transportation planning and other relevant conference theme areas. The conference has adopted double blind review process and after completion

of review a total of 84 papers were finally scheduled to present in the conference. A total of 74 papers were presented by the attendees during the conference.

Dr. Ashish Dhamaniya
Associate Professor, SVNIT Surat
Surat, India

Dr. Indrajit Ghosh
Associate Professor, IIT Roorkee
Roorkee, India

Dr. Sai Chand
Assistant Professor, IIT Delhi
New Delhi, India

Acknowledgements

The financial support for organising the conference has been received from various government and private agencies working in the field of traffic and transportation engineering. CSIR-Central Road Research Institute (CRRI), New Delhi is the diamond sponsor for the conference. M/s. R. N. Dobariya, Surat, M/s. J. M. Shah, Surat, Fortress Infracon Limited, Mumbai and Translink Infrastructure Consultants Pvt. Ltd., Ahmedabad has supported the conference as Gold Sponsors. Apart from that the conference has received Silver Sponsorship from The Setu Nirman structural consultant, Project iRASTE, ZEN Microsystems, D. D. Constructions, RTC Consultancy, JMC and Shantilal B. Patel, Surat.

We would like to acknowledge the efforts of authors for submitting and presenting quality papers in RATE 2022. We especially thank key note and inverted speakers Dr. Manoranjan Parida, Director CSIR-CRRI, New Delhi, Dr. Satish Chandra former Director CSIR-CRRI, New Delhi and Professor at IIT Roorkee, Dr. S. Gangopadhyay, former Director CSIR-CRRI, New Delhi, Dr. S.Velmurugan, Chief Scientist at CSIR-CRRI, New Delhi, Dr. Constantinos (Costas) Antoniou, Full Professor, Technology University of Munich and Prof. Dr.-Ing. Bernhard Friedrich from Institute of Transportation and Urban Engineering Technology University of Braunschweig, Germany for their valuable talk. We convey our gratitude to Dr. Anupam Shukla, Director SVNIT Surat for their support and motivation. We also covey sincere thanks to our Head of the Civil Engineering Department Professor Dr. G. J. Joshi and convenor of RATE 2022 for his guidance and support. We acknowledge colleagues Dr. Rakesh Kumar, Dr. Sriniwas Arkarkar, Organising Secretary of RATE 2022 and Sh. Amit J. Solanki who worked along with us for the success of the conference.

The review process of the papers was coordinated by the members of the scientific committee with the help of renowned researchers. We acknowledge the contribution of Dr. Indrajit Ghosh, IIT Roorkee, Dr. S. Velmurugan, CSIR-CRRI, Prof. Rajat Rastogi, IIT Roorkee, Prof. K. R. Rao, IIT Delhi, Prof. P. K. Agarwal, MANIT, Bhopal, Prof. Akhilesh Kumar Maurya, IIT Guwahati, Dr. Pradeep Kumar, CSIR-CRRI, Prof. Ashish Verma, IISc Bangalore, Dr. Ankit Gupta, IIT BHU and Dr. M. Harikrishna, NIT Calicut for their assistance in scientific committee. We thank the members of organising committee, advisory committee, student coordinator

Mr. Rajesh Chouhan, Mr. Rohit Rathod and other Ph.D. and Post Graduate Scholars of Transportation Engineering & Planning Section at SVNIT Surat and SVNIT administration for their valuable assistance in the successful organisation of the conference.

Dr. Ashish Dhamaniya
Associate Professor, SVNIT Surat

Dr. Indrajit Ghosh
Associate Professor, IIT Roorkee

Dr. Sai Chand
Assistant Professor, IIT Delhi

Contents

Pedestrian Level of Service: A Review of Factors and Methodology 1
Varsha Yadav and Rajat Rastogi

An Approach for Modelling Vehicular Pollution Using Artificial Neural Networks 19
Naina Gupta and Sewa Ram

Pedestrian Perception of Safety in Areas with Newly Provided Pedestrian Facility: The Case of Bangalore's Tender SURE (Specifications for Urban Utilities and Road Execution Project) 35
Aditya Saxena, P. S. Reashma, and Basavaraj Kabade

Plots to Identify the Rheological Properties of Polymer-Modified Warm Mix Binders 57
Rajiv Kumar and Vinod Kumar Sharma

Design Consistency Evaluation Tools for Rural Highways: A Review 69
Vinay Kumar Sharma and Gourab Sil

Artificial Intelligence (AI)-Based Assessment of Behavior of Bus Drivers in Nagpur City (India): A Case Study 89
Dev Singh Thakur, Mukti Advani, S. Velmurugan, Anbumani Subramanian, Neelima Chakrabarty, and Arun Goel

Effect of Pavement Roughness on Speed of Vehicles 107
Mithlesh Kumar, V. M. Ashalakshmi, M. V. L. R. Anjaneyulu, and M. Sivakumar

DSRC-Based Bus Trajectory Analysis and Prediction Near Signalized Intersection 119
Aswathi Chandrahasan, Aayush Jain, and Lelitha Vanajakshi

Development of Intercity Travel Demand Models for a Highly Industrialised Regional Corridor 137
Rohit Rathod, Sunil Parmar, Ashutosh Maurya, and Gaurang Joshi

Investigating Car User's Exposure to Traffic Congestion-Induced Fine Particles in Megacity Delhi 159
Vasu Mishra and Rajeev Kumar Mishra

Study on the Effect of Variation in the Geometric Parameters of the Work-Zone on Traffic Safety Using the Simulation Approach 173
Omkar Bidkar, Shriniwas Arkatkar, Gaurag Joshi, and Said M. Easa

Impact of the COVID-19 Pandemic on the Grocery Shopping Behavior of Individuals 181
Saladi S. V. Subbarao, B. Raghuram Kadali, B. C. H. Abhishek Kumar, and B. Semanth Reddy

Impact of Leading Vehicles of the Queue on Saturation Flow at Signalized Intersections 199
Rishabh Kumar and Mithun Mohan

Comparative Safety Assessment of Vehicle–Pedestrian Interactions at Urban Arterial and Highway Using UAV Data 211
Rajesh Chouhan, Abhi Shah, Rushabh Dalal, Jash Modi, Ashish Dhamaniya, and Chintaman Bari

Impact of Traffic Noise on the Teaching and Learning Process of School Environment 227
Avnish Shukla and B. N. Tandel

A Comprehensive Investigation of Pavement Evaluation Through Field and Laboratory and Prioritization 239
Rajkumar Muddasani, Ramesh Adepu, and Kumar Molugaram

On-Street Night Car Parking Demand Estimation in Residential Areas: A Case Study at Delhi 267
Ashwani Bokadia and Mokaddes Ali Ahmed

A Study of Indian Wholesalers for Mode Choice Decisions in Urban Goods Distribution 279
Pankaj Kant, Sanjay Gupta, and Ish Kumar

Mode Choice Behaviour in Leisure Travel: A Case Study of Indian Cities 295
Praveen Samarthi and Kumar Molugaram

Metro Rail Noise Analysis and Designing of Noise Barrier Along Selected MRTS Corridor in Delhi 311
Rajeev Kumar Mishra, Manoranjan Parida, and Kranti Kumar

Effect of Traffic Composition on Environmental Noise and Development of Noise Map of Roadside School, Colleges, and Hospital Buildings 327
Ramesh B. Ranpise and B. N. Tandel

Calibration of Microscopic Traffic Simulation for Signalized Intersections Under Heterogeneous Traffic Conditions 339
Rushikesh Katkar, Anagha Venugopal, Chithra A. Saikrishna, and Lelitha Vanajakshi

Design Optimization and Statistical Analysis of Parking Characteristics in a Commercial Area of Chandigarh 357
Kshitij Jassal, Kartick Kumar, and Umesh Sharma

Distance-Based Speed Prediction Models Using Naturalistic Driving Data on Two-Lane Roads in Mountainous Regions 373
Mikshu Bhatt, Rushiraj Gohil, Apoorva Gupta, Jaydip Goyani, and Shriniwas Arkatkar

An Integrated Approach to Assess Pavement Condition by Integrated Survey Vehicle as Replacement of Manual Assessment 387
Smit A. Savaliya, Avinash P. Satasiya, and Shivangkumar N. Dabhi

Pavement Design and Cost Analysis of Mine Waste Stabilized Low Volume Roads 405
Shravan A. Kanalli, Sureka Naagesh, and K. Ganesh

Driver Perception of Superimposed Horizontal and Vertical Road Curves for Bi-Directional Roads 421
Lekha Kosuri and Anuj Kishor Budhkar

Evolving Feasible Transportation Route from Cement Plant to the Proposed Mines: A Case Study 435
Nataraju Jakkula and Velmurugan Senathipathi

Effect of Lateral Shift of a Vehicle on Following Vehicles 449
Heikham Pritam Singh, Ashutosh Kasoundhan, Shubham Thapliyal, and R. B. Sharmila

Number of Aggregate Sizes and Aggregate Gradation Area: A Correlational Study 467
Ramu Penki, Subrat Kumar Rout, and Aditya Kumar Das

Simulation Approach for Analysis of Signalized Intersection Capacity Under the Influence of Access Point: A Case Study 481
J. Athira, K. T. Arshida, Yogeshwar V. Navandar, and K. Krishnamurthy

Area Based Cross Classification Measure of Social Vulnerability with Accessibility to Health Services and a Heterogeneous Customer Satisfaction Index for IPT Services in Imphal 499
S. Padma, S. Velmurugan, Ravindra Kumar, and Yendrembam Arunkumar Singh

Evaluation of Air Quality for Various Demand Management Scenario (Work from Home and Switch to Electric) for a Region in Delhi NCR 523
U. Gupta, S. Padma, R. Singh, A. Shukla, N. Dogra, and S. Ram

Study of Driver Behavior in Overtaking Maneuvers on Undivided Road in Indian Context 537
Indrajeet Kumar and Amit Kumar Yadav

Identification of Crash Severity Level of Unsignalized Intersection Blackspots in Mixed Traffic Scenario 559
Arpita Saha and Pratik Deshmukh

Use of Toll Transaction Data for Travel Time Prediction on National Highways Under Mixed Traffic Conditions 575
Chintaman Santosh Bari, Parth Jhaveri, Satyendra Kumar Sharma, Shubham Gupta, and Ashish Dhamaniya

Implementation of Airfield Pavement Management System in India 595
Pradeep Kumar, Sachin Gowda, and Aakash Gupta

Two-Lane Bidirectional Traffic Flow Patterns 607
Shreya Dey, Suresh Nama, and Akhilesh Kumar Maurya

About the Editors

Dr. Ashish Dhamaniya is an Associate Professor of Transportation Engineering in the Department of Civil Engineering at SVNIT, Surat. He has completed his Ph.D. in Traffic Engineering from Indian Institute of Technology (IIT) Roorkee. He has wide area of research interests in dynamic traffic flow modelling, highway capacity and level of service, GIS and GPS applications in transportation engineering, pedestrian flow modelling and facility design, road safety, pedestrians and motorists and drone data analysis. He is one of the pioneers in the study of toll plaza operation studies in India and abroad. He has guided number of Ph.D. and M.Tech. students. He has also been awarded with international collaborative research project with Technical University of Munich, Germany under DST-DAAD scheme. He has published more than 100 papers in reputed SCI and Scopus indexed journals and reputed conferences.

Dr. Sai Chand is an Assistant Professor at the Transportation Research and Injury Prevention (TRIP) Centre, Indian Institute of Technology (IIT) Delhi. Prior to that, he worked as a Postdoctoral Research Associate at Research Centre for Integrated Transport Innovation (rCITI), University of New South Wales (UNSW) Sydney, Australia, where he also obtained his Ph.D. in 2019. His research focuses on statistical modelling of traffic safety, applications of crowdsourced pervasive traffic data, traffic flow fluctuations, building strategic regional transport network planning models, and simulation modelling of the network-wide impacts of autonomous vehicles. Dr. Chand has managed several research and consultancy projects. He has helped develop traffic and safety management strategies for several global cities. He has authored more than 40 journals and conference papers with international presentations. He also taught courses on transport modelling and the fundamentals of traffic engineering.

Dr. Indrajit Ghosh is an Associate professor in the Department of Civil Engineering at the Indian Institute of Technology (IIT) Roorkee. He has completed his Ph.D. in Transportation Engineering area from Wayne State University, U.S.A. He has a wide area of research interests including road traffic safety using traffic conflict technique, ITS applications, traffic control devices, traffic operations, level-of-service

analysis, adoption of electric vehicle and e-mobility. He has more than 40 research papers published in peer reviewed journals and more than 60 papers in national and international conferences. He has supervised 7 Ph.D. scholars. He has been awarded with DUO-India fellowship, Thomac C. Rumble Fellowship, and Young Scientist Award by different national and international agencies.

Pedestrian Level of Service: A Review of Factors and Methodology

Varsha Yadav and Rajat Rastogi

Abstract Level of service (LOS) is a qualitative or quantitative measure of the operation condition of a facility. The quantitative assessment indicates the flow condition, and the qualitative assessment presents the satisfaction level of users with the facility. Generally, six categorizations are used for LOS. The LOS or the Measures of Effectiveness change with the type of facility. Despite the technological advancement in the transportation sector, the need to walk has not diminished. This warrants the evaluation of pedestrian facilities. This paper reviews the works done related to pedestrian facilities and focuses on the identification of the factors which influence the LOS and the methodologies adopted to arrive at the LOS for a facility. Various influencing factors being identified are pedestrians' personal characteristics, roadway characteristics, traffic characteristics, operational characteristics, pedestrian perception, pedestrian speed, pedestrian delay and pedestrian behavioural characteristics. Various approaches have been used by different researchers to arrive at categorized LOS for different pedestrian facilities. These are regression analysis, point system, GA Fuzzy clustering approach and C-mean clustering approach.

Keywords Pedestrians · Facilities · Factors · LOS · Methodologies

1 Introduction

The technological advancement in vehicle technology has assisted in the increased level of motorization across cities and countries. This is one pointer to improvement in the living standard of people, but it has negative externalities like environmental degradation, increase in social inequality, increase in expenditure on imported

V. Yadav (✉)
Transportation Engineering Group, Department of Civil Engineering, Indian Institute of Technology Roorkee, Roorkee 247667, India
e-mail: varsha_y@ce.iitr.ac.in

R. Rastogi
Department of Civil Engineering, Indian Institute of Technology Roorkee, Roorkee 247667, India
e-mail: rajat.rastogi@ce.iitr.ac.in

A. Dhamaniya et al. (eds.), *Recent Advances in Traffic Engineering*, Lecture Notes in Civil Engineering 377, https://doi.org/10.1007/978-981-99-4464-4_1

fuel, etc. So, there is a need to adopt efficient and safe modes of transportation. Walking has been reported as the preferred mode for short-distance commuting. Its share varies across countries. In Beijing, approximately 61% of total trips are by pedestrians [1, 2]. 40% of total trips are dependent on walking in rural households [2, 3]. In India, it is reported that 10.9% of trips are made by public transport, 0.7% by intermediate transport, 15.8% by bicycles and 64.7% on foot [2, 4].

Pedestrians can be defined as persons who sit, walk and stand in public spaces. They may use crutches, walking sticks or wheelchairs. They may be of any age group and profession like children, adults, teenagers, people with disabilities, elderly persons, workers, shoppers and residents. Pedestrian safety is a major problem, and many bottlenecks are experienced by pedestrians in mixed traffic conditions. The limited space available on the road leads to conflicts between pedestrians and vehicles. A study reveals that China, Russia and India is having the highest number of pedestrian deaths [5]. According to The Global Status Report on Road Safety [2, 6], "1.25 million deaths per year are reported in a total of 180 countries. 60% of pedestrian accidents in urban areas are reported in Low and Middle-Income countries". Since pedestrians are major road users, higher attention shall be given to increasing their walkability and safety.

Pedestrian facilities can be classified as interrupted or uninterrupted flow facilities. Various facilities are crosswalks, sidewalks, stairways, ramps, pedestrian overbridges, or underpasses and escalators. The operational quality of these facilities is measured by the LOS. Safety, delay, comfort and convenience are the important factors considered in determining the level of service for pedestrian facilities. HCM defines six levels of service from A to F, where 'A' represents the best possible condition while 'F' represents the worst possible condition of a facility.

The LOS is based on quantitative and qualitative measures. In terms of flow, it is closely related to capacity. It evaluates the facility based on certain measures of effectiveness. The measure of effectiveness varies with the type of facility. Categorisation of the LOS is done based on various methodologies. The measures and methodologies are discussed in the subsequent sections.

2 Factors and Methodologies for LOS at a Facility

2.1 Crosswalks

In this type of facility, there is an interaction between vehicular movement and pedestrian movement. These are more critical locations due to the interactions. These facilities can be classified as signalized, un-signalized and mid-block crosswalks. The crossings can also be classified as at-grade and grade separated. At-grade crossings are those at which pedestrians cross at the carriageway level or 100 mm above that, while grade-separated crossings are those where pedestrians cross the carriageway

at a different level. At-grade crossings are further classified as crossing at an intersection or at a mid-block (away from the intersection) which may be controlled or uncontrolled. At signalized crossings, a particular signal time is provided for the pedestrians to cross while for the rest of the time they have to wait at the kerb side. The influencing factors and methodologies for determining the LOS are discussed in the following sub-sections for different facilities.

Signalized crosswalks Delay is an important parameter for evaluating the LOS of pedestrian crosswalks at signalized intersections [7]. Traffic characteristics, delay, crossing behaviour of pedestrians and operational characteristics are the factors considered in the evaluation of LOS at signalized intersections in HCM 2010 [8]. Turning manoeuvres are complex movements because they increase pedestrian delay and reduce pedestrian safety. The effect of turning vehicles on pedestrians' safety as well as delay is also studied [9–11].

By using observational studies, pedestrian opinion surveys and simulation approaches, the effect of bidirectional flow on area occupancy and speed has been studied [12, 13]. It has been found that most of the studies have not given importance to pedestrian safety, comfort and convenience.

It has also been observed that the unsafe behaviour of pedestrians leads to many crashes [14, 15]. The thresholds are also being reported for bidirectional flows with consideration given to walking speed, pedestrian flow and pedestrians' opinions [16].

A fuzzy clustering technique is used to arrive at LOS [5]. The pedestrian delay, crossing time, speed, volume of pedestrians and density were also reported to affect the pedestrian LOS at signalized intersections under mixed traffic conditions [5].

Unsignalized crosswalks These are the intersections in which pedestrians are exposed to free-flow traffic. These are difficult to analyse because it is based on acceptable gaps in vehicular flow by the pedestrian. The pedestrian gap acceptance is the major factor in these cases. Other factors are found similar to crosswalks at signalized intersections. Pedestrians' perception of safety and comfort is considered in determining the LOS [17, 18].

Mid-block crosswalks These are hazardous crossing locations and are completely different from signalized and un-signalized intersection crosswalks. These are provided for a pedestrian to cross the street safely. These can be marked or unmarked, signalized or unsignalized, or assisted by a crossing volunteer. Controlled crossing locations may have simple traffic signals or pelican signals, or they are marked with zebra lines. Uncontrolled crossings are more critical locations. These may have higher chances of hazardous pedestrian-vehicle interaction due to uncontrolled speeds and higher waiting times [19, 20].

At mid-blocks, pedestrians have to wait for a longer time before getting the required gap in the vehicular stream. In developing countries, pedestrian behaviour is not considered while in developed countries, pedestrian behaviour, as well as driver behaviour, is reported. It is reported that with an increase in vehicle speed, volume, crossing width, and length of traffic signal cycles, pedestrians face higher difficulty in crossing the road, whereas the presence of marked crosswalks, restricted medians

and traffic signals reduces pedestrian difficulty [20, 21]. Group behaviour is also considered in the analyses [22, 23]. *The review of the literature indicates that none of the studies has considered pedestrian safety and crossing difficulty as the measure of effectiveness for evaluating the LOS.*

2.2 Sidewalks

Sidewalks are the facilities that are placed parallel to the traffic facilities. These are raised paths along the roadside, and these are separated from vehicular traffic. These are designed for universal access, i.e., by pedestrians of all age groups, persons with disabilities and persons using assistive devices. LOS of these facilities shall be defined considering all the users. Mostly, measurable attributes like pedestrian flow rate and pedestrian speed are used to define the LOS on sidewalks [24, 25]. It is reported that pedestrians face a problem when choosing walking speed on sidewalks [26]. Qualitative measures like pedestrian safety, sidewalk continuity, comfort, security and convenience are also used [27, 28]. It is also reported that appropriate safety and comfort guarantee a suitable environment for pedestrians irrespective of users' physical limitations [28]. Most of the studies have focused on users' perceptions and did not tell how to quantify combined methods or environmental factors. LOS is also defined based on factors like the availability of sidewalks, a lateral separation between pedestrians and vehicles, traffic volume, and the speed of vehicles [29, 30]. Pedestrian space and evasive movements are also considered in studies. It is reported that the evasive movement explains the pedestrians' LOS in a better way [31]. Recent studies have proposed LOS considering persons with disability and wheelchair users [32–34].

The design standards do not consider the diverse users like pedestrians with disability and wheelchair users in developing countries like India.

2.3 Stairways

Stairways are the facilities that are used to ascend or descend and allow vertical movements. A study conducted in the USA used pedestrian space and flow rate to define LOS quantitatively. Time-lapse photography was used to collect the data and a relationship between human convenience, speed and volume was developed. The study proposed to include illumination, riser dimension and location in the analysis [35]. Another study in China also used a quantitative approach and considered factors like safety, environment, conflict and accessibility. It concluded that the congestion level, presence of informatory signs and clear visibility affect the LOS [36].

Another study was conducted on undivided stairways at a suburban station in Mumbai, India. The variables used were pedestrian space, flow rate, walking speed

and volume/capacity ratio. The k-mean clustering approach was used. Pedestrian characteristics were classified based on age. The speed density relation was found non-linear, therefore for the speed-flow relation, two regime modal was developed. Average hourly pedestrian volume was used for the analysis. Further analysis was done with the help of STATISTICA. The study reported that pedestrians in China need more space in LOS D to F as compared to India and USA. It also reported that in India, the space tolerance is higher [37].

Another study was conducted at a metro station in Shanghai, China. The interaction index was used for the analysis. The whole area was divided into four locations. Further analysis was done by building EXODUS. Four parameters were used for analysis, namely volume, frequency rate (FR), distance travelled and congestion waiting time [38].

2.4 Walkways

Walkways are the paths or defined spaces used by pedestrians. A study conducted in India used a clustering algorithm to arrive at LOS categories based on flow rate, volume/capacity ratio, speed and average pedestrian space [39].

Another study, which was conducted in Rome and Munich, used qualitative analysis to arrive at LOS categories considering attributes like comfort, convenience, attractiveness, system coherence, safety, continuity and security [40]. A study conducted in the Philippines used both qualitative as well as quantitative approaches and considered factors like convenience, safety, continuity, system coherence, level of congestion and safety [41]. Another qualitative study used comfort as a major attribute for LOS categorisation [42].

A study conducted in China used horizontal distances, longitudinal distances, the frequency and behaviour of pedestrians who used the facility as variables. It concluded that safety, illegal vendors and security affects the LOS [43]. A study conducted in Malaysia developed a relationship between safety, connectivity, comfort and accessibility, and did a Pearson correlation analysis [44].

2.5 Foot-Over Bridge

A study was conducted in South Korea in which pedestrian area (m^2), pedestrian speed (m/min), pedestrian density (ped/m^2), delay and pedestrian flow rate (ped/min/m) were used as attributes [45].

Table 1 presents the attributes used by different researchers to arrive at LOS of a facility, and Table 2 presents the methodologies adopted by various researchers.

Table 1 Factors affecting the LOS of pedestrians' crosswalks, sidewalks, stairways and walkway facilities

Author, Country	Factors considered for LOS
Milazzo II et al. [7], The United States	Pedestrian crossings behaviour, crosswalk width, and length, crossing facilities, traffic conflicts, delays to pedestrians
Baltes and Chu [21], The United States	Turning movements, presence of pedestrian signals and cycle length, signal spacing, and width of painted medians
Zhang and Prevedouros [46], The United States	Perceived safety and comfort, corner radius dimension, crossing distance, roadway space allocation, presence/ absence of right-turn channelization island, traffic signal characteristics, pedestrian delay, conflicting and turning traffic flow, mid-block 85^{Th} percentile speed of the vehicle on street being crossed
Steinman and Hines [9], The United States	Crossing distance, roadway space allocation, presence/ absence of right-turn channelization island, and Perceived safety and comfort
Muraleetharan et al. [47], Japan	Crosswalk width and length, crossing facilities, traffic conflicts, delays to pedestrians
Petritsch et al. [48], United States	Corner radius dimension, crossing distance, roadway space allocation, presence/ absence of right-turn channelization island, and Perceived safety and comfort
Lee et al. [13], Hong Kong	Turning vehicles and through vehicles, pedestrian bidirectional flow, area occupancy, pedestrian delay, walking speed
Hubbard et al. [10], United States	Crosswalk characteristics, right-turn traffic volume, the pedestrian direction of travel, pedestrian arrival rate
Alhajyaseen et al. [12], Japan Nagraj and Vedagiri) [49], India	Turning vehicles and through vehicles, pedestrian bidirectional flow, area occupancy, pedestrian delay, walking speed
Chutani and Parida [23], India	Vehicular flow, pedestrian crossing speed, group size, waiting time
Zhao et al. [22], China	The volume of two-way motor vehicles, the distance between marked-unmarked crosswalks
Kadali and Vedagiri [50], India	Vehicle speed and number of vehicles encountered, age of rolling and gender of participants, rolling behaviour of pedestrian, and speed change behaviour of pedestrian
Mohan et al. [51], India	Space, and flow rate
Marisamynathan and Vedagiri [52], India	Pedestrian volume, Vehicle volume, Delay and land use
Asadi-Shekari et al. [53], Malaysia	Pedestrian speed
Tanaboriboon and Guyano [54], Thailand	Space and flow rate
Miler at el. [55], U.S.A	Safety and environment
Kim et al. [56], South Korea	Surface and environment
Yadav et al. [57], India	Safety, comfort, convenience and gender

(continued)

Table 1 (continued)

Author, Country	Factors considered for LOS
Muraleetharan and Hgiwara [58], Japan	Vehicle speed, crossing and traffic control
Saha et al. [59], Bangladesh	Gender and age
Botma [60], Netherlands	Vehicle characteristics and roadway geometry
Jensen [30], Denmark Asadi-Shekari et al. [53], Malaysia	Roadway geometry, pedestrian behaviour and environmental factors
Kang et al. [61], China Kim at el. [31], South Korea	Capacity-based factors, vehicle characteristics and roadway geometry
Muraleetharan et al. [47], Japan	Environmental factors, pedestrian behaviour and roadway geometry
Petritsch et al. [62], The United States	Environmental factors, vehicle factors and pedestrian behaviour
Polus et al. [24], Israel	Density, space and flow rate
Sisiopiku et al. [63], U.S.A	Flow rate, width, surface and v/c ratio
Al-Azzawi and Raeside [64], UK	Density, flow rate and delay
Christopoulou and Pitsiava-Latinopoulou [65], Greece	Width
Marisamynathan and Lakshmi [66], India	Width, vehicle volume, surface and obstructions/friction
Landis et al. [29], U.S.A	Lateral separation, vehicle speed, vehicle volume, safety, comfort and environment
Jaskiewicz et al. [67], U.S.A	Surface, obstructions, width and accessibility
Ferreira et al. [33], Brazil	Surface, width and crossing
Octaviana and Moreno Freydig [68], Indonesia	Comfort
Stairways	
Fruin [69], U.S.A	Pedestrian flow rate and pedestrian space
Lee and Lam [36], China	Accessibility, conflict, environment and safety
Shah et al. [37], India	Flow rate, space/pedestrian, walking speed and v/c ratio
Hu et al. [38], China	Interaction index
Walkways	
Sahani and Bhuyan [39], India	Flow rate, speed, average pedestrian space and v/c ratio
Sarkar [40], Italy	Attractiveness, safety, system coherence, security, convenience and continuity
Gacutan et al. [41], Philippines	Safety, continuity, level of congestion, convenience and system coherence
Sarkar [42], India	Comfort

(continued)

Table 1 (continued)

Author, Country	Factors considered for LOS
Shan et al. [43], China	Macro and micro level indicators (frequency, longitudinal distance before and after interactions, horizontal distance before and after interactions, etc.)
Zakaria and Ujang [44], Malaysia	Accessibility, comfort and safety

3 Level of Service Guidelines

3.1 IRC 103:2022—Guidelines for Pedestrian Facilities [73]

The guidelines have considered five principles for the safe design of pedestrian facilities. These are safety, security, continuity, comfort and liveability. It defined the level of service as a "qualitative measure used to determine how well a facility is operating from a traveller's perspective". Width is considered the main factor for designing facilities. The width will be dependent on the street type, expected and current pedestrian flow, and adjoining land use.

Table 3 presents the pedestrian LOS for walking infrastructure and index values according to walkability type.

3.2 Indo-HCM 2017 [74]

INDO-HCM 2017 provides methodologies to arrive at pedestrian LOS for four pedestrian facilities namely crosswalks, sidewalks, stairways and foot-over bridges. Pedestrian flow (ped/min/m) is suggested to define LOS on a sidewalk catering to different land uses like commercial, terminal, institutional, residential and recreational.

The following methodology is used to arrive at LOS threshold values:

(i) Identification of the type of land use
(ii) Sidewalk width measurement
(iii) Calculating the effective width of the facility
(iv) Recording pedestrian flow and identifying maximum flow rate (ped/min)
(v) Determination of the PLOS

In the case of a crossing facility, the delay is used as an influencing attribute. The average delay at a crossing facility is calculated and used to define the LOS. Flow (ped/min/m), speed (m/min) and space (m^2/ped) are used as the attributes to define LOS at stairs. The effective width of the stairs is used for this purpose. Speed (m/min), space (m^2/ped) and flow (ped/min/m) are used as attributes to define LOS on a foot over-bridge. The effective width of the stairs and bridge is used while calculating the

Table 2 Methodologies used for arriving at LOS for crossing, sidewalks, stairways and walkway facilities

Author, Country	Analysis method
Crossing facility	
Milazzo et al. [7], U.S.A	Linear relationship
Zhang and Prevedouros [46], U.S.A	Regression
Steinman and Hines [9], The U.S.A	Point system
Petritsch et al. [48], The U.S.A	Pearson correlation analyses and stepwise regression
Murraleetharan et al. [47], Japan	Stepwise multiple, regression model
Nagraj and Vedagiri [49], India	Stepwise regression
Jensen [70], Denmark	CLM stepwise regression
Bian et el. [18], China	Stepwise regression
Zhao et al. [22], China	Stepwise regression
Ye et al. [15], China	Linear regression technique
Sidewalk facility	
Polus et al. [24], Israel	Linear-speed density regression
Tanaboriboon and Guyano [25], Thailand	Linear relationship
Sarkar [27], U.S.A	Point system
Muraleetharan et al. [47], Japan	Linear relationship
Kim et al. [71], The U.S.A	Linear relationship
Hidayat et al. [72], Thailand	Multiple linear regression
Christopoulou and Pitsiava-Latinopoulou [65], Greece	Point system
Kang et al. [61], China	Ordered probit
Kim et al. [31], Korea	Multiple linear regression
Stairways	
Fruin [69], U.S.A	Quantitative analysis by time-lapse
Lee and Lam [36], China	Quantitative analysis
Shah et al. [37], India	K-mean clustering approach
Hu et al. [38], China	Analysis on Building Exodus Software
Walkways	
Sahani and Bhuyan [39], India	Affinity propagation clustering method
Sarkar [40], Italy	Qualitative analysis
Gacutan et al. [41], Philippines	Qualitative analysis
Sarkar [42], India	Qualitative analysis
Shan et al. [43], China	Quantitative survey
Zakaria and Ujang [44], Malaysia	Pearson correlation

Table 3 The LOS criteria for walking infrastructure and index values according to walkability type

LOS considered	Service volume of pedestrian facility of unit width, pedestrian/h/metre (ped/h/m) in both directions				
	Commercial	Institutional	Terminal	Recreational	Residential
LOS-B	1285	1145	1360	1360	1430
LOS-C	1800	1600	1900	1900	2000
Walkability type	*Index value*				
A	>4.5				
B	<4.5–4.2				
C	<4.2–3.8				
D	<3.8–3.5				
E	<3.5–3.1				
F	<3.1				

attributes' values determined. Table 4 presents the LOS criteria given in Indo-HCM (2017) for different facilities.

3.3 Highway Capacity Manual 2010 [8]

The guidelines provide the procedure for determining the LOS of the walkways and stairways, as well as for shared-use paths. Walkways are considered as paved paths, plazas and ramps that are located more than 35 feet from urban streets as well as the streets which are reserved for pedestrian traffic on a part-time basis or full basis. In the case of walkways, pedestrian zones, pedestrian paths, ramps (grade up to 5%), walkways and plaza areas are considered. The flow is considered random and platoon-type. Six categories of LOS are defined. Average space (ft^2/p), flow rate (p/min/ft) and average speed (ft/s) are used as attributes. Also, the V/C ratio is calculated and used for LOS categorisation.

For LOS categories on a stairway, average space (ft^2/p), flow rate (p/min/ft) and V/C ratio are used as attributes. These are presented in Table 5.

The guidelines which are followed in different countries are different in many respects. Indo HCM has considered the human ellipse as $0.35\text{m} \times 0.51\text{m} = 0.18\text{m}^2$ while US-HCM (HCM 2000) has considered the human ellipse as $0.46 \times 0.61\text{m} = 0.28\ \text{m}^2$. For Indian conditions, footpaths are designed for LOS-B and LOS-C (in case of resource constraints). The width of the footpaths varies with the type of facility. While the US guidelines have considered their analysis boundaries for designing pedestrian facilities. The manual has the formula for calculating the effective width of walkways. The guidelines have given separate LOS criteria for walkways with the random pedestrian flow and walkways with platoon flow.

Table 4 LOS criteria according to INDO-HCM 2017 for sidewalks, crosswalks, stairways and foot-over bridge

INDO HCM 2017						
Sidewalks (ped/min/m)						Crosswalks
LOS	Commercial	Institutional	Terminal	Recreational	Residential	Pedestrian delay (s)
A	≤13	≤13	≤15	≤12	≤16	≤5
B	>13–19	>13–19	>15–26	>12–20	>16–23	5–10
C	>19–30	>19–27	>26–32	>20–32	>23–34	11–25
D	>30–47	>27–36	>32–68	>32–54	>34–47	26–45
E	>41–69	36–42	>68–78	>54–91	>47–59	46–80
F	Variable	Variable	Variable	Variable	Variable	>80
Stairways						
LOS	*Flow (ped/min/m)*	*Speed (m/min)*	*Space (m^2/ped)*			
A	≤10	≥42.6	≥2.5			
B	>10–22	>37.2–42.6	>1.50–2.5			
C	>22–46	>31.2–37.2	>0.75–1.50			
D	>46–55	>28.2–31.2	>0.50–0.75			
E	>55–70	>24.2–28.2	>0.40–0.50			
F	Variable					
Foot over bridge						
LOS	*Flow (ped/min/m)*	*Speed (m/min)*	*Space (m^2/ped)*			
A	≤12	≥56.78	≥4.89			
B	>12–17	>55.03–56.78	>3.3–4.9			
C	>17–27	>51.08–55.03	>1.9–3.3			
D	>27–38	>45.65–51.08	>1.2–1.9			
E	>38–52	>30.91–45.65	>0.6–1.2			
F	Variable	<30.91	<0.6			

4 Discussion

A review of factors affecting LOS and methodologies used to arrive at the categorisation of LOS has been discussed in this paper. The following emerges out of the discussion:

Table 5 The LOS criteria according to HCM 2010 for walkways and stairways

Average flow criteria for walkways					Platoon adjusted criteria for walkways	
		Related measures				Related measures
LOS	Average space (ft^2/p)	Flow rate (p/min/ft)	Average speed (ft/s)	v/c	Average space (ft^2/p)	Flow rate (p/min/ft)
A	>60	≤5	>4.25	≤0.21	>530	≤0.5
B	>40–60	>5–7	>4.17–4.25	>0.21–0.31	>90–530	>0.5–3
C	>24–40	>7–10	>4.00–4.17	>0.31–0.44	>40–90	>3–6
D	>15–24	>10–15	>3.75–4.00	>0.44–0.65	>23–40	>6–11
E	>8–15	>15–23	>2.50–3.75	>0.65–1.00	>11–23	>11–18
F	≤8	Variable	≤2.50	Variable	≤11	>18
Stairways						
LOS	*Average space (ft^2/p)*	*Flow rates (p/min/ft)*	*v/c ratio*			
A	>20	≤5	≤0.33			
B	>17–20	>5–6	>0.33–0.41			
C	>12–17	>6–8	>0.41–0.53			
D	>8–12	>8–11	>0.53–0.73			
E	>5–8	>11–15	>0.73–1.00			
F	≤5	Variable	Variable			

a. More studies are being carried out on crosswalks, followed by studies on sidewalks and walkways. Quite a less studies are carried out on other pedestrian facilities. This needs to be strengthened (Refer to Fig. 1).

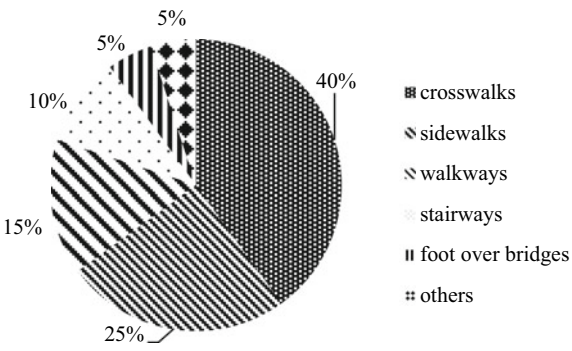

Fig. 1 Number of studies on different facilities

b. A regression-based analysis is done to arrive at LOS values in most of the studies. It is followed by the development of other types of pedestrian LOS models. Qualitative assessment is carried out in quite lesser studies. This needs to be incorporated along with the quantitative analysis to get an overall idea of a facility LOS (Refer to Fig. 2).
c. The influencing factors are examined concerning their effectiveness on the LOS of a facility [2]. Factors have been categorized and their influence on interrupted and uninterrupted pedestrian facilities has been summarized in Fig. 3. A scale of 0 to 5 is used for the purpose. '0' means there is no effect and '5' means it highly affects the LOS of a type of facility. It can be noted that pedestrian and traffic characteristics and geometric factors affect the LOS most. The rest of the factors are either not influencing or influencing either type of facility.

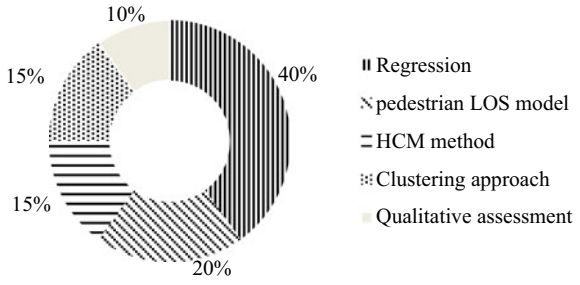

Fig. 2 Methods used for categorization of LOS for different pedestrian facilities

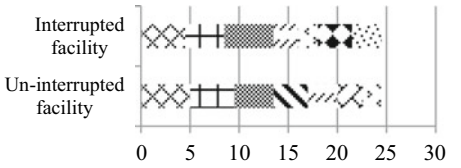

	Un-interrupted facility	Interrupted facility
pedestrian factors	5	4.5
geometric factors	4.5	4
traffic characteristics	4	5
pedestrian-vehicle interactions	3.5	0
land-use accessibility	3	2.5
environmental factors	2.5	0
Socio-demographic factors	2	2
pedestrian delay and compliance	0	3.5
operational characteristics	0	3

pedestrian factors
geometric factors
traffic characteristics
pedestrian-vehicle interactions
land-use accessibility
environmental factors
Socio-demographic factors
pedestrian delay and compliance
operational characteristics

Fig. 3 Categorization of factors and their influences on LOS of pedestrian facilities

5 Conclusion

A review of factors and methodologies is presented in this paper. The factors which influence pedestrian facilities are broadly classified as roadway characteristics, traffic characteristics, pedestrian personal characteristics, operational characteristics, and land use and accessibility characteristics.

For sidewalks facilities: density, flow rate, width, traffic volume, age, space and obstructions are used as quantitative factors while safety, the volume of pedestrians, and vehicle speed are used as qualitative factors. For crosswalks facilities: volume of vehicles and pedestrians, delay, space, and flow rate were used as quantitative factors while traffic control, safety, and surface were used as qualitative factors. For stairways facilities: flow rate, space and congestion were used as quantitative factors while comfort, accessibility and safety were used as qualitative factors. For walkways facilities, flow rate, space and width were used as quantitative factors while safety, accessibility and comfort were used as qualitative factors. Delay is the most important parameter at crosswalk locations.

The regression method is widely used for evaluating the LOS for crosswalks and sidewalks.

It is concluded from the literature that developed countries like the U.S.A., are focusing on the quantitative as well as qualitative methods for evaluating the LOS for sidewalks facilities while other countries like India, are focusing on qualitative methods. Qualitative as well as quantitative factors were used for determining LOS for crosswalk facilities in countries like the U.S.A., Japan, and India.

There is a difference between developed and developing countries in terms of operational conditions, roadway, pedestrian density at crosswalks locations, pedestrian behaviour, culture, and driver behaviour. Driving rules are different in different countries, so the behaviour of pedestrians is also different, which ultimately affects the LOS. It is very difficult to design pedestrian facilities in developing countries because these are populous countries and have a mixed mode of transport.

The important factor which is noticed in the literature is that the studies are less focused on the person with a disability. More studies are needed for pedestrians with disability at railway stations on stairs, circulation areas and ramps. For pedestrian with a disability, there is no common factor available to normalize their impact under mixed conditions in developing countries while designing such facilities because these type of pedestrians affects the speed and sight distances. Due to the lack of traffic regulations, the crossing behaviour of these pedestrians become very complex in developing countries. Further, the geometric dimensions are not properly designed keeping in mind the pedestrian with disability.

In developing countries, sidewalks are not properly available for pedestrians or there is discontinuity, so they share the lanes. Ultimately their proper evaluation is needed for the upgradation of the facility. Due to this, there is a change in mode shift. Further, due to the non-availability of adequate gaps, free left turns are more complicated at crossings and roundabouts, so studies are needed to cater to this issue.

More studies are needed on the combined effects of quantitative and qualitative factors in developing countries. There is a lack of studies with fewer traffic regulations at uncontrolled intersections in developing countries. Studies are lacking in proper evaluation of unprotected mid-block crosswalk locations. Further, there is a need to improve traffic rules, lighting at night, lighting by reflective markings, and provisions to improve street hawkers' conditions and improve pedestrian facilities.

Factors like pedestrian age, gender, walking with or without baggage and the purpose can be considered while evaluating the LOS at signalized mid-block locations. The effect of optimizing signal control on the LOS can be studied. LOS for pedestrian flows at escalators needs to be studied.

References

1. Tanaboriboon Y, Jing Q (1994) Chinese pedestrians and their walking characteristics: a case study in Beijing. Transp Res Board 16–26
2. Bansal A, Goyal T, Sharma U (2018) Level of service of pedestrian facilities in an urban area (a critical evaluation of factors). J Eng Technol 7:416–434
3. Kadali BR, Vedagiri P (2016) Review of pedestrian level of service: perspective in developing countries. Transp Res Rec 2581:37–47
4. Arasan VT, Rengaraju VR, Rao KVK (1994) Characteristics of trips by foot and bicycle modes in Indian city. J Transp Eng 120:283–294
5. Tallam T, Rao KML (2020) Determination of pedestrian level of service at signalized midblock locations for mixed traffic conditions. Int J Recent Technol Eng (IJRTE) 8:2751–2755
6. Global Status Report on Road Safety. World Health Organization (2015)
7. Milazo JS, Rouphail NM, Hummer JE, Allen DP (1999) Quality of service for uninterrupted-flow pedestrian facilities in highway capacity manual 2000 transportation research record. J Transp Res Board
8. Highway Capacity Manual (2010) Transportation Research Board. National Research Council (U.S.)
9. Steinman N, Hines DK (2004) Methodology to assess design features for pedestrian and bicyclist crossings at signalized intersections. Transp Res Rec J Transp Res 1878:42–50
10. Hubbard SML, Awwad RJ, Bullock DM (2007) Assessing the impact of turning vehicles on pedestrian level of service at signalized intersections: a new perspective. Transp Res Rec 27–36
11. Sisiopiku V, Akin D (2007) Modeling interactions between pedestrians and turning vehicles at signalized crosswalks operating under combined pedestrian-vehicle interval. Transp Res Board
12. Alhajyaseen WKM, Nakamura H, Asano M (2011) Effects of bi-directional pedestrian flow characteristics upon the capacity of signalized crosswalks. Proc Soc Behav Sci 526–535. Elsevier Ltd
13. Lee JYS, Goh PK, Lam WHK, Asce M (2005) New level-of-service standard for signalized crosswalks with bi-directional pedestrian flows. J Transp Eng 957–960
14. Bian Y, Ma J, Rong J, Wang W, Lu J (2009) Pedestrians' level of service at signalized intersections in China. Transp Res Rec 83–89
15. Ye X, Chen J, Jiang G, Yan X (2015) Modeling pedestrian level of service at signalized intersection crosswalks under mixed traffic conditions. Transp Res Rec 2512:46–55
16. Goh PK, Lam WHK (2004) Pedestrian flows and walking speed: a problem at signalized crosswalks. Inst Transp Eng ITE J 28–33
17. Vijayawargiya V, Rokade S (2017) Identification of factors affecting pedestrian level of service of crosswalks at roundabouts. Int Res J Eng Technol 342–346

18. Bian Y, Lu J, Zhao L (2013) Method to determine pedestrians level of service for unsignalized intersections. Appl Mech Mater 1936–1943
19. Gårder PE (2004) The impact of speed and other variables on pedestrian safety in Maine. Accid Anal Prev 36:533–542
20. Diogenes MC, Lindau LA (2010) Evaluation of pedestrian safety at midblock crossings, Porto Alegre, Brazil. Transp Res Rec 37–43
21. Baltes MR, Chu X (2002) Pedestrian level of service for midblock street crossings. Transp Res Rec J Transp Res Board 1818:125–133
22. Zhao L, Bian Y, Lu J, Rong J (2014) Method to determine pedestrian level of service for the overall unsignalized midblock crossings of road segments. Adv Mech Eng 1–9
23. Chutani C, Parida P (2013) LOS for pedestrian at uncontrolled mid-block crossings. In: Proceedings Urban Mobility India Conference, New Delhi, India
24. Polus A, Schofer JL, Ushpiz A (1983) Pedestrian flow and level of service. J Transp Eng 109:46–56
25. Tanaboriboon B, Guyano JA (1989) Level-of-service standards for pedestrian facilities in Bangkok: a case study. ITE J 39–41
26. Rahman K, Abdul Ghani N, Abdulbasah Kamil A, Mustafa A, Kabir Chowdhury MA (2013) Modelling pedestrian travel time and the design of facilities: a queuing approach. PLoS ONE 8:1–11
27. Sarkar S (1993) Determination of service levels for pedestrians, with European examples. Transp Res Rec 1405:35–16042
28. Khisty CJ (1994) Evaluation of pedestreian facilities: bayonnd the level-of-service concept. Transp Res Rec 45–50
29. Landis BW, Vattikuti VR, Ottenberg RM, McLeod DS, Guttenplan M (2001) Modeling the roadside walking environment: pedestrian level of service. Transp Res Rec J Transp Res Board 1773:82–88
30. Jensen SU (2007) Pedestrian and bicyclist level of service on roadway segments. Transp Res Rec 43–51
31. Kim S, Choi J, Kim S, Tay R (2014) Personal space, evasive movement and pedestrian level of service. J Adv Transp 48:673–684
32. Kochelman KL, Heard L, Kweon J, Rioux TW (2002) Analysis of accessibility for person with disabilities. J Transp Res Rec 108–118
33. Asadi-Shekari Z, Moeinaddini M, Shah MZ (2013) Disabled pedestrian level of service method for evaluating and promoting inclusive walking facilities on urban streets. J Transp Eng 139:181–192
34. Ferreira MAG, Da S, Sanches P (2007) Proposal of sidewalk accessibility index. J Urban Environ Eng 1:1–9
35. Fruin JJ (1971) Pedestrian planning and design. Metropolitan Association of Urban Designers and Environmental Planners, Newyork
36. Lee JYS, Lam WHK (2003) Levels of service for stairway in Hong Kong underground stations. J Transp Eng 129:196–202
37. Shah JH, Joshi GJ, Parida PM, Arkatkar SS (2016) Determination of pedestrian level of service for undivided stairways at suburban rail stations in developing countries
38. Hu M, Lu L, Yang J (2020) Exploring an estimation approach for the pedestrian level of service for metro stations based on an interaction index. Transp Lett 12:419–428
39. Sahani R, Bhuyan PK (2013) Level of service criteria of off-street pedestrian facilities in Indian context using affinity propagation clustering. Proc Soc Behav Sci 104:718–727
40. Sarkar S (1993) Determination of service levels for pedestrians, with European examples. Transp Res Rec 35–42
41. Gacutan A, Vallent JJ, Gacutan Maria AU, Tan JM (2012) Level of service of pedestrian facilities in the university of the Philippines diliman. Transp Eng Group
42. Sarkar S (2003) Qualitative evaluation of comfort needs in urban walkways in major activity centers. Transp Q 57:39–59

43. Shan X, Ye J, Chen X (2016) Proposing a revised pedestrian walkway level of service based on characteristics of pedestrian interactive behaviour in China. PROMET-Traf Transp 28:583–591
44. Zakaria J, Ujang N (2015) Comfort of walking in the city center of Kuala Lumpur. Proc Soc Behav Sci 170:642–652
45. Kim I, Kang H (2013) A study of delay-based level of service on pedestrian facility. Austr Transp Res Forum
46. Zhang L, Prevedouros PD (2003) Signalized intersection level of service incorporating safety risk. J Transp Res Rec 1852:77–86
47. Muraleetharan T, Student G, Adachi T, Hagiwara T, Kagaya S (2005) Method to determine pedestrian level-of-service for crosswalks at urban intersections. J East Asia Soc Transp Stud 6:127–136
48. Petritsch TA, Landis BW, Mcleod PS, Huang HF, Challa S, Guttenplan M, Petritsch TA, Landis BW, Mcleod PS, Huang HF, Challa S (1939) Level-of-service model for pedestrians at signalized intersections. Transp Res Rec J Transp Res Board 55–62
49. Nagraj R, Vedagiri P (2013) Modeling pedestrian delay and level of service at signalized intersection crosswalks under mixed traffic conditions. Transp Res Rec 70–76
50. Kadali BR, Vedagiri P (2018) Pedestrian quality of service at unprotected mid-block crosswalk locations under mixed traffic conditions: towards quantitative approach. Transp J 33:302–314
51. Mohan M, Chandra S, Rastogi R (2015) Development of level of service criteria for pedestrians. J Indian Road Congr
52. Marisamynathan S, Vedagiri P (2017) Modeling pedestrian level of service at signalized intersection under mixed traffic conditions. Transp Res Rec 2634:86–94
53. Asadi-Shekari Z, Moeinaddini M, Zaly SM (2014) A pedestrian level of service method for evaluating and promoting walking facilities on campus streets. Land Use Policy 38:175–193
54. Tanaboriboon Y, Guyano JA (1991) Analysis of pedestrian movements in Bangkok. Transp Res Rec 1294:52–56
55. Miller JS, Garber NJ, Bigelow JA, Garber NJ (2000) Calibrating pedestrian level-of-service metrics with 3-D visualization. Transp Res Rec 1705:9–15
56. Kim S, Choi J, Kim Y (2011) Determining the sidewalk pavement width by using pedestrian discomfort levels and movement characteristics. KSCE J Civ Eng 15:883–889
57. Singh Yadav J, Jaiswal A, Nateriya R (2015) Modelling pedestrian overall satisfaction level at signalised intersection crosswalks. Int Res J Eng Technol 2:2328–2237
58. Muraleetharan T, Hagiwara T (2007) Overall level of service of urban walking environment and its influence on pedestrian route choice behavior. Transp Res Rec J Transp Res Board 2002:7–17
59. Kumar Saha M, Rahman Tishi T, Sirajul Islam M, Kumar MS (2013) Pedestrian behavioral pattern and preferences in different road crossing systems of Dhaka City. J Bangl Inst Plan 6:149–160
60. Botma H (1995) Method to determine level of service for bicycle paths and pedestrian-bicycle paths. Transp Res Rec 1502:38–44
61. Kang L, Xiong Y, Mannering FL (2013) Statistical analysis of pedestrian perceptions of sidewalk level of service in the presence of bicycles. Transp Res Part A Policy Pract 53:10–21
62. Petritsch TA, Landis BW, Mcleod PS, Huang HF, Challa S, Skaggs CL, Guttenplan M, Vattikuti V, Petritsch TA, Landis BW, Mcleod PS, Huang HF, Challa S, Skaggs CL (2006) Pedestrian level-of-service model for urban arterial facilities with sidewalks. Transp Res Rec J Transp Res Board 84–89
63. Sisiopiku VP, Byrd J, Chittoor A (2007) Application of level-of-service methods for evaluation of operations at pedestrian facilities. Transp Res Rec J Transp Res Board 2002:117–124
64. Al-Azzawi M, Raeside R (2007) Modeling pedestrian walking speeds on sidewalks. J Urban Plan Dev 133:211–219
65. Christopoulou P, Pitsiava-Latinopoulou M (2012) Development of a model for the estimation of pedestrian level of service in greek urban areas. Proc Soc Behav Sci 48:1691–1701
66. Marisamynathan S, Lakshmi S (2018) Method to determine pedestrian level of service for sidewalks in Indian context. Transp Lett 10:294–301

67. Jaskiewicz F, Jackson G, Anglin K, Rinehart L (2000) Pedestrian level of service based on trip quality. Transp Res Rec
68. Octaviana S, Moreno Freydig H (2013) Evaluation of walkability on pedestrian sidewalk in Bandung. In: The second Planocosmo conference
69. Fruin JJ (1971) Pedestrian Planning and design. Technical report
70. Jensen SU (2013) Pedestrian and bicycle level of service at intersections, roundabouts and other crossings. Transp Res Rec
71. Kim KL, Hallonquist L, Settachai N (2006) Measuring pedestrian level of service in an urban resort district. Transp Res Rec 104–112
72. Hidayat N, Choocharukul K, Kishi K (2011) Pedestrian level of service model incorporating pedestrian perception for sidewalk with vendor activities. Proc East Asia Soc Transp Stud 9:1012–1023
73. IRC:103-2022 Guidelines for Pedestrian Facilities. Indian Roads Congress, New Delhi
74. Indo-HCM (2017) Indian Highway Capacity Manual. CSIR-CRRI, Delhi

An Approach for Modelling Vehicular Pollution Using Artificial Neural Networks

Naina Gupta and Sewa Ram

Abstract Vehicular pollution is one of the biggest concerns in urban areas across the globe. Several air pollution studies have been carried out based on deterministic, statistical and soft computing approaches. However, limited research has been carried out on understanding the non-linear and highly complex dispersion of vehicular pollution based on soft-computing approaches. Artificial neural networks (ANN) consisting of interconnected adaptive processing units can detect nonlinearity in incomplete or noisy datasets. This paper elaborates the methodology for developing an ANN-based vehicular pollution model. In this study, pollution model has been developed for Income Tax Office (ITO) intersection in Delhi, considering particulate matter ($PM_{2.5}$), meteorological variables and traffic flow. Several combinations of models have been tried for prediction of pollutant concentration considering solely traffic variables and varying meteorological and traffic variables have been attempted. The results reveal that neural network models cannot predict satisfactorily when only traffic variables are considered but are able to do so when combination of traffic and meteorological variables are considered. The combination of temperature, wind direction, wind speed, mixing height and traffic flow gives the best model results. In addition, the results also concluded that wind speed is the most sensitive variable followed by atmospheric pressure, traffic flow and temperature in predicting $PM_{2.5}$ concentration.

Keywords Vehicular pollution · Pollution modelling · Particulate matter · Neural network

1 Introduction

India is the world's 4th most significant greenhouse gas emitter and ranks fifth amongst countries with the world's worst air quality [1]. Transportation is the fastest growing source of carbon emissions and contributes nearly 11% of India's carbon

N. Gupta (✉) · S. Ram
School of Planning and Architecture, Delhi, India
e-mail: nainagupta9793@gmail.com

A. Dhamaniya et al. (eds.), *Recent Advances in Traffic Engineering*, Lecture Notes in Civil Engineering 377, https://doi.org/10.1007/978-981-99-4464-4_2

emissions [2]. In addition, eleven of the twenty most polluted cities in Central and South Asia, according to a recent study [3], are Indian cities.

This clearly demonstrates the need for a better understanding of pollution dispersion phenomena, as well as developing a reliable model for pollution prediction. Decades of research have been devoted to modelling the dispersion of pollution, but it is still difficult to develop a realistic vehicular pollution model due to the several dynamic and influencing meteorological variables that have a substantial impact on pollution dispersion [4, 5].

Vehicle pollution modelling approaches are widely classified as deterministic, statistical, hybrid of statistical and deterministic models, and soft-computing systems [6]. Several studies have indicated that deterministic models are reasonably good at predicting air pollution and are useful in long-term planning decisions. However, they do not do well in terms of modelling vehicular pollution [7]. The correctness of deterministic models is determined by whether or not their underlying assumptions are met. Similarly, statistical models outperform non-linear data sets for site-specific analysis.

Numerous modelling studies utilizing multi-layer neural networks to anticipate pollutant concentrations have been undertaken in recent years, however the application of neural networks to estimate vehicle pollution is limited [18–22].

Table 1 provides a summary of several case studies relating to air pollution/vehicular pollution modelling over the years. Based on the non-linear and complex relationships in the environment, these research publications argue that soft computing approaches, particularly neural networks, are better suited for air pollution modelling.

However, regarding vehicular pollution modelling, deterministic or statistical approaches predominate. In addition, the findings predicted by deterministic models are more reliable than those anticipated by statistical approaches if the plume model's boundary conditions are precisely defined. Overall, having a reliable model of vehicular pollution remains a challenge due to vast number of dynamic and influencing variables which has significant impact on pollution dispersion. This paper discusses the methodology to develop a neural network for predicting vehicular pollution-based traffic and meteorological variables.

2 Vehicular Pollution Modelling Using Artificial Neural Network (ANN)

ANN is an offshoot of artificial intelligence which was developed initially in 1950s that envisaged to mimic the biological brain architecture and thereafter it became an indispensable modelling tool for modelling non-linear dynamic processes. The neural network method shows promise as a replacement for more traditional models due to its inherent abilities of self-correction, self-learning, and parallel processing [7]. The basic architecture of ANN is shown in Fig. 1.

Table 1 Review of Indian case studies related to pollution modelling

Author, Year	Approach	Variables
Dass et al. [8]	Soft computing (fuzzy)	Pollutant and meteorological variables
Dutta and Jinsart [9]	Comparison of statistical (multi linear regression, MLR) and soft computing (ANN)	Pollutant and meteorological variables
Kaur and Mandal [10]	Soft computing (ANN)	Pollutant and meteorological variables
Agarwal et al. [11]	Soft computing (ANN)	Pollutant and meteorological variables
Yadav and Nath [12]	Comparison of statistical (principal component analysis, MLR) and soft computing approach (ANN)	Pollutant and meteorological variables
Dhyani et al. [13]	Deterministic model (CALINE-based Gaussian plume dispersion model)	Meteorological, Traffic and Road characteristics
Mishra et al. [14]	Comparison of statistical (MLR) and soft computing approach (neuro-fuzzy and ANN)	Pollutant and meteorological variables
Kumar et al. [15]	Deterministic model (CALINE-based Gaussian plume dispersion model)	Meteorological, land use, surface characteristics and source emission data
Singh et al. [16]	Statistical (decision tree)	Pollutant and meteorological variables
Prakash et al. [17]	Soft computing (recurrent neural network)	Pollutant and meteorological variables

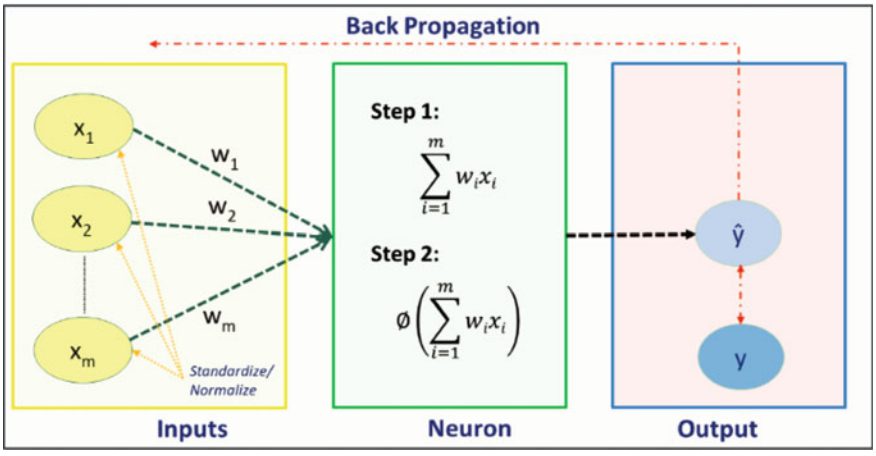

Fig. 1 ANN architecture

It comprises input layers (same as the number of independent variables), hidden layers and output layers. The neurons in the hidden layers, total layers, some other parameters such as learning rate, activation function, learning algorithm, number of epochs and batch size of the neural network are called hyper-parameters. These hyper-parameters are tuned to an optimum level to increase the efficiency of the model.

In ANN, the multi-layer neural network has been widely employed in air pollution research because of its ability to represent highly nonlinear relationships and generalize properly, when treated with new unseen data [23, 24]. To generate accurate model outputs, it is crucial to avoid overtraining neural networks, which causes the model to acquire inconsequential information from the training data, resulting in poor generalization when tested on new, untrained data [25].

To evade over training of neural networks, the model is often trained on a subset of inputs and outputs to determine weights, and then validated on the remaining dataset to verify the accuracy of model predictions. The dataset is divided into training dataset, test dataset and validation dataset. During training, the training dataset is utilized to evaluate the model's generalization performance. The training of the model is terminated when its performance on the test dataset reaches maximum. The test dataset is not used in the modelling process and is only used at the end of the modelling to test the predictability of the model beyond the training dataset. The final neural network model is evaluated using the validation dataset and hyper-parameter tuning. Further to carry out ANN-based vehicular pollution modelling six sequential steps are followed as mentioned below:

Step 1: Selecting Optimal Model-Architecture

The architecture of ANN-based vehicular pollution model consists of building interconnections between its input, hidden and output neurons. In the context of vehicular pollution modelling, the neurons in its input layer correspond to the number of meteorological and traffic input variables. The output layer consists of one neuron, i.e. pollutant concentration. However, the critical aspect is determining the number of neurons in its hidden layer which depends upon several factors like number of input/output neurons, noise in the data, network architecture, activation function employed in the hidden layer and the training process. Consideration of a small number of neurons in the hidden layer might result in underfitting and, thus, high training and testing mistakes. In contrast, taking into account an excessive number of neurons may result in overfitting and large variance, resulting in low error on training data set but high error on test dataset.

In the past, researchers have used the following criteria to determine optimal number of neurons (N) in the hidden layer, as listed below [7, 26, 27]:

(a) N = Summation of number of input neurons and output neurons;
(b) $N_{(max)}$ = Twice the number of neurons in its input layer;
(c) N = (Number of the training patterns)/(5 × number of neurons in its input and output layer);

(d) N = Adopting an iterative approach to determine optimal number of neurons which would yield minimum prediction error on the test data set.

Step 2: Selecting Activation/Transfer Function

The activation functions can be classified into two types: linear and non-linear activation function. Non-linear activation functions are the most often employed activation functions in ANN. The inclusion of activation functions enhances the non-linear approximation capabilities of ANN.

The activation/transfer function with a bound range is also known as squashing, or sigmoid functions. Sigmoid functions (hyperbolic tangent and logistic functions) have been predominantly employed for hidden neurons in ANN-based air pollution modelling, as a tiny change in weights will result in changes in the outputs that indicate whether the change in weight is converging or not. Further, linear or identity activation function does not transform its net input. In context of ANN-based vehicular pollution modelling, the sigmoid function is applied to the neurons of the hidden layer while the linear function is applied to the neurons of the input and the output layers [28, 29].

Step 3: Selecting Optimum Learning Parameters

The learning process in a neural network is carried out using several optimization algorithms with varied advantages and disadvantages in terms of memory, speed and precision. The most commonly used optimization algorithm includes Gradient descent; Newton technique; Conjugate gradient; Quasi-Newton method; Adam Optimizer and Levenberg-Marquardt algorithm.

In addition, the back-propagation technique is commonly used to train multi-layer neural networks, with learning rate and momentum rate considered to 'accelerate' or 'decelerate' error convergence, respectively. This training approach provides an 'approximation' of the gradient descent-calculated trajectory in weight space. The decrease in learning rate would result in a small change in synaptic weight after each iteration, resulting in slower training, whereas an increase in the value of the learning parameter would result in a large change in synaptic weight after each iteration, resulting in rapid training, but would render the network unstable or oscillatory. In order to avoid oscillation, the training algorithm for backpropagation takes momentum rate into account. The rates for 'learning' and' momentum' are between 0 and 1. The ideal values for 'learning' and' momentum' rates are determined using the convergence criteria like converging to local minima in error surface or network configuration with fewest number of epochs [7, 28].

Step 4: Initializing Network Weights and Bias

Before training the model, it is necessary to establish the synaptic weights and bias values of the network, which should be uniformly distributed within a small range of values to prevent premature saturation. The condition in which instantaneous sum-squared errors remain constant for a specified length of time during the

training process, but thereafter decrease. Therefore, it cannot be regarded as the local minimum.

In general, all network parameters are set to the random numbers distributed uniformly within small range of values to reduce likelihood of saturating neurons and developing small error gradients. For sigmoid functions, it is suggested to set random values for the weights which are uniformly distributed in the range ($\pm 2.4/\mathrm{Ni}$), where Ni represents total number of inputs [7, 30].

Step 5: Model Training and Generalization

Model training involves the process of estimating synaptic weights to accurately represent underlying patterns in training dataset and produce desired output with minimum model error. The training process involves initializing weights to small random values and then sequentially presents it to the network to perform the following steps.

(a) Multiply inputs by an initial random weight and calculate its summation;
(b) Transforming output of hidden layer by a sigmoid transfer function;
(c) Multiply the outputs of the hidden layer by the weight of the outputs of the hidden layer, and calculate the summation and
(d) Transforming the output using transfer function to estimate network outputs and compare the results with actual values.

In the context of back-propagation learning, the outputs are acquired by a series of iterations in which the weights are modified at each step so as to provide the smallest sum of squares error. There are two fundamental stopping criteria for the back-propagation algorithm:

(a) The method is deemed to have converged if there is no absolute rate of change in mean squared error (MSE) per epoch; however, this does not imply good generalization.
(b) After each repetition of the training set, the network's generalization performance is evaluated, and the process terminates when the performance on the test dataset as measured by prediction error achieves its maximum. If the error rate is more than the statistically acceptable level, the training process continues with additional epochs.

Step 6: Model Evaluation

Various statistical measures, such as Root Mean Square Error (RMSE), Mean Square Error (MSE), Mean Bias Error, Coefficient of determination (R^2), mean and standard deviations, and index of agreement, are used to evaluate the significance and performance of ANN models (d). In this study, the criteria examined for each phase are listed in Table 2.

Table 2 Criteria used for developing ANN-based vehicular pollution model

S. no.	Step	Criteria considered in the study
1	Selecting ANN architecture	• Input neurons = number of input variables (traffic and meteriological) • Input selection: Genetic algorithm and pruning • Output neurons: umber of output variable (Pollutant concentration) • Hidden neurons = minimum neurons that results in minimum prediction error on the test data set
2	Selecting activation/selection function	• Input and output neurons = linear function • Hidden neurons = sigmoid functions
3	Selecting learning parameters	Early stopping procedure wherein the learning parameters converge and give best performance on the test data with least number of epochs/iterations
4	Learning optimizer	Levenberg-Marquardt and Adam optimizer
5	Initializing network weights and bias	Random values for the weights which are uniformly distributed in the range ($\pm 2.4/N_i$), where N_i represents total number of inputs
6	Model training and generalization	Back-propagation
7	Stopping criteria	Early stopping procedure
8	Model evaluation	RMSE, MSE, R^2 and d value

3 Case Area: ITO Intersection, Delhi

Vehicular pollution model has been developed for one of the busiest junctions, i.e. Income Tax Office (ITO) Intersection in the National Capital, Delhi. Figure 2 shows the study area and the location of kerb side air quality monitoring station (about 3 m above the ground level) monitored by Central Pollution Control Board (CPCB). The source apportionment study (CPCB, [31] for Delhi also highlighted that traffic contributes to nearly 30% of the pollution observed at the junction. The predominant land use surrounding the site is institutional and commercial attracting large number of daily vehicular trips.

Fig. 2 Study area—ITO intersection, Delhi, India

3.1 Data Collection

3.1.1 Pollutant Data

The hourly pollution data set ($PM_{2.5}$ concentration, $\mu g/m^3$) for the month of January 2019 was obtained and used for training, validating and evaluating the ANN model's prognostic capacity. The pollutant concentration data for $PM_{2.5}$ was collected from CPCB for ITO junction, Delhi [32].

The dependent variable, $PM_{2.5}$ concentration has an average value of 156.5 $\mu g/m^3$ and varies between 24 $\mu g/m^3$ and 903.75 $\mu g/m^3$. Figure 3 depicts the variance in $PM_{2.5}$ concentration on a weekly and hourly basis. The weekly concentration peaks on Thursday and hourly variation shows that the concentration of $PM_{2.5}$ peaks at the midnight and reaches its lowest point around 5 pm.

3.1.2 Meteorological Data

The hourly meteorological data set for the month of January 2019 was collected for the nearest available weather station at Safdarjung (approximately 10 km from ITO Junction).

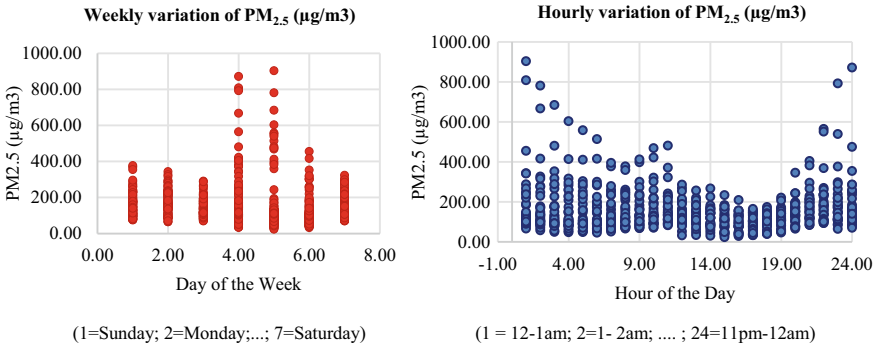

Fig. 3 Weekly and hourly variation of $PM_{2.5}$

3.1.3 Traffic Data

Using videographic surveys, 16 h of traffic data were collected on a weekday (Monday) and a weekend (Sunday) in January 2019. The data have been extrapolated to a 24-h count, and a factor for daily variance has been established based on historical traffic count data and fuel sales data. The daily volume average at this site is 1,45,355 PCUs. The percentage composition of the traffic on weekday and weekend is almost the same, wherein two-wheelers and four-wheelers occupy the maximum share of 77%.

Table 3 displays the average daily maximum, minimum, mean and median for each meteorological variable, whereas Table 4 displays the correlation between the variables.

The temperature ranges from an average of 13.06 °C to a minimum of 3.2 °C. Temperature and the concentration of the pollutant $PM_{2.5}$ are inversely proportional. The average dew point temperature, 10.3 °C, likewise exhibits an inverse association with $PM_{2.5}$ concentration, but one that is smaller than that of temperature. The relative humidity, which ranges from 40 to 100%, correlates positively with the $PM_{2.5}$ concentration. There is a modest inverse association between precipitation and $PM_{2.5}$ concentration. The major wind direction is west, and there is an inverse relationship between wind speed and $PM_{2.5}$ concentration. The air pressure, which ranges from 1008.6hPa to 1023.7hPa, correlates positively with the $PM_{2.5}$ concentration.

4 Model Development

The modelling procedure begins with the pre-processing of the data, which begins with data cleansing and inputs selection. As the ANN model can learn the pattern and adjust weights accordingly, it is not necessary to eliminate the insignificant variables.

Table 3 Average daily maximum, minimum, mean and median of meteorological variables

Code	Variable	Mean	Median	Maximum	Minimum
1	Temperature (°C), temp	13.06	12.80	22.60	3.20
2	Dew point temperature (°C), dwpt	10.33	10.35	15.80	3.20
3	Relative humidity, rhum	85.32	91.00	100.00	40.00
4	Precipitation (mm), prep	0.05	0.00	6.00	0.00
5	Wind direction (°), wdir	191.13	250.50	360.00	0.00
6	Wind speed (km/h), wspd	5.08	3.70	22.30	0.00
7	Atmospheric pressure (hPa), pres	1017.57	1017.90	1023.70	1008.60
8	Mixing height, mixh	442.3	–	900.00	50.00

Source Met Office [33]

Table 4 Correlation matrix

	temp	dwpt	rhum	prcp	wdir	wspd	pres	mixh	$PM_{2.5}$
temp	1								
dwpt	0.51	1							
rhum	-0.83	0.05	1						
prcp	0.11	0.26	0.05	1					
wdir	0.12	-0.13	-0.24	-0.1	1				
wspd	0.5	-0.04	-0.61	0.06	0.45	1			
pres	-0.44	-0.51	0.16	-0.27	0.03	-0.13	1		
mh	-0.36	-0.21	0.28	-0.05	-0.42	-0.41	0.32	1	
$PM_{2.5}$	-0.37	-0.2	0.29	-0.05	-0.41	-0.42	0.32	0.88	1

Genetic algorithm (GA) is used to incorporate the most pertinent characteristics of the dataset into the neural network selection for reducing dimensionality of data [34].

January 2019 one-month dataset was used for model training. The selected dataset is then divided into training, validation and test sets. The complete data set is separated into a training set and a test set with a 70:30 ratio. The test set is not utilized throughout the modelling procedure; rather, it is utilized at the conclusion of the modelling procedure to evaluate the model's ability to forecast beyond the training dataset. The validation set is extracted from the training set at a ratio of 70:30 for the purpose of hyper-parameter adjustment.

In this study, the 'Mean and Standard Deviation Scaling Method' was chosen for feature scaling of input using 'sci-kit learn' package in Python libraries.

The list of meteorological and traffic characteristic variables parameters considered as input variables include Temperature, Dew Point Temperature, Relative Humidity, Precipitation, Wind Direction, Wind Speed, Atmospheric Pressure, Mixing Height, vehicular flow and source strength ($PM_{2.5}$). A total of fifteen models with s with varied combinations of independent input variables and optimization algorithms were built. Five of these models with more importance are summarized in Table 2.

4.1 Hyper-Parameter Tuning of ANN

The hyper-parameters are the parameters that influence the efficiency of the ANN model. Determining the hyper-parameter could be based on theoretical basis or using optimization. However, optimizing all the hyper-parameters of the ANN is computationally expensive hence in this study just a subset of hyper-parameters is optimized and the rest are chosen on a theoretical basis. The optimization constraints considered for hyper-parameter tuning of ANN are presented in Table 5.

Various techniques, including random search, grid search, genetic optimization and so on, can be used to optimize hyper-parameters. The activation function, learning rule and batch size hyper-parameters were determined manually, and the remaining hyper-parameters were optimized using the 'random search' algorithm in the 'Keras tuner' module from the Python library. For each of the independent models, multiple computational runs were performed with random values of the number of neurons in the hidden layers, and the combination yielding the minimum Mean Square Error after the network stabilizes and having satisfactory statistical performance (in terms of 'd' and RMSE) was deemed to be the optimal number of neurons in the hidden layers. At repeated intervals of training epochs, the trained ANN-based model network is saved and its applicability is evaluated. The process continues until the performance of the trained model on the test dataset is optimal. After modelling with the selected hyper-parameters and visualizing the mean absolute error of the training and test datasets, the number of epochs was determined.

Table 5 Criterion of hyper-parameter tuning of ANN

Hyper-parameter	Optimization constraints
Number of hidden layers	1–25
Number of neurons in individual hidden layers	6–60
Learning rate	0.001/0.01/0.1

The incorporation of activation functions improves the ANN's nonlinear approximation skills. In this work, sigmoid (or logistic) and Tanh (or hyperbolic tangent) Activation Functions were utilized for hidden layers, whereas identity function was utilized for input and output layers.

Using the Python 'Keras' library, an ANN-based model for vehicle pollution has been constructed. Table 6 presents a summary of the five best model outputs that were produced using different techniques for input selection, transfer/activation function and learning. The modelling results indicate that Model 4 with a combination of temperature, wind direction, wind speed, mixing height and traffic flow gives best model results. The comparison of the observed and the predicted values for Model 4 is also presented in Fig. 4.

In addition to the models presented above, ANN model was also developed considering only traffic variables. The models with only traffic variables gave very poor results which indicated that the inability of ANN models to consider 'effect of background pollution' [4] in absence of meteorological variables. However, for overall predicting pollutant concentration considering traffic and meteorological variables, ANN can perform satisfactorily.

In addition, the model's sensitivity to changes in input variables with a 10% fluctuation in pollution concentration was analysed and presented in Fig. 5. Wind speed was determined to be the most important variable, followed by atmospheric pressure, traffic flow and temperature.

Table 6 Summary of model outputs

Final input layer		Model 1	Model 2	Model 3	Model 4	Model 5
		temp, dwpt, rhum, wspd, pres, tf	temp, rhum, wdir, wspd, pres, tf	temp, rhum, wspd wdir, tf	temp, wdir, wspd, pres, mh, tf	temp,wspd, pres, mh, tf
No. of hidden neurons		7	9	10	10	9
Input selection		GA	GA	GA	GA	Pruning
Transfer function		tanh	Logistic	tanh	tanh	logistic
Learning		Levenberg–Marquardt algorithm		Adam optimizer		
Testing	MSE	0.005	0.005	0.004	0.003	0.006
	RMSE	0.070	0.071	0.063	0.055	0.079
	d	0.85	0.87	0.81	0.94	0.85
	R^2	0.68	0.71	0.57	0.84	0.69

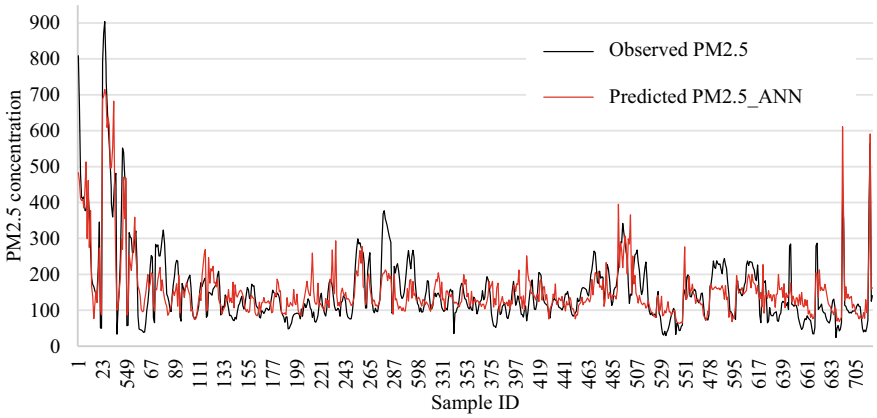

Fig. 4 Observed versus predicted PM2.5 concentrations

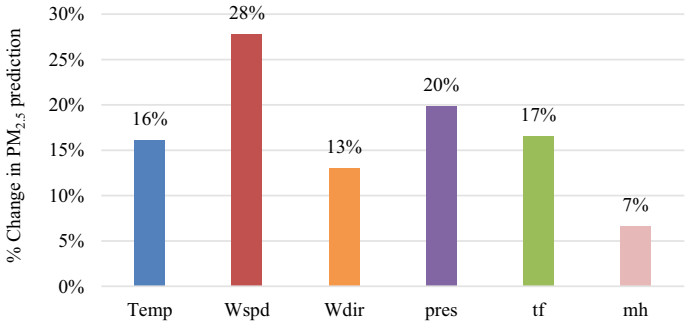

Fig. 5 Sensitivity analysis with respect to 10% variation in input variables

5 Conclusion

The majority of vehicle pollution modelling research conducted in the last decade was based on deterministic (especially plume-based dispersion model) and statistical methodologies, which do not adequately reflect the complex and non-linear connections. In order to examine the intricate interrelationships between traffic, meteorological variables and varied pollution concentrations in urban areas, ANN should be researched further. And the development of a dependable model of vehicular pollution could assist local governments in creating efficient air quality management policies.

In this study, the ANN method predicted good results for modelling vehicle pollution. However, additional traffic characteristics like as composition, speed and fuel type must be investigated further.

References

1. UN Environment Programme: Emissions Gap Report. UNEP (2019). https://www.unep.org/resources/emissions-gap-report-2019
2. Kamboj P et al (2022) India transport energy outlook. CEEW. https://www.ceew.in/publications/india-transport-energy-use-carbon-emissions-and-decarbonisation
3. IQAir (2021). https://www.iqair.com/world-most-polluted-cities/world-air-quality-report-2021-en.pdf
4. Gupta N, Ram S, Sudagani BG (2023) Environmental capacity of roads under mixed traffic conditions. In: Devi L, Errampalli M, Maji A, Ramadurai G (eds) Proceedings of the sixth international conference of transportation research group of India. CTRG 2021. Lecture notes in civil engineering, vol 273. Springer, Singapore. https://doi.org/10.1007/978-981-19-4204-4_6
5. Gupta N, Ram S (2023) Effects of traffic on particulate matter (PM2.5) in different built. Nat Environ Pollut Technol 22(2):887–894. https://doi.org/10.46488/NEPT.2023.v22i02.031
6. Shiva Nagendra SM, Khare M (2004) Artificial neural network-based line source models for vehicular exhaust emission predictions of an urban roadway. Transp Res Part D: Transp Environ 9(3):199–208
7. Khare M, Nagendra SMS (2007) Artificial neural networks in vehicular pollution modelling. Springer, Berlin
8. Dass A, Srivastava S, Chaudhary G (2021) Air pollution: a review and analysis using fuzzy techniques in Indian scenario. Environ Technol Innov 22:101441
9. Dutta A, Jinsart W (2021) Air pollution in Indian cities and comparison of MLR, ANN and CART models for predicting PM10 concentrations in Guwahati, India. Asian J Atmos Environ 15(1):68–93
10. Kaur M, Mandal A (2020) PM2.5 concentration forecasting using neural networks for hotspots of Delhi. In: 2020 International conference on contemporary computing and applications
11. Agarwal S et al (2020) Air quality forecasting using artificial neural networks with real time dynamic error correction in highly polluted regions. Sci Total Environ 735:139454
12. Yadav V, Nath S (2018) Novel hybrid model for daily prediction of PM10 using principal component analysis and artificial neural network. Int J Environ Sci Technol 16(6):2839–2848
13. Dhyani R, Sharma N, Maity AK (2017) Prediction of PM 2.5 along urban highway corridor under mixed traffic conditions using Caline4 model. J Environ Manage 198:24–32
14. Mishra D, Goyal P, Upadhyay A (2015) Artificial intelligence-based approach to forecast PM 2.5 during haze episodes: a case study of Delhi, India. Atmos Environ 102:239–248
15. Kumar A et al (2015) Application of WRF model for vehicular pollution modelling using AERMOD. Atmos Clim Sci 05(02):57–62
16. Singh KP, Gupta S, Rai P (2013) Identifying pollution sources and predicting urban air quality using ensemble learning methods. Atmos Environ 80:426–437
17. Prakash A et al (2011) A wavelet-based neural network model to predict ambient air pollutants' concentration. Environ Model Assess 16(5):503–517
18. Heydari A et al (2021) Air pollution forecasting application based on deep learning model and optimization algorithm. Clean Technol Environ Policy 24(2):607–621
19. Kumar A (2016) Modeling for vehicular pollution in urban region; a review. Pollution. https://jpoll.ut.ac.ir/article_58309.html
20. Rahimi A (2017) Short-term prediction of NO_2 and no X concentrations using multilayer perceptron neural network: a case study of Tabriz, Iran—ecological processes. Springer
21. Shams SR et al (2021) Artificial intelligence accuracy assessment in NO_2 concentration forecasting of metropolises air. Nat News. https://www.nature.com/articles/s41598-021-81455-6
22. Sofuoglu SC et al (2006) Forecasting ambient air SO_2 concentrations using artificial neural networks. Taylor and Francis. https://doi.org/10.1080/009083190881526
23. Abiodun OI et al (2018) State-of-the-art in artificial neural network applications: a survey. Heliyon

24. Gardner MW, Dorling SR (1998) Artificial Neural Networks (the multilayer perceptron)—a review of applications in the Atmospheric Sciences. Atmos Environ 32(14–15):2627–2636
25. Bilbao I, Bilbao J (2017) Overfitting problem and the over-training in the era of data: particularly for artificial neural networks. In: Eighth international conference on intelligent computing and information systems
26. Sheela KG, Deepa SN (2013) Review on methods to fix number of hidden neurons in neural networks. Math Prob Eng. https://www.hindawi.com/journals/mpe/2013/425740/
27. Xu S, Chen L (2008) A novel approach for determining the optimal number of hidden layer neurons for FNN's and its application in data mining. A novel approach for determining the optimal number of hidden layer neurons for FNN's and its application in data mining—Open Access Repository. https://eprints.utas.edu.au/6995/
28. Mlakar P, Boznar MZ (2011) Artificial neural networks—a useful tool in air pollution and meteorological modelling. Intech Open
29. Park J, Chang S (2021) A particulate matter concentration prediction model based on long short-term memory and an artificial neural network. Int J Environ Res Publ Health. https://www.ncbi.nlm.nih.gov/pmc/articles/PMC8297184
30. Yadav S (2020) Weight initialization techniques in neural networks. Medium. https://towardsdatascience.com/weight-initialization-techniques-in-neural-networks-26c649eb3b78
31. CPCB: Air quality monitoring, emission inventory and source apportionment studies—Delhi. https://cpcb.nic.in/displaypdf.php
32. CPCB: Central pollution control board (2019). https://www.cpcb.nic.in/automatic-monitoring-data
33. Met Office: New Delhi Safdarjung (India) weather (2019). https://www.metoffice.gov.uk/weather/forecast/ttnfsermf#?date=2022-08-23
34. Montri I, Veera B, Sarun I (2016) Artificial neural network and genetic algorithm hybrid intelligence for predicting Thai stock price index trend. Comput Intell Neurosci. https://doi.org/10.1155/2016/3045254

Pedestrian Perception of Safety in Areas with Newly Provided Pedestrian Facility: The Case of Bangalore's Tender SURE (Specifications for Urban Utilities and Road Execution Project)

Aditya Saxena, P. S. Reashma, and Basavaraj Kabade

Abstract According to India's Ministry of Road Transport and Highways (MORTH), every sixth person killed in a road accident is a pedestrian, making pedestrians vulnerable road users. The general approach to mitigating such an epidemic is to implement corrective infrastructure measures. However, pedestrian perceptions of such changes are often neglected. Although a few studies in the Indian context on pedestrian perceptions of safety have been conducted, the majority of them have been done with the goal of advocating for improvements to existing old infrastructure. This becomes a reactive approach, while the current study aims to examine the safety perceptions of pedestrians in newly pedestrianized zones as a proactive approach by determining the factors that influence pedestrians' perception of safety. The study area under consideration in this study is part of the newly constructed pedestrian zones as a part of the project Tender S.U.R.E. Bangalore. In the present study, principal component analysis (PCA) with a discrete choice model (ordinal logistic regression) was applied to determine the factors affecting the safety perception of pedestrians. Based on the results obtained it was found that pedestrian perceptions of safety were significantly affected by their income level, their frequency of walking, and the three factors derived from principal component analysis. The findings of this study also revealed that pedestrians were most concerned about the approaching speed of vehicles. Referring to the results obtained from the present study, government agencies can plan future interventions pertaining to infrastructural changes.

Keywords Pedestrian safety · Perception study · Principal component analysis · Ordinal logistic regression · Income levels · Frequency of walking

A. Saxena
Indian Institute of Technology, Mumbai, India

P. S. Reashma (✉)
Global Academy of Technology, Bengaluru, India
e-mail: psreashma@gmail.com

B. Kabade
Bruhat Bengaluru Mahanagara Palike (BBMP), Bengaluru, India

A. Dhamaniya et al. (eds.), *Recent Advances in Traffic Engineering*, Lecture Notes in Civil Engineering 377, https://doi.org/10.1007/978-981-99-4464-4_3

1 Introduction

The negative externalities of urban transport cause immense social and economic loss to the nation [1]. According to reports, there are 20–50 million serious injuries each year [2]. According to the World Health Organization (WHO), pedestrian fatalities accounted for 22% of all road-user deaths in 2019, globally [3]. It is imperative that research be conducted to reduce pedestrian crashes [4]. In India, every year almost 1.5 lakh (0.15 million) people lose their lives in road crashes. MORTH categorizes pedestrians and two-wheeler users within the vulnerable road users (VRUs) category [1, 5]. In total, VRUs account for 54% of fatalities. Approximately 55,000 pedestrians were killed in road crashes in just two years (13,400 deaths in 2016 to 22,700 deaths in 2018) [6]. In India, out of the total number of fatalities every year, 17% involve pedestrians, implying that every sixth person who dies in a traffic crash is a pedestrian. Such statistics are indicative of the importance of pedestrian safety studies and inventions in the Indian context. From the start of this century, the Indian government has taken up this matter as a priority. In this regard, amendment in motor vehicle act, approval of Good Samaritan law, allocation of funds for infrastructure improvement, and formation of National Road Safety Committee (NRSC) are some of the clinical measures adopted by the government [7]. MORTH recently initiated grants programs to non-governmental organizations (NGOs) for working on road safety at the advocacy level. In terms of urban design interventions, the Ministry of Housing and Urban Affairs has recently launched its campaign for Pedestrianization of at least three marketplaces in every million-plus city of India [8].

Even after the availability of extensive kinds of literature for pedestrian safety and design guidelines, there exists a gap. In the Indian Context, road safety studies are often worked out from an infrastructure engineering and design point of view, and the perspective of the road user is often left out in such studies. The present study is an attempt to bridge this existing gap by performing a pedestrian perception study and assessing the parameters affecting it. The city of Bangalore is taken up as a case for conducting pedestrian perception study towards road safety. The present study evaluated the influence of 12 parameters selected from the literature review for identifying pedestrian safety perceptions. Cronbach's alpha test was used to assess the reliability and internal consistency of the selected parameters; additionally, the selected parameters were subjected to principal component analysis to derive factors from the selected parameters. The derived factors were then subjected to ordinal logistic regression with perceived safety ratings of pedestrians as dependent and derived factors, other socio-economic variables as independent to establish the relationship.

Bangalore is the fifth largest metropolis in India, with a total population of 8.5 million [9]. Just like most of the metro cities in India, the pedestrian safety scenario in Bangalore is critical. As per the dataset released by the traffic police department of Bengaluru, the city witnessed 7019 fatal crashes which resulted in 7297 losses of lives from 2010 to 2020 [10]. To mitigate pedestrian fatalities and improve pedestrian safety, the government of Karnataka initiated Tender S.U.R.E. (Specifications

for Urban Road Execution) project in Bangalore [11]. As of yet, it has yet to be determined whether such a pedestrian safety initiative would be effective.

2 Literature Review

2.1 A Subsection Sample

In the context of urban transportation, global, perception studies have been extensively cited [12–[14]. Based on their literature study, Raad [15] highlighted comfort level, footpath width, obstructions to pedestrian flow, motor vehicle speeds and volumes, shoulder widths, and on-street parking as determinants of pedestrian perception towards infrastructure. In another study, it was found pedestrian perception as a powerful tool for evaluating the Quality of Service (QoS) at sidewalks [16]. Another attempted to explore the importance of public perceptions on road safety measures and rules and concluded that in order to build a safe scenario, public participation and their support is pivotal [17]. In a study conducted in Vietnam, the influence of attitudes towards traffic safety, risk perceptions, and pedestrian behaviors was explored [18]. Using regression analysis and structural equation modeling, the author determined that safer attitudes towards traffic safety and higher levels of traffic risk perception are associated with safer pedestrian behaviors.

Ram [19] performed a similar kind of study by applying exploratory factor analysis, followed by confirmatory factor analysis to understand the effect of drivers' risk perception and perception of driving tasks on road safety attitude. His study observed a significant positive correlation between drivers' risk perception and perception of driving tasks and found that both perceptions significantly affect drivers' road safety attitudes. Espinoza [20] also focused on driver's perception of road safety using confirmatory factor analysis and groped the selected 41 variables into 6 categories (human, vehicle, road infrastructure, regulatory framework and intervention measures, socio-economic and driving precautions). Another study of the same kind was performed by Anapakula [21] for assessing the parameters affecting the quality of the pedestrian environment and later on developing an index for the same. They advocated that such studies will assist governing bodies in progressive decision-making, as well as help them in prioritizing pedestrian-oriented investments. Balasubramanian [22] assessed pedestrians' perception while approaching vehicles crossing towards the road in the nighttime, and concluded that the effect of beam light from vehicles had a direct relation with safe crossing.

There can be multiple parameters and factors affecting pedestrian safety and their perception. Vijayawargiya [23] identified vehicle volume, vehicle speed, carriageway width, pedestrian refugee island, street lights, and road marking and signage as major parameters affecting pedestrian safety perception. In another study, Bendak [24] waiting time before crossing the road, sight distance, speed of approaching vehicle were considered as determining parameters. The world health organization (WHO)

in one of their study found that inadequate visibility, speed of approaching vehicles, and improper road sign and markings were the major reason for pedestrian crashes [25]. Barón [26] determined that properly raising median and curbs, availability of resting places, quality of footpath, cleanliness, and aesthetics are major motivating features for a pedestrian to perceive a secure walking environment.

In India, pedestrian safety research has received considerable attention in recent past years. Both reactive and proactive safety approaches were adopted and tried to quantify both actual as well perceived risk of pedestrian safety. Studies focused on reactive approach, investigated historical crash data, identified the high-intensity crash location (black spot) also the potential risky elements influencing pedestrian safety by correlating the crash data to infrastructure elements, built environment, traffic operational characteristics. One such reactive study was conducted by Rankavata [27], wherein forty-five crash spots were identified using past data, a primary survey was conducted to assess the pedestrians' perceived risk towards safety, and an ordered logit model was further used to evaluate the effect of various demographics on perceived road safety. While proactive safety studies were conducted by Bhaduri [28] and Kumar [29] where the focus was to study the perceived satisfaction of pedestrians towards the present infrastructural services.

Many studies focused on pedestrian behavior aspects and quantified the dynamics of pedestrian-vehicle interaction. Kumar [30] explored the yielding behavior of road users during conflicts and analyze the spontaneous order developed at intersections. The results obtained from their study suggested that vehicle volume, type of vehicle, noncompliance with signals by pedestrians, type of pedestrian-vehicle interaction, and size of intersection are some of the major factors that are significant predictors of the dominance of road users. In order to assess the reasons behind pedestrian-vehicle interaction at un-signalized junctions, a study was conducted by Kathuria [31] where severity levels were proposed under heterogeneous traffic conditions using Import Vector Machine (IVM) approach.

The proactive-based approach is gaining more attention as they promise in-depth safety analysis focusing on nearby pedestrian-vehicle interaction (near-miss collision events) and identifying the degree of severity of collisions by meaningfully relating it to actual crashes. Many researchers have combined both proactive and reactive safety approaches and assessed pedestrian safety. Chatterjee [32] identified several risk factors responsible for road crashes in rural roads using the principles of the road safety audit, developed a risk matrix using available crash data, and concluded that integrating the findings from reactive analysis with proactive safety management is more beneficial than just focusing on only proactive or reactive approaches. Mukherjee [33] proposed a methodology combining both reactive and proactive approaches to assess pedestrian safety at urban intersections using a combination of historical crash data, analysis of pedestrian-vehicle interaction, and pedestrian risk perception towards built environment and traffic characteristics.

For a pedestrian, safety is not limited to being safe but also to the extent of feeling safe. Perception studies are usually deployed to understand how pedestrians feel safe on roads. It also serves as input for decision-makers to improve the safety measures to achieve the safety target. Pedestrian perception safety studies were also

performed in the Indian context, but the nature of these studies and their objectives varied widely. Many research studies Kadali [34] performed perception studies with respect to specific pedestrian facilities and had developed models to evaluate the safety level and determining the respective level of service. Rankavata [27] conducted pedestrian perception studies in Delhi to understand the underutilization of pedestrian facilities like a zebra crossing, underpasses, and overpasses and also assessed the existing safety level of each of these facilities. Mukherjee [33] studied pedestrian perceived satisfaction level at signalized intersections in Kolkata city in the viewpoint of fatal pedestrian crash frequency. Pedestrian perception studies were performed by Banerjee [35] to identify the critical factors influencing the use of pedestrian skywalk facilities in an Indian context. Studies have reported the use of pedestrian perception to identify their impact on future travel decisions Rahul [36].

As noted in the reviewed literature, in the Indian context, it is logit models and structural equation modeling methods are most frequently used for assessing the perception of pedestrians. Contrary to other studies, the present study adopts a proactive approach by assessing the factors influencing pedestrians' perception of road safety by using a combination of principal component analysis and discrete choice model (ordinal logistic model), an approach that has not been previously explored extensively. The advantage of applying such an approach is that it has the ability to analyze pedestrian safety perception at an aggregate level by deriving factors out of the several selected parameters, thus making it easy for the government to implement future infrastructure change easily. The objective of the current study is (i) to identify the various factors that affect the pedestrian perception of road safety and (ii) to assess how satisfied they are with the selected factors.

3 Methodology and Data Collection

Based on the discussion with Bruhat Bengaluru Mahanagara Palike (BBMP), Twelve Central Business Districts (CBDs) were selected in Bangalore based on their high utility and footfall. After the selection of the study area, the sample size was determined using Slovin's Formula. All the selected twelve CBDs were considered as one study area and based on the cumulative footfall, a sample size of 384 samples was determined, at 95% confidence level and 5% margin of error. After extraction of the total number of samples to be obtained, the sample size was further distributed based on the footfall proportion of each CBD against the cumulative footfall. With the help of literature review, the present study considers twelve parameters (presence of road sign and marking, lighting at the crossing, presence of refuge island, pedestrian volume, waiting time while crossing the road, visibility and sight distance, cleanliness, and quality of footpaths, continuity of footpaths, obstruction-free footpaths, and speed of approaching vehicles) as the determining parameters for deriving principal component factors. The derived factors and the socio-economic variables of the respondents are then subjected to an ordinal logit model.

A survey questionnaire was designed for the purpose of assessing the impact of selected parameters on perceived satisfaction towards road safety for pedestrians. The samples were collected using the random sampling method. No specific group or class of people was targeted. The survey was conducted by 9 surveyors at the selected locations through Google forms filled by the respondents. A total of 384 samples were collected from selected locations. The data was collected using a 5-point Likert scale. Further, to capture the socio-economic profile of respondents, data regarding their age (0–15, 15–59, and older than 59) in an ordinal scale, gender (male, female) on a nominal scale, household income (0–25, 25–50, 50–100, and above 100k) in ordinal scale, and frequency of walking a week (every day, 3–4 days, 5 days, weekends only, and hardly ever) in ordinal scale were collected.

After the primary data collection, the obtained data were sorted and analyzed using statistical software Jamovi, which is a GUI for the R programming language. For performing statistical analysis, the initial step is to validate the reliability and measure the internal consistency of data. Cronbach's Alpha test was used for this purpose and the standardized value achieved was around 0.8, indicating a very good model fit. Based on the satisfaction rating of twelve selected parameters, collected from the Likert scale, principal component analysis was performed for the purpose of dimension reduction using the varimax rotation method. In our study, varimax rotation was applied since datasets were not correlated [37]. Twelve parameters were reduced into three factors. The three obtained factors were then utilized to understand the relation between them and perceived road safety using an ordinal logistic regression model. For the purpose of regression, respondents were asked to assess the pedestrian road safety condition in the survey area and rate it from "very low" (1) to "very high" (5).

The foremost task was the identification of parameters affecting perception towards safety. The survey questionnaire included questions about the socio-economic profile and travel behavior characteristics of respondents in the first part. In the second part of the survey questionnaire, respondents were asked to rate their satisfaction with the selected parameters. Twelve parameters for principal component analysis were identified from the literature review and were assigned codes for simplicity in analysis. The selected parameters and their respective coding are shown in Table 1.

The survey questionnaire was designed to capture the socio-economic profile and travel behavior of respondents along with their perceived satisfaction on selected parameters and road safety satisfaction level or rating with regard to the area where the survey was conducted. For the purpose of sampling, the total footfall of all the CBDs was considered and Slovin's formula was used to determine the sample size [38]. In Slovin's formula, a 95% confidence level was considered and a 5% margin of error.

Slovin's formula:

$$n = \frac{1}{Ne^2} \tag{1}$$

Table 1 Identified parameters for principal component analysis

Parameter	Respective infrastructure	Code
Speed of approaching vehicles	Midblock	Q1
Presence of road sign and marking	Midblock	Q2
Waiting time	Midblock	Q3
Lighting at crossing	Midblock	Q4
Presence of refuge island	Midblock	Q5
Visibility/sight distance	Midblock	Q6
Pedestrian volume	Footpath/sidewalk	Q7
Cleanliness of footpath	Footpath/sidewalk	Q8
Availability and quality of street lights	Footpath/sidewalk	Q9
Resting spaces	Footpath/sidewalk	Q10
Continuity of footpath	Footpath/sidewalk	Q11
Presence and quality of kerb height	Footpath/sidewalk	Q12

where, n-Sample size, N-Total population/Footfall, e-Margin of error.

From secondary data, total footfall was found to be around 4,80,000 per day, implying a sample size of 384 when equated in Eq. (1).

4 Results

This section details out the results obtained from descriptive and statistical analysis performed from the data collected.

4.1 Descriptive Statistics

In terms of socio-economic profile, from the collected data, it was observed that 61% of the respondents were male, while only 39% were female. Within the age category, the working-age group had a very significant share within the respondents with 91% of them between the age group of (15–59), followed by senior citizens with only 8% of them. Within the income category, the lower-income group (0–25 k/month) and the middle-lower income group (25–50 k/month) recorded a significant share with 46% and 27% respectively. Based on the data collected, 73% of the respondents walked every day. The data collected from the primary survey is depicted in Table 2.

Table 2 Socio-economic profile of respondents

Age	Number	Percentage share
0–15	3	1
15–59	349	91
60 and above	29	8
NA's	3	1
Gender		
Female	148	39
Male	233	61
Other	1	0
NA's	2	1
Monthly household income		
>100k	23	6
0–25k	177	46
25–50k	104	27
50–100k	72	19
NA's	8	2
Frequency of walking in a week (walking as a mode)		
1–3 days	46	12
4–5 days	26	7
Every day	281	73
Hardly ever	1	0
Weekends only	30	8
Total	384	100

4.2 Perception Study Details

Results from the perception study depict that overall, people were not satisfied with the current infrastructure provided or present prevailing conditions, as the mean obtained for most of the selected parameters was lower than 3 (which was described as average while conducting surveys). The highest mean was obtained for the twelfth parameter which was "Appropriate Kerb Height." While the people were most unsatisfied with the first parameter "speed of approaching vehicles." The selected parameters were coded for the purpose of simplicity in data analysis and representation, as shown in Table 3.

Table 3 Perception of respondents towards selected parameters

Parameter	Respective infrastructure	Code	Median	Mean
Speed of approaching vehicles	Midblock	Q1	2	2.402
Proper road sign and marking	Midblock	Q2	3	2.825
Waiting time	Midblock	Q3	3	2.517
Lighting at crossing	Midblock	Q4	3	2.836
Presence of refuge island	Midblock	Q5	3	2.559
Visibility/sight distance	Midblock	Q6	3	2.995
Pedestrian volume	Sidewalk	Q7	3	2.671
Cleanliness of footpath	Sidewalk	Q8	3	2.919
Availability and quality of street lights	Sidewalk	Q9	3	2.564
Resting spaces at footpaths	Sidewalk	Q10	3	2.705
Continuity of footpath	Sidewalk	Q11	3	2.817
Appropriate kerb height	Sidewalk	Q12	3	3.201

4.3 Statistical Analysis

4.3.1 Principal Component Analysis (PCA)

Principal Component Analysis was performed on all the twelve selected parameters for dimension reduction and extracting factors out of the selected parameters. Principal component analysis (PCA) is a technique for reducing the dimensionality of such datasets, increasing interpretability but at the same time minimizing information loss. The benefit of using PCA is that it removes correlation between different parameters, and improves visualization. Using "Jamovi" as a tool, component variances and component loading was obtained. Component variances refer to estimates of the contributions that different experimental factors make to the overall variability of the data while component loading is the contribution of the particular variable to the principal component [39]. As studied from the literature review, only those factors were retained whose Eigenvalue is above 1 [40]. Three factors were acquired from Component variances, as shown in Table 4. The correlation between factors and parameters was found from component loading and only those parameters were retained whose correlation value was above 0.5 [41], as depicted in Table 5. The following equation was used for computing covariance [42].

$$Cov(X, Y) = \frac{\left[\Sigma_{i=1}^{n}(\mathrm{Xi} - \overline{\mathrm{X}})(\mathrm{Yi} - \overline{\mathrm{Y}})\right]}{n - 1} \tag{2}$$

where X, Y are variables.

Table 4 Eigenvalues for components

Component variances	Eigenvalues	Importance of components (%)
Comp.1	3.79	31.60
Comp.2	1.562	44.60
Comp.3	1.002	53.00

Table 5 Parameter correlations with obtained factors

Parameters	Component loading			Uniqueness
	1	2	3	
"Q1"	0.691			0.44
"Q2"	0.604			0.57
"Q3"	0.645			0.52
"Q4"	0.539			0.65
"Q5"	0.712			0.47
"Q6"	0.552			0.41
"Q7"	0.597			0.61
"Q8"		0.60		0.37
"Q9"			0.794	0.34
"Q10"		0.643		0.53
"Q11"			0.595	0.39
"Q12"		0.799		0.34

The top three components were only retained. The retained three components explain 53% of the variance which is acceptable [43]. The respective component loading values are depicted in Table 6.

Furthermore, the Kaiser-Meyer-Olkin (KMO) measure of sampling adequacy is used to determine whether the data is sufficient for a stable factors solution. The KMO test considers the variance explanation of the indicators. Bartlett's sphericity test checks the validity of factor analysis by examining the whole correlation matrix, which identifies the correlation between variables. This is a measure of how strongly one variable is correlated with another. A KMO value greater than 0.5 and a significance level of less than 0.05 for Bartlett's test suggest that the data exhibit a strong correlation [44, 45]. Based on the KMO measure and Bartlett's Test of Sphericity, a value of 0.819 was evaluated with a significance level of less than 0.01.

Finally, obtained component values for component loading with respect to the corresponding factor. Factor 1 contains Q1, Q2, Q3, Q4, Q5, Q6, and Q7, Factor 2 comprises Q10 and Q11, while Factor 3 includes Q9 and Q12. Table 6 illustrates the obtained factors and their respective parameters.

Table 6 Obtained factors and their respective parameters

Parameter	Respective infrastructure	Code
Speed of approaching vehicles	Midblock	PCA 1
Proper road sign and marking	Midblock	
Waiting time	Midblock	
Lighting at crossing	Midblock	
Presence of refuge island	Midblock	
Visibility/sight distance	Midblock	
Pedestrian volume	Sidewalk	
Cleanliness of footpath	Sidewalk	
Appropriate kerb height	Sidewalk	PCA 2
Resting spaces at footpath	Sidewalk	
Continuity of footpath	Sidewalk	PCA 3
Availability of street lights	Sidewalk	

4.3.2 Cronbach's Alpha

To estimate the reliability of data and check its internal consistency of parameters under each factor, Cronbach's Alpha test was performed. Cronbach's Alpha measures reliability by comparing the amount of variance shared among the items that make up an instrument to the overall variance of the instrument. For statistical significance, a value of 0.7 is considered acceptable [46]. Majorly, Cronbach's alpha test is applied to the data collected through the Likert scale. Cronbach's alpha was performed between the selected parameters for the following purpose. The obtained reliability was around 0.8, which signifies a good fit or good reliability of data. The obtained results are shown in Table 7. Furthermore, to evaluate the multi-collinearity diagnostics, tolerance level and Variance inflation factor (VIF) value was estimated. The range for rejecting multi-collinearity in data was adopted as VIF value < 10 and tolerance value > 0.10 [47]. The dataset was found to be reliable and free from multi-collinearity after performing the tests.

4.3.3 Ordinal Logistic Regression

The ordinal logistic model develops the relationship between an ordinal response variable and one or more explanatory variables using ordinal logistic regression. After extracting Factors, ordinal logistic regression analysis was performed for assessing the relationship between the three Factors and the overall city safety rating given by respondents while conducting the survey. The safety ratings were kept as a dependent while the three factors were kept as independent variables. The equation used for performing ordinal logistic regression analysis is as follows [48]:

Table 7 Results obtained from Cronbach's alpha test

Parameter	Respective infrastructure	Factor	Mean
Speed of approaching vehicles	Midblock	PCA 1	0.787
Proper road sign and marking	Midblock		
Waiting time	Midblock		
Lighting at crossing	Midblock		
Presence of refuge island	Midblock		
Visibility/sight distance	Midblock		
Pedestrian volume	Sidewalk		
Cleanliness of footpath	Sidewalk	PCA 2	0.732
Appropriate kerb height	Sidewalk		
Resting spaces at footpaths	Sidewalk		
Continuity of footpath	Sidewalk	PCA 3	0.704
Availability of street lights	Sidewalk		

Table 8 Model fit statistics for ordinal logistic model

Model	Deviance	AIC		R^2_N	χ^2	Overall model test	
			R^2_{McF}			df	p
1	920	950	0.355	0.408	85.9	11	< 0.001

$$y_n = \beta^T x_n + \epsilon_n n = 1, \ldots, N \tag{3}$$

where y_n is given by the combination of variables, parameters, and random residuals that are taken into consideration in the estimated models, being n as the generic individual and N as the sample size. ϵ_n represents the random residuals. The vector x_n is a set of covariates, assumed to be independent of ϵ_n. β and y are vectors of estimated parameters.

The results obtained from ordinal logistics regression analysis (keeping safety rating as dependent variable and PCA1, PCA 2, PCA 3, gender, income and frequency of walking as independent variables) are shown in Tables 8 and 9.

From Table 9, it can be observed that while income, frequency of walking, and the three derived factors (PCA1, PCA2, PCA3) had a significant relationship with safety ratings, gender was found to have insignificant relation.

5 Discussion and Conclusion

The results indicate that PCA1, PCA 2, and PCA 3 do not support the null hypothesis, as a significant relationship exists between all three derived factors and perceived safety ratings. In addition, income levels and walking behavior (frequency of walking

Table 9 Results from ordinal logistics regression

Predictor	Estimate	SE	p	Odds ratio	95% confidence interval	
					Lower	Upper
PCA1	0.4232	0.102	<0.001	1.5268	1.25	1.869
PCA2	0.5115	0.101	<0.001	1.6678	1.37	2.037
PCA3	0.5915	0.102	<0.001	1.8066	1.482	2.211
"Monthly household income"						
50–100k – 0–25k	−0.815	0.276	0.003	0.4426	0.257	0.76
>100k – 0–25k	−0.1317	0.426	0.757	0.8766	0.381	2.035
25–50k – 0–25k	−0.4215	0.238	0.077	0.656	0.411	1.045
"Frequency of walking in a week"						
4–5 days–weekends only	−1.2236	0.497	0.14	0.2942	0.11	0.777
Every day–weekends only	−0.9904	0.371	0.008	0.3714	0.178	0.765
1–3 days–weekends only	−0.9522	0.441	0.031	0.3859	0.162	0.914
Hardly ever–weekends only	−4.0273	1.788	0.024	0.0178	4.22E-04	0.724
"Gender"						
Male–Female	−0.0959	0.2	0.631	0.9086	0.614	1.344

in a week) were also significantly related to perceived safety ratings. However, gender did not have a significant relationship. Based on the data analysis results, we can also conclude that all three derived factors had a greater influence on perceived safety than socio-economic variables. In terms of income bracket, respondents earning "50–100 k" per month were 0.44 times less satisfied with perceived safety as compared to those earning "0–25 k" per month. As for walking behavior, Respondents who only walk every day were found to be significantly more satisfied as compared to respondents who walk on weekends only. The results of this study also showed that in general, pedestrians were most anxious about the approaching speed of the vehicles.

The perception of pedestrian safety has been studied from a reactive and a proactive perspective [49–51]. The present study was a proactive approach-based study on the perception of pedestrians regarding the infrastructure changes in Bangalore under the TENDER SURE program. The results of the present study will assist the concerned authorities in identifying the areas on which they need to focus in the future to improve the perceived safety level of roads. The need to improve perceived safety levels has been justified by several studies, in order to enhance the mode share of non-motorized transport and reduce car dependency, safety perception directly influences the choice of mode of transportation [52–54]. According to the results of this study, all the selected parameters (road sign and marking, lighting at crossings,

presence of refuge islands, pedestrian volume, crossing time, visibility and sight distance, continuous footpaths, obstruction-free footpaths, and speed approaching vehicles) except for one (cleanliness on the footpath) had a notable impact on pedestrian safety perception. Furthermore, pedestrians were most concerned about the speed of approaching vehicles, which is consistent with the findings of other studies [22, 55–57]. Moreover, it was also found that people who walk only on weekends are more satisfied with safety levels than people who walk daily, frequently, or rarely. However, this is a distinct observation from the existing literature [58, 59]. The reason for this observation may be that people who walk only on weekends experience fewer safety issues than those who walk daily, frequently. Additionally, these respondents who walk only on weekends do not face the same traffic conditions as those who walk on weekdays.

The conclusion which can be drawn from the present study is that respondents feel unsafe while crossing the road because of the high speed of approaching vehicles while they comparatively seem to be satisfied with the infrastructure provided at sidewalk/footpaths. Additionally, the result of the work made under Tender S.U.R.E. can also be related to the project's major purpose, which was primarily about improving pedestrianization with urban design interventions. Based on the responses, it is determined that most respondents complained about difficulty crossing the street, lack of enforcement and policeman to regulate traffic, lack of resting areas on sidewalks, and poor quality of footpaths and streets. On the other hand, most respondents revealed no problems with obstructions on or continuity of the path. Many respondents even expressed a desire for more trees and greenery around the sidewalks. While, with Tender S.U.R.E., city authorities are attempting to meet the infrastructure users' needs, maintaining and ensuring the quality of the services provided are entirely different issues. In addition, respondents repeatedly pointed out the lack of a proper drainage system that causes waterlogging and unhygienic conditions. The issue needs to be addressed quickly so that pedestrians can be safe and secure all year round.

6 Research Contribution

Traditionally, pedestrian safety studies have been carried out with a view to suggesting improvements to the old infrastructure. Most studies have used pedestrian perception to examine the root causes of their safety perception and to identify the factors affecting their perception, while in this study, we examine the factors which influence pedestrian perception in areas that have recently been pedestrianized under a government project. The selected areas are under the project of Tender S.U.R.E. The goal of this study is to take a closer look at the areas or parameters that need further attention even after improving road infrastructure specifically for pedestrians. This was determined by selecting 14 parameters that can be directly related to pedestrian safety perception.

Furthermore, the present study employs an approach wherein we combine principal component analysis with the discrete choice model (ordinal logit model). The advantage of using this approach is that often it becomes difficult to interpret the results when several parameters have a significant influence on the dependent variable. By employing this method, we were able to derive 3 factors out of 14 parameters, thus making it easy for the city authorities and implementation agencies to prioritize which factors they need to improve further.

7 Future Scope and Limitations

The purpose of this study was to identify the factors that affect pedestrian perceptions of safety. Using principal component analysis and ordinal logistic regression, the current study examined the relationship between perceived safety levels and the contributing factors, as well as the socio-economic profile of respondents. Due to the perception-based nature of the present study, there may be a number of factors that influence pedestrians' perceptions of safety that may not have been taken into account in the current study. It is worth noting that because sampling was random, the socio-economic factor "age" of the respondent was not included in the analysis of the data since the data for age was found to be highly skewed. This is because in India, the category of "15–59" is considered as a working-age group and a vulnerable age group [7]. We kept this category as it is for the purposes of collecting samples in this model. This study is also limited by the fact that nearly 37% of the samples were collected from a specific location, meaning the perception of respondents in that location had a big impact on the overall results. Further, the extracted factors could explain up to 53 percent of the total variance, which is one limitation of using principal component analysis.

Response to Reviewers

The authors would like to thank the scientific committee for accepting our manuscript and suggesting important changes. The suggested changes have been incorporated. Please find the point-by-point response.

Comments	Revisions
Reviewer 1	
How sample representativeness is checked, how it's representing the population	Based on the discussion with Bruhat Bengaluru Mahanagara Palike (BBMP), Twelve Central Business Districts (CBDs) were selected in Bangalore based on their high utility and footfall. After the selection of the study area, the sample size was determined using Slovin's Formula. All the selected twelve CBDs were considered as one study area and based on the cumulative footfall, a sample size of 384 samples was determined, at 95% confidence level and 5% margin of error After extraction of the total number of samples to be obtained, the sample size was further distributed based on the footfall proportion of each CBD against the cumulative footfall
Is any pilot survey conducted?	Yes, the authors conducted pilot survey to check the adequacy and flow of survey questions. However, we did not include the samples collected from pilot survey for main data analysis
Only traffic safety is considered? What about personal security, i.e., security from crime?	The present study looks into the case of implementation of safety measures adopted under Tender S.U.R.E. project in Bangalore city. The scope of the present study was limited to assess the safety perception of pedestrians towards road crashes. Personal security related to other crimes were not considered in the present study
Mean perception is very low for all variables. What about the standard deviation?	The standard deviation for all the parameters ranged from 0.73 (minimum) to 1.87 (maximum)
Pearson correlation analysis need to conducted to assess the correlation among attributes	In order to account for the effect of collinearity, PCA was employed. The parameters that had high correlation among each other were reduced into a single factor. Table 5 depicts the same Regarding the correlation among the derived factors, PCA as a statistical method itself takes care of it

(continued)

(continued)

Comments	Revisions
What is research contribution and novelty? Similar studies are already conducted in Indian context	Traditionally, pedestrian safety studies have been carried out with a view to suggesting improvements to the old infrastructure. Most studies have used pedestrian perception to examine the root causes of their safety perception and to identify the factors affecting their perception, while in this study, we examine the factors which influence pedestrian perception in areas that have recently been pedestrianized under a government project. The selected areas are under the project of Tender S.U.R.E. The goal of this study is to take a closer look at the areas or parameters that need further attention even after improving road infrastructure specifically for pedestrians. This was determined by selecting 14 parameters that can be directly related to pedestrian safety perception Furthermore, the present study employs an approach wherein we combine principal component analysis with the discrete choice model (ordinal logit model). The advantage of using this approach is that often it becomes difficult to interpret the results when several parameters have a significant influence on the dependent variable. By employing this method, we were able to derive 3 factors out of 14 parameters, thus making it easy for the city authorities and implementation agencies to prioritize which factors they need to improve further
Reviewer 2	
In the Abstract, there are repetitions of sentences in lines from 20 to 28. Please check	Suggested change has been taken care off
Page 3, Line 30, World Health Organisation. W.H.O can be in capital letters	Suggested change has been incorporated
Page 3, line 32 [22]—while citing a reference in the starting of a sentence, parenthesis may be omitted. Please check	Suggested change has been incorporated
Page 3, line 32 [26]—same observation as in 3	Suggested change has been incorporated
Page 4, line 4, line 17, line 31, line 34—same observation as in 3	Suggested change has been incorporated
Page 5, line 3: Research contribution section may be located towards the end of the paper	As suggested by the reviewer we have moved the research contribution section towards the end

(continued)

(continued)

Comments	Revisions
Page 6, line 5, frequency of walking a week, if 4 days, it comes under which category? (3–4 days or 4–5 days?)	Thank you for highlighting this mistake. It will actually come under 3–4 days. To avoid any type of miscommunication we have made the necessary change in manuscript
Page 7, line 7, Slovin's formula is given as n = 1/Ne2. But it is found to be n = N/(1 + Ne2). From the following reference. https://www.statisticshowto.com/probability-and-statistics/how-to-use-slovins-formula/ please comment	By mistake, wrong citation was inserted. We have changed the source of information
Page 7, line 23, "Based on the data collected, walked every day (73%)." Please modify the sentence	Suggested change has been incorporated
Page 7, line 15, subsection 5.1, many details in the text (lines 19 to 23) are repeated in Table 2, which can be modified/omitted	Suggested change has been incorporated
Page 7, line 23–24, "The interpretation of data collected from the survey is depicted in Table 2." This sentence may be modified	Suggested change has been incorporated
Page 9, line 7, punctuation is missing	Suggested change has been incorporated
Page number 12, line 9, please correct the typing error "(frequency of walking in a weak)"	

Funding Not available.

Disclosure Statement The authors report there are no competing interests to declare.

References

1. Saxena A, Choudhury B (2022) Internalizing the externalities of urban private transport—a case of Gurugram, national capital region, India. Case Stud Transp Policy. https://doi.org/10.1016/j.cstp.2022.08.002
2. Mphela T, Mokoka T, Dithole K (2021) Pedestrian motor vehicle accidents and fatalities in Botswana—an epidemiological study. Front Sustain Cities. https://doi.org/10.3389/frsc.2021.666111
3. The World Bank (2017) The High Toll of Traffic Injuries: Unacceptable and Preventable. https://openknowledge.worldbank.org/bitstream/handle/10986/29129/HighTollofTrafficInjuries.pdf?sequence=5andisAllowed=y
4. Zegeer CV, Carter DL, Hunter WW, Richard Stewart J, Huang H, Do A, Sandt L (1982) Index for assessing pedestrian safety at intersections. Transp Res Rec J Transp Res Board 1982(1):76–83. https://doi.org/10.1177/0361198106198200110
5. Saxena A (2022) Is street design and infrastructure perceived differently by persons of different ages, genders , and hierarchy of street ? Innov Infrastruct Solut. https://doi.org/10.1007/s41062-022-00880-2

6. Dash DK (2019) 62 pedestrians die daily in India, up 84% in 4 years. https://timesofindia.indiatimes.com/india/62-pedestrians-die-daily-in-india-up-84-in-4-years/articleshow/72101003.cms
7. Transport Research Wing (2019) Road accidents in India—2019. Ministry of Road Transport and Highways, MORTH
8. MOHUA (2020) Pedestrianisation in market places: MoHUA recommends holistic planning for pedestrian friendly market spaces in consultation with stake holders. https://pib.gov.in/PressReleasePage.aspx?PRID=1630613
9. Registrar General & Census Commissioner., India (2011) 2011 Census data. https://censusindia.gov.in/2011-common/censusdata2011.html
10. Police (2021) Bengaluru traffic. Accident Statistics. http://www.bangaloretrafficpolice.gov.in/Accidentstats.aspx
11. Indian Urban space foundation (2012) Government of Karnataka project tender S.U.R.E. Report. Indian Urban space foundation
12. Pietrantonio H, Bornsztein LL (2015) Evaluating road safety audit procedures: some questions and a new method of study. Transp Plan Technol 38(8):909–34. https://doi.org/10.1080/03081060.2015.1079390
13. Qi Y, Zhao Q (2017) Safety impacts of signalized lane merge control at highway work zones. Transp Plan Technol 40(5):577–91. https://doi.org/10.1080/03081060.2017.1314499
14. Kim NS, Yoon SS, Yook D (2017) Performance comparison between pedestrian push-button and pre-timed pedestrian crossings at midblock: a Korean case study. Transp Plan Technol 40(6):706–21. https://doi.org/10.1080/03081060.2017.1325146
15. Raad N, Burke MI (2018) What are the most important factors for pedestrian level-of-service estimation? A systematic review of the literature. Transp Res Rec J Transp Res Board 2652(35). https://doi.org/10.1177/0361198118790623
16. Rodriguez-Valencia A, Barrero GA, Ortiz-Ramirez HA (2020) Power of user perception on pedestrian quality of service. Transp Res Rec J Transp Res Board 2674(5). https://doi.org/10.1177/0361198120914611
17. Mikušová M, Hrkút P (2014) Public perception of selected road safety problems. Proc Soc Behav Sci 330–339
18. Dinh D, Vũ NH, McIlroy RC (2020) Effect of attitudes towards traffic safety and risk perceptions on pedestrian behaviours in Vietnam. IATSS Res 238–247
19. Ram T, Chand K (2016) Effect of drivers' risk perception and perception of driving tasks on road safety attitude. Transp Res Part F Traf Psychol Behav
20. Espinoza F, del Valle Arenas Ramirez B, Izquierdo FA (2021) Road safety perception questionnaire (RSPQ) in Latin America: a development and validation study. International Journal of Environmental Research and Public Health
21. Anapakula KB, Eranki GA (2021) Developing an index to evaluate the quality of pedestrian environment: case study application in an Indian metro. Transp Res Interdisc Perspect
22. Balasubramanian V, Bhardwaj R (2018) Pedestrians' perception and response towards vehicles during road-crossing at nighttime. Accident Anal Prevent 128–135
23. Vijayawargiya V, Rokade S (2017) Identification of factors affecting pedestrian level of service of crosswalks at roundabouts. Int Res J Eng Technol (IRJET) 342–346
24. Bendak S, Alnaqb AM (2021) Factors affecting pedestrian behaviors at signalized crosswalks: an empirical study. J Saf Res 269–275
25. Bartolomeos K, Crof P (2013) Pedestrian safety—a road safety manual for decision makers and practitioners. The World Health Organization (WHO)
26. Barón L, da Costa JO, Soares F (2021) Effect of built environment factors on pedestrian safety in Portuguese urban areas. Applied System Innovation (Applied System Innovation)
27. Rankavata S, Tiwari G (2016) Pedestrians risk perception of traffic crash and built environment features—Delhi, India. Saf Sci 1–7
28. Bhaduri E, Manoj BS, Sen J (2019) Measuring user satisfaction of pedestrian facilities and its heterogeneity in urban India—a tale of three cities. J East Asia Soc Transp Stud

29. Kumar P (2007) The value of design : a study of pedestrian perception in New Delhi, India. Environment and Planning D-society & Space D
30. Kumar A, Ghosh I (2020) Analysis of spontaneous order of pedestrian–vehicle conflicts at signalized intersections. Transp Res Rec J Transp Res Board
31. Kathuria A, Vedagiri P (2020) Evaluating pedestrian vehicle interaction dynamics at un-signalized intersections: a proactive approach for safety analysis. Accident Anal Prevent
32. Chatterjee S, Mitra S (2019) Safety assessment of two-lane highway using a combined proactive and reactive approach: case study from Indian national highways. Transp Res Rec J Transp Res Board
33. Mukherjee D, Mitra S (2020) Pedestrian safety analysis of urban intersections in Kolkata, India using a combined proactive and reactive approach. J Transp Saf Secur
34. Kadali RB, Nivedan R, Perumal V (2015) Evaluation of pedestrian mid-block road crossing behavior using an artificial neural network (ANN). J Traf Transp Eng
35. Banerjee A, Maurya AK (2019) A comparative study of pedestrian movement behavior over foot over bridges under similar land-use type. Transp Res Proc. Elsevier
36. Rahula TM, Manoj M (2020) Categorization of pedestrian level of service perceptions and accounting its response heterogeneity and latent correlation on travel decisions. Transp Res Part A Policy Pract 40–55
37. Neumann DL, Chan RCK, Boyle GJ (2015) Measures of personality and social psychological constructs. In: Saklofske DH, Gregory GM, Boyle J (eds) Measures of empathy: self-report, behavioral, and neuroscientific approaches. Elsevier, pp 257–289. https://doi.org/10.1016/B978-0-12-386915-9.00010-3
38. Korkmaz IH, Özceylan A, Özceylan E (2019) Investigating the academic success of industrial engineering students in terms of various variables. Proc Comput Sci 158:9–18. https://doi.org/10.1016/j.procs.2019.09.022
39. Karamizadeh S, Abdullah SM, Manaf AA (2013) An overview of principal component analysis. J Signal Inf Process 173–175. https://doi.org/10.4236/jsip.2013.43B031
40. Jolliffe IT, Cadima J (2016) Principal component analysis: a review and recent developments. Philos Trans R Soc A
41. Maskey R, Fei J (2018) Use of exploratory factor analysis in maritime research. Use of exploratory factor analysis in maritime research, pp 91–111
42. Dubey A (2018) The mathematics behind principal component analysis. https://towardsdatascience.com/the-mathematics-behind-principal-component-analysis-fff2d7f4b643
43. Mishra S, Sarkar U (2017) Principal component analysis. Int J Livestock Res
44. Rossoni L, Engelbert R, Bellegard NL (2016) Normal science and its tools: reviewing the effects of factor analysis in management. Revista de Administração 51(2):198–211. https://doi.org/10.5700/rausp1234
45. Han W, Zhao J (2020) Driver behaviour and traffic accident involvement among professional urban bus drivers in China. Transp Res Part F Traf Psychol Behav 74:184–97. https://doi.org/10.1016/j.trf.2020.08.007
46. Birren JE (2007) Encyclopedia of gerontology. Elsevier
47. Fumagalli LAW, Rezende DA, Guimarães TA (2021) Challenges for public transportation: consequences and possible alternatives for the covid-19 pandemic through strategic digital city application. J Urban Manage 10(2):97–109. https://doi.org/10.1016/j.jum.2021.04.002
48. Coppola P, Silvestri F (2020) Assessing travelers' safety and security perception in railway stations. Case Stud Transp Policy 8(4):1127–1136
49. Baldwin C, Stafford L (2019) The role of social infrastructure in achieving inclusive liveable communities: voices from regional Australia. Plan Pract Res 34(1):18–46. https://doi.org/10.1080/02697459.2018.1548217
50. Behrens R (2005) Accommodating walking as a travel mode in south African cities: towards improved neighbourhood movement network design practices. Plan Pract Res 20(2):163–82. https://doi.org/10.1080/02697450500414686
51. Talen E (2002) Pedestrian access as a measure of urban quality. Plan Pract Res 17(3):257–278. https://doi.org/10.1080/026974502200005634

52. Guo Y, Yang L, Huang W (2020) Traffic safety perception, attitude, and feeder mode choice of metro commute: evidence from Shenzhen. Int J Environ Res Publ Health 17(24)
53. Nordfjærn T, Şimşekoğlu Ö, BrendeLind H (2014) Transport priorities, risk perception and worry associated with mode use and preferences among Norwegian commuters. Accident Anal Prevent 72:391–400
54. Nevelsteen K, Steenberghen T, Van Rompaey A (2012) Controlling factors of the parental safety perception on children's travel mode choice. Accident Anal Prevent 45:39–49
55. Papić Z, Jović A, Simeunović M, Saulić N (2020) Underestimation tendencies of vehicle speed by pedestrians when crossing unmarked roadway. Accident Anal Prevent 143:105586
56. Shi J, Wu C, Qian X (2020) The effects of multiple factors on elderly pedestrians' speed perception and stopping distance estimation of approaching vehicles. Sustainability 12(13):5308
57. Butler AA, Lord SR, Fitzpatrick RC (2016) Perceptions of speed and risk: experimental studies of road crossing by older people. PLoS One 11(4)
58. Lyu Y, Forsyth A (2021) Attitudes, perceptions, and walking behavior in a Chinese city. J Transp Health 21:101047
59. Yoh K, Khaimook S, Doi K, Yamamoto T (2021) Study on influence of walking experience on traffic safety attitudes and values among foreign residents in Japan. IATSS Res

Plots to Identify the Rheological Properties of Polymer-Modified Warm Mix Binders

Rajiv Kumar and Vinod Kumar Sharma

Abstract The present study describes the use of various plots to identify the rheological properties of polymer-modified warm asphalt binders, which are obtained from the dynamic shear rheometer (DSR). Isothermal Plot, Isochronal Plot, Cole-Cole Diagram, Black diagrams, and Master Curves are presented to detect the occurrence of inconsistencies in rheological data caused by material properties of warm mix additive. Polymer-modified binder (PMB-40) and Sasobit were used to make polymer-modified warm asphalt binder. The Sasobit was added in the dose of 2, 3, and 4% by weight of the binder, and the linear viscoelastic (LVE) region for each binder was determined at an angular frequency of 10 rad/s at a temperature ranging from 20 °C to 70 °C. The frequency sweep test was conducted at different frequencies and temperatures to produce different rheological plots. It is found that the rheological properties of PMB-40 get changed when Sasobit is added. The result further indicates that Williams-Landel-Ferry (WLF) equation which is generally used to calculate the shift factor for the normal binder is not valid for modified warm mix binders and the shift factor for complex modulus is different from that for phase angle.

Keywords Polymer modified binder (PMB) · Sasobit · Warm asphalt binders (WMA)

1 Introduction

Asphalt cement is a common binder used in the construction of flexible pavement. It is principally obtained as a residual product in petroleum refineries. In India, this material is typically called bitumen. The rheological characteristics of the asphalt cement binders in India are determined using some empirical tests. For example,

R. Kumar (✉)
CSIR-Central Road Research Institute, Delhi-Mathura Road, New Delhi 110025, India
e-mail: rajivkumar.crri@nic.in

V. K. Sharma
Dr. B.R. Ambedkar National Institute of Technology, G.T. Road, Jalandhar 144027, India
e-mail: vinodks.ce.18@nitj.ac.in

A. Dhamaniya et al. (eds.), *Recent Advances in Traffic Engineering*, Lecture Notes in Civil Engineering 377, https://doi.org/10.1007/978-981-99-4464-4_4

softening point is determined to predict the deformation properties of bitumen at high temperatures, the ductility test to find the cohesive properties of the asphalt binder, and the Frass breaking point test to judge the brittleness property of the asphalt binder at low temperature. Neat asphalt is classified based on viscosity at 60 °C as per current Indian specifications IS 73 [1]. It states that 7 days average maximum temperature in a year can decide the use of viscosity grade bitumen. In north India, the maximum temperature in summer reaches 45 °C and VG-40 can only be used in such conditions. Also, with the increases in axle loads and traffic volumes, polymer-modified asphalt (PMA) is increasingly used in India. Bahia et al. [2] reported unmodified binders to have major drawbacks like rutting, fatigue cracking, low-temperature cracking, and moisture-induced damage. This distress is relieved when polymer-modified bitumen is used. However, the mixing temperature for all modified binders is above 177 °C which is considered very high in the asphalt industry with consideration of emission problems. To reduce the mixing temperature, new technology like warm mix technology is quite popular nowadays.

Warm Mix Asphalt (WMA) refers to an asphalt concrete mixture that is produced at a lower temperature than Hot Mix Asphalt (HMA). Generally, it has been observed that Warm Mix Asphalt can be produced from 20 °C to 30 °C when compared with HMA [3–5]. As per IRC SP, 101-2019 temperature should be reduced by more than 30 °C in the case of warm mix asphalt.

Kok and Akpolat [6] modified B 50/70 bitumen with SBS, Sasobit, and SBS+Sasobit, and found that 3% SBS with 3% Sasobit gives better results than other combinations of modifiers. It showed a good elastic performance, with a 53% higher toughness index value than that achieved by 3% SBS modification alone. Zelelew et al. [7] also observed that the mixtures prepared with Sasobit give higher stiffness, a higher dynamic modulus rutting parameter (G*/Sinδ), and higher fatigue cracking parameter (G*.Sinδ) than those of the other mixes.

Wasiuddin et al. [8] found that in the case of PG 70-28, 2%, 3%, and 4% Sasobit reduces the mixing temperature by 10 ºC, 12 ºC, and 13 ºC respectively, from 163 ºC and also increases the high-temperature binder grading. Mallick et al. [9] showed that Sasobit helped in obtaining a uniform mix. Another research has also reported similar types of findings with Porras et al. [10], Bennert et al. [11], Saboundjian et al. [12], Middleton and Forfylow [13] have reported that the addition of Sasobit decreases the mixing and compaction temperature by 20 ºC to 30 ºC in Germany.

The rheological behavior of bitumen varies with time and temperature and the stiffness of the bitumen is time-dependent. The dynamic shear rheometer (DSR) test is used to measure the elastic and viscous nature of bituminous binders within a linear and nonlinear viscoelastic range of temperatures and frequencies. The rheological data of binders can be presented in many forms including Isothermal plots, Isochronal plots, Cole-Cole diagrams, Black Diagrams, and Master curves. Isothermal plots show the behavior of complex modulus (G*) with frequency (ω) at different temperatures. The isochronal plot is a curve that represents the behavior of complex modulus (G*) or phase angle (δ) with the temperature at a constant frequency. Cole-Cole diagram is drawn between the loss modulus (G”) and the storage modulus (G’). The black diagram is a graph drawn with the magnitude (norm) of the complex modulus

(G*), versus the phase angle (δ) obtained from a dynamic test, and the Master Curve is drawn with the complex shear modulus (G*) and the phase angle (δ) against frequency for various temperatures on a Log-log scale. The principle used to relate the equivalency between time and temperature and produce a master curve is known as the time-temperature superposition principle (TTSP).

TTSP theory is based on Schapery's work and also Park and Schapery [14] discovered that the solid propellant is thermos rheologically simple in the linear viscoelastic range. It implies that the same set of time-temperature shift factors can apply to both states. Elastic modulus is the function of time and temperature and the modulus-temperature relationship is described using TTSP which states that the relaxation modulus (E) at temperature (T) is equal to the modulus at the reference temperature (T_{ref}) at a scaled time by a shift factor of a_T (T) and this factor is a function of temperature difference only Williams et al. [15]. This relationship known as Williams-Landel-Ferry (WLF) relation is given in Eq. (1).

$$E(T,t) = E(T_{ref,a} - T^t(T)) \tag{1}$$

WLF equation can be written in a logarithmic relationship as Eq. (2).

$$\log 10\, \boldsymbol{a_T}(\boldsymbol{T}) = \frac{-c1(T - T_{ref})}{c2 + (T - T_{ref})} \tag{2}$$

where C1 and C2 are material constants.

The present study describes the use of various plots to identify the rheological properties of warm mix additive (Sasobit) with an Indian-specified grade of modified asphalt binder (PMB-40). Rheological tests were conducted on a dynamic shear rheometer (DSR) using a spindle 25 mm diameter and with a 1 mm gap. Isothermal Plot, Isochronal Plot, Cole-Cole Diagram, Black diagrams, and Master Curve are developed to detect the occurrence of inconsistencies in rheological data caused by testing irregularities and distinctive material properties of warm mix additive.

2 Experimental Design

2.1 Materials

In this study, PMB-40 binder has been compared with warm mix binder having 2%, 3%, and 4% Sasobit by weight of base asphalt binder. The additive was blended into the asphalt binder using a low-shear mixer for 15 min. The mixer speed was 300 revolutions per minute, and it was equipped with a four-blade propeller. The binder was heated to the blending temperature at 150 ℃, and it was stirred for 1 min to obtain a uniform temperature throughout the binder then warm mix additive was added and stirred for 15 min at 300 revolutions per minute.

2.2 *Dynamic Test*

The dynamic tests are conducted using the Anton Paar controlled strain Dynamic Shear Rheometer (DSR) at temperatures of 20–70 °C with 10 °C equal intervals. Testing was done in the linear viscoelastic region (LVE), which was found at an angular frequency of 10 rad/s with a range of strain levels of 0.01–100% for each temperature. It is observed that the strain level for linear viscoelastic is more at high temperatures and less at low temperatures. The obtained highest strain level for linear viscoelastic strain level is taken for the frequency sweep test and the frequency was varied from 0.1 rad/s to 100 rad/s.

3 Result and Discussion

An oscillatory test was conducted by using a Dynamic Shear Rheometer. The first step was to conduct the Amplitude sweep test to find the linear viscoelastic range (LVE Range). To find the LVE-Ranges, the stain was varied from 0.01% to 100% while the angular frequency was fixed at 10 rad/s. The profile in the setup was ramp log+point/decades with 6 point/dec at each temperature. The LVE ranges are given in Table 1. In this study, the linear viscoelastic region is considered as the strain at which the complex modulus dropped by 95% of the initial value. Table 1 shows the basic rheological properties and LVE range of polymer-modified warm asphalt binders.

Table 1 Basic rheological properties of asphalt binder

Rheological property	PMB-40	PMB-40+2% S	PMB-40+3% S	PMB-40+4% S
Softening point (ºC)	60	64	75	80
Penetration value (dmm)	54	30	30	24
Viscosity at 150 ºC (c.P)	685	577	387	210
PG-true grade	PG 85-X	PG 87-X	PG 89-X	PG 90-X
LVE range at 70 ºC (%)	10 (28.65)	5 (13.239)	1 (2.847)	1 (5.409)
LVE range at 60 ºC (%)	10 (26.45)	5 (11.2)	1 (2.637)	1 (4.782)
LVE range at 50 ºC (%)	10 (24.9)	5 (7.605)	1 (1.473)	1 (3.857)
LVE range at 40 ºC (%)	5 (8.001)	1 (4.416)	1(1.918)	1 (2.564)
LVE range at 30 ºC (%)	1 (2.811)	1(1.77)	1 (1.428)	1 (1.405)
LVE range at 20 ºC (%)	1 (1.806)	0.5 (1.113)	0.5 (0.8584)	0.5 (1.001)

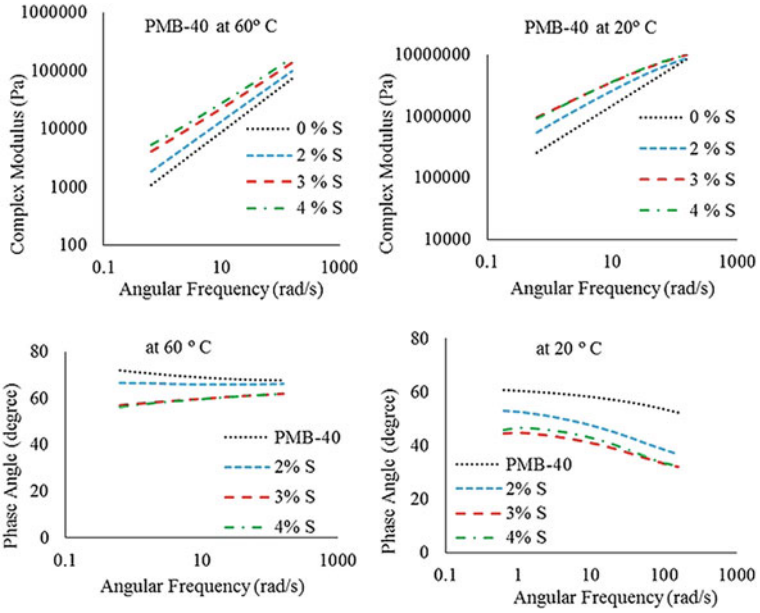

Fig. 1 Isothermal plot of complex modulus and phase angle for asphalt binder at 60 °C and 20 °C

3.1 Isothermal Plot

Figure 1 shows the isothermal plots of complex shear modulus and phase angle for PMB-40 and PMB-40 with Sasobit at 60 °C and 20 °C. The complex modulus of asphalt binder increases with frequency which shows that with the increase in frequency, the stiffness of the asphalt binder increases also the content of Sasobit increases the stiffness of the asphalt binder at 60 °C as well as 20 °C. However, at low temperatures, the rate of increase in the complex shear modulus reduces with the Sasobit content. Isothermal plots of phase angle show that the phase angle reduces with the addition of Sasobit in the PMB-40 binder. At a lower temperature of 20 °C, the phase angle reduces with frequency also. It implies that at a higher frequency and lower temperature the warm mix asphalt binder becomes stiffer and more elastic than a normal polymer-modified binder.

3.2 Isochronal Plot

Variation in complex modulus (G*) and phase angle (δ) with the temperature at low frequency (1.04 rad/s) and high frequency (157 rad/s) is shown in Fig. 2. As may be seen the complex modulus decreases sharply and the phase angle increases with an increase in test temperature. The complex shear modulus of PMB-40 increases

when 2% Sasobit is added but remains almost the same at higher doses of Sasobit. The same is the case with phase angles also. It is lower for warm mix asphalt binder, but an increase of Sasobit dose from 3 to 4% does not make any difference in the phase angle.

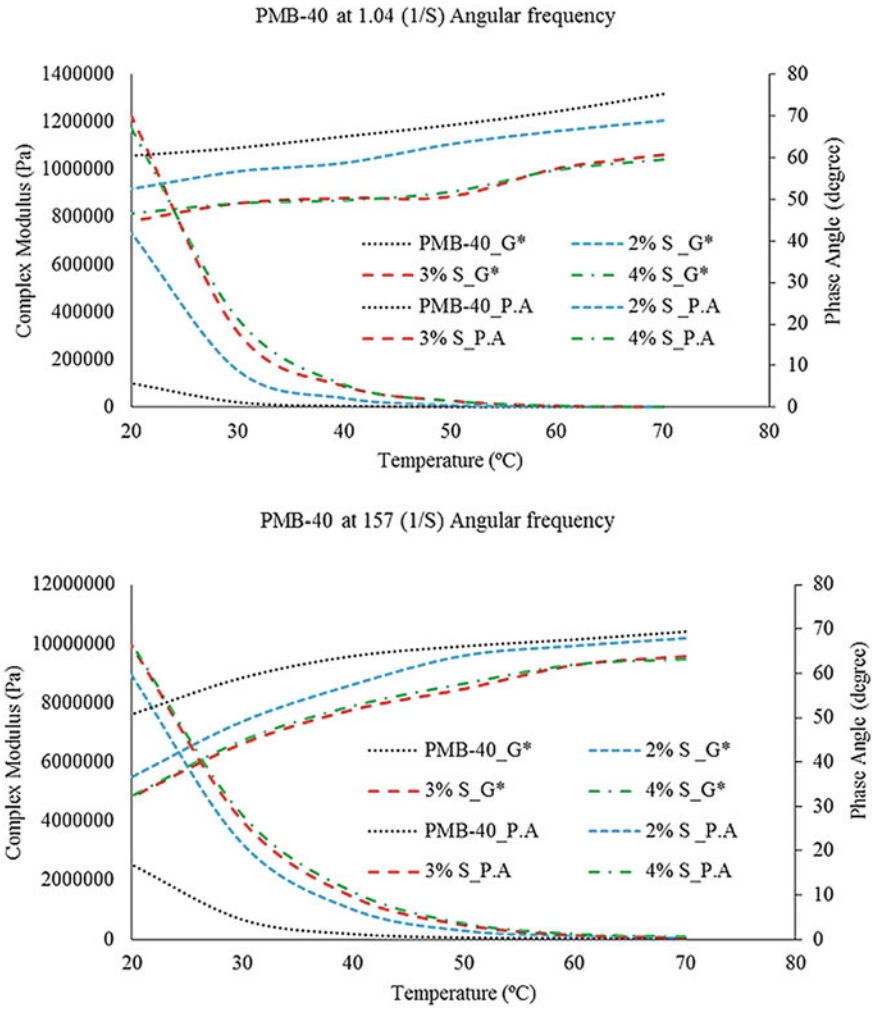

Fig. 2 Isochronal plot at angular frequency 1.04 and 157 rad/s for modified asphalt binders

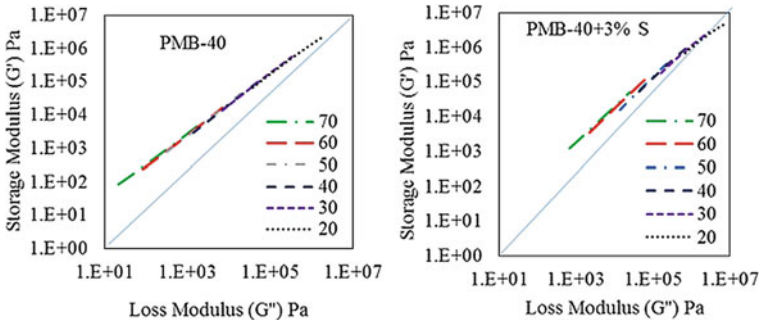

Fig. 3 Cole-Cole diagram for PMB-40 and PMB-40+3%S

3.3 Cole-Cole Diagram

Cole-Cole diagram is generally used to look into the structure of polymer and co-polymer in asphalt binder and a Cole-Cole curve shows (using linear axis), a semi-circular shape for thermoplastic, non-crosslinked polymers. Figure 3 represents the Cole-Cole diagram for polymer-modified binder and warm mix binder at 20–70 °C with an interval of 10 °C. The graph is divided into two halves by a diagonal line (at 45° line). All data points on the left and above the line except a few points of warm mix binder (PMB+3% S) at very low temperature. The distance of points from the 45° line is generally more in the case of PMB-40 than that in the case of a warm mix binder. It means PMB-40 behaves more elastically than warm mix binders. This is more evident at a higher temperature. At lower temperatures, both binders tend to have similar elastic/viscous behavior. At higher temperatures, warm asphalt binders are more viscous than a neat modified binder.

3.4 Black Diagrams

A black diagram represents the graph between complex modulus and phase angle, obtained from a dynamic test. In this graph, the frequency and temperature are eliminated and the time-temperature superposition principle is not applied so that the real value can be seen without manipulation. Al-Mansob et al. [16] state that a black diagram with the presence of high wax content asphalt binder, a high polymer-modified bitumen, or a high asphaltene structure indicates a disjointed curve. In Fig. 4, it is observed that PMB-40 asphalt binder is less susceptible to temperature in comparison to PMB-40+3% S. It is also observed that with modification of PMB-40 with Sasobit, the phase angle gets reduced. It means Sasobit can improve the rheological properties of PMB-40.

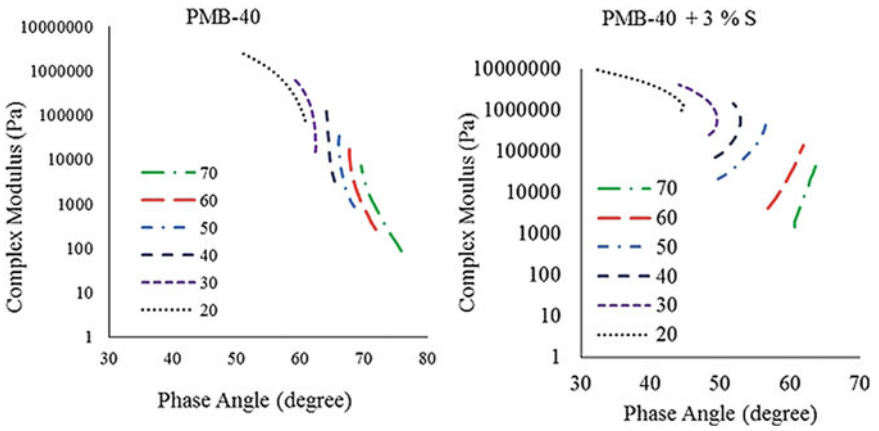

Fig. 4 Black diagram for PMB-40 and PMB-40+3%S

3.5 Master Curve

Construction of the master curve requires a shift factor to calculate the rheological parameter (G* or δ) at a range of temperatures. The shift factor in the present study was calculated using the WLF equation, but these values did not provide a smooth curve. It indicates that the rheological properties of modified binders and also of warm mix asphalt binders cannot be shifted by TTSP to produce a smooth continuous master curve. Therefore, the shift factor was manually calculated to obtain a single continuous curve for complex shear modulus (G*), and the same is given in Fig. 5. The corresponding master curve for G* is shown in Fig. 6. It is mentioned here that the shift factor for PMB-40 and warm binders with 2, 3, and 4% Sasobit followed a continuous curve, and a single value was adopted for all four binders. The shift factor given in Fig. 5 is also used to construct the master curve for phase angle, which is also given in Fig. 6. The master curve for phase angle is not a smooth construction curve for warm mix binder indicating that the shift factor for the phase angle is different from that for complex shear modulus.

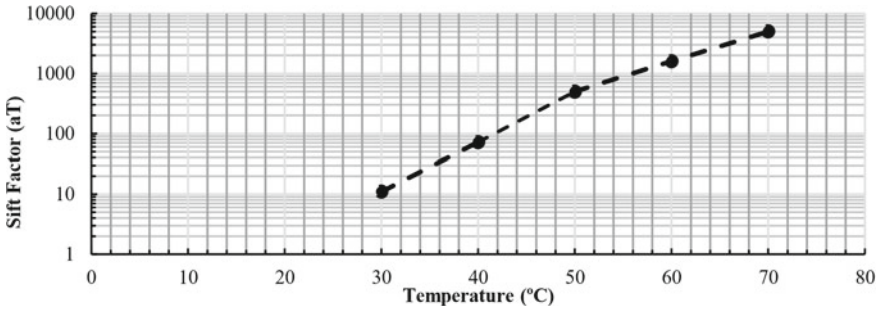

Fig. 5 Shift factor corresponding to reference temperature 20 ℃

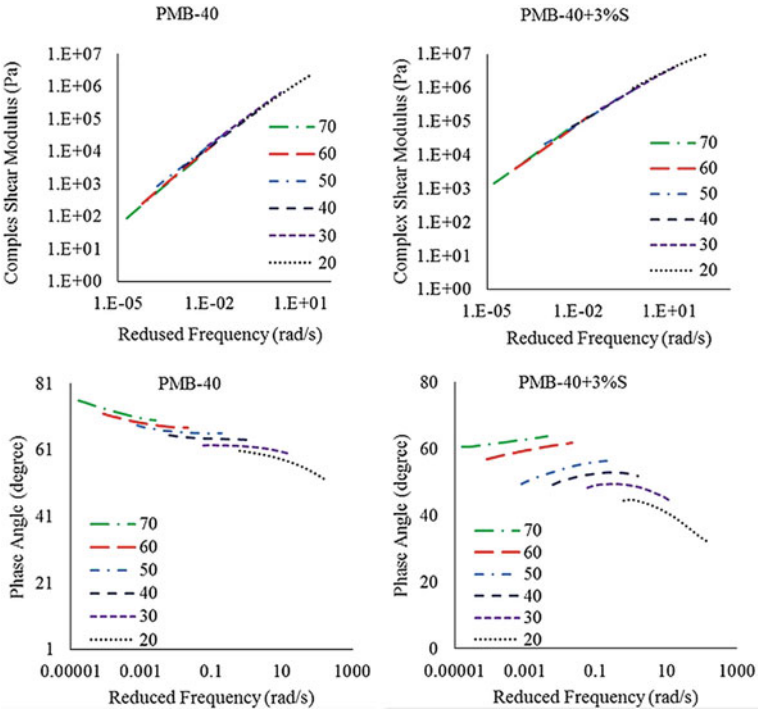

Fig. 6 Master curve with a reference temperature of 20 ℃ for PMB-40 and PMB-40+3%S

4 Conclusion

Polymer-modified binder of grade PMB-40 was blended with 2%, 3%, and 4% Sasobit by weight of asphalt binder to produce polymer-modified warm asphalt binder. A dynamic shear rheometer was used to measure the rheological and mechanical properties of these binders. Based on the data presented in this paper, the following conclusions are drawn.

- Amplitude sweep tests conducted on various formulations indicate that the LVE Range of a warm asphalt binder decreases with the temperature. It reduces with the increase of the content of Sasobit also the LVE range gets reduced. It has been found that the LVE range varies from 10% to 0.5% or different binders used in the present study.
- Isothermal plots show that the complex shear modulus of modified asphalt binder increases with frequency. It increases with Sasobit content also. At higher temperatures, the increase in complex modulus was distinctly visible at all frequency ranges, but at low temperatures, the influence of additive diminished at a higher frequency. The phase angle reduced with frequency for neat binder at both test temperatures but it slightly increases when Sasobit was added and tested at 60 ℃. The complex modulus and phase angle did not change much when the Sasobit dose was increased from 2 to 3%.
- Isochronal plots show the variation of complex modulus and phase angle with temperature and it is found that at a particular frequency, the complex modulus decreases and phase angle increases with the increase of test temperature. The phase angle was reduced and the complex modulus increased with an increase in the Sasobit dose. It suggested that a warm mix binder has better elastic properties than PMB-40.
- Cole-Cole diagrams plotted for PMB-40 and PMB-40+3% Sasobit show all data points above the 45º line, the points being further in case of modified asphalt binder than warm asphalt binder. It means a polymer-modified binder is more elastic than a warm binder with 3% Sasobit. However, at a lower temperature, both binders tend to behave similarly as all data points are close to the 45º line.
- The black diagram shows complex modulus and phase angle with the combined effect of preselected temperature and frequencies. It is found that the addition of Sasobit causes a disjointed curve, which implies that the content of Sasobit is highly asphaltene structure.
- For the development of the master curve for complex modulus and phase angle, the shift factor was calculated by using Williams Landel, and Ferry (WLF) equation but it failed to provide a single line curve. It indicates that the rheological properties of modified binder and modified warm asphalt binder cannot be shifted using the principle of time-temperature superposition to produce a smooth master curve. Therefore, shift factor was calculated manually for complex shear modulus. When the same shift factor was used for phase angle, it did not produce a smooth curve indicating that the shift factor for phase angle is different from that for complex modulus.

References

1. IS73 (2013) Paving bitumen—specification (fourth revision). The Bureau of Indian Standards, New Delhi (India)
2. Bahia HU, Hanson DI, Zeng M, Zhai H, Khatri MA, Anderson RM (2001) Characterization of modified asphalt binders in superpave mix design. Rep No 459, Transportation Research Board, National Research Council, Washington, DC.IS 73-2013
3. Caro S, Beltrán DP, Alvarez AE, Estakhri C (2012) Analysis of moisture damage susceptibility of warm mix asphalt (WMA) mixtures based on dynamic mechanical analyzer (DMA) testing and a fracture mechanics model. Constr Build Mater 35(2012):460–467
4. Wang C, Hao P, Ruan F, Zhang X, Adhikari S (2013) Determination of the production temperature of warm mix asphalt by workability test. Constr Build Mater 48(2013):1165–1170
5. Ahmed EI, Hesp SAM, Samy SKP, Rubab SD, Warburton G (2012) Effect of warm mix additives and dispersants on asphalt rheological, aging, and failure properties. Constr Build Mater 37(2012):493–498
6. Kok BV, Akpolat M (2015) Effect of using Sasobit and SBS on the engineering properties of bitumen and stone mastic asphalt. J Mater Civ Engi ASCE. https://doi.org/10.1061/(ASCE)MT.1943-5533.0001255
7. Zelelew H, Paugh C, Corrigan M, Belagutti S, Ramakrishnareddy J (2013) Laboratory evaluation of the mechanical properties of plant produced warm-mix asphalt mixtures. Road Mater Pavement 14(1):49–70
8. Wasiuddin MW, Selvamohan S, Zaman MM, Guegan MLTA (2007) A comparative laboratory study of sasobit® and aspha-min® in Warm mix asphalt. Transp Res Rec J Transp Res Board 1998/2007:82–88
9. Mallick RB, Kandhal PS, Bradbury RL (2009) Using warm-mix asphalt technology to incorporate high percentage of reclaimed asphalt pavement material in asphalt mixtures. Transp Res Rec J Transp Res Board 2051
10. Porras JD, Hajj EY, Sebaaly PE, Kass S, Liske T (2012) Performance evaluation of field-produced warm-mix asphalt mixtures in Manitoba, Canada. Transp Res Rec J Transp Res Board 2294
11. Bennert T, Maher A, Sauber R (2011) Influence of production temperature and aggregate moisture content on the initial performance of warm-mix asphalt. Transp Res Rec J Transp Res Board 2208
12. Saboundjian S, Liu J, Li P, Brunette B (2011) Late-season paving of a low-volume road with warm-mix asphalt an Alaskan experience. Transp Res Rec J Transp Res Board. https://doi.org/10.3141/2205-06
13. Middleton B, Forfylow RW (Bob) (2009) Evaluation of warm-mix asphalt produced with the double barrel green process. Transp Res Rec J Transp Res Board 2126
14. Park SW, Kim YR, Schapery RA (1996) A viscoelastic continuum damage model and its application to uniaxial behaviour of asphalt concrete. Mech Mater 24:241–255. https://doi.org/10.1016/S0167-6636(96)00042-7
15. Williams ML, Landel RF, Ferry JD (1955) The temperature-dependence of relaxation mechanisms in amorphous polymers and other glass-forming liquids. J Am Chem Soc 77:3701–3706
16. Al-Mansob RA, Ismail A, Alduri AN, Karim CHAMR, Md. Yusoff NI (2014) Physical and rheological properties of epoxidized natural rubber modified bitumens. Constr Build Mater 63:242–248

Design Consistency Evaluation Tools for Rural Highways: A Review

Vinay Kumar Sharma and Gourab Sil

Abstract Rural highway safety and efficient driver performance are usually associated with consistent highway geometric design. Inconsistency in the rural highway design is determined to be the primary cause of single-vehicle crashes at curve sites. The primary objective of the current review article is to summarize the various tools and their threshold values used in the literature and to discuss the various tools that evaluate the consistency of rural highways. Twenty-nine research articles along with a geometric design code were selected according to eligibility criteria. The eligibility for research articles was that they must include at least one consistency tool, consistency process, assumption of free flow condition and consistency evaluation must be on rural highways. The evaluation process is defined under four consistency measures: speed consistency, dynamic consistency, alignment consistency, and consistency through the driver's workload. The study found that most of the consistency evaluation tools are developed based on the speed and geometric data of two-lane rural highways. Speed consistency is found mostly explored measure since over-speeding is the prime reason for the single-vehicle crash. Moreover, input parameters were selected for consistency evaluation primarily based on the vehicle, road, and driver's characteristics such as speed, road geometry, and visual demand respectively. Roadside environmental factors, driver's real-time perception, and vehicle dynamic advancement are rarely explored to assess consistency.

Keywords Rural highway · Highway consistency · Design consistency · Consistency evaluation

V. K. Sharma (✉) · G. Sil
Indian Institute of Technology Indore, Indore 453552, India
e-mail: vksharma@iiti.ac.in

G. Sil
e-mail: silgourab@gmail.com

A. Dhamaniya et al. (eds.), *Recent Advances in Traffic Engineering*, Lecture Notes in Civil Engineering 377, https://doi.org/10.1007/978-981-99-4464-4_5

1 Introduction

Highway geometric design consistency is a surrogate measure of highway safety analysis without using any previous accident data. The consistency is found in the driver's behavior or by the existing geometry of the road (alignment indices calculations). The driver behavior is again determined based on three approaches: speed consistency (operating speed); dynamic consistency (lateral friction safety margin); and consistency through the driver's workload. Figure 1 represents the hierarchical classification of consistency measures.

The degree to which highway networks are designed and built to prevent critical driving maneuvers, that can increase the danger of a collision, is known as design consistency [1] or the ability to confirm the driver's expectations in the highway geometry [2]. Consistent highway design is that which makes certain that subsequent geometric features are coordinated in a way to generate a harmonious driving performance without unexpected events [3]. Road users may not be prepared for abrupt changes in design speed, cross-section, or alignment requirements between neighboring portions along a rural route [4]. Driver expectations are violated since the vehicle speed at the horizontal curve and tangent cannot be constant up to the design speed. The effect of inconsistency in design can be observed as 25–30% of the total fatal crashes occurred on horizontal curves, with 60–70% as runoff-road crashes [5]. Accidents occur when drivers make mistakes for a variety of causes, including poor perception, lack of expertise, attention, and higher workload due to complex geometry. Conventional geometric design practices in the developing countries like India are fundamentally based on design speed (allowable speed).

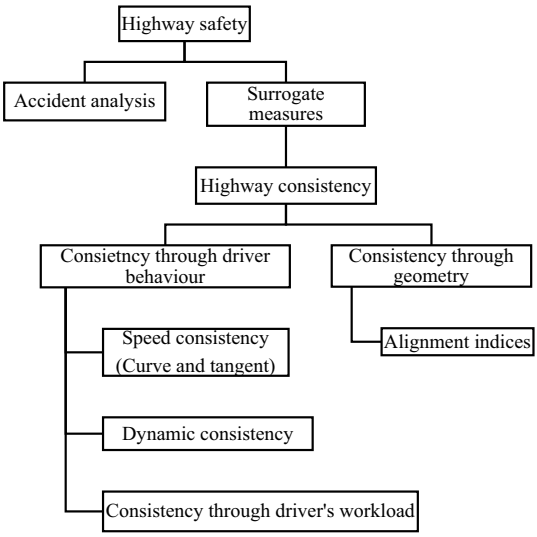

Fig. 1 Classification of different consistency measures

1.1 Conventional Geometric Design Process by IRC 73:1980

IRC 73:1980 [6] suggests the guidelines for the conventional methods of geometric design of rural highways. The design process involved the assumption of design speed. The type of the road and the topography both influence the design speed. All the geometric design aspects are determined by this fundamental characteristic of design speed. Preferably, the design speed should be constant throughout a specific highway. However, alterations in speed might not be averted due to terrain variances. When this is the case, it is preferable to modify the design speed gradually by introducing successive sections of increasing/decreasing design speed so that the road users become accustomed to the change over time. Design speed is the upper safe speed limit or allowable speed limit on rural highways. However, the free flow condition motivates the drivers to drive at higher speeds at tangents and suddenly decelerate into curves, after which the inconsistency occurs.

1.2 Review Objectives

The single-vehicle safety on rural routes could be increased by adding a consistency evaluation procedure as a supplemental step to the conventional geometric design approach. Several highway consistency evaluation studies were carried out [7–9]. Numerous studies suggested different approaches for evaluating consistency. There is a limited amount of information available in a complete review report of all this research that provides a critical analysis of the various consistency evaluation tools and methodologies. Therefore, the objective of the current article is as follows.

- To summarize the various tools and their threshold values used in the literature that evaluates the consistency of rural highways.
- To discuss the tools and synthesis the shortcomings.

The current paper road map consists of listing and summarizing all the consistency evaluation tools under speed consistency, dynamic consistency, alignment consistency, and consistency through driver's workload developed by highway researchers. Furthermore, a comprehensive systematic review is given of these tools and applications. Additionally, a brief discussion has been made over the vehicle functional advancement which can be used to evaluate consistency.

2 Review Methodology

The review method was adopted according to the PRISMA statement. Figure 2 represents the steps involved in the methodology to select the articles. At first, the eligibility criteria were designated. Only those articles included contain at least one

consistency tool, consistency evaluation process, rural highways along with free flow conditions. Articles containing case studies on consistency evaluation are also eligible for further steps. Information sources were fixed as research articles, review articles, and design codes. Online search engines like Google Scholar, ResearchGate, and ScienceDirect were decided for initial searches. Additionally, the keywords "Highway consistency"; "Consistency models"; "Consistency evaluation threshold"; and "Surrogate safety measures" was planned to search the articles. However, eligibility check is planned in further step. Backward referencing was also proposed to locate any further consistency evaluation literature if required.

3 Results

Once the review approach is completed, document selection based on the designated eligibility criteria begins. Results included the selection of the number of articles and consistency evaluation process from each tool (Fig. 2 and Table 1). Additionally, consistency evaluation tools (Table 2) and their threshold values (Table 3) are summarized.

3.1 Study Selection

The complete process for the study selection is shown in Fig. 2. At first, fifty-five research articles were searched out. Out of those, twenty-two research articles were found eligible after the first overview of the abstract and methodology. Thirty-three articles were screened out due to non-eligibility. Furthermore, twenty-nine documents are finally carefully chosen based on the designated eligibility. Most of the papers are published in the transportation research record and journal of transportation engineering (ASCE) (Table 1).

3.2 Consistency Evaluation Tools

Consistency evaluation tools extracted from the literature have been listed in Table 2. The tools are listed for each classified consistency measure as shown in Fig. 1. The tools for which threshold values are available are also listed separately in Table 3. All the threshold values are enumerated for good, fair, and poor consistency levels.

A total of twenty-seven tools (Table 2) are listed in the literature. Out of which threshold values are available for fifteen tools (Table 3). A comprehensive systematic review is given in further sections for these tools and applications. These consistency tools may be incorporated in the conventional design process to improve the safety of highways.

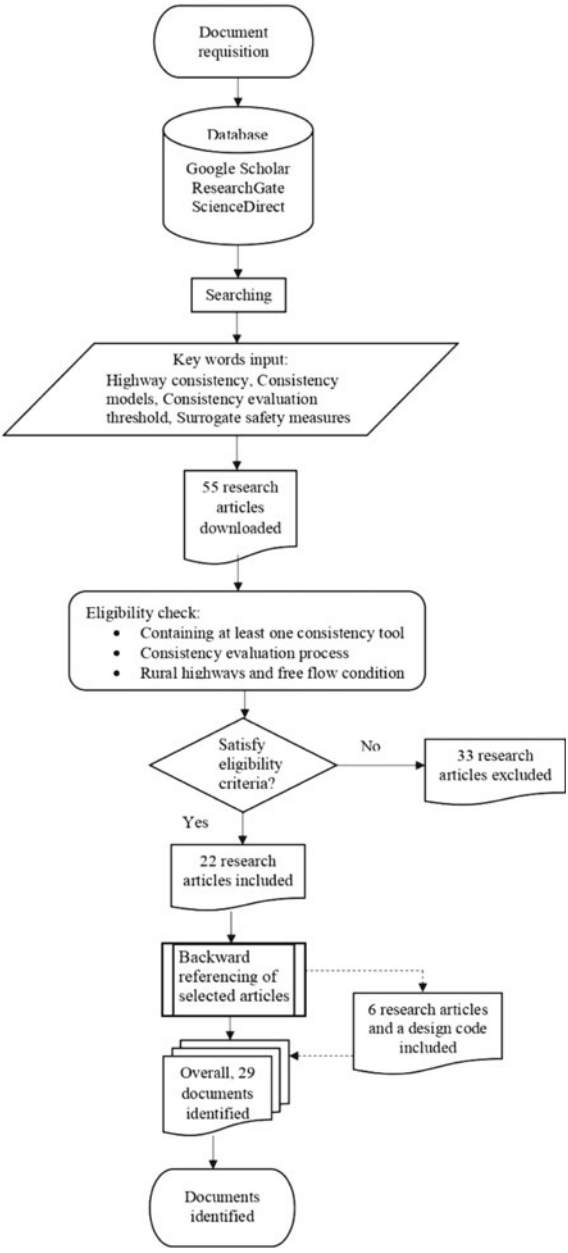

Fig. 2 Study selection methodology for literature review

Table 1 Publication of selected articles

Publication	No. of articles
Transportation research record	14
Journal of transportation engineering (ASCE)	9
Accident analysis and prevention	1
Procedia-social and behavioral sciences	1
International journal of civil engineering	1
Transport, Vilnius Gediminas technical university	1
Canadian journal of civil engineering	1
Proceedings of 4th international symposium on highway geometric design	1

4 Discussion

Consistency tools can be applied as a supplemental step to the conventional design methods. Evolution of the consistency tools from 1980 to 2022 is discussed along with some shortcomings in further sections.

4.1 Speed Consistency

Lamm et al. [10] opined that driving at geometric feature on two-lane rural highway with significantly higher speed than the allowable speed or design speed cause inconsistencies. Lamm et al. [10] developed a consistency tool (also called safety criterion I) as the speed differential between 85th percentile speed and design speed (Single element). For such tool they defined the consistency threshold values as good, fair, or poor consistency level (Table 3). Hassan et al. [11] used this tool on a case study of 18 km length road stretch. Additionally, they analyzed speed profile for both the lanes (upstream and downstream). The allowable speed was found based on the two criteria,stopping sight distance and vehicle stability (speed required for friction). Further sight distance consideration was spilt into two dimensional and three-dimensional analysis. Two-dimensional stopping sight distance was simple formula based, while in three dimensional, all types of obstruction in small elemental level was considered for better accuracy on finding the allowable speed. Cafiso et al. [12] also applied this tool using naturalistic driving experiment and speed profile data were collected by using instrumented vehicle. In this case study, Cafiso and Cava [7] suggested the lower threshold values (Table 3) for the tool as suggested by Lamm et al. [10]. They concluded that higher threshold values of speed variations based on 85th percentile speed for single element and successive element can underestimate the effective change in the driving task, which creates the need to use lower threshold values to judge the consistency level. Luque and Castro [13] split the consistency of road as “local” and “global” consistency. The local consistency included isolated

Table 2 Design consistency evaluation tools

	References	Evaluation tools	Equation
Speed consistency	Lamm et al. [10]	Design speed and 85th percentile speed differential (single geometric element)	$\lvert V_{85} - V_D \rvert$
	Hassan et al. [11]		
	Cafiso et al. [12]		
	Cafiso and Cava [7]		
	Luque and Castro [13]		
	Sil et al. [14]		
	Goyani et al. [8]		
	Lamm et al. [10]		
	Al-Masaeid et al. [1]	85th percentile speed differential calculated as the difference between 85th percentile speed between two geometric elements	$\Delta V_{85} = \lvert V_{85i} - V_{85\,i+1} \rvert$
	Cafiso et al. [12]		
	Cafiso and Cava [7]		
	Jacob et al. [9]		
	Luque and Castro [13]		
	Goyani et al. [8]		
	McFadden and Elefteriadou [15]	85th percentile differential of speed calculated as 85th percentile value of speed differentials of individual drivers	Δ_{85} V or $(V_{85i} - V_{85i+1})^{85th}$
	Mishaghi and Hassan [16]		
	Cafiso and Cava [7]	Difference between minimum speed on curve and average speed on entire test stretch	$\lvert V_{\text{curve min}} - V_{\text{tangent max}} \rvert$
	Cafiso and Cava [7]	Difference between minimum speed on curve and maximum speed at tangent	$\lvert V_{\text{curve min}} - V_{\text{stretch mean}} \rvert$
	Garcia et al. [17]	85th percentile and inertial speed differential	$\lvert V_{85\text{inertial}} - V_{85} \rvert$
	Polus and Habib [18]	Relative area of speed deviation obtained from speed profile	R_a

(continued)

Table 2 (continued)

	References	Evaluation tools	Equation
	Polus and Habib [18]	Standard deviation of speed obtained from speed profile	σ
	Polus and Habib [18]	Direct consistency value	Equations (3 and 4) under Sect. 4.1
	Garach et al. [19]		
	Luque and Castro [13]		
	Camacho-Torregrosa et al. [20]		Equation (5) under Sect. 4.1
Dynamic consistency	Lamm et al. [21]		$\Delta f_{vehicle}$
	Cafiso et al. [12]	Safety margin on skidding	
	Maljkovi and Cvitani [22]	Safety margin on front and rear axles	$\Delta f_{front\ axle}$, $\Delta f_{rear\ axle}$
Alignment consistency	Polus and Dagan [23]	Three combined alignment indices	$\frac{RL_c}{TL_c+TL_t}$; $\frac{R_{min}}{R_{max}}$; $\frac{R_{Avg}}{R_{\min(V_D)}}$
	Lamm et al. [10]	Difference between degree of curve for two successive curves	ΔDC
	Lamm et al. [24]	Curvature change rate	CCR
	Cafiso and Cava [7]	Curve mean radius ratio	R_{mean}/R_i
	Cafiso and Cava [7]	Length to radius of curve ratio	L/R_i
	Altamira et al. [25]	Sight distance (stopping, passing and available)	SD
Consistency through driver's workload	Messer [26]	Workload value for a geometric feature	W_L (Eq. 10 under Sect. 4.4)
	Krammes and Glascock [27]		
	Wooldridge et al. [28]	Workload due to visual demand of familiar and unfamiliar driver	W_{VDLU}, W_{VDLF} (Eqs. 11 and 12 under Sect. 4.4)

Note $V_{85\ inertial}$ = inertial operating speed (average operating speed over 1 km length just before start of curve);V_D = design speed; V_{85i} and $V_{85\ i+1}$ = 85th percentile speed of successive geometric features; R_a = relative area of speed deviation; σ = standard deviation of speed; R_{Avg} or R_{mean} = average radius (m); R = radius of isolated horizontal curve (m); R_{min} = minimum radius of curve on entire selected stretch; R_{max} = maximum radius of curve on entire selected stretch L = length of horizontal curve; ΔDC = difference between degree of curve for two successive curves; CCR = curvature change rate; $V_{curve\ min}$ = minimum speed at curve; $V_{stretch\ mean}$ = average speed over entire stretch; Vtangent max = maximum speed at tangent; $\Delta f_{vehicle}$ = safety margin for a vehicle; Δffront axle = safety margin for front axle, Δfrear axle = safety margin for rear axle; W_L = workload value; W_{VDLU} = workload dure to visual demand of unfamiliar road; W_{VDLF} = workload due to visual demand of familiar road; SD = sight distance; $R_{min\ (VD)}$ = minimum radius calculated by design speed

Table 3 Threshold values for consistency evaluation tools

	References	Consistency thresholds			
Speed consistency	Lamm et al. [10]	$\Delta V_{85} \leq 10$ km/h, Good design consistency			
		$10 < \Delta V_{85} \leq 20$, fair design consistency			
		$\Delta V_{85} > 20$, poor design consistency			
	Lamm et al. [10]	$\lvert V_{85} - V_D \rvert \leq 10$ km/h, Good design consistency			
		$10 < \lvert V_{85} - V_D \rvert \leq 20$, Fair design consistency			
		$\lvert V_{85} - V_D \rvert > 20$, Poor design consistency			
	Polus and Habib [18]	Good	Fair	Poor	
		$R_a \leq 1$ m/s	$1 < R_a \leq 2$	$R_a > 2$	
		$\sigma \leq 5$	$5 < \sigma \leq 10$	$\sigma > 10$	
		$C > 2$	$1 < C \leq 2$	$C \leq 1$	
	Cafiso and Cava [7]	Parameter	Good	Fair	Poor
		$\lvert V_{curve\ min} - V_{stretch\ mean} \rvert$	0–10	10–20	≥20
		$\lvert V_{85} - V_D \rvert$	0–7.5	to 15	≥15
		$\lvert V_{curve\ min} - V_{tangent\ max} \rvert$	0–6	6–18	≥18
		$\lvert V_{85i} - V_{85\ i+1} \rvert$	0–7.5	7.5–15	≥15
	Garcia et al. [17]	$\lvert V_{85inertial} - V_{85} \rvert \leq 10$ km/h, Good design consistency			
		$10 < \lvert V_{85inertial} - V_{85} \rvert \leq 20$, fair design consistency			
		$\lvert V_{85inertial} - V_{85} \rvert > 20$, poor design consistency			
	Jacob et al. [9]	Δ_{85} V	Tangent/curve	Curve/Curve	
		Good	≤15	≤10	
		Acceptable	16–30	11–20	
		Poor	>30	>20	
	Garach et al. [19]	Good	Acceptable	Poor	
		$C_1 > 2$	$1 < C_1 \leq 2$	$C_1 \leq 1$	
Dynamic consistency	Lamm et al. [21]	$\Delta f_{vehicle} \leq 0.01$, Good design consistency			
		$0.01 > \Delta f_{vehicle} \geq -0.04$, fair design consistency			
		$\Delta f_{vehicle} < -0.04$, poor design consistency			
Alignment consistency	Lamm et al. [10]	$\Delta DC \leq 5°$, Good design consistency			
		$5° < \Delta DC \leq 10°$, fair design consistency			

(continued)

Table 3 (continued)

	References	Consistency thresholds			
		$\Delta DC > 10°$, poor design consistency			
	Lamm et al. [24]	$\lvert CCR_{s(i)} - CCR_{s(i+1)} \rvert \leq 180$ gon/km, Good			
		$180 < \lvert CCR_{s(i)} - CCR_{s(i+1)} \rvert \leq 360$ gon/km, fair			
		$\lvert CCR_{s(i)} - CCR_{s(i+1)} \rvert > 360$ gon/km, poor			
	Cafiso and Cava [7]	Parameter	Good	Acceptable	Poor
		R_{mean}/R	<1.5	1.5–2	≥2
		L/R	<1	1–2	≥2
Consistency through driver' workload	Messer [26]	W_L	LOC of feature		
		≤1	A	Good	
		≤2	B		
		≤3	C	Fair	
		≤4	D		
		≤5	E	Poor	
		≤6	F		

C = consistency model by Polus and Habib [18], C_1 = consistency model by Garach et al. [19]

and successive road geometry elements, while the global consistency includes the complete road segment. Safety criteria I and II [10] were considered as the indicator of local consistency. Sil et al. [14] used this tool for four-lane divided rural highways. The developed V_{85} model has only two independent variables, radius, and preceding tangent length. Using V_{85} model and safety criterion I [10], they evaluated the consistency level. Moreover, they suggested the process to design radius for good consistency level. Goyani et al. [8, 29] opined that vehicle category also affects the consistency level. They evaluated the consistency for three different categories of vehicle, two wheelers, cars, and heavy commercial vehicles (HCVs). Operating speed deviation from the design speed was found lower for two wheelers and cars as compared to HCVs.

The above tool was limited to consistency evaluation of single geometric element. Lamm et al. [10] developed the 85th speed differential tool for successive geometric elements. The threshold values for good, fair, and poor consistency level are given in Table 3. Al-Masaeid et al. [1] opined that speed reduction is not only affected by road geometry, also by pavement condition as well. Pavement condition was judged by pavement serviceability rating (PSR) as an input parameter. They developed speed reduction models for three different vehicle categories: car, light truck, truck, and all vehicles. Moreover, three successive transitions were observed for each category as follows.

(a) Tangent—curve
(b) curve—curve without tangent

(c) curve—curve with long tangent.

Speed reduction was found highly correlated with the degree of horizontal curve, gradient, and pavement condition for the first transition. Moreover, speed reduction was found highly correlated with radius of the curve for second transition phase. In the last transition phase, speed reduction was found greatly affected by length of common tangent and deflection angle of curve. Cafiso et al. [12] also applied this tool using naturalistic driving experiment and speed profile data were collected by using instrumented vehicle. Furthermore, Cafiso and Cava [7] suggested the threshold values for different consistency levels (Table 3). [9] developed speed reduction tool for two different transitions: when transition from approach tangent to the mid of the successive curve and transition mid-point of the successive curves. When approaching from a tangent to the curve, speed reduction reduces with an increase in radius and curve length as well as with a decrease in tangent speed [9]. They also calculated the threshold values for different consistency levels (Table 3). Luque and Castro [13] called it "local" consistency tool since it included only operating speeds of successive road geometry elements. Goyani et al. [8, 29] applied this tool for three different categories of vehicle, two wheelers, cars, and heavy commercial vehicles (HCVs).

Individual driver's speed profile was not included in the above speed differential tool. McFadden and Elefteriadou [15] developed 85th percentile speed reduction models using individual driver speed profiles. In other words, model evaluates the amount of speed reduction incurred by 85% of the drivers. Tangent to curve transition was selected up to the length of 200 m straight tangent before starting the curve and after end of the curve. Moreover, radius of horizontal curve, length of approach tangent, and the 85th percentile speed at tangent section 200 m before the beginning of the curve were found most significant variables. Mishaghi and Hassan [16] agreed with McFadden and Elefteriadou [15]. They also developed speed reduction model with significant input parameters as approach tangent speed, deflection angle of curve, shoulder width, curve negotiation direction, curve intersection presence, and longitudinal gradient.

Cafiso and Cava [7] developed two new consistency tools from speed profile: difference between minimum speed at curve and average speed over the stretch ($V_{curve\ min} - V_{stretch\ mean}$),difference between minimum speed at curve and maximum speed on tangent ($V_{curve\ min} - V_{tangent\ max}$). Distribution plot of ($V_{curve\ min} - V_{stretch\ mean}$) followed the normal distribution and distribution plot of ($V_{curve\ min} - V_{tangent\ max}$) followed gamma distribution. 50th percentile value and 85th percentile values from the cumulative plots were suggested as lower and upper threshold values respectively (Table 3).

Garcia et al. [17] opined inertial speed as an important indicator for consistency evaluation since driver slowed down at the tangent section just before negotiation of the curve. They defined vehicle inertial speed as the average operating speed on the previous 1 km road segment before the beginning point of the curve arrives. Moreover, the threshold values for different consistency levels were calculated (Table 3).

Polus and Habib [18] suggested a speed dependent tool, relative area (area bounded between operating speed and average speed) as consistency indicator of rural highway. The relative area from speed profile was calculated as follows (Eq. 1).

$$Relative\ area = \frac{\sum individual\ bounded\ between\ the\ operating\ speed\ and\ the\ average\ speed}{Total\ length\ of\ segment} \quad (1)$$

They concluded as the radius of curve increased, the relative area decreased exponentially. Moreover, the threshold values for different consistency levels were calculated (Table 3).

Polus and Habib [18] suggested another consistency indicator as standard deviation. It was extracted from speed profile and calculated by Eq. (2). This tool can be used as an initial supplemental check for consistency.

$$St.\ deviation\ of\ O.S. = \sqrt{\frac{(O.S.\ along\ a\ single\ geometric\ element - average\ weighted\ speed\ by\ length)}{number\ of\ geometric\ elements}} \quad (2)$$

They concluded that as the radius of curve increased, the value of standard deviation decreased exponentially. The threshold values for different consistency levels were calculated (Table 3).

Moreover, Polus and Habib [18] combined the relative area and standard deviation. Hence developed an aggregated exponential tool (Eq. 3) to find the consistency values. It can be observed that the tool completely utilized the driver's speed profiles.

$$Polus\ and\ Habib\prime sC = 2.808 * e^{-0.278\left[relative\ area * \left(\frac{Standard\ deviation\ of\ speed}{3.6}\right)\right]} \quad (3)$$

The model was based on the exponential function relationship with relative area and standard deviation, characterized by large slopes variations, in which the consistency value decreases rapidly when input value increases. The threshold values for different consistency levels were calculated (Table 3). Garach et al. [19] proposed a new consistency value model (Eq. 4). Unlike the previous model, this was not an exponential model, while represented as the hyperbolic functions with relative area and standard deviation.

$$Garach\prime sC_1 = \frac{195.073}{\left(\frac{st.\ deviation\ of\ speed}{3.6} - 5.7933\right)(4.1712 - relative\ area) - 26.6047} + 6.7823 \quad (4)$$

The sensitivity shows the consistency value decreases more slowly than exponential functions, because of having smoother slopes, and having an opposite concavity.

Luque and Castro [13] used the direct consistency value tool suggested by Polus and Habib [18] and Garach et al. [19]. Luque and Castro [13] called it a global consistency tool since these tools utilized the complete speed profile and evaluated the consistency of entire stretch, not for a single isolated element. The only limitation that did not consider was design speed.

Camacho-Torregrosa et al. [20] developed a direct consistency value indicator (kmph) for a given geometric feature based only on the 85th percentile speed. They called it the design consistency index. The study also included a new parameter as percentage of road segment (length) under deceleration conditions. The input parameters were average 85th percentile speed and its average speed reduction (Eq. 5).

$$Consistency\ value = \frac{(Average\ 85th\ percentile\ speed)^2}{Average\ 85th\ percentile\ speed\ reductio} kmph \tag{5}$$

4.2 Dynamic Consistency

Transition from tangent to the horizontal curve creates a centrifugal force. If available side friction is not sufficient, it might result in a slide or overturning of the vehicle [30]. Gibreel et al. [3] opined insufficient side friction at a horizontal curve could result in a skid out, rollover, or head-on collision. Lamm et al. [21] developed third safety criterion ($\Delta f_R = f_R - f_{RD}$) against dynamic stability. Threshold values for this tool were also calculated to find the different consistency levels (Table 3). However, it is a difference between the side friction difference between demanded friction and assumed friction. Demanded friction was calculated by operating speed (Eq. 7). Assumed and tangential frictions were calculated by design speed (Eqs. 6 and 8).

$$f_{Assumed} = n \times 0.925 \times f_{Tandential\ friction} \tag{6}$$

$$f_{Demanded} = \frac{{V_{85}}^2}{127R} - e \tag{7}$$

$$f_{Tangential\ friction} = 0.59 - 0.0485 V_{design} + 0.0000151 V_{design}^2; \quad n = utilisation\ ratio \tag{8}$$

The limitation of safety criterion III [21] was that it assumed a vehicle as a point mass and single value of friction was estimated for entire vehicle. Cafiso et al. [12] also applied this tool using naturalistic driving experiment and speed profile data were collected by using instrumented vehicle. Maljkovi and Cvitani [22] opined that the friction values for front and rear axles were different during the applications of brake at curve the weight of the vehicle was different at front and rear axle. Maljkovi and

Cvitani [22] developed bicycle friction model to overcome the limitation. The model was also applied to evaluate the safety margin on upward gradient and downward gradient, as the weights of the axles shifted slightly on the gradient. The friction circle of longitudinal and lateral friction was assumed as ellipse (Eq. 9).

$$\left(\frac{f_{demand\ longitudinal}}{f_{max\ longitudinal}}\right)^2 + \left(\frac{f_{demand\ lateral}}{f_{\max\ lateral}}\right)^2 = n^2 \leq 1 \tag{9}$$

Note n = utilization ratio, which is a factor with no physical significance, and is based on practical experience for different topographic conditions and road category groups.

They concluded the safety margin decreases rapidly with decreasing curve radius for curves with radii smaller than approximately 250 m. Moreover, they found braking on a sharp curve on a steep downgrade is the most critical situation for the loss of lateral vehicle stability. The use of this bicycle model found insignificant for larger radius curve since drivers chooses path radii more freely under such conditions [22].

4.3 Alignment Consistency

Polus and Dagan [23] developed the three types of alignment consistency rating models for horizontal alignment (hilly and flat terrain): Geometric models, spectral models, and compound models (Table 4). All the consistency models were made by combination of three alignment indices as follows.

$$\frac{RL_c}{TL_c + TL_t}; \frac{R_{min}}{R_{max}}; \frac{R_{Avg}}{R_{\min(V_D)}}$$

Table 4 Consistency rating models developed by Polus and Dagan [23]

Geometric models	Geo-Spectral models (Compound)
$Model\ 1 = \frac{RL_c}{TL_c+TL_t} + \frac{R_{min}}{R_{max}}$	$Model\ 6 = S + \frac{RL_c}{TL_c+TL_t} + \frac{R_{min}}{R_{max}} + \frac{R_{Avg}}{R_{\min(V_D)}}$
$Model\ 2 = \frac{RL_c}{TL_c+TL_t} + \frac{R_{min}}{R_{max}} + \frac{1}{4}(\frac{R_{Avg}}{R_{\min(V_D)}})$	$Model\ 7 = S + \frac{RL_c}{TL_c+TL_t} + \frac{R_{min}}{R_{max}} + \frac{1}{2}(\frac{R_{Avg}}{R_{\min(V_D)}})$
$Model\ 3 = \frac{RL_c}{TL_c+TL_t} + \frac{R_{min}}{R_{max}} + \frac{1}{3}(\frac{R_{Avg}}{R_{\min(V_D)}})$	Spectral model
$Model\ 4 = \frac{RL_c}{TL_c+TL_t} + \frac{R_{min}}{R_{max}} + \frac{1}{2}(\frac{R_{Avg}}{R_{\min(V_D)}})$	$S = Log_{10} * (Deviation\ of\ alignment\ from\ centre)$
$Model\ 5 = \frac{RL_c}{TL_c+TL_t} + \frac{R_{min}}{R_{max}} + \frac{R_{Avg}}{R_{\min(V_D)}}$	

Note RL_c = relative length of curve; TL_c = total length of curve; TL_t = total length of tangent; R_{min} = minimum radius; R_{max} = maximum radius; R_{avg} = average radius; $R_{min(VD)}$ = minimum radius calculated by design speed

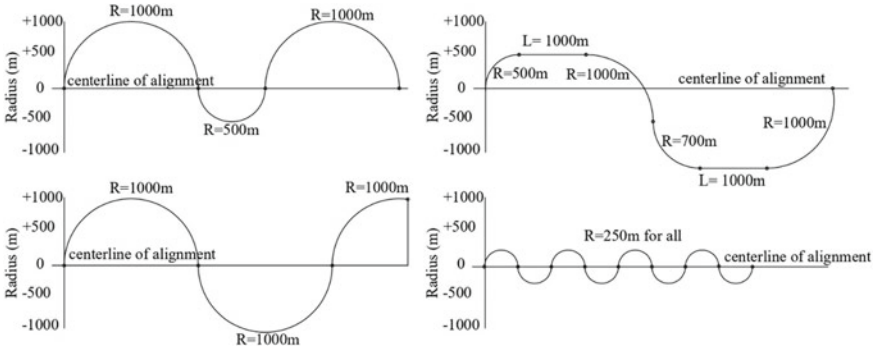

Fig. 3 Typical theoretical road spectral pattern drawn by Polus and Dagan [23]

Initially they drawn spectral road alignment (centerline layout) pattern (Fig. 3) to observe the nature of alignment, whether it is of repeating pattern or not. A total of 23 theoretical spectral roads were made and grouped into six, before applying the consistency rating tools. Moreover, consistency analysis is done by finding the relation between two ratings for each group: model output rating and logical rating. Logical rating of geometric features was quoted as per previous studies and engineering judgment. For achieving the good consistency of road design, they suggested the radius and similarity against the curve should be higher. However tangent length between the curves and equal radius curves should be minimized to have a good consistency [23].

Lamm et al. [10] observed as the degree of curve increases from DC = 0° (when driver at tangent element) to beyond values (when driver at curve), speed decreases. However, it depends on the length of the tangent. They opined that if the length of tangent between the curves is small, it can be neglected. Consistency level between such curves they evaluated by difference between the degree of curves. However, if the tangent length is enough, the consistency level they evaluated by the difference between degree of curve and tangent (DC = 0°). Moreover, they determined the threshold values for different consistency levels (Table 3).

Lamm et al. [24] employed curvature change rate of a curve as a consistency tool. The tool was the difference between curvature change rate values (angle measured in 400 angle units instead of 360: gon per km) between two successive curves. Threshold values also they defined (Table 3).

Cafiso and Cava [7] reported two alignment consistency indices: ratio of average radius to individual radius (R_{mean}/R_i) and ratio of length of curve to radius of curve (L/R_i). These two indices were selected because of significant correlation with speed differentials ($V_{curve\ min} - V_{stretch\ mean}$) and ($V_{curve\ min} - V_{tangent\ max}$). The corresponding quantitative threshold values for both the tools were obtained (Table 3) by the simple regression check between (R_{mean}/R_i) and ($V_{curve\ min} - V_{tangent\ max}$). Similarly, for ($L/R_i$) and ($V_{curve\ min} - V_{stretch\ mean}$). Moreover, they suggested that it is a more accurate approach to check the consistency level by multiple tools as compared to single tool.

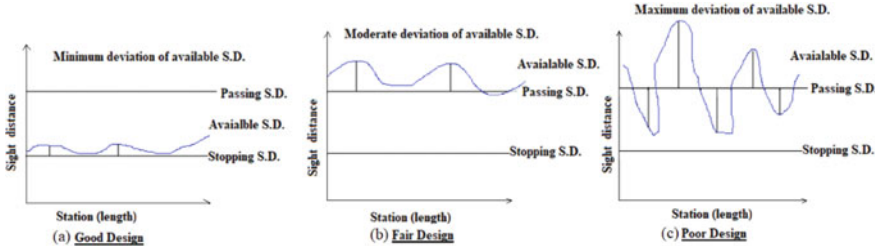

Fig. 4 Qualitative consistency judgment from available sight distance by Altamira et al. [25]

Altamira et al. [25] evaluated the consistency by available sight distance ahead to the driver and called it a good indirect indicator of consistency. They opined that the ability of driver to adjust the vehicle speed is affected by the available sight distance, which modifies the expectations and perception of driver. Three types of sight distances,stopping, passing, and available were calculated to find the consistency of road. Figure 4 represents the qualitative measure of consistency as good, fair, and poor by the absolute differences among stopping, passing, and available sight distances. Passing sight distances and stopping sight distances were calculated theoretically (i.e., from design speed) for a given road stretch. Available sight distances were calculated from operating speed. The assessment of available sight distances (from driver's view) along the road axis was performed by a simulation software. They created a visibility diagram of continuous variation of available sight distance with the chainage by means of simulation software. Moreover, the diagram identified the locations where the available sight distance deviated so frequent with large amount with the stopping sight distances or passing sight distances. These geometric sections were at poor design consistency level (Fig. 4c). On the other hand, the available sight distance was almost constant for a good design consistent geometric element (Fig. 4a).

4.4 Consistency Through driver's Workload

Driver's workload is defined as the individual driving task, performed by the driver in a particular time interval under a certain environmental condition which changes continuously until it is completed [26]. Moreover, he developed a model (Eq. 10) to evaluate the workload value for existing geometric feature.

$$W_{L(i)} = DUF * FEF * SDF * WPR + WCOF * W_{L(i-1)} \tag{10}$$

Note DUF = Driver's unfamiliarity factor; FEF = Feature expansion factor; SDF = Sight distance factor; WPR = Workload potential rating; = WCOF = Workload value of previous feature; $W_{L(i-1)}$ = Workload value of previous geometric feature.

Workload potential rating between zero (No problem) to six (big problem). Geometric features were identified based on type, sight distance available, and separation distance between previous feature to the next feature. Stopping sight distance was calculated by design speed and adjusted by V_{85} (80–113 kmph). Workload carry over factor was calculated by V_{85} and separation distance. Feature expansion factor was introduced if the next feature was not like the last one. Moreover, threshold values were determined for different consistency levels (Table 3). Krammes and Glascock [27] also applied the workload value model as developed by Messer et al. [26] and found the level of consistency for low volume rural highways.

Moreover, Woodridge et al. [28] opined that since driver's visual demand continuously changed with the geometry of the ahead road, it could be a good consistency indicator. Visual is defined as the amount of visual information needed by a driver to maintain an acceptable path on the roadway. The hypothesis statement said that drivers feel more comfortable (i.e., feel lesser workload), while driving on a familiar road as compared to unfamiliar road. Always visual demand is higher for the unfamiliar road. Using the visual occlusion technique, they developed analytical models that relate driver's visual demand to the inverse of radius of curve (Eqs. 11 and 12).

$$W_{DLU} = 0.173 + \frac{43.0}{R} \tag{11}$$

$$W_{DLF} = 0.198 + \frac{29.2}{R} \tag{12}$$

Speed consistency was found mostly explored as over-speeding is the prime reason for single-vehicle crash. Many consistency tools are developed based on the speed and geometric data of two-lane rural highways. However, most of the tools evaluate the consistency only for the passenger cars. Majority of the tools used for consistency evaluation were primarily based on the vehicle, road, and driver's characteristics such as speed, road geometry, and visual demand respectively.

5 Conclusions and Future Research Directions

This paper presented a comprehensive review on the concept of highway geometric design consistency and evaluation tools for rural highways. Several consistency tools are listed, and threshold values are outlined. Moreover, enhancements of the tools from 1980 to 2022 are discussed along with some shortcomings. However, consistency tools can be applied as a supplemental step to the conventional design methods. Even though some research has already been done, more is still needed to successfully address these challenges on a global scale:

- Although the radius of multilane highway is higher (i.e., flat curve), chances of over-speeding are more on multilane highways. So, speed consistency tools might be a good indicator of the consistency of multilane highways.

- Apart from abrupt changes in road geometry, abrupt changes in the roadside environment may lead to single-vehicle crash. Roadside environmental characteristics such as density of trees and density of access entries may create inconsistency.
- Vehicle age may also account for the consistency evaluation. Since the consistency level may be different for an old vehicle as compared to an advanced vehicle for the same existing geometric feature. Moreover, the day-by-day advancement in vehicular characteristics may also change the consistency level.
- Driver's real-time perception may also be a good consistency indicator. However, it is challenging to quantify but still by adopting appropriate human perception theory, it can be achieved.

Dynamic consistency evaluation process may include the vehicular functional advancements such as brake assist, anti-lock braking system, hill hold control, cruise control since these functions help drivers to control the vehicle at curve and hilly areas. The researchers need to work and update frequently to keep the highway design parameters on track with the ever-evolving automobile industry. A further challenge is to make the already constructed highways consistent for the drivers. However, for a new proposed highway, it is easier to adopt the consistency tool to achieve a good consistency level.

Acknowledgements The authors are grateful to both anonymous reviewers for their thorough and helpful comments. This study is a part of the project entitled "Analysis and Modelling of Drivers' Perception and Performance of Operational Measures for Geometric Design Consistency and Safety Evaluation of High-Speed Roadways", sponsored by Science and Engineering Research Board (SERB), project no. SRG/2021/002117, Government of India. The project is sponsored by Department of Civil Engineering, Indian Institute of Technology Indore.

References

1. Al-Masaeid HR, Hamed M, Ela MA, Ghannam AG (1995) Consistency of horizontal alignment for different vehicle classes. Transp Res Rec 1500:178–183. Transportation Research Board, Washington, DC
2. Anderson IB, Bauer KM, Harwood DW, Fitzpatrick K (1999) Relationship to safety of geometric design consistency measures for rural two-lane highways. Transp Res Rec 1658:43–51. Transportation Research Board, Washington, DC. https://doi.org/10.3141/2F1658-06
3. Gibreel GM, Easa SM, Hassan Y, El-Dimeery IA (1999) State of the art of highway geometric design consistency. J Transp Eng 125(4):305–313. https://doi.org/10.1061/(ASCE)0733-947X(1999)125:4(305)
4. Hassan Y (2004) Highway design consistency: Refining the state of knowledge and practice. Transp Res Rec 1881(1):63–71. https://doi.org/10.3141/1881-08
5. Srinivasan R, Baek J, Carter DL, Persaud B, Lyon C, Eccles KA, Gross F, Lefler N (2009) Safety evaluation of improved curve delineation (No. FHWA-HRT-09-045), U.S. Department of Transportation Federal Highway Administration, New Jersey Avenue SE Washington, DC
6. IRC: 73 (1980) Geometric design standards for rural (non-urban) highways. Indian Roads Congress, New Delhi

7. Cafiso S, La Cava G (2009) Driving performance, alignment consistency, and road safety: real-world experiment. Transp Res Rec 2102(1):1–8. https://doi.org/10.3141/2102-01
8. Goyani J, Chaudhari P, Arkatkar S, Joshi G, Easa SM (2022) Operating speed prediction models by vehicle type on two-lane rural highways in Indian hilly terrains. J Transp Eng Part A Syst. ASCE, ISSN 2473-2907. https://doi.org/10.1061/JTEPBS.0000644
9. Jacob A, Dhanya R, Anjaneyulu MVLR (2013) Geometric design consistency of multiple horizontal curves on two-lane rural highways. Proc Soc Behav Sci 104. 2nd Conference of transportation research group of India (2nd CTRG), pp 1068–1077. https://doi.org/10.1016/j.sbspro.2013.11.202
10. Lamm R, Choueiri EM, Hayward JC, Paluri A (1988) Possible design procedures to promote design consistency in highway geometric design on two lane rural roads. Transp Res Rec 1195:111–122. Transportation Research Board, Washington, DC
11. Hassan Y, Gibreel G, Easa SM (2000) Evaluation of highway consistency and safety: practical application. J Transp Eng 126(3):193–201. https://doi.org/10.1061/(ASCE)0733-947X(2000)126:3(193)
12. Cafiso S, Di Graziano A, La Cava G (2005) Actual driving data analysis for design consistency evaluation. Transp Res Rec 1912(1):19–30. https://doi.org/10.1177/0361198105191200103
13. Luque R, Castro M (2016) Highway geometric design consistency: speed models and local or global assessment. Int J Civ Eng 14(6):347–355. https://doi.org/10.1007/s40999-016-0025-2
14. Sil G, Maji A, Nama S, Maurya AK (2019) Operating speed prediction model as a tool for consistency based geometric design of four-lane divided highways. Transport ISSN 1648-4142 34(4):425–436. https://doi.org/10.3846/transport.2019.10715
15. McFadden J, Elefteriadou L (2000) Evaluating horizontal alignment design consistency of two-lane rural highways: development of new procedure. Transp Res Rec 1737:9–17. Transportation Research Board, Washington, DC. https://doi.org/10.3141/1737-02
16. Misaghi P, Hassan Y (2005) Modeling operating speed and speed differential on two-lane rural roads. J Transp Eng 131(6):408–418. ASCE. https://doi.org/10.1061/(ASCE)0733-947X(2005)131:6(408)
17. García A, Llopis-Castelló D, Camacho-Torregrosa FJ, Pérez-Zuriaga AM (2013) New consistency index based on inertial operating speed. Transp Res Rec 2319:105–112. https://doi.org/10.3141/2391-10
18. Polus A, Mattar-Habib C (2004) New consistency model for rural highways and its relationship to safety. J Transp Eng 130:3(286):286–293. ASCE. https://doi.org/10.1061/(ASCE)0733-947X(2004)130:3(286)
19. Garach L, Calvo F, Pasadas M, Ona J (2014) Proposal of a new global model of consistency: application in two-lane rural highways in Spain. J Transp Eng 140:04014030–1. American Society of Civil Engineers. https://doi.org/10.1061/(ASCE)TE.1943-5436.0000683
20. Camacho Torregrosa FJ, Pérez Zuriaga AM, García García A (2013) New geometric design consistency model based on operating speed profiles for road safety evaluation. Accid Anal Prev 61:33–42. https://doi.org/10.1016/j.aap.2012.10.001
21. Lamm R, Choueiri E, Mailaender T (1991) Side friction demand versus side friction assumed for curve design on two-lane rural highways. Transp Res Rec 1303:11–21. TRB, National Research Council, Washington, DC
22. Maljkovi B, Cvitani D (2022) Improved horizontal curve design consistency approach using steady-state bicycle model combined with realistic speeds and path radii. J Transp Eng Part A: Syst. ASCE, ISSN 2473-2907. https://doi.org/10.1061/JTEPBS.0000723
23. Polus A, Dagan D (1987) Models for evaluating the consistency of highway alignment. Transp Res Rec 1122:47–56. Transportation Research Board, Washington, DC
24. Lamm R, Wolhuter K, Beck A, Ruscher T (2001) Introduction of a new approach to geometric design and road safety. In: Proceedings, 20th Annual South African transport conference, Pretoria, South Africa, July 16–19
25. Altamira AL, Marcet JE, Graffigna AB, Gómez AM (2010) Assessing available sight distance: an indirect tool to evaluate geometric design consistency. In: Proceedings of 4th international symposium on highway geometric design, Valencia, Spain

26. Messer CJ (1980) Methodology for evaluating geometric design consistency. Transp Res Rec 757:7–14. Transportation Research Board, Washington, DC. https://trid.trb.org/view/165801
27. Krammes RA, Glascock SW (1992) Geometric inconsistencies and accident experience on two-lane rural highways. Transp Res Rec 1356
28. Wooldridge MD (1994) Design consistency and driver error. Transp Res Rec 1445:148–155. Transportation Research Board, Washington, DC
29. Goyani J, Chaudhari P, Arkatkar S, Joshi G, Easa SM (2022) Speed-based reliability analysis of 3D highway alignments passing through two-lane mountainous terrain. J Risk Uncertainty Eng Syst Part A Civ Eng. ASCE, ISSN 2376-7642. https://doi.org/10.1061/AJRUA6.0001271
30. Fitzpatrick K, Collins JM (2000) Speed-profile model for two-lane rural highways. Transp Res Rec 1737:42–49. Transportation Research Board, Washington, DC. https://doi.org/10.3141/2F1737-06

Artificial Intelligence (AI)-Based Assessment of Behavior of Bus Drivers in Nagpur City (India): A Case Study

Dev Singh Thakur, Mukti Advani, S. Velmurugan, Anbumani Subramanian, Neelima Chakrabarty, and Arun Goel

Abstract An assessment of road crash statistics of Nagpur city revealed that the annual number of road crashes ranges between 1000 and 1100, with heavy vehicles (buses) accounting for 8–14% of the total. Many of these road crashes are caused by large vehicles like buses and trucks, creating several blind spots for the drivers. In this study, an Artificial Intelligence *(AI)* powered Collision Alert System *(CAS)* was deployed. The study revealed that CAS offers the driver many visual and audio alerts when the vehicle encounters various obstacles while driving on the road. Further, Vienna Test was conducted to understand ground decisions by the drivers, *i.e., referred to as "subjects" henceforth* regarding these alerts, and a detailed questionnaire survey (DQS) was also performed to collect the basic attributes of these subjects. Using these data, namely, CAS alerts, Vienna results, and driver attributes of 33 drivers, correlation analysis was performed, and a linear regression model was developed to establish the Road Safety Index *(RSI)* based on their driving experience, eye condition, and generated alerts. This index can be used as a significant indicator for the evaluation of drivers, potentially leading to a reduction in road crashes involving buses and assisting in the allocation of duties to bus drivers on various bus routes.

Keywords Driver · Vienna · ADAS · CAS · Artificial intelligence · RSI · Nagpur · Bus

D. S. Thakur (✉)
iHUB-Data, IIIT Hyderabad, Hyderabad 500032, India
e-mail: devsinghthakur219@gmail.com

M. Advani · S. Velmurugan · N. Chakrabarty
CSIR-CRRI, New Delhi 110035, India

A. Subramanian
INAI-Applied AI Research Centre, IIIT Hyderabad, Hyderabad 500032, India
e-mail: anbumani@iiit.ac.in

A. Goel
NIT Kurukshetra, Kurukshetra 136119, India

A. Dhamaniya et al. (eds.), *Recent Advances in Traffic Engineering*, Lecture Notes in Civil Engineering 377, https://doi.org/10.1007/978-981-99-4464-4_6

1 Introduction

1.1 Preamble

Nagpur is the geographical center of India and 3rd largest city of Maharashtra state. Also, Nagpur is one of the important Tier-II metropolitan cities located in the central part of the country. Two major national highways, namely, NH-44 and 53 intersect, and State Highways, 248, 255, and 260 passes through the city. The overall length of the road network, including Nagpur's suburbs, is around 1,907 km, of which 1,150 km is under the control of the Nagpur Municipal Corporation (NMC) [12], and the remainder is under the jurisdiction of the Nagpur Metropolitan Region [10].

Despite having a good road network, Nagpur city lags in terms of road safety. As per the road crash statistics [1], the safety situation is not looking good in the city except for a marginal decrease witnessed during the year 2020 due to the COVID-19 lockdown. But subsequently, road crashes especially the number of fatalities show increasing trends in 2021 as depicted in Fig. 1. Further, a close look at the above statistics for the year 2021 that road crashes involving heavy vehicles accounted for 8–14% which is a cause of concern. Since the buses invariably share the available road space with other vehicle types especially, Vulnerable Road Users *(VRUs)* like motorized 2-wheelers, cycles, and pedestrians during the peak and off-peak periods of traffic movement, the severity level of crashes involving buses is usually high. This can be attributed to the enormity of its dimension contributing to several blind spots around the bus making it difficult for the drivers. Considering the above, apart from the road and vehicle, the major parameter is the driver [1].

It is an established fact that the capability of the driver to resort to defensive driving to achieve safer driving practice is important. At the same time, in case a driver makes a mistake, the provision of road environs as well as the in-vehicle aids in the form of Advanced Driver Assistance System *(ADAS)* can make the road "forgiving". On the first aspect of the capability of the drivers, timely information/alerts regarding

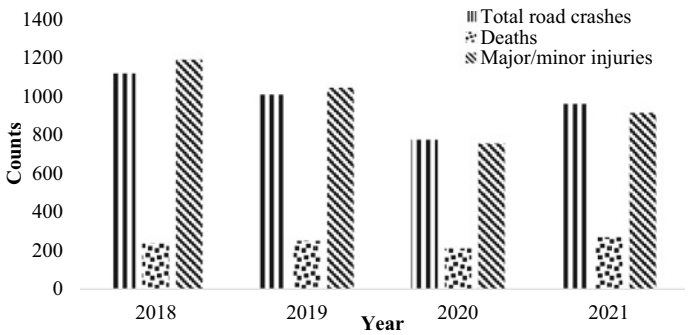

Fig. 1 Road crash statistics of Nagpur Metropolitan Area (*Source* Accident Research Cell, Mumbai)

any possible risk can help the driver in taking safer driving decisions. Such timely alerts to drivers are possible through the ADAS such as Collision Avoidance System *(CAS)* which provides several visual and audio alerts to drivers, whenever any vehicle, obstruction, or pedestrian comes in the path of the subject vehicles wherein ADAS is installed. Conceptually, this is a system covering camera(s) which capture the images/videos of the road ahead and thus detect static/moving objects within the predefined distance/time range and lane of the subject vehicle. Due to the communication of the alerts, potential crash events are averted as the driver gets instant alerts in the form of audio and visual alerts and thus aiding them while driving [9].

1.2 Collision Avoidance System (CAS)

Mobileye 8 Connect Collision Avoidance System *(CAS)* was employed in this study, which is also widely deployed on various domestic and commercial automobiles across the world. The type of visual and audio alerts communicated to the driver includes Forward Collision Warning *(FCW)*, Pedestrian Collision Warning *(PCW)*, Headway Monitoring Warning *(HMW)*, Lane Departure Warning *(LDW),* and Speed Limit Indication *(SLI)* alert so that driver can handle this adverse condition in advance. It also provides driver information such as alert generation timing with driver ID, as well as geographical coordinates of incidents and thus doing real-time mapping [9].

1.3 Literature Review

Various research studies were conducted to understand driver behavior aimed at enhancing road safety and in some of these investigations, questionnaire surveys, machine learning, deep learning, and artificial intelligence were utilized and a brief on them is discussed in the succeeding section.

Mishra & Bajaj (2015) conducted a comprehensive investigation into the prevalence of any type of secondary activity to narrow down the characteristics that cause driver distraction while driving and determined the parameters that directly or indirectly determine a certain type of driver's behavior, such as driver's attitude and temperament [8].

Farooq et al. (2020) used the FAHP (Fuzzy Analytical Hierarchy Process) framework to examine and compare the important driving behavior characteristics among defined driving cultures *(countries)* and the Driver Behavior Questionnaire *(DBQ)* survey, which is developed on a fuzzy scale, is used to examine evaluators' responses to perceived road concerns [6].

Bhalerao et al. (2020) investigated driver behavior and predicted whether the driver is a safe driver, and they built a system that forecasts whether a motorist is a safe driver or not by taking into consideration several characteristics such as attentiveness and drowsiness, driver background data and driving data, and surrounding situations [5].

Aksjonov et al. (2020) developed a methodology for detecting and evaluating driver distraction *(DD)* while conducting secondary tasks is explained, as well as an appropriate hardware and software environment that is supplied and investigated. The system incorporates a normal driving model, a subsystem for monitoring secondary task mistakes, and a module for overall distraction evaluation. This technique is used as a standard for safe and transparent in-vehicle information systems design [2].

Alkinani et al. (2020) found that since the introduction of deep learning algorithms, a substantial amount of research has been done to anticipate and evaluate driver behavior or action-related data using neural network methods. It contributed to the first classification and discussion of Human Driver Inattentive Driving Behavior *(HIDB)* into two key categories: Driver Distraction *(DD)* and Driver Fatigue *(DF)* in this study [3].

Voinea et al. (2020) looked at the usage of a smartphone-based ADAS in terms of driving performance and driver acceptance to improve road safety. The researchers used paired *t*-tests to look for statistical differences between the baseline and ADAS conditions. All items were scored on a seven-point Likert scale, with scores ranging from one to seven in which the system's acceptability is moving from Strongly Disagree to Strongly Agree on a scale of 1–7. The results show that employing a driver assistance system has a favorable effect on the driver's conduct [13].

Ye Xu et. al. (2021) discovered that during naturalistic driving scenarios, drivers typically ignore or overreact to ADAS signals. They next investigated bus driver responses to lane departure warning *(LDW)* and forward-collision warning *(FCW)* using 20 days of naturalistic driving data and discovered that employing LDW and FCW systems has several drawbacks. According to the study's mathematical analysis, drivers' reactions to FCW are typically more favorable at night, and the coefficients of variation for LDW and FCW are higher. Acceptance of LDW and FCW is higher on freeways than on city streets, and the disparity is much bigger at night [14].

Azman et al. (2021) did research in Malaysia with 20 drivers who consented to have an In-vehicle Monitoring System *(IVMS)* installed in their ADAS along with onboard diagnostics devices (OBD)—compliant private vehicles. The methodology used in this study includes data collection, device installation, "Blind-Unblind-Reblind" testing, and data analysis on MS Excel. The parameters examined encompassed FCW, SLI, LDW, and HMW coupled with OBD examinations, severe braking, and acceleration, as well as journey duration, time of travel, and distance traveled [4].

The findings described in Table 1 demonstrate that the examination of driver behavior using AI tools is the way forward in the Indian context as it can act as a force multiplier which is being attempted for the first time on Indian roads.

1.4 Objective, Scope, and Methodology of the Study

The objective of this study is to develop a Road Safety Index (RSI) that can be used to assess bus drivers by integrating with the AI-based CAS device data. Such alerts based on the travel along the road network traversed by buses have been maintained

Table 1 Summary of literature

Author	Title	Source	Findings
Mishra & Bajaj (2015)	Driver behavior monitoring on urban roads of a tier 2 city in India	7th International Conference on Emerging Trends in Engineering & Technology	Identified the factors that characterize a driver's attitude and temperament, such as age, gender, old-school views vs current understanding, and so on
Farooq, D., Moslem, S., Tufail, R. F., Ghorbanzadeh, O., Duleba, S., Maqsoom, A., & Blaschke, T. (2020)	Analyzing the importance of driver behavior criteria related to road safety for different driving criteria. Budapest, Hungary	Int. J. Environ. Res. Public Health 2020, 17, 1893	Examine and compare the important driving behavior characteristics among defined driving cultures (countries) and the Driver Behavior Questionnaire (DBQ) survey, which is developed on a fuzzy scale
Bhalerao, J., Kadam, A., Shinde, A., Mugalikar, v., & Bhan, H. (2020)	Proposed design on driver behavioral analysis	International Journal of Engineering Research & Technology (IJERT)	Prepared a system that forecasts whether a motorist is a safe driver or not by taking into consideration several characteristics such as attentiveness and drowsiness, driver background data and driving data, and surrounding situations
Aksjonov, A., Nedoma, P., Vodovozov, V., Petlenkov, E., & Herrmann, M. (2020)	Detection and Evaluation of Driver Distraction Using Machine Learning and Fuzzy Logic	IEEE transactions on intelligent transportation systems	Developed a methodology for detecting and evaluating driver distraction (DD) while conducting secondary tasks by using a safe and transparent IVIS (in-vehicle information systems) design with minimal driver load

(continued)

Table 1 (continued)

Author	Title	Source	Findings
Alkinani, M. H., Khan, W. Z., IEEE, S., & Arsad, Q. (2020)	Detecting Human Driver Inattentive and Aggressive Driving Behavior Using Deep Learning: Recent Advances, Requirements, and Open Challenges: Jeddah	IEEE Access, Special section on Artificial intelligence (AI)-empowered	Contributed to the first classification and discussion of Human Driver Inattentive Driving Behavior (HIDB) into two key categories: Driver Distraction (DD), Driver Fatigue (DF), or Drowsiness in this study (DFD)
Voinea, G. D., Postelnicu, C. C., Duguleana, M., Mogan, G. L., & Socianu, R. (2020)	Driving Performance and Technology Acceptance Evaluation in Real Traffic of a Smartphone-Based Driver Assistance System	Int. J. Environ. Res. Public Health 2020	Looked at the usage of a smartphone-based ADAS in terms of driving performance and driver acceptance to improve road safety. The results show that employing a driver assistance system has a favorable effect on the driver's conduct
Ye, W., Xu, Y., Zhou, F., Shi, X., & Ye, Z. (2021)	Investigation of Bus Drivers' Reaction to ADAS Warning System: Application of the Gaussian Mixed Model	MDPI, Sustainability 2021	Discovered that during naturalistic driving scenarios, drivers typically ignore or overreact to ADAS. Drivers' reactions to FCW are typically more favorable at night, and the coefficients of variation for LDW and FCW are higher
Azman, N. S., Hashmin, H. H., Shabadin, A., Abd ghani, M. R., Abu kassim, K. A., & Mohammad radzi, M. (2021)	A Study of Driver Behavioral Adaptation to Advanced Driver Assistance System (ADAS) in Malaysia	Journal of Advanced Vehicle System 11. Retrieved from	Forward Collision Warning, Speed Limit Warning, Lane Departure Warning, and Headway Monitoring Warning were among the indicators examined in this study through ADAS, and OBD examinations included severe braking, cornering, and acceleration, as well as journey duration, time of travel, and distance traveled

centrally through cloud storage for later data analysis so that the performance of the subjects can be assessed based on the integration of the generated alerts with the associated road parameters. The scope of the present study encompassed 33 buses running on 76 defined bus routes of NMC covering more than 3,00,000 km during the 3-month period from September 2021 to November 2021. The alerts generated during the observation period were intended to assess drivers.

The above data has been compiled on an Excel database and a detailed analysis of the driver performance covering the evaluation of their characteristics based on Vienna outcomes (refer Table 2), driver attributes, and CAS alerts of all 33 drivers. In addition, a correlation analysis between Vienna results, driver attributes, and CAS alerts was also conducted to understand whether there is the existence of multi-collinearity among the various independent variables. After ascertaining that there is an optimal amount of multi-collinearity among the considered independent variables, RSI for driver evaluation was developed by formulating a linear regression model. Figure 2 depicts the approach devised in this study.

2 Material & Methods

2.1 Data Collection

To develop the RSI, data was gathered from the following sources:

- The Vienna test results revealed the response time of drivers toward various visual and audio alerts and the characteristics of a sample of 33 drivers.
- Driver's attributes were gathered through a Detailed Questionnaire Survey (DQS).
- CAS alerts (namely PCW, HMW, FCW, LDW) are generated by drivers.

The Vienna test system is a computerized psychological test of the 15-min time period (Fixed duration type test) or of any period, in which the drivers are exposed to visual (through various lights) and audio (through high & low tones) signals at various speed and time intervals which is as similar associated with many natural events which occur on roads such as various lights operation of front vehicle, traffic lights and signals, clutch and brake action (foot movements), various sounds from other vehicles, and so on. This provides information on the number of correct responses, number of incorrect responses, number of omitted signals, and delayed responses during the testing (correct responses but delayed) [11]. By using this, 33 drivers were assessed in this study to capture their different responses. These transmitted signals and associated responses were exported in a matrix format at the end of the test. Table 2 represents the typical sample of the Vienna output matrix for a driver. It contains the driver names, reactions requested, and various visual & audio signals, which can be analyzed simply as a matrix analysis. For understanding, if the white color signal requested by the Vienna system is matched with the driver's reacted

Table 2 Typical output of Vienna output matrix for a subject

Parameter	Score level								
Reactions (requested)	White	Yellow	Red	Green	Blue	Right foot	Left foot	High tone	Low tone
White answers	18								
Yellow answers		18							
Red answers			18						
Green answers				17					
Blue answers					18			1	
Right foot answers			1			13			
Left foot answers	1		1			3	3		
High tone answer								13	
Low tone answers								1	17
Omitted	1	1	1	2		6	16	5	1
Sum of wrong answers	1		2		1	3		2	
Complete correct	17	18	16	17	18	10	3	11	17
Omitted	1	1	1	2	0	6	16	5	1
Wrong	1	0	2	0	1	3	0	3	1
Total	19	19	19	19	19	19	19	19	19

white color, then it is the correct signal otherwise it will be a wrong, omitted, or delayed signal. Similarly, all signals were checked.

In addition, during the Vienna test, a DQS was completed with the consent of each driver that their data will be used for research, which helped in obtaining the socio-economic profile of the subjects. Under this, the drivers were asked about their name, age, experience, educational background, exposure to driving, the consumption of toxic things, any past assistantship work experience during their beginning stage of driving, previous involvement in road crashes, any eye illness, and so on. Only reliable and significant information that would be useful in driver assessment and for developing a RSI were considered, such as driving experience, any past driver assistantship work experience, and eye illnesses.

This study made use of the CAS alerts, which encompassed the PCW, FCW, HMW, and LDW alerts. During the observation period, 33 buses generated 84195

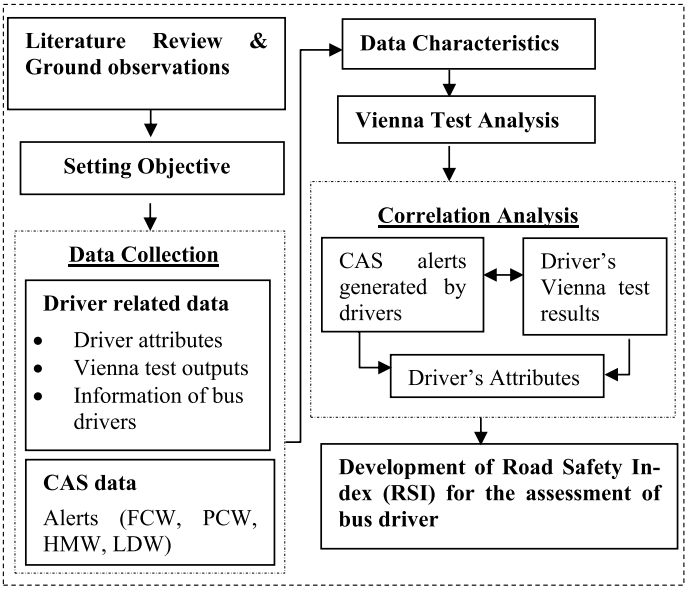

Fig. 2 Overall study methodology

alerts, of which 25561 PCW, 8633 FCW, 45084 HMW, and 4917 LDW alerts were generated and then imported it to the GIS platform, as shown in Fig. 3.

Fig. 3 CAS alerts (indicated by black circles) on road network (Black line) *(Alerts are denoted by black circles in hindsight it may appear as a black bold line as the generated alerts are high)*

2.2 Data Characteristics

In this section, the characteristics and significance of various output data from the Vienna Test, DQS data, and CAS alerts have been analyzed. Additionally, the relationship between the data from the Vienna test and the CAS alerts data has been examined, which will be useful for assessing the drivers. It can be understood from Table 2 that the responses are related to two kinds of signals *(audio & visual)*, and these are randomly given to the subjects. Various lights are included as part of the visual signals of different colors (white, red, yellow, green, and blue), as well as signals of left and right leg movement which included two types of audio signals namely, high and low tones. Based on the above studies and the Vienna output matrix given in Table 2, the following inferences have been drawn:

- The incorrect responses occurred more frequently in the case of audio signals as well as foot movement signals than visual signals.
- When left and right leg motions happened visually, the Complex Reaction Time (CRT) for eye-to-foot movement became longer than eye-to-hand movement which resulted in foot movements becoming increasingly incorrect. The various reactions/responses of the subjects at the Laboratory level Vienna testing have been carefully examined which helped in formulating strategies to analyze the CAS alerts which is generated during driving on the road.
- It is evident that there is a strong relationship between the results of the Vienna test system and CAS device because both produce audio and visual alerts seeking coordinated and timely reactions in terms of eye-to-hand, eye-to-foot, ear-to-hand, and ear-to-foot movement. This relationship can be used to evaluate the behavior of the driver.

In addition, relevant data were extracted after systematically reviewing the DQS data that could be utilized in further research, such as age/driving experience, assistantship work in the early stages of their driving field, and any eye issues. The DQS study revealed that 30% of the subjects had eye issues. When the alert generation was examined in relation to the driver's driving experience, it was shown that even experienced drivers generated more alerts, except for middle-aged drivers who possessed driving experience of 5 years or less.

To understand more about CAS alert characteristics, the 3-month data were normalized in terms of per-subject-per-day to investigate the average generation of different alerts generated by drivers. Figure 4 represents the average characteristics of generated CAS alerts by each driver during the observation period of 91 days.

It can be inferred from Fig. 4 that the total average alerts generated from a driver are increasing continuously from LDW to FCW, FCW to PCW, and PCW to HMW per day. In the case of day and night-time, the same trend of alert generation was seen, but during night-time, LDW alert is more prevalent than FCW alert, this might be due to a lack of visibility, insufficient lighting along the road, or due to driver carelessness. Following that an Excel database was created that had the Vienna outputs of the drivers, normalized CAS alerts produced by the drivers (CAS alerts/

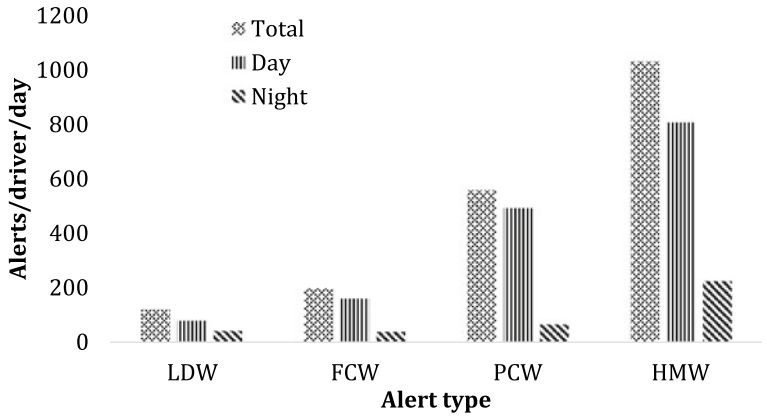

Fig. 4 Average statistics of CAS alerts during the observation period

distance traveled in km), and various other attributes, which aided in the driver behavior assessment. To accomplish the task, a linear regression model using the above data and from which a RSI has been developed for the evaluation of drivers. The equation derived from this model was used to analyze the driver, and based on this data, the function can be applied throughout Indian roads.

2.3 Data Analysis

The analysis of driver behavior assessment is divided into two parts: First, the outputs of the Vienna test of drivers are analyzed, and then the correlation is examined between the Vienna outputs, attributes of drivers, and CAS alerts.

From the Vienna test, a report for each subject was prepared based on the output matrix (refer, Table 2), which is then computed individually for its overall correct responses and individual correct responses toward visual and audio signals. Five categories have been defined for the subjects based on correct responses toward combined alerts as well as individual visual and audio alerts. So, when a subject responded less than 50% correct responses toward visual and audio signals of Vienna test individually, then the driver was categorized into the "WEAK" category, whereas if the correct response in individual visual and audio signals falling between 50% and 75%, the subject is in the "AVERAGE" category. Similarly, if the total correct response is between 75% and 85%, then the subject is categorized under the "GOOD" category whereas if the driver is between 85% and 95%, the driver is in the "VERY GOOD" category; and "EXCELLENT" if the score is more than 95%. This allows the categorization of drivers based on their percentage correct response toward total and individual Vienna signals.

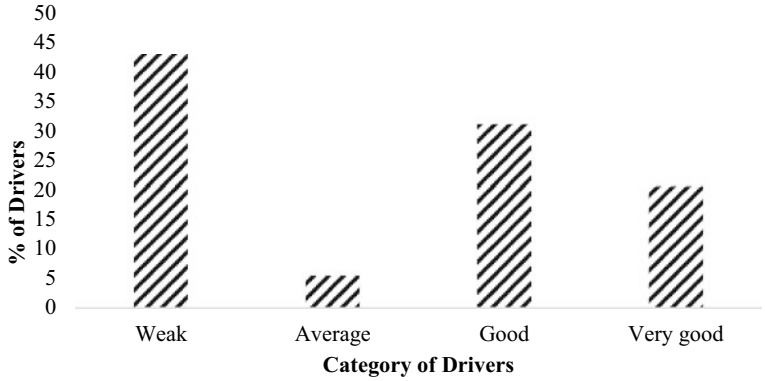

Fig. 5 Categorizing drivers based on total Vienna test responses

Figure 5 shows that out of the 33 subjects, 20.57% of drivers fall under the "VERY GOOD" group, 31.07% have scores in the "GOOD" category, 5.44% have scores in the "AVERAGE" category, and 42.93% have their Vienna score in the "WEAK" category.

Drivers' performance in the Laboratory-based Vienna test serves as a precursor toward understanding the level of compliance for CAS by the subjects. In other words, subjects securing better Vienna scores are expected to generate less CAS alerts. To validate this, after evaluating the Vienna outcome of the outcome, using IBM-SPSS software [7], a correlation analysis of the drivers with their Vienna scores, attributes like their age, driving experience, any assistantship work, any eye disease, etc., and several normalized CAS alerts such as PCW, FCW, LDW, and HMW were performed to understand whether there is multi-collinearity among the independent variables.

Table 3 represents the correlation matrix, in which each variable was assessed based on its significant coefficient (Sig.) and the Pearson Correlation beta (B) coefficient.

Following that a correlation analysis was performed between the three forms of data, which was useful in assessing the subjects, and the following inferences have been drawn from this analysis:

- Total Vienna signals *(visual & audio)* with correct responses exhibited multi-collinearity with PCW *($p = 0.007$)* and HMW alerts *($p = 0.036$)*. Similarly, based on the close look at each alert type *(visual/audio)* independently, it can be observed that the Vienna score specific to visual alerts, i.e., correct responses toward visual alerts exhibit collinearity with LDW alerts *($p = 0.075$)*, as with increase in the correct responses to visual alerts, number of LDW alerts are being observed to be decreasing. Similarly, correct response toward audio alerts in Vienna system is significantly correlated with the sum of all CAS alerts *($p = 0.001$)*.
- It is observed that there is a significant correlation between the age of the driver and the driving experience *($p = 0.000$)* and nearly correlation between the age of the driver and the diseases related to eye *($p = 0.047$)*. With increasing age, number

Table 3 Correlation matrix

Correlation matrix												
		% Corrected response to signals	% Corrected response to visual alerts	% Corrected response to audio alerts	Driving experience	Worked as an assistant to driver	Any eye disease	Sum of CAS (Alerts/km)	Sum of FCW (Alerts/km)	Sum of PCW (Alerts/km)	Sum of HMW(Alerts/km)	Sum of LDW(Alerts/km)
% Corrected response to signals	B	1	0.687**	0.687**	−0.087	−0.055	0.003	0.202*	0.146	0.271**	0.213*	−0.119
	Sig		0.000	0.000	0.395	0.595	0.979	0.048	0.155	0.007	0.036	0.247
% Corrected response to visual alerts	B	0.687**	1	−0.053	−0.117	−0.035	−0.145	−0.055	0.007	0.164	−0.067	−0.182
	Sig	0.000		0.606	0.254	0.737	0.156	0.591	0.947	0.107	0.517	0.075
% Corrected response to audio alerts	B	0.687**	−0.053	1	0.020	−0.034	0.146	0.321**	0.192	0.192	0.350**	0.014
	Sig	0.000	0.606		0.843	0.742	0.153	0.001	0.059	0.060	0.000	0.893
Driving experience	B	−0.087	−0.117	0.020	1	0.148	0.133	−0.176	−0.142	−0.191	−0.154	−0.057
	Sig	0.395	0.254	0.843		0.148	0.193	0.085	0.166	0.061	0.133	0.578
Worked as an assistant to driver	B	−0.055	−0.035	−0.034	0.148	1	−0.096	−0.132	−0.225*	−0.229*	−0.089	−0.015
	Sig	0.595	0.737	0.742	0.148		0.348	0.198	0.027	0.024	0.387	0.887
Any eye disease	B	0.003	−0.145	0.146	0.133	−0.096	1	−0.150	−0.085	−0.027	−0.145	−0.140
	Sig	0.979	0.156	0.153	0.193	0.348		0.142	0.407	0.794	0.156	0.171

(continued)

Table 3 (continued)

Correlation matrix												
		% Corrected response to signals	% Corrected response to visual alerts	% Corrected response to audio alerts	Driving experience	Worked as an assistant to driver	Any eye disease	Sum of CAS (Alerts/km)	Sum of FCW (Alerts/km)	Sum of PCW (Alerts/km)	Sum of HMW(Alerts/km)	Sum of LDW(Alerts/km)
Sum of distance (Km)	B	−0.081	−0.035	−0.088	−0.015	0.062	0.256*	−0.036	−0.037	0.050	0.000	−0.214*
	Sig	0.429	0.733	0.392	0.882	0.544	0.011	0.727	0.721	0.623	0.999	0.036
Sum of CAS (Alerts/km)	B	0.202*	−0.055	0.321**	−0.176	−0.132	−0.150	1	0.762**	0.573**	0.971**	0.461**
	Sig	0.048	0.591	0.001	0.085	0.198	0.142		0.000	0.000	0.000	0.000
Sum of FCW (Alerts/km)	B	0.146	0.007	0.192	−0.142	−0.225*	−0.085	0.762**	1	0.560**	0.682**	0.280**
	Sig	0.155	0.947	0.059	0.166	0.027	0.407	0.000		0.000	0.000	0.005
Sum of PCW (Alerts/km)	B	0.271**	0.164	0.192	−0.191	−0.229*	−0.027	0.573**	0.560**	1	0.465**	−0.071
	Sig	0.007	0.107	0.060	0.061	0.024	0.794	0.000	0.000		0.000	0.491
Sum of HMW (Alerts/km)	B	0.213*	−0.067	0.350**	−0.154	−0.089	−0.145	0.971**	0.682**	0.465**	1	0.334**
	Sig	0.036	0.517	0.000	0.133	0.387	0.156	0.000	0.000	0.000		0.001
Sum of LDW (Alerts/km)	B	−0.119	−0.182	0.014	−0.057	−0.015	−0.140	0.461**	0.280**	−0.071	0.334**	1
	Sig	0.247	0.075	0.893	0.578	0.887	0.171	0.000	0.005	0.491	0.001	

of HMW, PCW, FCW, and LDW alerts are also being observed to be decreasing. This can be due to the increased experience leading to safer driving practices.

- The driving experience exhibited multi-collinearity with PCW alerts *($p = 0.061$)* which implies when driving experience increases generation of PCW alerts are decreasing as depicted from correlation matrix.
- Further, driver assistantship experience exhibited multi-collinearity with FCW *($p = 0.027$)* & PCW *($p = 0.024$)* alerts which indicated that if a subject has worked as a driver's assistant prior to working as a driver, it had a positive impact on the number of alerts being generated.

Considering the above correlation analysis, it was observed driving experience, his work as an assistant to driver, and the details of his eye condition have a direct influence on the visual and audio signals of Vienna test and these signals are significantly inversely correlated with CAS alerts. Hence a linear regression has been performed to formulate a mathematical model for the evaluation of the subjects in which the % Corrected Responses to Vienna Signals *(% CRVS)* is considered as a dependent variable whereas the driver's experience on driving & assistantship work, eye disease related data are considered as independent variables that are used to develop the multiple linear regression model which is given in Eq. 1.

$$\%\,CRVS = (3.672 * D_E) + (27.576 * A_D) - (12.59 * E_D) \tag{1}$$

where % CRVS is the Percentage Corrected Responses to Vienna signals, D_E is the Driving Experience (in years), A_D is Assistantship work to Driver (in years), and E_D is related with Eye Disease (Yes = 1 or No = 0).

As mentioned in Eq. (1), driver's experience as an assistant has the maximum impact on its performance toward correct answers, as the beta coefficient value is maximum, i.e., 27.6. Positive sign associated with driver's driving experience is as expected. Negative sign for the parameter of eye disease indicates that driver with some visual limitation may not be able to respond correctly and/or timely.

3 Results

First, the data from the Vienna test was evaluated, which indicated how the driver reacts to the arrival of any individual or combined visual and audio signals in terms of their response time and described the driver's attentiveness toward various signals/alerts which is illustrated in Fig. 5. Further analysis was conducted to understand responses of the subjects toward visual and audio signals of Vienna test individually which is presented in Fig. 6. It can be noted from Fig. 6 that 84.2% of drivers generated 80–100% correct visual signals, whereas 15.2% drivers generate 60–80% correct visual signals.

It was inferred that from above Vienna analysis, visual alerts received better responses than audible alerts and hence the key takeaway is that the response of the

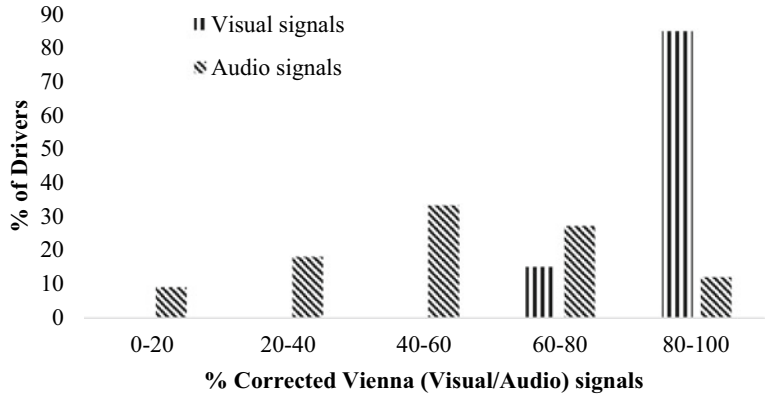

Fig. 6 Categorizing drivers based on responses toward visual & audio signals of the Vienna test

subjects to the video alerts will far exceed the audio alerts. Further, it is inferred that the subjects who generated less CAS alerts while driving on the road will have a better Vienna score, as well as significant experience of driving and assistantship work for the driver and will not have any eye-related concerns, which can help in driver's assessment and recruitment of drivers for various bus routes of Nagpur city. Also, the characteristics of the driver have been evaluated based on the generated CAS alerts of the drivers to determine how this driver will perform on various bus routes or corridors. Taking this into account, the mathematical maximum value for this Eq. (1) for preparing an index for challenging situations, such as driving and assistant-ship work experience of 30 and 3 years, respectively, and considering existing eye disease condition (ED = 1) % CRVS value of 180.3 which has been taken up to a maximum value of 200, then five scale categorization of the driver has been done and an RSI as presented in Table 4 has been prepared. It is evident from Table 4 that if the % CRVS value is between 161 and 200, the driver is in the "EXCELLENT" category, between 121 and 160, the driver is in the "VERY GOOD" category, between 81 and 120, the driver is in the "GOOD" category, between 41 and 80, the driver is in the "AVERAGE" category, and between 0 and 40, the driver is in the "WEAK" category.

A comparison of the % corrected Vienna scores in the ascending order of its arrangement with that of the CAS alert generated for each driver revealed that the driver-generated CAS alerts are decreasing, which indicated that the driver is

Table 4 RSI for the categorization of driver

% CRVS value	Category of driver
0–40	Weak
41–80	Average
81–120	Good
121–160	Very good
161–200	Excellent

performing well. On the other hand, if everything is all right, but the CAS alerts are increasing, which implied that certain deficiency in road geometry contributes to the generations of alerts.

Based on the outputs, subjects can be allocated travel routes and corridors in a structured way depending on the score obtained by them. For instance, the subjects who have scored less percentage of CRVS can be assigned to a less congested route; on the contrary, the subjects who have secured more percentage of CRVS, they may be assigned to a more congested route. Considering the above analogy, the subjects who secure fewer CAS alerts will generate, which can ultimately help avert the incidence of road crashes/fatalities involving buses. With other types of road users especially VRUs.

4 Conclusion & Recommendations

In this study, an effort has been made to integrate AI-based CAS data with Vienna test coupled with a conventional detailed questionnaire survey. In this research 33 driver's data were utilized for the development of RSI which allows Nagpur bus drivers to be appropriately classified so that they may perform well in a disciplined manner with the use of Advanced Driver Assistance System (ADAS) on the roads. From the research, it can be clearly seen that there is a perfect inverse correlation present between Vienna & CAS device visual and audio signals, and practically visual signals are more attended by drivers as compared to audio signals. Based on the results of the correlation analysis, it was observed driving experience, his work as an assistant to driver, and the details of his eye condition have a direct influence on the visual and audio signals of Vienna test. Hence a linear regression has been performed to formulate a mathematical model for the evaluation of the subjects in which the % Corrected Responses to Vienna Signals *(% CRVS)* is considered as a dependent variable, whereas the driver's experience on driving & assistantship work, eye disease related data are considered as independent variables that are used to develop the multiple linear regression model given in Eq. 1. After that, taking the maximum value of variables of that equation, a five-scale categorization has been done to prepare a RSI (refer, Table 4).

In summary, it is recommended that weaker drivers can be improved by imparting proper training. Further, among the drivers with average and good scores, drivers with vision limitations can be identified and improved with proper rectification strategies (eye checkups followed by medication and supply of spectacles).

Acknowledgements This study was carried out as part of Project iRASTE (Intelligent Solutions for Road Safety through Technology and Engineering) by the consortium of CSIR-CRRI, Intel India, Mahindra & Mahindra Group, INAI Centre & iHUB-data at IIIT-Hyderabad, and Nagpur Municipal Corporation. Authors are thankful to the data collection team consisting of Ms. Kamini Gupta, Mr. Mohammad Akil, Mr. Abhi Mandal, and Mr. Sikandar.

References

1. Accident research cell (2018, 2019, 2020, 2021) Road accidents in Maharashtra. Mumbai: Accident research cell
2. Aksjonov A, Nedoma P, Vodovozov V, Petlenkov E, Herrmann M (2019) Detection and evaluation of driver distraction using machine learning and fuzzy logic. IEEE Trans Intell Transp Syst **20**(6): 2048–2059. doi:https://doi.org/10.1109/TITS.2018.2857222.
3. Alkinani MH, Khan WZ, IEEE S, Arsad Q (2020) Detecting human driver inattentive and aggressive driving behavior using deep learning: Recent advances, requirements and open challenges. IEEE Access **8**(8): 105008–105030. doi:https://doi.org/10.1109/ACCESS.2020.2999829
4. Azman NS, Hashmin HH, Shabadin A, Abd ghani MR, Abu kassim KA, Mohammad radzi M (2021) A study of driver behavioral adaptation to advanced driver assistance system (adas) in Malaysia. J Adv Veh Syst **11**(1): 1–12. Retrieved from http://www.akademiabaru.com/submit/
5. Bhalerao J, Kadam A, Shinde A, Mugalikar V, Bhan H (2020) Proposed design on driver behavioral analysis. Int J Eng Res & Technol (IJERT) **9**(5): 1–5. Retrieved from http://www.ijert.org
6. Farooq D, Moslem S, Tufail RF, Ghorbanzadeh O, Duleba S, Maqsoom A, Blaschke T (2020) Analyzing the importance of driver behavior criteria related to road safety for different driving criteria. Int J Environ Res Public Health **17**(6): 1893. doi :https://doi.org/10.3390/ijerph17061893
7. IBM Corp. (n.d.) IBM SPSS statistics for windows, Version 22.0. (IBM Corp.) Retrieved June 17, 2013, from https://www.ibm.com/support/
8. Mishra A, Bajaj P (2015) Driver behaviour monitoring on urban roads of a tier 2 city in India. 7th Int Conf Emerg Trends Eng & Technol 15: 134–140. doi:https://doi.org/10.1109/ICETET.2015.13
9. Mobileye-8-connect (2021) Products. Retrieved from Mobileye: https://www.mobileye.com/us/fleets/products/mobileye-8-connect/
10. Nagpur metropolitan region development authority (2017) NMRDA. About us. Retrieved from nmrda: http://www.nmrda.org/aboutNMR.aspx
11. Schuhfried G (2011) Wiener test system (Vienna Test System) modelling. Schuhfried, Austria
12. Urban mass transit company limited (2018) Comprehensive mobility plan for Nagpur. Nagpur Improvement Trust, Nagpur
13. Voinea GD, Postelnicu CC, Duguleana M, Mogan GL, Socianu R (2020) Driver performance and technology acceptance evaluation in a real traffic of smartphone based driver assistance system. Int J Environ Res Public Health **17**. doi: https://doi.org/10.3390/ijerph17197098
14. Ye W, Xu Y, Zhou F, Shi X, Ye Z (2021) Investigation of bus drivers' reaction to ADAS warning system: application of the Gaussian mixed model. MDPI, Sustainability **13**(8759): 13–16. doi: https://doi.org/10.3390/su13168759

Effect of Pavement Roughness on Speed of Vehicles

Mithlesh Kumar, V. M. Ashalakshmi, M. V. L. R. Anjaneyulu, and M. Sivakumar

Abstract The surface condition of pavement influences traffic safety, operating speed, manoeuverability, driver comfort and service volume. Generally, the service quality provided by pavement surface is evaluated based on its roughness. International Roughness Index (IRI) is a roughness indicator used globally. Even though the measurement of IRI is very costly, it gives a standardised method of pavement unevenness evaluation. This study attempts to relate pavement roughness with the speed of different classes of vehicles. Pavement roughness and traffic flow characteristics were collected from thirteen sites in Calicut city. Traffic data was collected using a Transportable Infrared Traffic logger (TIRTL), while geometric data was collected manually. Surface roughness was measured using the Machine for Evaluating Roughness Using Low-cost Instrumentation (MERLIN), and the Cundill roughness equation was used for IRI calculation. As IRI increases, the Free-Flow Speed (FFS) and Peak Hour Speed (PHS) of different vehicle classes reduce. The reduction in FFS is linear with IRI, whereas a negative logarithmic relationship can be observed in the case of PHS.

Keywords International roughness index · TIRTL · MERLIN · Free flow speed · Peak hour speed

1 Introduction

Pavements are constructed to provide good serviceability to road users in their design life. After opening to the traffic, the pavement surface starts deteriorating due to the repetition of loads and varying environmental conditions. Consequently, different types of surface distress appear on the pavement and affect traffic operations, riding

M. Kumar (✉) · V. M. Ashalakshmi · M. V. L. R. Anjaneyulu · M. Sivakumar
Department of Civil Engineering, National Institute of Technology, Calicut, Kerala 673601, India
e-mail: kmithlesh23@yahoo.com

M. Kumar
Department of Civil Engineering, Indian Institute of Technology Bombay, Mumbai 400076, India

A. Dhamaniya et al. (eds.), *Recent Advances in Traffic Engineering*, Lecture Notes in Civil Engineering 377, https://doi.org/10.1007/978-981-99-4464-4_7

quality, route selection and quality of service. The deterioration of pavement increases as the age of the pavement increases. This deterioration is generally measured in terms of pavement roughness which adversely affects riding comfort. Therefore, as roughness increases, the driver tends to reduce the speed accordingly to reduce passenger discomfort.

Driving on a rough road is tricky because the normal speed limits are provided for good road surfaces. If the vehicle is driven at the normal speed, it may result in accidents, as rough road necessitates the driver to drive more slowly and cautiously [10, 14]. If the speed is reduced beyond a limit, it will create unnecessary congestion and reduce the capacity of the road stretch [13]. Other than these effects, the reduced speed will result in higher fuel consumption and vehicular emissions ([11, 16]). Therefore, it is very important to analyse how pavement roughness affects the speed of different classes of vehicles.

Earlier studies concentrated on how traffic affects pavement, but later many researchers worked on how pavement surface characteristics affect traffic flow. But little research has been carried out on how this effect varies between different classes of vehicles. The studies on the effect of pavement roughness on different classes of vehicles limit their study to cars and heavy vehicles. Other types of vehicles were not considered. Also, the development of the automobile industry improved vehicle suspension systems in such a way that vehicles can move over rough roads with more speed.

This study is limited to straight and level sections on two-lane, two-way non-urban flexible pavements in the Calicut district of state of Kerala to efficiently measure how pavement roughness affects the speed of various classes of vehicles. This study excludes skid resistance and its effect on traffic flow. The International Roughness Index (IRI) was selected as the roughness indicator, and speed is the only macroscopic traffic flow characteristic chosen for the study. Therefore, the study's primary goal is to determine and quantify the effect of pavement roughness on the speed of traffic flow during free-flow and peak-hour flow situations.

2 Literature Review

Apart from studying the impact of traffic on pavement, Karan et al. [9] study is the first attempt to introduce the concept of the effect of pavement condition on traffic flow characteristics. The roughness was collected from 72 sites in Canada and represented in terms of a Riding Comfort Index (RCI), along with which volume-capacity (v/c) ratio and speed limit also affected FFS. It was determined that the degree of roughness substantially impacts speed. This impact of roughness on vehicles will be different for different types of vehicles, which was studied by Chandra [3]. According to the study, roughness significantly impacts the capacity of two-lane roads in India. Equations (1) and (2) show that the influence of roughness is more pronounced at the speed of passenger cars than at the speed of heavy vehicles.

$$FFS_{CAR} = 66.9 - 0.0034 \times UI \ (R2 = 0.91) \quad (1)$$

$$FFS_{HV} = 51.6 - 0.0019 \times UI \ (R2 = 0.84) \quad (2)$$

where

FFS = Free flow speed in km/hr and

UI = Unevenness Index in mm/km.

Indo HCM [6] gives a single relationship for the operating speed of vehicles with IRI on two-lane interurban roads, as given in Eq. (3).

$$V_{OS} = 104 - 6.8 \times IRI \quad (3)$$

where

V_{OS} = Operating speed in km/hr and

IRI = International Roughness Index in m/km.

This type of variation in speed is observed, when the IRI is very low (3 m/km). Similar study concluded that when IRI increases, speed decreases linearly such that an unit change in IRI will lead to a speed reduction of 0.48–0.64 km/h [17]. IRI greater than 7 m/km causes a sharp decline in FFS on horizontal curves and mid-block sections of roadway, although only linear relationships are observed at intersections [1].

Vehicle speed may be influenced by a variety of other variables in addition to pavement roughness. Yu and [18], using an empirical model, found different variables including the volume-capacity (v/c) ratio, pavement type (flexible/rigid), number of lanes and speed limit. Preliminary analysis, however, revealed that neither the pavement type nor the posted speed restriction had any impact on the average speed of a vehicle. For each unit increase in roughness, the developed regression model showed that the average speed of vehicles drops by 0.84 km/hr. According to the authors, the model did not consider vehicle type as an independent variable, which might make the model less reliable. Summary of literature is given in Table 1.

While this review of the literature reveals that the work has been done studying the impact of pavement roughness on vehicle speed, although very few of these studies considered different types of vehicles. The primary goal of this research is to investigate the relationship between IRI and traffic speed in various vehicle classes.

3 Methodology and Data Collection

The methodology of the study is given in Fig. 1.

From the literature review, roughness is one of the significant factors affecting speed. Speed was collected using TIRTL, and roughness using MERLIN. Free flow

Table 1 Summary of literature

Sl no.	Authors & year	Dependent variable	Indices used	Model selected
1	Karan et al. [9]	FFS	RCI	Linear regression model
2	Chandra [3]	FFS, Capacity	UI	Linear regression model
3	Madhu et al. [12]	FFS	IRI	Linear regression model
4	Wang et al. [17]	FFS	IRI	Linear regression model
5	Yu and Lu [18]	Average speed	IRI	Linear regression model
6	Chandra et al. [2]	Speed	IRI	Linear regression model
7	Ghuzlan et al. [5]	Std. speed, FFS	PCI, IRI	Linear regression model
8	Sekhar et al. [15]	Speed	IRI	Linear regression model
9	Kalan et al. [8]	Operating speed	IRI	Exponential model
10	Kakara and Chowdhary [7]	Speed	IRI	Linear regression model

Fig. 1 Flowchart of the methodology

and operating speed were collected and modelled with pavement roughness. Thirteen study locations were selected in the Calicut district, where 200m long straight sections were chosen on each site. Images of a few study sites are given in Fig. 2, and the geometric details of study sites are given in Table 2.

Straight and level sections were selected to eliminate the impact of other geometric constraints such as curvature, speed hump, longitudinal gradient and intersections. Other hindrances, such as parking lots, bus-stop and service roads were also avoided during the selection of sites.

Mainly two types of data collection were carried out: traffic data and roughness data. The Infrared Traffic Logger (TIRTL) was used for traffic flow recording, which was carried out on working days from 6.00 am to 12.00 pm and under clear weather conditions to eliminate extraneous effects on traffic flow. It is a multifunctional traffic

Fig. 2 Images of study sites (a) Malaparamba and (b) NIELIT

Table 2 Geometric details of study site

Sl No.	Site	Carriageway Width [CW] (m)	Shoulder Width [SW] (m)
1	Manaserry	7.0	2.1
2	Dayapuram	5.0	1.8
3	NIELIT	7.2	1.4
4	Malayamma (Shiva temple)	5.0	1.0
5	Eranjikoth	6.2	0.65
6	Karanthur	7.2	1.7
7	Velliparamba	7.3	2.3
8	Peruvayal	7.2	2.1
9	Cheroopa	6.1	0.7
10	Vellalassery	5.6	1.1
11	Malaparamba	9.6	1.7
12	Karuthaparamba	5.65	1.6
13	KMCT Engg. College Road	5.5	1.0

sensor that can function as a traffic counter, speed sensor, heavy vehicle tracker, over-height vehicle sensor, rail crossing sensor and network management system. The data extracted from TIRTL is in Excel format, which can be directly used for analysis.

For roughness data collection, 600 m level and straight sections were selected and equally divided into 200 m sections, as shown in Fig. 3. The central 200 m section represents the study stretch, where the prior and after 200 m sections were considered to ensure no drastic change in pavement surface condition before and after the study section, which may affect traffic flow parameters. If the roughness of the preceding or succeeding sections is less compared to the mid-section, then vehicles

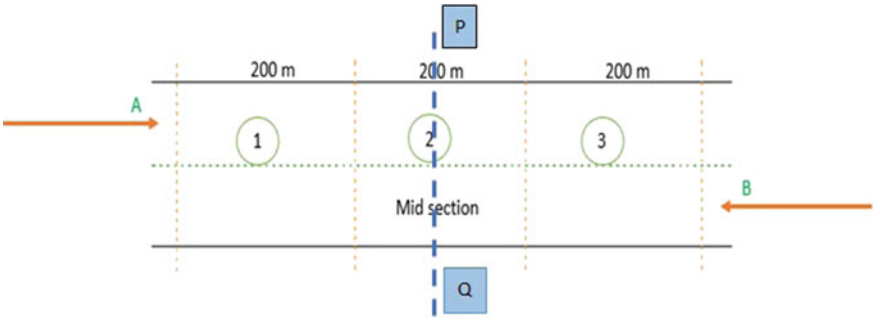

Fig. 3 The layout of the study section

will be entering the mid section at high speed. Due to this high variation in pavement roughness, these drivers may traverse the section at a higher speed than they should generally adopt. If roughness is more, vehicles will be entering the mid section at a lower speed.

The roughness survey was performed using MERLIN (Machine for Evaluating Roughness using Low-cost Instrumentation) on all three sections in both A and B directions shown in Fig. 3. A cumulative value of pavement roughness is obtained by moving MERLIN along the wheel path of the road. IRI is calculated using the MERLIN dispersion (D) value based on the Cundill [4] equation given below.

$$\text{IRI} = 0.593 + 0.0471\text{D} \tag{4}$$

where

IRI = International Roughness Index in m/km.

D = Dispersed width of central 90% histogram from MERLIN chart in mm.

The IRI values of pavement in both directions are calculated using Eq. 4 and the IRI values of mid-section are given in Table 3.

The sites with IRI less than 3 m/km are found to have very good condition. Most of the roads considered come under the hypothesis of good condition. When IRI is greater than 6 m/km, the roads are more deteriorated, having distresses with high severity.

4 Data Analysis

The details obtained from TIRTL in spreadsheet format were used to calculate the FFS of different classes of vehicles with minimum lead and lag headway of 8 seconds and 5 seconds, respectively. The remaining data was considered as peak hour flow. Different classes of vehicles, such as two-wheelers (2W), three-wheelers (3W), cars,

Table 3 IRI values of study sites

Sl no.	Location	IRI		Average
		Direction A	Direction B	
1	Manaserry	2.21	1.98	2.1
2	Dayapuram	6.89	8.01	7.45
3	NIELIT	2.62	2.1	2.36
4	Malayamma (Shiva temple)	10.72	7.78	9.25
5	Eranjikoth	2.44	2.65	2.55
6	Karanthur	1.93	1.96	1.95
7	Velliparamba	2.42	2.34	2.38
8	Peruvayal	2.3	2.85	2.58
9	Cheroopa	4.07	4.28	4.18
10	Vellalassery	6.88	7.19	7.04
11	Malaparamba	4.05	4.13	4.09
12	Karuthaparamba	2.95	3.97	3.46
13	KMCT Engg. College Road	7.38	9.71	8.55

Light Commercial Vehicles (LCV), Small Commercial Vehicles (SCV), Medium Commercial Vehicles (MCV) and Heavy Commercial Vehicles (HCV), are considered. The observed speeds under free-flow and peak hour conditions were plotted as a cumulative percent frequency distribution curve to find each study section's 98^{th} percentile of FFS and PHS.

Consistency in the roughness of 600 m selected study stretches is examined using the IRI of Sects. 1, 2 (mid-section) and 3 (200 m each). It has been observed that if the highly uneven surface is lying before the mid-section, the speed of vehicles will reduce in the prior section, and the actual dependence of traffic speed on the study section distresses (or roughness) could not be projected. Similar difficulties arise when the preceding section is very smooth compared to the mid-section. ANOVA is performed to identify the difference in the roughness over the different sections. The outcome is provided in Table 4, which demonstrates no appreciable variation among the IRI of Sects. 1, 2 and 3.

Similarly, the difference in IRI values of the two directions of the roads were also analysed. If there is a significant difference, then the driver will try to move on a relatively smoother surface for better ride quality. This phenomenon will cause

Table 4 Results of ANOVA for different sections

Source of variation	SS	df	MS	F	P-value	F crit
IRI in different sections	13.647	2	6.823	0.738	0.485	3.259
Within groups	332.754	36	9.243	–	–	–
Total	346.401	38	–	–	–	–

hindrance to the traffic running on the road due to unnecessary vehicle-vehicle interaction. The results presented in Table 5 show that there is no statistically significant difference between IRI values in the two directions.

Correlation analysis was done for different categories of vehicles to identify the relation between the speed of each class of vehicles and IRI, which is given in Table 6.

FFS of all classes of vehicles were found to be depending on IRI as well as CW. At the same time, the FFS of most of the vehicle classes is independent of SW. Correlation analysis results of PHS of different class vehicles are given in Table 7.

Different transformed forms of IRI were considered, such as IRI, ln(IRI), IRI^2 and e^{IRI}, among which ln(IRI) is found to have significantly substantial correlation coefficient with PHS of different classes of vehicles. The CW affects the speed of

Table 5 Results of ANOVA for both directions

Source of variation	SS	df	MS	F	P-value	F crit
IRI in the lanes A and B	0.168	1	0.168	0.023	0.881	4.260
Within Groups	177.018	24	7.376	–	–	–
Total	177.186	25	–	–	–	–

Table 6 Correlation matrix for free flow speed

	FFS ALL	FFS 2W	FFS 3W	FFS CAR	FFS LCV	FFS SCV	FFS MCV	FFS HCV	AVG IRI	CW	SW
FFS ALL	1.00	–	–	–	–	–	–	–	–	–	–
FFS 2W	0.91	1.00	–	–	–	–	–	–	–	–	–
FFS 3W	0.55	0.52	1.00	–	–	–	–	–	–	–	–
FFS CAR	0.96	0.77	0.53	1.00	–	–	–	–	–	–	–
FFS LCV	0.92	0.92	0.58	0.85	1.00	–	–	–	–	–	–
FFS SCV	0.77	0.75	0.77	0.73	0.79	1.00	–	–	–	–	–
FFS MCV	0.76	0.88	0.65	0.66	0.89	0.73	1.00	–	–	–	–
FFS HCV	0.64	0.55	0.65	0.68	0.79	0.61	0.73	1.00	–	–	–
AVG IRI	−0.80	−0.74	−0.62	−0.79	−0.76	−0.80	−0.70	−0.66	1.00	–	–
CW	0.63	0.61	0.53	0.63	0.70	0.74	0.61	0.69	−0.62	1.00	–
SW	0.23	0.18	0.62	0.31	0.35	0.60	0.48	0.48	−0.43	0.45	1.00

Table 7 Correlation matrix for peak hour speed

	PHS ALL	PHS 2W	PHS 3W	PHS CAR	PHS LCV	PHS SCV	PHS MCV	PHS HCV	ln (AVG IRI)	CW	SW	% CV
PHS ALL	1.00	–	–	–	–	–	–	–	–	–	–	–
PHS 2W	0.89	1.00	–	–	–	–	–	–	–	–	–	–
PHS 3W	0.51	0.57	1.00	–	–	–	–	–	–	–	–	–
PHS CAR	0.98	0.84	0.48	1.00	–	–	–	–	–	–	–	–
PHS LCV	0.87	0.80	0.64	0.87	1.00	–	–	–	–	–	–	–
PHS SCV	0.68	0.73	0.71	0.70	0.71	1.00	–	–	–	–	–	–
PHS MCV	0.59	0.62	0.36	0.62	0.78	0.47	1.00	–	–	–	–	–
PHS HCV	0.55	0.34	0.53	0.63	0.65	0.45	0.58	1.00	–	–	–	–
ln(AVG IRI)	−0.68	−0.57	−0.51	−0.68	−0.72	−0.63	−0.66	−0.67	1.00	–	–	–
CW	0.62	0.65	0.56	0.64	0.53	0.52	0.62	0.71	−0.55	1.00	–	–
SW	0.23	0.18	0.62	0.31	0.35	0.60	0.48	0.48	−0.43	0.45	1.00	–
% CV	−0.30	−0.52	−0.33	−0.32	−0.20	−0.49	−0.05	0.10	−0.01	−0.28	−0.22	1.00

Table 8 Regression models for Free Flow Speed

Vehicle category	Regression equation	R^2	Adjusted R^2	F
ALL	$FFS_{ALL} = 61.52 - 1.71 \times IRI + 1.2 \times CW$	0.67	0.60	9.97
2W	$FFS_{2W} = 57.94 - 1.52 \times IRI + 1.29 \times CW$	0.579	0.495	6.87
3W	$FFS_{3W} = 47.01 - 1.08 \times IRI + 1.04 \times CW$	0.420	0.305	3.63
Car	$FFS_{Car} = 62.89 - 1.59 \times IRI + 1.16 \times CW$	0.647	0.577	9.18
LCV	$FFS_{LCV} = 45.02 - 2.25 \times IRI + 3.30 \times CW$	0.670	0.604	10.14
SCV	$FFS_{SCV} = 39.43 - 2.12 \times IRI + 3.09 \times CW$	0.741	0.689	14.29
MCV	$FFS_{MCV} = 27.23 - 1.44 \times IRI + 4.68 \times CW$	0.562	0.464	5.76
HCV	$FFS_{HCV} = 22.98 - 0.44 \times IRI + 4.07 \times CW$	0.275	0.034	1.14

vehicles, but SW and the percentage of commercial vehicles (% CV) will not have any impact on PHS.

4.1 Effect of Pavement Roughness on FFS

For all classes of vehicles, the significant variables influencing FFS were identified as IRI and Carriageway Width (CW). Using data from thirteen sites, models were developed, which are given in Table 8.

The models reliability are statistically supported by high R^2 and F-values for each type of vehicles, except for HCV. Therefore, all the FFS prediction models, except the model for HCV, can be used to determine the impact of roughness on FFS. The negative sign of IRI indicates that as the IRI increases, speed decreases. For example, one unit change in IRI can cause a 1.59 km/h reduction in the speed of the car. The speed of 3Ws are the least affected by roughness, whereas speed of LCVs are the most affected class of vehicles.

4.2 Effect of Pavement Roughness on Peak Hour Speed

In the peak hour condition, CW and IRI significantly impact PHS. Among different transformed variables, ln(IRI) is highly related to PHS, and the developed models are given in Table 9.

Table 9 Regression models for peak hour speed

Vehicle category	Regression equation	R^2	Adjusted R^2	F
ALL	$PHS_{ALL} = 54.25 - 6.21 \times \ln(IRI) + 1.907 \times CW$	0.55	0.454	5.51
2W	$PHS_{2W} = 45.79 - 3.41 \times \ln(IRI) + 2.36 \times CW$	0.50	0.375	4.31
3W	$PHS_{3W} = 38.05 - 2.75 \times \ln(IRI) + 1.65 \times CW$	0.615	0.526	2.69
Car	$PHS_{Car} = 53.75 - 6.14 \times \ln(IRI) + 2.14 \times CW$	0.562	0.464	5.77
LCV	$PHS_{LCV} = 57.28 - 10.31 \times \ln(IRI) + 1.42 \times CW$	0.54	0.534	5.29
SCV	$PHS_{SCV} = 47.44 - 6.18 \times \ln(IRI) + 1.35 \times CW$	0.628	0.534	3.523
MCV	$PHS_{MCV} = 30.79 - 14.71 \times \ln(IRI) + 4.95 \times CW$	0.521	0.416	4.912
HCV	$PHS_{HCV} = 31.37 - 2.63 \times \ln(IRI) + 1.64 \times CW$	0.544	0.418	2.78

Among different types of vehicles, speed of HCVs are the least affected by roughness, whereas speed of MCVs are the most affected. Researchers has given little consideration about this variation for the impact of roughness study among different commercial vehicle categories in the past. Conclusion from the modeling depict that it will be benificial to explore this findings further.

5 Summary and Conclusion

The current study shows the impact of pavement surface roughness on the free flow speed and peak hour speed of different classes of vehicles. Data from various parts of two-lane, two-way undivided roadways across thirteen sites in Calicut are analysed. From the results of the study, pavement surface roughness is found to have a considerable impact on the 98th percentile of FFS and PHS along with carriageway width, but shoulder width and percentage of commercial vehicles do not have any effect on speed.

An increase in roughness has a different impact on different classes of vehicles. FFS is linearly related to IRI, and a logarithmic relationship is observed between PHS and IRI. One unit increase in IRI will result in only a 1 km/h reduction in the FFS of 3Ws, but in the case of LCVs, a speed reduction of 2.25 km/h is observed for a unit increase in IRI. The least affected class of vehicles in both free flow and peak hour conditions are 3W and HCVs. As the radius of the tyre is very large in the case of HCVs, the roughness-induced vibrations are not well pronounced. This confirms the results obtained by Chandra [3]. But the speed of small, light and medium commercial

vehicles is more affected by roughness compared to other classes. Considering the results of this study, it is recommended that different commercial vehicle categories be considered separately in FFS and PHS prediction models.

This study is limited to two-lane, two-way undivided non-urbanised roads, where further studies can be carried out on the other categories of roads.

References

1. Abeygunawardhana C, Sandamal RMK, Pasindu HR (2020) Identification of the Impact on Road Roughness on Speed Patterns for Different Roadway Segments. *Moratuwa Engineering Research Conference (MERcon) 2020,* DOI: https://doi.org/10.1109/MERCon50084.2020.9185387
2. Chandra S, Sekhar CR, Bhatti AK, Kangadurai B (2013) Relationship between pavement roughness and distress parameters for Indian highways. J Transp Eng 139(5):467–475
3. Chandra S (2004) Effect of road roughness on capacity of two-lane roads. J Transp Eng 130(3):360–364
4. Cundill MA (1991) The MERLIN low-cost road roughness measuring machine. *Transport Research Laboratory*
5. Ghuzlan KA, Al-Omari BH, Mahmoud MA (2015) Effect of Pavement Condition on Multilane Highway Free Flow Speed. Inst Transp Engineers ITE J 85(8):31
6. Indo HCM (2017) Indian Highway Capacity Manual. Council of Scientific & Industrial Research (CSIR). India
7. Kakara S, Chowdary V (2020) Effect of pavement roughness and transverse slope on the magnitude of wheel loads. Arab J Sci Eng 45(5):4405–4418
8. Kalan O, Ozbay K, Kurkcu A, Gao J, Desai V, Joshi D (2020) Network-wide life cycle cost analysis that takes into account the effect of road roughness on road capacity. Transportation
9. Karan MA, Haas R, Kher R (1976) Effects of pavement roughness on vehicle speeds. Transp Res Rec 602:122–127
10. Kawamura A, Tomiyama K, Rossi R, Gastaldi M, Mulatti C (2017) Driving on rough surface requires care and attention. Transp Res Procedia 22:392–398
11. Louhghalam A, Akbarian M, Ulm F-J (2016) Carbon management of infrastructure performance: integrated big data analytics and pavement-vehicle-interactions. J Clean Prod 142:956–964
12. Madhu E, Senathipathi V, Ravinder K, Nataraju J (2011) Development of free speed equations for assessment of road user cost on high speed multi-lane carriageways of India. Curr Sci 100(9):1362–1372
13. Mate VP, Hon P (2020) To study impact of road roughness on free flow speed of vehicle. Aegaeum J 8(6):373–379
14. Popoola MO, Apampa OA, Adekitan O (2020) Impact of pavement roughness on traffic safety under heterogeneous traffic conditions. Niger J Technol Dev 17(1):13–19
15. Sekhar ChR, Nataraju J, Velmurugan S, Kumar P, Sitaramanjaneyulu K (2016) Free flow speed analysis of two-lane inter urban highways. Transp Res Proceedia 17:664–673
16. Setyawan A, Kusdiantoro I, Syafi I (2015) The effect of pavement condition on vehicle speeds and motor vehicles emissions. Proceedia Eng 125:424–430
17. Wang T, Harvey J, Lea JD, Kim C (2013) Impact of pavement roughness on vehicle free-flow speed. J Transp Eng 140(9)
18. Yu B, Lu Q (2014) Empirical model of roughness effect on vehicle speed. Int J Pavement Eng 15(4):345–351

DSRC-Based Bus Trajectory Analysis and Prediction Near Signalized Intersection

Aswathi Chandrahasan, Aayush Jain, and Lelitha Vanajakshi

Abstract The current study aims to identify all possible factors influencing bus travel time near signalized intersections and predict the arrival time to stop line under the heterogeneous and lane free traffic conditions. Preliminary analysis of the bus trajectories grouped them based on uniform and non-uniform movement and whether the bus stopped or not. The prediction model is formulated considering all possible events in which a bus can get detected near an intersection, especially when the bus arrival is during the later green and early red phases. The algorithm is developed integrating the bus, traffic, and control information. Implementation and evaluation of the models developed has been carried out to understand their performance under varying conditions. Bus information is collected using the DSRC (dedication short range communication) devices. Results showed very good prediction performance with the errors reducing as the bus approached the stop line. The findings of this study can be used to predict the arrival time of the bus at the stop line, which can further be used for various applications including bus signal priority.

Keywords Bus arrival time prediction · Trajectory analysis · Signalized intersection

1 Introduction

Severe traffic congestion has become a major challenge to tackle by transportation agencies all over the world. Cities have been witnessing significant developments in the field of transportation as a consequence of rapidly growing economy, increasing levels of vehicle ownership and high expectations for superior infrastructure and services. These are more challenging in developing countries like India where uncontrolled growth of vehicle population, relatively slow infrastructure growth, and rampant encroachment of carriageway are leading to traffic snarls on a daily

A. Chandrahasan · A. Jain · L. Vanajakshi (✉)
Department of Civil Engineering, Indian Institute of Technology, Madras, India
e-mail: lelitha@civil.iitm.ac.in

A. Dhamaniya et al. (eds.), *Recent Advances in Traffic Engineering*, Lecture Notes in Civil Engineering 377, https://doi.org/10.1007/978-981-99-4464-4_8

basis. One way to address this inefficient and inadequate system is to improve the public transport system in an effective and sustainable way.

One of the major drawbacks of the public transport bus service is its unreliability. Buses face maximum delay in urban arterials near signalized intersections. Thus, if bus delay at intersections can be reduced, more people may shift to public transport from personal vehicles. This in turn will help to reduce traffic congestion because of the high occupancy of the buses than personal vehicles. Bus Signal Priority (BSP) system helps to achieve the same by detecting a bus as it approaches the intersection and providing green time to that approach so that the bus can pass the intersection without much delay. The reliability of bus services can be improved if such a BSP system is implemented accurately. This would be a more desirable and sustainable strategy than the infrastructure expansion to meet rapid traffic growth needs.

For the successful performance of the BSP system, a better understanding of the behavior of buses near intersections and in turn an accurate bus arrival time prediction to the stop line is crucial. This will help to decide how much the present green phase is to be prolonged or the current red phase is to be truncated. The present study focuses on these two aspects of understanding the behavior of bus near intersection and quick and reliable prediction of its arrival to the stop line. One major requirement for these is high-resolution, real-time data collection. The common sensors used for this purpose include intrusive sensors such as inductive loops [7], magnetometers [23], piezoelectric sensors [7], pneumatic tubes [9] and non-intrusive sensors like video cameras [3], microwave radar [6], LiDAR (Light detection and ranging) [16], ultrasonic [12], and hybrid sensor technologies [17]. Intrusive sensors are installed beneath the road surface and hence invasive to the pavement. Location-specific non-intrusive sensors though useful to detect the presence, speed, type of vehicle, lane crossing, etc., are expensive and their performance gets affected by traffic and climatic conditions. On the other hand, onboard tracking solutions like global positioning systems (GPS) help to determine the exact location of a vehicle and are more efficient under heterogeneous and less lane disciplined traffic conditions such as the one in India. A detailed literature review of data collection, data analysis, and prediction near signalized intersections is conducted to understand the gaps in this area of research.

2 Literature Review

Bus arrival time can be predicted either for a midblock section or near intersections. The studies on the prediction of bus travel time for midblock sections, especially to the next bus stop reported the use of different prediction methods such as time series analysis [4], ANN technique [11], SVR technique [21], Kalman filtering technique [20].

Most of these studies were developed for the purpose of prediction to bus stops. However, for the BSP application, the requirements are different with the prediction focusing on a small stretch of roadway near to the intersection, at high resolution,

where the stochasticity is more. This means that the space span of prediction is shorter and prediction accuracy must be stricter for the same [8].

Lee et al. [13] reported a more advanced method of bus signal priority control which consisted of two parts: a high-performance online microscopic simulation model for prediction of transit travel time up to the stop line using sensor data and a priority operation model to select the best priority strategy based on the prediction results. Another related research work was reported by Tan et al. [19] using both historical and adaptive model. Automatic Vehicle Location (AVL) data and wheel speed data were taken as inputs for this study. However, this method was reported to be not suitable for heavily congested traffic.

Ekeila et al. [5] used AVL systems which are mostly installed on many transit buses for the dynamic BSP strategy. Li et al. [15] reported a predictive BSP control that predicted the arrival time of the bus until the stop line of the subject intersection by detecting the transit vehicles upstream (e.g., immediate upstream intersection of the subject intersection). Bie et al. [2] developed an analytical model using the traffic flow and time headway-based equations based on the field data. Yu et al. [22] presented an estimation algorithm based on the equations of motion for the arrival time prediction of buses to the stop line. Gang et al. [8] proposed a deep learning-based model for bus travel time prediction to the stop line. They presented a stacked auto-encoder (SAE) neural network, which is a pre-training model and included logistic regression model as the predictor. The limitation of this study is that the experimental data used was created through traffic simulations rather than being gathered in the actual world.

There are various factors which affect arrival time prediction namely, spatial and temporal factors, conditions of traffic, driving behavior, and vehicle characteristics. Travel time is correlated with characteristics of the route such as road segment, road/route length, intersections, bus stops near the intersection and turning movements. The main temporal factors considered for arrival time prediction for BSP include dwell time and intersection delay. Prediction accuracy can be enhanced by improving the dwell time and intersection delay estimates [1]. Yu et al. [22] considered bus dwell time for the estimation of arrival time. Analytical models were developed by Bie et al. [2] for the estimation of arrival time of bus up to the stop line, taking into account the bus delay at the intersection. However, the model needed detailed speed and signal settings data. For the prediction of arrival time, the average delay at intersection has also been calculated in some studies [9]. However, intersection delay modeling by an average value can sometime reduce the accuracy of bus travel time prediction models.

Traffic information such as speed, flow, density, and queue length has a direct impact on arrival time prediction. Studies based on historical data used constant average speed [9]. Adaptive average speed based on real time data was used by Yu et al. [22]. Only a few studies have considered arrival rate, discharge headway, and signal timing details for the arrival time prediction to the stop line [2].

Driving and vehicle characteristics can also contribute to variation in arrival time. Lee et al. [13] presented an arrival time prediction model which incorporated driving characteristics (i.e., aggression level) and behavior of the adjacent vehicle

(lane changing and queuing at the stop line). Based on these factors, the prediction model included a set of driving rules (initialization rules, free-flow driving rules, car-following rules, lane changing rules, traffic signal reaction rules, and transit vehicle rules) using real-time traffic count and transit location information.

It can be observed that most of the above studies on bus arrival time prediction for implementation of BSP are based on traffic conditions in western countries and these studies cannot be directly implemented in India where lane discipline is not followed and too many vehicle types are sharing the road space. Hence, a research study on arrival time prediction to stop line near signalized intersection under mixed traffic conditions is needed for a successful BSP implementation under the heterogeneous and lane less traffic conditions.

3 Study Site, Data Collection, and Preliminary Analysis

3.1 Study Site

The study area selected is Tidel Park junction connecting Rajiv Gandhi IT expressway and East coast road (Fig. 1a). This is one of the nine major intersections in Rajiv Gandhi Road which is a busy arterial road in Chennai. IT-enabled service companies, industrial estates, educational institutions, and residential developments are located around this roadway. There is also a local railway line that runs parallel to this road section.

The Tidel Park intersection is a four legged one with Madhya Kailash to the north at a distance of 2.2 km, East Coast Road (ECR) to the east at a distance of 1 km, SRP tools to the south at a distance of 1.5 km and Tidel park service road to the west at a distance of 0.6 km. Since Tidel park service road is a free left road, this intersection can be taken as three legged. A six-lane roadway is in the north–south direction with three lanes in each direction having a width of 3.5 m/lane. The east bound ECR

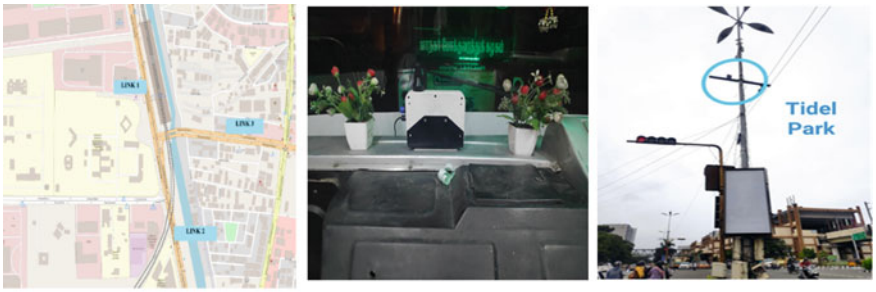

Fig. 1 **a** Study Area (*Source* https://www.openstreetmap.org/), **b** OBU installed in Bus **c** RSU installed on signal pole

approach is a four-lane divided carriageway. The traffic volume was observed to be around 4000 veh/hr for north bound, 3800 veh/hr for south bound, 1200 veh/hr for west bound, and 100 veh/hr for east bound.

3.2 Data Collection

Continuous information on position, speed, direction and acceleration and deceleration characteristics of buses are required for the successful implementation of BSP. This high-resolution data was guaranteed by using Dedicated Short Range Communications (DSRC) based devices. DSRC devices include On-Board Units (OBU), which communicates with Road Side Units (RSU) fixed at the intersection, when they are in the line of sight. Along with bus information, traffic and signal information are concurrently collected from video recordings.

Bus Data. For the present study, DSRC devices were used for bus detection and tracking near the intersection. The RSU is fixed at Tidel Park signal and OBUs were fixed in seven buses of route number 19 that are crossing this intersection, with OBU IDs 21, 22, 23, 25, 26, 27, and 28. When OBU installed bus comes in the vicinity (roughly around 300 m) of the RSU location, the OBU starts sending data packets to RSU and the RSU, in turn, would send that information to the server. Figure 1b&c shows OBU device installed inside a bus and the RSU that is installed at Tidel Park signal.

Data collected for five days—08/02/2022, 09/02/2022, 10/02/2022, 11/02/2022, and 14/02/2022 was used. Table 1 shows the details of the DSRC data collection period and number of trips made on each day.

Continuous information on speed, position, acceleration, or deceleration of buses was communicated till the bus leaves the intersection area. The type of movement (turning or straight) and route of each bus was obtained based on the changes observed in latitude and longitude values.

Signal and traffic data. Manual data collection using video recordings was done for signal timing details, arrival rate, and saturation discharge headway. For the proposed study, two video cameras were installed. One camera was placed facing the signal head along with vehicles crossing the stop line, to collect the signal timing details and saturation headway. Another one was installed facing the arriving vehicles

Table 1 DSRC data details

Date	DSRC Data Collection Period	No. of trips made by buses
08-02-2022	5 am to 8 pm	29
09-02-2022	6 am to 10 pm	25
10-02-2022	5.30 am to 11 pm	31
11-02-2022	5 am to 9.30 pm	36
14-02-2022	6 am to 9.30 pm	24

about 250–300 m away from signal, to collect the arrival rate of vehicles. These manually collected traffic counts were converted into Passenger Car Unit (PCU) using PCU factors suggested in IRC 106 [10].

3.3 Data Cleaning and Preliminary Analysis

Duplicate values were removed from raw data as part of data cleaning. After that, check for outliers was done on the basis of speed thresholds, i.e., speed cannot be less than zero km/h and the upper threshold was taken as the 95th percentile speed.

Next level data cleaning was done using Quantum Geographic Information System (QGIS) software. By importing latitude and longitude values into QGIS, a dynamic display of bus position was created. By analyzing the routes of buses in QGIS software, the trips which do not pass through the study area were identified. Such trips were removed, and remaining trips were selected for the bus arrival time prediction to the stop line. Table 2 shows the details of the final data set used.

As part of the preliminary analysis, using the information of continuous positions of buses with timestamp, bus trajectories were created. Then trajectories of each bus were plotted in tableau software. The trajectories were found to be falling into the following two groups: Uniform trajectories, and non-uniform trajectories with/without stopping.

Figure 2 shows sample trajectories falling under these groups. Prediction was done separately for each of these groups.

Table 2 Final data set

Description	Date of data collection				
	08/02/2022	09/02/2022	10/02/2022	11/02/2022	14/02/2022
Total number of trips after preliminary data cleaning	29	25	31	36	24
Number of trips available in signal video data	17	20	21	19	13
Number of trips which shows error in QGIS	5	7	8	3	3
Remaining number of trips for implementation	12	13	13	16	10
Number of trips from Madhya Kailash	1	2	1	4	3
Number of trips from Thiruvanmiyur	1	0	0	1	1
Number of trips from SRP Tools	10	11	12	11	6

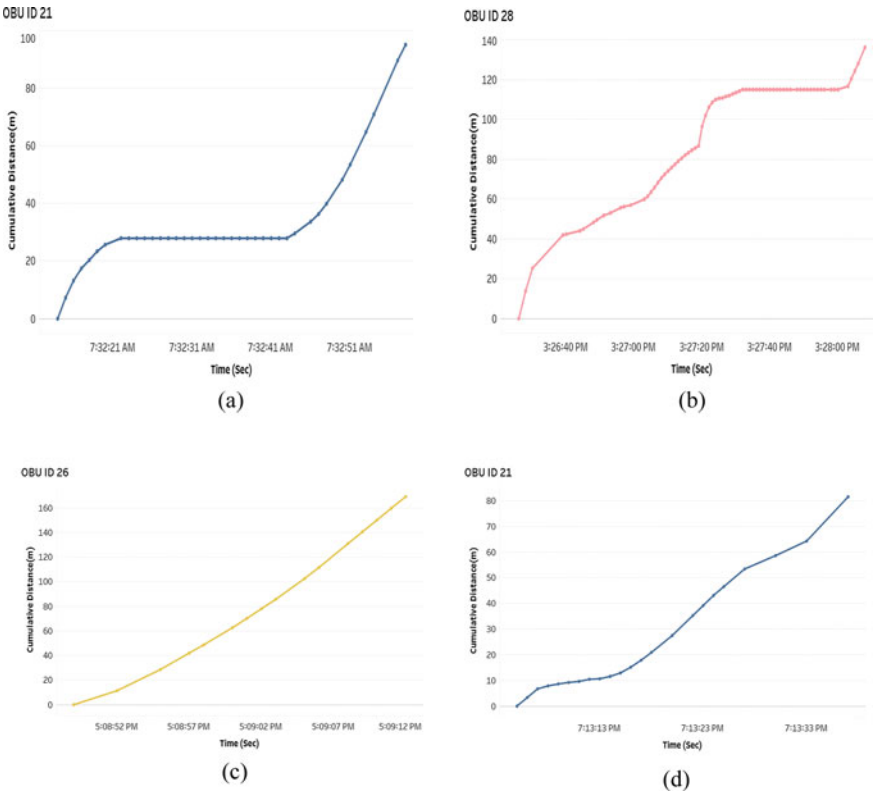

Fig. 2 Sample trajectories of the identified groups **a** Uniform trajectory with stopping, **b** Non-uniform trajectory with stopping, **c** Uniform trajectory without stopping, **d** Non-uniform trajectory without stopping

4 Bus Travel Time Prediction Model

The prediction model assumes that the intersection is under-saturated such that queuing vehicles clear within the cycle without any residual queue. The model splits the travel time into three parts from the advanced detection position to stop line, as travel time from detection point to the end of queue, waiting time in the queue, and time for discharging of queued vehicles in front of the bus. A model proposed in Bie et al. [2] was used as the base model for the present study. An advantage of this model is that it takes into account all possible outcomes, especially when the bus arrives in the later green light and early red-light stages. Modifications were made to this base model to take into account the heterogeneous traffic conditions and the lane free movement in the study area.

4.1 Model Formulation

Suppose the signal has n phases and current green phase is k. Let the bus placing the priority request is on phase j. Let G denotes green time, Y denotes yellow time, and R denotes red time. Based on the signal operating status when a bus is detected, the model is classified into different categories as discussed below.

Priority phase as current green phase ($k = j$). In this category, when the bus is detected first, phase j is having green time or in other words, the bus is detected during the green signal. The main concern in this situation is whether the bus can arrive at the stop line before the end of current green signal. If bus can reach stop line within available residual green time, bus need not make a stop and anterior queue length determines its arrival time to stop line. If it cannot reach within the given residual green time, it needs to make a stop and wait for green signal in the next cycle. Free-flow travel time from the current position to the stop line determined as in Eq. (1) can be used to check whether the given residual green time is sufficient to cross.

$$T_f = \frac{D}{V_f}, \tag{1}$$

where D = Distance between the current location of the bus and stop line in m, and V_f = Free-flow speed in m/s. This V_f is taken as 95th percentile speed of buses in that link.

When free-flow travel time is more than residual green time ($Tf > Gr$), bus cannot pass the stop line in the current cycle. For this case, bus arrival time T from the current position to the stop line, including waiting time for green in next cycle and anterior queue length to discharge, can be obtained as shown in Eq. (2).

$$T = G_r + Y + \overline{R_c} + R_n + N\bar{t} + \varphi, \tag{2}$$

where T = Predicted arrival time of the bus in seconds;

Gr = Residual green time of phase j in seconds;

Y = Yellow time of phase j in seconds;

$\overline{R_c}$ = Red time in current cycle after detection point in seconds;

Rn = Red time in next cycle before start of green time in seconds;

$\bar{t}$ = Saturation discharge headway in seconds per PCU;

φ = Time interval between front end of the bus and rear end of adjacent anterior vehicle in seconds (it is nearly a constant number when vehicles are discharging at saturation flow rate and can be obtained by field survey);

N = Queue length in front of the bus up to the stop line.

Since no residual queue is left at the end of each cycle and vehicles at the intersection arrive randomly, N can be expressed as

$$N = \left(T_f - G_r\right)q, \tag{3}$$

where q is the average vehicle arrival rate of phase j in PCU/second, and $(Tf - Gr)$ is elapsed red time of phase j in seconds.

When free-flow travel time is less than residual green time ($Tf \leq Gr$), bus need not stop before reaching the stop line since sufficient residual green time is available. The key issue for this case is whether the bus can move forward without being hampered by the queue length. Intuitively, if the queue is short, the bus can arrive at the stop line freely. Otherwise, it has to alter its speed. Therefore, it is necessary to determine the critical number of anterior vehicles that could affect the bus. However, for the bus to arrive at the stop line freely, the number of anterior queue vehicles should be such that.

$$N_c = \frac{T_f}{\bar{t}}, \tag{4}$$

where Nc = critical number of queue vehicles in front of the bus,

Tf = free-flow travel time from the current position to the stop line in seconds and $\bar{t}$ = saturation discharge headway in Seconds/PCU.

Since the bus is coming during the green time, vehicles in front of it are discharging. Hence, actual anterior queue length up to the stop line can be calculated as

$$N = \left[R_p + R_c^{'} + G_e\right]q - \left[\frac{G_e}{\bar{t}}\right], \tag{5}$$

where R_p = Red time in the previous cycle after end of green time in seconds;

R'_c = Red time in the current cycle before detection in seconds;

G_e = Elapsed green time in the current cycle in seconds.

The number of vehicles that arrived since red light of phase j started is the first term of the Eq. (5) and the second term is the number of vehicles that have been released since the green light started. To avoid negative N, the above equation can be modified as.

$$N = \max\{\left[R_p + R_c^{'} + G_e\right]q - \left[\frac{G_e}{\bar{t}}\right], 0\}. \tag{6}$$

If $N \leq Nc$, the bus arrival time $T = Tf$. Otherwise, arrival time will be affected by queue length and arrival time can be updated as

$$T = N\bar{t} + \varphi. \tag{7}$$

Priority phase as red phase ($k \neq j$). In this case, phase j has red time when the bus places a priority request or in other words, bus is detected during the red indication. Since the signal is not a fixed time one, the timings in adjacent cycles are different making the waiting time for the green varying. If bus is placing a priority request after the green time of phase j in the current cycle, it needs to wait for the green signal in the next cycle. However, if bus is placing priority request before the green time of phase *j* in current cycle, it can wait for its right of way in the current cycle itself. It can be noted that the waiting time for the latter case will be less compared to the former.

Priority phase before the current green phase ($k > j$). In this case, the green time of phase *j* has ended in the current cycle and bus needs to wait for the green in the next cycle. Since bus is coming during the red time, there will be two types of vehicles in front of the bus—vehicles which already formed the queue during the red time and vehicles which are moving in front of the bus to join the end of queue. Out of these, the number of vehicles in front of the bus which already formed the queue during the elapsed red time can be calculated as.

$$N_1 = R_e q, \tag{8}$$

where R_e = Elapsed red time in seconds.

Travel time needed from current bus location to the end of this queue is.

$$T_f^{'} = \frac{D - (N_1 \times \overline{L})}{V_f}, \tag{9}$$

where $\overline{L}$ = average vehicle length in meters. During this time interval, vehicles will be moving in front of the bus to join the end of queue. Number of such vehicles will be

$$N_2 = T_f' q. \tag{10}$$

Thus, the total number of vehicles in queue in front of the bus will be

$$N = N_1 + N_2 = \mathrm{Re} \cdot q + \left(\frac{D - (\mathrm{Re} \times q \times \overline{L})}{V_f} \right) q. \tag{11}$$

Sometimes, the second term in Eq. (11) can be negative and in such cases, it may indicate that bus made a lane change. In such cases when $D < (R_e q \overline{L})$, the anterior queue length is updated as shown in Eq. (12).

$$N = \left(\frac{D}{V_f} \right) q = T_f q. \tag{12}$$

Finally, the time for bus to reach stop line is

$$T = \overline{R}c + R_n + N\bar{t} + \varphi, \tag{13}$$

where R_n = Red time in the next cycle before the starting of green.

Priority phase after the current green phase ($k < j$). In this case, green time of phase j has not started in the current cycle and the bus has to wait for its right of way in the current cycle itself.

Queue length calculation in this case is similar to that of case $k > j$. The number of vehicles which already formed queue in front of the bus is

$$N_1 = \left(R_p + R_e\right)q, \tag{14}$$

where R_p = Red time in the previous cycle after the end of green time in seconds;

R_e = Elapsed red time seconds.

In this case, the bus travel time from the current position to the end of queue is calculated as in Eq. (9) and number of vehicles arriving to join the queue is calculated as in Eq. (10). Thus, the total number of vehicles in queue in front of the bus is

$$N = (R_P + R_e)q + \left(\frac{D - \left[\left(R_p + R_e\right) \times q \times \overline{L}\right]}{V_f}\right)q \tag{15}$$

Here also when $D < \left(\left(R_p + R_e\right)q\overline{L}\right)$, anterior queue length is updated as in Eq. (12).

Then, the time for bus to reach stop line can be obtained by substituting queue length value in.

$$T = \overline{R_c} + N\bar{t} + \varphi. \tag{16}$$

If queue length value obtained in any of the above-mentioned cases is closer to zero, the arrival time to stop line can be updated as T_f, irrespective of the signal in which the bus is detected.

The overall methodology for arrival time prediction model is given in Fig. 3.

5 Implementation and Evaluation

Evaluation of the model was done by comparing the actual arrival time, with the predicted arrival time at different distances from the stop line. Madhya Kailash to Tidel Park approach was selected for implementation and evaluation. The phase plan of the selected signal is shown in Fig. 4. Since the priority phase is the 3rd phase in the phase plan, case c (waiting time > threshold value) does not exist. Trajectories are classified into case a, b, and d by comparing bus detected time with actual signal time.

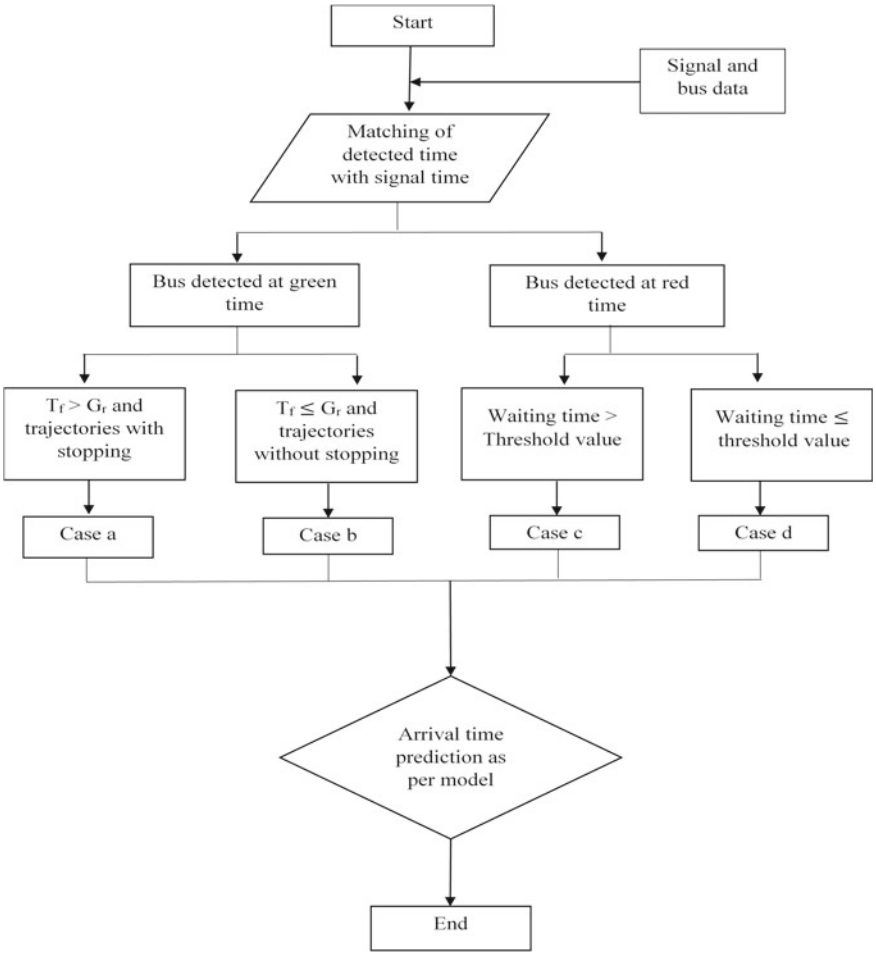

Fig. 3 Methodology for arrival time prediction model

Performance evaluation was done at 300, 250, 200, 150, and 100 m away from the stop line to see how prediction varies as the bus comes closer to the stop line. Thus, five detection points were there for each trajectory. From the detection time at mentioned distances and comparing it with signal time, bus trajectories were classified as per the model and 3.63% were found to fall in case a, 40% in case b and 56.36% in case *d*. As the bus is moving after the first detection, the signal status may change. Hence, the same trajectory may show different cases at different positions. Table 3 shows sample classification details of OBU 21 detected on 11/02/2022 at different distances from stop line. It can be seen that the status was *d* when the bus was first detected, which changed to b as it was traveling.

Performance of the developed analytical model was checked by observing the error between actual and predicted arrival times for each individual bus at 300 m,

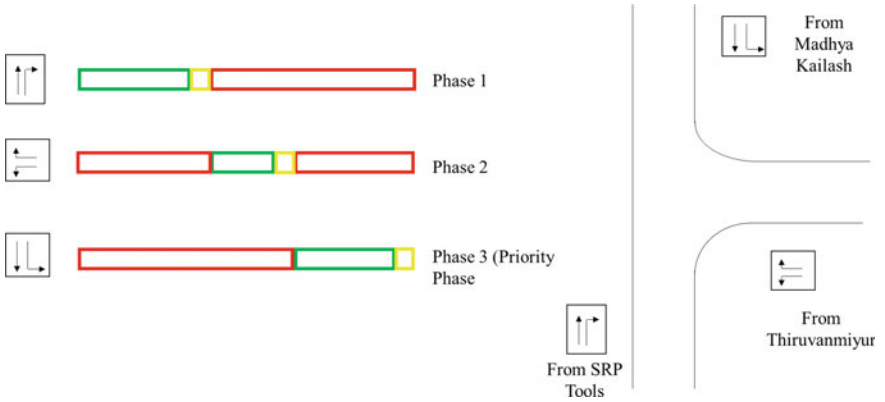

Fig. 4 Phase diagram for the study area

Table 3 Classification details of OBU 21 at different distances

Detected time	Distance from current position to stop line D (m)	Free-Flow speed V_f (m/s)	Free-flow travel time T_f (s)	Signal status at detected time	Residual green time G_r (s)	Category
10:52:22	300	15.06	19.92	Red	–	Case d
10:52:33	250	15.06	16.60	Green	66	Case b
10:52:40	200	15.06	13.28	Green	59	Case b
10:52:46	150	15.06	9.96	Green	53	Case b
10:52:55	100	15.06	6.64	Green	44	Case b

250 m, 200 m, 150 m, and 100 m away from stop line. Then the variation of this error with distance from the stop line (Fig. 5) was analyzed to understand the prediction accuracy.

Average errors were analyzed next by considering all *11* trajectories together at different distances from the stop line. Figure 6 shows average error values along with maximum and minimum error value observed for varying distances from the stop line. From Fig. 6, it can be observed that error value is decreasing as the distance from the stop line decreased.

Mean Absolute Error (MAE) and Mean Absolute Percentage Error (MAPE) were calculated to quantify the errors for all predictions from each category using Eqs. (17) and (18) respectively [18].

$$MAE = \frac{1}{n}\sum |x_o - x_p|, \tag{17}$$

$$MAPE = \frac{1}{n}\sum \left[\frac{|x_o - x_p|}{x_o}\right] 100, \tag{18}$$

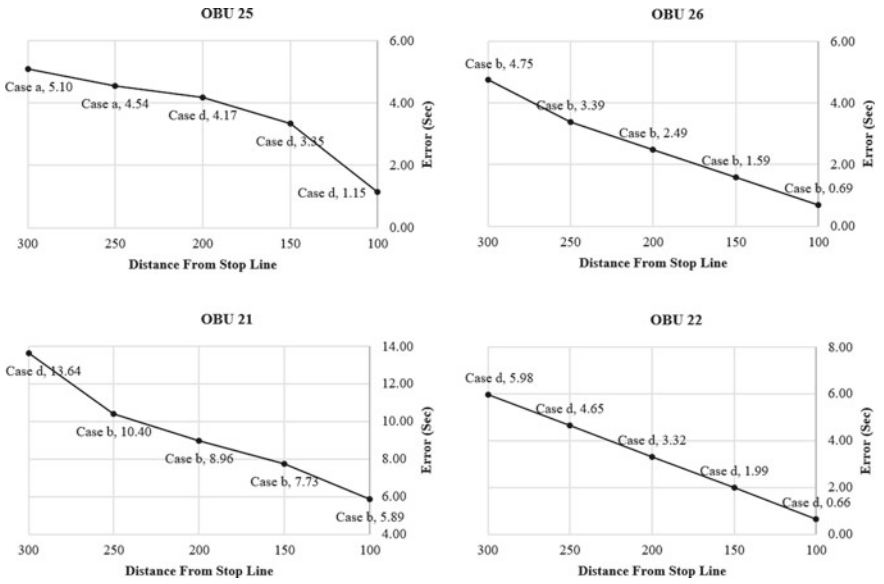

Fig. 5 Variation of the error for each bus coming on 11/02/22 with distance from the stop line

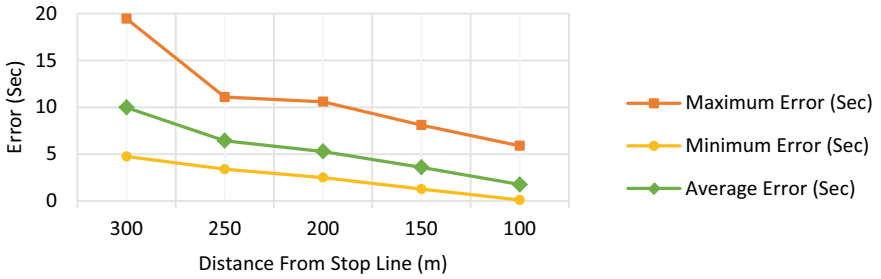

Fig. 6 Plot of maximum, minimum, and average error values at different distances from the stop line

where n is the number of observations; x_o is the observed value; and x_p is the predicted value.

Figure 7 shows the variation of MAE and MAPE values for all predictions from each category (case a, case b, and case d). It can be seen that the MAE is below 5 s for cases a and d. MAPE also shows acceptable range (Lewis et al., 1986) of values for all cases. A higher MAPE value can be observed for case b compared to other categories since its arrival time prediction was mainly based on the constant free-flow speed value, which is an assumption that needs verification.

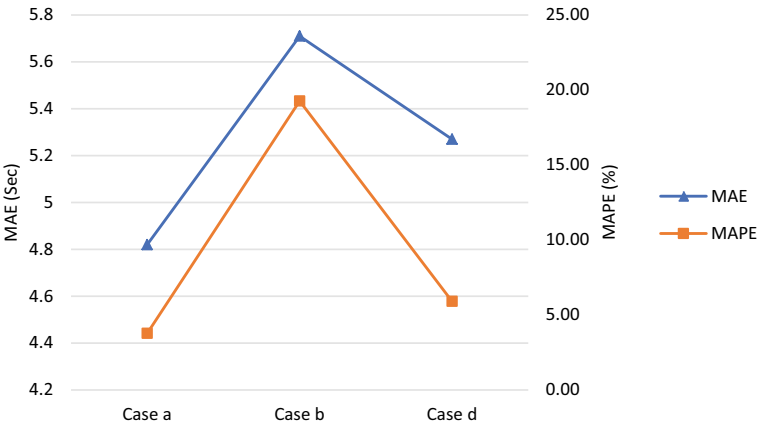

Fig. 7 MAE and MAPE for cases a, b and d

6 Summary and Conclusions

The goal of the present study was to accurately predict the time of arrival of buses, which are detected in the vicinity of an intersection, to the stop line, that can be used for the development of an efficient BSP solution. The bus data were collected using DSRC-based OBU and RSU devices. On the other hand, traffic data were collected from video recordings and signal timings by manual observation.

Preliminary analysis of the data showed different types of trajectories, which were grouped based on uniform and non-uniform movement and whether the bus stopped or not. Analytical models were developed for each group separately considering the signal timings and queue condition. Performance evaluations were conducted for each group at different distances from the stop line. It was found that the errors reduce as the bus comes closer to the stop line. MAPE values calculated for all scenarios of the model were within 20%, indicating good performance of the model (Lewis et al., 1986).

As future extension, the queue length calculation can be done by incorporating actual speeds, which will capture the deceleration and acceleration characteristics of the bus, instead of a constant free-flow speed value.

Acknowledgements The authors acknowledge the support of the Ministry of Information Technology, Government of India, for this study as part of the funded project through Project Number CE/19-20/331/MEIT/008253. The authors also acknowledge the "Connected Intelligent Urban Transportation Lab," funded by the Ministry of Human Resource Development, Government of India, through project number CEMHRD008432.

References

1. Baptista AT, Bouillet EP, Pompey P (2012) Towards an uncertainty aware short-term travel time prediction using GPS bus data: case study in Dublin. IEEE Conference on Intelligent Transportation Systems, Proceedings, ITSC, 1620–1625. https://doi.org/10.1109/ITSC.2012.6338633
2. Bie Y, Wang D, Qi H (2011) Prediction model of bus arrival time at signalized intersection using GPS data. J Transp Eng 138(1):12–20. https://doi.org/10.1061/(ASCE)TE.1943-5436.0000310
3. Chellappa R, Qian G, Zheng Q (2004) Vehicle detection and tracking using acoustic and video sensors. ICASSP, IEEE International Conference on Acoustics, Speech and Signal Processing – Proceedings 3(4), 1–4. https://doi.org/10.1109/icassp.2004.1326664
4. D'Angelo MP, Al-Deek HM, Wang MC (1999) Travel-time prediction for freeway corridors. Transp Res Rec 1676:184–191. https://doi.org/10.3141/1676-23
5. Ekeila W, Sayed T, El Esawey M (2009) Development of dynamic transit signal priority strategy. Transp Res Rec 2111:1–9. https://doi.org/10.3141/2111-01
6. Fang J, Meng H, Zhang H, Wang X (2007) A low-cost vehicle detection and classification system based on unmodulated continuous-wave radar. IEEE Conference on Intelligent Transportation Systems, Proceedings, ITSC 715–720. https://doi.org/10.1109/ITSC.2007.4357739
7. Gajda J, Piwowar P, Burnos P, Stencel M, Żegleń T, Sroka R (2007) Measurements of road traffic parameters using inductive loops and piezoelectric sensors. Metrol Meas Syst 14(2):187–203
8. Gang X, Kang W, Wang F, Zhu F, Lv Y, Dong X, Riekki J, Pirttikangas S (2015) Continuous travel time prediction for transit signal priority based on a deep network. IEEE Conference on Intelligent Transportation Systems, Proceedings, ITSC 523–528. https://doi.org/10.1109/ITSC.2015.92
9. Guerrero-Ibáñez J, Zeadally S, Contreras-Castillo J (2018) Sensor technologies for intelligent transportation systems. Sensors (Switzerland) 18(4):1–24. https://doi.org/10.3390/s18041212
10. Indian Roads Congress (1990) Guidelines for Capacity of Urban Roads in Plain Areas. New Delhi. In *IRC Code of Practice* (Vol. 106)
11. Jeong R, Rilett LR (2005) Prediction model of bus arrival time for real-time applications. Transp Res Rec 1927:195–204. https://doi.org/10.3141/1927-23
12. Jo Y, Choi J, Jung I (2014) Traffic information acquisition system with ultrasonic sensors in wireless sensor networks. Int J Distrib Sens Netw. https://doi.org/10.1155/2014/961073
13. Lee J, Shalaby A, Greenough J, Bowie M, Hung S (2005) Advanced transit signal priority control with online microsimulation-based transit prediction model. Transp Res Rec 1925(1):185–194
14. Lewis FL, Lewis FL (1986) Optimal estimation with an introduction to stochastic control theory. J. Wiley
15. Li J, Wang W, Van Zuylen HJ, Sze NN, Chen X, Wang H (2012) Predictive strategy for transit signal priority at fixed-time signalized intersections: Case study in Nanjing, China. Transp Res Rec 2311:124–131. https://doi.org/10.3141/2311-12
16. Luo Z, Habibi S, Mohrenschildt MV (2016) LiDAR based real time multiple vehicle detection and tracking. Int J Comput Inf Eng 10(6), 1125–1132. https://waset.org/publications/10004678/lidar-based-real-time-multiple-vehicle-detection-and-tracking
17. Odat E, Shamma JS, Claudel C (2018) Vehicle classification and speed estimation using combined passive infrared/ultrasonic sensors. IEEE Trans Intell Transp Syst 19(5):1593–1606. https://doi.org/10.1109/TITS.2017.2727224
18. Sohil F, Sohali MU, Shabbir J (2022) An introduction to statistical learning with applications in R. In *Statistical Theory and Related Fields,* (2022), (Vol. 6, Issue 1). https://doi.org/10.1080/24754269.2021.1980261
19. Tan CW, Park S, Liu H, Xu Q, Lau P (2008) Prediction of transit vehicle arrival time for signal priority control: Algorithm and performance. IEEE Trans Intell Transp Syst 9(4):688–696. https://doi.org/10.1109/TITS.2008.2006799

20. Vanajakshi L, Subramanian SC, Sivanandan R (2009) Travel time prediction under heterogeneous traffic conditions using global positioning system data from buses. IET Intel Transport Syst 3(1):1–9. https://doi.org/10.1049/iet-its:20080013
21. Wu CH, Ho JM, Lee DT (2004) Travel-time prediction with support vector regression. IEEE Trans Intell Transp Syst 5(4):276–281. https://doi.org/10.1109/TITS.2004.837813
22. Yu G, Li Y, Sun W, Yu H, Wang Y (2015) Bus priority signal control strategy for intersections without bus lanes. In *CICTP* (pp. 2097–2107)
23. Zhu H, Yu F (2016) A cross-correlation technique for vehicle detections in wireless magnetic sensor network. IEEE Sens J 16(11):4484–4494. https://doi.org/10.1109/JSEN.2016.2523601

Development of Intercity Travel Demand Models for a Highly Industrialised Regional Corridor

Rohit Rathod, Sunil Parmar, Ashutosh Maurya, and Gaurang Joshi

Abstract To generate cash flow in the economy, it is essential to develop the skillset of people in the country. This is done by taking care of induced travel demand generating year on year since it keeps on increasing with urbanisation. Hence, it is indispensable to provide effective and adequate transport infrastructure at the right time by analysing demand. As a service operator, it is equally important to provide the supply in the form of transport infrastructure like wide road width, flyovers, bridges, bus stops, and railway stations in the country. In the case of the movement of people and goods, the railway comes as the predominant and reliable mode of transport. For this study, the highly industrialised regional corridor covering Surat, Ahmedabad, and Vadodara is considered to develop the intercity passenger demand models and observe its sensitivity. To analyse the demand at the regional level, a direct demand model is developed, and it is found that the demand is going to almost double in 2030. The sensitivity analysis showed that a one percent change in travel time shows higher passenger demand compared to a unit change in travel cost and annual frequency.

Keywords Direct demand modelling · Demand elasticity · Travel demand · Ridge regression · Sensitivity analysis

1 Introduction

The economy of any country is the backbone of its peoples' livelihood. It is essential to make the cash flow in the economy for the survival and growth of any country. This cash flow happens through the movement of people and goods from one place to the other because of the spatial distribution of the resources in the country. For all such valuable economic activities, there is an indispensable and induced need for a transportation system. To boost economic growth, it is important to provide sufficient facilities for the smooth conduct of activities. While focusing on supplying

R. Rathod (✉) · S. Parmar · A. Maurya · G. Joshi
Department of Civil Engineering, S.V. National Institute of Technology, Surat, India
e-mail: rohit.rathod2230@gmail.com

A. Dhamaniya et al. (eds.), *Recent Advances in Traffic Engineering*, Lecture Notes in Civil Engineering 377, https://doi.org/10.1007/978-981-99-4464-4_9

the goods and passengers the transport facilities, it is required to know the demand beforehand. Since the activities take place in the physical world, to cater to its demand it is favourable to take decisions for the supply of the transportation system for the future years. In this process, there is a need of modelling the transport demand so that decision makers can be assisted in forming transportation planning decisions. This demand can be generated within the city (Intracity) as well as between the cities (Intercity).

The urban and regional contexts are totally different in the case of transportation systems. Urban travel generally demands a single mode of transportation, mostly road transport, whereas regional travel demands a different pattern with multiple modes of transportation. This further comes with more complexions with a number of modes available for access, egress, and trunk route journey. To analyse and alleviate the complexion of travel demand, it is required to perform the modelling which will support the decisions taken by the decision makers. Again, there is a different modelling approach for urban and regional contexts.

Multimodal inter-regional travel demand models can be made through various approaches. If the behavioural responses are considered at the aggregate level, then a direct demand model and elasticity analysis can be developed. If not considered, then only origin–destination estimation without behaviour theory is made. Furthermore, if disaggregated individual behaviour is considered, then a four-stage model is used. From therein, for analysing trips, the trip-based four-step models and for analysing tours/activity chains, activity-based modelling is done. At the regional level, developing an aggregate model is more sensible considering the complexities in the behavioural responses.

Urban travel demand can be approached by disaggregate modelling where each behavioural measure is analysed. Conventionally, the urban travel demand is modelled through the four-step modelling or sequential modelling which are trip generation, trip distribution, modal choice, and trip assignment. While doing so for regional context, it requires a huge dataset and at such a macrolevel, the homogeneity can be perceived and hence, for regional travel demand aggregate models are used.

In the conventional modelling approach, the estimation of relatively well-defined submodels is necessary which requires disaggregated data of the entire study area. This makes the task complicated at the regional level. Also, there is a challenge of calibrating the gravity model which creates problems with the errors in trip end totals and for those generated poorly from intrazonal trips. This drawback is eliminated in the case of direct demand model where it is calibrated simultaneously for all the three submodels, i.e., trip generation, trip assignment, and mode choice.

2 Literature Survey

Wirasinghe and Kumarage attempted to formulate an aggregate total demand model for estimating the inter-district passenger travel by public transport in Sri Lanka. Limitations of the model proposed were large calibration error, correlation between

socio-economic variables, correlation between impedance variables, inappropriate functional forms, and spatially non-transferable [1]. Ibe modelled an intercity travel demand model for Nigeria. The study found that passenger traffic is closely related to the frequency of vehicle trips, available bus fare, vehicular capacity, distance between origin and destination, and journey time performance of vehicles [2]. A log-linear relationship between travel demand and the explanatory variables was developed.

Woldeamanuel compared the intercity bus service with other competing modes. It concluded that intercity buses are environment-friendly, economically viable, and socially inclusive modes of long-distance travel. Intercity bus provides services to many rural areas which are far apart from the other intercity transit services [3]. Peers and Bevilacqua stated that the separate formulation of models by mode provides the opportunity to achieve the maximum flexibility in the model specification in direct demand modelling [4]. One of the initial formulations for the direct demand models was the Kraft-SARC model which had later on been modified by Mc-Lynn. Filippini and Deb studied 22 Indian states to estimate the log-linear travel demand function using panel data over the period of 1990–2001 [5]. It stated that the population has a positive and significant impact on travel demand. Fouquet studied the behaviour of real income and the price elasticity of demand for aggregate transport [6].

The report of "Transit and Quality Service Manual, third edition" provides the quality of service measure for the transit mode for comfort and convenience as passenger load, reliability, and transit auto travel time. Other factors mentioned were safety, security, and employee interactions with customers. Sinha identified that the key quality of service parameters of public transport is i) Cost, ii) Time, and iii) Quality of attributes of onboard comfort, ease of transfer, and information availability [7]. The report on "Understanding Transport Demands and Elasticities" mentions the elasticity of travel with respect to travel time for various modes and time periods, based on Portland, Oregon, data. It indicates that each 1% increase in AM peak drive-alone travel time reduces vehicle travel by 0.225% and increases demand for shared ride travel by 0.037% and transit by 0.036%. Frank found that transit riders are more sensitive to the change in travel time or waiting time compared to transit fare. A 10% increase in the in-vehicle travel time will reduce the transit demand by 2.3%, whereas a 10% increase in the transit fare will reduce the transit demand by 0.8% only [8].

Gaudry and Wills investigated the different forms of travel demand models that have been part of the different studies. It found that the sequential urban travel demand model is linear whereas the intercity travel demand model is generally of the log-linear form. This states that incorrect form of modelling can lead to erroneous results of the important parameters in the model [9]. Semeida developed the travel demand forecasting models for low population areas using two different methods, multiple linear regression, and generalised linear modelling (GLM) and then compared them which suggested that the GLM procedure offers a more suitable and accurate approach than linear regression for developing number of trips [10].

Filippini and Deb report that the aggregate transit demand can be estimated from a linear function model, semi-log linear model, log-linear model, and generalised log-linear model. The most common functional form used is the log-linear model

Fig. 1 **a** Ahmedabad TAZ, **b** Surat TAZ, and **c** Vadodara TAZ

because it reduces the number of coefficients to be estimated and the coefficient of the log-linear model directly estimates the elasticity [5].

Yahya carried out the study on modelling the variables when the data shows multi-collinearity and overfit to the testing data. For the stable and efficient estimates of the parameters in the presence of multi-collinearity in the data, it is suggested that the variables should be scaled at unit length or have zero means and unit standard deviation. Studies suggested that it is necessary and desirable to scale the predictor variables in ridge regression modelling when the presence of multi-collinearity is suspected [11].

3 Study Area

The economy of Gujarat state is the third largest in the country with a per capita GDP of 1,57,000. Also, Gujarat has been in the top five contributors to Indian GDP.

Moreover, in this state the corridor of three districts in the central and south regions, Ahmedabad, Vadodara, and Surat, have been taken for this study considering the heavily populated and industrialised corridor. The municipal areas have been delineated based on TAZ in the municipal area. Surat, Ahmedabad, and Vadodara have been divided into 7, 6, and 4 TAZs, respectively, as shown in Fig. 1.

4 Demography

The demographic profile of all three cities is mentioned in Table 1.

Table 1 Demographic profile of all cities

City	Population (2011 census)	Area (Sq. km.)	Decadal growth (2001–2011)
Surat	4,466,826	326.515	55.29%
Ahmedabad	5,577,940	466.000 (2006)	58.46%
Vadodara	1,752,371	230.660	34.16%

4.1 Linkages Between Cities

All three cities are well connected through Rail, Road, and Air Transport. Rail transport is considered for the study and study corridors are mentioned below.

(1) ST-ADI Rail Corridor
(2) ST-BRC Rail Corridor
(3) ADI-BRC Rail Corridor.

5 Data Collection

The following sections are provided for the secondary data collected for the present study.

5.1 Railways Secondary Data

For the current study, secondary data were collected such as for railways; historical passenger travel demand has been collected from the Ministry of Indian Railways (Railway Board), New Delhi, for the past 11 years from January 2009 to December 2019. Railway passenger demand data has been collected for all types of trains (passenger, Mail, Express, superfast, Shatabdi, Special trains, etc.) with 1A, 2A, 3A, CC, EC, FC, SL, and 2S. Later, for ease of analysis and evaluation, the data is segregated into Non-AC and AC classes.

5.2 Population

Historical population data was collected from the official website of Surat Municipal Corporation. The population of municipal areas of all three cities has been listed on a decadal basis from 1901 to 2011. For the construction of Direct Demand Models, the population is estimated from 2011 to 2019.

5.3 Annual Income Per Capita

Annual Income Per Capita has been collected from the national high-speed rail feasibility report. The report has published the annual income per capita of the city for the year 2006.

5.4 Travel Time

Access and Egress Travel time has been collected from the centroid of every zone to the intercity terminal such as railway stations and bus stands with the help of Google Maps. Travel time for the trunk route journey has been taken as per the published schedule of the services.

5.5 Travel Cost

Travel cost has been estimated based on fuel prices. The fuel prices have been collected from the petrol pump.

5.6 Service Frequency

The frequency of the railways has been collected as per the timetable provided by the railway board.

6 Data Analysis

After the data collection, irrespective of the type of data (qualitative or quantitative), analysis may consist of following steps:

1. Describe and summarise the data
2. Identify relationships between variables
3. Compare variables
4. Identify the difference between variables
5. Forecast outcomes.

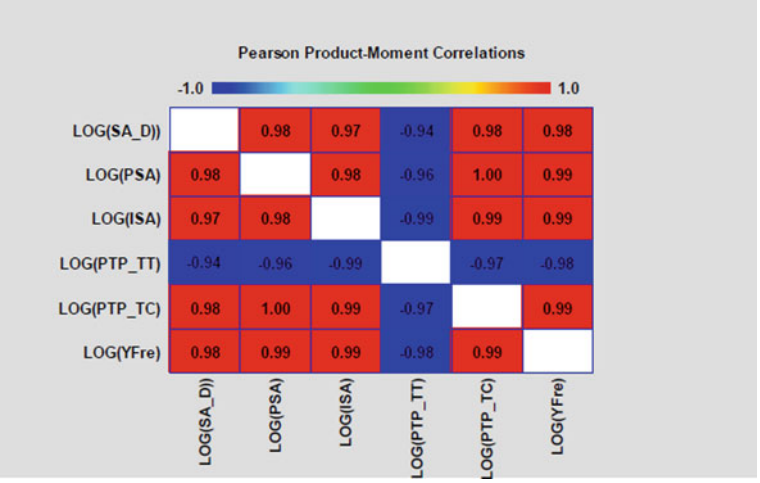

Fig. 2 Multi-collinearity in dataset

6.1 Ridge Regression

To identify the relationships between the variables, the Pearson correlation method was used. But the results showed that it is an overfit model which is shown in Fig. 2 and cannot be used reliably over the forecasting.

Hence, to alleviate the variance in the model, another statistical method called Ridge Regression was used. In this method, it changes the line of least squared fit to ridge regression line that will compromise on the bias but reduces the variance that is needed for the model. It adds an additional term in the least squared fit equation as the product of the lambda value and square of the slope of the line. The lambda value can be obtained by ten-fold cross validation.

6.2 Passenger Demand Analysis

The secondary data obtained from the Ministry of Railway Board gives passenger demand for the last 11 years. The railway passenger demand (RPD) variation over the years is shown in the following figures. Figure 3 shows the overall demand variation, whereas Figs. 4 and 5 are showing demand variation for AC and Non-AC classes, respectively. It can be observed that Surat-Ahmedabad is having the highest demand compared to Surat-Vadodara and Vadodara-Ahmedabad sections.

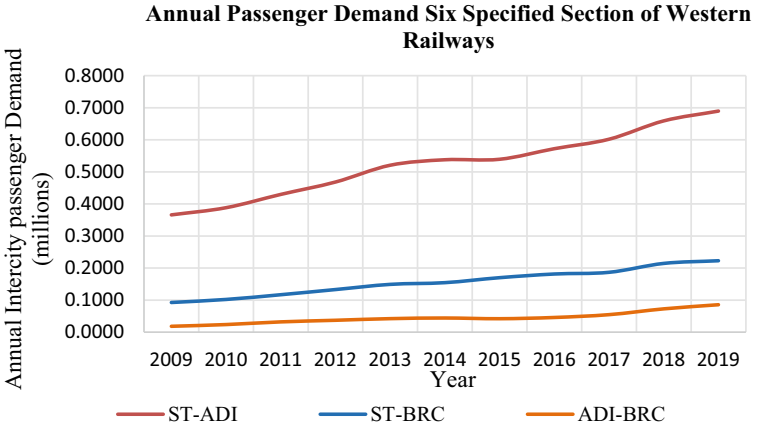

Fig. 3 Railway passenger demand variation from 2009 to 2019

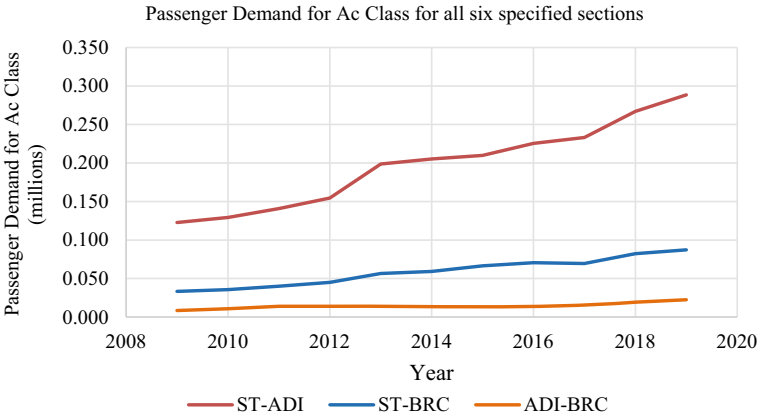

Fig. 4 RPD AC variation from 2009 to 2019

6.3 AC Class Passenger Demand

6.4 Non-AC Passenger Demand

As shown in the above Fig. 5, Non-AC class passenger demand is highest in all sections. The relative demand of Non-AC class passenger demand with respect to AC class passenger demand is shown below:-

i. ST-ADI—1.71
ii. ADI-ST—1.86
iii. ST-BRC—1.70

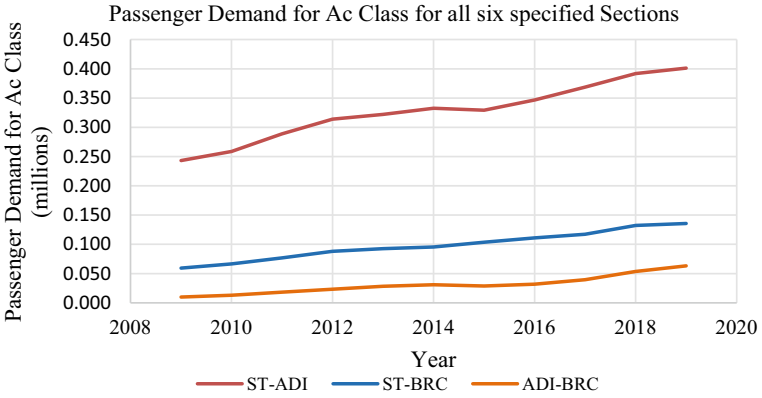

Fig. 5 RPD non-ac variation from 2009 to 2019

iv. BRC-ST—1.81
v. ADI-BRC—2.03
vi. BRC-ADI—1.89.

6.5 Input Variables for Direct Demand Model

For the direct demand model, the intercity demand has been correlated with the product of the population of two cities, product of annual income per capita of two cities, travel time between two cities, travel cost for the chosen mode, and annual frequency of the services for the chosen between two cities. Because of the difficulty in predicting the population of a specific age group who make the intercity trips, the total population is considered for the forecasting.

There can be many measures of income to include in the model: Income distribution, median income, or mean income. Using income groups for the model will be quite unpredictable for forecasting. To forecast median income would require either a projection of the total income distribution or a model relating the median income to some other, more readily forecast, variable such as aggregate personal income. This model will definitely lead to a more complex model than using a mean income. Income can be measured at different scales such as the income of a person, household, or city. The population and annual income per capita are taken in the log scale for the model.

To develop the model, the total travel time is considered for one way. In this study, total travel time considers access time, transfer time, waiting time, trunk route journey time, and egress time. The access and egress travel times for the three cities are mentioned in Table 2.

Table 2 Access and egress travel time in minutes

City	Bus	Car	2W	Auto	Walk
Surat	24	19	18	19	10
Ahmedabad	39	17	16	18	10
Vadodara	25	16	12	15	10

7 Minutes of Walking Time Has Been Considered Based on the 1.2 m/s Pedestrian Speed

Waiting time at different terminal stations has been taken from the feasibility report of national high-speed rail. A waiting time of 24 min is considered for the railway stations. A transfer time of 5 min is considered for the study.

The variation in trunk route journey travel time in minutes is shown in Fig. 6 for the past 11 years. It shows that over the years the travel time is decreased for Surat to Ahmedabad more than the other sections.

In this study, the travel cost is considered as access travel cost, trunk route travel, and egress travel cost. Access and egress travel cost has been estimated from the fuel prices in the city. The trunk route travel cost is available through secondary data, and it is given in terms of average travel cost per passenger. It was found that the travel cost has increased drastically for the railways over the years.

As per the transit capacity quality of the service manual, the service frequency was consistently reported as the top factor influencing overall trip satisfaction. It is also taken from the secondary data provided. This shows that over the years, the frequency has increased with increased demand.

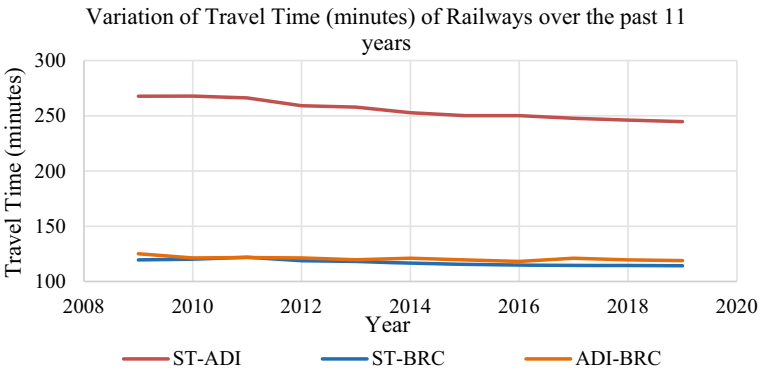

Fig. 6 Variation of travel time (minutes) for rail corridors

8 Passenger Demand Modelling

Direct Demand Models have been constructed for the different corridors by using the five variables as explanatory variables and the passenger demand as the response variable. The following types of direct demand models have been constructed:

1. Railway models without access and egress consideration for all three sections (RPDM—XEA)
2. Railway AC models without access and egress consideration for all three sections (RPDM AC—XEA)
3. Railway Non-AC models without access and egress consideration for all three sections (RPDM NAC—XEA)
4. Railway AC models with access and egress consideration for all three sections (RPDM AC—WEA)
5. Railway Non-AC models with access and egress consideration for all three sections (RPDM NAC—WEA).

8.1 RPDM—XEA

Table 3 shows the coefficients for every explanatory variable used in the model. The coefficients for the product of population, product of income per capita, average travel cost, and annual frequency are positive because of having a positive correlation with annual passenger demand, whereas the coefficient of travel time is negative, because of the negative correlation with annual passenger demand. The model has been constructed based on the log-linear model hence the coefficient itself shows the elasticity value of that variable.

For intercity travel, the elasticity value of travel cost is positive. Mathematically, it represents that by increasing the travel cost the travelling demand will get increased, which never justifies the behaviour of transit users. Generally, the user responds to the travel cost when it exceeds his travel expenditure limit. In the case of railways, there are 30 types of trains which are running with multiple classes with different

Table 3 RPDM—XEA

Section	RP	LOG(PSA)	LOG(ISA)	LOG(R_TT)	LOG(R_TC)	LOG(R_YFre)	Constant
ST-ADI	0.1	0.193	0.059	–0.473	0.061	0.242	2.467
	RP	LOG(PSB)	LOG(ISB)	LOG(R_TT)	LOG(R_TC)	LOG(R_YFre)	CONSTANT
ST-BRC	0.25	0.327	0.065	–1.144	0.199	0.404	0.439
	RP	LOG(PAB)	LOG(IAB)	LOG(R_TT)	LOG(R_TC)	LOG(R_YFre)	CONSTANT
ADI-BRC	0.55	0.537	0.094	–0.429	0.030	0.457	–4.461

Table 4 RPDM—XEA performance statistics

Corridor	RP	MSE	MAE	MAPE	ME	MPE	R^2
ST-ADI	0.10	0.000	0.009	0.154	0.000	–0.001	95.035
ST-BRC	0.25	0.001	0.011	0.201	0.000	–0.002	92.667
ADI-BRC	0.55	0.008	0.038	0.793	0.000	–0.019	73.552

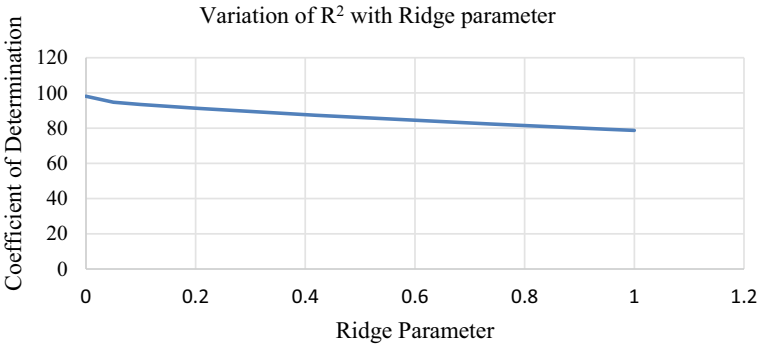

Fig. 7 Variation of R^2 value with the ridge parameter

travel costs. Hence, If the travel cost increases for the railways, then the passengers will shift to the other classes which will not show a decrease in demand.

Table 4 shows the residual analysis results for the above model.

Likewise, the models for the AC class and Non-AC class were developed without considering access and egress time. And similar results were obtained.

8.2 Ridge Parameter

It was found that with the increase of the ridge parameter, there was a higher error observed in the model in terms of R^2 value. The relationship between the R^2 value and the ridge parameter is shown in Fig. 7. Hence, it is necessary to find the appropriate value of the ridge parameter for the optimum results of the model.

8.3 RPDM AC—WEA

This section describes the direct demand model of railway passenger demand considering access and egress modes. Access and egress modes have been kept in 4 categories. Private car and 2W have been mentioned as Private mode, BRTS and City Bus are considered as Buses, Cab and Auto are categorised as Auto, and Walk has

been taken as Non-motorised Transport. A total of 16 possible mode chains have been taken in the model as PTP, PTB, PTA, PTN, BTP, BTB, BTA, BTN, ATP, ATB, ATA, ATN, NTP, NTB, NTA, and NTN where P = Private Mode, T = Train, B = Bus, A = Auto, and N = Non-motorised Transport.

Hence, PTP indicates a mode chain for a passenger as follows:

First Alphabet: It denotes the access mode in the origin city.

Second Alphabet: It denotes the trunk route mode between the cities.

Third Alphabet: It denotes the egress mode in the destination city.

8.3.1 ST-ADI Rail Corridor

This model considers the access and egress modes with AC class in the trip and the regression coefficient for all explanatory variables used in the model which are shown in Table 5. These coefficients show the elasticity value in that particular variable.

The performance measures of this model are shown in Table 6.

In this way, models for other corridors ST-BRC and ADI-BRC were developed. And similar results were found.

Table 5 RPDM AC—WEA ST-ADI

Mode chain	RP	LOG (PSA)	LOG (ISA)	LOG (TT)	LOG (TC)	LOG (Y_Fre)	CONSTANT
PTP	0.15	0.222	0.084	−0.919	0.333	0.238	1.275
PTB	0.15	0.224	0.084	−0.929	0.327	0.242	0.876
PTA	0.15	0.221	0.082	−0.967	0.358	0.235	0.581
PTN	0.1	0.230	0.095	−0.609	0.333	0.217	0.293
BTP	0.15	0.222	0.083	−1.019	0.320	0.238	0.935
BTB	0.15	0.222	0.083	−1.047	0.315	0.239	0.616
BTA	0.15	0.219	0.082	−1.080	0.345	0.233	0.308
BTN	0.1	0.228	0.094	−0.758	0.319	0.213	0.126
ATP	0.2	0.215	0.077	−1.148	0.349	0.247	0.345
ATB	0.2	0.215	0.077	−1.199	0.345	0.247	0.099
ATA	0.25	0.210	0.072	−1.333	0.356	0.250	0.125
ATN	0.2	0.214	0.076	−1.249	0.332	0.245	0.624
NTP	0.2	0.218	0.078	−1.109	0.304	0.252	0.788
NTB	0.2	0.218	0.078	−1.145	0.300	0.254	0.491
NTA	0.2	0.216	0.077	−1.156	0.328	0.248	0.120
NTN	0.15	0.222	0.084	−0.973	0.300	0.241	0.322

Table 6 RPDM AC—WEA ST-ADI performance statistics

Mode chain	MSE	MAE	MAPE	ME	MPE	R^2
PTP	0.001	0.015	0.316	0.000	−0.003	93.110
PTB	0.001	0.015	0.350	0.000	−0.003	93.069
PTA	0.001	0.015	0.365	0.000	−0.004	93.201
PTN	0.001	0.015	0.308	0.000	−0.002	94.175
BTP	0.001	0.015	0.366	0.000	−0.004	93.119
BTB	0.001	0.015	0.411	0.000	−0.004	93.088
BTA	0.001	0.015	0.435	0.000	−0.005	93.222
BTN	0.001	0.015	0.357	0.000	−0.003	94.186
ATP	0.001	0.015	0.474	0.000	−0.007	92.176
ATB	0.001	0.016	0.552	0.000	−0.009	92.148
ATA	0.001	0.015	0.622	0.000	−0.013	91.327
ATN	0.001	0.015	0.485	0.000	−0.007	92.199
NTP	0.001	0.016	0.431	0.000	−0.005	92.040
NTB	0.001	0.016	0.491	0.000	−0.007	92.006
NTA	0.001	0.015	0.528	0.000	−0.008	92.149
NTN	0.001	0.015	0.425	0.000	−0.005	93.051

8.4 RPDM NAC—WEA

This model considers Non-AC class of railway and includes access and egress modes of travel. The results and performance measures are shown for each corridor considered in this study in the subsequent tables below.

8.4.1 ST-ADI Rail Corridor

Tables 7 and 8 are showing the model results in terms of coefficients of ridge regression and the performance measures.

In a similar manner, models for other corridors were developed. And satisfactory results were obtained.

9 Sensitivity Analysis

The sensitivity analysis based on the elasticity values of the level of service parameters used in the model was carried out. The following **Table 9** shows the percentage change in the passenger demand for railways with respect to the unit change of LOS parameters while keeping other factors constant.

Table 7 RPDM NAC—WEA ST-ADI

Mode chain	RP	LOG (PSA)	LOG (ISA)	LOG (TT)	LOG (TC)	LOG (YFre)	CONSTANT
PTP	0.10	0.122	0.025	−0.056	0.150	0.203	2.009
PTB	0.10	0.125	0.025	−0.126	0.133	0.204	1.783
PTA	0.10	0.109	0.022	−0.079	0.226	0.183	1.400
PTN	0.10	0.127	0.026	−0.103	0.120	0.208	2.049
BTP	0.10	0.123	0.025	−0.065	0.141	0.203	1.409
BTB	0.10	0.125	0.025	−0.139	0.125	0.204	1.188
BTA	0.10	0.109	0.022	−0.084	0.215	0.184	0.793
BTN	0.10	0.128	0.026	−0.114	0.112	0.208	1.449
ATP	0.15	0.105	0.023	−0.231	0.213	0.168	1.103
ATB	0.10	0.108	0.022	−0.035	0.228	0.183	0.083
ATA	0.10	0.098	0.021	−0.057	0.300	0.169	−0.216
ATN	0.10	0.109	0.023	−0.013	0.215	0.186	0.373
NTP	0.15	0.118	0.026	−0.244	0.126	0.185	1.570
NTB	0.10	0.128	0.026	−0.070	0.114	0.210	0.512
NTA	0.10	0.111	0.023	−0.024	0.203	0.189	0.163
NTN	0.10	0.131	0.027	−0.045	0.102	0.214	0.768

Table 8 RPDM NAC—WEA ST-ADI performance statistics

Mode chain	MSE	MAE	MAPE	ME	MPE	R^2
PTP	0.000	0.007	0.132	0.000	0.000	93.860
PTB	0.000	0.007	0.142	0.000	−0.001	93.750
PTA	0.000	0.006	0.141	0.000	−0.001	94.460
PTN	0.000	0.007	0.132	0.000	0.000	94.460
BTP	0.000	0.006	0.147	0.000	−0.001	93.840
BTB	0.000	0.007	0.165	0.000	−0.001	93.840
BTA	0.000	0.006	0.167	0.000	−0.001	94.430
BTN	0.000	0.007	0.152	0.000	−0.001	93.660
ATP	0.000	0.006	0.179	0.000	−0.001	93.500
ATB	0.000	0.006	0.194	0.000	−0.001	94.650
ATA	0.000	0.005	0.192	0.000	−0.001	95.230
ATN	0.000	0.006	0.176	0.000	−0.001	94.440
NTP	0.000	0.006	0.165	0.000	−0.001	92.650
NTB	0.000	0.007	0.187	0.000	−0.001	93.650
NTA	0.000	0.006	0.192	0.000	−0.001	93.650
NTN	0.000	0.007	0.171	0.000	−0.001	93.650

Table 9 Railway passenger demand sensitivity analysis

Additional railway passenger demand due to			
Corridor	−1% change in travel time (min)	1% change in average travel cost (Rupees)	1% change in annual frequency
ST-ADI	4452	1424	1365
ST-BRC	2494	553	865
ADI-BRC	1085	188	271

The results show that the reduction in travel time shows higher passenger demand compared to a unit change in travel cost and annual frequency. Hence, passengers are more sensitive to travel time during the travel compared to the other two parameters.

10 Scenario Analysis

After the construction of the above models, attempts were made to check the future demand with the three scenarios with the different combinations of three parameters, i.e., travel time, travel cost, and annual frequency.

Three scenarios related to all LOS parameters were generated as Business As Usual (BAU), Scenario-1 (S-1), and Scenario-2 (S-2).

The different combinations of these parameters with different scenario analysis combinations are shown below.

(1) (BAU_TT) and (BAU_TC) and (BAU_Fre)
(2) (S1_TT) and (S1_TC)
(3) (S1_TT) and (S1_Fre)
(4) (S1_TC) and (S1_Fre)
(5) (S1_TT) and (S1_TC) and (S1_Fre)
(6) (S2_TT) and (S2_TC)
(7) (S2_TT) and (S2_Fre)
(8) (S2_TC) and (S2_Fre)
(9) (S2_TT) and (S2_TC) and (S2_Fre)

where

BAU_TT = Business as Usual for Travel Time.

BAU_TC = Business as Usual for Travel Cost.

BAU_Fre = Business as Usual for Annual Frequency.

S1_TT = Scenario—1 for Travel Time.

S1_TC = Scenario—1 for Travel Cost.

S1_Fre = Scenario—1 for Annual Frequency.

S2_TT = Scenario—2 for Travel Time.

S2_TC = Scenario—2 for Travel Cost.

S2_Fre = Scenario—2 for Annual Frequency.

Business As Usual: This scenario shows a do-nothing case where only the historical trends are observed.

S1_TT: In this scenario, the speed of trains increases by 15% and 25% for the years 2025 and 2030, respectively.

S2_TT: Speed has been changed by 20% and 30% for the years 2025 and 2030, respectively.

S1_TC: (BAU-10%): This scenario considers there will not be any investment towards the new trains with new technology, and the travel cost will change due to the change in the source of energy with renewable energy so the cost might increase with decreased rate than the BAU.

S2_TC: (BAU + 10%): It considers new investment towards new technology trains with better comfort and convenience, with renewable energy sources hence increasing the cost of travel at a greater rate than BAU, considered for the years 2025 and 2030.

S1_Fre: (BAU-10%): Since the semi-high-speed train has been planned in the same corridor, it will attract passengers from railways as well as from buses hence these may experience an increase in frequency with a lower rate than BAU, considered for the years 2025 and 2030.

S2_Fre: (BAU + 10%): If some new technology train has been operated through Indian railways with an affordable price than semi-high-speed rail, then it might see some increase in demand, and hence increase in frequency with a greater rate than BAU, considered for the years 2025 and 2030.

Table 10 shows the different scenarios of LOS parameters for the years 2025 and 2030.

Table 11 suggests that scenarios S1_TT and S1_TC and S1_TT and S1_Fre have resulted in almost the same percentage change in demand for all three study corridors. Similarly, S2_TT and S2_TC, S2_TT and S2_Fre, and S2_TT and S2_TC and S2_Fre have also resulted in almost equal percentage increase in demand.

The similar analysis was carried out for the year 2030 and results are shown in Tables 12 and 13.

The above table suggests that scenario S1_TT and S1_TC and S1_TT and S1_Fre have resulted in almost the same percentage change in demand for all three study corridors. Similarly, S2_TT and S2_TC, S2_TT and S2_Fre, and S2_TT and S2_TC and S2_Fre have also resulted in almost equal percentage increase in demand. As most of the scenarios resulted in around a 100% increment, this indicates that in the next 10 years the passenger demand may get doubled.

Table 10 Scenario analysis for RPD for the year 2025

		ST-ADI	ST-BRC	ADI-BRC
Travel time (based on speed)	BAU	−5.589%	−2.564%	−3.268%
	Scenario 1	−13.043%	−13.043%	13.043%
	Scenario 2	−16.667%	−16.667%	16.667%
		Scenario 1: 15% speed increment		Scenario 2: 20% speed increment
Average travel cost	BAU	27.781%	22.066%	20.284%
	Scenario 1	17.781%	12.066%	10.284%
	Scenario 2	37.781%	32.066%	30.284%
		Scenario 1 = BAU − 10%		Scenario 2 = BAU + 10%
Annual frequency	BAU	23.279%	21.005%	27.284%
	Scenario 1	13.279%	11.005%	17.284%
	Scenario 2	33.279%	31.005%	37.284%

11 Conclusion

Direct Demand Models have been constructed for the 5 different combinations with and without consideration of access and egress modes. Four different modes have been considered in the cities for access and egress to and from the intercity terminal in the cities. The elasticity values are found less than the unity for most of the cases which shows the inelastic nature of the railway passenger demand. As mentioned in previous studies that travel time and travel cost generally show negative elasticity values for the change in demand but in this study, it is found that travel cost is having positive elastic value. This indicates that there is no decrease in passenger demand with travel cost increased. This is justified by the thought that whenever the travel cost exceeds the travel expenditure of an individual, he will shift the class (AC to Non-AC) of the train journey rather than shifting to other modes.

Scenario Analysis has shown that in 2025, the passenger demand will get increased by around 40% whereas by the year 2030, this demand will be nearly doubled. It can be observed that scenarios S1_TT and S1_TC and S1_TT and S1_Fre have resulted in almost the same percentage change in demand for all three study corridors. Similarly, S2_TT and S2_TC, S2_TT and S2_Fre, and S2_TT and S2_TC and S2_Fre have also resulted in almost equal percentage increase in demand.

Table 11 Change in passenger demand for the year 2025 based on scenario analysis

Corridor	BAU_TT & BAU_TC & BAU_Fre	S1_TT & S1_TC	S2_TT & S2_TC	S1_TT & S1_Fre	S2_TT & S2_Fre	S1_TC & S1_Fre	S2_TC & S2_Fre	S1_TT & S1_TC & S1_Fre	S2_TT & S2_TC & S2_Fre
ST-ADI	27.397%	32.103%	40.254%	32.114%	40.237%	23.190%	31.409%	29.909%	42.436%
ST-BRC	40.861%	56.629%	71.107%	54.722%	73.045%	33.362%	48.139%	51.472%	76.463%
ADI-BRC	16.728%	31.071%	43.487%	30.186%	44.401%	11.604%	21.664%	27.728%	46.955%

Table 12 Scenario analysis for RPD for the year 2030

		ST-ADI	ST-BRC	ADI-BRC
Travel time (based on speed)	BAU	−8.597%	−4.533%	−4.982%
	Scenario 1	−20.00%	−20.00%	−20.00%
	Scenario 2	−23.08%	−23.08%	−23.08%
		Scenario 1: 25% speed Increment		Scenario 2: 30% speed increment
Average Travel Cost	BAU	60.206%	51.813%	60.009%
	Scenario 1	50.206%	41.813%	50.009%
	Scenario 2	70.206%	61.813%	70.009%
		Scenario 1 = BAU − 10%		Scenario 2 = BAU + 10%
Annual Frequency	BAU	68.233%	34.345%	79.647%
	Scenario 1	58.233%	24.345%	69.647%
	Scenario 2	78.233%	44.345%	89.647%
		Scenario 1 = BAU − 10%		Scenario 2 = BAU + 10%

Table 13 Change in passenger demand for the year 2030 based on scenario analysis

Corridor	BAU_ TT & BAU_ TC & BAU_ Fre	S1_TT & S1_TC	S2_TT & S2_TC	S1_TT & S1_Fre	S2_TT & S2_Fre	S1_TC & S1_Fre	S2_TC & S2_Fre	S1_TT & S1_TC & S1_Fre	S2_TT & S2_TC & S2_Fre
ST-ADI	62.889%	75.176%	84.367%	75.382%	84.170%	58.796%	66.835%	73.063%	86.487%
ST-BRC	90.643%	128.441%	146.641%	125.468%	149.624%	81.900%	99.161%	100.086%	153.610%
ADI-BRC	71.836%	110.672%	127.571%	109.848%	128.436%	66.382%	77.142%	72.108%	131.497%

References

1. Wirasinghe SC, Kumarage AS (1998) An aggregate demand model for intercity passenger travel in Sri Lanka. Transportation (Amst) 25(1):77–98. https://doi.org/10.1023/A:1004985506022/METRICS
2. Dike D, Ibe C, Ejem E, Erumaka O, Chukwu O (Dec.2018) Estimation of inter-city travel demand for public road transport in Nigeria. J Sustain Dev Transp Logist 3(3):88–98. https://doi.org/10.14254/JSDTL.2018.3-3.7
3. Woldeamanuel M (2012) Evaluating the competitiveness of intercity buses in terms of sustainability indicators. J Public Transp 15(3):77–96. https://doi.org/10.5038/2375-0901.15.3.5
4. Peers JB, Bevilacqua M (1976) Structural travel demand models: an intercity application. Transp Res Rec 569:124–135
5. Deb K, Filippini M "Public Bus Transport Demand Elasticities in India"
6. Fouquet R (2012) Trends in income and price elasticities of transport demand (1850–2010). Energy Policy 50:62–71. https://doi.org/10.1016/J.ENPOL.2012.03.001
7. Sinha S, Shivanand Swamy HM, Modi K (2020) User perceptions of public transport service quality. Transp. Res. Procedia 48:3310–3323. doi: https://doi.org/10.1016/J.TRPRO.2020.08.121
8. Frank L, Bradley M, Kavage S, Chapman J, Lawton TK (2008) Urban form, travel time, and cost relationships with tour complexity and mode choice. Transportation (Amst) 35(1):37–54. https://doi.org/10.1007/S11116-007-9136-6/TABLES/4
9. Wills G "1978-2 Transpn Res CRT 63.pdf."
10. Semeida AM (2014) Derivation of travel demand forecasting models for low population areas: the case of Port Said Governorate, North East Egypt. J Traffic Transp Eng (English Ed., vol. 1, no. 3, pp. 196–208. doi: https://doi.org/10.1016/S2095-7564(15)30103-3
11. Yahya WB, Olaifa JB (2014) A note on ridge regression modeling techniques. Electron J Appl Stat Anal 7(2):343–361. https://doi.org/10.1285/I20705948V7N2P343

Investigating Car User's Exposure to Traffic Congestion-Induced Fine Particles in Megacity Delhi

Vasu Mishra and Rajeev Kumar Mishra

Abstract Air pollution and traffic congestion have become a significant concern for all urban cities. This study aims to find a relationship between the congestion zone and the Particle Number Concentration (PNC) of Fine Particulates. During the study, a direct relation was observed between traffic densities, congestion, and the PNC. Heavy congestion causes an average increase of 3×10^5 to 6×10^5 #/cc in PNC, while the light congestion zone causes an average growth of 1.3×10^5 to 1.8×10^5 #/cc. A relation between the traffic signal duration and PNC was also observed. Shorter duration signals resulted in negligible impact, while longer duration signals have a noticeable impact on PNC.

Keywords Air pollution · Commuter exposure · Fine particles · Particulate matter · qUFP · Traffic congestion

1 Introduction

Traffic congestion and commuter exposure to Particulate Matter (PM) are becoming new norms, and while both are related to each other in one way or another, not much study has been done to understand how the two are related to each other. This study aims to analyse better how traffic congestion impacts the in-cabin concentration of fine particulate matter in cars and determine the risk of commuter exposure.

The seriousness of this issue can be understood by the fact that in recent years, commuter exposure to air pollution has become a topic of concern across the globe [1–3]. Developing countries like India [4] witness rapid urbanization and industrialization. India has a large number of urban cities facing overcrowding and severe air pollution, resulting in many Indian cities regularly featuring in the list of most polluted (9 cities in the list of 10 most polluted cities in the world [5]) and congested cities (4 out of 10 most congested cities [6]) in the world.

V. Mishra · R. K. Mishra (✉)
Department of Environmental Engineering, Delhi Technological University, Delhi, India
e-mail: rajeevkumarmishra@dtu.ac.in

A. Dhamaniya et al. (eds.), *Recent Advances in Traffic Engineering*, Lecture Notes in Civil Engineering 377, https://doi.org/10.1007/978-981-99-4464-4_10

On average, Indians spend 7% of their day commuting to the office [7], while the situation is much worse in Delhi. As per a report [6] published in Delhi, the average commuting time is increased by 56% due to traffic congestion, while in terms of air pollution, bad and severe Air Quality Index (AQI) days have become the new normal in the city, while good air days have become rare occurrences [3, 5, 8]. As a result, people living in Delhi are at greater risk of commuter exposure to air pollution.

Amongst the various pollutants, PMs have become a significant concern amongst people due to serious health risks like respiratory allergies, asthmas, and bronchitis [9]. As per World Health Organization's (WHO) latest report [10], 9 out of 10 people living in urban areas are exposed to PM2.5, while almost 4.5 million premature deaths are attributed to PM exposure. Also, almost 2.7% of global illnesses can be linked to respirable PM [11].

Amongst the various PMs, fine particles ($dp < 1\ \mu m$) have recently become particularly interesting as they contribute to up to 70–80% of the total particle number in the ambient air [12, 13]. Fine particles tend to have a varying chemical composition and very small size, which allows them to remain in the air for a long period and penetrate deep into the respiratory tract and have profound implications (directly as well as indirectly) on the health and contributing to issues like arrhythmia, hypertension, reduced lung function, etc. [14–16]. Exposure to fine particles is a well-known risk [17–19], and the risk increases further while commuting [8, 20, 21].

Fine particles, quasi-Ultra Fine Particles (qUFP), and Ultra Fine Particles (UFP) are a sub-fraction of PM 2.5, contributing up to 90% of total Particle Number Concentration (PNC, i.e., the total number of particles present per unit volume of air) of PM2.5 [13]. While fine particles are defined as particles having a size less than 1000 nm, at the moment, there is a lack of agreement amongst scholars regarding the definition of the UFP and qUFP; as a result, the boundary conditions are not well established. Over the years, various researchers have used different meanings for these particles. For this study, we have considered UFP as particulate matter with at least one dimension less than 100 nm [13] and qUFP particles as particulates in a size range of 100–360 nm [22].

In Indian urban areas, people spend a considerably large amount of time commuting from one place to another place. Most of the Indian metro cities are highly congested and regularly ranked very high on the list of cities with the most polluted air, which translates to the fact that people living in Indian metro cities (especially Delhi) are at a relatively higher risk of facing serious health implications (directly and indirectly) related to air pollution due to increased risk of commuter exposure.

2 Methodology

2.1 Route Selection

The study was conducted on two different routes located in the National Capital Territory (NCT) of Delhi; both routes were selected to provide a realistic representation of the traffic scenario NCT of Delhi and contain different traffic densities. Both routes were similar in length; route-1 was from Delhi Technological University (DTU) to Indira Gandhi International (IGI) airport Terminal-2 (Fig. 1a), a 37 km long route connecting North Delhi to South West Delhi. This route had a variable traffic density and contained more greenery and less unplanned stoppage and congestion zone as it included the open area near the airport. The route-2 covered a 36 km long stretch from Mohan Nagar metro station to DTU (Fog 1b), connecting North Delhi with East Delhi, and Ghaziabad. This route included the Kashmiri Gate Inter-State Bus Terminus (ISBT) area, one of the busiest terminus in Delhi, the industrial area of Mohan Nagar/Sahibabad, and covers parts of Grand Trunk (GT) road. The route has a high traffic density and unplanned stoppage while also including the crossing of the river Yamuna. The average duration of both the routes was around 2 h 45 min for a round trip.

2.2 Instrumentation

The sampling was done inside the vehicle (car) using "GRIMM Technik, model 11-A portable aerosol spectrometer", a portable Optical Particle Counter (OPC) (refer to Table 1[1] for technical specs). For this study, 12 particulate-size channel bins (corresponding to <1 μm particle size) were used, i.e., <0.25 μm, 0.25–0.28μ, 0.28–0.30 μm, 0.30–0.35 μm, 0.35–0.40 μm, 0.40–0.45 μm, 0.45–0.50 μm, 0.50–0.58 μm, 0.58–0.65 μm, 0.65–0.7 μm, 0.7–0.8 μm, and 0.8–1.0 μm, while the reading interval was set to 6 s (the least frequency). The vehicle used was a 2010 model, white Maruti Suzuki Dzire, with a working AC (non-HEPA air filter); the vehicle underwent servicing a week before sampling and was in excellent condition. The instrument and the sampling probe were set up on the front passenger seat next to the driver (as shown in Fig. 2) at a distance similar to the passenger breathing zone (although the height of the sampling probe was lower) to measure the driver exposure.

[1] https://pdf.directindustry.com/pdf/grimm-aerosol-technik/model-11-a/69071-654475.html".

a) Route 1- DTU to IGI T2 parking

b) Route 2- DTU to Mohan Nagar

Fig. 1 Route used for the data collection

2.3 Sampling Protocols

The data was collected twice each day during morning and evening peak hours for two days on each route (one working day and one non-working day). The peak hours were selected based on Delhi's traffic flow data [6], with morning peak hours being 9 AM to 11 AM and 11 AM to 1 PM, while evening peak hours were 5 PM to 8 PM and 4 PM to 7 PM, respectively for weekdays and weekends.

The car was vacuum cleaned before starting each trip, and OPC was calibrated and allowed to warm up for 15 min before the trip. The sampling was done with closed windows (as it is the most common setting in winter), while the ventilation setting used were fan—off, re-circulation (RC)—off, and AC—off as this was found to be the highest exposure setting with windows closed [23]. The same driver drove the

Table 1 Technical specification of GRIMM Technik, model 11-A portable aerosol. spectrometer

Technical parameter	Range
Supply voltage	18–24 VDC
Maximum current	2.5 A
Temperature range (operating)	0 to + 40 °C
Max relative humidity (operating)	r.H. < 95% (not condensing)
Sample air temperature	0 to 40 °C
Laser	Wavelength: $\lambda = 600$ nm, Power $P_{max} = 40$ mW
Size channel (μm)	31 channels: 0.25/0.28/0.3/0.35/0.4/0.45/0.5/0.58/0.65/0.7/0.8/1.0/1.3/1.6/2/2.5/3/3.5/4/5/6.5/7.5/8.5/10/12.5/15/17.5/20/25/30/32
Particle concentration	1 to 3,000,000 particles/litter
Sample flow rate	1.2 l/min, ±5% constantly through control
Dust collection	47 mm PTFE filter (without supporting tissue)

Fig. 2 GRIMM Technik, model 11-A portable aerosol spectrometer

car to minimize the variation due to the driver's behaviour. Also, efforts were made to avoid any sudden acceleration or deceleration of the vehicle, while top speed was limited to 50kmph to maintain a constant wind flow inside the car [24–26]. Also, the traffic congestion zone was monitored and marked visually and using Google Maps, while the traffic behaviour was also observed visually. The congestion zones were divided into three categories:

(a) Planned congestion zone (grey columns in Fig. 4): they include traffic signals or manually controlled intersections where the local authorities regulate the traffic stoppage in a planned way.

b) The orange congestion zone (orange columns in Fig. 4): it includes the zone where traffic density was high and the vehicles were moving at a speed below 30 kmph.
c) The red congestion zone (red columns in Fig. 4) includes the zones where the traffic density was dense and the vehicles were halted completely or were moving below 10 kmph.

Both the Orange congestion zone and the Red congestion zone were unplanned zones, and the study only included the unplanned congestion zones having a duration of more than 60 s. The data was collected in the form of PNC as a number per cm^3 from the aerosol spectrometer and stored in an MS Excel spreadsheet. All the data was filtered, sorted, and analysed using the analysis tools of MS Excel, while data interpretation was made using a visual interpretation of the graph.

3 Results and Discussions

3.1 Particle Size Distribution

The PNC data was collected for different size bins which were <0.25 μm, 0.25–0.28 μm,0.28–0.30 μm, 0.30–0.35 μm, 0.35–0.40 μm, 0.40–0.45 μm, 0.45–0.50 μm, 0.50–0.58 μm, 0.58–0.65 μm, 0.65–0.7 μm, 0.7–0.8 μm, and 0.8–1.0 μm. Inside the cabin, it was found that the particle size distribution for PM 1 was dominated by the quasi-UFP, contributing nearly 74–80% of the PNC, while the particles having Dp < 0.5 contributed 96–98% of total PNC for PM-1 (as shown in Fig. 3a). This can be attributed to the fact that the smaller size particles are more capable of infiltrating the vehicle cabin [27] and are also in accordance with the general fact that smaller particles make up the bulk of PNC in total PMs [13, 27]. The dominance of small particles in heavy traffic density can also be attributed to the fact that, in Indian metropolitan cities like Delhi, people tend to drive bumper to bumper and as per a study by Xu et al. in 2020, the PNC of smaller particles is higher near the vehicle exhaust and reduces as we move further away [28]. In the study, it was also noticed that the particles having a size range of <0.25 μm, 0.25–0.28 μm, 0.28–0.30 μm, and 0.30–0.35 μm follow a similar trend (as shown in Fig. 3b) and hence they were combined to form a single bin range of <0.35 μm.

3.2 Impact of Traffic Congestion

A direct impact of the congestion zone on the PNC can be seen in Fig. 4a and 4b. During the study, the average PNC was found to be relatively high when the traffic density was high. As per Fig. 4b, Higher PNC was found on weekdays (high traffic density) compared to weekends (low traffic density). A direct link between

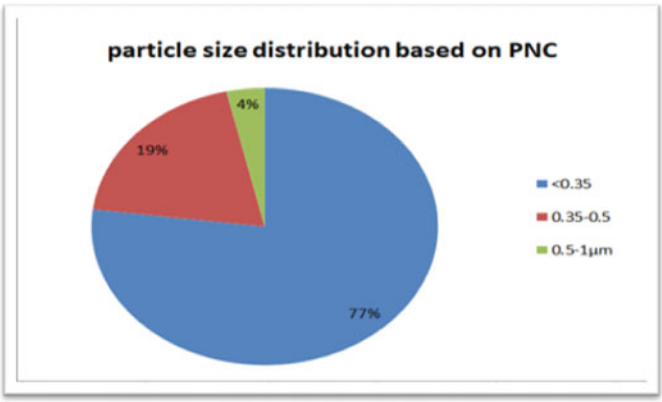

a) Particle size contribution based on PNC

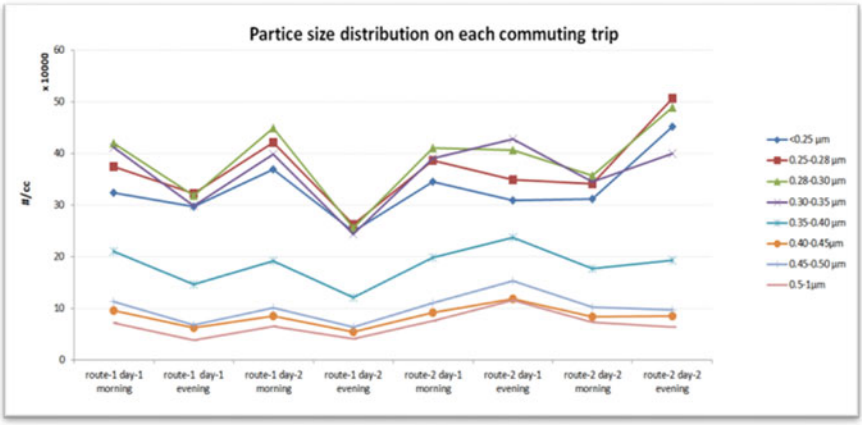

b) Particle size distributions on each commuting trip

Fig. 3 Particle size distribution

the traffic congestion zone and PNC was observed. It was also observed that the traffic congestion could cause a sudden increase in PNC concentration for quasi-UFP having a size of <0.35 µm. Higher traffic congestion has resulted in higher variation in PNC for qUFP with a standard deviation being as high as 6.6×10^5 #/cc on weekdays while on weekends, the standard deviation was found to be 1.1×10^5 #/cc.

The larger particles (having size > 0.5 µm), on the other hand, show a negligible relationship with traffic congestion as they show a maximum standard deviation of 3.5×10^4 #/cc. This discrepancy between the finer and coarse particles may be due to the different penetration abilities of both particles [29] as well as the fact that in

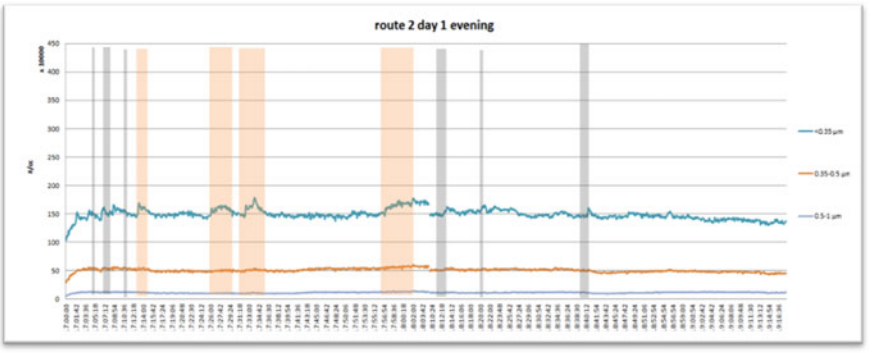

a) Route-2 evening weekend

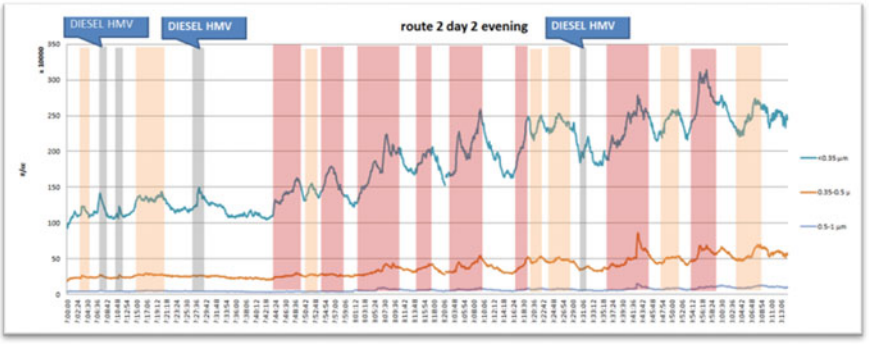

b) Route-2 evening weekday

Fig. 4 Impact of traffic congestion zone on PNC (#/cc) weekday versus weekend

the near exhaust environment, the particles emitted from the vehicular exhaust are finer [30, 31].

3.3 Impact of Congestion Zones

For this study, we categorize the congestion zones into three categories, i.e., red zone, orange zone, and planned congestion zone (i.e., traffic signal). During the study, it was observed that amongst the planned and unplanned (red and orange) congestion zones, the planned congestion zone showed a slight increase (i.e., 0.5×10^5–1.5×10^5 #/cc) in the PNC, while the unplanned congestion zone contributed to a significant increase (4×10^5 to 6×10^5 for red zone and 2×10^5 for orange zone) in the PNC of qUFP.

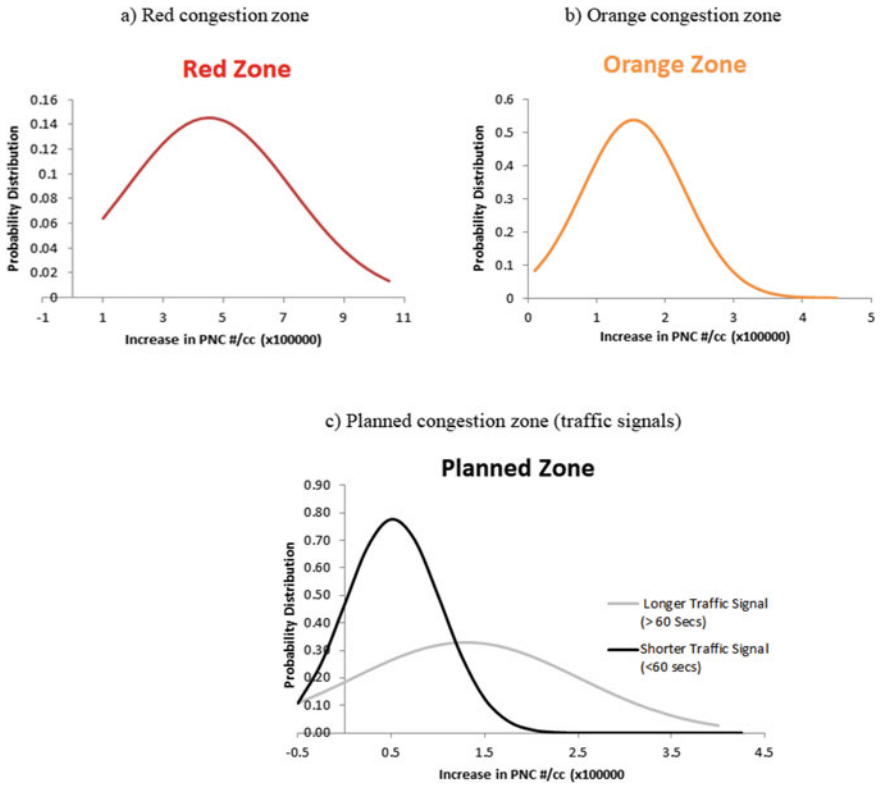

Fig. 5 Probability Distribution of Increase in PNC in different congestion zones

3.3.1 Impact of Red Zones

During the red zone, a quite significant increase was observed in the concentration of qUFP, with an increase as high as 75%, while in terms of PNC, the peak concentration of 3.1×10^6 #/cc was observed during a single red zone. The maximum increase of PNC was noted to be 1×10^6 #/cc, while as Fig. 5a shows, an average increase in the order of 4×10^5 to 6×10^5 #/cc (25–30%) was observed during the red zone. This high increase may be due to the slow speed of vehicles (which contributes to higher PNC formation [32] coupled with the stop-start movement of cars during the red zone and bumper-to-bumper driving) (Rodriguez et al. 2020).

3.3.2 Impact of Orange Zones

A moderate increase was observed during the orange zone in the qUFP concentration. As shown in Fig. 5 b, an average rise of 1.5×10^5 to 2×10^5 #/cc was observed in the orange zone, which was lower than the increase during the red zone. The lower

intensity of growth can be attributed to the fact that traffic density was still moving at some pace in the orange zone and there was a relative distance between the vehicles, which allowed for some degree of dilution of particles [33, 34].

3.3.3 Impact of Planned Congestion Zone (Traffic Signals)

A relationship between traffic signal duration and PNC was observed during the study. Traffic signals with a short duration (less than 60 s) show a minor or negligible impact on PNC, as can be seen in Fig. 5c, with a shorter duration signal having a sharper peak and resulting in an average increase of just 0.5×10^5 #/cc. On the other hand, in the case of traffic signals with longer duration (>60 secs), the peak is much damper and, on the right, the average measurable increase in PNC was observed in the order of 1.5×10^5 to 2×10^5 #/cc (Fig. 5 c). A similar rise in PNC was also found by Wang et al. [35].

3.4 Impact of Leading Vehicle or Nearby Vehicles

During the study, a strong relationship was noticed between the increase in PNC and the characteristics of the leading vehicle (i.e., the vehicle in front of the test car) as well as that of nearby vehicles. It was observed that when a large diesel Heavy Motor Vehicle (HMV) like a truck or tractor was present in the vicinity of the test vehicle, it caused a sudden increase in the PNC of quasi-fine particles. An average spike of 20–40% was observed during the study. This can be attributed to diesel engines generating more PNC due to the high sulphur content in diesel [30]. The max increase observed was 75% (9×10^5 #/cc) on the 18th morning. This high peak may be due to the combined effect of the Red zone and the presence of HMV. A similar trend was also observed in the study conducted by [36, 37]. While all the vehicles resulted in some increase in PNC, E-vehicles show the most negligible impact on the PNC, which can be attributed to the fact that E-Vehicle has zero direct emissions.

4 Conclusion

Various studies have shown that whenever a person commutes and spends only a small portion of his daytime, it can contribute up to 50% of their daily fine particle exposure. As per the study conducted by [38], one hour of in-cabin commuting can contribute to up to 50% of fine particle exposure, while a study by [39] in LA found a similar result in which 33–45% of daily fine particle exposure can be linked directly to time spent in commuting (6% of day which is less than Indian average of 7%). This exposure can further increase during congestion, as congestion increases commuting time. This study established a direct relation between congestion and

in-cabin concentration of qUFP. During the investigation, it was observed that the PNC was higher (with peak concentration 3.1×10^6 #/cc) on route 2, which has higher traffic density and more congestion zone. Impact on PNC was also found higher (almost 10 times more deviation) on a working day than on a non-working day. The study revealed that unplanned congestion zones (red congestion zone) cause a more potent increase (15% more average increase) in PNC as compared to planned congestion zones. A secondary relationship between the duration of the planned zone was also discovered, with traffic signal having short duration (<60 s) showing a negligible or low impact on PNC of qUFP, while long duration signals (>60 s) showing a visible increase. The impact of the type of nearby vehicle was also visible in the study as the presence of diesel HMV resulted in a massive and sharp spike in PNC for qUFP. Based on the study outcomes, it can be concluded that by reducing the congestion zones and having shorter duration traffic signals, we can reduce the commuter exposure to qUFP by a great extent. During this study, it has been found that the traffic congestion mainly affected the smaller size particles ($Dp < 0.35\ \mu m$) while having no or negligible impact on larger size particles ($Dp > 0.5\ \mu m$).

Due to the limitation of the monitoring instrument, this study focuses on particles up to the range of qUFP, while the Covid conditions limited the sample size to just 1 season. Furthermore, the study's scope was limited to studying the impact of congestion only, and the impact of vehicle condition and driving behaviour were kept constant. Based on the trend observed in this study, it can be assumed that traffic congestion could have a significant impact on the concentration of UFP, further research studying the impact of traffic zone on UFP is needed to be carried out.

References

1. Health Effects Institute. State of Global Air 2019. Heal Eff Institute 24 (2019). https://www.stateofglobalair.org/sites/default/files/soga_2019_report.pdf
2. Kumar P, Robins A, Vardoulakis S, Britter R (2010) A review of the characteristics of nanoparticles in the urban atmosphere and the prospects for developing regulatory controls. Atmos Environ 44:5035–5052. https://doi.org/10.1016/j.atmosenv.2010.08.016
3. IQAir. World Air Quality Report (2019) 2019. World Air Qual Rep 1–35
4. Beig G, Ghude SD, Deshpande A (2010) Scientific evaluation of air quality standards and defining air quality index for India. Indian Inst Trop Meteorol 1–31
5. IQAir. World Air Quality Report (2020) 2020, World Air Qual Rep 1–35
6. Tomtom (2019) Traffic Index results. https://www.tomtom.com/traffic-index/ranking
7. MoveInSync (2019) Indians Spend 7% of Their Day in Office Commute. Travel Time Rep Q1 2019 vs Q1 2018 8
8. Mishra RK, Mishra AR, Pandey A (2020) Commuters' exposure to fine particulate matter in Delhi City. Lect Notes Civ Eng 69:369–377. https://doi.org/10.1007/978-981-15-3742-4_23
9. Nagar J, Akolkar A, Kumar R (2014) A review on airborne particulate matter and its sources, chemical composition and impact on human respiratory system. Int J Environ Sci 5:447–463. https://doi.org/10.6088/ijes.2014050100039
10. World health statistics (2019) WHO world heatlh statistics 2019, 2019th ed. WHO
11. Junaid M, Syed JH, Abbasi NA, Hasmi MZ, Malik RN, Pei DS (2018) Status of indoor air pollution (IAP) through particulate matter (PM) emissions and associated health concerns in South Asia. Chemosphere 191:651–663. https://doi.org/10.1016/j.chemosphere.2017.10.097

12. Hussein T, Hämeri K, Aalto PP, Paatero P, Kulmala M (2005) Modal structure and spatial-temporal variations of urban and suburban aerosols in Helsinki - Finland. Atmos Environ 39:1655–1668. https://doi.org/10.1016/j.atmosenv.2004.11.031
13. Air Quality Expert Group (2018) Ultrafine Particles (UFP) in the UK. 96. https://uk-air.defra.gov.uk
14. Kelly FJ, Fussell JC (2015) Air pollution and public health: emerging hazards and improved understanding of risk. Environ Geochem Health 37:631–649. https://doi.org/10.1007/s10653-015-9720-1
15. Franchini M, Mannucci PM (2007) Short-term effects of air pollution on cardiovascular diseases: Outcomes and mechanisms. J Thromb Haemost 5:2169–2174. https://doi.org/10.1111/j.1538-7836.2007.02750.x
16. Delfino RJ, Sioutas C, Malik S (2005) Potential role of ultrafine particles in associations between airborne particle mass and cardiovascular health. Environ Health Perspect 113:934–946. https://doi.org/10.1289/ehp.7938
17. Das A, Kumar A, Habib G, Vivekanandan P (2020) Insights on the biological role of ultrafine particles of size PM<0.25: A prospective study from New Delhi. Environ Pollut 268:115638. https://doi.org/10.1016/j.envpol.2020.115638
18. Sotty J, Kluza J, Sousa C De, Tardivel M, Antherieu S, Alleman LY, Canivet L, Perdrix E, Loyens A, Marchetti P, Guidice JM Lo, Gorcon G (2020) Mitochondrial alterations triggered by repeated exposure to fine (PM2.5-0.18) and quasi-ultrafine (PM0.18) fractions of ambient particulate matter. Environ Int 142:105830. https://doi.org/10.1016/j.envint.2020.105830
19. Chen R, Hu B, Liu Y, Xu Z, Yang G, Xu D, Chen C (2016) Beyond PM2.5: The role of ultrafine particles on adverse health effects of air pollution. Biochim Biophys Acta – Gen Subj 1860:2844–2855. https://doi.org/10.1016/j.bbagen.2016.03.019
20. Pant P, Habib G, Marshall JD, Peltier RE (2017) PM2.5 exposure in highly polluted cities: A case study from New Delhi, India. Environ Res 156:167–174. https://doi.org/10.1016/j.envres.2017.03.024
21. Onat, B., Şahin, Ü.A., Uzun, B., Akin, U., Özkaya, F., Ayvaz, C.,: Determinants of exposure to ultrafine particulate matter, black carbon, and PM2.5 in common travel modes in Istanbul. Atmos Environ 206:258–270 (2019). https://doi.org/10.1016/j.atmosenv.2019.02.015
22. Li F, Kreis JS, Cyrys J, Wolf K, Karg E, Gu J, Orasche J, Abbaszade G, Peters A, Zimmermann R (2018) Spatial and temporal variation of sources contributing to quasi-ultrafine particulate matter PM0.36 in Augsburg, Germany. Sci Total Environ 631–632:191–200. https://doi.org/10.1016/j.scitotenv.2018.03.041
23. Leavey A, Reed N, Patel S, Bradley K, Kulkarni P, Biswas P (2017) Comparing on-road real-time simultaneous in-cabin and outdoor particulate and gaseous concentrations for a range of ventilation scenarios. Atmos Environ 166:130–141. https://doi.org/10.1016/j.atmosenv.2017.07.016
24. Zhu S, Marshall JD, Levinson D (2016) Population exposure to ultrafine particles: Size-resolved and real-time models for highways. Transp Res Part D Transp Environ 49:323–336. https://doi.org/10.1016/j.trd.2016.09.010
25. Chawla, K., Singh, R., Singh, J (2020) Segregation and recycling of plastic solid waste: a review. In: Lecture Notes in Mechanical Engineering. pp 205–221
26. Campagnolo D, Cattaneo A, Corbella L, Borghi F, Buono LD, Rovelli S, Spinazzé A, Cavallo DM (2019) In-vehicle airborne fine and ultra-fine particulate matter exposure: The impact of leading vehicle emissions. Environ Int 123:407–416. https://doi.org/10.1016/j.envint.2018.12.020
27. Knibbs LD, de Dear RJ, Morawska L (2010) Effect of cabin ventilation rate on ultrafine particle exposure inside automobiles. Environ Sci Technol 44:3546–3551. https://doi.org/10.1021/es9038209
28. Xu G, Wang J, Qiao X (2020) Numerical study on evolution of ultrafine particles emitted from vehicle exhaust with multi-dynamical behaviors. Atmos Environ 244:117916. https://doi.org/10.1016/j.atmosenv.2020.117916

29. Lee ES, Stenstrom MK, Zhu Y (2015) Ultrafine particle infiltration into passenger vehicles. Part I: Experimental evidence. Transp Res Part D Transp Environ 38:156–165. https://doi.org/10.1016/j.trd.2015.04.025
30. Banerjee T, Christian RA (2018) A review on nanoparticle dispersion from vehicular exhaust: Assessment of Indian urban environment. Atmos Pollut Res 9:342–357. https://doi.org/10.1016/j.apr.2017.10.009
31. Zhong J, Nikolova I, Cai X, MacKenzie AR, Harrison RM (2018) Modelling traffic-induced multicomponent ultrafine particles in urban street canyon compartments: Factors that inhibit mixing. Environ Pollut 238:186–195. https://doi.org/10.1016/j.envpol.2018.03.002
32. Bhardawaj A, Habib G, Kumar A, Singh S, Nema AK (2017) A review of ultrafine particle-related pollution during vehicular motion, health effects and control. J Environ Sci Public Heal 01:268–288. https://doi.org/10.26502/jesph.96120024
33. Chang VWC, Hildemann LM, Chang CH (2009) Dilution rates for tailpipe emissions: Effects of vehicle shape, tailpipe position, and exhaust velocity. J Air Waste Manag Assoc 59:715–724. https://doi.org/10.3155/1047-3289.59.6.715
34. Rodriguez R, Murzyn F, Mehel A, Larrarte F (2020) Dispersion of ultrafine particles in the wake of car models: A wind tunnel study. J Wind Eng Ind Aerodyn 198:104109. https://doi.org/10.1016/j.jweia.2020.104109
35. Wang Y, Zhu Y, Salinas R, Ramirez D, Karnae S, John K (2008) Roadside measurements of ultrafine particles at a busy urban intersection. J Air Waste Manag Assoc 58:1449–1457. https://doi.org/10.3155/1047-3289.58.11.1449
36. Strawa AW, Kirchstetter TW, Hallar AG, Ban-Weiss GA, McLaughlin JP, Harley RA, Lunden MM (2010) Optical and physical properties of primary on-road vehicle particle emissions and their implications for climate change. J Aerosol Sci 41:36–50. https://doi.org/10.1016/j.jaerosci.2009.08.010
37. Tsang H, Kwok R, Miguel AH (2008) Pedestrian exposure to ultrafine particles in Hong Kong under heavy traffic conditions. Aerosol Air Qual Res 8:19–27. https://doi.org/10.4209/aaqr.2007.09.0041
38. Zhu Y, Eiguren-Fernandez A, Hinds WC, Miguel AH (2007) In-cabin commuter exposure to ultrafine particles on Los Angeles freeways. Environ Sci Technol 41:2138–2145. https://doi.org/10.1021/es0618797
39. Fruin S, Westerdahl D, Sax T, Sioutas C, Fine PM (2008) Measurements and predictors of on-road ultrafine particle concentrations and associated pollutants in Los Angeles. Atmos Environ 42:207–219. https://doi.org/10.1016/j.atmosenv.2007.09.057

Study on the Effect of Variation in the Geometric Parameters of the Work-Zone on Traffic Safety Using the Simulation Approach

Omkar Bidkar, Shriniwas Arkatkar, Gaurag Joshi, and Said M. Easa

Abstract From a safety and capacity perspective, road transit is a crucial means of transportation. It is one of the difficult components to comprehend the performance of the road network, especially in terms of efficiency and safety on the roads. The need for road transportation is very high because of a constant increase in traffic demand. Road maintenance and construction activities are fairly prevalent and produce a variety of work-zones. Work-Zone of any road is critical from both safety and capacity points of view. Work-Zone safety-related issues are very critical from both operation and maintenance points of view. Work-Zone geometry has a significant effect on both traffic safety and capacity. Various work-zone geometric parameters are length of work-zone, lane-drops of work-zone and tapering length of work-zone. The research paper studies the effect of variation in the geometric parameters of the work-zone on traffic safety using a simulation approach. The research paper studies the geometric parameter variation of work-zone on traffic safety at the microscopic level using various microscopic parameters such as box and whisker plots, descriptive statistics, trajectories, hysteresis plots and conflict probability.

Keywords Work-zone · Geometric parameters · Traffic safety · Conflict probability · Trajectories

O. Bidkar (✉)
SKN Sinhgad College of Engineering, Korti, Pandharpur 413304, India
e-mail: omkar.bidkar93@gmail.com

S. Arkatkar · G. Joshi
Sardar Vallabhbhai National Institute of Technology, Surat 395007, India

S. M. Easa
Ryerson University, Toronto 66777, Canada

A. Dhamaniya et al. (eds.), *Recent Advances in Traffic Engineering*, Lecture Notes in Civil Engineering 377, https://doi.org/10.1007/978-981-99-4464-4_11

1 Introduction

Since everyone is either directly or indirectly connected to road transportation, it performs a crucial role for all people. It is one of the difficult components to comprehend the performance of the road network, especially when looking at road efficiency and safety. Traffic in developing nations like India is diverse, which leads to accidents of various severity. As a result, traffic safety is becoming increasingly important in daily life. Therefore, it is important to research traffic safety in both the WZ and WWZ sections under a variety of highway conditions. A work-zone (WZ) is an area where there are road construction activities taking place that involve lane closures, detours and moving equipment (IRC SP: 55). Depending on the state of the roadways, different sections of the highway may not be as safe for traffic. In India, WZ collisions and confrontations happen frequently. In a nation like India, work on WZ traffic safety is really minimal. Studying transportation safety at both the macroscopic and microscopic levels is therefore crucial. As a result, for both the WWZ and WZ sections, traffic safety is examined at both the macroscopic and microscopic traffic levels in this study.

2 Literature Review

The prevalence and characteristics of crashes at various WZ were researched by Garber et al. [1]. Five WZ locations—advance warning, transition, longitudinal buffer, activity and termination—were used to analyse crashes. The proportionality test was performed to identify significant differences at the 5% significance level at various WZ locations. The findings show that, regardless of the type of highway, the activity area is the crucial site for WZ crashes, and rear-end collisions are the most common crash type. The findings also show that there are much more sideswipe-in-the-same-direction crashes in the transition region than in the warning area. Zheng et al. [2] concluded that traffic safety for rear-end collision could be computed using conflict probability using the GEV distribution of TTC and DRAC. The method incorporates traffic conflicts from various locations and times to create a consistent generalized extreme value (GEV) model for estimating the treatment effect. A hierarchical Bayesian framework also accommodates unobserved heterogeneity between different sites by connecting potential factors to GEV parameters. Miller et al. [3] studied the safety of construction WZ during night-time. He has developed various threshold levels for operating speed on rods. The threshold level involves the average speed of different categories of vehicles with standard deviation. Wang et al. [4] studied rear-end conflicts at various intersections. He found that rear-end conflicts are the most common accident type at signalized intersections. The rear-end accident probability is dependent upon the aggressive type. The aggressive type is high risk followed by conservative, followed by normal. Tarko et al. [5] justified the Lomax distribution to predict the crash probability for given critical conflicts. The maximum

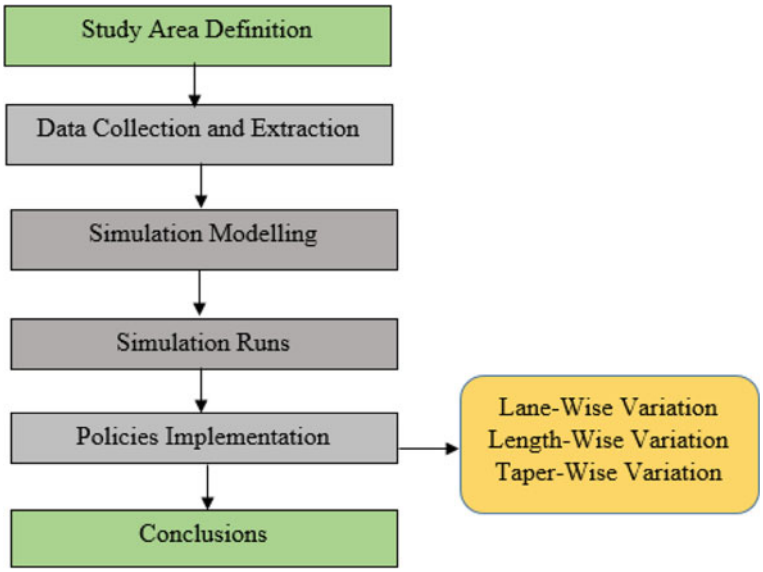

Fig. 1 Descriptive methodology of the study

likelihood estimate (MLE) method and the probability-weighted moment's method calculate the crash probability. The above study finally found that the threshold value for Time to Collision calculates the number of crashes on the field. Guo et al. [6] studied variables at motorway diverge locations that affect crash rates by collision type. For the purpose of safety modelling, the author created a novel random parameter multivariate Tobit model. The effects of risk factors on various collision types were estimated to have separate effects after taking into account the correlation between collision types and unobserved heterogeneity across observations.

3 Methodology

Figure 1 describes the methodology of the study in a detailed manner.

4 Analysis and Results

This section is divided into three types which are Box and Whisker plots, Trajectories and Conflict Probability.

4.1 Box and Whisker Plots

Box and Whisker plots of Following Time (FT) are studied at the microscopic level. Taper-wise, Length-wise and Lane-drop-wise box and whisker plots are drawn and shown in Fig. 2. It is found from the figure that the following time increases with an increase in the rate of taper. As the following time of the section is less, there are more chances of conflicts and crashes. Hence, there are more conflicts and crashes with less tapering length. The number of conflicts and crashes increases with an increase in the tapering length of the section. It is found from the figure that the following time increases with an increase in the length of the work-zone. Hence, it is found that the number of conflicts and crashes increases with an increase in the number of work-zone lengths. It is found from the figure that the following time decreases with an increase in the number of lane-drops. As the following time of the section is less, there are more chances of conflicts and crashes. Hence, there are more conflicts and crashes with an increase in the lane-drops of the section.

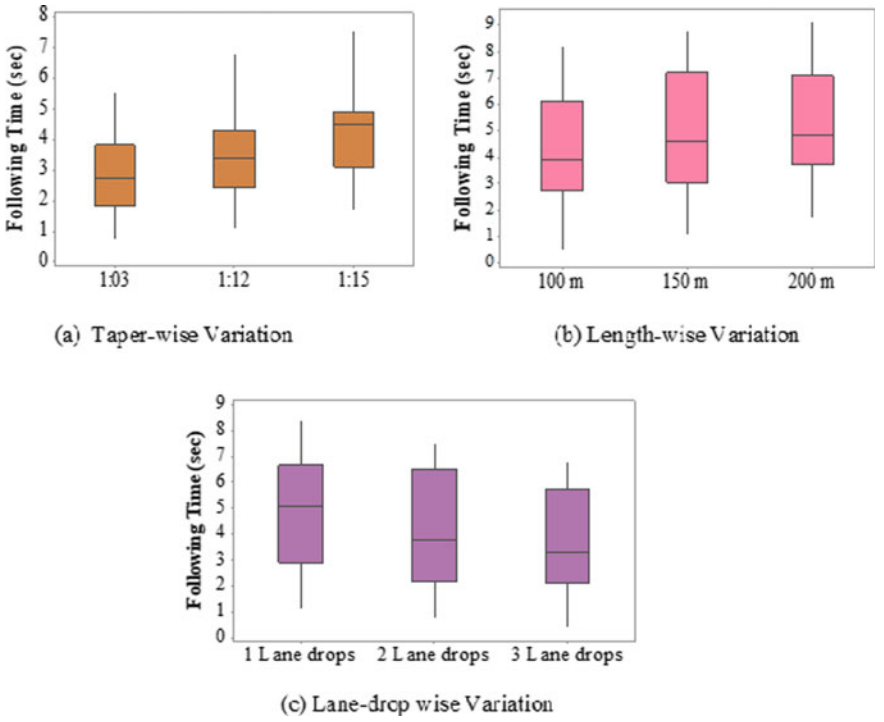

Fig. 2 Taper-wise, lane-drop-wise and length-wise box and whisker plots of following time (FT)

4.2 Trajectories

Traffic Behaviour at the microscopic level is studied by using the microscopic analysis. Length-wise, Taper-wise and Lane-drop-wise trajectories are plotted at the microscopic level.

Figure 3 shows the trajectories for various lane-drops, tapers and lengths of a work-zone. It is found from the figure that vehicles are closely spaced with each other both laterally and longitudinally for 2 and 3 lane-drops than 1 lane-drop. It is found from the figure that vehicles are closely placed with each other with less tapering rate of the work-zone. As the rate of taper increases, vehicles are separated from each other in both lateral and longitudinal directions. It is found from the figure that vehicles are closely placed with each other for a small length of the work-zone. As the length of the work-zone increases, vehicles separate each other laterally and longitudinally. Hence, it is proved that as the length of the work-zone increases, then there is a reduction in the number of conflicts and crashes.

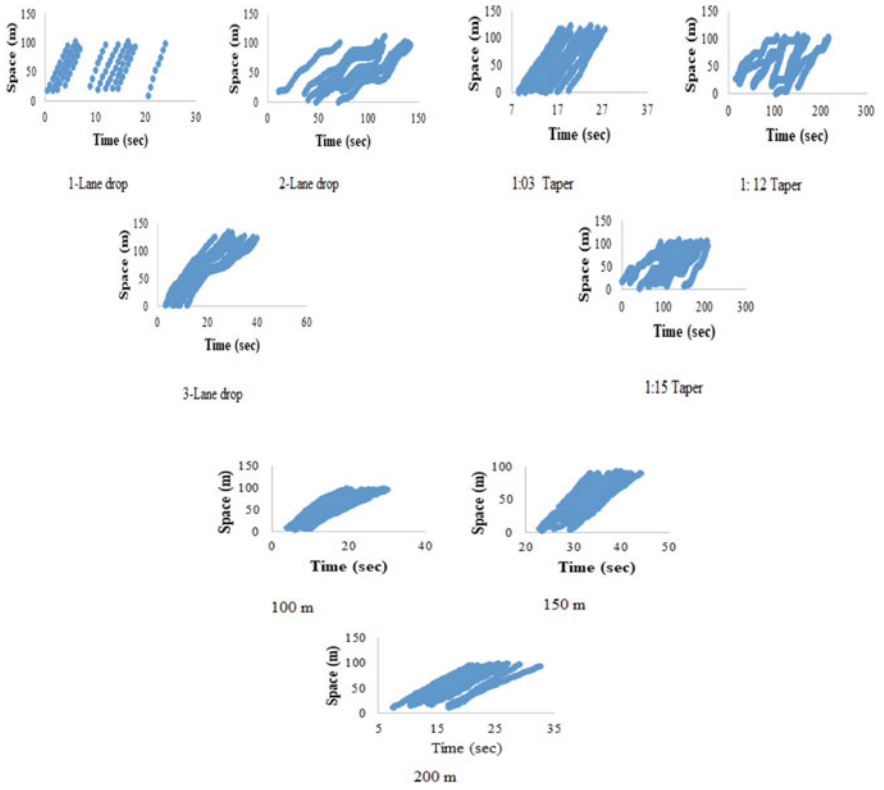

Fig. 3 Trajectories for various lane-drops, tapers and lengths of work-zone

Table 1 Lane-wise, taper-wise and length-wise conflict probability is calculated for different volumes of work-zones

Type of section	Type of volume		
Section type	High	Medium	Low
1-lane-drop, 100 m and 1:3 taper of WZ	0.33 (0.012)	0.26 (0.031)	0.21 (0.022)
2-lane-drops, 100 m and 1:3 taper of WZ	0.41 (0.041)	0.34 (0.034)	0.29 (0.024)
3-lane-drops, 100 m and 1:3 taper of WZ	0.48 (0.034)	0.41 (0.074)	0.35 (0.028)
01:03, 2 lane-drops and 100 m length of WZ	0.46 (0.014)	0.38 (0.025)	0.32 (0.031)
01:12, 2 lane-drops and 100 m length of WZ	0.34 (0.027)	0.28 (0.031)	0.21 (0.041)
01:15, 2 lane-drops and 100 m length of WZ	0.29 (0.014)	0.22 (0.031)	0.16 (0.029)
100 m, 2 lane-drops and 1:3 taper of WZ	0.44 (0.044)	0.34 (0.014)	0.29 (0.031)
150 m, 2 lane-drops and 1:3 taper of WZ	0.35 (0.022)	0.23 (0.041)	0.18 (0.031)
200 m, 2 lane-drops and 1:3 taper of WZ	0.29 (0.011)	0.15 (0.042)	0.11 (0.033)

4.3 Conflict Probability

Table 1 shows the length-wise conflict probability for different volumes. It is found from Table 1 that conflict probability decreases with increases in the length of the work-zone. It is also found from the table that conflict probability for High volume is greater than for Medium and Low volumes.

5 Conclusion

The following are important conclusions that are drawn from the given study:

(I) There is an effect of geometric parameters of the work-zone on traffic safety at the microscopic level.

(II) Trajectories have a greater effect on the work-zone geometry of the section. Trajectories are closely placed with each other with respect to both lateral and longitudinal directions for 2 and 3 lane-drops as compared to 1-lane-drop. Trajectories are closely placed with each other both laterally and longitudinally with decreasing rates of taper. Trajectories are closely placed with each other both laterally and longitudinally with decreasing length of taper.

(III) Conflict probability increases with an increase in the lane-drop for all types of volume. Conflict probability decreases with an increase in the rate of taper and conflict probability decreases with an increase in the length of the work-zone.

References

1. Garber NJ, Zhao M (2002) Distribution and characteristics of crashes at different work zone locations in Virginia. Transp Res Rec 1794(1):19–25
2. Zheng L, Sayed T, Essa M (2019) Validating the bivariate extreme value modelling approach for road safety estimation with different traffic conflict indicators. Accid Anal Prev 123:314–323
3. Miller L, Mannering F, Abraham DM (2009) Effectiveness of speed control measures on night-time construction and maintenance projects. J Constr Eng Manag 135(7):614–619
4. Wang W, Li Y, Lu J, Li Y, Wan Q (2019) Estimating rear-end accident probabilities with different driving tendencies at signalized intersections in China. J Adv Transp
5. Tarko AP (2018) Estimating the expected number of crashes with traffic conflicts and the Lomax distribution—A theoretical and numerical exploration. Accid Anal Prev 113:63–73
6. Guo Y, Li Z, Liu P, Wu Y (2019) Modeling correlation and heterogeneity in crash rates by collision types using full Bayesian random parameters multivariate Tobit model. Accid Anal Prev 128:164–174

Impact of the COVID-19 Pandemic on the Grocery Shopping Behavior of Individuals

Saladi S. V. Subbarao, B. Raghuram Kadali, B. C. H. Abhishek Kumar, and B. Semanth Reddy

Abstract Understanding the mobility patterns of human beings is important during the pandemic to assess the spread of ineffectual diseases. The present study attempted to explore the grocery shopping behavior of consumers before and during the COVID-19 pandemic conditions. To achieve this objective, a Google Forms-based online survey has been conducted (viz., the survey form has been circulated through electronic and social media) to understand consumer behavior and their daily mobility. The data is analyzed based on the socioeconomic characteristics and their impact on the frequency of shopping, shopping duration, mode of shopping, distance traveled for shopping, etc. From the analysis, it was inferred that the majority of individuals are restricting their shopping trips to nearby grocery shops and making shorter trips. The results of this study provide some insights into grocery shopping behavior, and it might be extended to other shopping-related activities.

Keywords Grocery shopping · Pandemic · COVID-19 · Consumer behavior · Chi-square test · Online survey

1 Introduction

The pandemic situation due to Corona Virus Disease (COVID-19) has begun in India in March 2020. However, many countries such as China, Italy, Spain, and the United States of America (USA) have experienced and been impacted severely by this outbreak of COVID-19, while the World Health Organization has initiated different pandemic plans and the entire globe has started rethinking the condition of COVID-19 by considering different preventive measures including the lockdown of the severely

S. S. V. Subbarao (✉) · B. C. H. A. Kumar · B. S. Reddy
Department of Civil Engineering, Ecole Centrale School of Engineering, Mahindra University, Hyderabad, Telangana 500043, India
e-mail: saladi.subbarao@mahindrauniversity.edu.in

B. R. Kadali
Department of Civil Engineering, NIT Warangal, Warangal, Telangana, India
e-mail: brkadali@nitw.ac.in

A. Dhamaniya et al. (eds.), *Recent Advances in Traffic Engineering*, Lecture Notes in Civil Engineering 377, https://doi.org/10.1007/978-981-99-4464-4_12

affected regions, travel bans, restrictions on recreational trips, imposing work-from-home, etc. Further, many others include shopping malls, schools, and public events that are shut down during this pandemic. In India, the countrywide lockdown started in March 2020, and subsequently, the lockdown has been lifted based on the number of cases. In India, essential services-based shopping trips (viz., particularly grocery and vegetables/fruits-related trips) are allowed during the lockdown period with strict enforcement of social distancing and limited operational hours. Research studies have explored the effectiveness of travel restrictions in controlling the spread of the outbreak of COVID-19 [1, 2], whereas many countries have imposed a travel ban which is one of the important measures to prevent the widespread infectious flu virus like COVID-19. It is essential to understand human travel patterns during the restricted travel bans and fulfilling the daily needs of human beings [3]. Researchers have also explored the impact of travel bans on the mobility patterns of people in China during different stages of COVID-19, and the results concluded that travel bans have a significant impact on the control of spreading diseases and such travel patterns may be useful for the healthcare professionals to understand the possible way of the spread of flu-based infectious diseases during a pandemic [4].

Viral diseases have a significant impact on the travel pattern due to the risk perception of the public [5]. To control the spread of the virus, it has been suggested to implement social distancing norms, and this social distancing leads to an increase in waiting time at shopping places in the form of long queues at the entrance, inside the shopping places, and also at the cash counters. These specific conditions might influence the consumer's psychological behavior and it may change their shopping trip behavior significantly. Though this kind of pandemic condition might be there for the short term and also it can't be denied in the future, it is necessary to understand consumer behavior and its impact on changes in travel behavior which gives an idea about the different strategies to face the future pandemic conditions. In this context, the objective of the proposed study is to estimate the impact of COVID-19 on shopping behavior and its related travel attitudes during the pandemic condition. The remainder section of the study is as follows. The literature review about the pandemic conditions and related travel behavior is given in Sect. 2, and the data collection and survey questionnaire are discussed in Sect. 3. Detailed descriptive analysis is provided in Sect. 4. Section 5 provides the potential conclusions from the study observations.

2 Literature Review

In general, travel is derived from demand, and it exhibits various activity-travel patterns and different travel behaviors [6]. Several research studies have explored the various factors that influence travel behavior including land-use characteristics, availability of transport modes, fear, and flu-type infectious diseases. Studies have shown that demographic variables, urban density, transit infrastructure, and land use factors have a significant impact on travel decisions [7]. Researchers have explored that

the increasing lifestyle and socio-demographic variables have significantly impacted individual accessibility within the geographic location in an urban environment [8]. Further, Kim et al. explored the impact of fear on travel behavior during the Middle East Respiratory Syndrome (MERS), and study results concluded that traveler fear has significantly influenced travel behavior during flu diseases [9]. The outbreak of diseases is one of the pandemic conditions, and there are other kinds of pandemic conditions such as cyclones and war that have a different level of impact on travel behavior.

Some studies found that Information and Communication Technologies (ICTs) influence travel patterns, and they concluded that change in technology makes a change in travel patterns over spatial and temporal [10]. Further, from past studies, it was observed that tourist consumer behavior largely affects travel behavior and they have proven that ICT has a significant role in tourist behavior which has an impact on the economy of a particular area [11, 12]. Researchers have identified that frequent Internet users will travel more frequently as compared to the non-Internet users due to various activities (viz., product search) on the Internet and which further changes their travel patterns [13]. Some research studies have identified that the travel time ratio is a predominant factor in the change in travel patterns of urban commuters which further impacts the activities of social changes [14]. In travel activities, shopping is a complex travel activity, and it has a significant impact on travel behavior [15, 16]. Grocery shopping has varied travel behavior related to mode choice and destination patterns for weekdays and weekends also. Online-based grocery shopping potentially changes user travel behavior, and many studies have focused on the quantification of this online shopping over store-based shopping [17]. Researchers have further focused on the individual choice between online versus store-based shopping, and the results concluded that choice-making is a complex task in particular grocery-based items [18]. Studies also focused on various factors such as the number of goods, time of the day shopping, weekend/weekday shopping, delivery cost, and impact of promotions and found that these situation-based factors in a particular quantity of goods have a positive impact on online grocery shopping choice [19]. Another research study explored the choice of travel mode for making grocery shopping trips, and the study results concluded that the household size and location of the grocery shop significantly influence the mode choice [20].

In general, during restricted movements, people plan to make fewer out-of-home activities and also give importance to comfort when making those activities. Further, these restricted movements have a negative impact on planning activities [21]. Also due to restricted travel, the active travel modes will be stimulated for short trips, and there will be a change in travel patterns and mode choice for making these patterns [22]. With the travel restrictions as well as the social distance norms, there is a significant drop in demand for travel which results in more activities that have been carried work from home and there are fewer trips for shopping as well as leisure [23]. However, people may use online-based shopping for their daily needs in major cities which results in some freight activity; still, it can be observed as the reduction in the number of trips due to restricted movements. Also, studies have proven that flu-based infectious diseases might change commuter travel mode choices [24]. It is also

important to understand the mode choice of commuters during the pandemic of the outbreak of infectious diseases. Researchers have studied the impact of social changes on travel behavior by using household travel survey data, and the results concluded that temporal and spatial characteristics significantly change travel behavior [25]. Researchers have also studied the pandemic situation of terror threats, and the results concluded that the pandemic of terror threats is significantly influenced by fear and risk perception of the public, particularly women, and the same resulted in the usage of personalized vehicles [26]. Another research study explored the pandemic impact of terror and ineffectual disease on travel behavior, and results revealed that travelers are much more fearful of ineffectual diseases while they travel in public transportation [27]. Other research studies explored that fear has a significant impact on travel behavior analysis [28]. Further, researchers have explored consumer behavior during pandemic conditions of Severe Acute Respiratory Syndrome (SARS), and the results concluded that pandemic conditions severely impacted the travel patterns of people's daily needs [29].

Based on the above studies, it can be inferred that a significant contribution was done by the researchers in understanding the impact of risk perception and pandemic conditions on travel behavior. Also, there is a good number of works related to shopping trips, and their associated activities during pandemic conditions are identified. But with the self-experience during the COVID-19 pandemic conditions, the authors felt that it is necessary to study grocery shop-based trips during pandemic conditions and the risk perception of the users during such trips. In this direction, the proposed study aims to identify the behavior of people for making daily essential-based trips and the impact of socioeconomic characteristics on their shopping patterns during pandemic conditions.

3 Data Collection

The survey instrument is designed in such a way that it is suitable for online administration by keeping the pandemic COVID-19 in view, and a random sampling technique was adopted for the administration. The survey questionnaire was administered to a wide group of people using various electronic and social media like E-mails, Facebook, WhatsApp, and LinkedIn. The survey has been conducted during April 10–30, 2020, and approximately 840 samples were used for the analysis after removing incomplete samples. The primary purpose of the survey is to obtain information on individual grocery shopping behavior during and before the lockdown conditions due to the pandemic, COVID-19.

3.1 Design of Survey Instrument

The survey instrument contains four-folded questions which include socio-demographic characteristics, grocery trip-related information before lockdown, grocery trip-related information during the lockdown, and the anticipated user behavior post lockdown conditions. The socio-demographic characteristics include gender, age, income, and vehicle ownership. Grocery trip-related information before and during lockdown contains the mode of shopping (online or offline), distance traveled for shopping, shopping duration, frequency of shopping, the amount spent on shopping, type of payment at shopping destinations (cash or card or payment apps), etc. The same information collected from the individuals before lockdown as well as during lockdown will be useful for observing the behavior of individuals before and during the lockdown. Further, the survey instrument contains the anticipated behavior of the individuals after the lockdown. This section contains questions related to changes in travel patterns, perception of public transportation, etc.

3.2 Data Collection

The present study included 840 samples from the participants out of 860 samples collected after performing data mining, and all individuals in the sample data are aged between 24 and 54 years. Survey questionnaires are circulated online, and data is received in the form of Excel sheets. Among these participants, nearly 40% are workers, 24% are students, and the remaining are non-workers. Further, it has been observed from the data that more than 60% of individuals have a monthly income range of less than Rs. 50,000, but, at the same time, nearly 18% of the individuals belong to the high-income group, which are having a monthly income range of more than Rs. 1,00,000. Of the total respondents, it has been observed that more than 70% have a minimum education level of Graduation, and nearly 90% of individuals have at least one car at home. Table 1 shows the descriptive statistics of the sample collected, and it also shows the mean and standard deviation values of the collected data.

4 Data Analysis

The basic methodology adopted for this study is to understand the individual behavior before and during COVID-19 for making their grocery shopping trips. In this process, the study analyzed the socioeconomic characteristics of the individuals and their impact on the frequency of shopping, mode of shopping, the amount spent on shopping, and distance traveled for shopping before and during COVID-19. Figure 1 depicts the distribution of age groups among respondents, and Table 2 depicts the

Table 1 Descriptive statistics of the data collected from the survey

Factor	Description (code)	Number of responses	Percentage (%)	Mean	Standard deviation
Gender	Male (1)	636	77	1.77	0.42
	Female (0)	191	23		
Age	<20 years (1)	101	12.21	37.43	13.39
	20–30 years (2)	339	40.99		
	31–40 years (3)	209	25.27		
	41–50 years (4)	105	12.7		
	>50 years (5)	73	8.83		
Occupation	Student (1)	195	23.6	2.12	0.76
	Non-worker (2)	335	40.5		
	Worker (3)	297	35.9		
Monthly income	<Rs. 10,000 (1)	141	17.04	2.18	1.11
	<Rs. 10,001–20,000 (1)	162	19.6		
	Rs. 21,000–50,000 (2)	216	26.12		
	Rs. 51,000–100,000 (3)	162	19.59		
	>Rs. 100,000 (4)	146	17.65		
Education	Matriculation (10th)	116	14.03	3.27	1.02
	10 +2/Diploma	103	12.45		
	Graduation	255	30.83		
	Post-graduation and above	353	42.68		
Vehicle ownership	0	114	13.78	1.39	0.91
	1	394	47.64		
	2	220	26.6		
	>2	99	11.97		

distribution of income ranges among respondents. From Fig. 1, it has been observed that the majority share of respondents belongs to the age group of 20–30 years. From Table 2, it can be observed that nearly 17% of the individual's monthly income is less than Rs. 10,000, and nearly 18% of the individuals are earning more than Rs. 1,00,000 per month, which clearly shows the variation between the economic levels of the individuals.

Further, nearly 53% of individuals are working from home due to COVID-19. Among these people, nearly 18% of the individuals belonging to the high-income group (earning more than Rs. 1,00,00 per month) are working from home and at the

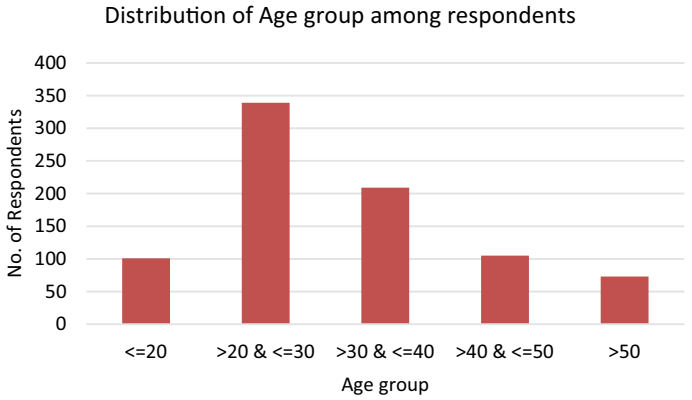

Fig. 1 Distribution of age group among respondents

Table 2 Distribution of income ranges among respondents

Income level	No. of respondents	% no. of respondents
<10,000	141	17
10,001–20,000	162	19.6
20,001–50,000	216	26.1
50,001–100,000	162	19.6
>100,000	146	17.7

same time, a mere 30% of the individuals from the low-income group (earning less than Rs. 10,000 per month) are working from home. These statistics clearly show that people working on a daily wage basis or in small-scale industries don't have the luxury of working from home. The majority of the individuals who are working in managerial or executive positions are getting a choice of working from home.

4.1 Mode Choice Behavior of Individuals

Regarding the mode choice behavior of individuals, a considerable difference was observed between the participants before the pandemic and during the pandemic. Nearly 10% of individuals are making trips using PT, Ride-hail, and auto-rickshaw before pandemic conditions, but during the pandemic the share of these modes is nil. Further, a considerable increase in the mode share was observed for private modes like cars and two-wheelers. Walking trips increased from 19 to 31% which shows that people are inclined to make shorter trips or maintenance trips during the pandemic time. Table 3 shows the percentage share of the mode choice of individuals before and during pandemic conditions.

Table 3 Percent share of the mode choice of individuals before and during pandemic conditions

Mode choice	The percentage share of individuals	
	Before pandemic	During pandemic
Public transit	4.7	0
Ride hail (Ola/Uber)	0.6	0
Auto-rickshaw	3.1	0
Car	6.9	8
Two-wheeler	65.8	60.7
Walk	18.9	31.3

4.2 The Shopping Behavior of Individuals

Regarding shopping destinations, it was observed that due to the COVID-19 pandemic, individuals constrain themselves to nearby grocery shops for purchasing essential goods. Individual shopping trips to nearby grocery shops are increased by 14% and supermarkets are reduced by 10%. Regarding the frequency of shopping for essential goods, nearly 50% of the individuals reported that they used to do shopping at least twice a week before the pandemic, whereas during the pandemic it was reduced to 20%. These statistics clearly show that individuals are very cautious about the pandemic. Also, interestingly it was observed that a pandemic does not have any impact on money spent on essential goods. On average, individuals are spending the same amount on their shopping before and during the pandemic. Moreover, it was observed that individuals preferred more for making short-distance shopping trips during the pandemic situation. Nearly 60% of individuals made shopping trips of a distance less than 2 km before the pandemic, whereas it increased to 80% during the pandemic. It clearly shows the people's apathy toward making long-distance trips during pandemic conditions.

4.2.1 Impact of Socioeconomic Characteristics on the Frequency of Shopping

To further understand the shopping behavior of individuals due to COVID-19, it is necessary to analyze the impact of socioeconomic characteristics on the frequency of shopping-related activities. Table 4 shows the average frequency of shopping before and during the pandemic. From the table, it was observed that nearly 50% of the individuals used to make shopping trips at least twice a week before the pandemic and it was reduced to 23% during pandemic conditions which clearly shows an individual tendency to be cautious about the pandemic, COVID-19.

Regarding the impact of the age of the individual on their shopping activities, the data clearly shows that individuals having age more than 50 years considerably reduced their shopping frequency. Comparing the individuals performing shopping activities every day, during the pandemic their frequency reduced to 1% whereas

Table 4 Percent distribution of the trips as per their shopping frequency

Shopping frequency	Percent distribution of trips	
	Before pandemic	During pandemic
Daily	8.5	0.7
Thrice a week	15	4.8
Twice a week	23.6	17.9
Once a week	31.7	47.4
Once in two weeks	11.5	29.1
Once a month	9.8	0

it is 10% before the pandemic. Analyzing the impact of individual income on their frequency of shopping, an interesting observation is that middle-income class people (income level ranges Rs. 20,000–Rs. 50,000) are making more frequent trips even before the pandemic and during the pandemic, which infers that their income level might not allow them to buy groceries and vegetables for longer durations. Another interesting observation is that people with an education level of at least graduation are making more frequent shopping trips during the pandemic when compared with the before-pandemic statistics, perhaps due to their awareness of the pandemic among other members of the family.

4.2.2 Impact of Socioeconomic Characteristics on the Shopping Attitude of Individuals Before and During Lockdown

From the above section, it is evident that the socioeconomic characteristics of the individuals are influencing the frequency of shopping before and during the lockdown. For the statistical understanding of the association between socioeconomic characteristics and shopping attitudes of individuals before and during the lockdown, the Chi-square test was administered. From the test results, it was observed that education level, household income, occupation level, number of workers in the household, and vehicle ownership are significant in making more frequent shopping before lockdown which is shown in Table 5. Interestingly, household income is the only variable observed to have a significant contribution in making more shopping trips during the lockdown, perhaps due to the COVID-19 pandemic lockdown making people panic, and restrictions imposed by the local authorities discouraging people to go out frequently for shopping. Table 6 describes the household income level that has a significant impact on individual shopping behavior irrespective of the pandemic lockdown.

Table 5 Association of socioeconomic characteristics and frequency of shopping before lockdown

S. No	Respondent profile variable	Chi-square (p-value)	Result
1	Education level	0	Significant
2	Household income	0	Significant
3	Gender	0.462	Not significant
4	Age	0.99	Not significant
5	Occupation	0.022	Significant
6	Household size	0.168	Not significant
7	Number of workers in the HH	0	Significant
8	Vehicle ownership	0	Significant

Table 6 Association of socioeconomic characteristics and frequency of shopping during lockdown

S. No	Respondent profile variable	Chi-square (p-value)	Result
1	Education level	0.813	Not significant
2	Household income	0.011	Significant
3	Gender	0.19	Not significant
4	Age	0.148	Not significant
5	Occupation	0.128	Not significant
6	Household size	0.846	Not significant
7	Number of workers in the HH	0.789	Not significant
8	Vehicle ownership	0.486	Not significant

4.2.3 Variation in Other Shopping-Related Characteristics Before and During Pandemic Conditions

Table 5 provides the details of the mode of shopping before and during pandemic conditions. It depicts that during pandemic conditions, individuals prefer to do shopping nearby grocery shops which makes them more comfortable. As the study was conducted during the lockdown, the statistics did not show any values related to shopping in malls and fewer values online as online platforms are operated in a limited way (Table 7).

The Fig. 2 shows the percent variation in the amount spent by individuals before and during pandemic conditions. More percentage of people are spending about Rs. 200–500 on groceries during the pandemic and the percentage is higher when compared with the pandemic conditions. Table 6 provides data about the shopping behavior of individuals in terms of their travel distance before and during the pandemic. Interestingly, it was observed that no individual is making a shopping trip of distance more than three kilometers during pandemic conditions, whereas it was nearly 25% before the pandemic. And also people making shorter trips (less than 5 km) increased from 17 to 25% during pandemic conditions (Table 8).

Table 7 Percent distribution of mode of shopping before and during pandemic conditions

Mode of shopping	Percent distribution of mode of shopping	
	Before pandemic	During pandemic
Nearby grocery shops	52.96	66.26
Nearby supermarkets	37.12	27.45
Shopping malls	4.23	0
Online	5.68	6.29
Total	100	100

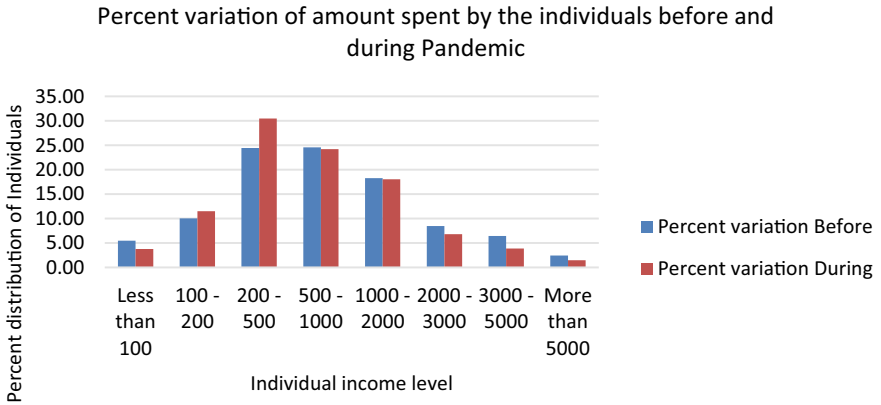

Fig. 2 Percent variation in the amount spent by the individuals

Table 8 Percent distribution of individuals as per their distance traveled for shopping

Distance traveled for shopping (km)	Percent distribution of individuals	
	Before pandemic	During pandemic
Less than 0.5	17.41	25.03
0.5–1.0	25.15	32.53
1.0–2.0	21.52	22.01
2.0–3.0	11.12	10.64
3.0–5.0	10.28	0
5.0–10	11.49	0
More than 10	3.02	0

5 Summary, Conclusions, and Future Scope

The study aims at understanding the shopping behavior of individuals and the impact of COVID-19 on their shopping behavior. In this process, an online survey instrument was designed and circulated to different individuals who are having different socioeconomic characteristics for the near representation of the population. A total of 840 samples are used for the data analysis out of 860 samples received from the survey after data mining. Data related to socioeconomic characteristics, shopping behavioral characteristics of the individuals before and during pandemic conditions, and anticipated behavior of the individuals after the pandemic is collected from the survey.

Data analysis started with the descriptive analysis of socioeconomic characteristics. From this analysis, it was observed that nearly 40% of the individuals are in the age group of 20–30 years and more than 17% of the individuals are having an income level of more than Rs. 1,00,000. As a next step, the mode choice and shopping behavior of individuals are analyzed in the next section. COVID-19 has a clear negative impact on shopping frequency, and a drastic reduction in the percentage share of daily grocery trips was observed. Moreover, it was observed that low- and medium-income people are making high-frequency shopping trips compared with high-income people during pandemic conditions. And individuals prefer to use their vehicles for making shopping-related trips during pandemic conditions. Further, a rise in the percentage of shopping trips to nearby grocery shops during pandemic conditions was also observed when compared with the pandemic conditions. From the data, it was also inferred that individuals making shorter trips for shopping and the pandemic do not have any impact on the amount spent on grocery shopping.

As the present study concentrates on descriptive analysis of socioeconomic characteristics and their impact on shopping behavior, there is a huge scope for further detailed analysis for understanding the behavior. At present, all kinds of businesses are in operational mode; now the study can be extended to analyze individual shopping behavior after the pandemic conditions. This kind of analysis is going to provide a clear picture of individual shopping behavior before, during, and after pandemic conditions. The study can extend to analyzing the behavior of individuals during shopping for other goods in addition to grocery shopping.

Reviewer 1 Comments:

Sl.No.	Comment	Response
1	The introduction part of the paper seems to be slightly long and it talks about many general details. It may be slightly revised	Revised the introduction section by making it concise

(continued)

(continued)

Sl.No.	Comment	Response
2	Page 6, it is mentioned that "…….but at the same time, nearly 18 percent of the individuals belong to the high-income group, which are having a monthly income range of more than Rs. 1,00,000." And in page 8, it is mentioned that "….of the individuals belonging to the high-income group (earning more than Rs. 2,00,00 per month)…." The author may clearly define the income range of the 'High-income category'	For maintaining consistency, the income range of the High-Income category was modified to Rs. 1,00,000 and the same was changed in the text and table
1	Page 7, it is mentioned that "From Table 2, it can be observed that nearly 17 percent of the individual's monthly income is less than Rs. 10,000 and nearly 18 percent of the individuals are earning more than Rs. 1,00,00 per month". Please check whether there is a typing error (Rs. 1,00,00 instead of Rs. 1,000,00 in the second place)	The typo error was rectified
2	Page7, page 8, Table 1 and Table 2 gives two different income ranges. If there is any specific reason, please mention	It was a typo error and the same was rectified
3	Page 11, it is mentioned that "…..Another interesting observation is that people with an education level of at least graduation are making more frequent shopping trips during the pandemic when compared with the before pandemic statistics. This result clearly shows the irresponsible behavior of educated people towards others." The last sentence may be omitted/revised. We cannot make a general conclusion like this, out of the above observation	Modified in the text as per the suggestions
4	Page 12, Table 5: Usually, the p-values are mentioned as "<0.05" or ">0.05" in technical papers. The actual values are not written	The authors' opined that indicating the exact p-values will be useful to decide on significant or not significant and it is not necessary to mention <0.05 or >0.05
5	Page 12, Table 6: same observation as above	The explanation provided in question 4 is applicable here too
6	Page 2, it is stated that "In this context, the objective of the proposed study is to estimate the impact of COVID-19 on shopping behaviour and its related travel attitudes during the pandemic condition". However, calculation of such estimates are missing in the paper	The authors' intention of giving that statement is the impact of COVID-19 on shopping behaviour with their Mode choice, socioeconomic characteristics, frequency of shopping, etc. The same was analysed in the article

(continued)

(continued)

Sl.No.	Comment	Response
7	This paper presents an exploratory study, however, it would be better, if the authors could develop some mathematical models to estimate the influence of various socio-demographics on the grocery shopping behaviour, by which, it is possible to quantify the impact of explanatory variables	The Authors' intention in conducting this study is to understand the shopping behaviour of individuals during and before the pandemic. Further, the authors attempted to develop various models to understand the shopping behaviour of individuals but the model results are not significant due to crucial behavioural data

Reviewer 2 Comments:

Sl.No.	Comment	Response
1	In the last paragraph of the literature review, the authors stated that the previous researchers had contributed significantly to understanding the impact of risk perception and pandemic conditions on travel behavior. Also, there is a good number of works related to shopping trips and their associated activities during pandemic conditions. So, why this study?	The necessity of the study is also provided in the subsequent section of the literature review. Further, the study concentrated only on grocery shopping trips, which were not much explored
2	What are the identified gaps? What makes this study relevant?	Due to COVID-19, a complete lockdown was announced in India and many struggled to get their daily groceries. As these lockdown conditions are new to the existing generation, the existing study substantially contributes to the grocery shopping behaviour of Individuals
3	The authors said that they had circulated google forms for collecting data to a wide range of people. How can authors make sure the reliability of collected data?	As the study was conducted during the Pandemic, traditional methods of data collection had become superfluous to adapt to the restrictions and quarantine protocols implemented by the local governments around the world. Still, for the reliability of data, the Authors verified the responses by comparing their behavioural responses with socioeconomic characteristics
4	The sample size seems small since it does not require any field data collection	Though the study does not require field data collection, in the fear of the pandemic authors' put their best effort to get the sample
5	Whether it represents the grocery shopping behavior of a particular city?	No, the study represents the general grocery shopping behaviour of people from India during COVID-19

(continued)

(continued)

Sl.No.	Comment	Response
6	Does this study significantly contribute to leading any incremental advance in the field?	The study attempted to explain the grocery shopping behaviour of the people during the COVID-19 pandemic and it is an exploratory study
7	The transferability and generalization of the findings are questionable	The study findings are suitable for any developing countries
8	Section 5 looks like a summary of the study. Better to change the section heading to summary and conclusions. Otherwise, the authors should concentrate only on the main conclusions from the study in this section	Modified accordingly to "Summary, Conclusions and Future scope"

Acknowledgements The authors express sincere thanks to those who have responded to the online as well as offline survey. We also extend thanks to the surveyors Mr. D. Mayur, Mr. S. Akshay, and Ms. P. Krishnadeepthi for helping in the intercept survey.

References

1. Kraemer MU, Yang CH, Gutierrez B, Wu CH, Klein B, Pigott DM (2020) The effect of human mobility and control measures on the COVID-19 epidemic in China. Science, 4218
2. Chinazzi M, Davis JT, Ajelli M, Gioannini C (2020) The effect of travel restrictions on the spread of the 2019 novel coronavirus (COVID-19) outbreak. Science 368:395–400
3. Pepe E, Bajardi P, Gauvin L, Privitera F, Lake B, Cattuto C, Tizzoni M (2020) COVID-19 outbreak response: a first assessment of mobility changes in Italy following national lockdown. Sci Data 7:1–16
4. Gibbs H, Liu Y, Pearson CA, Jarvis CI, Grundy C, Quilty BJ, Diamond C, Eggo RM (2020) Changing travel patterns in China during the early stages of the COVID-19 pandemic. In: LSHTM CMMID COVID-19 working group. Department of Infectious Disease Epidemiology, London School of Hygiene & Tropical Medicine, UK
5. Lindahl JF, Grace D (2015) The consequences of human actions on risks for infectious diseases: a review. Infection Ecol Epidemiol 5(1):1–11
6. Timmermans HJP, Arentze TA, Joh CH (2002) Analysing space-time behaviour: new approaches to old problems. Prog Hum Geogr 26:175–190
7. Shay E, Khattak AJ (2012) Household travel decision chains: residential environment, automobile ownership, trips and mode choice. Int J Sustain Transp 6:88–110
8. Dijst M, Kwan MP (2005) Accessibility and quality of life: time-geographic perspectives. In: Donaghy KP, Poppelreuter S, Rudinger G (eds) Social dimensions of sustainable transport: transatlantic perspectives. Ashgate, Aldershot, pp 109–126
9. Kim C, Cheon SH, Choi K, Joh CH, Lee HJ (2017) Exposure to fear: changes in travel behavior during MERS outbreak in Seoul. KSCE J Civil Eng 1–8
10. Yu H, Shaw SL (2007) Revisiting Hägerstrand's time-geographic framework for individual activities in the age of instant access. In: Miller H (ed) Societies and cities in the age of instant access. Springer, Dordrecht, pp 103–118
11. Guo Y, Zhang H (2002) The analysis of tourist decision making behavior. Tour Sci 4:24–27
12. Gossling S, Scott D, Hal CM (2020) Pandemics, tourism and global change: a rapid assessment of COVID-19. J Sustain Tour 1–21
13. Corpuz G, Peachman J (2003) Measuring the impacts of internet usage on travel behaviour in the sydney household travel survey. In: Paper presented at the Australasia transport research forum conference, Wellington
14. Dijst M, Vidakovic V (2000) Travel time ratio: the key factor of spatial reach. Transportation 27:179–199
15. Handy S (1996) Methodologies for exploring the link between urban form and travel behavior. Transp Res Part D 1(2):151–165
16. Visser EJ, Lanzendorf M (2004) Mobility and accessibility effects of B2C ecommerce: a literature review. Tijdschr Econ Soc Geogr 95:189–205
17. Mokhtarian PL (2003) Telecommunications and travel. The case for complementarity. J Ind Ecol 6:43–57
18. Crocco F, Eboli L, Mazzulla G (2013) Individual attitudes and shopping mode characteristics affecting the use of e-shopping and related travel. Transp Telecommun 14:45–56
19. Chintagunta PK, Chu J, Cebollada J (2012) Quantifying transaction costs in online/off-line grocery channel choice. Mark Sci 31:96–114. https://doi.org/10.1287/mksc.1110.0678
20. Jiao J, Moudon AV, Drewnowski A (2011) Grocery shopping: how individuals and built environments influence choice of travel mode. Transp Res Rec: J Transp Res Board, No 2230, Transportation research board of the national academies, Washington, D.C., pp 85–95
21. De Vos J (2020) The effect of COVID-19 and subsequent social distancing on travel behaviour. Transp Res Interdiscip Perspect 5:100121
22. Singleton PA (2019) Walking (and cycling) to well-being: modal and other determinants of subjective well-being during the commute. Travel Behav Soc 16:249–261
23. Shi K, De Vos J, Yang Y, Witlox F (2019) Does e-shopping replace shopping trips? Empirical evidence from Chengdu, China, Transp Res Part A 122:21–33

24. Troko J, Myles P, Gibson J, Hashim A, Enstone J, Kingdon S, Packham C, Amin S, Hayward A, Nguyen Van-Tam J (2011) Is public transport a risk factor for acute respiratory infection? BMC Infect Dis 11–16
25. Choi J, Lee WD, Park WH, Kim C, Choi K, Joh C-H (2014) Analyzing changes in travel behavior in time and space using household travel surveys in Seoul metropolitan area over eight years. Travel Behav Soc 1:3–14
26. Elias W, Albert G, Shiftan Y (2013) Travel behavior in the face of surface transportation terror threats. Transp Policy 28:114–122. https://doi.org/10.1016/j.tranpol.2012.08.005
27. Rittichainuwat BN, Chakraborty G (2009) Perceived travel risks regarding terrorism and disease: the case of Thailand. Tour Manag 30(3):410–418. https://doi.org/10.1016/j.tourman.2008.08.001
28. Church A, Frost M, Sullivan K (2000) Transport and social exclusion in London. Transp Policy 7(3):195–205. https://doi.org/10.1016/S0967-070X(00)00024-X
29. Wen Z, Huimin G, Kavanaugh RR (2005) The impacts of SARS on the consumer behaviour of Chinese domestic tourists. Curr Issue Tour 8(1):22–38. https://doi.org/10.1080/13683500508668203

Impact of Leading Vehicles of the Queue on Saturation Flow at Signalized Intersections

Rishabh Kumar and Mithun Mohan

Abstract Saturation flow is an essential component in the design and capacity estimation of signalized intersections. The saturation flow rate is influenced by several factors, including intersection geometry, speed limit, the proportion of heavy vehicles, parking activities, bus stops adjacent to the intersection area, lane utilization, pedestrian volume, etc. Estimation of saturation flow is well-established for homogeneous traffic conditions. However, measuring and modelling saturation flow are challenging in mixed traffic conditions due to the non-lane-based traffic flow and the presence of multiple types of vehicles. Typically, Passenger Car Unit (PCU) adopted should be enough to account for the variation among the vehicles that constitute the queue while estimating saturation flow. However, field observation at Indian intersections indicated that the vehicles at the front of the queue might profoundly influence the queue discharge at the onset of green phase, thereby exposing the shortcoming of PCUs. This influence is clearly visible when heavy vehicles make up the front of the queue and owing to their inferior operational performance and larger size, they deny the following vehicles the opportunity to attain their desired acceleration. To investigate this, the present study simulated the operation of a typical four-legged signalized intersection in VISSIM software. The subsequent analysis revealed a strong relationship between leaders of the queue and the saturation flow of the approach. This result from the simulation was then verified based on field data. The study concluded that the PCU factors adopted at signalized intersections fail to account for the effect of the queue leader's composition, which has a marked influence on the saturation flow.

Keywords Signalized intersection · Saturation flow · VISSIM · Queue composition

R. Kumar (✉) · M. Mohan
Department of Civil Engineering, National Institute of Technology Karnataka, Surathkal 575025, India
e-mail: rishabhgupta1301153@gmail.com

M. Mohan
e-mail: mithun@nitk.edu.in

A. Dhamaniya et al. (eds.), *Recent Advances in Traffic Engineering*, Lecture Notes in Civil Engineering 377, https://doi.org/10.1007/978-981-99-4464-4_13

1 Introduction

Signalized intersections are one of the integral elements of an urban road network, and an efficient design is essential to improve the overall traffic flow across the network. Saturation flow is the most basic parameter that governs the capacity of a signalized intersection. However, estimating saturation flow based on field measurements is often time-consuming and tedious. Further, many developing nations are facing difficulties in providing efficient vehicular traffic operations due to the mixed nature of traffic. Several types of vehicles operate on the same carriageway width without any physical segregation between motorized and non-motorized vehicles, and these operate without proper lane discipline. Despite these difficulties, it is essential to estimate the saturation flow accurately to design signalized intersections properly.

The rapid increases in traffic volume, poor lane discipline, and the introduction of newer vehicle types alongside older vehicles have warranted a better understanding of traffic flow in developing countries. Signalization is a traffic control strategy to ease the competition at intersections through the cyclical allocation of right-of-way to conflicting traffic streams. However, estimating saturation flow is crucial in designing a signalized intersection. Saturation flow is influenced by a variety of factors like vehicle composition, intersection geometry, driver behaviour, etc. Indo-HCM [1] has recommended a saturation flow model primarily based on homogeneous conditions with limited ability to address heterogeneity. Though the manual provides Passenger Car Units (PCU) for the conversion to equivalent homogeneous conditions, it still fails to address the complete complexity of mixed traffic. Field observations indicated that the positions of different vehicle types within the queue might also impact saturation flow, which Indo-HCM has not considered in the estimation of PCU and saturation flow.

It is seen that the presence of heavy vehicles at the front of the queue often disrupts the flow of streams as these larger sized vehicles perform poorly and denies the overtaking opportunity for trailing vehicles owing to their larger size. This highlights the shortcoming of adopting static PCU values for signalized intersections. This research investigates the effects of the leading vehicles that discharge from a queue at a signalized intersection on the saturation flow. The study models a 4-legged signalized intersection in PTV VISSIM to replicate the traffic characteristics of Indian intersections. A number of cases with varying queue compositions were tested to understand the variation in saturation flows. The data collected from one of the signalized intersections were used to verify the existence of a similar relationship in the field.

2 Background and Literature

To formulate the need and objective of the current study, a detailed survey of previous literature was performed to discuss the saturation flow estimation for heterogeneous traffic conditions. This study used traffic microsimulation software, PTV VISSIM, for simulation. Hence, the literature that used VISSIM for traffic simulation in mixed traffic conditions was referred to identify and adopt various parameters required for calibrating the traffic model to suit Indian conditions.

The Transport Road Research Laboratory [2] put an approach for calculating saturation flow in the field. The flow corresponding to a steady-moving queue that crosses the stop line is used to estimate the saturation flow. It is assumed that the flow representing the 98th percentile is a saturation flow. Mathew and Radhakrishnan [3] proposed a methodology for describing non-lane-based driving behaviour and calibrating VISSIM for highly heterogeneous traffic at the signalized intersection. Calibration parameters were identified using sensitivity analysis. The optimum values for these parameters were obtained using a genetic algorithm that minimizes the error between the simulated and field delay. Jie et al. [4] investigated the calibration of VISSIM parameters for mixed traffic. A sensitivity study showed that the following VISSIM parameters have a significant impact: desired speed, acceleration, safety distance, and vehicle length. In VISSIM, car-following behaviour based on Wiedemann's design was used. These characteristics explain 37% of the variations in the saturation flow rate.

The effect of different vehicle types on saturation flows at signalized intersections is rather well documented. Chand et al. [5] summarized the significance of PCU values and found PCU values at signalized intersections as highly sensitive to given geometric conditions such as approach width, traffic flow, composition, and stream speed. The study summarized that, except for the PCU of LCV and truck/bus, the dynamic PCU value for all vehicle categories has a negative correlation with the stream speed. During the green phase, it was discovered that the PCU values of cars, two-wheelers, and three-wheelers decrease as stream speed increases. Majhi [6] proposed a field procedure for measuring saturation flow and the effect of typical mixed traffic behaviour at signals. The most important aspect of this study was the presence of a high discharge rate at the start of the green interval, which was caused by zero start-up lost time. In the case of heterogeneous traffic, the movement is haphazard and mostly occurs due to non-lane-based movement by different drivers, but, more importantly, two-wheelers play a pivotal role as they sneak through the traffic and always try to stay ahead of the fleet, causing the discharge rate to be erroneous. Arasan and Vedagiri [7] proposed the model to estimate the saturation flow rate of heterogeneous traffic with the specific goal of investigating the effect of road width on saturation flow measured in PCU per unit width of the road. According to this model, the saturation flow rate per unit width increases marginally as the width of the approach increases. The reason for the increase in saturation flow rate per unit width with increasing approach width may be attributed to the fact that vehicles of

heterogeneous traffic with wide variations in overall dimensions can effectively use the road space under saturated conditions as the road width increases.

Sushmitha and Ravishankar [8] developed a model for signalized intersections to provide sequential movements of vehicular traffic from one leg to another leg. This study presented the results of a saturation flow analysis conducted at eight signalized intersections of similar geometry in three different cities in India. According to the model, the saturation flow increases with an increase in green time and the percentage of two-wheelers. At the same time, it decreases with an increase in the percentage of heavy vehicles. Anusha et al. [9] examined how two-wheelers affected the saturation flow rate at signalized intersections. The measurement of saturation flow rate and the percentage of two-wheelers were shown to be strongly correlated. The outcomes demonstrated that the saturation flow determined by the modified HCM equation was more in line with the observed saturation flow values.

Chodur et al. [10] investigated the effect of bad weather on the entry lane capacity. The saturation flow at particular intersection traffic signal cycles was discovered to be a random variable that can be characterized by gamma or normal distribution. The study's findings demonstrate a trustworthy influence of various weather conditions on the saturation flow. Shrestha and Marsini [11] estimated the PCU values for various vehicle categories from a multiple linear regression model developed between the saturated green time and the number of different vehicle types. The PCU value for a vehicle category was determined from the model by taking the ratio of the coefficient corresponding to the subject vehicle type and that of standard cars. Patel and Patel [12] examined the effects of mixed traffic behaviour on PCU and saturation flow. The study examined arrival rate, compositions, and intersection geometry to determine the queue release rate during saturated green times. According to the results of the study, the saturation flow increases as the arrival rate per meter width and the percentage of two-wheelers increase. Nguyen [13] investigated the impact of motorcycles on the heterogeneous traffic flow at signalized intersections. A saturation flow model was created to transform the entire volume into motorbike units. It was discovered that the homogeneous motorbike saturation flow rate in the 3.5 m width is around 11,300 MCU/h, which is more than 5.8 times the homogeneous vehicle flow's 1900 PCU/h saturation flow rate. Rajgor et al. [14] studied the saturation flow rate by counting the number of cars during the saturated green intervals. The saturation flow model was developed considering three variables: approach width, percentage of cars, and two-wheelers. Saha et al. [15] proposed a formula based on road width, traffic composition, and the proportion of right-turning cars to determine the saturation flow rate in mixed traffic conditions. The number of cars crossing the stop line during the effective green time was divided by the effective green time and multiplied by 3600 to compute the saturation flow rate.

This study looks into a possible relationship that might exist between queue leaders and the saturation flow of the approach. The variation in saturation flow with the type of queue leaders depicts the drawback associated with the static PCU values used for signalized intersections. As the presence of smaller vehicles at the front of the queue may increase the discharge from a signalized approach, having larger vehicles as queue leaders may have a negative impact.

3 VISSIM Model

The study intends to investigate the effect that the presence of smaller and large-sized vehicles has on queue discharge characteristics and saturation flow. This will require the data collected from a number of queues having varying shares of different types of vehicles at the front of the queue. However, capturing such conditions with different queue compositions in the field is difficult and rarely feasible. Hence, this study used VISSIM to simulate the various scenarios to be checked.

This study started by modifying the default parameters in VISSIM to simulate the behaviour of Indian traffic at the signalized intersection. This was done based on inputs from previous studies performed by researchers who investigated Indian traffic. In VISSIM, the vehicles were allowed to take any position on the lane, and diamond queuing was enabled. The values of each vehicle category's speed distribution were chosen to ensure the curve follows an 'S' shape. Based on previous literature [2] that calibrated VISSIM for Indian conditions, the minimum and desired acceleration and deceleration functions were designed to be similar to those of Indian vehicle categories. Further, the following aspects were also modified to replicate Indian mixed traffic conditions such as vehicle class and dimensions (length and width), desired speed distribution, acceleration and deceleration functions, and driving behaviour.

The Wiedemann-74 car model was chosen as the driving behaviour for signalized intersections, as it falls into the category of an interrupted facility. The heterogeneous traffic condition was simulated by modifying the parameters in VISSIM based on previously calibrated values. The study [2] recommended 1.33 m as the average standstill distance and additive and multiplicative components of 0.28 and 0.16, respectively. In the model, the minimum lateral distances were set to 0.3 m and 0.42 m for speeds of 0 kmph and 50 kmph, respectively.

4 Network Design of Signalized Intersections

A four-legged signalized intersection was created in VISSIM, with all the approaches having a four-lane divided configuration, as shown in Fig. 1.

The signal consists of four main signal groups and eight signal heads, with two signal heads for each approach. A signal cycle time of 120 s was considered for each approach, with an amber time of 2 s and a lost time of 4 s, such that the effective green time for each approach is set to 22 s. The data collection points are strategically placed next to the stop line, and the simulation was performed for 60 min following a warmup period of 120 s. The traffic inputs were set high to ensure that the approaches were saturated throughout the simulation runs. The dimensions of vehicles and their composition used as input in the created network are given in Table 1.

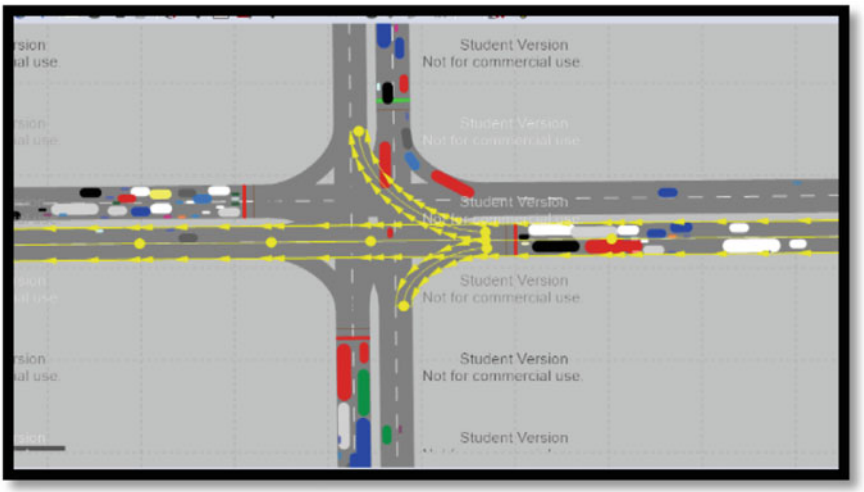

Fig. 1 Four-legged signalized intersection created in VISSIM

Table 1 Vehicle dimensions and their proportion in the traffic stream

Vehicle type	Length (m)	Width (m)	Proportion (%)
Two-wheeler (2W)	1.80	0.68	40
Three-wheeler (3W)	2.36	1.08	5
Car	4.36	1.97	30
LCV	5.00	2.05	5
Bus	11.55	2.69	10
HCV	10.21	2.50	10

5 Model Simulation

The default values of all parameters in the VISSIM model for mixed traffic were substituted with previously calibrated values [2]. To ensure stochasticity, simulations were run for random seeds 42, 44, 46, and 50 to investigate the various effects on saturation flow. All of the approaches were loaded with high-traffic inputs in VISSIM so that they were completely saturated throughout the simulation period. To achieve a stable queue of vehicles, a start-up lost time of 4 s was considered for each green phase. PCU conversion factors were taken directly from the Indian Highway Capacity Manual [1]. Turning traffic from each approach forming the intersection was varied during the simulation runs. Various proportions of left-turn, straight-turn, and right-turn combinations of vehicles from each approach were permitted at the same time.

6 Analysis of Simulation Results

The results of simulation runs were obtained in the form of mer files from the VISSIM software. These files were opened in MS Excel, and vehicles were counted by filtering the data for each approach during each cycle's effective green time. The vehicle counts were then converted into equivalent passenger car units, and the saturation flow for each signal cycle time was calculated using Eq. 1:

$$S = \Sigma N_i * P_i * \left(\frac{3600}{g_i}\right) \tag{1}$$

where S = Saturation Flow in PCU per hour, N_i = Number of Vehicles of type 'i', P_i = Passenger Car Unit of the vehicle type 'i', and g_i = Effective Green Time (in seconds).

The saturation flow was calculated from the output of VISSIM simulation using Eq. (1) and with PCU value from Indo-HCM. The saturation flows computed for different queues revealed a significant variation despite converting to the equivalent number of passenger cars. This might be due to the deficiency of the static PCU values given in Indo-HCM that fails to consider the condition present in the field, which might be the composition of the vehicles in front of the queue.

7 Investigating the Effect of Leaders of Queue on Discharge from Approach

The main objective of the study was to investigate the effect of leaders of the queue on the saturation flow of the approach. However, owing to the presence of a wide variety of vehicle types in the traffic mix, it will be difficult to derive sufficient samples of each vehicle type at the front of the queue. Hence, all the vehicles were broadly divided into three categories: Small Vehicles (SV), Medium Vehicles (MV), and Large Vehicles (LV). Motorized Two-Wheelers (2w) and Motorized Three-Wheelers (3w) were considered as Small Vehicles, while Cars were included in the Medium Vehicle category. Due to their size, Buses, Light Commercial Vehicles (LCV), and Heavy Commercial Vehicles (HCV) were included in the Large Vehicle Category. Analysis of the VISSIM output indicated a large variation in the values of saturation flow across different cycles for the same approach. This indicated the effect of some unaccounted factors that are causing the variation. As the geometric and control conditions at the intersection were unaltered, it must be the composition of the queues that resulted in the variation of saturation flow.

The leaders of the queue were identified as the first 10 vehicles that crossed the stop line of the intersection. Since the approaches had 2 lanes, the first 5 vehicles crossing the stop line respectively from each of the lanes were identified and classified into the three categories as mentioned earlier. Then, the saturation flow was estimated for

each of the approaches for different cycles and was plotted against the number of vehicles of each class that constituted the leaders of the queue. These are presented in Fig. 2. The plots depict a linear trend between saturation flow and the number of SV, MV, and LV as the leaders of the queue. However, it can also be observed that while the graph for HV has a negative slope (in Fig. 2c), SV and MV have a positive slope. This indicates that as more number of HV are present at the front of the queue, the overall saturation flow drops. Further, the slope of the trend line corresponding to SV is relatively higher than that of MV, indicating that a higher proportion of SV as the leader will increase the overall saturation flow than MV.

Thus, through simulation in VISSIM, it is established that the presence of HV at the front of the queue dissipating from an approach negatively influences the saturation flow. But when a greater number of SV and MV constitute the leaders of the queue, the saturation flow increases. Hence, it could be inferred that the composition of the front of the queue significantly affects the saturation flow of the approach. However, these deductions were made based on the simulations in VISSIM that was calibrated for Indian traffic; hence, it is essential to see if the same holds good for data collected in the field. The following section describes the collection and analysis of field data.

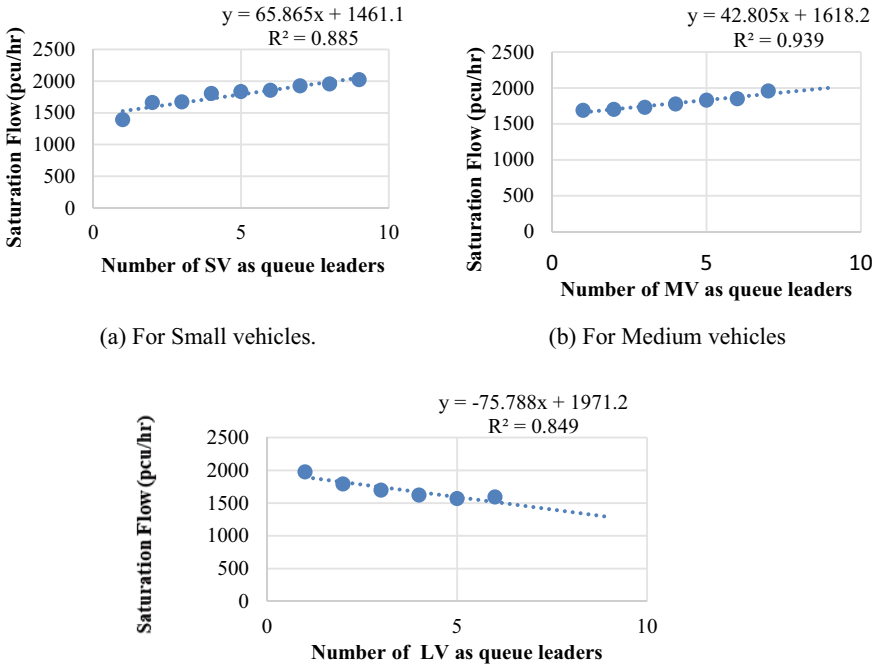

(a) For Small vehicles.

(b) For Medium vehicles

(c) For Large vehicles

Fig. 2 Variation in saturation flow with various compositions of queue leaders

8 Field Data Analysis

Shivaji Chowk intersection in Mumbai is a signalized intersection with four approach arms intersecting at right angles. Video data were collected at this intersection as a part of the CSIR-funded project on Developing the Indian Highway Capacity Manual. Each of the approaches had different widths ranging from 8 to 10 m. All of the approaches to the intersection had no gradient, with the least amount of interference to traffic entering or exiting due to pedestrians, bus stops, and parked vehicles. Figure 3 shows two of the approaches to the Shivaji Chowk intersection. Some steps are considered for field data extraction:

- Data from the recorded video were manually extracted for each signal cycle during each green phase of the approach. They were categorized into six: Motorized Two-Wheeler (2w), Three-Wheeler (3w), Car, Light Commercial Vehicle (LCV), Bus, and Heavy Commercial Vehicle (HCVs—including all regular Goods Vehicles).
- Only those signal cycles with substantial vehicle queuing were considered for data collection. The time for dissipation of the queue was measured after 4 s from the onset of green (start-up lost time) till the time when the queue completely dissipates or the end of green time, whichever occurs first.
- The composition of the queue, as well as starting 10 vehicles of the queue for each of the signal cycles, was noted.
- The available data were collected during the morning and evening, respectively, from 8:00 a.m. to 12:00 p.m. and 2:00 p.m. to 6:00 p.m. The approach width of the Shivaji Chowk intersection was 8.8 m and had a green time of 30 s.

As traffic flow is very heavy during peak hours, all of the approaches to the intersections function in near-saturated conditions. Traffic data was extracted from recorded video manually for each green phase of the approach, and the vehicles that constituted the leaders of the queue were categorized into SV, MV, and LV as

Fig. 3 Signalized intersection at Shivaji Chowk, Mumbai

adopted for the analysis of simulated data. The vehicles that constituted the queue were counted after omitting the initial 4 s (as start-up lost time) of green interval till the instant when the queue completely dissipates or the end of green time, whichever occurs earlier. This was used to estimate the saturation flow rate and to find the composition of the leaders of the queue. As discussed in the previous section, a similar analysis was performed between saturation flow and the number of vehicles that constitutes the leaders of the queue, and the results are presented in Fig. 4.

The plot above depicts the trends for all three vehicle classes at Shivaji Chowk, and these trends are similar to that of the simulated data (Fig. 2). In Fig. 4a, the slope of the trend line for SV was positive, indicating that when there are more small vehicles at the front of the queue, the queue dissipates quickly. In contrast, when large vehicles are present at the front of the queue, it dissipates slowly, as shown by the negative slope of Fig. 4c. The plot for medium vehicles also showed an increasing trend, but its slope was relatively flat compared to the one for small vehicles. Thus, it could be confirmed that the composition of vehicles at the front of the queue definitely impacts the saturation flow estimated for the approach. This clearly shows that the

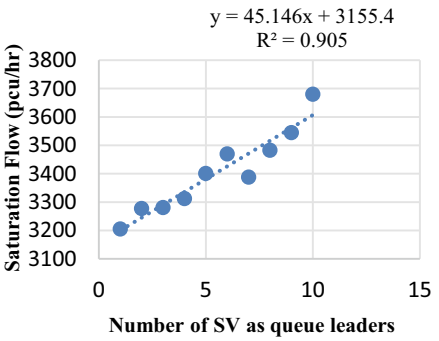

(a) For Small vehicles.

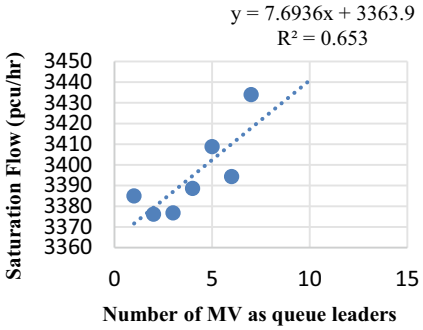

(b) For Medium vehicles

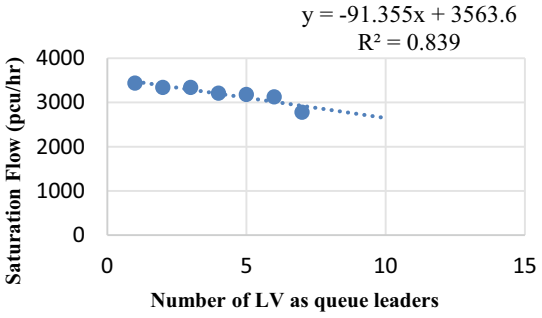

(c) For Large vehicles

Fig. 4 Variation in saturation flow with the composition of queue leaders at Shivaji Chowk

static PCU values normally adopted for signalized intersections are inadequate to capture the effect of queue leaders on the saturation flow.

9 Conclusions

The estimation of saturation flow is one of the foremost steps in the capacity analysis of signalized intersections. Researchers have considered a number of factors that potentially affect saturation flow. However, observing the manner in which a queue of vehicles dissipates from an approach of signalized intersection indicated that the leaders of the queue have a potential impact on the saturation flow. This was not considered in any of the previous research, as it would have been assumed that the use of PCU for conversion to equivalent homogeneous traffic would have nullified the presence of different types of vehicles at the head of the queue. This is the research gap being investigated in this study.

The research initially simulated the operation of a typical signalized intersection in India. PTV VISSIM was used to perform the simulation by adopting the calibrated values of various parameters from previous research. The first ten vehicles of the approach were considered as the leaders of the queue, and the vehicles were broadly classified into Small, Medium, and Large Vehicles based on their sizes. The saturation flow was computed in terms of PCU/h by measuring the vehicles crossing the stop line during the effective green period and using the PCU factors given in Indo-HCM. However, it was found that the saturation flows varied across the cycle for the same approach, indicating that some unaccounted factors affect the saturation flow. This factor must be the composition of the queue, as the rest of the likely parameters that tend to affect saturation flow were kept constant.

Using the output of the VISSIM simulation, the variations in saturation flows were plotted against the number of the three classes of vehicles as leaders of the queue. It was established that as the number of small vehicles at the front of the queue increased, there was also a substantial increase in the saturation flow. The slope of the trend line depicted an increasing trend, indicating when more number of small vehicles are present at the head of the queue, the queue dissipates quickly. In contrast, a similar plot for large vehicles exhibited a declining trend. This indicated that if large-sized vehicles are present at the front of the queue, the queue dissipates very slowly. This may be due to the poor acceleration characteristics of large vehicles compared to other vehicles in the queue, causing the delay for the following vehicles as they have limited opportunity to overtake. This further reduces the saturation flow value. The plot for medium vehicles also showed an increasing trend, but its slope was less steep than that of small vehicles. Analysis of data collected from the field on a signalized intersection of similar geometry also indicated a similar trend, indicating the effect of queue composition on saturation flow.

According to this analysis, a higher percentage of two-wheelers occupied narrow gaps during the formation of the queue, increasing the saturation flow rate. On the contrary, large vehicles occupied wider space across the approach width during the

queue formation, decreasing the saturation flow rate. All of these indicate the deficiency of static PCU factors to account for the variation in saturation flow as per the leader's composition. Future research will explore how the PCU factors could be modified and propose an adjustment factor for saturation flow estimation to account for the impact of leading vehicles on saturation flow.

References

1. Indian Highway Capacity Manual (Indo-HCM) (2017) Council of Scientific and Industrial Research (CSIR), New Delhi
2. A Method of Measuring Saturation Flow at Traffic Signals (1963) Transport and Road Research Laboratory, Road Note No. 34, London
3. Mathew TV, Radhakrishnan P (2010) Calibration of microsimulation models for nonlane-based heterogeneous traffic at signalized intersections. J Urban Plan Dev 136(1):59–66
4. Li J, Zheng F, Van Zuylenb H, Lu S (2011) Calibration of a microsimulation program for a Chinese city. Procedia Soc Behav Sci 20:263–272
5. Chand S, Gupta NJ, Velmurugan S (2017) Development of saturation flow model at signalized intersection for heterogeneous traffic. Transp Res Procedia 25:1662–1671
6. Majhi RC (2017) Field saturation flow measurement using dynamic passenger car unit under mixed traffic condition. Int J Traffic Transp Eng 7(4):475–486
7. Arasan VT, Vedagiri P (2006) Estimation of saturation flow of heterogeneous traffic using computer simulation. In: 20th European conference on modelling and simulation (ECMC), vol 9553018, pp 7–15
8. Ramireddy S, Ravishankar KVR (2019) Effect of vehicle composition on saturation flow at signalized intersections in mixed traffic conditions. In: World Congress for Transport Research (WCTR), pp 647–656
9. Anusha CS, Verma A, Kavitha G (2013) Effects of two wheelers on saturation flow at signalized intersections in developing countries. J Transp Eng 139(5):448–457
10. Chodur J, Olstrowski K, Tracz M (2016) Variability of capacity and traffic performance at urban and rural signalized intersections. Transp. Res. Procedia 15:87–99
11. Shrestha S, Marsini A (2014) Development of saturation flow and delay model at signalized intersection of Kathmandu. In: Proceedings of IOE graduate conference Kathmandu, Nepal
12. Patel N, Patel SG (2012) Capacity analysis of signalized intersections by use of saturation flow rate under mixed traffic conditions. PariPex—Indian J Res 7:33–35
13. Nguyen HD (2016) Saturation flow rate analysis at signalized intersections for mixed traffic conditions in motor cycle dependent cities. Transp Res Procedia 15:694–708
14. Rajgor TB, Patel AK, Gundaliya PJ (2016) Development of saturation rate model for heterogeneous traffic at urban signalized intersection. Int J Innov Res Technol 12:151–155
15. Saha A, Ghosh I, Chandra S (2017) Saturation flow estimation at signalized intersections under mixed traffic conditions. WIT Trans Built Environ 387–393. ISSN 1743-3509

Comparative Safety Assessment of Vehicle–Pedestrian Interactions at Urban Arterial and Highway Using UAV Data

Rajesh Chouhan, Abhi Shah, Rushabh Dalal, Jash Modi, Ashish Dhamaniya, and Chintaman Bari

Abstract According to the WHO Global Road Safety Report [10] and the MoRTH Accident Report [12], fatal road accidents involving pedestrians are increasing yearly. The primary factor contributing to these rising statistics is vehicle speed, which calls for a thorough examination of the overall situation. The current study compares the interactions between vehicles and pedestrians on two separate roadway facilities in Gujarat, India, with varying vehicle speeds and pedestrian behavior characteristics. This study compares the severity of interactions at the two roadway facilities, which is primarily based on speed and safety analysis. An automatic trajectory extractor is used to retrieve the speeds and Time to Collision (TTC) of both the entities involved in interactions. It was observed that the pedestrians keep a higher distance from the interacting vehicle on National Highway (NH) because of the higher speed of the interacting vehicles. The present study revealed that although Time-to-Collision (TTC) is lower in urban settings, and higher on National Highways even than fatality rates are significantly higher on National Highways due to elevated vehicular speeds. This underscores the complex relationship between speed, collision risk, and outcome severity. A new risk factor is introduced as the fatality risk Index to assess the overall risk of different traffic facilities. This study can work as a means to measure the safety

R. Chouhan (✉) · A. Shah · R. Dalal · J. Modi · A. Dhamaniya · C. Bari
Department of Civil Engineering, S.V. National Institute of Technology, Surat, India
e-mail: rajeshchauhan.321992@gmail.com

A. Shah
e-mail: shahabhi031@gmail.com

R. Dalal
e-mail: rushabhdalal56@gmail.com

J. Modi
e-mail: JashM40@gmail.com

A. Dhamaniya
e-mail: adhamaniya@gmail.com

C. Bari
e-mail: chintamanbari@gmail.com

A. Dhamaniya et al. (eds.), *Recent Advances in Traffic Engineering*, Lecture Notes in Civil Engineering 377, https://doi.org/10.1007/978-981-99-4464-4_14

of different traffic facilities and develop safer options for the movement of pedestrians across different facilities involving interaction between vehicles and pedestrians.

Keywords Speed · Risk index · Pedestrian · Vehicle–pedestrian interactions · Safety · Surrogate safety measure

1 Introduction

Pedestrians and vehicles mostly share a common space while the pedestrian undergoes road crossing maneuvers if a dedicated grade-separated pedestrian infrastructure is not provided at the designated location. In such situations, it is inevitable for pedestrians and vehicular traffic to interact with one another. The vehicle and pedestrian negotiate their way around each other by following the traffic control devices or by social rules and understandings. These interactions, in many cases, lead to conflict between the two interacting parties, which in some cases often leads to accidents or other risky conditions. According to the Ministry of Road Transportation and Highways [1], it has been reported that in the year 2020, 31.8% of the total accidents occurred on National Highways. Among the total fatal accidents, 35.9% were on National Highways (NHs) [1]. At the same time, pedestrian accidents on NHs were 12%, out of which 16.3% resulted in fatalities. Road accidents are multi-casual and often result from human error, road environment, and vehicular conditions. This study presents a comparative analysis of the vehicle–pedestrian interactions on an Urban (U) Road and a National Highway in mixed traffic conditions. Overall, 272 vehicle–pedestrian interactions on the Urban Road are compared with 158 vehicle–pedestrian interactions on the National Highway. It is observed that the decision of pedestrians to undergo an illegal crossing is different at different facilities. Post Encroachment Time (PET) and Time to Collision (TTC) are some of the frequently used Surrogate Safety measures. A research work employed Surrogate Safety measures into groups using the Time-To-Collision (TTC), the Post Encroachment Time (PET), and the deceleration families, plus two extra groups for other and unspecified indicators and found that Time to Collision is frequently used, followed by PET [2]. Conflict points, pedestrian and vehicle velocity, vehicle class, conflict type, and Time to Collision (TTC) are the parameters that have been identified and estimated. TTC is defined as the time taken by the later entity, either pedestrian or vehicle, to arrive at the conflict point, provided that the conflicting entity continues with its speed and direction [3]. This paper is presented in two sections, the first section summarizes the comparative speed characteristics of the two roadway facilities, and the second section focuses on the safety and severity levels of the identified interactions. The findings of this study can augment current pedestrian safety recommendations and offer guidance to those who design safe and effective traffic facilities. Lastly, the variability index (VI) and severity level of the obtained vehicle–pedestrian interactions are used to provide a new safety index to compare the risk of crossing at Urban and National Highways.

2 Literature Review

Previously, researchers have employed the idea of surrogate safety measures utilizing one or a combination of characteristics for the interaction between pedestrians and vehicles. It is advantageous to use TTC as a Surrogate Safety Measure (SSM) because of its ability to quantitatively capture the severity of interaction [4]. Researchers have studied the vehicle–pedestrian interactions on Urban Roads with mixed traffic conditions by extracting trajectory data [3]. It was observed that the ratio of aggressive to non-aggressive behavior was more prominent in the case of vehicles, while pedestrians were seen to exhibit less aggression. A distance-based surrogate safety metric known as Safe Distance (SD) is established which is identified based on vehicle–pedestrian interactions [5]. The findings demonstrated that SD rises as vehicle size and speed increase. A study was conducted to analyze the behavior of vehicle–pedestrian interactions on midblock crossings with a High-resolution LiDAR [6].

A study that was conducted to determine the severity levels of vehicle–pedestrian interactions concluded that due to male pedestrians' tendency to take more risks, interactions involving male pedestrians had a higher severity level while for the same pedestrian gender and vehicle type, the severity level falls as pedestrian crossing speed increases [7]. Conflict risk evaluation models and their thresholds are developed based on the vehicle–pedestrian interaction data to be used in real-time risk evaluation models [8].

Few studies have also focused on the studies done to improve the existing pedestrian facilities. Some researchers have re-examined the pedestrian crossing warrants by analyzing pedestrian safety and vehicle delays at vehicle–pedestrian intersections at urban midblock sections [9]. The study suggested using PV^2 values (where P is the volume of pedestrians crossing the roadway facility per hour and V is per-hourly vehicular traffic volume) to define thresholds for various types of pedestrian crossing facilities. In Global Status on Road Safety 2018 by WHO, it was mentioned that over 1.35 million people die each year in traffic crashes, and about 50 million are injured. Road accident is the eighth leading cause of death for people of all age groups, while it stands first for children and young adults in the age group of 5–29 years. In addition to this, low-income countries have three times higher death rates when compared to high-income countries [10].

As per the Ministry of Road Transportation and Highways [1] report, for the third consecutive year [11], the fatal road accident victims largely constitute young people in the productive age groups [1]. Young adults aged 18–45 years accounted for 69% of victims in 2020. Regarding road user categories, the share of Motorized 2-Wheeler (2W) riders in total fatality has been the highest (43.5%) during 2020, followed by the Pedestrian road users with 17.8% of persons killed in road accidents, as shown in Table 1.

As per the MoRTH Accident Report—2020, it was reported that pedestrian fatalities are increasing by 0.5–2.0% every year, as shown in Fig. 1, which is of significant concern and shows the gravity of the problem [12]. Also, it is important to mention

Table 1 Pedestrians killed in accidents classified by the type of impacting vehicles in 2020 [1]

Victim	Impacting vehicle category								
	Bicycle	2W	3W	Cars, taxis, vans & LMV	Trucks/ lorries	Buses	Non-motorized vehicle	Others	Total
Pedestrian	107	6489	954	5511	4142	1161	305	4808	23,477
% Share in total fatalities	8.4	18.3	16.8	17.5	15	15.8	14.4	23.2	17.8

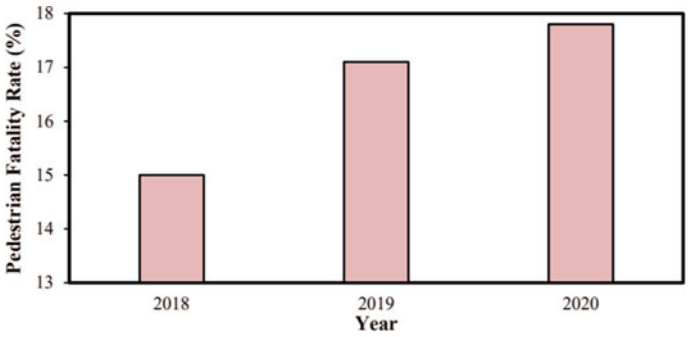

Fig. 1 Yearly pedestrian fatalities rate

that in the year 2020, traffic was constrained due to the lockdowns; even then, the fatalities were relatively high for pedestrians, which shows the need to study the safety aspects of vehicle–pedestrian interactions.

This study aims to present the vehicle–pedestrian interactions with the severity levels, which can be used in favor of pedestrians to reduce the number of accidents and provide solutions for the safer movement of pedestrians. The critical situation of vehicle–pedestrian interactions is studied using the data collected using Unmanned Aerial Vehicles (UAVs) to get accurate and precise analysis.

3 Methodology

Traffic conflict is generally defined as the event in which at least one of the interacting entities has to deviate from its path to avoid a collision. To study conflicts, proactive techniques like the use of surrogate safety methods have been followed by various researchers at different traffic facilities [13, 14].

The study presented in this paper is divided into two sections, with one section dedicated to comparative speed study and the second to the safety and severity analysis, which presents certain conditions that can be used to determine the severity levels of a particular interaction at a particular road type. The concept of surrogate safety measures is used in the present study to perform the safety analysis. The methodology adopted for the present study is shown in Fig. 2.

The analysis results of Speed, Time to collision (TTC) analysis (surrogate safety measure for the study), and Severity are then used to compare and give recommendations which the field engineers can use to plan for improving the present infrastructure facilities for pedestrians to reduce the risk levels and fatalities. Different planning approaches should be adopted for both Urban roads and National highways as the severity of vehicle–pedestrian interaction is different in both cases.

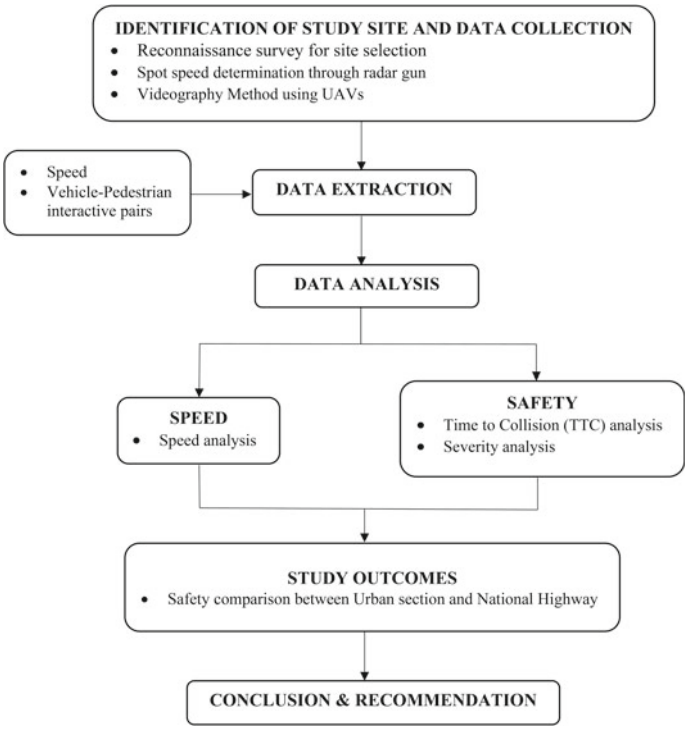

Fig. 2 Methodology adopted for the present study

4 Data Collection

Videography data was collected from the selected study sections under clear weather conditions using a UAV. The required pedestrian and vehicle data, including the type of interaction (Vehicle Passing First (VPF) or Pedestrian Passing First (PPF)), the speeds of vehicles and pedestrians during their interaction, and the distance between them, were extracted from video using automatic trajectory extractor software. TTC was determined based on the noted distances.

The two interaction cases of vehicle passing first and pedestrian passing first have been shown in Fig. 3. Past studies have mentioned that UAVs' advantages include time and money savings, enhanced data measurement accuracy, and improved data recording security [15]. Hence, the use of UAVs was preferred for data collection over static data collection.

The spot speed data were collected through a radar gun for a short period of different vehicle classes (Fig. 4), which was later used to validate the speeds obtained from the UAV video through an automatic trajectory extraction tool. Vehicles' spot speeds in urban and NH study sections were extracted from video using DataFromSky software.

The significance of the difference between both the spot speed data is checked using the F-Test for all the vehicle classes separately. It was observed that there is no significant difference between them at 5% level of significance as the P-value for all the vehicle classes came to be less than 0.05 as shown in Table 2. Thus, the spot speeds extracted from UAV data resemble the actual spot speeds on the field and can be used for analysis.

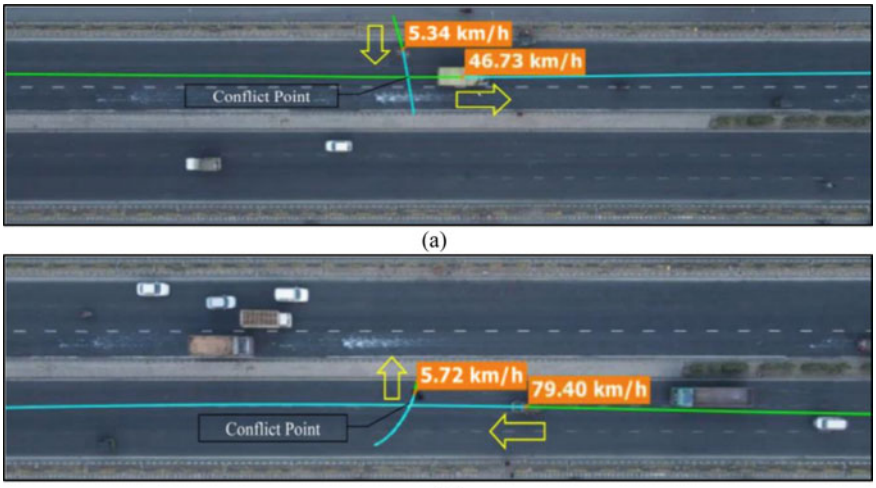

Fig. 3 Vehicle passing first (VPF) and pedestrian passing first (PPF) interaction observed in NH study section

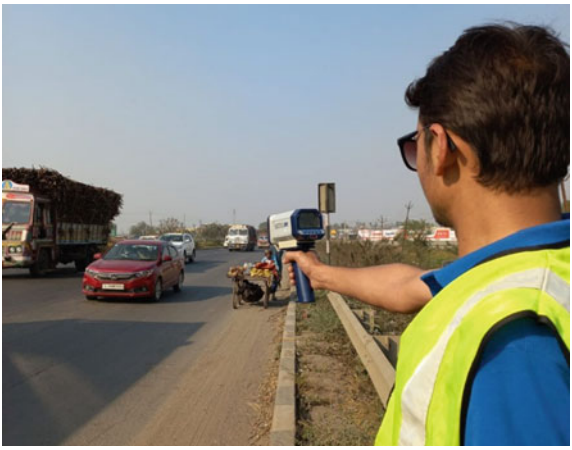

Fig. 4 Spot speed data collection through radar gun

Table 2 F-test results

Vehicle type	F_{value}	$F_{Critical}$	p-value	Remark
2W	0.504	0.603	0.014	Statistically insignificant difference
3W	0.795	0.837	0.017	Statistically insignificant difference
Car	0.555	0.661	0.010	Statistically insignificant difference
HV	1.214	1.199	0.039	Statistically insignificant difference

5 Data Processing and Analysis

5.1 Speed Analysis

Different drivers choose different speeds depending on various factors such as vehicle limitations, roadway conditions, and driver ability. A single speed value cannot correctly represent all the speeds at a specific location. Different drivers react differently to the same driving conditions, and these differences also affect their choice of speed. Hence, it is important to study speed as a separate entity. The vehicle classes considered in this study were Motorized 2-Wheeler (2W), Motorized 3-Wheeler (3W), Car, and Heavy Vehicles (HV), which include LCV, Bus, and Heavy commercial vehicle (HCV)) are the majority of vehicles in the overall traffic composition. Figure 5 shows the heat map in the NH study section at different speeds.

To have confidence that the speed difference is there at U and NH sections, F-test is conducted, and it is observed that there is a significant difference between speeds at both sections for different vehicle categories at 5% level of confidence (Table 3).

Figure 6 shows the cumulative frequency distribution of speed on the Urban (U) road section and National Highway section (NH) for different vehicle classes. Table 4 shows that the mean speed of cars is highest for both the road sections and the mean

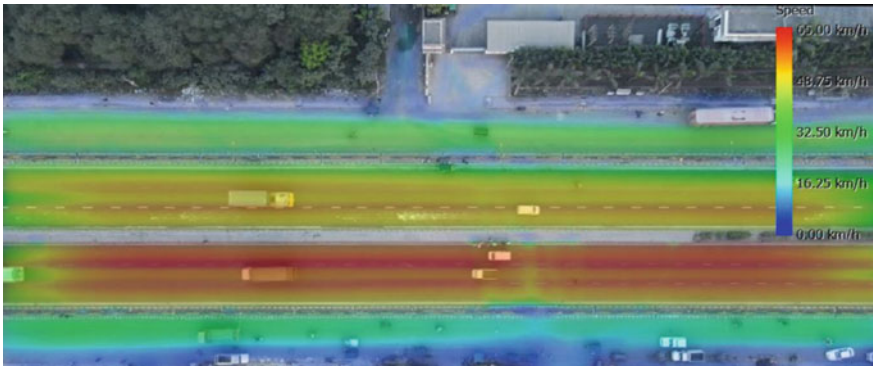

Fig. 5 Heat map showing speed variation across the NH study section

Table 3 F-test results for speed difference at the U and NH for different vehicle classes

Vehicle type	F	$F_{Critical}$	P-value	Remark
2W	1.101	1.698	0.394	Significant result
3W	0.632	0.537	0.111	Significant result
Car	0.599	0.537	0.087	Significant result
HV	1.738	1.861	0.071	Significant result

speed of 3W is the least in the case of NH and HVs have the least speed in U section. It can be because the 3Ws drove mostly near the curb lanes and constantly picked up and dropped pedestrians near the NH study section. The variation in speed is high in cars on urban roads and NH.

The 15th, 85th, and 98th percentile speeds are determined by analyzing the spot speeds of different vehicle classes, as shown in Table 4. The maximum observed speed is 77 km/h for 2W on the NH. The 15th percentile speed, which signifies slow-moving vehicles, for cars is 27.5 km/h and for HV is 20.63 km/h for U road section, whereas for NH, the same for cars is 46.16 km/h (67.85% higher) and for HV is 34.81 km/h (68.73% higher). For 2W on the U road section, the 15th percentile speed is 43.31% lower than on NH. Also, the 98th percentile speed of cars for the Urban Road Section is 34.89% lower than in NH. The mean speed of 3W for the U road section is 24.12% lower than in NH, whichh is the least among all vehicles due to its repetitive stop-and-go conditions.

Table 5 depicts that the vehicles traveling with speeds greater than or equal to the 85th percentile speed for the interacting vehicles in NH are 59.32% higher than in the Urban road section. It shows higher aggression in driving style in NH as compared to the urban road section.

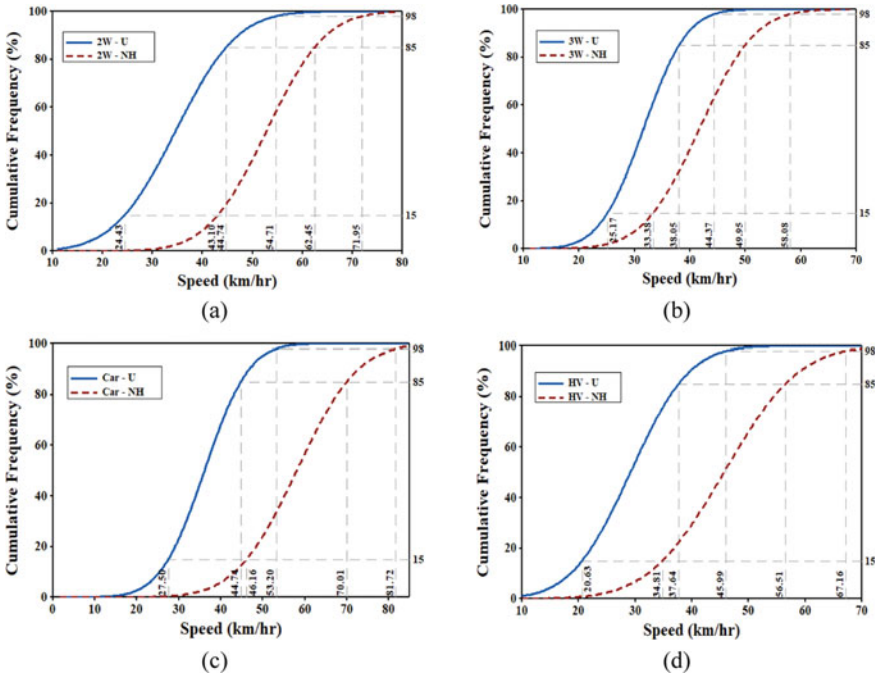

Fig. 6 Cumulative distribution function (CDF) of speed data for **a** 2W, **b** 3W. **c** Car. **d** HV

Table 4 Speed characteristics for different vehicle classes

Speed characteristics (km/h)	2W		3W		Car		HV	
	U	NH	U	NH	U	NH	U	NH
Max	58.00	77.00	54.00	55.00	54.00	83.00	50.00	65.00
Min	11.00	38.00	13.00	25.00	13.00	39.00	11.00	25.00
Mean speed	34.58	52.77	31.61	41.66	36.12	58.08	29.13	45.65
15th percentile	24.43	43.10	25.17	33.38	27.50	46.16	20.63	34.81
85th percentile	44.74	62.45	38.05	49.95	44.74	70.01	37.64	56.51
98th percentile	54.71	71.95	44.37	58.08	53.20	81.72	45.99	67.16

Table 5 Descriptive statistics of vehicles involved in interactions

Categories	Number of vehicles							
	2W		3W		Car		HV	
	U	NH	U	NH	U	NH	U	NH
Speed <15th percentile speed	17	4	13	6	24	9	18	5
Speed >85th percentile speed	15	4	10	5	22	7	12	8
Speed >98th percentile speed	1	2	2	0	1	1	3	0

5.2 Variability Index

To predict the variability of Spot Speed data, a parameter known as Variability Index (VI) is used [16]. It is the ratio of the difference between the 90th percentile and 10th percentile to 50th percentile speed. It signifies the given data is how much variable between 10 and 90th percentile speed to 50th percentile speed shown in Eq. 1.

$$\lambda = \frac{P_{90} - P_{10}}{P_{50}} \tag{1}$$

According to Table 6, the highest variability index in urban roads is about 0.74 for 2W, which is 60.81% more than NH, and the lowest is 0.57 for 3W. Whereas in NH, the highest variability index is 0.59 for HV, which is 18.05% less than Urban Road because lane changing operation is more in urban roads than in NH. Another reason can be that the value of the variability index is lower on NH than on Urban Road because the speed of vehicles on NH is more consistent as fewer obstruction to traffic is observed there.

Figure 7 shows the cumulative frequency distribution of the variability index on the Urban (U) road section and National Highway section (NH) for different vehicle classes.

Speed Spread Ratio (SSR) is used to check the normality of speeds [17]. It is the ratio of the difference between the 85th percentile and 50th percentile to the difference between the 50th percentile and 15th percentile speed. As per the SSR, the vehicles having an SSR range between 0.86 and 1.1 follows the normal distribution. In the present case, SSR for all the vehicle classes on both Urban Road and NH is almost equal to 1, signifying it follows a normal distribution.

Table 6 Variability index for different vehicle types

Categories	Vehicle type	Spot speed (Percentile)			Variability index
		10th	50th	90th	
National highway (NH)	2W	40.81	52.77	64.74	0.45
	3W	31.42	41.67	51.91	0.49
	Car	43.34	58.09	72.84	0.51
	HV	32.24	45.66	59.07	0.59
Urban road (U)	2W	22.03	34.59	47.74	0.74
	3W	21.64	31.61	39.57	0.57
	Car	25.46	36.12	46.77	0.59
	HV	18.61	29.13	39.65	0.72

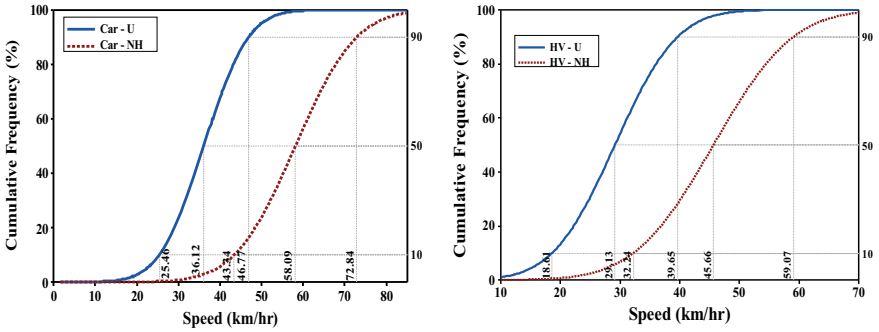

Fig. 7 Cumulative distribution function (CDF) of variability index for **a** Car. **b** HV

5.3 Time to Collision (TTC)

The safety analysis of any traffic facility should be done through proactive techniques. One of these techniques is the use of surrogate safety measures. In the present study, time to collision is taken as the surrogate safety study. The time taken by the later entity (pedestrian or vehicle) to arrive at the conflict point provided that the conflicting entities continue with their speed and direction is known as the time to collision (TTC).

It should be observed that the calculations are based on the assumption that the driver and the pedestrian, respectively, are not distracted while driving a vehicle and crossing a roadway.

As shown in Fig. 8, Time to collision (TTC) is less for Urban roads compared to the NH as the pedestrians take a higher risk due to the lower speeds of vehicles in the urban sections. However, due to the higher speeds of vehicles at the NH, pedestrians keep a higher distance from vehicles while crossing roads to ensure safety, leading to higher TTC values.

As observed from the box plots presented in Fig. 9, it can be said that the variation in TTC is less on the Urban road in both the cases—VPF and PPF as compared to that on the NH as the decision of pedestrians to cross the roadway facility is more rigid for an Urban road because of the less vehicular speeds which is just an opposite scenario to that observed on an NH. It can also be observed that the mean TTC values for pedestrians passing the first case are higher for both road sections. It can be attributed that while pedestrians pass the first case, pedestrians maintain a higher distance from the interacting vehicle but for vehicles passing the first case, pedestrians respond quickly and start crossing the road as soon as the vehicle passes the point of conflict as he feels safe afterward.

As observed from the distribution plots shown in Fig. 10, it can be said that the mean TTC lies in the range of 0–1 s for the Urban road, whereas for NH, it can be observed between 2 and 4 s. Because the vehicular speeds are high on NH and pedestrians try to keep larger gaps with the interacting vehicle while crossing the

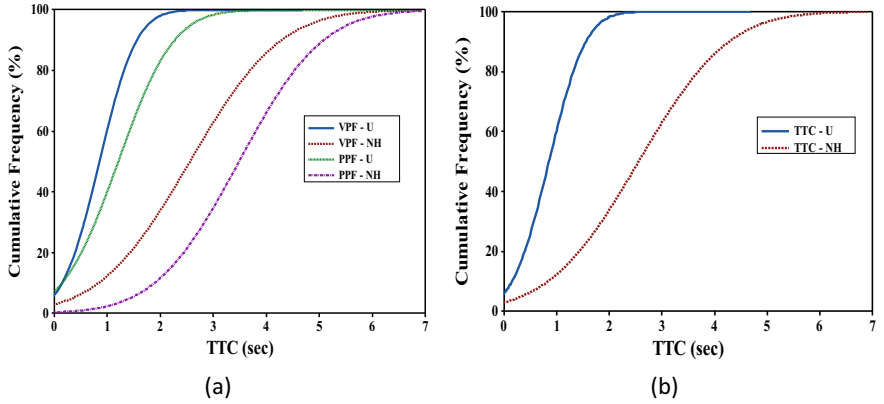

Fig. 8 Cumulative distribution frequency (CDF) for **a** VPF and PPF for U and NH. **b** TTC for U and NH

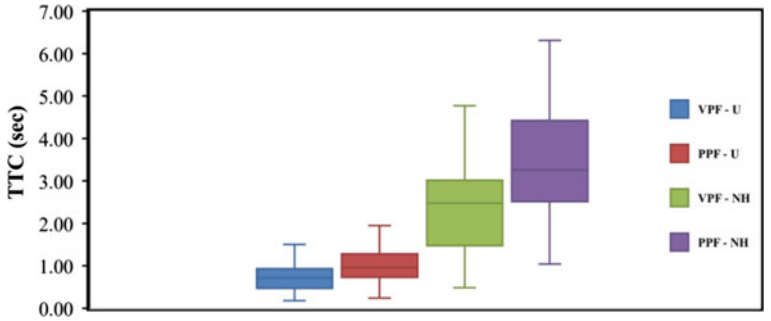

Fig. 9 Box plot for TTC for different road sections

road; thus, higher values of TTC are observed for such cases. The analysis indicated that it is difficult to assess the risk just by observing the TTC as different speeds are observed for both sections. Hence, further analysis is carried out to evaluate the risk and severity of vehicle–pedestrian interaction.

5.4 Severity Analysis

Speed is a major factor that is related to the safety of pedestrians on roads. It mainly depends on factors like roadway conditions, vehicle limits, and driver's ability or experience. The probability of pedestrian deaths resulting from various vehicle speeds, as shown in Table 7, is given in Speed Concepts: Informational Guide by the Federal Highway Administration. Higher operating speeds result in more severe

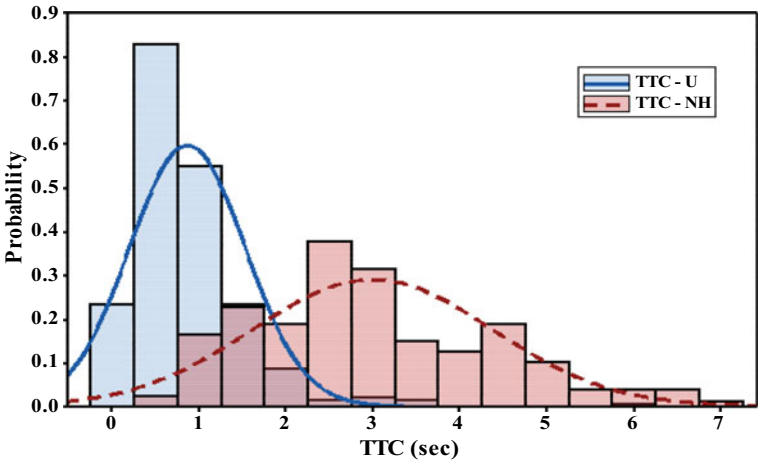

Fig. 10 Probability distribution frequency (PDF) for TTC on U and NH

crashes. If pedestrians are involved in crashes, the fatality risk increases as the impact speed increases. Cars and HV have a major impact on pedestrian collisions.

From Fig. 11, it can be observed that vehicle speed varies between 25 and 50 km/h on the Urban road, and the average value of TTC varies in the range of 0–1 s, whereas on NH, it is 3–4 s. If speeds are, then the average speed on interaction varies in the range of 40–60 km/h, which is quite high as compared to urban sections. Hence, the risk of crossing also depends on the speeds of vehicles involved in the crossing event. To study the probability of a pedestrian getting into a fatal conflict a new risk index is proposed in this study as the Fatality Risk Index (FRI).

$$\text{Fatality Risk Index} = \frac{\text{No.of probable fatal interactions}}{\text{Total no.of interactions}} \tag{2}$$

FRI is the ratio of the number of probable interactions that could lead to fatality to total interactions between all classes of vehicles and pedestrians. In the present study, 272 and 158 vehicle–pedestrian interactions on the Urban Road and the National Highway respectively are considered. Total number of fatal interactions are calculated based on vehicular speeds involved in the vehicle–pedestrian interactions as per Speed Concepts: Informational Guide by the Federal Highway Administration.

Table 7 Probability of pedestrian fatality based on vehicle speed [18]

Vehicle speed (km/h)	Probability of pedestrian fatality (%)
35–50	5
50–65	45
>65	85

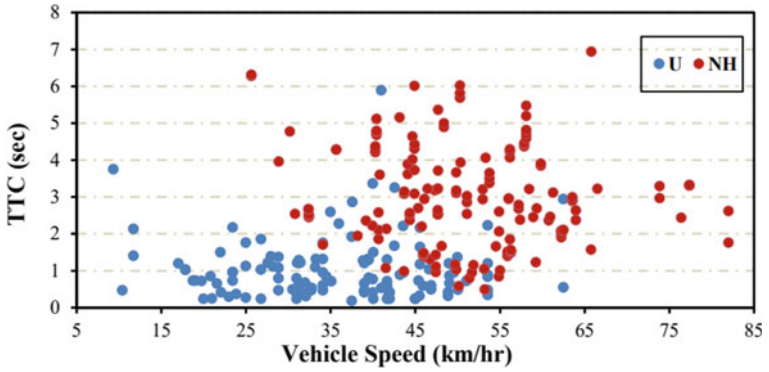

Fig. 11 Variation of TTC with speed on U and NH

Table 8 Fatality risk index for U and NH

Category	Vehicle type	No. of vehicles				Fatality risk index
		Speed less than 35 km/h	Speed between 35 and 50 km/h	Speed between 50 to 65 km/h	Speed more than 65 km/h	
National highway (NH)	2W	0	13	15	3	0.27
	3W	8	18	5	0	
	Car	0	13	20	13	
	HV	5	24	14	1	
Urban roads (U)	2W	47	45	6	0	0.06
	3W	70	30	1	0	
	Car	71	84	6	0	
	HV	73	26	1	0	

From Table 8, it can be concluded that the chances of pedestrians being involved in fatal accidents on NH are 4.5 times higher than on the Urban road as the number of vehicles with speed greater than 65 km/h is higher in the case of NH. The number of vehicles with a speed lower than 35 km/h is more in the case of Urban roads. So, the Urban road has a lower risk with less Fatality Risk Index when compared to NH.

6 Conclusion and Way Forward

This paper includes a comparative study of vehicle–pedestrian interactions on an Urban Road and an NH. The conclusions and recommendations are based on the speed and safety analysis by introducing specific useful parameters and a risk index that give reasonable insights about the present study.

The Conclusions made from the study are as follows:

(1) It is found that there is a significant difference between the speeds of vehicles on Urban Road and NH, which further yielded that the 15th percentile speed of 2W on Urban Road is 43.31% lower than that on the NH while the 98th percentile speed of Car on Urban Road is 34.89% lower than that on NH.
(2) Based on the 85th percentile speed, it is deduced that the drivers are 59.32% more aggressive on Urban Road than on NH.
(3) From the CDFs, it was concluded that the variation in the speeds of HV is high compared to other vehicle classes. It is then validated using the term Variability Index which resulted that HV was possessing a greater Variability Index with NH having 18.05% less variability than that on the Urban Road.
(4) Pedestrians maintain a mean TTC of 0–1 s on the Urban Road as the vehicular speeds are less, while it is 2–4 s in the case of NH as the vehicular speeds are high on the NH and pedestrians act more cautious while traversing on NH.
(5) Chances of accidents are high on Urban Roads as the TTC values observed are lower, but the severity will be less, and the fatality rate will also be lower. But as the speeds observed for NH are high, thus the chances of meeting a fatal accident are higher at NH. Thus, NH can be said to be riskier than the Urban road.

The study's future scope includes a comparison of vehicle–pedestrian interactions on expressways and the formulation of policies that can be used for the development of pedestrian-friendly infrastructure in order to lower the number of fatal accidents resulting from such interactions.

References

1. Ministry of Road Transportation and Highways: Road Accidents in India 2020 (2022)
2. De Ceunynck T (2017) Defining and applying surrogate safety measures and behavioural indicators through site-based observations
3. Golakiya HD, Chauhan R, Dhamaniya A (2020) Mapping pedestrian-vehicle behavior at urban undesignated mid-block crossings under mixed traffic environment—A trajectory-based approach. Transp Res Procedia 48:1263–1277. https://doi.org/10.1016/j.trpro.2020.08.148
4. Chen P, Zeng W, Yu G, Wang Y (2017) Surrogate safety analysis of pedestrian-vehicle conflict at intersections using unmanned aerial vehicle videos. J Adv Transp. https://doi.org/10.1155/2017/5202150
5. Golakiya HD, Chauhan R, Dhamaniya A (2020) Evaluating safe distance for pedestrians on urban midblock sections using trajectory plots. Eur Transp 2015:1–17
6. Vasudevan V, Agarwala R, Tiwari A (2022) LiDAR-based vehicle-pedestrian interaction study on midblock crossing using trajectory-based modified post-encroachment time. Transp Res Rec J Transp Res Board 2676:036119812210832. https://doi.org/10.1177/03611981221083295
7. Govinda L, Sai Kiran Raju MR, Ravi Shankar KVR (2022) Pedestrian-vehicle interaction severity level assessment at uncontrolled intersections using machine learning algorithms. Saf Sci 153:105806. https://doi.org/10.1016/j.ssci.2022.105806
8. Amini RE, Yang K, Antoniou C (2022) Development of a conflict risk evaluation model to assess pedestrian safety in interaction with vehicles. Accid Anal Prev 175:106773. https://doi.org/10.1016/j.aap.2022.106773

9. Golakiya HD, Dhamaniya A (2021) Reexamining pedestrian crossing warrants based on vehicular delay at urban arterial midblock sections under mixed traffic conditions. J Transp Eng Part A Syst 147:1–18. https://doi.org/10.1061/jtepbs.0000538
10. Groot K (2018) WHO—Global Status on Road Safety
11. Transport Research Wing G. of I (2020) Road Accidents in India 2019. Ministry of Road Transportation and HighwaysResearch Wing
12. MoRTH: Road Accidents in India (2020)
13. Chauhan R, Dhamaniya A, Arkatkar S (2021) Spatiotemporal variation of rear-end conflicts at signalized intersections under disordered traffic conditions. J Transp Eng Part A Syst 147:14. https://doi.org/10.1061/jtepbs.0000589
14. Xing L, He J, Abdel-Aty M, Cai Q, Li Y, Zheng O (2019) Examining traffic conflicts of up stream toll plaza area using vehicles' trajectory data. Accid Anal Prev 125:174–187. https://doi.org/10.1016/j.aap.2019.01.034
15. Cvitanic D (2020) Drone applications in transportation. In: 2020 5th international conference on smart sustainable technologies split 2020. https://doi.org/10.23919/SpliTech49282.2020.9243807
16. Van Lint JWC, Van Zuylen HJ (2005) Monitoring and predicting freeway travel time reliability: using width and skew of day-to-day travel time distribution. Transp Res Rec 54–62. https://doi.org/10.3141/1917-07
17. Dey PP, Chandra S, Gangopadhaya S (2006) Speed distribution curves under mixed traffic conditions. J Transp Eng 132:475–481. https://doi.org/10.1061/(ASCE)0733-947X(2006)132:6(475)
18. Donnell ET, Himes SC, Mahoney KM, Porter RJ, McGee H (2009) Speed concepts: informational guide, vol 59

Impact of Traffic Noise on the Teaching and Learning Process of School Environment

Avnish Shukla and B. N. Tandel

Abstract Long-term exposure to noise causes various health problems, including hypertension, depression, distressed cognition, and hearing impairment. The existing literature indicates rapid industrialization, population, and uncontrolled growth in vehicular traffic as the main causes of outdoor noise generation. In this study, measurements were conducted by monitoring the noise levels outside/inside of two school campuses, named A and B. Class-2 precision sound level meter was used to find out the exposure of students to noise inside classrooms in both prevailing (PC) and silence (SC) condition. Noise maps developed from these measurements reflect an alarming situation for both schools with high noise exposure. Furthermore, there is an average noise level reduction of 6.15 and 6.72 dB(A) in school A & B respectively, when situation changed from prevailing to silence. Results also indicate that the measured noise levels (L_{Aeq}) were nearly twice as high as the recommended limit set by World Health Organization (WHO) for classrooms occupied with students. The z-test indicates a significant difference in noise levels for PC and SC. The questionnaire survey investigates the perception and awareness of the students towards the health consequences of high noise exposure. Results indicate higher distraction in the classroom due to road traffic noise. Around 67% of students experienced difficulty in speech intelligibility and 78% found it difficult to concentrate in classrooms. The study has shown a significant impact of traffic noise on the school environment which leads to detrimental effects on the academic performance and well-being of school children. Hence, it is strongly recommended to mitigate road traffic noise generated outside these schools in the form of thick vegetation/noise barriers, thereby ensuring healthy learning conditions inside the classrooms.

Keywords Noise pollution · Road traffic noise · School children · Health consequences · Noise maps

A. Shukla (✉) · B. N. Tandel
Department of Civil Engineering, S.V. National Institute of Technology, Surat 395007, India
e-mail: avnishshukla1706@gmail.com; d20ce027@ced.svnit.ac.in

B. N. Tandel
e-mail: bnt@ced.svnit.ac.in

A. Dhamaniya et al. (eds.), *Recent Advances in Traffic Engineering*, Lecture Notes in Civil Engineering 377, https://doi.org/10.1007/978-981-99-4464-4_15

1 Introduction

Over the years, rapid industrialization has grown, which had led to polluting the ambient atmosphere [1]. Urban noise is one of the main sources that makes life hard to sustain in metro cities [2]. It is the unwanted sound that may be acceptable to an individual but not to others [3–5]. Most of the research used to be done on water and air pollution because noise is invisible [6], and the type of pollution that cannot be seen is thought to be less dangerous [4] than the pollution that can be seen. But in the last few years, noise has also come to be seen as a major problem. Most of this noise comes from unbalanced growth and a sudden rise in traffic [7]. In recent years, most of the studies have focused to look at how traffic noise affects roadside shopkeepers, traffic police, and roadside vendors. Most of these studies found a positive correlation between noise exposure and physical and mental distress [8]. It is also clear that loud noise can cause psychological trauma [9], sleep problems, cardiovascular diseases, and high blood pressure (BP), including a wide range of other health problems that can last for a long period of time. Hearing impairment, mental health issues, heart disease, and coronary illness have all increased in the past five years [10–12]. This reflects the severe nature of traffic-related noise pollution in the surrounding environment. Limited studies were observed on school environment and children's exposure to noise [13]. However, most of the children under the age of 12 were not able to realize the damaging impact of noise pollution on their ability to learn, concentrate, perform, and react until it's too late [14–16]. According to federal regulations, schools and hospitals must be situated in a noise-free environment [17–19], but it is still a challenging situation in urban areas. The WHO permissible limit for noise in school playground is 55 dB(A), while it is 35 dB(A) for classrooms [20] (Table 1).

Considered literature indicate that the measured noise levels in schools were typically neither below the permissible value nor even close to that number [5, 12, 16, 21, 22]. A detailed questionnaire survey was conducted to determine the student's perception of noise and its impact on their health [23]. The CPCB noise guidelines [24] were shown in Table 2.

Table 1 World health organization-recommended decibel levels for classrooms [20]

Certain situation	L_{Aeq} dB(A)	Health impact (s)
Indoors, in preschool and elementary school classrooms	35 (during class)	Problems in understanding speech, interpreting meaning, and conveying messages
Outdoors, school, and playground	55 (during play)	Annoyance (external source)

Table 2 Ambient noise standards (CPCB) [24]

Area code	Category of area	L_{Aeq} dB(A)	
		Day time	Night time
A	Industrial area	75	70
B	Commercial area	65	55
C	Residential area	55	45
D	Silence area	50	40

2 Study Area

Surat, with an approximate area of 474.2 km^2, is one of Gujarat's most developed cities in India. According to the census 2011, the city has a population of around 4,645,384 people and a population density of 10,052 people/Km^2. In addition to this, it is widely recognized as the commercial capital of the diamond and textile industries. The city is situated in western Gujarat on the Tapi River at 210°12′00.00″ North and 72°52′00.00″ East.

The study was conducted in two secondary schools, which is shown in Fig. 1. School A is located across the six-lane arterial road which is possessing heavy traffic due to a large number of commercial vehicular transportation as compared to school B. Since the school is located in a fast-developing commercial zone of the city, its topographical area is smaller than School B. The school operates in two shifts and offers English and Gujarati as a medium of study for standard 1–12. Small food courts, walkways, city transportation, commercial cars, and personal vehicles near the school area are all sources of noise pollution from outside school A. School B is a three-storied building located across the arterial and sub-arterial road, it is well-developed with a spacious playground and parking area. It consists of students from grade 1–12. The medium of instruction is in English. The school was at a significant distance from arterial road, but adjacent to the sub-arterial road which was the main source of traffic noise. The small food court vendors and pedestrians were the other sources of noise.

3 Methodology

The detailed methodology is shown in Fig. 2. It includes taking permission from the principal of schools to conduct the experiments in the school premises. The schools are so selected that the location of schools should be near to a street of any urban/main road, i.e., only schools which are highly prone to traffic noise. Children of these schools (located along moderate to high-traffic roads in a busy commercial locality) were likely to be in a critical stage of noise exposure. Students in grades 7, 8, 9, and 11 were considered due to the fact that lower-grade students may not provide answers with logical thinking. For measurement of road traffic noise, two Sound

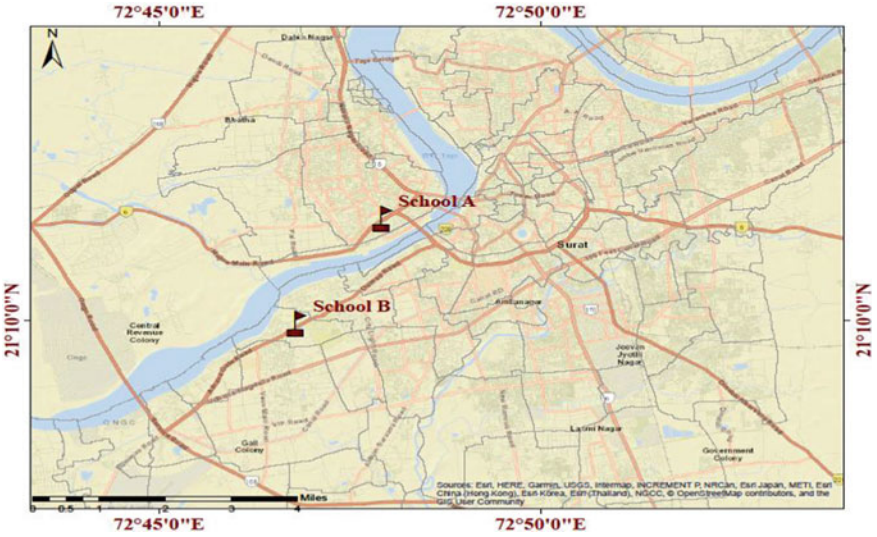

Fig. 1 Location map of the study area

level meters—class-2 precision (Kimo-dB300) were used, one sound level meter was placed outside of the school boundary facing towards the road traffic with a minimum distance of 1.2–1.5 m from the boundary wall and another sound level meter was placed inside the classroom which was mounted over the tripod at the height of 1.5 m (Fig. 3) and with the minimum distance of 1.5 m from the wall. Measurement of sound was performed simultaneously from both sound level meters and further extracted by the computer software of Kimo-dB300. The classroom noise levels were measured at two different noise conditions, i.e., in prevailing condition (when the study was done with all doors, windows open and noisy electrical equipment was operating, it was referred as prevailing condition (PC)) and in silence condition (when the study was done with all doors, windows closed with closing noisy electrical equipment it was referred as silence condition (SC)).

It was observed that school A was having high road traffic noise due to nearby vehicle stopping zone (traffic light) causing horn honking, acceleration–deceleration vehicular engine noise, and tire-pavement noise generated by vehicles on the main arterial road and flyover. School B is having moderate noise exposure due to the lesser number of vehicles on the sub-arterial road as compared to the main arterial road.

The average classroom size was 7 m × 11 m, well equipped with wooden benches with a maximum of two occupancies per bench, half-glazed windows of size 1.8 m × 1 m, wooden blackboard, six fans, speakers, wooden platform of size 1.8 m × 1.2 m × 0.5 m near to the writing board, teacher's table, and chair was present in the classroom. The responses to the questionnaire were analyzed through IBM-SPSS (Statistical Package of Social Science). The school's location and noise maps were prepared through ArcGIS 10.8 and Google Earth Professional. The questionnaire

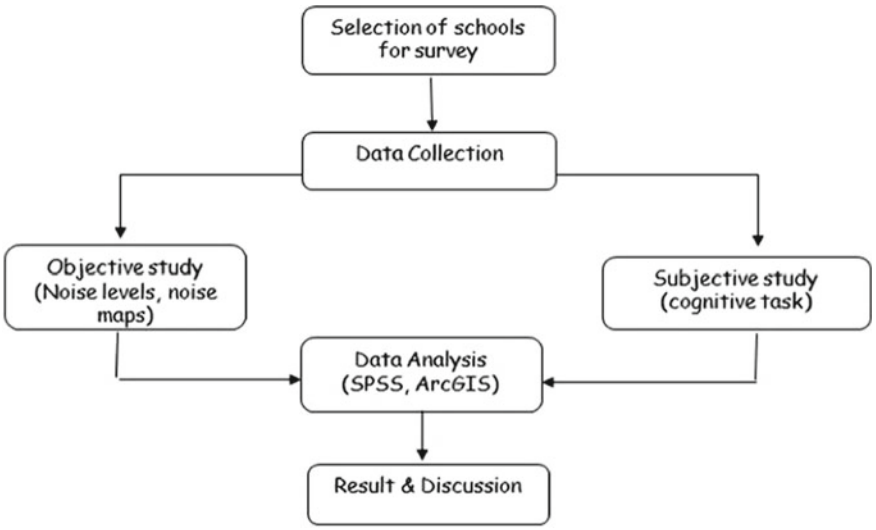

Fig. 2 Methodological framework

Fig. 3 Class-2 precision sound level meter

consists of ten questions, which are based on major factors of learning directly/indirectly affected by ambient noise.

The sound level measurement inside the classroom was taken for 15 min for the prevailing condition, 15 min for the silence condition, and 10 min have been given for the questionnaire survey. Figure 4 shows the photographs of data collection in classrooms and roadside of schools for traffic noise.

(a)

(b)

Fig. 4 Data collection through class-2 precision sound level meters, **a** inside classroom, **b** roadside

4 Noise Measurement Results

The result of noise inside a classroom with the prevailing condition and silence condition and road traffic noise was shown in Table 3. The measured noise levels in all observed classes were much beyond the WHO recommended guidelines (35 dB during ongoing class). RT refers to the decibel level of noise generated by vehicles on the road.

The noise levels in the classrooms were observed to decrease by an average value of 6.15 dB(A) and 6.72 dB(A) in schools A and B respectively, when all doors and windows were closed and noisy electrical equipments were turned off (SC). This

Table 3 Measurements of ambient noise dB(A)

Parameters	Class 7			Class 8			Class 9			Class 11		
	PC	SC	RT	PC	SC	RT	PC	SC	RT	PC	SC	RT
School A												
L_{Aeq}	77.0	72.8	79.8	74.2	68.2	78.3	74.9	67.3	77.8	76.4	69.6	78.5
L_{Amax}	87.2	76.3	84.2	89.1	76.9	86.8	82.1	82.8	82.6	82.5	73.8	91.1
L_{Amin}	65.3	62.7	64.3	66.7	62.0	65.6	58.9	53.4	65.1	54.2	56.1	68.4
L_{95}	67.6	63.4	68.7	61.4	64.3	65.6	64.2	58.9	63.6	61.4	58.2	59.8
School B												
L_{Aeq}	62.3	56.2	65.8	67.2	58.2	65.7	71.2	65.1	64.2	62.2	56.5	68.2
L_{Amax}	73.4	62.4	82.8	74.9	61.8	82.2	84.0	71.2	78.1	74.8	66.4	81.4
L_{Amin}	44.5	48.4	56.8	57.2	43.4	57.4	58.2	48.4	52.4	47.2	41.2	62.4
L_{95}	48.2	44.5	47.8	58.7	44.4	52.4	64.2	48.6	51.4	52.8	42.4	50.2

* *PC: Prevailing condition, SC: Silence condition, RT: Road traffic noise levels*

Table 4 Z-test results of measured noise levels in prevailing and silence conditions

Parameter	Class 7th	Class 8th	Class 9th	Class 11th
School A				
Z-value (P-value)	**8.71(0.00)**	**10.1(0.00)**	**7.24(0.00)**	−0.63(0.52)
Variance PC (SC)	26.1(14.6)	17.7(30.0)	28.0(37.9)	14.6(31.0)
Mean PC (SC)	74.5(72.2)	74.2(71.3)	70.4(67.6)	68.8(69.0)
School B				
Z-value (P-value)	**49.8(0.00)**	**32.4(0.00)**	**61.4(0.00)**	**48.6(0.00)**
Variance PC (SC)	35.0(15.3)	37.7(15.0)	39.5(15.3)	33.9(18.8)
Mean PC (SC)	64.7(53.1)	63.7(56.0)	68.0(53.1)	64.8(53.1)

Note Bold features indicate the statistical difference between the samples

indicates that maintaining acoustic conditions within the classroom have resulted in a significant reduction in noise levels.

The z-test was performed on measured noise levels in prevailing and silence conditions inside the classrooms and the results were shown in Table 4. In almost all considered classes, a significant statistical difference was found.

5 Noise Maps of School Premises

Based on the measurements, the noise maps were developed through Google Earth Professional and ArcGIS to represent the exposure of road traffic noise to the ongoing classrooms inside the schools. It was found that classes near to roadside, i.e., class

7 and class 8 of school A and class 8 and class 9 of school B are more influenced as compared to the classes far from the road. This indicates that the impact of noise reduces as it propagates away from roadside traffic. Figures 5a, b shows the developed noise maps for School A and school B, respectively, where the boundary of the map is the school premises.

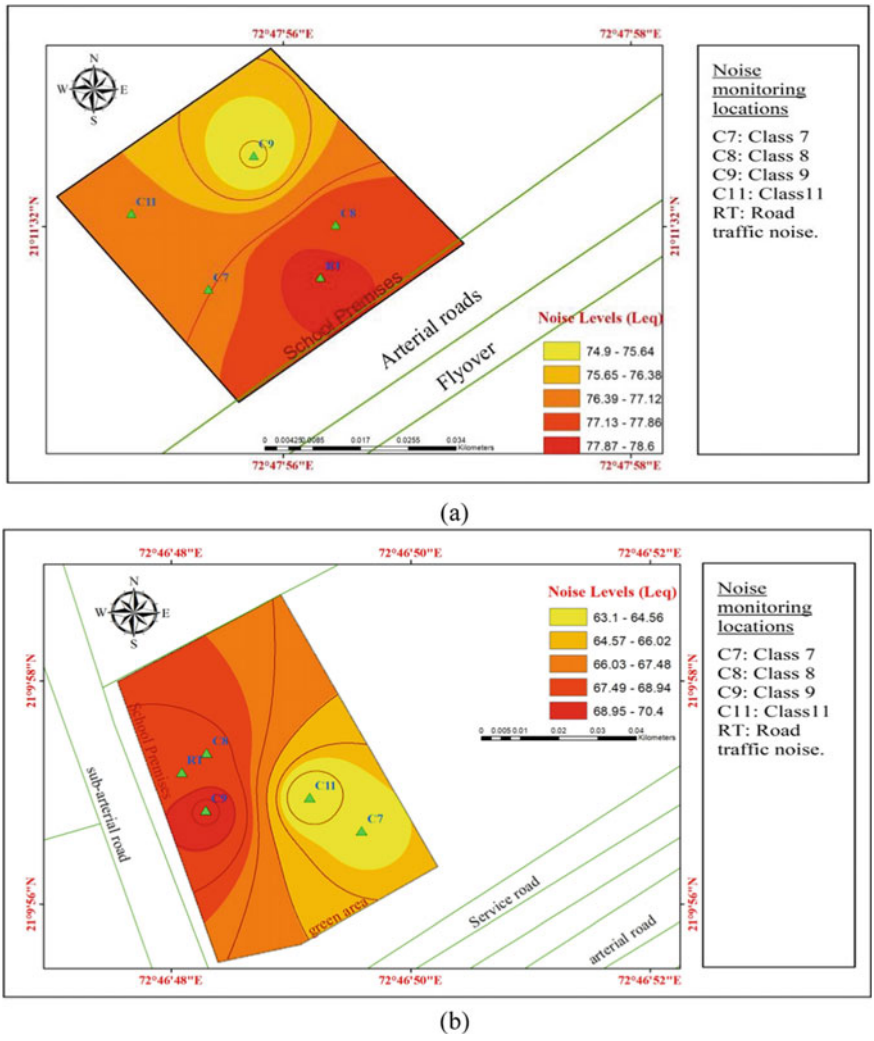

Fig. 5 Noise map for **a** School A. **b** School B

6 Assessment Through Questionnaire Survey

As per the responses to the questionnaire survey, the road traffic noise shows a higher level of disturbance which becomes a cause of loss of concentration and distraction, and sometimes leads to hearing loss. It was found that 50.1% ($n = 105$) of the students thought the classroom atmosphere was sometimes loud, while 28.2% ($n = 59$) said it was always noisy and difficult to concentrate in the classroom owing to noise. Similarly, 40.2% ($n = 83$) of students found it difficult to understand conversation in a full classroom, which increases the level of interior noise, although only 27.2% ($n = 58$) of students encountered this on a regular basis. Excessive conversational noise may also hinder speech comprehension and create disruptions. Due to the presence of ambient noise, 35.2% ($n = 75$) of students found it difficult to comprehend the discussion on the cell phone. However, just 20.6 percent (n = 43) of students thought this happened on a regular basis. This might be because school students are not permitted to carry or often use cell phones (Fig. 6).

It can be inferred that 34.2% ($n = 72$) of students occasionally found hearing impairment or less hearing, whereas 12.2% ($n = 24$) of students found this every time or on a regular basis by combining two questions—"do you frequently need to ask people what they are saying" and "do your family or friends occasionally complain about your low hearing ability." More than half of the students ($n = 106$) were affected by noise in the classroom, with 37.4% ($n = 63$) reporting issues sometimes and 19.3% ($n = 42$) suffering problems on a regular basis.

7 Conclusion

This study tries to determine how road traffic noise affects the academic performance of schoolchildren. Using noise level measurements, maps, and questionnaire responses from students, the impact of ambient (traffic) noise on the teaching and learning process in the classroom was measured. The major source of noise in schools is road traffic noise, which includes engine, tire-pavement interaction, and horn honking. However, teachers have confirmed that it is not the only source of disturbance in the regulation of proper classes; other sources such as disturbance from another class, students running in corridors, dusters hitting a table, ill-maintained electric fans, furniture shifting, and playground noise were also sources of indoor noise. The results reveal that more than fifty percent of students experienced hearing difficulties throughout class and that more than forty percent of students found it tough to converse in a noisy classroom. Both the teaching and learning processes need heightened focus; also, questionnaire data indicates a positive association between increasing noise levels and students' declining performance. The measured noise levels outside the school building facades were much higher than the WHO limits (55 dB(A)) for noise-sensitive areas. The average reduction in noise levels is 6.15 and 6.725 dB(A) in schools A and B when the situation changed from prevailing to

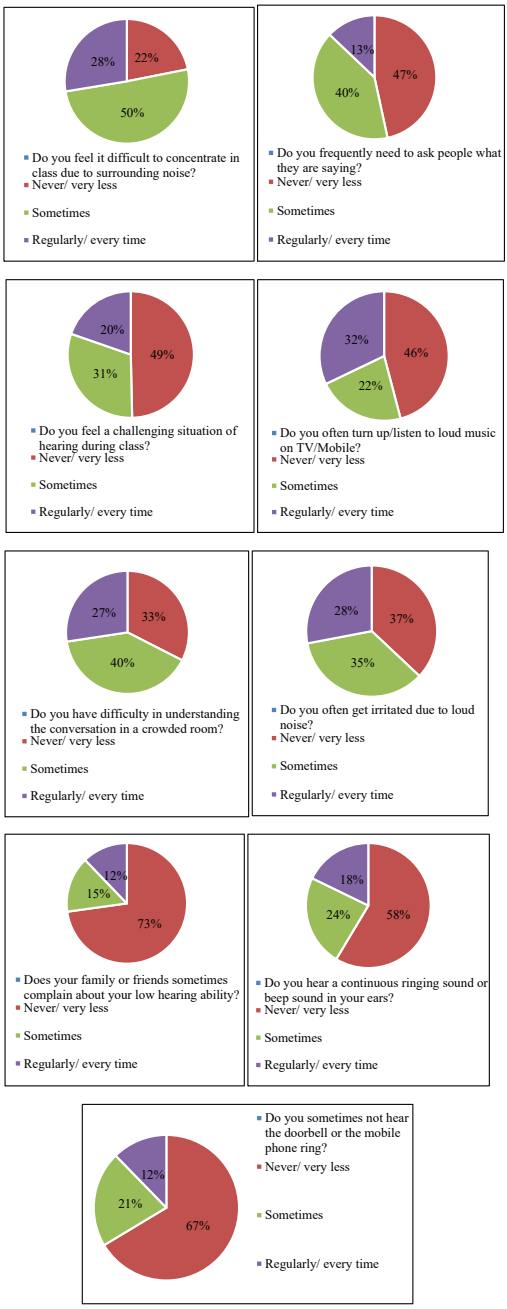

Fig. 6 Results of questionnaire analysis

silence indicating a substantial difference in noise exposure settings (PC and SC). The z-test indicates a significant difference in noise levels for PC and SC. In addition, the results show that school A needs immediate noise reduction in the form of a noise barrier or a class relocation away from the road, as increased noise levels in the classrooms impede student learning. This study concludes that if rigorous noise pollution reduction approaches and scrupulous legislative measures are applied, there is a greater chance that student performance will improve. The use of noise barriers, noise-absorbing materials, double-glazed glass windows, and soundproof doors could also help to limit roadside noise penetration into classrooms, whereas the government authorities should conduct public awareness programs to encourage the use of public transportation, which reduces the number of personnel vehicles, and consequently, road traffic noise.

Acknowledgements The authors gratefully acknowledge the principals, teachers, and students of schools for their cooperation and participation in the research.

Funding Details No financial grant from any authority or organization has been received for this work.

References

1. Foraster M, Eze IC, Vienneau D, Brink M, Cajochen C, Caviezel S, Héritier H, Schaffner E, Schindler C, Wanner M, Wunderli JM, Röösli M, Probst-Hensch N (2016) Long-term transportation noise annoyance is associated with subsequent lower levels of physical activity. Environ Int 91:341–349. https://doi.org/10.1016/J.ENVINT.2016.03.011
2. Fiedler PEK, Zannin PHT (2015) Evaluation of noise pollution in urban traffic hubs—Noise maps and measurements. Environ Impact Assess Rev 51:1–9. https://doi.org/10.1016/J.EIAR.2014.09.014
3. Francis CD, Ortega CP, Cruz A (2009) Noise pollution changes avian communities and species interactions. Curr Biol 19:1415–1419. https://doi.org/10.1016/J.CUB.2009.06.052
4. Singh N, Davar SC (2017) Noise pollution-sources, effects and control. Kamla Raj Enterp 16:181–187. https://doi.org/10.1080/09709274.2004.11905735
5. Stansfeld SA, Matheson MP (2003) Noise pollution: non-auditory effects on health. Br Med Bull 68:243–257. https://doi.org/10.1093/BMB/LDG033
6. Bronzaft AL, Hagler L (2010) Noise: the invisible pollutant that cannot be ignored. Emerg Environ Technol 2:75–96. https://doi.org/10.1007/978-90-481-3352-9_4
7. Tandel BN, Macwan J (2011) Urban corridor noise pollution: a case study of Surat city, India. In: International conference on environment and industrial innovation (ICEII 2011), vol 12, pp 144–148
8. Yadav M, Tandel B (2021) Structural equation model-based selection and strength co-relation of variables for work performance efficiency under traffic noise exposure. Arch Acoust 46:155–166. https://doi.org/10.24425/aoa.2021.136569
9. Sahu AK, Nayak SK, Mohanty CR, Pradhan PK (2021) Traffic noise and its impact on wellness of the residents in Sambalpur city—A critical analysis. Arch Acoust 46(2)
10. Thakur N, Batra P, Gupta P (2016) Noise as a health hazard for children, time to make a noise about it. Indian Pediatr 53:111–114. https://doi.org/10.1007/s13312-016-0802-7
11. Gupta D, Gulati A, Gupta U (2015) Impact of socio-economic status on ear health and behaviour in children: a cross-sectional study in the capital of India. Int J Pediatr Otorhinolaryngol 79:1842–1850. https://doi.org/10.1016/J.IJPORL.2015.08.022

12. Gupta A, Gupta A, Jain K, Gupta S (2018) Noise pollution and impact on children health. Indian J Pediatr 85:300–306. https://doi.org/10.1007/S12098-017-2579-7.
13. Mikulski W, Radosz J (2011) Acoustics of classrooms in primary schools–results of the reverberation time and the speech transmission index assessments in selected buildings. Arch Acoust 36(4):777–793
14. Basner M, Babisch W, Davis A, Brink M, Clark C, Janssen S, Stansfeld S (2014) Auditory and non-auditory effects of noise on health. Lancet 383:1325–1332. https://doi.org/10.1016/S0140-6736(13)61613-X
15. Crombie R, Clark C, Stansfeld SA (2011) Environmental noise exposure, early biological risk and mental health in nine to ten year old children: a cross-sectional field study. Environ Health A Glob Access Sci Sour 10. https://doi.org/10.1186/1476-069X-10-39
16. Forns J, Dadvand P, Foraster M, Alvarez-Pedrerol M, Rivas I, López-Vicente M, Suades-Gonzalez E, Garcia-Esteban R, Esnaola M, Cirach M, Grellier J, Basagaña X, Querol X, Guxens M, Nieuwenhuijsen MJ, Sunyer J (2016) Traffic-Related air pollution, noise at school, and behavioral problems in barcelona schoolchildren: a cross-sectional study. Environ Health Perspect 124:529–535. https://doi.org/10.1289/EHP.1409449
17. Ranpise RB, Tandel BN (2022) Noise monitoring and perception survey of urban road traffic noise in silence zones of a Tier II City—Surat, India. J Inst Eng Ser A 103:155–167. https://doi.org/10.1007/S40030-021-00598-X
18. Berglund B, Lindvall T, Schwela DH (2000) New who guidelines for community noise. Noise Vib Worldw 31:24–29. https://doi.org/10.1260/0957456001497535
19. Athirah B, Nurul Shahida MS (2022) Aircraft noise exposure and effects on the health of nearby residents: a review. In: Lecture notes in mechanical engineering, vol 01. Springer, Singapore, pp 361–378. https://doi.org/10.1007/978-981-16-4115-2_29
20. WHO: WHO | World Health Organization
21. Clark C, Crombie R, Head J, Van Kamp I, Van Kempen E, Stansfeld SA (2012) Does traffic-related air pollution explain associations of aircraft and road traffic noise exposure on children's health and cognition? A secondary analysis of the United Kingdom sample from the RANCH project. Am J Epidemiol 176:327–337. https://doi.org/10.1093/AJE/KWS012
22. Andersen ZJ, Sram RJ, Ščasný M (2016) Newborns health in the Danube region: environment, biomonitoring, interventions and economic benefits in a large prospective birth cohort study. Env Int 88:112–122. https://doi.org/10.1016/j.envint.2015.12.009
23. Crandell CC, Smaldino JJ (2000) Classroom acoustics for children with normal hearing and with hearing impairment. Lang Speech Hear Serv Sch 31(4):362–370
24. Central Pollution Control Board: CPCB | Central Pollution Control Board. https://cpcb.nic.in/who-guidelines-for-noise-quality/. Accessed 15 June 2022

A Comprehensive Investigation of Pavement Evaluation Through Field and Laboratory and Prioritization

Rajkumar Muddasani, Ramesh Adepu, and Kumar Molugaram

Abstract The structural and functional aspects of a pavement must be regularly evaluated because this improves the pavement's functionality and riding quality Field samples tested in the lab would improve the pavement evaluation process. This article's aim is to evaluate the selected pavement sections from field and laboratory studies for maintenance priority. In order to determine the importance of pavement maintenance, a study was carried out in the Hyderabad city along the National Highway (NH 44). Both functional and structural elements were considered. For the purpose of functional evaluation, distress parameters, road roughness, and skid resistance were factored in. The structural performance considers deflection measurement on the pavement sections and pavement performance results of field samples. 100 mm and 150 mm wide core samples were collected on study sections, for the assessment of moisture sensitivity, tensile strength, stiffness, and fracture properties. The investigation's findings demonstrate that there relates a high correlation between structural and functional parameters. Additionally, the study attempted to develop a Maintenance Priority Index (MPI), which is mostly based on the structural and functional parameters of field and laboratory results. The use of artificial neural network has helped in pavement maintenance priority. The findings of this study shall help the maintenance engineer for prioritization of pavement sections of similar categories.

Keywords Functional and structural evaluation · Tensile strength ratio · Resilient modulus · Fracture properties · ANN technique

R. Muddasani (✉)
PG Student, Department of Civil Engineering, VNR Vignana Jyothi Institute of Engineering and Technology, Hyderabad, Telangana, India
e-mail: 20071d8706@vnrvjiet.in

R. Adepu
Professor, Department of Civil Engineering, VNR Vignana Jyothi Institute of Engineering and Technology, Hyderabad, Telangana, India
e-mail: ramesh_a@vnrvjiet.in

K. Molugaram
Professor of Civil Engineering, University College of Engineering, Osmania Univeristy, Hyderabad, India

A. Dhamaniya et al. (eds.), *Recent Advances in Traffic Engineering*, Lecture Notes in Civil Engineering 377, https://doi.org/10.1007/978-981-99-4464-4_16

1 Introduction

India has the largest road network in the world, with 1.5 lakh km categorized as National Highways as of 2021, which would make up 40% of the country's entire transportation infrastructure. In the fiscal year 2022–2023, an additional 25,000 km are expected to be added to the National Highway network. The majority of the existing road network and the length of the new roads constructed during this phase both have asphalt surfaces. Regular maintenance is another issue the road administration is working with. Damage to the pavement's structural strength is the most frequent reason for deficiencies. Rainwater, one of the main causes of accidents, will increase the progression of defects and create traps for driving vehicles once pavement cracks appear. According to National Crime Records Bureau (NCRB 2020), a total of 11,386 people died in the country as a result of road defects, which implies that approximately seven people are met with fatalities due to road surface defects. As a consequence, maintaining safer roads and timely development of a pavement maintenance strategy that will safeguard road users and their property depend greatly on this parameter. Sunny et al. [1] conducted a comparative subgrade moduli study using a lightweight deflectometer (LWD) and conventional Benkelman beam deflectometer (BBD) on low volume roads. The results a closer relationship which are being validated with the laboratory samples tested on repeated triaxial test. Vaibhav et al. [2] performed structural evaluation of flexible pavement using BBD and LWD processes. The study results show that there exists a linear correlation with the use of central deflection values through the LWD test and results also show that there exists a strong relation between them. Ashwini et al. [3] has conducted a deflection test using BBD and a few samples in the laboratory tests for the estimation of overlay thickness. Raj et al. [4] evaluated the pavement surface modulus with the help of a developed lightweight deflectometer and dynamic cone penetration. The results developed a correlation from the collected deflection values which were observed at different test locations. Sung et al. [5] selected four site locations and calculated the stiffness of pavement subgrade by using the LWD test and determined the Resilient modulus of the soil surface, later compared with the results, and found that the relation between both appreciable. Siegfried et al. [6] evaluated the flexible pavement structure by using FWD and LWD, the structural number and surface modulus of the subgrade was attributed for predicting the performance. Amir et al. [7] considered studying different pavement stretches using equipment like PFWD and FWD and the study compared the moduli values to that of laboratory CBR results. The results indicated that there exists a decent correlation between PFWD moduli, FWD, and CBR results. Reddy et al. [8] carried investigation on fracture properties for modified mixes, the fracture resistance and index were improved, compared to control mixes at intermediate temperatures. This study explains that fracture properties are required to assess the performance of mixes. Ramesh et al. [9] studied the fracture characteristics of DBM and BC mixes with modified binders and compared them with the control mixes for evaluation of pavement performance. Janani et al. [10] devised a

unique technique for prioritizing road management segments based only on operational pavement attributes. Following then, these authors were investigated using an enterprise digital, Artificial Neural Network (ANN). Most of the studies were trying to understand the structural capacity of the pavements through field investigations. However, in this case study, an attempt is made to demonstrate how functional and structural performance correlates with insight gained from laboratory studies and the development of sectional priorities.

1.1 Objectives of Study

In order to prioritize maintenance, the study tries to quantify the field performance of pavement sections. The following process is been described below.

- *Field investigation:* To determine the Functional performance from pavement roughness, Skid Resistance and the Structural Performance is measured from deflection studies using BBD and LWD test methods.
- *Laboratory Investigation:* Tensile strength, moisture sensitivity, resilient modulus, and fracture properties are estimated from core samples collected in the field. The test results will aid in the development of a priority model using the ANN technique.

2 Methodology

The current investigation discusses a comprehensive methodology and step-by-step procedure used in this study. It provides information regarding the field and laboratory investigation that shall be carried out in this research (Fig. 1).

3 Data Collection and Methods

The Year of construction of the existing pavement was 2012 and there were several in situ non-destructive testing methods for the measurement of the structural capacity of the pavement. The fundamental idea is to apply a load to the pavement with a specified mass and then assess the size and direction of the resulting deformation on it [11]. The vertical direction exhibits the most frequent distortion [12, 13]. There are three common ways to measure defection in field tests: Moving dynamic defection measurement, such as the laser dynamic deflectometer (LDD) [14, 15], which records the defection along a line on the pavement as the vehicle moves, is an example of moving dynamic deflection measurement. Static load-based deflectometer, which provides the maximum deflection under a static load

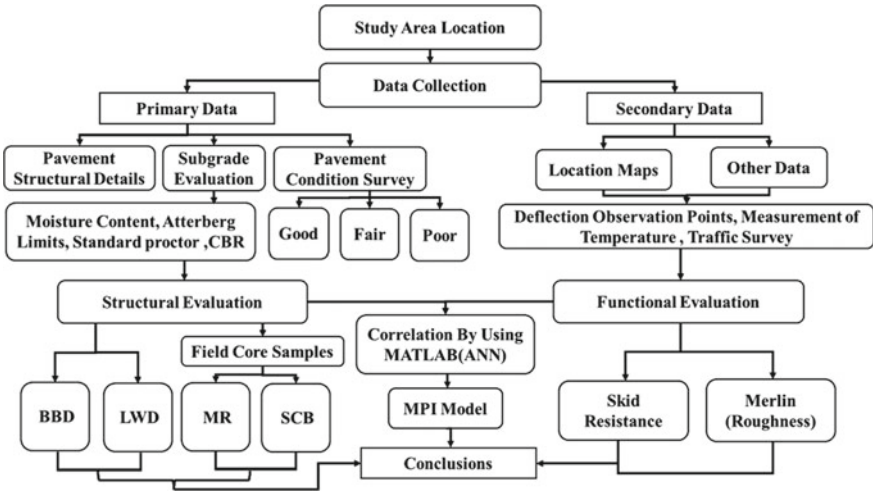

Fig. 1 Schematic flow chart of the methodology adopted for the study

[16]. Although in India and several other countries have employed the static load-based Benkelman beam extensively to assess the structural performance of in-service pavements [11, 17–22].

3.1 Study Area Location

The study investigation was carried out on Kallakal to Jeedipally stretch, Medchal Dist. of NH 44, (National Highways Authority of India's − NHAI) 454 + 000 km. at Kallakal village and terminates at 462 + 000 km at Jeedipally village on NH 44. The stretch passes through an urban corridor of Hyderabad city and is also under due consideration for improvement as shown in Fig. 2. The existing pavement is of four lanes with 3.5 m width on each lane and has a paved shoulder. The width of the median is 1.5 m and the width of the paved and earthen shoulder varies from 2.5 m (1.5 m + 1.0 m) to 3.0 m (1.5 m + 1.5 m).

3.2 Functional Performances

The functional performance of the existing pavements was evaluated using distress surveys, skid resistance tests, and assessments of pavement roughness.

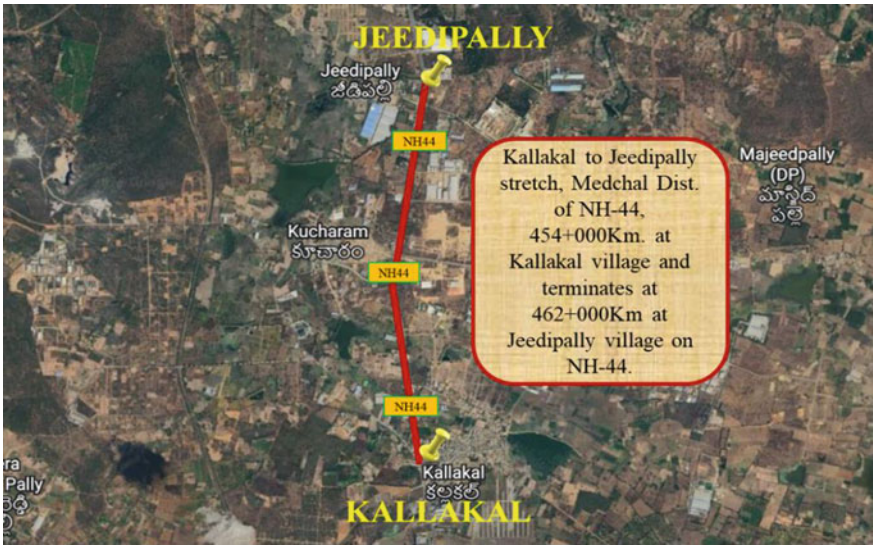

Fig. 2 Study location considered on NH−44

Roughness test

The roughness data was collected from Machine for Evaluating Roughness using a Low-cost Instrument (MERLIN) as depicted in Fig. 3, and is often used for direct roughness measurements or for calibrating response-type sensors, in accordance with Transport and Research Laboratory (TRL), research report 301 and IRC: SP:16–2004 [23, 24].

Fig. 3 Roughness survey carried out at the study location

Fig. 4 Skid resistance test conducted on study locations

Skid Resistance Study of Pavement

Road user has always a sincere concern over the safe passage of vehicles on the road traversed path as shared provided by road designers and engineer. A vehicle's skid resistance is used to assess its level of road safety. Numerous vehicular accidents and fatalities have been associated with pavement skid. The complex interaction of the pavement, vehicle, and environment is necessary for skid resistance [25]. Figure 4 depicts the skid resistance data collected from the study stretches [26–29].

4 Structural Assessment

Benkelman Deflection Test

Deflection measurements were taken in accordance with the guidelines of IRC: 81–1997 [30] for the calculation of pavement's rebound deflection. Using the deflection data, the characteristics deflection was estimated, and the outputted parameters from the test results shall be used for the design overlay thickness (Fig. 5).

The structure number (SN) is an index that gives an indication of the thickness of the pavement layers and the overall pavement structure. The deflections were measured from the field with the use of BBD apparatus as shown in Fig. 6 and the collected data shall also be helpful for arriving at the SN of the pavements. Equations (1) and (2) explain the mathematical formula for calculating SN utilizing Characteristics Deflection (DEF) values [15].

$$\mathrm{SN} = 3.2\,\mathrm{DEF}^{-0.63}\,(\text{Base is not cemented}) \tag{1}$$

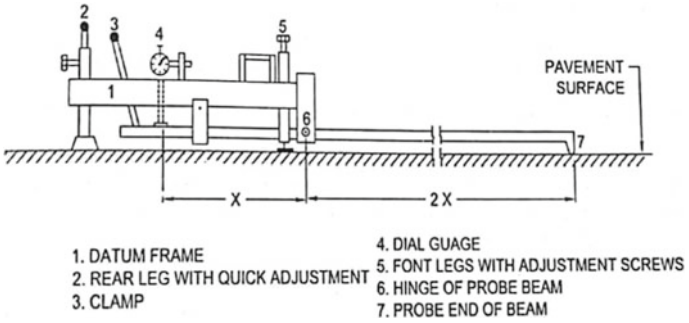

Fig. 5 Schematic view of Benkelman beam apparatus. (*Source* Highway materials and pavement testing-fifth edition, 2015)

$$\mathrm{SN} = 2.2\,\mathrm{DEF}^{-0.6}(\text{Base is cemented}) \tag{2}$$

Indigenous lightweight deflectometer (ILWD) designed in a research facility

The ILWD is a portable device used to evaluate the deflection of thin asphalt layers and unpaved surfaces. The ILWD equipment was designed in the laboratory with unique characteristics such as a trigger assembly, used for the release mechanism (20−25 kg of mass drop) and a base cylinder with load cell arrangements on the top and bottom parts that have fixture arrangements for housing the central geophone. Above the load cell, a rubber buffer is designed and installed in order to provide an impulsive load with a load pulse rate time range of 15–40 ms. For the purpose of estimating the stiffness of the relevant layer, the instrument also includes two extra geophone

Fig. 6 Collection field deflection data using BBD test -static method

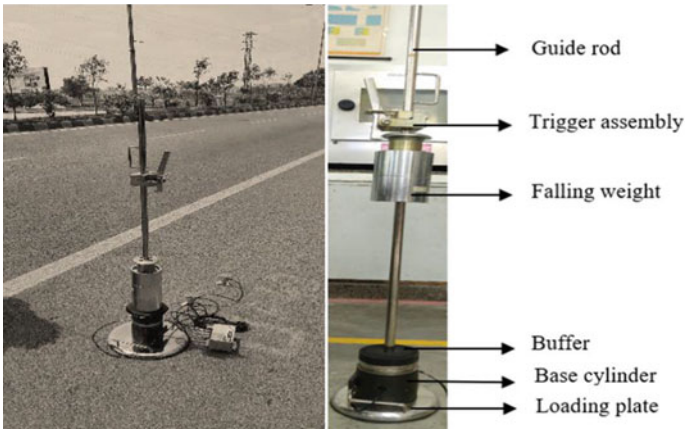

Fig. 7 ILWD Test process at study location

sensors in the radial direction at 30 cm c/c. Also, in order to measure the deflection, a base plate with a diameter ranging from 150 to 300 mm is employed. A handle is also supplied for the convenience of the equipment, and the guide rod is designed for a height range of 70–130 cm and to direct the drop mass's descent. The observed deflection at the center of the plate and radial must be used to calculate the dynamic deformation modulus of unbound and thin asphalt pavement layers. According to ASTM E2583-07 2011 [14, 31], the instrument was created and constructed. When developing highway sections, the utilization of LWD is essential due to the quality of the integrated subgrade and sub-base. Relying on the stiffness and durability of the pounded pavement structure, LWD could be often used to evaluate quality control (QC) and quality assurance (QA) procedures. Figure 7 presents the ILWD's component parts.

In the AASHTO 1993 formula, the effective Structural Number ($SN_{eff.)}$ was determined from Eq. 3.

$$SN_{eff} = 0.0045\, D\sqrt{Ep} \tag{3}$$

where Ep is the effective modulus of the pavement layers above the subgrade and D is the overall thickness of the pavement system above the subgrade level in inches.

5 Field Cores

Field core samples were collected from various points along the study length as depicted in Fig. 8. The core locations were stratified at random along the section's length and width. Each core was assessed for layer thickness, in-direct tensile (IDT)

Fig. 8 Core samples collection on the existing pavement, NH–44

(ASTM D 6931), Resilient Modulus (ASTM 4123), and Fracture properties as outlined in ASTM 8044 [13, 16].

6 Laboratory Investigations

Soil Index Properties

The soil samples were also collected from study stretches at selected locations. Soil tests like Atterberg limits, standard proctor compaction test, and CBR test were performed as part of this study as per IS guidelines. The laboratory investigation helps to identify the engineering parameters used in the designs [32–34]. The section-wise Atterberg limits and standard proctor tests were conducted from 454 + 000 to 462 + 000. The following results were obtained from the test results.

- The average liquid limit (WL) is 26.645.
- The average plastic limit (WP) is 15.033.
- The total average plasticity index (PI = WL-WP) is 11.611 which is less than 15.
- Annual rainfall <1300 mm.
- The optimal dry density is 1.92 g/cm^3 and the average optimal moisture content is 12.5% according to the proctor test.

In-Direct Tensile Strength and Moisture Sensitivity Test

The collected core samples were loaded vertically in the diametric plane with a compressive force, and the loading plane will be where they fail. The maximum load that the sample could withstand was used to compute the mixture's tensile strength using Eq. (4) as outlined in ASTM D 6931 [13]. Figure 9 presents the test process for conditioned and unconditioned samples which shall also explain the moisture

(a)In-direct tensile test process (b)In-direct tensile test process (c)field sample

Fig. 9 In-direct tensile test process for field samples collected

sensitivity.

$$\mathrm{IDT} = 2\mathrm{P}/\pi\mathrm{DT} \tag{4}$$

where P—max load; D—diameter of the sample; T—thickness of sample.

Tensile strength ratios ranging from 0 to 1 value, in the range of 0.8− 1 indicate the asphalt mix is doing well in terms of moisture susceptibility. A TSR value less than 0.7 infers that the mixture has low resistance toward moisture sensitivity, however, a value greater 0.7 provides better resistance toward moisture. TSR is obtained from conditioned and un-conditioned samples test process as outlined in ASTM D 7369–11 and is determined as presented in Eq. (5).

$$\mathrm{TSR}\ (\%) = \mathrm{C}/\mathrm{UC} \tag{5}$$

where TSR—Tensile strength Ratio; C—Conditioned sample; UC—Unconditioned sample.

Repeated Load Cyclic Test

Using the repeated load Cyclic (RLCT) test in line with ASTM 4123 [16] standards, the resilient modulus of the obtained core specimens was assessed. The RLCT test specimens were 100 mm in diameter with 40 and 50 mm in height. The modulus value for core specimens was calculated using repeated compressive cyclic load with a haversine waveform applied vertically to measure the horizontal and vertical strain measured at 35 °C as presented in Fig. 10. The samples were in a repeated haversine load form with a load period of 0.1 s and a rest period of 0.9 s. Compressive load magnitude is determined by a 10% failure load obtained from in-direct tensile carried out at 35 °C. Trials were run at each location in order to calculate the robust modulus values. After the initial 100 cycles were completed, a total of 1000 cycles were used; the next five cycles were taken into account to determine the resilient modulus of

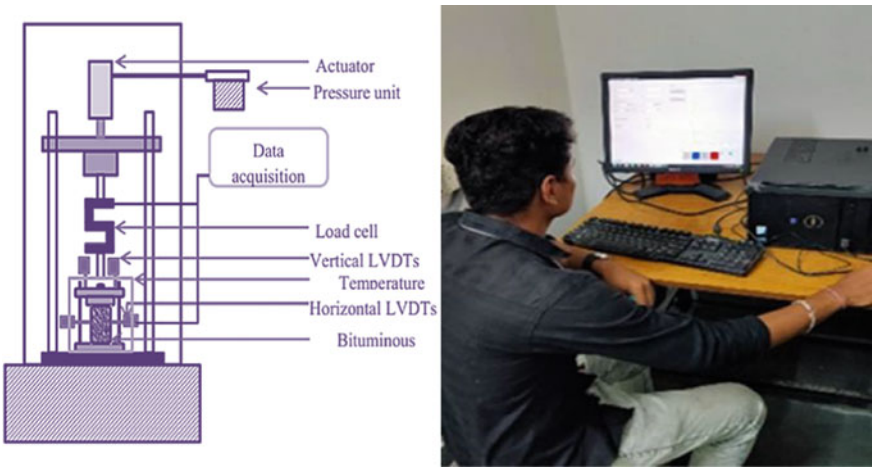

Fig. 10 Resilient modulus test for the collected core samples in the field

mixes (M_R). Resilient modulus was calculated from Eq. (6).

$$MR = (P(0.27 + \mu))/(t \times \Delta h) \tag{6}$$

where MR = bituminous mix resilient modulus (MPa), 'P' = applied load (N), μ-'Poisson's ratio', 'T' = sample thickness (mm), and Δh = horizontal deformation (mm).

Fracture properties

In the current investigation, an intermediate temperature of 25 ^{O}C was employed to analyze the fracture properties of asphalt core sample mixtures using the Semi-Circular Bending (SCB) test. Cylindrical specimens of 150 mm diameter were divided in half to create semi-circular test specimens having dimensions of 75 mm in diameter and 50 mm in thickness. Additionally, 5 mm and 10 mm deep notches were carved halfway through the flat side of the semi-circular specimens using an appropriate diamond cutter. A SCB test is carried out to evaluate asphalt mixes with regard to cracking resistance because fatigue failure is one of the most frequent causes of failure in asphalt layers. This test measures the fracture resistance of asphalt mixtures in terms of (i) fracture toughness (K), (ii) fracture energy (G), (iii) cracking resistance index (CRI), and (iv) critical strain energy release [14]. According to ASTM D 8044–16 [22], the test was carried out with a monotonic loading rate of 0.5 mm/min (Fig. 11).

The equations listed below (Eq. 7–11) were used for the computation of fracture properties. The fracture toughness, fracture energy, flexibility index, critical strain energy rate, and cracking resistance index.

Fracture Toughness (K):

Fig. 11 Fracture properties conducted through semi-circular bending test

$$K = \sigma \times YI\ (\text{sqrt}\ (\pi \times a) \tag{7}$$

YI (t/d) = YI (100/150) = YI (0.66).
YI (0.66) = 4.782 + 1.219(c/r) + 0.063e^ (7.045 × c/r).
Where c—notch length, r—radius.

Fracture energy (Gf):

$$Gf = (W0 + mg\delta 0)/A_{lig} \tag{8}$$

where W0—Fracture work area below load displacement curve,

M—mass (negligible because small samples are used), g—gravitational acceleration.

$\delta 0$ = deformation, A_{lig} = Ligament area = t(r–c).

Where t—thickness, r—radius, c—notch length of SCB specimen.

Flexibility Index (F.I):

$$F.I = 0.01((\text{Fracture energy})/(\text{post peak slope at inflection point})) \tag{9}$$

Crack Resistance Index (C.R.I):

$$C.R.I = Gf / Pmax \tag{10}$$

Critical strain energy release rate (JC kJ/m2 integral):

For Two notch lengths:

$$\text{Jc} = (\text{A1}/\text{t1} - \text{A2}/\text{t2}) \times 1/(\text{a2} - \text{a1}) \tag{11}$$

where A1, A2 = Area under the curve up to maximum load Pmax; a1, a2—initial notch lengths. t1, t2—thickness of samples.

7 Prioritization Technique

The ultimate goal of this work shall lead to the development of a Maintenance Management plan for the chosen pavement segment that is solely based on the pavement's functioning characteristics. The major indicators for building a Maintenance Priority Index are commonly recognized as Deflection and Ride Quality.

The SN of the pavement was determined using the ANN connection from the material characteristics and roughness of the pavement. Roughness Index and Deflection Index Eqs. (12) and (13) were used for the assessment of ride quality.

$$\text{Deflection Index} = (\text{Predicted Deflection} \div \text{Maximum Permissible Deflection}) \times 5 \tag{12}$$

$$\text{Roughness Index} = (\text{Present Roughness} \div \text{Maximum Permissible Roughness}) \times 5 \tag{13}$$

The maximum traffic value was set at 10 million standard axles (msa), and the maximum allowed deflection value was computed according to IRC 81–1997 [30] and was 1.05 mm. The maximum allowable roughness value was set at 2.55 m/km. The following Eq. (14) was used to compute the Road Condition Index (RCI).

$$\text{RCI} = (\text{Maintenance Priority Index} \div \text{Traffic Factor}) \tag{14}$$

The Traffic Element was also taken into account while constructing the Repair Priority Index since it is an essential assessment factor for prioritizing the roads that require maintenance. According to IRC SP: 72, Equivalent Standard Axle Load (ESAL) was computed for the design life of the roads using current traffic data. The Traffic Factor was explored from the cumulative ESAL applications. Equation (15) was used to find the Maintenance Priority Index (MPI).

$$\text{Maintenance Priority Index} = \text{RCI} \times \text{Traffic Factor} \tag{15}$$

The Service Priority Ranking was used to assess the specified roadways for maintenance and rehabilitation work (MPI). Table 5 explains the MPI for all of the specified sections [see Table 1]. Using Eqs. (12) and (13), the Roughness Index and Deflection Index were derived from the average IRI and deflection values of each section. The MPI of road sections was estimated using Eq. (15).

Table 1 Functional characteristics of the study locations

Toward Jeedipally				
Sections	Skid number (Sn)			Roughness IRI value (m/km)
	Conventional Sn	Water Sn	Oil Sn	
462	30	26	23	1.55
460	32	28	22	1.49
461	35	29	24	1.57
459	23	23	24	1.64
458	41	51	48	1.53
457	40	39	35	1.67
456	41	40	36	1.57
455	42	39	36	1.55
454	32	29	27	1.52
Toward Kallakal				
454	32	29	27	1.52
455	42	39	36	1.55
456	41	40	36	1.57
457	40	39	35	1.63
458	41	51	48	1.53
459	23	23	24	1.74
460	25	24	22	1.54
461	30	26	23	1.5
462	29	36	37	1.55

The Artificial Neural Network (ANN) Approach

In this study, a comprehensive method to investigate the link across asphalt pavement material qualities, surface integrity, and structural capacity has been suggested. The Artificial Neural Network (ANN) approach was used as it has several advantages, including the capacity to learn and model non-linear and complicated interactions. ANNs are computational models that imitate physiological characteristics to simulate how the brain makes decisions. These are helpful for estimating and approximating unknown functions using a variety of input values (Fig. 12).

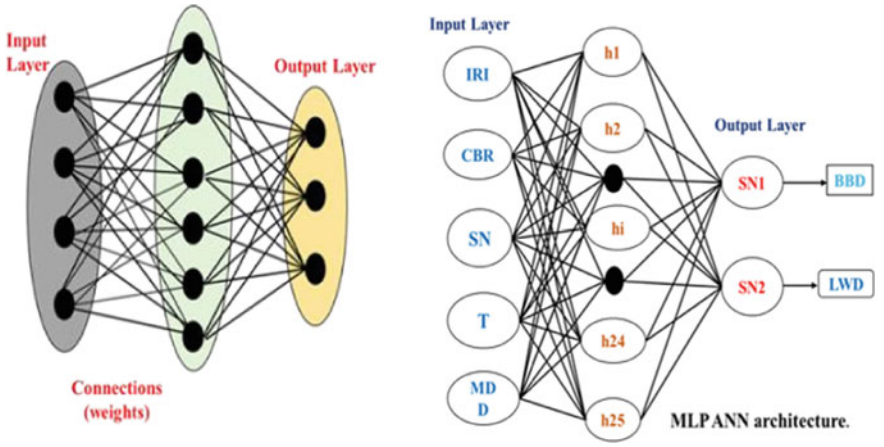

Fig. 12 MLP ANN structure and architecture

8 Results and Discussions

8.1 Functional and Structural Characteristics

The functional characteristics of the study locations, including skid resistance and roughness measurements, were measured, and the results are shown in Table 1.

Non-destructive test approaches such as deflection studies data were used to assess structural characteristics in the field. This also necessitates soil characteristics, and samples were collected from both directions. In the laboratory, moisture content, density, and CBR values were also determined. This data was used to compute Characteristic Deflection (CD), and the results are shown in Table 2 [a and b] for ready reference.

The surface deflection was measured using a lightweight deflectometer (LWD) from Kallakal to Jeedipally in both directions. This shall help in determining the structural number of pavement sections. In this study, a 300 mm dia. base plate was used in the field to calculate surface deflection, as shown in Fig. 13.

According to the test results, the surface modulus for the jeedipally toward 458 section is 640 Mn/m2 when tested using a 200 mm plate, whereas the surface modulus values for the kallakal toward likewise high at 458 section is 680 Mn/m2. And observe the load and central deflection of jeedipally and kallakal sections were 8.23 kn, 0.055 mm and 8.20 kn, 0.060 mm, respectively.

Table 2 Deflection data along the study stretches

(*a*) *Toward Jeedipally*				
Sections	Moisture content (%)	Dry density (g/cc)	CBR (%)	Characteristic Deflection (mm)
462	11	1.9	4.15	0.56
461	15	2.06	3.57	0.6
460	10	1.8	4.4	0.71
459	17	2.08	3.85	0.57
458	15	2.06	3.74	0.64
457	13	2.07	4.25	0.65
456	11	1.9	4.1	0.64
455	10	1.8	3.5	0.69
454	7	1.79	4.26	0.68
(*b*) *Toward kallakal section*				
454	7	1.79	3.34	0.463
455	10	1.8	3.15	0.57
456	11	1.9	2.97	0.602
457	13	2.07	3.25	0.517
458	15	2.06	3.05	0.409
459	17	2.08	2.09	0.592
460	10	1.8	3.26	0.834
461	15	2.06	3.1	0.508
462	11	1.9	2.95	0.5

8.2 Field Mixes Evaluation From Laboratory Studies

The pavement mix characterization was done in the lab using the core samples that were collected from the study locations. As a result, TSR tests on conditioned and unconditioned samples were carried out at 35 ^{0}C to determine moisture sensitivity. Tensile strength ratios were comparing the tensile strength of conditioned and unconditioned samples. The results are depicted in Fig. 14.

The resilient modulus (M_R) of the samples collected from the study sites was also determined. The test was carried out on a repeated load test setup in accordance with ASTM D7369-11 guidelines, as shown in Fig. 15. The sum of immediate and time-dependent continuous recoverable deformation during the test phase of one cycle. Table 3 and Fig. 16 show the M_R results for various sections.

Again, field samples of 150 diameter were used to assess fracture properties using a semi-circular bending test on a section of samples collected from the site. Load–displacement curves for 5 and 10 mm notch depths were measured at four Chainages. The fracture characteristics are calculated using these two variables and are presented in Fig. 17.

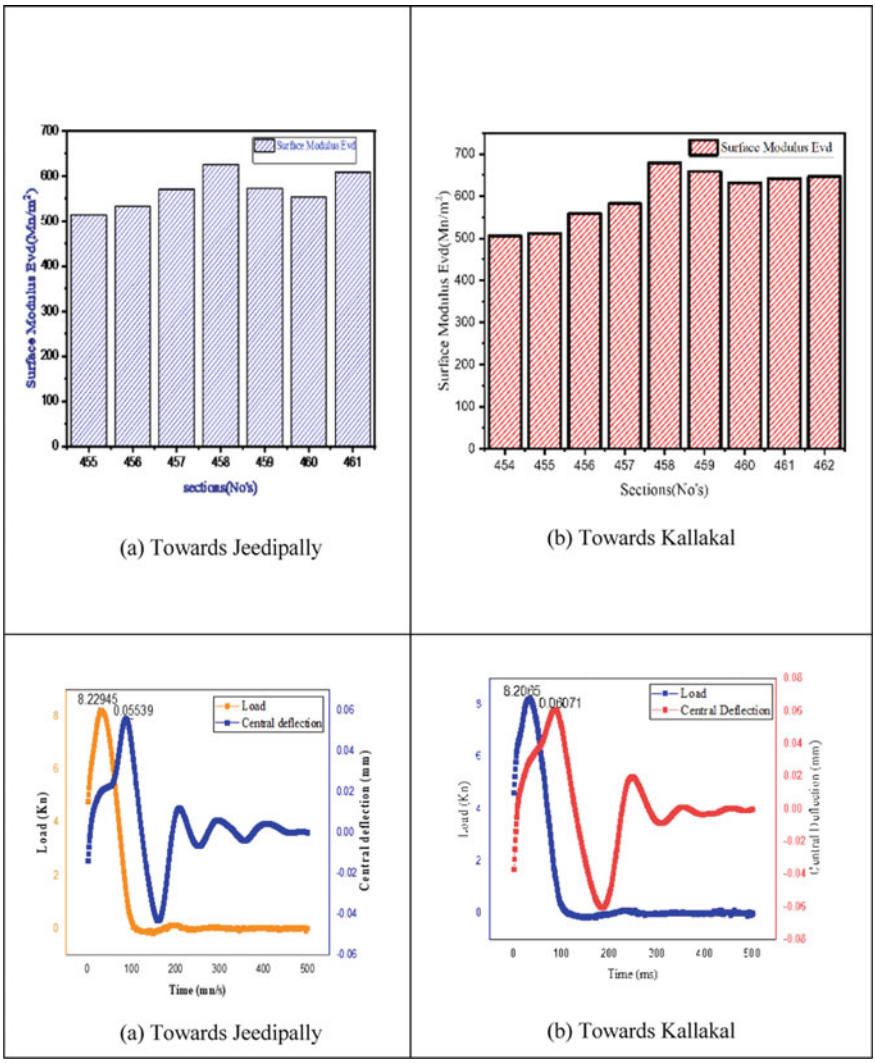

Fig. 13 LWD field test results on study locations

8.3 Correlation of Functional and Structural Characteristics and Prioritization

The Following characteristics and parameters were considered for correlation and maintenance priority.

IRI, Skid number, Pavement Temperature(°C), CBR, density, BBD–SN, LWD–SN.

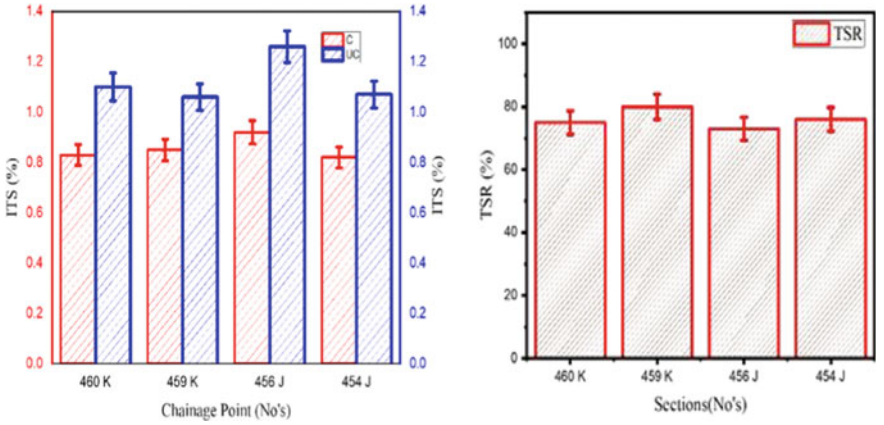

Fig. 14 Conditioned, unconditioned samples and TSR

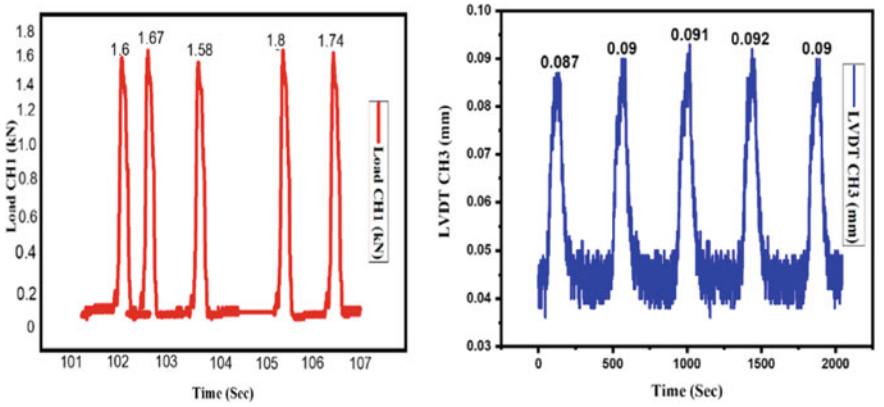

Fig. 15 Load and deflection data from repeated load test

- The soil subgrade's maximum dry density (MDD) in g/cc.
- MERLIN's International Roughness Index (IRI) in m/km.
- Skid number (Sn).
- Structure Number (SN).

The Multilayer Feed forward Neural Network is the most common form of ANN (MFNN). It is made up of three types of linked neuron layers: input, concealed, and output. Each neuron assesses the received inputs and creates an output based on an activation function, which is conveyed to neurons in the subsequent layer via the network topology's specified connections. Each connection is given a weight (w_i) that increases or reduces the input. A single neuron's relationship between inputs (x_i) and outputs (y_i) is characterized using a specific transfer function, which commonly has the logistic sigmoidal shape, as shown in equation.

Table 3 Resilient modulus of study sections

Toward Jeedipally			
sections	Load (N)	Deflection (Δh)	MR (mpa)
462 BC mix	1700	0.07	3011
458 BC mix	2000	0.075	3306
454 BC mix	1950	0.08	3022
462 DBM mix	1740	0.08	2697
458 DBM mix	1620	0.08	2511
454 DBM mix	1598	0.079	2508
Toward Kallakal			
463 BC mix	1875	0.074	3142
464 BC mix	1950	0.08	3023
465 BC mix	1987	0.078	3160
463 DBM mix	1768	0.085	2579
464 DBM mix	1678	0.08	2600
465DBM mix	1871	0.09	2578

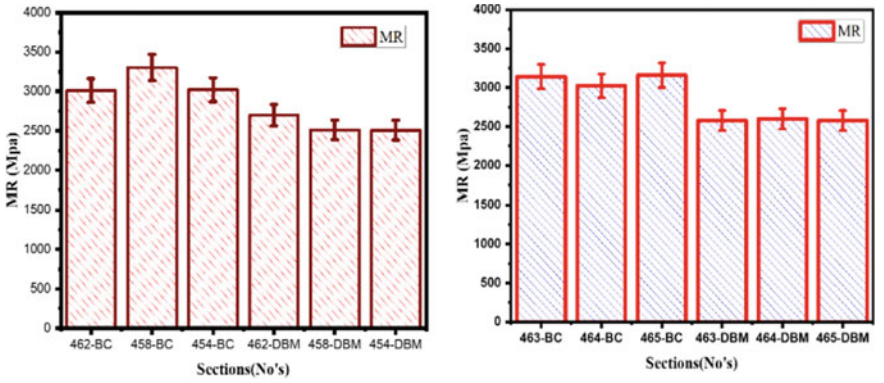

Fig. 16 Resilient modulus test results for study sections

$$F(I) = 1/(1 + e^{\wedge}(-1)) \tag{16}$$

For each location, the database has the following characteristics. $I = (w_i\ x_i)$ represents the total of the preceding neurons' weighted inputs x_i.

The training approach of a supervised technique, such as MFNN, involves modifying the various weights to produce acceptable output given a large set of input and output data. The output should resemble what was supplied for training. By considering consolidated values, the ANN correlation technique was developed, which is presented in Table 4 for both directions, and Fig. 18 represents the correlation between structural and functional characteristics.

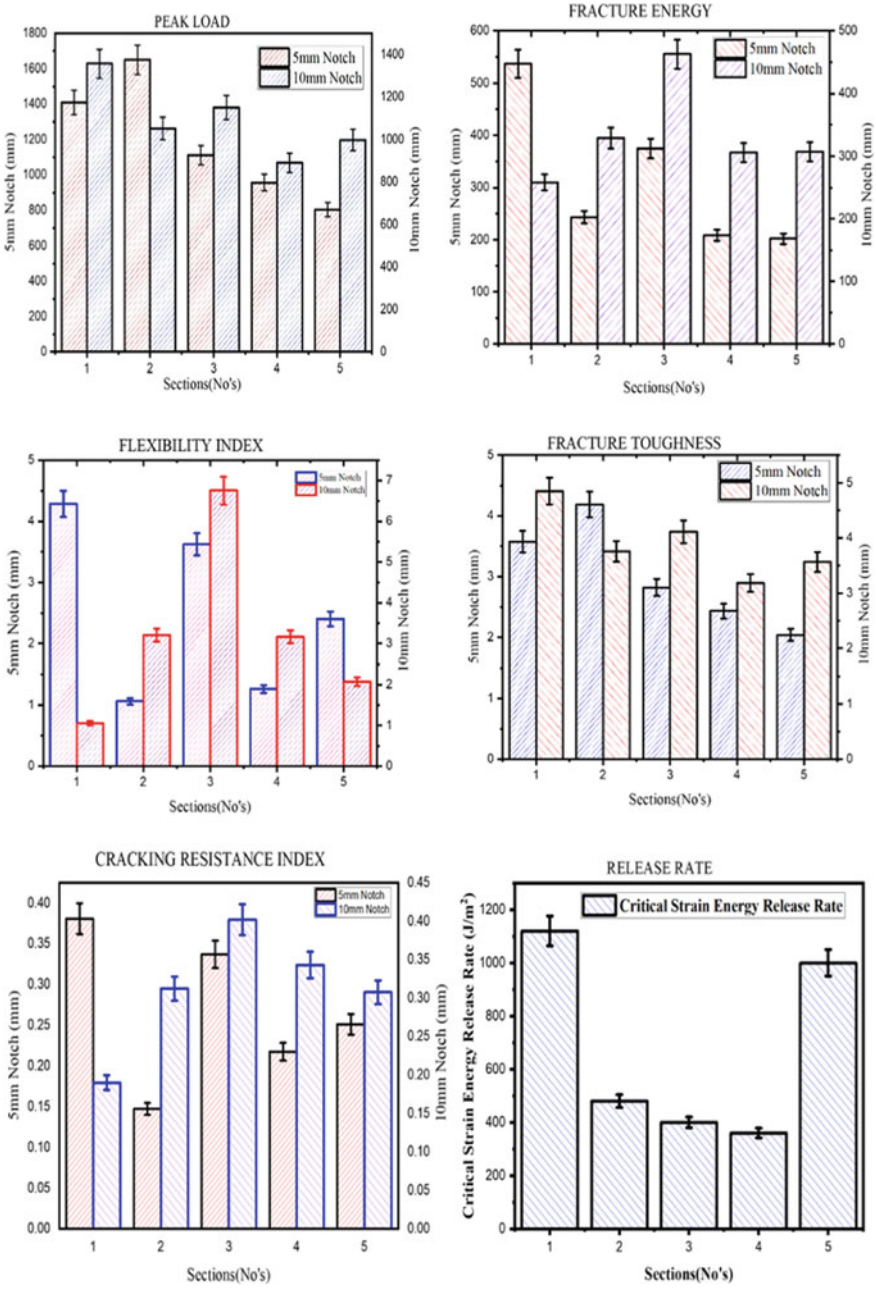

Fig. 17 Fracture parameters for test samples collected at study locations

Table 4 Database values for ANN technique

(*a*) *Toward Jeedipally*

Sections	IRI (m/km)	C Sn	W Sn	O Sn	Temp.	CBR %	MDD (g/cc)	BBD SN	LWD SN
462	1.58	29	36	37	41.28	4.15	1.91	4.60	4.92
461	1.62	43	37	30	41.3	3.57	1.89	4.44	4.9
460	1.68	35	33	36	41.3	4.4	1.76	3.97	5.19
459	1.58	44	67	64	41.27	3.85	1.75	4.56	5.02
458	1.68	46	44	42	41.75	3.74	1.89	4.25	4.95
457	1.55	31	34	32	42	4.25	1.96	4.20	4.9
456	1.46	47	45	42	41.69	4.1	1.95	4.23	5.08
455	1.67	44	60	39	42.9	3.5	1.82	4.05	4.95
454	1.54	65	55	46	42.9	4.26	1.9	4.10	4.97

(*b*) *Toward Kallakal*

Sections	IRI (m/km)	C Sn	W Sn	O Sn	Temp.	CBR %	MDD (g/cc)	BBD SN	LWD SN
454	1.52	32	29	27	40.9	3.34	1.79	5.20	4.71
455	1.55	42	39	36	40.95	3.15	1.8	4.56	4.72
456	1.57	41	40	36	40.26	2.97	1.9	4.41	4.86
457	1.63	40	39	35	37.7	3.25	2.07	4.85	4.93
458	1.53	41	51	48	37.5	3.05	2.06	5.62	5.19
459	1.74	23	23	24	37.65	2.09	2.08	4.45	5.14
460	1.54	0	0	0	37.7	3.26	1.8	3.59	5.07
461	1.5	30	26	23	38.3	3.1	2.06	4.90	5.09
462	1.55	29	36	37	38.35	2.95	1.9	4.95	5.11

Where SN—Structural Number, C—Conventional Sn, W—Water Sn, O—Oil Sn, T—Temperature, MDD—Maximum Dry Density, BBD SN—BBD Calculated SN, LWD SN—LWD Calculated SN.

The ANN approach is used to establish the predicted BBD Deflections. The predicted BBD deflection values are correlated with the measured BBD deflection values, and the correlation between the measured BBD deflection and the anticipated BBD deflection values is extremely strong, as illustrated in Fig. 19.

Based on the MPI, pavement maintenance engineers can prioritize the road sections for repair work. A high MPI value indicates that a specific stretch of road requires special attention. However, regardless of MPI, if a road has a DI or RI value greater than 4, corrective actions should be implemented as soon as possible. as shown in Table 5.

The DI value determines the priority index network in both directions; if the DI value is greater than 4, that section receives the first priority for rehabilitation and maintenance. If the DI value is less than 4, the MPI value is used. The higher the MPI

Table 5 Priority network for study sections

(*a*) *Jeedipally section*						
Sections	DI	RI	RCI	TF	MPI	PI Network
454	2.62	2.98	5.60	7	39.21	8
455	3.30	3.04	6.33	7	44.34	5
456	3.26	3.08	6.34	7	44.37	4
457	4.01	3.20	7.21	7	50.44	2
458	2.32	3.00	5.32	7	37.21	9
459	3.21	3.41	6.63	7	46.38	3
460	4.69	3.02	7.71	7	53.97	1
461	2.82	2.94	5.76	7	40.30	7
462	2.77	3.04	5.81	7	40.68	6
(*b*) *Kallakal section*						
462	2.72	3.10	5.82	8	46.57	8
461	2.83	3.18	6.01	8	48.06	6
460	3.54	3.29	6.83	8	54.65	1
459	2.72	3.10	5.82	8	46.56	9
458	3.22	3.29	6.51	8	52.11	3
457	3.10	3.04	6.13	8	49.08	5
456	3.11	2.86	5.97	8	47.74	7
455	3.26	3.27	6.53	8	52.26	2
454	3.23	3.02	6.25	8	49.98	4

value, the higher the priority of that section. Because there are no DI values greater than 4 in the kallakal section, the priority is determined by the MPI value.

9 Summary and Conclusions

Following a thorough functional and structural study of the chosen pavement, the following findings are reached:

- Based on a visual assessment of the road stretch, the bulk of the pavement portions, from 454 + 000 to 462 + 000 (in both directions) were evaluated as outstanding. Because there are no distresses on the pavement, its general state is likewise regarded as good.
- The acquired skid resistance data shows that the pavement is fully adequate for heavy traffic in both dry and wet conditions; however, because the skid resistance number is lower in wet conditions than in dry conditions, regular monitoring is required.

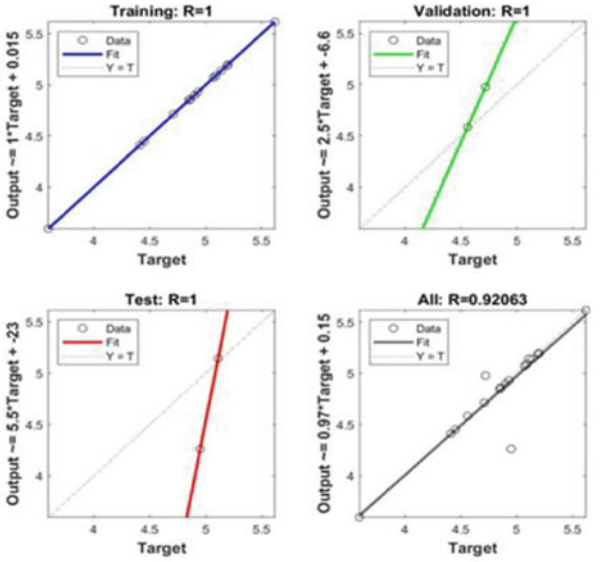

(a) Regression chart for Jeedipally section

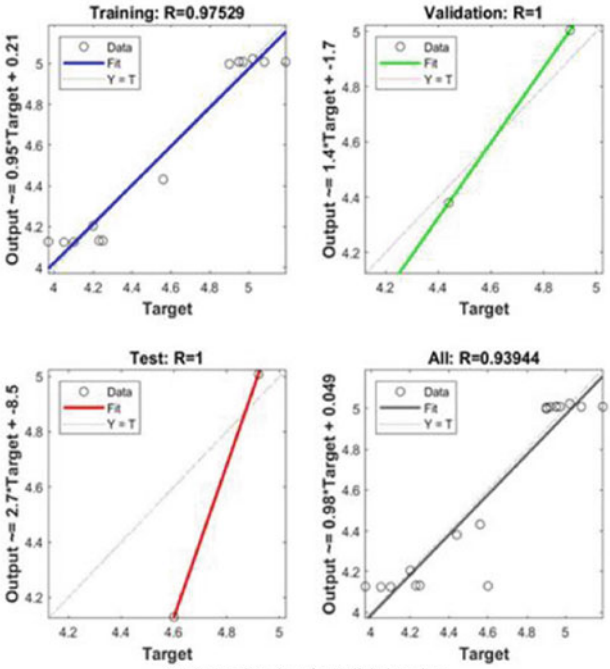

(b) Regression chart for Kallakal section

Fig. 18 Regression charts for both sections

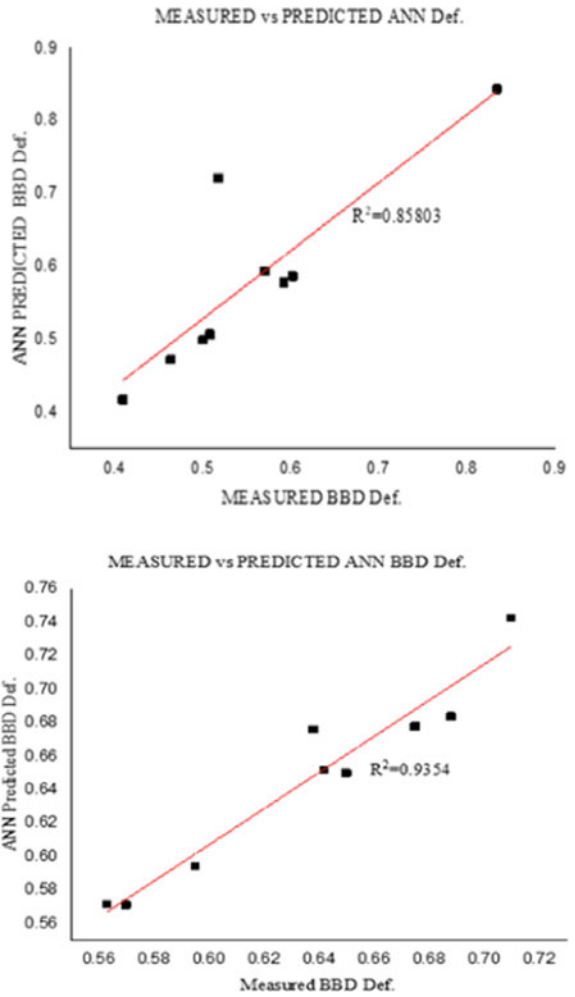

Fig. 19 Measured and projected deflection values for both sections

- According to IRC: SP 16–2019, the pavement's International Roughness Index (IRI) is 1.57 m/km, which is less than the maximum permitted roughness value of 2.55, indicating that the pavement is in "good" condition.
- The TSR (%) of the kallakal road segment is greater than that of the jeedipally road section, and the TSR ratio is evaluated using an IDT test on conditioned and unconditioned samples.
- Resilient modulus is a theoretical ideal elastic modulus that only considers recoverable strain. The average MR value of BC and DBM samples along Kallakal road section is 3000Mpa and 2600 MPa, respectively, with the same range as the Jeedipally road section.

- Composite fracture qualities directly offer an impediment to asphalt top-down breaking. The fracture energy of the BC sample is 536 J/m2, while that of the DBM sample is 462 J/m2. BC and DBM have peak load fracture parameters of 1651 N and 1357 N, respectively. The flexibility index was used to evaluate the failure behavior of BC and DBM samples. As the flexibility index rises, the likelihood of cracking decreases. The fracture resilience index increases the toughness of pavement fractures. And fracture toughness was discovered to be nearly identical in both areas.
- The correlation value for the ANN model is as high as 0.92, demonstrating the significant association between the structural and functional aspects of pavement sections.

This study proposes a different method for establishing a statistically reliable and exact connection between the structural and functional properties of asphalt pavement.

The ANN model has a correlation value as high as 0.92, demonstrating a significant relationship between the structural and functional aspects of pavements. This method reduces the frequency of costly and time-consuming tests for determining the structural features of pavements using Benkelman Beam Deflectometers, light Weight Deflectometers, and other devices.

The highest Maintenance Priority Index was reported in the current investigation on the Jeedipally to Kallakal segment at 460 and 457 sections. As a result, it is advised that this road portion be prioritized for maintenance and rehabilitation work. It is worth noting that if a road has a deflection or ride quality value that is more than its allowable maximum, that road should be prioritized for maintenance work regardless of its MPI. It is also advised that if a road has a DI or RI value of more than 4, remedial actions should be implemented on a priority basis and regardless of MPI.

The current technique will be extremely helpful to the maintenance department in prioritizing the road sections that require repair; it can also help in establishing a maintenance schedule that planned and looks forward for the next several years.

Acknowledgements The authors would like to extend their gratitude to the Device Development Scheme, Technology Development Programme, sanctioned by the Department of Science and Technology, Govt. of India, Ministry of Science and Technology for providing financial support for this research project. (Sanction order No. D.O. No. DST/TDT/DDP-12/2018 dt: 11.04.2019).

References

1. Guzzarlapudi SD, Adigopula VK, Kumar R (2016) Comparative studies of lightweight deflectometer and Benkelman beam deflectometer in low volume roads. J Traffic Transp Eng (Engl Ed) 3(5):438–447

2. Goyal MP, Karli S, Solanki VK (2017) Comparative studies between benkelman beam deflections (BBD) and Falling weight deflect meter (FWD) Test for flexible road pavement. IJSTE—International J Sci Technol & Eng 3(10)
3. Prabhu A, Arpith SP, Vahida KK, Kumar D, Bhat A, Kumar A (2021) Overlay design of flexible pavements using benkelman beam deflection method—a case study. Trends Civ Eng Chall Sustain, 475–491
4. Gunde R, Adepu R, Rachakonda P, Ch NR (2022) Laboratory evaluation of an indigenous developed light weight deflectometer as a quality control tool for pavement construction. Materials Today: Proceedings 60:431–439
5. Park SS, Bobet A, Nantung TE (2018) Correlation between Resilient Modulus (MR) of Soil, Light Weight Deflectometer (LWD), and Falling Weight Deflectometer (FWD). Jt Transp Res Program
6. Mulyawati F (2020) Comparative study of the use of FWD and LWD for flexible pavement evaluation". J Phys: Conf Ser, vol 1517, no 1. IOP Publishing, p 012031
7. Kavussi A, Rafiei K, Yasrobi S (2010) Evaluation of PFWD as potential quality control tool of pavement layers. J Civ Eng Manag 16(1):123–129
8. Reddy GS, Ramesh A, Ramayya VV (2022) Effect of nano-modified binder on fracture properties of warm mix asphalt containing RAP. Int J Pavement Res Technol:1–14
9. Ramesh A, Ramayya VV, Reddy GS, Ram VV (2022) Investigations on fracture response of warm mix asphalt mixtures with Nano glass fibres and partially replaced RAP material. Constr Build Mater 317:126121
10. Janani L, Dixit RK, Sunitha V, Mathew S (2020) Prioritisation of pavement maintenance sections deploying functional characteristics of pavements. Int J Pavement Eng 21(14):1815–1822
11. González A, Chamorro A, Barrios I, Osorio A (2018) Characterization of unbound and stabilized granular materials using field strains in low volume roads. Constr Build Mater:176, 333–343. ASTM. ASTM D4695–03 (2020). Standard guide for general pavement defection measurements
12. ASTM. ASTM D4694–09 (2020) Standard test method for defections with a falling-weight-type impulse load device
13. Bertulienė L, Laurinavičius A (2008) Research and evaluation of methods for determining deformation modulus of road subgrade and frost blanket course. Balt. J. Road Bridge Eng. 3:71–76
14. ASTM E2583–07 (2015) Standard test method for measuring deflections with a light weight deflectometer (LWD). Am Soc Test Mater
15. ASTM D4695–03 (2020) Standard guide for general pavement deflection measurements
16. ASTM D6931 (2017) Standard test method for indirect tensile strength of asphalt mixtures. Am Soc Test Mater
17. Manual series-2, Asphalt mix design methods, 7th edn
18. IRC: 66−1976 Recommended practice for sight distance on rural highways
19. IRC: 62−1976 Guidelines for control of access of highways
20. IRC: 32–1969 Standard for vertical and horizontal clearances of overhead electric power and telecommunications lines as related to roads
21. IRC: SP: 84–2019/IRC SP 87–2019 Manual of specifications and standards for four /six laning of highways
22. Saha G, Biligiri KP (2015) Fracture damage evaluation of asphalt mixtures using Semi-Circular Bending test based on fracture energy approach. Eng Fract Mech 142:154–169
23. Cundill MA The MERLIN low-cost road roughness measuring machine, Transport and research laboratory, research report 301
24. IRC, guidelines for surface evenness of highway pavements, IRC: SP:16–2004.
25. Zaid NBM, Hainin MR, Idham MK, Warid MNM, Naqibah SN (2019) Evaluation of skid resistance performance using British pendulum and grip tester. In: IOP conference series: earth and environmental science, vol 220, No 1. IOP Publishing, p 012016

26. IS 1203, Methods for Testing Tar and Bituminous Materials— Determination of Penetration, Bureau of Indian Standards, 1978 27
27. IS 1205, Methods for testing tar and bituminous materials—determination of softening point. Bureau of Indian Standards, 1978 28
28. IS 1206—Part II, Methods for testing tar and bituminous materials—determination of absolute viscosity. Bureau of Indian Standards, 1978
29. IS 1206—Part III, Methods for testing tar and bituminous materials—determination of kinematic viscosity. Bureau of Indian Standards, 1978 30
30. IRC: 81−1997 Guidelines for strengthening of flexible road pavements using benkelman beam deflection technique
31. ASTM D 8044–16 Standard test method for evaluation of asphalt mixture cracking resistance using the semi-circular bend test (SCB) at intermediate temperatures
32. IRC: 86−1983 Geometric design standards for urban roads in plains
33. Bureau of Indian standards, IS method of test for soils (part-5), determination of liquid and plastic limit (second revision), IS:2720(part-5)-1985 (reaffirmed 1995)
34. BIS, IS Classification and identification of soils for general engineering purposes, IS: 1498–1970
35. ASTM D4123 (1995) Standard test method for indirect tension test for resilient modulus of bituminous mixtures. Am Soc Test Mater

On-Street Night Car Parking Demand Estimation in Residential Areas: A Case Study at Delhi

Ashwani Bokadia and Mokaddes Ali Ahmed

Abstract The parking problem is a huge issue everywhere in the world. Delhi is one of India's biggest cities, which is affected by parking problems. The gradual growth in income and vehicle ownership per family is also the reason for the increase in parking demand. Day by day, the parking demand is also increasing in residential areas during nighttime due to insufficient space for car parking in most houses in residential areas, which leads to roadside parking at night. An appropriate management strategy should therefore be put into place for on-street night parking demand. In this study, three residential areas—Ber Sarai, Jia Sarai, and Katwaria Sarai, Delhi, have been selected as the case study areas. Parking demand models are developed to estimate the parking demand and determine the important parameters. The demand model's formation includes parameters like the number of cars owned, the presence of garage facilities, future car ownership, etc. The parking accumulation is found from field surveys such as in–out survey and license plate survey. The parking volume and peak hours for each location are obtained using a questionnaire survey. The parking demand model is generated using linear regression analysis using a statistical package for social sciences (SPSS). Using regression analysis, the good parking demand model with less error is found. In this study, a parking policy is also suggested to reduce and control parking demand during night-time based on vehicles' locations and parking demand.

Keywords Parking demand · On-street night parking · Parking accumulation · SPSS software · Regression analysis · Parking policy

A. Bokadia (✉) · M. A. Ahmed
Research Scholar, Department of Civil Engineering, NIT, Silchar, India
e-mail: ashwanibokadia1994@gmail.com

A. Dhamaniya et al. (eds.), *Recent Advances in Traffic Engineering*, Lecture Notes in Civil Engineering 377, https://doi.org/10.1007/978-981-99-4464-4_17

1 Introduction

Nowadays, due to the metro cities' worldwide rapid growth, there is an increasing rate of parking, which causes major parking issues in the majority of urban areas. On-street night parking demand in residential areas is increasing daily due to insufficient parking space and vehicle ownership. Also, It has been observed that car owners park their vehicles on-street at night in metro cities such as Chennai, Kolkata, and Mumbai. One of the largest cities, Delhi, has a similar issue with parking in residential neighborhoods. The city, which covers an area of 1,484 km^2, is the greatest commercial center in northern India and is situated in the northern region of the country. The demand cannot be satisfied by the availability of parking space in many residential areas of Delhi due to the insufficient parking system and facilities there. This will create more demand for parking in residential areas. A town planner must thus do a thorough analysis of parking in order to manage on-street parking.

The objective of the study is to find the important factors that affect the night car parking demand in residential areas, to study the present parking condition in residential areas, to develop a night parking demand model, and to suggest some policies to reduce on-street night car parking demand.

2 Literature Review

Developed an approach, according to cluster analysis, to create profiles of aggregate parking accumulation in parking lots, to improve the effectiveness of surveys' data gathered. According to the authors, accumulation profiles might help transportation experts make decisions and evaluate parking demand models. Furthermore, such profiles can help in the creation of parking information systems in real-time as well as the assessment of various traffic management tactics [1]. Conducted a campus study at the Beijing University of Aeronautics and Astronautics. The research collected data flow into and out of the university campus at the main university entrance and exit in order to analyse demand at different times of the day. Parking duration was calculated for each car by withdrawing entering time from exit time. A basic analysis of parking demand, duration, and turnover was carried out in the research [2, 3]. The research was done on three different land use patterns, including downtown, malls, and seaside parks. The study used a continuous investigation of license plate numbers gathered for a minimum of 3 h and recorded every 5 min. According to one study, license plates should be observed less than every 30 min in urban areas and every 60 min in coastal parks to identify all potential ideal parking features and cost-effective surveying [4]. Investigated the alteration in occupancy as a result of parking charge changes for a San Francisco study area where a parking policy based on performance was introduced. The authors determined that there is a considerable negative correlation between changes in occupancy and parking charges [5–7]. Created a method that may be used uniformly to analyse the potential savings in cruising time brought on by adopting

intelligent parking services (IPS). Using probability macroscopic parking models and theory, the authors investigated cruising situations with and without IPS. The authors calculated that IPS might save up to 15.6 h (17%) of traveling time in a normal, typical workday in a small downtown area (0.28 km^2) [8, 9]. Studied the efficacy of urban on-street parking charging schemes. The authors found that improving enforcement of on-street parking is possible to prevent negative parker attitudes. Such behavioral methods decrease overall traffic safety and accessibility, particularly in metropolitan areas. Furthermore, raising awareness of different alternative offerings in the respective field (PT, P&R, shared mobility, walkability, etc.) allows for the reduction of uncontrolled use of personal cars and the development of a co-modal strategy for sustainability [10–12]. Investigated the efficacy of parking strategies in reducing parking demand and vehicle use. The authors observe that visitors respond to parking restrictions by shifting to a new parking lot instead of transferring to another form of transportation. Based on simulations of various policies, authors concluded that when pricing and measure policies are combined, they have a greater overall impact on shaping parking demand than if they were used alone [13–15].

3 Study Area

Parking locations in various Delhi neighborhoods have been chosen for this study in residential areas. The areas of study were selected based on on-street night parking demand. The three areas, namely, Ber Sarai, Jia Sarai, and Katwaria Sarai, Delhi, are all residential areas of Delhi City and are under the municipal corporation of Delhi, as shown in Figs. 1, 2, and 3. The majority of residents in these neighborhoods drive their own automobiles, and they typically leave them in the street overnight close to houses or flats. People may encounter several issues in these places at night, such as congestion, accidents, delays, etc., as a result of on-street night parking.

4 Methodology

This study developed a methodology to calculate the impact of residential parking on car demand. Utilize the initial phase survey data collection methods like in–out survey and license plate to find out the all-over idea about the location and parking demand. Moreover, from a questionnaire survey, obtain the data from houses with the help of parameters. In the second step, with the help of SPSS software and regression analysis, estimate the parking demand equation and formulate the parking demand model for the study and the overall methodology shown in Fig. 4.

The quantity of parking space required in a specific location at a given time is known as the parking demand. When demand exceeds parking availability, the issue for the transportation system becomes more serious. The data gathered from various

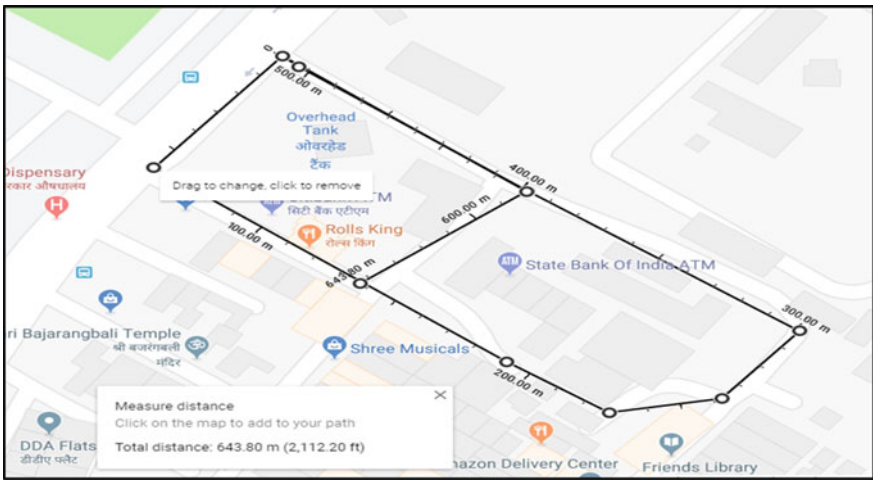

Fig. 1 Survey location map: Ber Sarai, Delhi

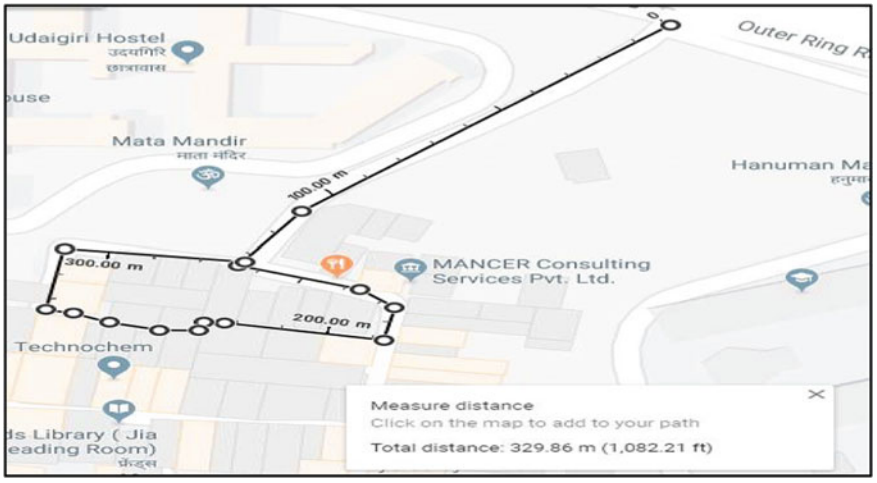

Fig. 2 Survey location map: Jia Sarai, Delhi

surveys are examined to create the parking demand model. This study includes variables such as the number of four-wheelers owned, the presence of garage facilities, and future car ownership. The standard regression equation form (by incorporating the parameters mentioned earlier) is shown below in Eq. 1. The following equation gives the demand equation:

$$N = \alpha_0 + a_1 \times x_1 + a_2 \times x_2 + a_3 \times x_3 \tag{1}$$

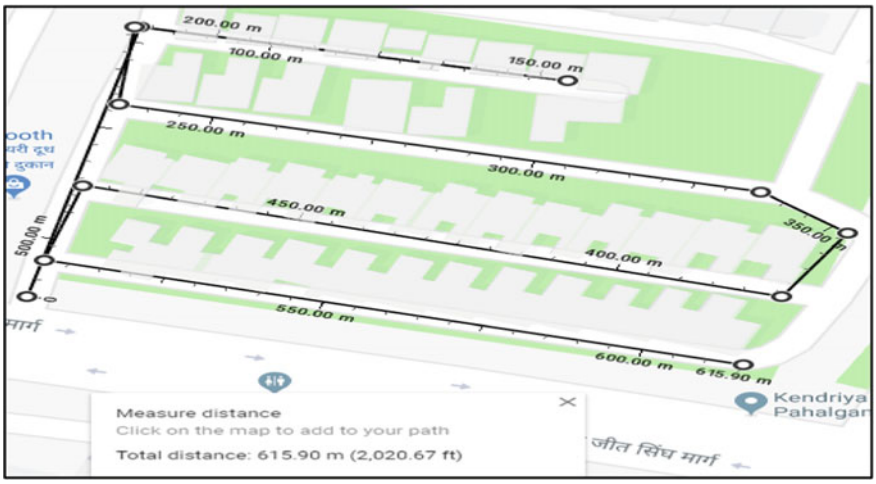

Fig. 3 Survey location map: Katwaria, Sarai, Delhi

where

N = parking demand.

$\alpha_{0,}a_{1,}a_{2,}a_3$ are constant values.

x_1= No. of cars owned.

x_2=Availability of garages at home.

x_3= Future car ownership.

Number of car owned increase in vehicle ownership leads to requirement for parking space in buildings or apartments. Parking space requirement directly influences parking demands. If sufficient parking space isn't available in the structure or apartments, at that point, there will be an increase in on-street night parking demand. Availability of garages at home will decrease the night parking demand at nighttime. If the resident has no garage facilities for car parking in our building and apartment, there will be more chances they park their vehicle on-street during nighttime. And this will directly affect parking demand. And future car ownership increase in car ownership but fixed is available in parking space in buildings and apartments. Parking spot requirements indirectly affect parking demands.

5 Survey and Data Collection

5.1 In–Out Survey

An in–out survey is conducted to determine the parking area's occupancy and track the accumulation profile. From the survey, the initial number of the space-occupied area is used, after which the number of cars entering the parking area for a specific

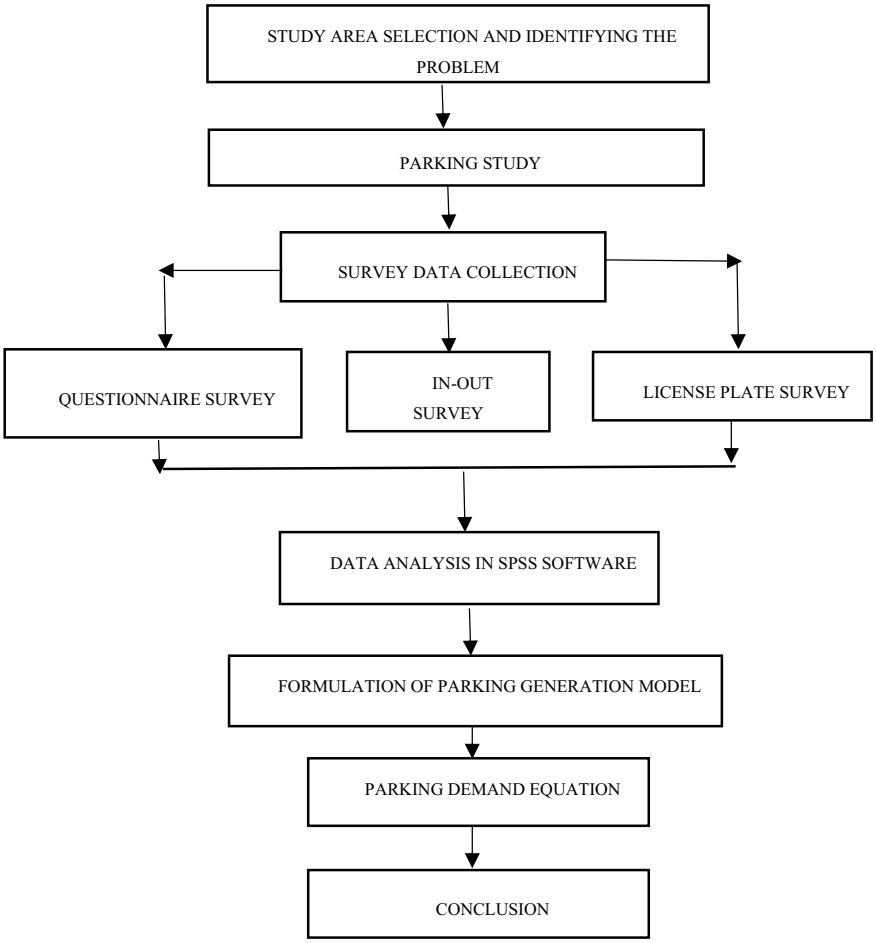

Fig. 4 Methodology flow chart

time period is counted. The quantity of cars leaving the parking area is also taken. The final occupancy is recorded at the survey's location. The poll was taken at three locations, Ber Sarai, Jia Sarai, and Katwaria Sarai in Delhi, from 9 PM to 6 AM to determine the parking accumulation as shown in Fig. 5.

5.2 Questionnaire Survey

It has been conducted at various survey locations so that the survey form has a minimum number of questions and gets the full user information. Seventy respondents from each location were collected and a detailed summary was prepared, as

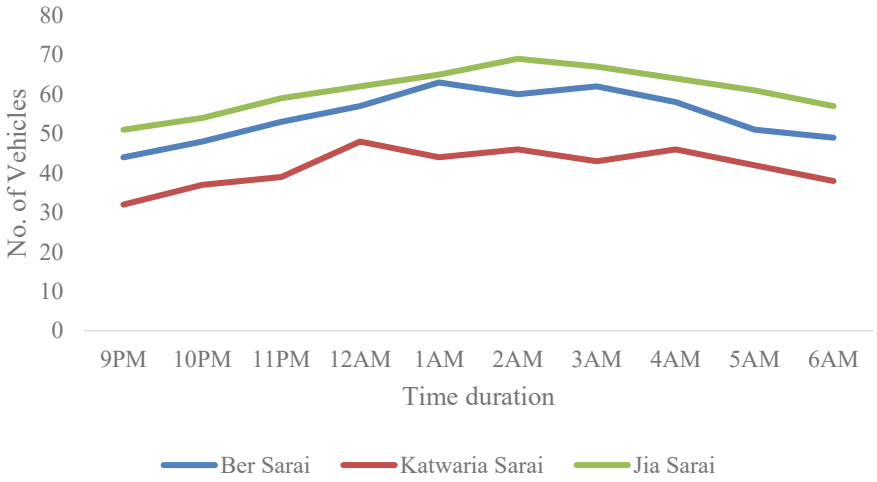

Fig. 5 Parking accumulation profile for all three locations

Table 1 Data collected

Data collected by questionnaire survey	Responders -in numbers total no. of sample (70)
Ber Sarai	
No. of four-wheelers owned	(a) 0 (5) (b)1 (61) (c) 2 (1) (d) > 2 (0)
Presence of garage facilities	(a) Yes (11) (b) No (59)
Do you wish to buy a car in future	(a) Yes (39) (b) No (31)
Jia Sarai	
No. of four-wheelers owned	(a) 0 (14) (b) 1 (44) (c) 2 (9) (d) > 2 (3)
Presence of garage facilities	(a) Yes (4) (b) No (66)
Do you wish to buy a car in future	(a) Yes (46) (b) No (24)
Katwaria Sarai	
No. of four-wheelers owned	(a) 0 (17) (b) 1 (40) (c) 2 (6) (d) > 2 (7)
Presence of garage facilities	(a) Yes (16) (b) No (54)
Do you wish to buy a car in future	(a) Yes (52) (b) No (18)

shown in Tables 1 and 2. Using the extracted data, linear regression analysis in SPSS has been used to evaluate the parking demand equation (Eq. 1).

6 Results and Discussions

Data from several types of surveys have been examined and presented as follows.

Table 2 Descriptive summary of the survey locations

Survey locations	Registered number of families	Total width of the road (in m)	Width available after parking (in m)	Type of parking
Ber Sarai, Delhi	602	7.73	3.73	Two side parallel parking
Jia Sarai, Delhi	690	7.62	4.02	Two side parallel parking
Katwaria Sarai, Delhi	2348	7.54	3.94	Two side parallel parking

6.1 Parking Accumulation

It refers to the total number of parked cars at any particular moment. The peak parking accumulation for each survey location is shown in Fig. 6. From the figure, it can be seen that Jia Sarai is more congested than the other two areas.

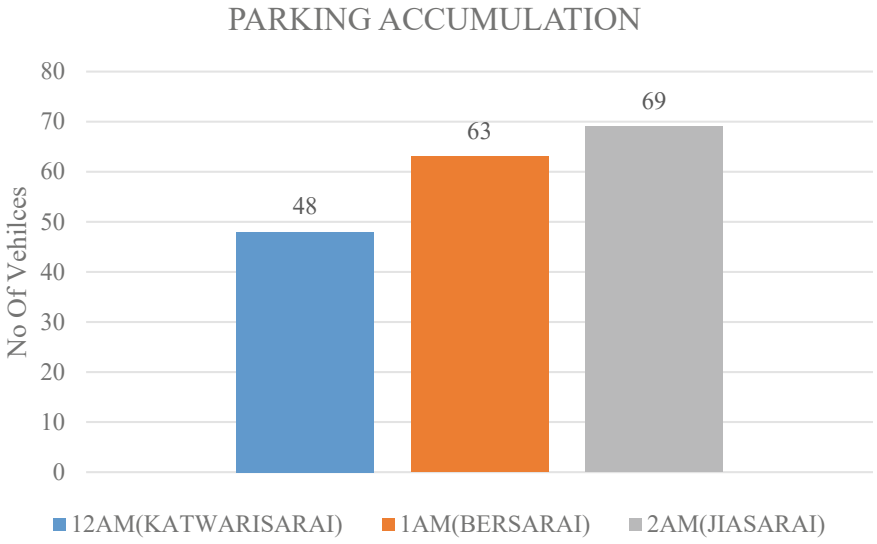

Fig. 6 Peak night parking accumulation profile

6.2 Parking Demand Model

The information gathered through the questionnaire survey was utilized in SPSS, a linear regression analysis was performed, and the regression equation for the three locations was obtained.

The model summary for the locations is shown in Table 3. The R-Squared values shows the correlation between the dependent and independent variables and the standard error of the estimate shows the accuracy of the predicted value.

The model coefficients are shown in Table 4. These are the independent variables found from the model, where the number of vehicles owned by a family and future car ownership are all significant. The presence of any garages is also significant enough to affect the parking demand. The significant value of less than 0.05 shows that the variables are significant, thereby developing a good relationship with the dependent variables and hence the predicted model is suitable for the study. The small value of standard error also signifies that the variables are positively related to the dependent variables.

The final demand equation for all three locations is equated using regression analysis with the help of SPSS software, as shown in Table 5.

ANOVA is also done for the locations and the results are shown in Table 6. The significant value is less than 0.05, which shows that the predicted model is suitable for all the locations.

Table 3 Model summary

Location	Model summary				
	R	R squared	Adjust R squared	Std. error of the estimate	Durbin watson
Ber Sarai	0.657	0.431	0.406	0.391	1.910
Jia Sarai	0.821	0.675	0.660	0.296	2.071
Katwaria Sarai	0.739	0.546	0.525	0.350	2.208

Table 4 Model coefficients

Location	Model	Unstandardized coefficient		Standardized coefficient	T	Sig.
		B	Std. error	Beta		
Ber Sarai	(Constant)	−1.461	0.451		−3.241	0.002
	No. of cars owned	0.561	0.097	0.542	5.804	0.000
	Home garages	0.503	0.198	0.237	2.538	0.014
	Future car ownership	0.339	0.095	0.333	3.553	0.001
Jia Sarai	(Constant)	−1.603	0.330		−4.860	0.000
	No. of cars owned	0.667	0.065	0.722	10.270	0.000
	Home garages	0.500	0.150	0.236	3.340	0.001
	Future car ownership	0.269	0.074	0.258	3.655	0.001
Katwaria Sarai	(Constant)	−1.304	0.384		−3.395	0.001
	No. of cars owned	0.558	0.072	0.647	7.711	0.000
	Home garages	0.555	0.177	0.261	3.135	0.003
	Future car ownership	0.189	0.091	0.174	2.067	0.043

Table 5 Parking demand equation

Location	Demand equation
Ber Sarai	$N = -1.461 + 0.561 \times X_1 + 0.503 \times X_2 + 0.339 \times X_3$
Jia Sarai	$N = -1.603 + 0.667 \times X_1 + 0.500 \times X_2 + 0.269 \times X_3$
Katwaria Sarai	$N = -1.304 + 0.558 \times X_1 + 0.555 \times X_2 + 0.189 \times X_3$

Table 6 ANOVA results

Location	ANOVA			
	Sum of squares	Mean square	F	Sig.
Ber Sarai	7.666	2.555	16.688	0.000
Jia Sarai	11.989	3.996	45.618	0.000
Katwaria Sarai	9.701	3.234	26.442	0.000

7 Conclusion

Car parking demand has been evaluated using the demand equation, and a multilinear regression model has been used to determine the parking demand during night-time. Three types of surveys have been conducted at Ber Sarai, Jia Sarai, and Katwaria Sarai, Delhi, to collect data on parking vehicle accumulation and peak time. The result shows that Jia Sarai is highly congested compared to the other two locations, with a maximum number of parked vehicles of 69 and a peak time of 2 am. Factors that affect on-street parking demand have been analysed. The number of cars owned, the presence of garage facilities, and future car ownership are the parameters that are used to generate the demand model, and the result shows that all of these parameters are found to be significant. In this study, Jia Sarai shows less error than Katwaria Sarai and Ber Sarai, signifying that the Jia Sarai model predicts better results for the study location. This model and demand equation will help reduce and control future on-street night parking demand in residential areas.

A policy that controls or reduces the increase in car ownership and legislation that encourages public transit instead of private vehicles should be introduced. It is recommended that a parking fee should be charged in order to reduce the use of private cars in the city. A study in Hong Kong shows that only 7% of all commuters use personal cars (Travel characteristics survey, 1993) [16]. This is because car ownership is so low and expensive parking fees are enforced at the workplace. Therefore, this strategy is beneficial for decreasing car ownership and usage in cities. The land value should determine the parking cost in a specific location or the rent being charged for the same. Promoting the use of public transportation and reducing the use of private cars is also beneficial from the perspective of equitable transportation.

References

1. Tong CO, Wong SC, Leung BSY (2004) Estimation of parking accumulation profiles from survey data. Transportation 31(2):183–202
2. Shang H, Wenji LIN, Huang H (2007) Empirical study of parking problem on university campus. J Transp Syst Eng Inf Technol, 7(2):135–140
3. Young W (2007) Modelling parking. Emerald Group Publishing Limited, In Handbook of transport modeling
4. Chimba D, Onyango M (2012) Optimization of short-term on-street park-pay license plate surveying. J Infrastruct Syst, 18(3):194–201
5. Pu Z, Li Z, Ash J, Zhu W, Wang Y (2017) Evaluation of spatial heterogeneity in the sensitivity of on-street parking occupancy to price change. Transp Res Part C: Emerg Technol 77:67–79
6. Maternini G, Ferrari F, Guga A (2017) Application of variable parking pricing techniques to innovate parking strategies. The case study of Brescia. Case Stud Transp Policy 5(2): 425–437
7. Ma R, Chen S, Zhang HM (2017) Relationships between parking garage occupancy and traffic speeds in cities: results from a data-driven study. Transp Res Rec 2643(1):74–83
8. Cao J, Menendez M (2018) Quantification of potential cruising time savings through intelligent parking services. Transp Res Part A: Policy Pract, 116:151–165

9. Sehdehi R, Henderson T, Nadeem M (2018) A novel inductively powered intelligent parking solution. In: 2018 IEEE International conference on industrial electronics for sustainable energy systems (IESES) (pp. 391–396). IEEE
10. Piccioni C, Valtorta M, Musso A (2019) Investigating effectiveness of on-street parking pricing schemes in urban areas: An empirical study in Rome. Transport Policy, 80:136–147
11. Alemi F, Rodier C, Drake C (2018) Cruising and on-street parking pricing: A difference-in-difference analysis of measured parking search time and distance in San Francisco. Transp Res Part A: Policy Pract 111:187–198
12. Ahangari S, Chavis C, Jeihani M, Moghaddam ZR (2018) Quantifying the effect of on-street parking information on congestion mitigation using a driving simulator. Transp Res Rec, 2672 (8):920–929
13. Yan X, Levine J, Marans R (2019) The effectiveness of parking policies to reduce parking demand pressure and car use. Transport Policy, 73:41–50
14. Kondor D, Zhang H, Tachet R, Santi P, Ratti C (2018) Estimating savings in parking demand using shared vehicles for home–work commuting. IEEE Trans Intell Transp Syst, 20 (8):2903–2912
15. Ou S, Lin Z, He X, Przesmitzki S (2018) Estimation of vehicle home parking availability in China and quantification of its potential impacts on plug-in electric vehicle ownership cost. Transport Policy, 68:107–117
16. Asia MVA (1993) Travel characteristics survey: Final report May. report for Transport Department, Territory Transport Planning Division (MVA Asia, Hong Kong)

A Study of Indian Wholesalers for Mode Choice Decisions in Urban Goods Distribution

Pankaj Kant, Sanjay Gupta, and Ish Kumar

Abstract Shippers make key decisions about shipment size and mode selection to lower total logistics costs. In this study, discrete choice models are developed for the urban distribution of commodities from wholesalers to retailers in the Indian city of Jaipur. To analyse market variance, the freight mode choice model selects two wholesale markets: building hardware (BHM) and electronics (EM). A structured questionnaire and a face-to-face, pencil-and-paper survey were employed to gather primary data. For all wholesale markets, binary logit models comprised of non-mortised transport (NMT), three-wheel commercial vehicle (3W), four-wheel commercial vehicle (4W), and light commercial vehicle (LCV) modes were developed for various time, cost, and distance combinations. Tonne-kilometre travelled (TKT) across commodity distribution and vehice kilometres travelled (VKT) are more suitable variables for intracity good distribution.

Keywords Urban freight · Mode choice · Wholesalers

1 Introduction

Urban goods distribution's effects on traffic, externalities, the fragility of the infrastructure, and compatibility with land use are all very concerning. The primary policy goal of many nations is the sustainability of urban goods transit [1]. Freight mode choice modelling is vital for policymakers to perform policy actions like reducing

P. Kant (✉) · S. Gupta · I. Kumar
Department of Transport Planning, School of Planning and Architecture, 4-Block-B Indraprastha Estate, New Delhi 110002, India
e-mail: pankaj179phd17@spa.ac.in

S. Gupta
e-mail: s.gupta@spa.ac.in

I. Kumar
e-mail: ish.phd.273tp21@spa.ac.in

A. Dhamaniya et al. (eds.), *Recent Advances in Traffic Engineering*, Lecture Notes in Civil Engineering 377, https://doi.org/10.1007/978-981-99-4464-4_18

externalities and congestion. Understanding and replicating urban freight stakeholder's behaviours and attributes is an essential research topic. Policy planners need to consider the effects of freight transportation on urban mobility from the perspective of sustainability [2]. The relationship between policy measures and stakeholder behaviours is still an area of investigation in the urban freight sector [3]. Associated urban freight traffic is significantly influenced by the flow of commodities and the frequency of shipments. The mode share and percentage of final commodities delivered by alternative transportation modes are determined by the type of infrastructure investment [4].

For the efficiency of the urban freight transport network and local sustainability, freight transport and urban freight strategies require better culmination. However, city planners procrastinated about the freight issues, transport operators and the last mile problem is often neglected to a large extent [5]. There are enough opportunities and scope to improve the efficiency of urban freight distribution as compared to long-haul freight (regional freight transport) without having additional costs to consumers and businesses [6]. Disaggregating models by commodity type can produce better estimates for freight mode choice [7]. Passenger transport is in a prime focus in cities of India in recent decades owing to National Urban Transport Policy, and urban freight is not adequately focused on in transport system development plan proposals in Indian cities [8]. Even the flagship smart cities mission programme of the Government of India, which has earmarked budgetary support for 100 smart cities to date has very limited priorities for urban freight transport proposals being taken up for implementation in these cities [9]. The explicit consideration of the urban commodities movement may help achieve the objectives of urban transportation. The goal of city planning, in particular, is to facilitate the efficient circulation of goods at targeted levels [10].

The diversity of urban freight stakeholders and the characteristics of urban goods movement present a significant barrier to policymakers seeking to implement interventions in city logistics. One of the topics that India hasn't covered enough is freight mode choice for intracity goods. The rest of the paper covers a literature review on mode choice for goods movement, research methodology, choice model formulation, characteristics of case city and wholesale markets, an overview of descriptive statistics of the data set, model estimation; and summing up with conclusions.

2 Literature Review

Econometric models such as discrete choice models are used at the shipment level for freight mode choice with modal attributes like cost, travel time, and distance [11]. To assess the variables impacting the selection of the freight modes, the probit with logit model was used for shipments among three zones in Maryland by revealing preference data. According to the findings, model choice decisions are critically influenced by mileage, the value of time, and fuel cost [12]. Microeconomic models are used to study how shippers select the size and mode of their shipments [13].

Time is the most critical variable for the shipper to determine freight mode choice for regional goods distribution [14]. For the shippers, the cost and quality factors of transport service, such as transit duration and damage rate, are significant, yet modality plays a significant part that is a fundamental aspect of their decision. For the end-shipper, a transport service's cost and quality factors like transit duration, dependability, and damage rate are important, but mode also has a non-negligible impact [15]. The taste characteristics of the shippers exhibit significant unobserved variation, according to the findings of multinomial logit models (MNL). Time and cost are subject to shipment size [16]. There is a greater need to analyse the changes in the firm's logistics for evaluating mode split and evaluation of transport infrastructure decisions [17].

Shippers have a high preference for the mode's service. The firm's inventory cost increases with an increase in transit mode time. Disaggregate models provide more accurate analyses and user satisfaction with a particular mode but are subject to the availability of data [18, 19]. The variables that may affect whether to use a rented truck, a personal truck or the rail mode were assessed using linear logit models. Rail mode is preferred for the long haul, and trucks are preferred for the short haul. Transit time, reliability in transit time, and length of hauls as essential factors for freight mode choice [20]. Binary choice models, along with sensitivity analysis, were used to evaluate the choices between truck and rail modes. Shipment cost is a critical factor for rail, whereas haulage time is for road shipments. No significant change in modal shift is observed with an increase in fuel cost [21]. A discrete–continuous model was used to analyse joint shipment size and mode choice with parameters of freight rate, transit time, frequency, and reliability. Logistics patterns are disturbed with policy-induced modal shifts, and shipment size needs to be adjusted accordingly [22]. A discrete–continuous model was used for evaluating factors affecting freight mode choice. Study results suggest that small vehicles are chosen for the higher value of shipment commodities and large vehicles for long-haul shipments [23]. A discrete–continuous model, along with elasticity analysis, was used for the choice of truck type by transport operators. Changes in shipment size or cost have a negative impact on the mode share in the market. Imposing an axle load ban increases the number of trips and thus causes more congestion [24].

The Multinomial logit model was used to analyse shippers' preferred freight mode. Shippers do not tend to use hire-carrier for high-value goods but have a high tendency to use LTL due to speed and reliability [25]. The degree of heterogeneity for the small truck, large truck, and rail modes for various commodities was assessed using a mixed MNL model. There is significant heterogeneity among shippers regarding service attributes, quality, and flexibility [26].

An MNL model was used to evaluate the probability of mode share for shipment size. Shipping cost is the highest among other variables [27]. A logit model with stated preference data was used to evaluate freight mode choice by shippers and carriers. The cost of transportation is a crucial factor in determining how popular a new transport mode will be [28]. A utility-random regret mixed MNL model to assess the heterogeneity of LOS variables. Truck transportation can significantly

be improved by assigning dedicated routes, access control, and other freight infrastructure provision parking and loading–unloading facilities [29]. The mode choice model using elimination-by-aspect was used to evaluate the factors affecting mode choice between rail and manufacturers and non-manufacturers. Reliability is the most crucial attribute for manufacturers and freight rates for non-manufacturers [30]. The factors influencing French shippers' choice of freight method were evaluated using a nested logit model with revealed preference. An increase in shipment frequency and haulage distance would increase the probability of using both rail and combined modes. An increase in shipment size only leads to the probability of choosing rail only [31].

The factors influencing the decision for the shipper in Canada were evaluated using the logit mode choice model with data gathered from the stated preference survey. The choice of mode is positively impacted by an increase in reliability. An increase in cost and damage risk hurt the selection of mode [32]. To explore the variables influencing the allocation of truck size for transport operators, a discrete–continuous model (MNL) was utilised. The probability of choosing a heavy vehicle increases with the increase in haulage distance [33]. To account for the heterogeneity in shipment size choices for intracity shipments for the Tokyo metropolitan area, an empirical model was applied. Decisions on the size of the shipment and the operation of the vehicle must be made simultaneously [34].

The logit model was used to estimate freight transport demand for road and sea transport. The main determinants of mode choice are frequency of shipments, haulage cost, and transit time [35]. A mode choice model with service quality variables like price and speed was used to assess the shift in mode choice [36]. For truck transfers, a discrete shipment size selection model based on logistical costs was created. The findings imply that the choice of cargo sizes can be largely explained by commodity flows [37].

The Phoenix-Tucson mega-region used the joint shipment size and mode choice model, which was created with CFS Public Use Microdata. The shipment size and selection were evaluated using the nested model structure [38]. Externalities caused by trucks and rail were compared for their consideration. Externalities associated with trucks are three-time to rail mode. For the creation of comprehensive strategies, a more dependable analytical instrument is needed [39]. Eight cities in two different Indian states have undergone thorough establishment freight surveys. In terms of scope, the research project is unique and offers a plan for low-cost data gathering. According to research, the physical properties of goods and city demography are largely related to response rates from establishment surveys [40].

Freight mode choice variables have been extensively explored with disaggregated models. By and large, these studies are focused on intercity movement by various transport modes. A few studies have also looked at urban freight mobility and freight mode selection. A large research vacuum exists because urban freight and mode choice have not been examined in the Indian setting.

3 Research Methodology

This study covers electronics and building hardware wholesale markets in case city to identify the variables impacting the selection of freight modes in intracity goods distribution. The research study hypothesis is that freight mode selection factors differ in relevance and significance across two commodity distributions in the case city. Binary logit models based on revealed preference were used to assess choice variables for shippers (wholesalers). Selected variables for freight mode choice consideration are related to cost and time from the literature review. Various combinations of both time and cost variables have been modelled in IBM SPSS Statistics 21 software to arrive at the final utility equation of modes for both markets. Time and cost variables are significant factors since they are crucial to the efficiency and flow of freight in cities. Figure 1 shows the adopted framework for the mode choice model along with the combination of choice variables for this research study.

At wholesale markets, both for-hire and private carriers have been surveyed. Primary data was collected from wholesalers and truck operators (carriers) through in-person surveys. The quantum of samples collected from stakeholders is depicted in Tables 1 and 2.

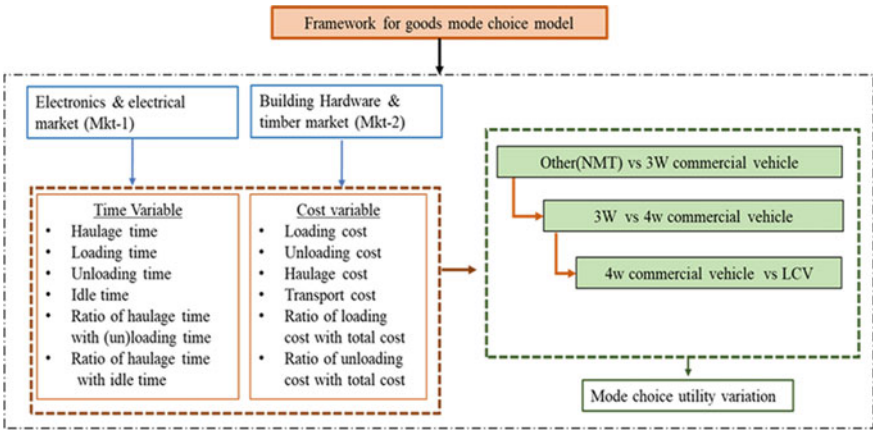

Fig. 1 The proposed framework for urban freight mode choice

Table 1 Quantum of samples

	Wholesalers	Carriers
Method of sampling	Stratified survey	Stratified survey
Samples collected	110	323

Source Author

Table 2 The sample size of transport operators

Mode	Electronics market	Building hard. market	Total sample size
Other (NMT)	35	30	65
3W	35	31	66
4W	32	35	67
LCV	31	30	61

Source Author

4 Case City Profile

The Indian state of Rajasthan's capital city is Jaipur. Jaipur covers a total area of 2939 km^2, of which the walled city (ancient area) takes up 17 km^2. Of the remaining 2650 square kilometres, the city of Jaipur is administered by the Jaipur Development Authority. 30.5 lac people are living in Jaipur city overall (yr. 2011). 44.8% of the city's land is used for residential purposes (13,825 ha), 6.7% for commercial purposes (2064 ha), 6.6% for industrial purposes (1862 ha), 2.6% for governmental purposes (602 ha), 3.3% for mixed purposes (1034 ha), 10.5% for public and semi-public use (3241 ha), 11.3% for recreational use (3461 ha), and 15.4% for circulation (4741 ha). The important wholesale markets at various location in Jaipur city including the walled city area along with intercity and intracity freight network is depicted in Fig. 2.

The building hardware market and electronics market was selected for the intracity mode choices exercised by wholesalers for respective commodities distribution. The Jaipur development authority recently created the building hardware market area. The building hardware industry bases the distribution of its goods based on weight. The electronics market is situated in a walled city area with restricted connectivity compared to the building hardware market. The electronics sector bases its distribution on the number of items.

5 Mode Choice Model Formulation

The likelihood that the shipper or wholesaler will select a particular mode of delivery for the consignment is determined by mode choice models. Mode choice models are disaggregate models with discrete dependent variables. The utility maximisation theory of economics is the fundamental behind discrete choice models. The decision made by the user maximises the utility gained from it. The choice mode is stated in probabilistic terms as an output from discrete choice models. Equation (1) depicts the utility equation of the binary discrete choice model. Equation (2) illustrates how the binary logit model framework yields the likelihood of selecting an option [41].

$$U = (b0 + b1x1, i + ... + bkxk, i) \tag{1}$$

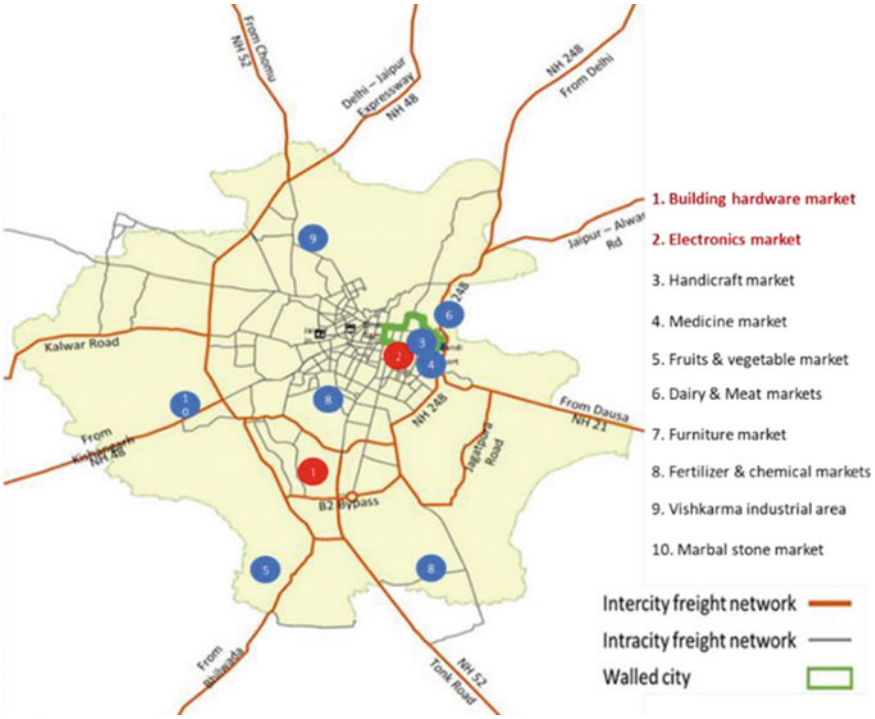

Fig. 2 Wholesale markets location (*Source* Author)

$$Pi = \frac{1}{1 + e^{-(b0+b_{1,i}+\ldots+b_{kxk,i})}} \tag{2}$$

In equations:

- U denotes the utility of individual I for a specific choice.
- b0 is constant.
- b1, b2, …bk are parameters that need calibration.
- x1i, x2i, … xki are variables associated with the choice set.

The initial universal set of variables for binary logistics regression taken into consideration for present freight mode choice modelling was based on the literature review, modal attributes, and case markets stakeholder's input. A total of 30 variables have been selected as possible predictors in mode choice across commodity distribution and modes. The final selection of modal attributes in the calibrated utility equations of modes is based on various statistical tests associated with binary logistics regression like the significance p-value of individual attributes of modes. The final utility equations incorporated the results of statistical tests such as the -2 Log-likelihood, Cox & Snell R Square, Nagelkrke R Square value, Hosmer and Lemeshow Test, and classification tables for several binary choice modes.

6 Descriptive Analysis

A descriptive analysis of the wholesaler's attributes is shown in Table 3. In the electronics market, the mean value of the shop area (square metres) is higher than in the building hardware market. The employment rate per 100 m^2 in the electronics market is 5, whereas it is 3 in the building hardware market. The total weekly tonnage handled in the building hardware market, including incoming and outgoing tonnage per 100 sqm, is 52.4 tonnes, whereas it is 26.6 tonnes in the electronics market. Total weekly trip frequency, including incoming and outgoing trips per 100 sqm of shop area, is 24 trips in the building hardware market and 27 trips in the electronics market. In the building hardware market, incoming weekly freight trips are nearly twice as high as in the electronics market. Compared to the building hardware market, the electronics market has more weekly outbound trips. As would be predicted, the building hardware sector has higher outgoing and entering tonnage than the electronics market.

Table 4 displays the descriptive analysis of transport operator characteristics. For all modes in both marketplaces, loading takes a little longer than unloading. For 3W and 4W modes, idle time is practically identical in both commodities, however, for LCV modes, the building hardware market (BHM) has longer idle times than the electronics market (EM).

There is not much significant difference in haulage cost for both markets except LCV modes. Compared to the electronics business, the haulage cost of LCV mode is higher in the building hardware sector. LCV is occasionally used for intercity (suburb) shipments. In both markets, the cost of loading and unloading an LCV does not significantly vary.

Table 3 Descriptive analysis of wholesalers

Variables	Unit	Electronics wholesalers			Building hardware wholesalers		
		M	Mdn	SD	M	Mdn	SD
Area of shops	Sq.m	140	149.5	67.7	89.1	80	62.5
Employment	Per 100 sqm	5	4	2.1	3.1	3	1.5
Incoming trips	weekly	4.1	4	1.4	9	9	2.7
Incoming tonnes	weekly	14.1	15	3.04	27.6	23	15.5
Outgoing trips	weekly	22.1	23	4.1	14.9	15	3.2
Outgoing tonnes	weekly	11.8	12	2.04	24.8	20	13.8

Source Author (M = mean, Mdn = median, SD = standard deviation)

Table 4 Descriptive statistics of transport carriers

Mode	Wholesale market	Haulage time (Hour)		Loading time (Hour)		Unloading time (Hour)	
		M	Sdn	M	Sdn	M	Sdn
NMT	EM	0.8	0.4	0.2	0.05	0.18	0.04
	BHM	0.9	0.3	0.2	0.04	0.19	0.04
3W	EM	0.7	0.2	0.3	0.05	0.27	0.06
	BHM	0.7	0.4	0.6	0.2	0.51	0.07
4W	EM	0.7	0.2	0.4	0.08	0.34	0.09
	BHM	0.8	0.3	0.6	0.17	0.49	0.15
LCV	EM	0.9	0.4	0.7	0.07	0.66	0.07
	BHM	1.4	0.6	0.7	0.12	0.69	0.09

Idle time (Hour)		Haulage cost (INR)		Loading cost (INR)		Loading time (Hour)	
M	Sdn	M	Sdn	M	Sdn	M	Sdn
0.09	0.03	228	87	50.9	8.6	50.9	8.6
0.67	0.13	207	68	96	25.1	97.9	25.8
0.95	0.15	597	186	109	101	109	101
0.9	0.17	584	343	168	47	142	49.8
1.15	0.16	853	304	150	12.1	150	12.1
1.13	0.2	834	241	159	47.5	135.7	21.4
1.4	0.14	1856	692	197	21.3		21.3
1.85	0.22	2627	832	202	39.7	194.1	26.1

Source Author
Note EM = Electronics market
BHM = Building hardware market
INR = Indian national rupee

7 Results and Discussions

The final calibrated utility functions of freight modes for both wholesale markets (commodities) are shown in Table 5.

Table 5 Calibrated utility equations

Mode	Market	Utility equation
NMT–3W	BHM	U = −6.8 (Total Time)−0.083 (Loading Cost) + 31.49
	EM	U = −14.8 (Unloading Time)−0.03 (Transport Cost) + 13.7
3W–4W	BHM	U = −2.03 (Travel Time)−0.15 (Loading & unloading Cost) + 4.99
	EM	U = −50.9 (Total Time) + 0.002 (Transport Cost) + 4.8
4W–LCV	BHM	U = 2.38 (Travel Time) + 0.39 (Unloading Cost)−15.8
	EM	U = 1.91 (Travel Time) + 0.001 (Transport Cost)−16.7

Source Author

Among all the variables considered for modelling freight mode choice, the main variables affecting mode choice among various freight modes across commodity distribution are loading cost, transport cost, loading & unloading cost, total time, travel time, and unloading time. Variables are differing across commodities and modes.

In the case of building hardware distribution, the signs associated with total time and loading cost are negative indicating that an increase in travel time and loading cost would result in the stakeholder being less likely to use a 3W commercial vehicle. Further, the impact of the loading cost variable is higher compared to the travel time variable in the selection of mode between commercial NMT and commercial 3W in building hardware distribution.

In the case of electronics goods distribution, the signs associated with unloading time and transport cost are negative indicating that an increase in transport cost and unloading time would result in less likely to select a 3W commercial vehicle similar to building hardware distribution. When choosing between a 3W commercial vehicle and an NMT for the distribution of electronics items, the influence of the unloading time variable is greater than that of the transport cost variable.

The signs associated with travel time and loading–unloading cost are negative for a choice between 3 and 4W, less likely to select a 4W commercial vehicle with an increase in variables in building hardware distribution. Further, the impact of the loading–unloading cost variable is lesser compared to the travel time variable in the selection of mode between commercial 3W and commercial 4W for building industry goods distribution.

For mode selection between 3 and 4W modes in electronics goods distribution, the signs associated with total time are negative and transport cost is positive indicating that an increase in total travel time results in the stakeholder being less likely to use a 4W commercial vehicle and an increase in transport cost are more likely to use a 4W commercial vehicle. Further, the impact of the haulage cost or transport is higher compared to the total transport time in mode selection between commercial 3W and commercial 4W modes in electronic goods distribution.

It is observed that the signs associated with travel time and loading cost are positive for 4W and LCV mode selection in building hardware distribution. An increase in travel time and loading cost would result in the more likely use of LCV. Further, the impact of the unloading cost variable is less compared to the travel time variable in the selection of mode between 4W and LCV in building hardware distribution.

The signs associated with travel time and transport cost are positive for LCV and 4W in electronics goods distribution similar to building hardware distribution. An increase in travel time and transport cost would result in the stakeholder being more likely to use LCV. When choosing between the 4W commercial and LCV modes of transportation for the distribution of electronic goods, the influence of the transport cost variable is far less significant than that of the travel time variable.

Statistical results associated with calibrated utility functions are shown in Table 6. Related statistical test associated with the final calibrated utility equations of the binary logit models qualifies all tests for the robustness of models. Only Hosmer and L. test has a value of 0.67 for the choice between NMT and 3W, but it is retailed as the value is nearer to 0.7.

Sensitivity analysis for 3W, 4W, and LCV has been shown in Table 7. Sensitivity analysis of the freight mode choice has been performed by incrementally increasing and decreasing the variable's value by 10%. Sensitivity analysis results are based on the mean values of various variables of transport operators (carriers) involved in respective commodity distribution in Jaipur city.

It is seen that loading and unloading cost is more sensitive in building hardware distribution as compared to electronics goods distribution, whereas time is more sensitive in electronics distribution compared to building hardware distribution in the selection of modes between 3 and 4W. The travel time variable is less sensitive compared to travel cost in the selection of modes between 3w, 4W, and LCV across commodity distribution in the case city. NMT mode is not considered in sensitivity analysis as there are various varieties of NMT modes ranging from a tricycle to a bullock cart, which makes it difficult to generalise NMT modal attributes.

Table 6 Statistical results

Mode	Market	–2 loglikelihood	Nagelkerke R square	Hosmer & L. test	Predicted (%)
NMT–3W	BHM	15.2	0.91	0.99	93
	EM	29.04	0.8	0.67	90
3W–4W	BHM	23.7	0.85	0.92	96
	EM	13.71	0.92	0.98	89
4W–LCV	BHM	13.05	0.92	0.98	98
	EM	9.88	0.94	0.97	95

Source Author

Table 7 Sensitivity analysis

Variable	Mode	Electronic market					
		-30(%)	-20(%)	-10(%)	10(%)	20(%)	30(%)
Cost	3W	-16	-10	-4	4	7	10
	4W	-18	-11	-5	4	8	11
Time	3W	1.3	0.9	0.4	-0.4	-0.9	-1.4
	4W	2.4	1.3	0.7	-0.7	-1.4	2.1
Cost	4W	-12	-7	-3	3	6	8
	LCV	-14	-8	-4	3	6	9
Time	4W	1	1	0	0	-1	-1
	LCV	2	1	-1	-1	-2	-3
Variable	Mode	Building hardware market					
		-30 (%)	-20(%)	-10(%)	10(%)	20(%)	30(%)
Cost	3W	-11	-6.7	-3.2	2.8	5.4	7.7
	4W	-11	-6.8	-3.2	2.8	5.3	7.5
Time	3W	0.3	0.2	0.1	-0.1	-0.2	-0.3
	4W	0.4	0.2	0.1	-0.1	-0.2	0.4
Cost	4W	-10	-6	-3	3	5	8
	LCV	-10	-6	-3	2	5	6
Time	4W	-0.1	-0.1	0.0	0.0	0.1	0.1
	LCV	-0.1	-0.1	0.0	0.0	0.1	0.1

Source Author

8 Conclusion

This study uses binary logit models to investigate the selection of road-based freight modes used in the distribution of urban goods in Jaipur city. The model incorporated several combinations of variables relating to time and the cost of intracity freight trips.

The key finding of the study suggests that mode choice variables differ from one commodity to another commodity distribution. Mode choice variables also differ according to mode due to the difference in tonnage carrying capacities. Travel time, unloading time, and transport cost variables are essential for electronics goods intracity shipment, whereas loading cost, unloading cost, and travel time are also crucial in building hardware shipments. Travel time and loading–unloading cost are the primary determinants in selecting 3W and 4W modes in building hardware distribution, whereas total time and transport cost are the key variables in the selection between 3 and 4W modes in electronics goods distribution. In the distribution of building hardware, the choice decision between 4W and LCV modes primarily depends upon unloading costs and travel time, whereas in the distribution of electronic items, the key concerns are travel time and transport cost. Variables that affect

the choice between a 3W and NMT mode in the electronics goods distribution are transport cost and unloading time, whereas it is loading cost and total time in the building hardware distribution. It is also observed that loading/unloading cost is relevant to building goods distribution whereas loading/unloading time in electronics goods distribution. Mode choice variables for intercity shipments are sensitive to VKT compared with TKT.

The appropriate modal share and parking-related infrastructure at wholesale marketplaces are directly impacted by the freight mode choice. For effective policy intervention for sustainable urban freight transportation, road-based urban freight mode choice variables are always for city planners and local policymakers. There is a further need to evaluate the freight mode choices within and across cities of different sizes, and more wholesale commodity markets need to be investigated.

References

1. OECD (2003) Delivering the goods: 21st century challenges to urban goods transport. [Online] Available at https://www.itf-oecd.org/sites/default/files/docs/03deliveringgoods.pdf. [Accessed 12 April 2019]
2. Dablanc L, Giuliano G, Holliday et al. (2013) Best practices in urban freight management: lessons from an international survey. TRB, Transp Res Rec (TRR):29–38
3. Comi A, Russo F (2012) City characteristics and urban goods movements: A way to the environmental transportation system in a sustainable city. Procedia Soc Behav Sci 39:61–73
4. Tsai YY (2009) Strategic choice of freight mode and investments in transport infrastructure within production networks. ADBI Working Paper Series, Tokyo
5. Lindholm M (2010) A sustainable perspective on urban freight transport: Factors affecting local authorities in the planning procedures. Procedia Soc Behav Sci 2:6205–6216
6. Brogan J et al (2013) Freight transportation modal shares: scenarios for a low-carbon future. U.S. Department of Energy, Washington, DC
7. Nam KC (1997) A study on the estimation and aggregation of disaggregate models of mode choice for freight transport. Transp Res Part E: Logist Transp Rev 33(3):223–231
8. MOUD (2006) National urban transport policy. Government of India, New Delhi
9. MoUA (2015) http://smartcities.gov.in. [Online] Available at http://smartcities.gov.in/content/area_development.php [Accessed 20 April 2019].
10. MoUD (2014) https://smartnet.niua.org/. [Online] Available at https://smartnet.niua.org/sites/default/files/resources/National%20Urban%20Transport%20Policy.pdf [Accessed Mar 2018].
11. NCFRP report 14, 2012. Guidebook for understanding urban goods movement. Transportation Research Board 2011, Washington, D.C.
12. Wang Y, Ding C, Liu C, Binglei. Xie (2013) An analysis of Interstate freight mode choice between truck and rail: A case study of Maryland, United States. Procedia Soc Behav Sci 96:1239–1249
13. Combes F (2009) The choice of shipment size in freight transport, Français: Economies et finances Paris-Est.
14. Kofteci S (2009) Trade-off analysis based freight mode choice model: a case study of Turkey. Int J Nat Eng Sci, 3(3):37–42
15. Fries N, Zachary P (2008) Carrier or Mode?—The dilemma of shippers' choice in freight modelling. Ascona, STRC
16. Jong DJ, Johnson D (2011) Heterogeneous response to transport cost and time and model specification in freight mode and shipment size choice. Int Choice Model Conf

17. Jiang F, Johnson P, Calzada C (1999) Freight demand characteristics and mode choice: an analysis of the results of modeling with disaggregate revealed preference data. J Transp Stat, (2):149–158
18. Winston C (1981) A disaggregate model of the demand for intercity freight transportation. Econometrica, 49(4):981–1006
19. Winston C (1983) The demand for freight transportation: models and applications. Transp Res Part A: Policy Pract, 17A(6):419–427
20. Wilson FR, Bisson BG, Kobia KB (1986) Factors that determine mode choice in the transportation of general freight. Transp Res Rec 1061:26–31
21. Samimi AK (2011) A behavioral analysis of freight mode choice decisions. Transp Plan Technol, 34(8):857–869
22. McFadden D, Winston C, Boersch-Supan A (1986a) Joint estimation of freight transportation decisions under non-random sampling. (Discussion Paper) Harvard University
23. Cavalcante R, Roorda MJ, Macabe S et al (2010) A disaggregate urban shipment size/vehicle-type choice mode. In: Presented at the 89th Annual meeting of the transportation Rrsearch board. Washington, D.C.
24. Holguín-Veras J (2002) Revealed preference analysis of commercial vehicle choice process. J Transp Eng 128(4):336
25. Mcginnis MA (1989) A comparative evaluation of freight transportation choice models. Transp J 29(2):36–46
26. Arunotayanun K, Polak JW (2011) Taste heterogeneity in freight shippers' mode choice behaviour. Transp Res Part E: Logist Transp Rev: 47(2):138–148
27. PourabdollahiB., Mohmmadian A., ZK (2013) Joint model of freight mode and shipment size choice. Transp Res Rec: J Transp Res Board 2378:84–91
28. Shin S, Roh HS, Hur SH (2019) Characteristics analysis of freight mode choice model according to the introduction of a new freight transport system. Sustainability: 1–1329. Nowreen Keya, Anowar
29. Keya N, Anowar S, Eluru N (2018) Freight mode choice: a regret minimization and utility maximization based hybrid model. Transp Res Rec, 2672(9):107–119
30. Young W, Richardson AJ, Ogden KW, Rattray AL (1982) Road and rail freight mode choice: application of an elimination-by-aspects model. Transp Res Rec 838:39–44
31. Kim KS (2002) Inherent random heterogeneity logit model for stated preference freight mode choice. J Korean Soc Transp 20(3):1–10
32. Patterson Z, Ewing GO, Haider M (2007) Shipper preferences suggest strong mistrust of rail: results from stated preference carrier choice survey for Quebec city–Windsor corridor in Canada. Transp Res Rec: J Transp Res Board, (2008):67-71
33. Abate M, Jong De (2014) The optimal shipment size and truck size choice—the allocation of trucks across hauls. Transp Res Part A: Policy Pract 59:262–277
34. Sakai T (2020) Empirical shipment size model for urban freight and its implications. Transp Res Rec: J Transp Res Board: 036119812091489.35. Leandro García-Menéndez et al. (2004) Determinants of mode choice between road and shipping for freight transport: Evidence for four Spanish exporting sectors. J Transp Econ Policy, 38(3):447–466
35. Tavasszy LA, van Meijeren J (2011) Modal shift target for freight transport above 300 km: an assessment. Netherland.
36. Piendl R, Liedtke G, Matteis T (2017) A logit model for shipment size choice with latent classes—Empirical findings for Germany. Transp Res Part A: Policy Pract:188–201
37. Stinson M, Zahra P, Vladimir L, Jeon K, Nippani S, Zhu H (2017) A joint model of mode and shipment size choice using the first generation of commodity flow survey public use microdata. Int J Transp Sci Technol 6(4):330–343
38. Forkenbrock D (2001) Comparison of external costs of rail and truck freight transportation. Transp Res Part A 35(4):321–337
39. Pani A, Sahu PK (2019) Planning, designing and conducting establishment-based freight surveys: A synthesis of the literature, case-study examples and recommendations for best practices in future surveys. Transp Policy:58–75

40. JDA (2011). http://jda.urban.rajasthan.gov.in. [Online] Available at https://jda.urban.rajasthan.gov.in/content/raj/udh/jda---jaipur/en/town-planning/master-development-plan-2011.html [Accessed 23 May 2019]
41. Ben-Akiva M, Lerman SR (2010) Discrete choice analysis. MIT Press

Mode Choice Behaviour in Leisure Travel: A Case Study of Indian Cities

Praveen Samarthi and Kumar Molugaram

Abstract Travel behaviour exploration of Mode choice is burdensome for leisure travel and is influenced by the heterogeneity of traveller preferences. One of the indicators of improvement in living standards is an increase in leisure travel. The research is an effort to comprehend the mode choice process of domestic tourists in India, which has witnessed rapid growth in the last 20 years. Data required for the study is collected through on-site personal interviews at selected tourist destinations having a distinct leisure value, viz., cultural and historical heritage. Two cities, Hyderabad and Delhi and are chosen as the study cities. Logit models depicting the mode choice decision of a tourist are developed for the two cities. In addition to traveller characteristics and mode characteristics, the level of importance accorded to modal characteristics is incorporated into the model framework. Analysis of modal share indicates that train takes a predominant share among the travel modes. The mode choice models developed indicate that all the modes are competing in Delhi, while in Hyderabad, paid modes of transportation w.r.t road (bus and taxi car), train, and self-driven car are in competition with one another. The value of travel time is found to be comparatively higher when compared to commuter travel for both destinations. Household income and the importance factor associated with hand budget are found to be significant variables influencing the choice of a mode while travelling to a historical heritage destination. The study results highlight the need to incorporate qualitative attributes in modelling of mode choices. The need to evolve specific strategies to improve the patronage of the public transport system is emphasised.

Keywords Destination choice · Leisure travel · Mode choice · Models · Traveller preferences

P. Samarthi (✉) · K. Molugaram
Civil Engineering Department, Osmania University, Hyderabad, India
e-mail: samarthipraveen@gmail.com

P. Samarthi
Civil Engineering Department, CVR College of Engineering, Hyderabad, India

A. Dhamaniya et al. (eds.), *Recent Advances in Traffic Engineering*, Lecture Notes in Civil Engineering 377, https://doi.org/10.1007/978-981-99-4464-4_19

1 Introduction

Travel behaviour research entails determining how people plan their trips, including the destination they choose, the time they travel, the kind of transportation they use, and the route they take. Travel behaviour studies are a useful link in transportation planning as the motivations for the traveller in transportation choices are to be ascertained. Among the various trip purposes, like travel to work, shopping, education, etc., leisure travel has received less attention on account of its inherent heterogeneity and flexibility. This is so, even in developed countries like Germany, where in 1997, 48% of all the person-kilometers has travelled for leisure and holiday purposes, which was twice the amount for commuting [1]. Developing countries like India are also witnessing a number of domestic tourist visits which steadily increased from 66 million in 1991 to 560 million in 2019, an increase of 740% over a 28-year period [2]. Because of the large range of leisure activities sites and flexibility associated with personalised modes which are coupled with an inefficient public transport system, therefore individual motorised modes are being widely used for domestic leisure travel. This has a bearing not only on the congestion on the existing road network, but also on energy use and emissions of greenhouse gases [3].

Leisure travel, often known as tourism, refers to excursions taken by a traveller outside of his or her typical surroundings for less than a year and a primary purpose other than to work for a resident entity in the destination [4]. Travellers undertaking the trip for the purpose of leisure are referred to as tourists and qualify as a domestic tourist. In this paper, the travellers undertaking travel for the purpose of leisure are referred to as tourists. Leisure trips are characterised by greater flexibility and the choice of mode may involve a single or combination of modes which cannot be classified as primary and secondary based on travel distances as in commuter travel. Network connectivity is also an influencing factor. This makes the modelling of mode choices more challenging.

A review of earlier studies on mode choice aspects of commute trips indicate that the factors influencing mode choice can be classified as user characteristics such as age, gender, socio-demographics, etc.; transport system characteristics such as access time and cost, frequency of service, etc., and travel characteristics such as total travel time and total travel cost. Modelling structures such as multinomial logit and nested logit are also attempted by researchers to study the intercity and commuter mode choice scenario [6–21]. Variables used in utility function specification include travel time, travel cost, departure time and frequency, access time, and socio-demographic characteristics like household income, group size, occupation, etc. The use of artificial intelligence methods like neural networks, fuzzy logic, multi-recursive partitioning, bayesian network, and neuro-fuzzy techniques are also used in the prediction of mode choice selection [21–24].

A few studies are also conducted in the aspect of mode selection in the leisure travel context. The mode choice decision for leisure travel is found to depend on the Trip type, destination, travel party size, travelling with children, and trip length are all factors to consider [25]**.** The forces driving leisure travel demand are identified

as determinants and motivators [26]. Income, free time, and pricing, as well as the quantity and quality of the product provided by service providers, are all determinants. Motivators are linked to personality traits and attitudes, and they're likely to be influenced by the consumer's socioeconomic and demographic features. It is emphasised that when assessing determinants and motivators, it is also necessary to recognise the special role that modes play in leisure travel. Constraint variables such as age, income, and life stage have also been proven to influence travel preferences [27]. The sensitivity to the distance of tourists was also investigated, and it was discovered that household income, the number of children on the trip, the size of the city of residence, the mode of transportation, the desire to discover new places, variety-seeking behaviour, and the motivations for taking the trip will influence the sensitivity to distance [28]. The influence of trip context on the mode choice decision of leisure tourists in Australia was also explored [29].

Researchers have studied transportation mode decisions in depth for a variety of travel purposes, but leisure trips and, in particular, tourism, have not been studied due to heterogeneity in travel preferences and, most likely, because transportation authorities have given the work commute top priority. Furthermore, the majority of the studies are based on data from rich countries; only a few studies from developing countries have been reported. Due to disparities in vehicle ownership levels, mobility needs, infrastructure provisions, and travel and activity characteristics, mode choice options in industrialised and developing countries may differ significantly. Several context-specific elements of mode choice behaviour in developing nations, such as leisure context, must be explored. In such conditions, research in this direction is required to understand the effect of different variables on mode choice in the Indian context. This study analyses the mode choice behavior of domestic leisure tourists to two historical heritage destinations in India, namely Delhi and Hyderabad, and aims to identify the influencing dimensions. Models were developed for two destinations, namely Delhi and Hyderabad. Significant factors affecting the choice behaviour are identified. The mode choice model aids in determining the current trend in leisure travel destination selection as well as the necessity for any improvements at the destinations in order to enhance the number of visitors to a specific region [33]. The effect of new transportation facilities on other forms of transport and people's mode choice is studied in the central zone of Hyderabad. The mode choice model aids in comprehending the current mode competition trend in the research region as well as the effects of new transportation systems on existing modes of transportation and people's mode preferences [34]. The factors considered include household traits such as household income, vehicle ownership, and the number of elderly or children in a family; trip traits such as travel time and travel cost; and behavioral intents measured on an importance rating scale for variables related to social aspects, destination values, travel, and other factors [35].

2 Methodology Adopted

This section is divided into sections that describe the study cities and sample and the study instrument used for the study.

2.1 Study Areas and Sample

The mode choice behaviour of domestic tourists visiting two renowned tourist destinations in India, United Delhi and Hyderabad, having historical significance are considered for the study. United Delhi includes Old Delhi and New Delhi, Old Delhi comprising of the formidable mosques, monuments, and forts, while New Delhi displays the fine architecture of the British Raj. The famous attractions in Delhi include the Red Fort, Qutub Minar, India Gate, and Raj Ghat. Hyderabad, popularly known as the Pearl City, is home to a plethora of tourist attractions including heritage sites, lakes, parks, and museums, as well as excellent cuisine and a pleasurable shopping experience. Hyderabad gives an interesting glimpse into the past, with a 400-year-old cultural and historical legacy. The Charminar, Hussain Sagar Lake, Salar Jung Museum, and other tourist sites in Hyderabad. Domestic tourists are interviewed at locations within the study cities. The eligibility criteria fixed for the selection of a respondent is that he/she should not be a resident of the city in which the data is collected and he/she should be staying in the city for at least one night. 300 tourists in each study city are interviewed.

2.2 Study Instrument

A self-administered questionnaire is used to collect the relevant information from the tourists. Although the aspect of mode choice behaviour of domestic tourists is part of a larger study to analyse the travel behaviour of domestic tourists, this section describes aspects relevant to mode choice only. The aspects influencing mode choice are grouped under four categories namely characteristics of the decision maker like household income, vehicle ownership; household demographics, etc., journey characteristics, which include a budget for the trip, trip sponsor, trip planner, group size, etc., features of transportation facilities such as journey time by main and other modes; cost of trip; service offered, etc., and qualitative factors which include the level of importance in a 5 point type scale. Travel-related dimensions include direct connectivity, availability of affordable travel modes, comfort and convenience of travel, distance from home, and safety during travel; social dimensions include the budget available and the number of elderly or children in the family; and social dimensions include direct connectivity, availability of affordable travel modes, comfort and convenience of travel, distance from home, and safety during travel.

3 Sample Characteristics

The socio-demographic details and mode share of the tourists are given in Table 1. The sample data indicates that the majority of tourists visiting the two cities are of the middle-income group. The family size in general ranges between 5 and the majority of the tourists have a car as well as a two-wheeler. The majority of tourists visiting Hyderabad are in groups of 3–4 members, while those visiting Delhi have a group size of 1–2. The train is found to have the highest patronage, followed by air in the case of Delhi and bus in the case of Hyderabad. The average travel distance travelled by tourists to Delhi is higher than those to Hyderabad. However, the average unit cost per 100 km distance is higher for the train mode at Hyderabad, while it is higher by bus mode for Delhi. The average travel time is similar for air, hired car, and self-driven car at both destinations.

4 Model Development

This section presents the details of the model development with respect to the variables considered for modelling, selection criteria for variables, and details of model estimation and validation. Multinomial logit (MNL) and Nested logit (NL) models are based on random utility techniques provided by Domencich and Mcfadden [20]. Ben-Akiva and Lerman developed discrete choice (logit analysis) which stated that visit to multiple destinations was viewed as a rational behaviour pattern that reduces the time and cost associated with travel [4].

4.1 Variable Specifications

The measurable part of the utility equation consists of unique variables, specific variables-alternate and specific constant-alternate. In this study, time of travel and cost of travel are considered as unique variables; personal or household characteristics like household income, vehicle ownership, etc., are considered alternative-specific variables. The details of the variables used in the development of the model are given in Table 2.

4.2 Selection Criteria of Variables

The minimal utility function definition is studied first, which comprises variables that are regarded as fundamental to any realistic model. Such variables included travel time, travel cost, household income, group size, travel frequency, etc. Each stage

Table 1 Leisure travel characteristics of tourists visiting different cities

Characteristics	Delhi	Hyderabad
Monthly household income (')	(%)	(%)
LIG-upto Rs.20,000	8.0	6.0
MIG-Rs.20,001—75,000	81.0	93.0
HIG- > Rs.75,001	11.0	1.0
Household size	(%)	(%)
1–2	0.0	0.0
3–4	13.0	34.0
5–6	60.0	66.0
7–8	19.0	0.0
> 8	8.0	0.0
Vehicle ownership	(%)	(%)
Only car	9.0	5.0
Only Two-wheeler	16.0	14.0
Both car and two-wheeler	72.0	80.0
No vehicle	3.0	1.0
Group size	(%)	(%)
1–2	42.0	22.0
3–4	33.0	51.0
5–7	10.0	23.0
8–10	6.0	2.0
> 10	9.0	2.0
Trip frequency	2.7 (1.0)	2.8 (0.9)
Modal share	(%)	(%)
Air	12	2
Train	77	68
Bus	6	21
Hired car	1	6
Self-driven car	4	3
Average travel distance travelled (km)	985.9 (590.5)	641.4 (407.2)
Average unit cost paid by distance (')	1.8 (1.2)	2.0 (1.8)
Avg. Travel time per distance of 100 km (Hours)	0.19	0.21
Air transport	2.15	2.73
Train transport	2.90	1.92
Bus transport	1.96	2.50
Hired car transport Self car	2.24	
Average rating based on the importance of qualitative dimensions	4.52 (0.61)	4.30 (0.71)

(continued)

Table 1 (continued)

Characteristics	Delhi	Hyderabad
Travel safety		
Travel comfort and convenience	4.00 (0.67)	3.81 (0.83)
Hand-Budget for making the trip	3.95 (0.89)	3.59 (0.88)
Affordability of transportation modes	3.60 (0.99)	3.52 (0.79)
Involvement of the elderly/children in the family	3.40 (1.00)	3.19 (0.90)
Direct communication	3.83 (0.87)	(0.99)
The distance from your residence	3.20 (1.06)	3.32 (0.95)

Table 2 Variables used in the development of model

Factors name	Definition	Details of data coding
Cost of travel	Cost of travel in Rs	In numbers as actual
Travel time	Time taken in travel in minutes	In numbers as actual
Monthly Household Income	Taken in Rs. Per month in seven categories	In increasing order from 1 to 7 as income increases
Vehicle Ownership	Total number of vehicles in the family	In numbers as actual
Persons accompanying	Number of people accompanying the respondent	In numbers as actual
Trip frequency	Average number of times in a year a leisure is made	In increasing order as frequency increases
Service used	Service class availed in a mode	In decreasing order as cost and comfort increases
Rating given to factors	Importance given in a 5 point Likert type scale	1 indicates 'Extremely Unimportant' to 5 indicates 'Extremely important'

of the model creation process introduces incremental changes to the modal utility functions, and the model is re-estimated to arrive at a more precise model specification. A variable's inclusion or exclusion is determined by its sign and statistical importance. The variable's sign should be logically correct. For any variable, t-ratio should always be more than +1.960 and less than –1.960 for 95% confidence level.

4.3 Model Estimation and Validation

The software, 'ALOGIT' is used for estimation of the model and validation. The statistical importance of the estimation results is checked by maximum likelihood values and their convergence. Also the value of ρ^2 value, more than 0.25 is considered reasonably good [32]. A nested structure that improved the model convergence (given

by likelihood ratio) and ρ^2 value is considered to be good. With this reasoning, various nested structures are attempted in search of a more refined model. In case, the log sum value is found to as equal to one, multinomial logit (MNL) structure is considered. About 15% of the total sample is randomly selected to carry out the validation process. The significance of validation results is checked by total likelihood and prediction success. The validation percent right of value of more than 50% is considered satisfactory.

5 Results

The mode choice models for Delhi and Hyderabad are discussed in the following sections.

5.1 Mode Choice Model for Delhi

A MNL structure is found to be the best-fit structure defining the mode choices of the tourists visiting Delhi. The estimated values of various variables and other statistical parameters of the Multinomial Logit (MNL) model are provided in Table 3.

Travel time is found to influence tourists more than travel cost. Household income and service preference are highly significant variables. It is clear that a small change in household income may affect the use of air travel. The increase in the importance given to comfort and convenience by tourists affects the use of bus adversely as a long-distance travel mode. The presence of children or elderly on a trip encourages the use of car category (owned car or hired car), though not in a proportionate manner. In case the service quality of the train reduces, the use of the train as a long-distance travel mode also reduces. This also implies that these tourists place a higher value on comfort and ease throughout their travels than on cost. When choosing a means of transportation, the presence of the elderly or youngsters in the family is given a higher priority than comfort and convenience during travel. The calculated values of the air and car category constants suggest that some unanticipated characteristics impede the utilisation of those modes.

The results obtained from statistical tests are found to be logically correct. Log likelihood with variables values showed good convergence as compared to log likelihood with constants only. Rho-squared values indicate towards high good-fit model ($\rho^2 > 0.25$). Percent right (59%) found to be satisfactory. The SVT is perceived by the tourists in Delhi to be quite high. In terms of 'per family' or 'per person', it comes out to be 1.04 times and 5.25 times, respectively, of the SVT in general. A higher value of time may be perceived by the tourists due to the large number of historical and cultural monuments present in the city for their visit and the value they derive out of the visit.

Table 3 Statistical values for the best fitting model of tourists visiting Delhi

Factor	Coefficient estimates	Variable relevancy
Travel time	−0.1082 (−3.5)	Generic
Travel cost	-0.4347×10^{-3} (−2.0)	Generic
Household income	1.430 (4.7)	Air
Service	−0.5325 (−5.2)	Train
Importance factor for comfort and convenience during travel	−0.3704 (−1.6)*	Bus
Importance factor for the presence of aged and children in family	0.8262 (2.2)	Car category
Constants		
Beta 10	−11.76 (−6.2)	Air specific constant
Beta 30	−3.311 (−2.8)	Bus specific constant
Beta 40	−8.610 (−5.2)	Car category-specific constant
Structural parameters		
Coefficient of utility of nest (logsum)	MNL model	
L(0)	−234.9540	
L(c)	−194.1346	
Initial likelihood	−234.9540	
L(θ)	−149.0469	
ρ^2 with respect to zero	0.3656	
ρ^2 with respect to constant	0.2322	
Sample size	222	
% Right	59.04	
Subjective Value of Time (SVT) (‘/Hr)	248.90	
Average Income/month (‘)	47,646	
Average household size	5.023	
SVT per family	1.04	
SVT per member	5.25	

* Not significant at 95% confidence level Values in parentheses are t–statistics
L (0): Likelihood ratio with zero coefficients L(c): Likelihood ratio with constants
L (θ): Likelihood ratio at convergence ρ^2: Rho-squared statistics

5.2 Mode Choice Model for Hyderabad

The best fit nested mode choice model for tourists visiting Hyderabad is shown in Fig. 1. Air mode was not considered for model formulation on account of the small sample size. Bus and hired car are found competing with each other in a nest named as ‘road based paid’, while train and self-driven cars are competing separately at the root. Air is not included as a choice due to the very small sample size (2%). The

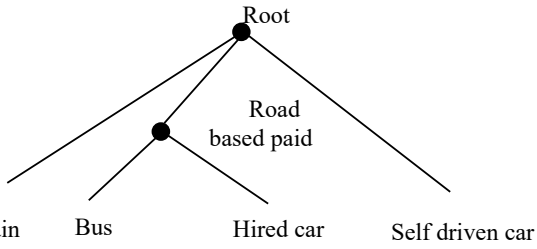

Fig. 1 Nested structure for mode choices for Hyderabad

estimated values of various variables and other statistical parameters are given in Table 4.

Travel time to Hyderabad by tourists is perceived as more significant and found to be more influencing than travel cost. All the estimated variables are found to be significant. The positive influence of household income and the importance of the budget available in hand for the trip are found in the choice of train and bus, respectively. An increase in household income is found to increase the probability of the use of train for long distance travel by tourists. Similarly, higher importance to budget is expected to bring a substantial increase in bus use for the same. This may be attributed to the large number of tourists of middle-income tourists visiting Hyderabad. AC services are least preferred in hired car due to higher fare charges. Higher household size is found to discourage the use of personalised vehicles, as it may cause discomfort in travel. Household size is found highly estimated which indicates that small changes in household size may bring more changes in the utility of self-driven cars. Household income and importance factor for budget are the next highly influencing variables after household size. The constant for self-driven car is found to be quite high and positively influences the use of self-driven car. The results of the statistical analyses are good. The logsum value is between 0 and 1, thus defining the nest in which bus and hired car are taken together, while train and self car competed separately. Log likelihood values showed higher convergence with variables as compared to with constants only or otherwise. Rho-squared values are indicating towards high goodness-of-fit of the model, according to the literature. The percent right (73%) is found to be good indicating towards better accuracy of the model in the prediction of mode choices.

The SVT for tourists in Hyderabad is higher than that at Delhi. This may be due to the shopping potential, for which the city is known. The perceived value of time by family or a member is also found to be higher (1.68 times and 7.91 times with respect to SVT in general) as compared to Delhi.

5.3 Discussion of Results

Mode choices made by tourists visiting Delhi and Hyderabad, both historical heritage cities, are studied. Multinomial and nested logit models are developed to explain the

Table 4 Statistics for best fit mode choice model for tourists visiting Hyderabad

Variable	Coefficient estimates	Relevance of variables
Travel time	−0.2645 (−3.3)	Generic
Travel cost	-0.7789×10^{-3} (−2.2)	Generic
Household income	1.481 (4.0)	Train
Importance factor for budget available in hand for the trip	1.179 (4.0)	Bus
Service	0.4202 (3.0)	Hired car
Household size	−2.032 (−2.3)	Self-driven car
Constants		
Beta 20	−6.216 (−3.5)	Bus specific constant
Beta 40	12.74 (3.0)	Self car specific constant
Structural Parameters		
Coefficient of utility of nest (logsum)	0.7592	
L(0)	−227.6983	
L(c)	−124.8566	
Initial likelihood	−90.8189	
L(θ)	−90.4536	
Structural parameters		
ρ^2 with respect to zero	0.6027	
ρ^2 with respect to constant	0.2755	
Sample size	223	
% Right	72.50	
Subjective Value of Time (SVT) (‘/Hr)	339.59	
Average Income/month (‘)	40,355	
Average household size	4.70	
SVT ratio per family	1.68	
SVT ratio per member	7.91	

* Not significant at 95% confidence level Values in parentheses are t–statistics
L (0): Likelihood ratio with zero coefficients L(c): Likelihood ratio with constants
L (θ): Likelihood ratio at convergence ρ^2: Rho-squared statistics

mode choices and to identify the significant variables influencing mode choices. The influence of socioeconomic characteristics like household income in influencing mode choice is observed. Household income is found to have a positive influence on the choice of air mode in Delhi. It is evident from Table 1 that the HIG tourists use air as their travel mode. Moreover, an increase in household income increases the utility associated with air mode. This implies that an increase in household income and associated disposable income can increase the patronage of air mode for tourists visiting Delhi. In case of Hyderabad, household income is found to influence the train mode and is a highly significant variable in the model. It is observed that the

majority of the MIG tourists visiting Hyderabad use train and bus as their travel modes. It is presumed that an increase in income can cause a shift from bus to train mode. The service availed by the tourists is observed as another significant factor. For the train users in Delhi, the influence of service on the use of train is negative in nature, indicating that lower-level services decrease the utility of train usage. This implies that a decrease in the comfort level of train can reduce the patronage of train. This is substantiated by the higher score for dimensions 'comfort and convenience during travel' by the tourists in Delhi. At Hyderabad, the variable 'service' is found influencing the usage of hired car. A decrease in service quality is found to positively influence the usage of hired car. The service quality in hired car relates to the use of air-conditioned car for travel, which translates into greater cost. It is seen from Table 1 that the average cost of travel per km at Hyderabad is comparatively higher and the rating for 'comfort and convenience during travel' is comparatively less. This implies that the tourists visiting Hyderabad are less likely to use comparatively high class services offered in hired car mode as they do not want to incur greater cost and also because the travel distances are comparatively less. Household size is also found to have a negative influence on the use of self-driven car and families having higher household sizes are less likely to use the self-driven car in Hyderabad.

The influence of qualitative attributes in mode choice is highlighted by the study results. 'Comfort and convenience during travel' is found to have a negative influence on the choice of bus for tourists visiting Delhi. This implies that tourists who give a higher rating for the variable are less likely to choose the bus as their travel mode. This is logical as travel for longer distances is not preferred by bus and the average distance travelled by tourists visiting Delhi is also comparatively high. 'The presence of aged or children in the family' is found to have a positive influence on car category users visiting Delhi. The importance rating given by the tourists visiting Delhi to this factor is also high. This implies that tourists having elderly or children in the family are more likely to use the car modes to access Delhi. The importance given to the comfort of the elderly and children in the family by Indian households is emphasised in this context. The importance rating for 'budget available in hand for the trip' is found to positively influence the choice of bus mode for tourists visiting Hyderabad. A relatively high modal share and less travel time for the bus mode may be prompting the use of the bus as a viable travel option.

The best-fit model for Delhi indicates that there is competition between modes in Delhi and all the modes compete with each other. Delhi, being the national capital, is well connected by road, rail, and air modes and hence the competition between modes is not surprising. Although the modal shares indicate a predominant preference for train as the travel mode, all the modes are found to compete with each other. On the other hand, in Hyderabad, bus and hired car are competing with each other in a 'road-based paid' nest and compete with train and self-driven car at the root. It is observed that the average travel time of 100 km for bus and hired car is almost the same for tourists visiting Hyderabad. It is presumed that the similarity in time for travelling is the reason for both the modes competing with each other in a nest. On the other hand, although train and self-driven car take comparative average travel time,

they are found to compete at the root with the 'road-based paid' mode on account of the differences in travel cost, travel time, and comfort level.

6 Conclusions

Various combinations of alternate travel modes to leisure cities are observed to define the mode choice decisions of the tourists. The presumption that mode choice characteristics of tourists visiting cities with similar leisure values are similar is found to be invalid, based on the developed models. Destination-specific policy initiatives are recommended for improving mode patronages. The nested structures developed indicate that in the case of Delhi, since all the modes compete with each other, policy initiatives that focus on all the available modes, viz., air, train, bus, and car categories are to be evolved so that competition between modes will improve patronage for all the modes. On the other hand, in case of Hyderabad, competition between train, road-based paid modes (bus and hired car), and self-driven car is seen. This implies that strategies that aim to improve competition and patronage of these modes with distinct policy strategies for train, road-based paid alternatives and personalised modes are to be evolved. Since the use of public transport facilities for travel is to be encouraged for sustainable travel, patronage for train can be improved by evolving special package tours for domestic tourists. The models also illustrate the use of qualitative attributes in mode choice modelling and emphasise their importance in the mode selection context. Studies on combined mode and destination choice relating to leisure travel can also be undertaken to explore the travel behaviour of domestic tourists in greater detail.

Funding Funding is not applicable.

References

1. Algers S (1993) Integrated structure of long-distance travel behaviour models in Sweden. Transp Res Rec, 1413:141–149. Transportation Research Board of National Academics, Washington, D. C
2. Allen D, Yap G, Shareef R (2008) Modelling interstate tourism demand in Australia: A co-integration approach. J Math Comput Simul, (79):2733–2740. Elsevier Science Ltd., London
3. Andrade K, Uchida K, Kagaya S (2006) Development of transport mode choice model by using adaptive neuro-fuzzy inference system. Transp Res Rec, Transp Re-Search Board Natl Acad, Washington 1977:8–16
4. Ben-Akiva M, Lerman SR (1985) Discrete choice analysis: theory and application to travel demand. The MIT Press, Cambridge
5. Buckeye KR (1992) Implications of high-speed rail on air traffic. Transp Res Rec, 1341:19–27. Transportation Research Board of National Academics, Washington, D.C

6. Cantarella G, Luca S (2003) Modelling transportation mode choice through artificial neural networks. In: Fourth International symposium on uncertainty modeling and analysis (ISUMA'03), IEEE Computer Society
7. Dhruvarajan PS, Srinivasan R, Subramaniam S (1980) Demand for short-haul air travel in India. In: Proceedings of International conference on transportation. New Delhi, pp AT 23–AT–43
8. Domencich T, McFadden D (1975) Urban travel demand-a behavioral analysis. North Holland, New York
9. Goulias K, Brog W, Erl E (2008) Perceptions in mode choice using situational approach: trip-by-trip multivariate analysis for public transportation. Transp Res Rec 1645: 82–93. Transportation Research Board, Washington, D. C
10. Graham A (2006) Have the major forces driving leisure airline traffic changed? J Air Transp Manag, 12: 14–20. Elsevier Science Ltd., London
11. Hensher A, Johnson L (1981) Applied discrete choice modelling. Croom-Helm, London
12. https://www.indiastat.com. Last accessed on 15th May 2019
13. Karlaftis M (2004) Predicting mode choice through multivariate recursive partitioning. J Transp Eng, 130(2):245–250. American Society of Civil Engineers, U. S.
14. Kattiyapornpong U, Miller K (2008) A practitioner's report on the interactive effects of socio-demographic barriers to travel. J Vacat Mark, 14(4):357–371. Elsevier Science Ltd., London
15. Kelly J, Haider W, Williams P (2007) A behavioral assessment of tourism transportation options for reducing energy consumption and greenhouse gases. J Travel Res, 45(3):297–309. Sage Publications, U. K.
16. Khanna SK, Kumar V, Gopal M (1983) Intercity modal split analysis. J Indian Highw 10:7–14
17. Koo T, Wu C, Dwyer L (2010) Transport and regional dispersal of tourists: is travel modal substitution a source of conflict between low-fare air services and regional dispersal? J Travel Res, Sage Publications. U K 49(1):106–120
18. Koppelman FS (1989) Multidimensional model system for intercity travel choice behavior. Transp Res Rec 1241:1–8. Transportation Research Board, Washington, D. C
19. Limtanakool N, Dijst M, Schwanen T (2006) The influence of socioeconomic characteristics, land use and travel time considerations on mode choice for medium- and longer-distance trips. J Transp Geogr 14:327–341. Elsevier Science Ltd., London
20. McFadden D (1973) Conditional logit analysis of qualitative choice behavior. In: Zarembka P (ed) Frontiers in econometrics. Academic Press, New York, pp 105–142
21. McFadden D (1978) Modelling the choice of spatial location. In: Karlqvist A, Lundqvist L, Snickars F, Weibull J (eds) Spatial interaction theory and planning models. North-Holland, Amsterdam, pp 75–96
22. Nicolau J (2008) Characterising tourist sensitivity to distance. J Travel Res, 47(1):43–52. Sage Publications, U. K.
23. Oheda Y, Sumi T, Nakanisi K, Tubaki S (1997) A model for choosing a departure time by Air travel passengers on Business. J Infrastruct Plan Manag, 15:83–90. Elsevier Science Ltd., London
24. Praveen S, Rastogi R (2012) Mode choice models defining Travel to Leisure Destinations. Research Academia, p 16
25. Quandt R (1992) Estimation of modal splits. The Collected Essays of Richard E. Quandt, vol 1. Edward Elgar Publishing House, England, pp 289–298
26. Recker W, Golob T (1976) An attitudinal modal choice model. Transp Res Rec 1645:299–310. Transportation Research Board, Washington, D. C
27. Praveen S, Kumar M (2018) A case study of mode choice analysis in Hyderabad city. Int J Emerg Technol Adv Eng, 8(5). ISSN 2250–2459
28. Praveen S, Kumar M (2018) Development of mode choice model using ALOGIT. J Emerg Technol Innov Res, 5(6). ISSN 2349–5162
29. Schlich R, Schonfeldera S (2004) Structures of leisure travel: temporal and spatial variability. Trans Review 24:219–237. 30th Anniversary Issue, Routledge Informa, England
30. Sheldon PJ, Mak J (1987) The demand for package tours: A mode choice model. J Travel Res, 25(3):13–17. Sage Publications, U. K.

31. Srinivasan S, Bhat C, Holguin-Veras J (2005) Empirical analysis of the impact of security perception on intercity mode choice a panel rank-ordered mixed logit model. Transp Res Rec, 1942:9–15. Transportation Research Board of the National Academies, Washington, D.C
32. United Nations Statistical Commission (2008) International recommendations for tourism statistics, pp 1–152. Statistical Papers Series M No. 83/Rev.1
33. Verhoeven M, Arentze T, Timmermans H, Waerden P (2005) Modelling the impact of key events on long-term transport mode choice decisions: decision network approach using event history data. Transp Res Rec, 1926:106–114. Transportation Research Board of National Academics, Washington D. C
34. Yanez M, Raveau S, Rojas M, Ortuzar J (2009) Modelling and forecasting with latent variables in discrete choice panel models. Publ Assoc Eur Transp Contrib
35. Yao E, Morikawa T, Kurauchi S, Tokida T (2003) A study on nested logit mode choice model for intercity high-speed rail system with combined RP/SP data. Transp Traffic Theory: 461–476. Elsevier Science Ltd., London

Metro Rail Noise Analysis and Designing of Noise Barrier Along Selected MRTS Corridor in Delhi

Rajeev Kumar Mishra, Manoranjan Parida, and Kranti Kumar

Abstract Noise has become an unwanted part of today's urban life. Rapid urbanization and, in turn, an increase in the number of different transport modes in megacities have raised the noise pollution problem. Different countries have formulated rules and guidelines to control and mitigate noise levels up to a certain level to minimize harmful impacts associated with high noise pollution. Various approaches are applied to reduce the noise level as per the geographical, geospatial, and traffic conditions of a country's particular location. These approaches may vary from location to location due to noise level dependence on several factors like the source of noise, distance between source and receiver, background noise, and meteorological and geospatial conditions. This study applies the Federal Transit Administration (FTA) manual guidelines to analyze and design a noise barrier for the selected corridors of the Delhi Metro Rail Transit System (MRTS). Field measurements were carried out to collect the noise level and other required data. The maximum noise level (86.6 dB) was observed at the Rithala metro station. Barrier height was optimized, keeping in mind the barrier's insertion loss and allowed noise level by Central Pollution Control Board (CPCB), India. The developed model was validated using the experimental data. Study results suggest that the FTA model gives satisfactory results for noise level L_{eq} calculation, and it can be applied successfully to design the noise barrier for the Delhi metro.

Keywords Barrier · FTA model · MRTS · Noise

R. K. Mishra (✉)
Department of Environmental Engineering, Delhi Technological University, Delhi 110042, India
e-mail: rajeevkumarmishra@dtu.ac.in

M. Parida
CSIR-Central Road Research Institute (CRRI), Delhi 110025, India
e-mail: m.parida@ce.iitr.ac.in

K. Kumar
School of Liberal Studies, Dr. B. R. Ambedkar University Delhi, Delhi 110006, India
e-mail: kranti@aud.ac.in

A. Dhamaniya et al. (eds.), *Recent Advances in Traffic Engineering*, Lecture Notes in Civil Engineering 377, https://doi.org/10.1007/978-981-99-4464-4_20

1 Introduction

As transport needs grow, the environmental impact of different modes of transport is coming under critical review. Railways are one of the most eco-friendly modes for large volumes of both passenger and freight traffic. Expansion of the high-speed railway network can help to curb growth in road and air journeys; if freight is transferred back onto the rails, this can remove heavy vehicles from the roads. New light rail and tramway schemes are being proposed in densely populated areas to solve traffic congestion issue [8].

Unfortunately, noise is regarded as an environmental shortcoming of railways [14]. The new railway projects have led to residents' protests, generally due to land acquisition concerns and noise and air pollution-related issues. Reducing the noise generated by trains up to the prescribed standards by restricting train services or speed will lead to other challenging issues like degraded train services and speed performance. The noise produced by the interaction between the wheel and rail often dominates the overall noise signature. Forces that are the consequence of that interaction are generated in a small contact region, throughout which the wheel and rail are in initiate contact. Several techniques for controlling wheel/rail noise directly reduce the excitation force in the contact region instead of modifying the wheels and rails to reduce response and sound radiation [4, 33].

Noise barriers are commonly seen as a routine solution to control excessive noise from roads and railway lines [16]. It is one of the important ways to reduce noise levels. However, these have the disadvantage that they can block the view of nearby residents as well as travelers. Apart from these issues, the high cost and limited noise reduction ability of noise barriers are other important parameters [37]. Regarding the transportation system, the noise barriers typically attenuate noise at the receiver up to 5 to 15 dBA, which depends on the height of the source and receiver, the height of barrier, and the distance between the source and receiver. Noise attenuation relies on the frequency of the sound. In this study, first, we calculate the barrier height using the FTA manual guidelines and then optimize the barrier height by calculating the insertion loss provided by it. The developed model was tested using experimental data at three selected locations of the Delhi Metro.

2 Literature Review

Various strategies have been employed by different researchers for mitigating/reducing noise levels up to permissible limits. Noise barrier has been used extensively in most countries for noise pollution control. Various researchers have made several attempts to design noise barriers and optimize their height and shape to get the maximum possible noise reduction [36]. Ekici and Bougdah [5] presented a thorough review of the environmental noise barrier. Several types of noise barriers, along with their relative acoustic benefits, were discussed in detail. The performance of noise

barriers with different edge shapes under several acoustical conditions was tested by Ishizuka and Fujiwara [9] using Boundary Element Method (BEM).

On the other hand, Grubesa et al. [7] investigated noise barriers' performance having different cross-sections. Simulated annealing (SA) algorithm was used by Mun and Cho [29] to design the desired noise barrier. Their prime focus was on optimizing the barrier dimensions keeping in mind construction cost, and achieving prescribed noise levels at the receiver end. On the other hand, Baulac et al. [1] used an optimization method to design a noise barrier by using different parameters. Cianfrini et al. [3] experimentally tested the acoustic performance of pairs of diffusive roadside barriers. The performance of the diffusive barriers was compared with traditional secularly reflecting barriers. The shadowing effect of barriers of infinite as well as the finite length was investigated by Menounou and Papaefthymiou [26]. Menounou [25] suggested a correction to Maekawa's curve for the insertion loss calculation behind noise barriers.

BEM is an important method to calculate the insertion loss for noise barriers in the absence of turbulence. Lam [17] applied a modified BEM to calculate the insertion loss of a noise barrier. To incorporate the theory of diffraction and sound reflection between surfaces of a room, a new formula was derived by Lau and Tang [18]. This formula was used to calculate insertion loss for rigid noise barriers in an enclosed space. Study results confirm that the modified formula gives more accurate barrier insertion loss than the present models. Ma and Li [22] proposed an optimization method for the design of an L-shaped noise barrier. The cost of the noise barrier was chosen as an objective function.

An optimal design method for noise barriers was presented by Ma et al. [24]. The distance was found as an essential parameter in determining the cost of a noise barrier. They reported that to get the desired reduction in noise level, the barrier height is a more important parameter than the distance between the receiver and the source. Weber and Atkinson [38] developed a method to determine the proper height and location for noise barriers adjacent to railway lines. An optimal design method by considering the cost of noise barrier as an objective function was proposed by Ma and Li [23]. It was concluded that the sound source's finite length is notable for shortening the noise barrier's length, which is essential to noise reduction and the cost of a noise barrier. Karimi and Younesian [11] analyzed the performance of T-shape and Y-shape inclined noise barriers for the mitigation of railway noise. For this purpose, a numerical model was proposed, and the Steepest Descent Method (SDM) was used for optimization purposes. Analysis of reflected noise from transparent noise barriers was done by Lee et al. [19].

The acoustic efficiency of several thin noise barrier designs was assessed by Toledo et al. [32]. Optimization methodology, along with 2D-BEM formulation, was proposed. Simulations using BEM were conducted by Kasess et al. [12] with combinations of 7 different barrier types, different heights, widths, and three different absorptive configurations. The efficiency of noise barriers to reduce noise was studied by Jiang and Kang [10] by considering different aspects of moving traffic. Wang et al. [34] developed a method to calculate the insertion loss of noise barriers based on varied vehicular frequencies. Experimental data verified the developed method.

The effects of wells mounted on the top edge of a barrier for noise reduction were investigated by Wang et al. [35]. To calculate the insertion loss of different types of barriers, 2D-BEM was applied. Zanin et al. [39] used ANN for noise barrier optimization. Their study demonstrates that ANN and the design of experiments provided consistent results. The absorption coefficient strongly influences the noise barrier's attenuation, and barrier height was correlated with the acoustic shadow area. Kim and Yoon [13] presented a novel topology optimization method to design a noise barrier's top shape based on Lighthill's acoustic analogy approach. Li et al. [20] applied the scale modeling method and 2.5 D BEM approach to analyze the nearly-enclosed noise barrier's acoustic performance. A statistical energy method (SEA) was proposed by Li et al. [21] to evaluate the noise reduction performance of vertical noise barriers alongside railway bridges.

Few studies on noise barriers were reported from India also [28]. Sharma [30] applied ANN to determine the height of the noise barrier. Mishra et al. [27] designed noise barriers along the bus rapid transit corridor in Delhi, India, to reduce noise. A modified Federal Highway Administration (FHWA) model was used to design the noise barrier along a flyover in Lucknow by Shukla [31]. Kumar et al. [15] used ANN to determine the optimized height of the noise barrier. Barrier attenuation was calculated using the FHWA model. Results of the study indicate that ANN can be applied to determine the height of noise barriers.

3 Methodology of the Study

The entire adopted methodology for evaluating noise levels and design of noise barrier is presented in Fig. 1.

The various steps adopted to conduct this study are described in the following sections.

3.1 Data Collection

Multiple data (Sound level, metro-related data, etc.) has been collected through field measurement and from a secondary source like the Delhi Metro Rail Corporation (www.delhimetrorail.com). Sound levels were measured using a sound level meter at selected locations. The collected input data are presented in Table 1.

3.2 Standard Equivalent Sound Level (L_{eq})

To check the noise levels obtained at various locations, the permissible noise limits of the Central Pollution Control Board (CPCB), New Delhi, India [2] and Federal

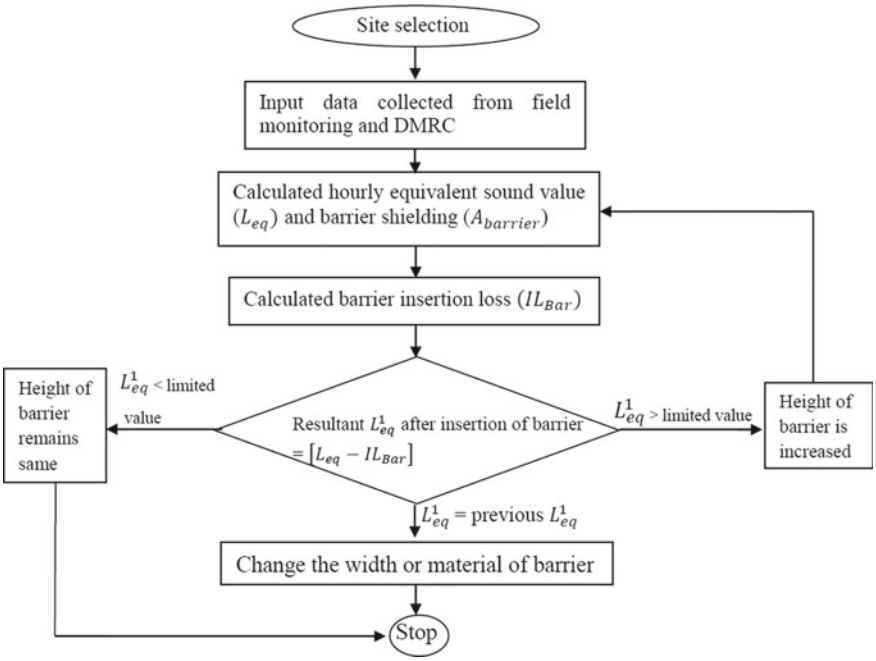

Fig. 1 Methodology of the study

Table 1 Input data collected during monitoring

S. no	Parameter	Data
1	Number of cars per metro train	4–6
2	Average speed of a metro train	50 mph
3	Average hourly train volume	20 trains/hour
4	Height of elevated track from the ground	varies between 12 and 13 m up to a maximum of 17 m
5	Distance between the center line of the track to the barrier	12 ft

Transit Administration (FTA) [6] are adopted (for example, the noise level in terms of L_{eq} in the vicinity of residential buildings should not exceed 55 dBA in the day and 45 dBA at night time).

3.3 Noise Levels Estimation

Noise levels at different conditions are predicted using the FTA model [6]. The model development is explained briefly in the model development section. A comparative analysis was done between measured and predicted noise levels during this study.

3.4 Evaluation of Barrier Effectiveness

To evaluate the efficacy of the barrier, noise levels were predicted as if there were no barriers at the site under consideration and with a barrier as well using FTA guidelines. It was useful to assess the noise level reduction due to the barrier.

3.5 Design of Noise Barriers

At the locations where noise barriers were not present, the reduction in noise levels was calculated by increasing the barrier height. The procedure is continued until the noise is reduced to permissible values given by CPCB. In other locations where noise barriers are already present, it was investigated whether the noise levels are reduced enough not to cause any disturbance to the people living in the vicinity of the area. As per the FTA model's limitations, the noise level can be further reduced to 20 dB by increasing the barrier's height. Further noise reduction can be possible only by changing the width or material used in the barrier.

4 Model Development

In this study, the FTA noise prediction model has been used as a base model to compute the selected receptor locations' noise levels. As input data in the model, the maximum noise levels at 50 ft for each type of noise source are used. The reference source noise levels along with sound exposure levels are presented in Table 2.

Each of the applicable noise metrics and criteria has been used to evaluate the noise impacts at identified receptor locations.

Table 2 Reference noise levels and sound exposure levels

S. no	Group	Description		
			L_{max}	SEL
1	Rail	Rapid transit car passbys	80	82
2		Rapid transit car horns	90	93
3		Locomotives—Diesel	88	92
4		Locomotives—Electric	86	90
5		Commuter rail car passbys	80	82
6		Locomotive horns	105	108
7		Wheel squeal	100	136
8		Aux. Equip.—Rapid transit	67	103
9		Locomotive Idle	80	116
10		Aux. Equip.—Commuter car	65	101
11		Grade crossing signal	73	109
12		Maintenance facility	82	118

4.1 FTA Rail Noise Calculations (for Rail Cars)

FTA has been used to predict the train noise levels at receptor sites. As per FTA guidelines, the noise prediction from passenger rail cars can be made by the following steps:

4.1.1 Hourly Equivalent Sound Level @ 50 ft

As per FTA, hourly L_{eq} at 50 ft can be calculated by using the following equation.

$$L_{eq@50feet} = SEL_{ref} + 10\log(N_{cars}) + 20\log\left(\frac{S}{50}\right) + 10\log(V) + C_{adj} - 10\log(3600) \tag{1}$$

where

$L_{eq@50ft}$ = hourly L_{eq} noise level at 50 ft (in dBA);
SEL_{ref} = reference SEL noise level at 50 ft (in dBA).
N_{cars} = average consist size (i.e., number of locomotives or rail cars per train);
S = train speed (in mph);
V = average hourly train volumes as follows (in trains/hour):

$$V_D = \left[\frac{\sum_{7AM}^{10PM} no\ of\ trains}{15}\right][Average\ hourly\ day\ time\ volume] \tag{2}$$

$$V_N = \left[\frac{\sum_{10PM}^{7AM} no\ of\ trains}{9}\right][Average\ hourly\ night\ time\ volume] \quad (3)$$

$$V_{PK} = \left[\sum_{PK-HR} number\ of\ trains\right][Average\ hourly\ peak\ hour\ volume] \quad (4)$$

C_{adj}= adjustment factor applied to track type as follows (in dBA):
= + 5 for jointed rail track;
= + 4 for aerial structure with slab track;
= + 3 for embedded track on grade.
10log(3600) = $L_{eq}(h)$ adjustment factor based on the number of seconds in one hour (in dBA).

4.1.2 Hourly Equivalent Sound Level @ Distance D ft

Equation 5 has been used to calculate the distance adjustment to the receiver.

$$L_{eq@Dfeet} = \left[L_{eq@50feet}\right] - \left[15log^{\left(\frac{D}{50}\right)}\right] \quad (5)$$

where D is the distance between the receiver and the track center line in feet

4.1.3 Barrier Shielding

Barrier shielding is estimated using Eq. 6. The schematic diagram of the barrier shielding is depicted in Fig. 2.

$$A_{barrier} = min\left\{20or\left[20\log\left[\frac{3.54\sqrt{p}}{\tanh\left[6.27\sqrt{p}\right]}\right] + 5\right]\right\} \quad (6)$$

where

$A_{barrier}$ = barrier shielding (in dBA);

p= barrier path length difference (in feet).

$$p = A + B - C \quad (7)$$

$$A = \sqrt{D_{SB}^2 + (H_B - H_S)^2} \quad (8)$$

$$B = \sqrt{D_{BR}^2 + (H_B - H_R)^2} \quad (9)$$

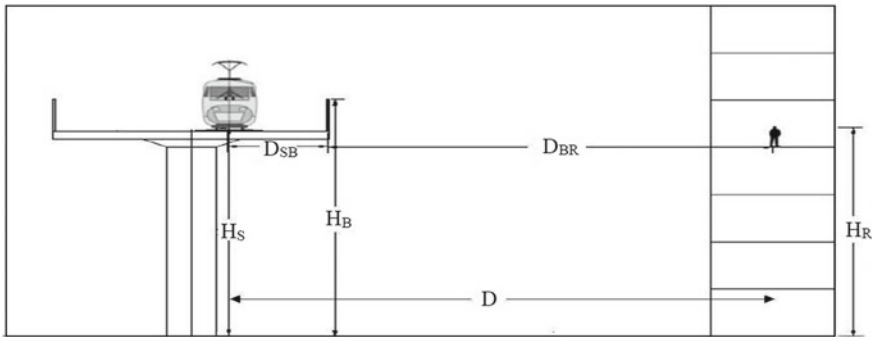

Fig. 2 Schematic diagram for barrier shielding

$$C = \sqrt{(D_{SB} + D_{BR})^2 + (H_S - H_R)^2} \tag{10}$$

where

$A + B$ = path length over the barrier;

C = path length through the barrier.

Barrier Insertion Loss. The Below Eq. (11) Has Been Used to Determine the Overall Barrier Insertion Loss.

$$IL_{Bar} = A_{barrier} - 10(G_{NB} - G_B)\log\left(\frac{D_s}{50}\right) \tag{11}$$

where

IL_{Bar} = barrier insertion loss (in dBA);
$A_{barrier}$ = barrier shielding (in dBA);
G_{NB} = ground factor computed without a barrier;
G_B= ground factor computed with a barrier; and.
D_s = closest distance between the receptor and the source (in feet).

Ground Attenuation: Effective Height. The Effective Height Between the Source and the Receptor is Computed According to the Below Equation.

$$H_{eff} = \frac{H_S + 2H_B + H_R}{2} \tag{12}$$

where

H_{eff} = effective height (in ft);
H_S = height of noise source with the following acoustical heights (in ft);
H_B = height of the intervening barrier (in ft); and,

H_R = height of receptor (in feet).

Ground Attenuation: Ground Factor. An Appropriate Ground Attenuation Factor May Be Computed Using the Eq. 13.

$$G = \begin{cases} 0.66 & H_{eff} < 5 \\ 0.75 \times \left(1 - \frac{H_{eff}}{42}\right) & 5 < H_{eff} < 42 \\ 0 & 42 < H_{eff} \end{cases} \quad (13)$$

where

G = ground factor (dimensionless); and,

H_{eff} = computed effective height (in ft).

4.1.4 Building Shielding

During this study, shielding due to rows of buildings is also calculated using the equation mentioned below.

$$A_{Bldg} = \left\{ Min\, 10\, or \left[1.5 \times (N_{Row} - 1) + C_{Gap} \right] \right\} \quad (14)$$

where

A_{Bldg} = building shielding (in dBA);

N_{Row} = number of rows of buildings that intervene between the source and receptor; and,

C_{Gap} = building shielding adjustment factor as follows (in dBA):

= 5 dBA if the gap between a row of buildings is less than 35% of the row length;

= 3 dBA if gaps between the row of buildings are between 35 and 65% of the row length; and,

A_{Bldg} = 0, if gaps between the row of buildings are greater than 65 percent of the row length.

4.1.5 Maximum Allowable Shielding

The total allowable shielding was calculated using Eq. 15.

$$A_{Shld} = Max\left\{ IL_{Bar} or A_{Bar} or A_{Bldg} \right\} \quad (15)$$

where

A_{Shld} = total shielding allowed (in dBA);
IL_{Bar} = barrier insertion loss (in dBA);
A_{Bar} = barrier shielding (in dBA);
A_{Bldg} = building shielding (in dBA).

4.1.6 Final L_{eq}^{1} After the Insertion of a Barrier

Final L_{eq}^{1} after barrier insertion can be obtained using the following relation:

$$FinalL_{eq}^{1} = L_{eq}@distanceD - IL_{Bar} \tag{16}$$

Final L_{eq}^{1} should be within the standards of CPCB and FHWA.

5 Results and Analysis

This section describes the noise level prediction at different distances, heights and the model results' validation.

5.1 Noise Level Prediction

Based on the above-discussed methodology, the noise levels are predicted at various selected points using the FTA model, and the results are presented in Fig. 3. In addition to that, the noise levels are also estimated at different heights at a distance of 50 ft. The entire profile of noise level variations with height is depicted in Fig. 4.

5.2 Model Validation

To validate the functionality of the above-discussed model, the field studies are conducted at three different locations (Rithala metro station, the residential building beside the elevated metro track, and the elevated track moving from Kashmere gate to Shastri Park over Yamuna River) to observe the noise levels and to evaluate the effectiveness of existing barrier at the particular location.

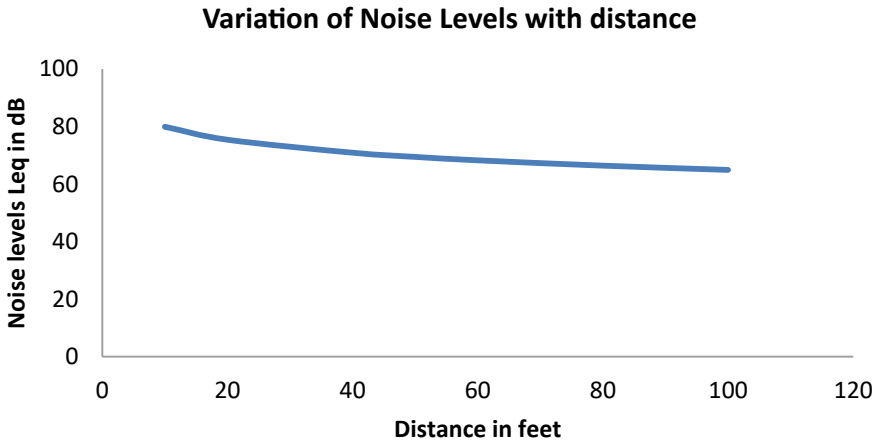

Fig. 3 Variation of noise level with distance

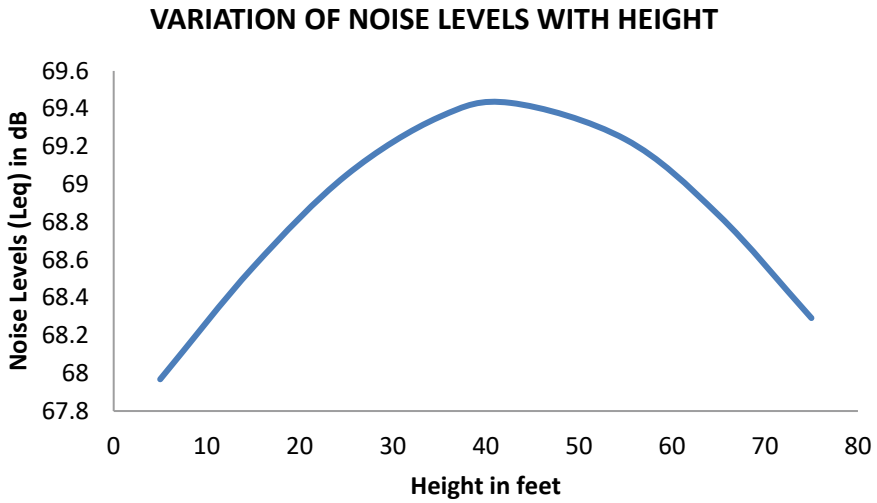

Fig. 4 Noise level variation with height at a distance of 50 ft

5.2.1 Location 1 (Rithala Metro Station)

Noise levels are observed using the Sound Level Meter by standing 6 ft away from the track's center. The calculations are done manually using the FHWA model, and both the observed and predicted values are shown in Table 3.

Table 3 Observed versus predicted noise level at Rithala metro station

Observed L_{eq} in dB	Predicted L_{eq} in dB	Percentage error
86.6	82.04	−5.26

5.2.2 Location 2 (Residential Apartments Beside Rithala Metro Rail Track).

Noise levels are observed standing on the fourth floor of a residential apartment at a distance of 120 ft from the center line of the track (Table 4).

The noise level observed at the selected location is also influenced by the road traffic noise moving beside the track at ground level, so the percentage error is more in Table 4. From the study of the location and analysis, it is found that the existing height of the noise barrier at the specific location can reduce the noise level up to 47.68 dB, which is less than the maximum daytime noise level given by CPCB, but for night time, this value is more than permissible (45 dBA), so the noise barrier height needs to be increased by 1.61 ft as shown in Fig. 5.

Table 4 Observed versus predicted noise level at residential apartments beside Rithala

Observed L_{eq} in dB	Predicted L_{eq} in dB	Percentage error
73.3	63.73	−13.06

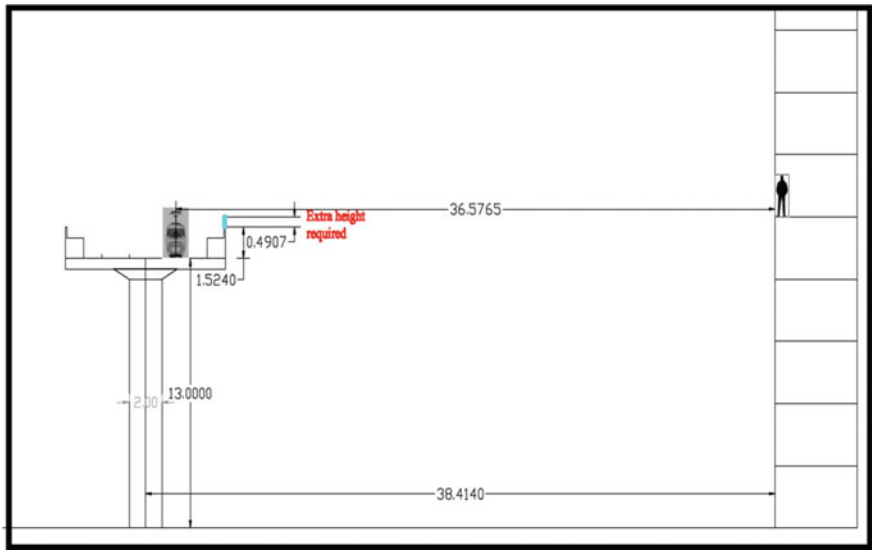

Fig. 5 Cross-section showing the elevated track at Rithala Delhi

Table 5 Observed and predicted noise level variation with different heights and distances at the selected location

S. no. of the point at the location	Height above the ground level (ft)	Distance from the outer face of the barrier (ft)	Observed L_{eq} in dB	Predicted L_{eq} in dB	Percentage error
1	9	45	71	68.20	−3.94
2	4	20	68.88	69.76	+ 1.28
3	4	10	68.66	70.54	+ 2.74

5.2.3 Location 3 (Elevated Track Moving from Kashmere Gate to Shasthri Park Over Yamuna River)

Noise levels are monitored at three different points at this location. The details of observed and predicted noise levels according to vertical height and horizontal distance are presented in Table 5.

The percentage error varies from −5.26 to + 2.74, which is considerable; this shows that the proposed model for FTA's noise prediction is validated and can be used to design the noise barrier at the selected metro corridor of Delhi. The noise levels from metro rails are calculated for the worst condition, and it is found that in Delhi during the night period, the values are more than 45 dBA (CPCB permissible limit) up to 200 ft from the center of the track, in which residential buildings are present at 50 ft distance. So there is a need to redesign the existing noise barriers for the Delhi metro. The study shows that a change in the height of the barrier cannot serve the purpose, so care should also be taken about the thickness and material of the barrier.

6 Conclusion

Based on collected data analysis and model validation, the noise level variation is observed increasing faster at closer distances; after that, noise levels reduce comparatively at a slow rate. The maximum noise level is found at the elevation, same as the source, which reduces above and below that level in the vertical plane. It is found from the analysis that the existing height of the noise barrier for the elevated metro track at Rithala can reduce the noise level above permissible limits given by CPCB, so there is a need to increase the barrier height by 1.61 ft. The L_{eq} values calculated in the Rithala metro platform give 82.04 dB, which is considered very high. The noise levels predicted using the FTA model give less percentage error with the field study's values; this shows the model is validated. At worst condition, it is found that during the night period, the noise values are more than 45 dB (CPCB permissible value) up to 200 ft from the center of the track, in which residential buildings are present at 50 ft distance. So there is a need to redesign noise barriers for the Delhi

metro. The maximum noise level a barrier can reduce is limited to 20 dB by FTA; over that, we have to concentrate on the barrier's width and material.

Conflict of Interests The authors declare no conflict of interest. The results, conclusions, and recommendations presented in this study do not represent the official view of DMRC, Delhi. The authors independently carried out this study for research and academic purpose only.

References

1. Baulac M, Defrance J, Jean P (2008) Optimisation with genetic algorithm of the acoustic performance of T-shaped noise barriers with a reactive top surface. Appl Acoust 69(4):332–342
2. Central Pollution Control Board (2022) [online] Available at https://www.cpcb.nic.in. [Accessed 23 August 2022]
3. Cianfrini C, Corcione M, Fontana L (2007) Experimental verification of the acoustic performance of diffusive roadside noise barriers. Appl Acoust 68(11–12):1357–1372
4. Transit Link Consultants (2008) Noise and vibration methodology report. Technical report NJT Contract #03–118
5. Ekici I, Bougdah H (2003) A review of research on environmental noise barriers. Building Acoustics 10(4):289–323
6. Transit Noise and Vibration Impact Assessment Manual., 2006. Federal Transit Administration.
7. Grubeša S, Domitrović H, Jambrošić K (2011) Performance of traffic noise barriers with varying cross-section. Promet-Traffic & Transp 23(3):161–168
8. Limited HMR (2007) Manualofspecifications and standards. Elevated mass rapid transit system through public-private partnership, Government of Andhra Pradesh
9. Ishizuka T, Fujiwara K (2004) Performance of noise barriers with various edge shapes and acoustical conditions. Appl Acoust 65(2):125–141
10. Jiang L, Kang J (2016) Combined acoustical and visual performance of noise barriers in mitigating the environmental impact of motorways. Sci Total Environ 543:52–60
11. Karimi M, Younesian D (2014) Optimized T-shape and Y-shape inclined sound barriers for railway noise mitigation. J Low Freq Noise, Vib Act Control J Acoust Soc Am 33(3):357–370
12. Kasess CH, Kreuzer W, Waubke H (2016) Deriving correction functions to model the efficiency of noise barriers with complex shapes using boundary element simulations. Appl Acoust 102:88–99
13. Kim KH, Yoon GH (2020) Aeroacoustic topology optimization of noise barrier based on Lighthill's acoustic analogy. J Sound Vib 483:115512
14. Krylov VV ed. (2001) Noise and vibration from high-speed trains. Thomas Telford
15. Kumar K, Parida M, Katiyar VK (2014) Optimized height of noise barrier for non-urban highway using artificial neural network. Int J Environ Sci Technol 11(3):719–730
16. Kurze UJ (1974) Noise reduction by barriers. J Acoust Soc Am 55(3):504–518
17. Lam YW (2004) A boundary element method for the calculation of noise barrier insertion loss in the presence of atmospheric turbulence. Appl Acoust 65(6):583–603
18. Lau SK, Tang SK (2009) Performance of a noise barrier within an enclosed space. Appl Acoust 70(1):50–57
19. Lee J, Kim I, Chang S (2015) Analysis of highway reflection noise reduction using transparent noise barrier types. Environ Eng Res 20(4):383–391
20. Li Q, Duhamel D, Luo Y, Yin H (2020) Analysing the acoustic performance of a nearly-enclosed noise barrier using scale model experiments and a 2.5-D BEM approach. Appl Acoust, 158: 107079
21. Li X, Hu X, Zheng J (2020) Statistical energy method for noise reduction performance of the vertical noise barrier alongside railway bridges. Appl Acoust 170:107503

22. Ma X, Li S (2009) Optimization design of L-shaped road noise barrier and cost-effectiveness analysis. In: IEEE Intelligent vehicles symposium, Xi'an, China, pp 988–993
23. Ma X, Li S (2011) Optimization of road noise barrier based on finite length of traffic flow. In: International conference on electric information and control engineering, Wuhan, China, pp 2441–2444
24. Ma X, Yang S, Xu B (2005) Optimization design of road noise barrier. In: IEEE International Conference on Vehicular Electronics and Safety, Shaanxi, China, pp 276–280
25. Menounou P (2000) A correction to Maekawa's curve for the insertion loss behind noise barriers. J Acoust Soc Am 108(5):2477–2477
26. Menounou P, Papaefthymiou ES (2010) Shadowing of directional noise sources by finite noise barriers. Appl Acoust 71(4):351–367
27. Mishra RK, Parida M, Rangnekar S (2010) Evaluation and analysis of traffic noise along bus rapid transit system corridor. Int J Environ Sci Technol 7(4):737–750
28. Mohan SA, Dutta N, Sarin SM (2002) Need for construction of noise barriers in India. Indian Highw, 30(12)
29. Mun S, Cho YH (2009) Noise barrier optimization using a simulated annealing algorithm. Appl Acoust 70(8):1094–1098
30. Sharma MKD (2007) Artificial neural network in transport-related pollution modeling. MTech thesis. Indian Institute of Technology Roorkee, India
31. Shukla AK (2011) An approach for design of noise barriers on flyovers in urban areas in India. Int J Traffic Transp Eng 1(3):158–167
32. Toledo R, Aznárez JJ, Maeso O, Greiner D (2015) Optimization of thin noise barrier designs using evolutionary algorithms and a Dual BEM formulation. J Sound Vib 334:219–238
33. US Department of Transportation, Federal Railroad Administration (1983) Railroad noise emission compliance regulations. Final Rule, 48 Federal Register, pp 56756–5676. (23 Code of Federal Regulations 210)
34. Wang H, Luo P, Cai M (2018) Calculation of noise barrier insertion loss based on varied vehicle frequencies. Appl Sci 8(1):100
35. Wang Y, Jiao Y, Chen Z (2018) Research on the well at the top edge of noise barrier. Appl Acoust 133:118–122
36. Watson D (2006) Evaluation of benefits and opportunities for innovative noise barrier designs. Technical report, Arizona Department of Transportation, Report No. FHWA-AZ-06–572
37. Watts GR (1996) Acoustic performance of a multiple edge noise barrier profile at motorway sites. Appl Acoust 47(1):47–66
38. Weber C, Atkinson K (2008) A systematic approach for arriving at reasonable heights and locations for noise barriers adjacent to railway lines. Noise and Vibration Mitigation for Rail Transportation Systems. Springer, Berlin, Heidelberg, pp 243–249
39. Zannin PHT, Do Nascimento EO, Da Paz EC, Do Valle F (2018) Application of artificial neural networks for noise barrier optimization. Environments 5(12):135

Effect of Traffic Composition on Environmental Noise and Development of Noise Map of Roadside School, Colleges, and Hospital Buildings

Ramesh B. Ranpise and B. N. Tandel

Abstract Urbanization, industrialization, and poor urban planning are the prime sources of noise pollution in cities. Traffic noise is escalating at a high rate in metro cities. Surat is the fastest growing city categorized into tier-II, located in the western part of Gujarat state of India. This study aims to enumerate the propagation of noise levels near the roadside school and college buildings by monitoring and mapping. Noise mapping is an effective tool to fulfill the noise impact analysis in the metropolitan area. In this study, five institutional buildings consisting of four colleges and one school were selected as study locations. Diurnal noise assessment was done by utilizing a KIMO sound level meter. The equivalent noise levels at all sites vary between 61.4 dBA to 75.7dBA. The highest noise level is observed at V.T. Choksi College. The collected data were mapped using ArcGIS software that represents the propagation of noise levels over the monitoring location. This study discloses that noise levels at all monitoring points surpass the standard limits given by the government of India. The noise map shows that the students, teachers, and other people in this area are exposed to urban road traffic noise. Therefore, instant strategic planning is required to decrease noise pollution levels in these areas.

Keywords Traffic composition · Urban Road traffic noise · Urban planning · Noise maps · ArcGIS

R. B. Ranpise (✉) · B. N. Tandel
Sardar Vallabhbhai National Institute of Technology Surat, Surat, Gujarat 395007, India
e-mail: d18ce017@ced.svnit.ac.in

B. N. Tandel
e-mail: bnt@ced.svnit.ac.in

A. Dhamaniya et al. (eds.), *Recent Advances in Traffic Engineering*, Lecture Notes in Civil Engineering 377, https://doi.org/10.1007/978-981-99-4464-4_21

1 Introduction

Noise pollution is defined as ambient noise, it is nothing but the distribution of noise levels with injurious impact on human activities [1]. The main origin of outside noise is generated by machines, transport, and other manmade activity. Indigent town planning, unprecedented growth, and rapid increment in the use of private vehicles may promote noise pollution in the urban region.

Noise is a disturbance to the human environment that is rising at such a high rate because it will turn into a significant threat to the quality of living of people [2]. Noise pollution influences both well-being and conduct, it may cause anxiety, tinnitus, hypertension, hearing loss, sleep disturbances, and other effects [3, 4].

The main Source of outdoor noise is transportation [5]. Due to the increment in the population, the rate of personal vehicles also increased, ultimately causing increment in traffic which directly causes high traffic noise. Noise pollution is not an uncommon problem for developing countries like India only. Traffic noise is produced from various sources such as horn honking, engine noise, ambulance siren, tire pavement interaction, etc.

Road traffic noise has a serious impact on dwellers.

Surat city has so many suburban areas as well as arteries which help in the systematic connection of every part of the city. Road transportation plays a crucial role in the generation of traffic noise. In Surat city, various Schools, Colleges, and hospitals are facing the main stream of traffic. It must be situated in silence zone also noise level in this region is exceeding the permissible limit which is given by CPCB [6], these buildings and shops near this area are exposed to high traffic noise.

In this study, traffic composition, traffic noise measurement, and generation of noise maps have been done. It will be helpful to investigate the effectiveness of different noise reduction strategies and possible reductions of noise propagation from road vehicles, focusing on traffic flow. Also it will helps in effective traffic and transportation planning, policy makers and town planners.

1.1 Urban Traffic and Noise Level

Urban road traffic and its congestion became a big subject of discussion among researchers for many years. While the increasing ambient noise levels in public areas due to traffic congestion, unauthorized parking, road construction and its maintenance activity, public address system, horns, and other devices destructively affect human well-being and the mental health of individuals. It is important to manage and control noise-producing sources to maintain ambient air quality standards in respect of noise [3, 7].

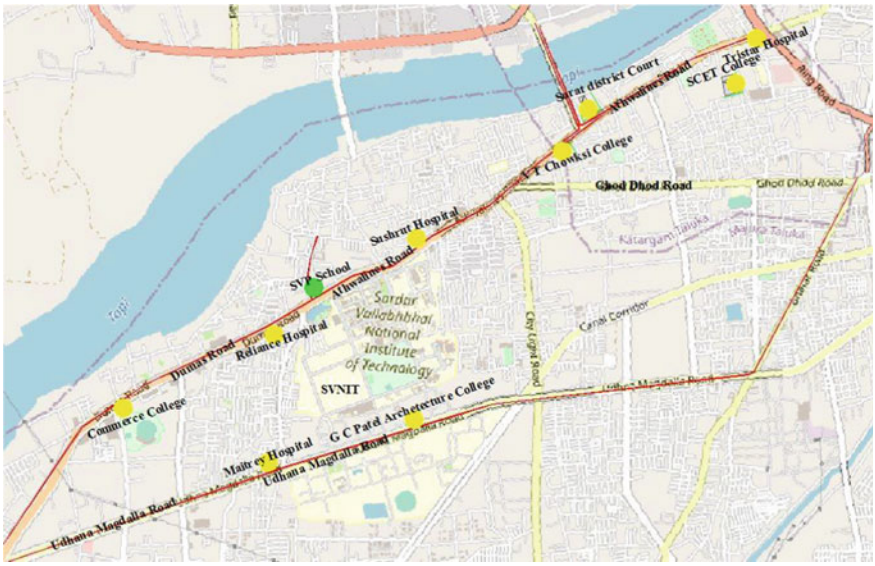

Fig. 1 Study location on Surat City's road

2 Methodology

2.1 Study Area

Surat city is the fastest growing city in India, the topographical area of Surat city is 210°12′00.00"N and 72°52′00.00"E close to the bank of Tapi River. Ten noise measurement points close to metropolitan roads in Surat City were chosen for the study. The determination of the measurement points depended on the site and road function. The study location includes three colleges, three hospitals, one school, and one regional court. These referenced areas fall under the silence zone (Fig. 1).

2.2 Instrument Used

Noise monitoring was carried out in the official days through Monday to Friday as considered working days. On-site measurement has been done by utilizing the KIMO DB 300 sound level meter. The Falcon HR radar gun has been utilized for on-spot speed measurement. The latitude and longitude have been noted by using mobile GPS.

2.3 Data Collection

Noise level (dBA): noise level readings were gathered for every minute of interval for 12 measuring hours with noise level meter. Noise level meter was held at 1.5 m over the surface of the road [8].

Traffic volume count: Handy cam was used for recording the videos for continuously 12 h, and after that, the traffic was counted by playing the recordings on the PC, i.e., manual counting for various classes of vehicle.

Traffic speed measurement: The speed for various categories of vehicles was assessed by using a Radar gun, i.e., on-site measurement and the width of the road was measured by meter tape.

A detailed noise measurement was carried out at various 10 measurement points. The selected location consists of one school building and four colleges which are situated along the major arterial road of Surat city. Continuous 12 h noise monitoring was performed to get good results.

2.4 Preparation of Noise Map

Noise maps are developed by utilizing ArcGIS 10.8 software. This map can help to visualize the spatial distribution of noise due to urban road traffic.

3 Results and Discussion

At Maitrey Hospital (MP-1), buildings were high from 9.00 am to 1.00 pm and quite constant from 4.00 Pm to night time 9.00 pm. As compared morning and evening noise levels at afternoon period it was low it may be due to the busy office hours and at afternoon period there was having low traffic.

At Sushrut Hospital (MP-2), the noise levels reading at outside the premises and inside the premises were almost the same; the reason could be the short distance from the main traffic stream as well as the road is quite busy for the whole day as it was connected to various suburban parts of the city. And the noise level inside the building was comparatively high than the outside the premises from morning 11.00 am to afternoon 4.00 pm, it may be due to the movement of vehicle which moving on the adjacent road of the hospital building and due to the entering the vehicle and movement of people inside the premises of hospital building [9, 10] (Fig. 2).

At Commerce College, there is no big difference between the inside and outside of the premises but the noise levels inside the campus were quite high as compared to the outside noise level readings. The reason may be the entering the two-wheeler inside the gate and the height of compound wall of the college is less. Also, there are

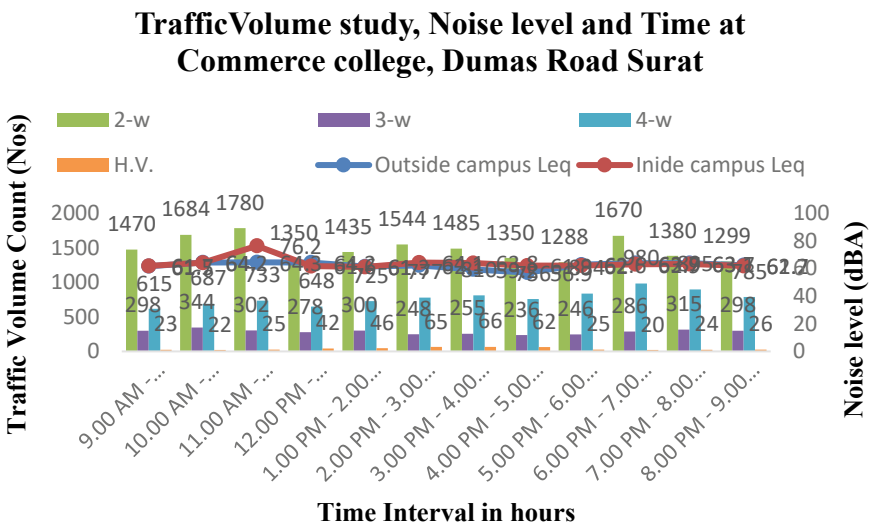

Fig. 2 Traffic volume count versus noise levels at Commerce College

two roads bearing the college area; one is just adjacent to the compound wall of the building and the other one was at the front side of the building.

Tristar Hospital building is situated at one of the busiest circles of Surat city name having Aero plane circle, Athwa gate, the traffic situation at this location became very crowd at morning and evening period also just near to the Tristar hospital building a flyover bridge was there which connect to Adajan-Patiya. Tristar Hospital is a multispecialty hospital so the movement of patients and the incoming and outgoing of the Ambulance could be the reason. Also, there is no closed compound wall around the hospital [10].

At MP-5, noise level measurement shows a remarkable increase in noise level in the morning period, i.e., 9.00 am to 1.00 pm, inside the premises of the school building; the main reason could be the building is just away from the traffic stream and entering the vehicles of staff inside the gate as well as the movement of the staff and students.

There is no significant difference in noise levels between inside and outside the campus of Sarvajanik College, the equivalent noise level is 62.8 dBA. But the maximum equivalent noise level is 89.7 and the minimum was 41dBA. The number of 2-w, 3-w, 4-w, and heavy motor vehicles are higher in the morning than afternoon hours and evening.

The noise level nearby V.T. Choksi Law College has noticed a moderate decreasing noise with time from morning 10.00 am to night 9.00 pm. The highest noise level was observed in the morning and the lowest during the evening. Therefore, the entire change in noise level is around 3 dB from morning to afternoon period.

During the afternoon period, the maximum traffic count and massive crowd adjacent to the court could be one of the reasons for the maximum noise. Also, during

morning furthermore evening hours the lesser number of vehicles count and low noise was observed as compare to afternoon. Noise levels for continuous 12 h period exceeding the permissible limit.

3.1 Preparation of Noise Map

To prepare the noise contour map, ArcGIS 10.8 software has been utilized. The shape file consisting road network of the study location was downloaded from geoinformatics world database, then it is imported into the GIS tool. To plot the noise levels concerning contours, the interpolation (Inverse Distance Weighted) method has been adopted in the ArcGIS tool. This interpolation technique displays noise levels at monitoring points by different color codes. The maps indicate more sensitive areas to the threat of noise pollution and provide more useful graphic details of the areas with greater noise levels and traffic congestion [10, 11]. The 2.5 dBA bandwidths have been used to construct the noise maps. Each band displays a distinct color, which on the map represents a different noise level. The sound scale ranges from 60 to 78 dBA. The coordinate system projection for Surat City is UTM-WGS 1984-Zone 45N. The prepared noise map has been shown below (Fig. 3).

The above graphical representation indicates the noise monitoring location along the arterial road and the propagation of sound waves at all 10 locations. The developed noise map visualizes the picture of noise pollution surroundings the location due to

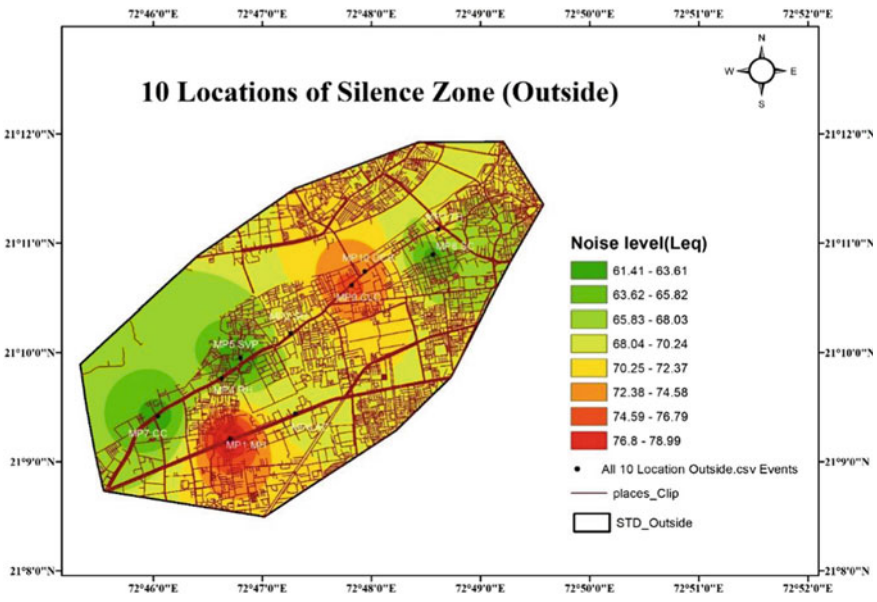

Fig. 3 Noise map for all 10 Locations outside the campus (12 h)

Table 1 Noise standards given by the government of India [6]

Area code	Category of area or zone	Limits in dB (A) Leq*	
		Day	Night
(A)	Industrial Area	75	70
(B)	Commercial Area	65	55
(C)	Residential Area	55	45
(D)	Silence Zone	50	40

present traffic conditions. The noise standards prescribed by the Central Pollution Control Bord of India has mentioned below (Table 1).

Red color indicates the highest noise level in a particular region and green color indicates the noise levels are below 60 dBA. According to the standards, the noise levels at all location surpasses the limit given by the government of India. Out of 10 locations, the maximum noise level was observed at MP-1, MP-3, MP-4, MP-8, MP-9, and MP-10. Yellow to red color represents the very noisy environment in that indicated region. The monitoring point number 1, 9, and 10 are noisy for the whole day and it may be due to the heavy traffic as they are situated alongside the major arterial road of the city.

4 Proposed Solutions for Noise Mitigation and Traffic Management

Noise mitigation strategies such as noise barrier, dense vegetation, steel railing, partition wall, sound absorption material, etc., for schools and college buildings can apply. Traffic management authorities, municipal corporations, town planners, and other administrators can rigidly enforce the vehicle speed limits. Banning heavy vehicles, musical horn systems, and unwanted horn honking must be strictly implemented. Proper land use planning, orientation of buildings, road lane discipline, and roadside hedges can help in the reduction of noise levels and smoothen the traffic flow. Some of the effective strategies are also mentioned below.

Noise Barriers: Installation of a noise barrier obstructs the direct path of noise between the receiver and the source, thereby attenuating the noise at the receiver's end.

Low Noise Engines: Major noise generated by an automobile is due to engine noise. These are generated due to internal and external vibrations. Internal vibration includes noise from the inertia of moving parts and external vibration includes noise from the entire engine system as a block. Low-noise engines should be installed to mitigate this noise.

Traffic Composition: In this strategy, the composition of traffic was considered such that, if the major noise-making vehicle class was adjusted according to the working hours, an appreciable reduction in noise could be achieved.

Low Noise tires: Changes in conventional tire design can be made to reduce the tire vibrations like increasing external diameter, increasing the weight, tread stiffness, and many others.

Low Noise Pavements: Pavements play a very important role and slight variations like the amount of binder used, the mix, and surface treatment can reduce the noise level considerably. The noise levels (Leq) of study location has mentioned below (Table 2).

Table 2 List of study locations along with coordinates and noise levels in dBA

Sr. no	Name	Noise level (Leq)	Latitude	Longitude
1	Maitrey Hospital	79	21.15351	72.77834
2	Sushrut Hospital	68.4	21.16956	72.78764
3	Tristar Hospital	68.8	21.1854	72.8102
4	Reliance Hospital	73.8	21.16268	72.71711
5	SVP School	61.4	21.16583	72.77994
6	Gijubhai Patel Institute of Architecture College	69.4	21.15733	72.78837
7	Commerce College	62.7	21.1569	72.76734
8	Sarvajanik Engineering College	62.8	21.18155	72.80932
9	Choksi Law College	75.7	21.17681	72.79694
10	District Court	73.8	21.17896	72.79894

5 Conclusion

The increment in road traffic noise in the urban region has an environmental concern. Urban road traffic is a remarkable source of noise in living as well as in active environments [10].

In this study, the traffic composition and its volume with respect to road width have been presented (Table 3). The spatial distribution of noise levels generated by arterial road traffic in urban areas has been visualized by means of noise monitoring and mapping as an effective tool for the appraisal of impact.

According to the developed noise map, the color codes are mentioned in consideration of the silence zone, and the standard values for the silence zone prescribed by the CPCB are considered in the graphical representation of sound level distribution and the propagation of sound waves at all 10 locations. In accordance with the principles, the decibel levels in silence zones shouldn't surpass 50 dB during the day and 40 dB at night. The sound levels at all locations varied from 50 to 79 dBA for the day.

At MP-2, MP-3, and MP-9, the level of noise is about 65 to 71.9 dBA inside the premises of that buildings. The difference in the maximum and minimum levels of noise is very big at all monitoring points.

The foremost area of noise abatement is transportation noise control, urban planning through zoning code, architectural design, and industrial noise control. Expeditious urbanization and improved social status from recent years have emerged in high vehicular development. The issue becomes more serious with heterogeneous traffic conduct on metropolitan roads as pedestrians, bikes, vehicles, auto carts, and cycle carts share a similar road space making incapable mobility conditions. Estimation of noise levels due to traffic, development, and visualization of noise maps, and traffic composition and road width in urban areas are the key elements to conduct effective transportation and traffic planning. It assists in traffic controlling guidelines too.

Table 3 Traffic volume count with class of vehicle and equivalent noise levels at Commerce College, Athwa Dumas Road, Surat

Time interval	Equivalent noise level (dBA)		Volume count (Nos.)				Avg. speed (Km/ h)				Avg. building height (meter)	Road width (meter)
	Outside campus	Inside campus	2-w	3-w	4-w	H.V	2-w	3-w	4-w	H.V		
9.00 AM–10.00 AM	61.5	61.7	1470	298	615	23	34	32	42	27	30	18
10.00 AM–11.00 AM	64.2	64.0	1684	344	687	22	36	33	35	29	30	18
11.00 AM–12.00 PM	64.3	76.2	1780	302	733	25	40	35	44	30	30	18
12.00 PM - 1.00 PM	64.2	61.6	1350	278	648	42	37	30	46	30	30	18
1.00 PM–2.00 PM	61.3	61.0	1435	300	725	46	44	22	47	28	30	18
2.00 PM–3.00 PM	62.1	64.1	1544	248	777	65	42	32	36	26	30	18
3.00 PM–4.00 PM	59.2	63.8	1485	255	810	66	39	28	38	30	30	18
4.00 PM–5.00 PM	56.9	61.9	1350	236	756	62	32	29	32	28	30	18
5.00 PM–6.00 PM	62.6	62.0	1288	246	834	25	31	32	44	26	30	18
6.00 PM–7.00 PM	63.7	62.9	1670	286	980	20	41	30	42	30	30	18
7.00 PM–8.00 PM	63.7	63.1	1380	315	895	24	44	29	40	28	30	18
8.00 PM–9.00 PM	62.2	61.7	1299	298	785	26	38	28	44	25	30	18

References

1. Florindo TJ, Florindo GD, Talamini E, da Costa JS, de Léis CM, Tang WZ, Schultz G, Kulay L, Pinto AT, Ruviaro CF (2018) Application of the multiple criteria decision-making (MCDM) approach in the identification of Carbon Footprint reduction actions in the Brazilian beef production chain. J Clean Prod 196:1379–1389. https://doi.org/10.1016/j.jclepro.2018.06.116.
2. Myllyntausta S, Virkkala J, Salo P, Varjo J, Rekola L, Hongisto V (2020) Effect of the frequency spectrum of road traffic noise on sleep: a polysomnographic study. J Acoust Soc Am 147:2139–2149. https://doi.org/10.1121/10.0000985
3. De SK, Swain BK, Goswami S, Das M (2017) Adaptive noise risk modelling: Fuzzy logic approach. Syst Sci Control Eng 5:129–141. https://doi.org/10.1080/21642583.2017.1294118
4. Eze IC, Foraster M, Schaffner E, Vienneau D, Héritier H, Pieren R, Thiesse L, Rudzik F, Rothe T, Pons M, Bettschart R, Schindler C, Cajochen C, Wunderli JM, Brink M, Röösli M, Probst-Hensch N (2018) Transportation noise exposure, noise annoyance and respiratory health in adults: a repeated-measures study. Environ Int 121:741–750. https://doi.org/10.1016/j.envint.2018.10.006
5. Nourani V, Gökçekuş H, Umar IK (2020) Artificial intelligence based ensemble model for prediction of vehicular traffic noise. Environ Res 180:108852. https://doi.org/10.1016/j.envres.2019.108852
6. Ministry of Environment and forest, The Noise Pollution (Regulation and Control) Rules (2000) 12311(1110):1088–1569. http://cpcbenvis.nic.in/noisepollution/noise_rules_2000.pdf
7. CPCB (2015) July 2015 Protocol for Ambient Level Noise Monitoring CENTRAL POLLUTION CONTROL BOARD. 10
8. Banerjee D, Chakraborty SK, Bhattacharyya S, Gangopadhyay A (2009) Appraisal and mapping the spatial-temporal distribution of urban road traffic noise. Int J Environ Sci Technol 6:325–335. https://doi.org/10.1007/BF03327636
9. Cunha M, Silva N (2015) Hospital noise and patients' wellbeing. Procedia Soc Behav Sci 171:246–251. https://doi.org/10.1016/j.sbspro.2015.01.117
10. Laib F, Braun A, Rid W (2019) Modelling noise reductions using electric buses in urban traffic: a case study from Stuttgart, Germany. Transp Res Procedia 37:377–384. https://doi.org/10.1016/j.trpro.2018.12.206

Calibration of Microscopic Traffic Simulation for Signalized Intersections Under Heterogeneous Traffic Conditions

Rushikesh Katkar, Anagha Venugopal, Chithra A. Saikrishna, and Lelitha Vanajakshi

Abstract One commonly used modeling approach for traffic systems is based on simulation. However, most of the traffic simulation solutions available are for homogeneous and lane-based traffic conditions. Some of them allow calibration of the model parameters to make it work for heterogeneous and lane-less conditions. One such solution, which is available as open-source, is SUMO (Simulation of Urban Mobility), a microscopic and continuous multi-modal traffic simulation package developed for homogeneous lane-based traffic. The present study focuses on calibrating SUMO for heterogeneous and lane-less traffic conditions. The study site selected is from Chennai, India. The calibration was done in two steps: in the first step significant parameters were identified and optimal values were found by trial and error. In the next stage, most influencing parameters were optimized using Genetic Algorithm (GA) by minimizing the error between the simulated and field travel time. Results showed an improvement of 82% compared to the default settings while simulating the heterogeneous and lane-less traffic conditions. The validated network can be used for various applications, including proper design and analysis of signals.

Keywords Simulation · Heterogeneous traffic · SUMO · Calibration · Travel time · Genetic algorithm

1 Introduction

Traffic in many of the developing countries is attributed to its heterogeneous and lane-less characteristics. Heterogeneous traffic consists of both motorized and non-motorized vehicles of varied composition with diverse static and dynamic characteristics. Lack of lane discipline is characterized by the vehicles occupying any space of the road width without following the one vehicle per lane concept. Traffic in India is an example of this. Modeling, management, and control of such traffic is highly challenging.

R. Katkar · A. Venugopal · C. A. Saikrishna · L. Vanajakshi (✉)
Department of Civil Engineering, Indian Institute of Technology Madras, Chennai, India
e-mail: lelitha@civil.iitm.ac.in

A. Dhamaniya et al. (eds.), *Recent Advances in Traffic Engineering*, Lecture Notes in Civil Engineering 377, https://doi.org/10.1007/978-981-99-4464-4_22

Traffic flow modeling, management, and control require an understanding of the system properly. Simulations are one of the tools to experiment and study traffic and its characteristics. Depending on the level of detail, traffic simulation software can be divided into three categories: microsimulation, mesosimulation, and macrosimulation [24]. Out of these, microsimulation is preferred to model and study heterogeneous traffic [18]. Microsimulation software that are currently available include TRANSIMS [30], Transmodeler [31], MATSim [9], MITSIMLab [33], AIMSUN [7], CORSIM [8], Paramics [6], SimTraffic [11], VISSIM [22], SUMO [5], etc. Continuous traffic simulation is performed using VISSIM, MATSim, SUMO, and AIMSUN. However, TRANSIMS, CORSIM, Paramics, and ARCHISIM adopt a discrete system for simulation [25]. SUMO, VISSIM, Paramics, and AIMSUN are more flexible than others in modeling various infrastructure elements. Out of these, SUMO is an open-source software, while others are licensed. However, SUMO has been developed primarily for homogenous traffic conditions with lane discipline. Hence, the parameters used in SUMO may not suit the traffic in India, which is heterogeneous and non-lane-based. The objective of this study is to calibrate various parameters of SUMO to make it work better for the simulation of heterogeneous and non-lane-based traffic conditions by conducting a case study in a study site from Chennai, India. This study focuses on calibrating the various parameters of SUMO to make it perform better for the simulation of heterogeneous and non-lane-based traffic conditions.

Initially, the simulation of the developed model is carried out in a setting where all the model parameters have default values. The need for calibration was ascertained by comparing the simulated and field travel times. The calibration was done in two steps: in the first step significant parameters were identified and optimal values were selected by trial and error. In the next stage, most influencing parameters were optimized using GA by minimizing the error between the simulated and field travel time. The output of the process includes a microsimulation model, a list of significant parameters in SUMO, and their calibrated values.

2 Literature Review

The process of adjusting and fine-tuning simulation model parameters using real-world data to reflect field traffic conditions is what is called model calibration [20]. Several studies were reported on the calibration of VISSIM [2, 13, 20, 34]. There were studies on the calibration of other simulation software such as AIMSUN [10, 23] Paramics [4] and MITSimLab [3, 12]. Sha et al. [27] used SUMO to simulate a section of the New Jersey Turnpike. They calibrated vehicles' maximum speed, acceleration, deceleration, and minimum gap parameters using Bayesian Optimization. It can be observed from these studies that the majority of the leading microsimulation packages and their calibration methodologies have been developed considering less complex homogeneous and lane-based traffic.

However, studies on calibrating microscopic traffic simulations for heterogeneous and non-lane-based traffic conditions are limited. Mathew and Radhakrishnan [18] propose an approach for the calibration of VISSIM in the case of heterogeneous traffic conditions. The methodology included a procedure for representing traffic, identification of sensitive parameters, setting the parameter ranges by trial and error, and calibrating them by minimizing the error between the simulated and field delays. The methodology was applied for signalized intersections and stopped delay was considered the performance measure for calibration and validation. Siddarth and Ramadurai [29] calibrated the model parameters for an intersection in Chennai using the Visual C++ COM interface of VISSIM. The significant parameters were identified using Elementary Effects (EE) and GA was used to find the optimal parameter combination. Anand et al. [1] did a study on a mid-block section from Rajiv Gandhi Salai from Chennai, India. They calibrated the VISSIM model for Indian traffic conditions by tuning the parameter values heuristically to reduce the error between field and simulated data while ensuring an adequately representational simulation of traffic behavior. Manjunatha et al. [15] calibrated VISSIM to simulate signalized intersections in Mumbai using GA to minimize the error between actual and simulated intersection delay. They used multi-parameter sensitivity analysis to find the significant parameters in the psychophysical car-following model.

Although researchers have been predominantly using VISSIM to model non-lane- based and heterogeneous traffic conditions, SUMO has certain advantages over VISSIM. SUMO includes a number of car-following models for urban areas. However, this gets restricted to the Wiedemann model with VISSIM. Also, each lane could be subdivided into the desired number of strips in SUMO. This aids in knowing the number of vehicles shared in a lane, which wouldn't be feasible with VISSIM [28]. This feature is critical in incorporating the parallel and non-lane-based movement. SiMTraM is such an adaptation made in SUMO, where each vehicle can take up one or more strips [16, 21]. However, studies on the calibration of SUMO in the context of Indian traffic are limited. Shashank et al. [28] presented an approach for calibrating SUMO for a mid-block section in Chennai. Parameters that influence the driving behavior were pinned out using a combination of sensitivity analysis and a one-way ANOVA test. The optimal parameter combination was identified using GA. However, calibration for intersection areas is not yet reported for heterogeneous and non-lane-based traffic conditions. This study focuses on the calibration of SUMO for a signalized intersection under Indian traffic conditions.

3 Methodology

The first step in the simulation modeling is the development of the traffic model in SUMO. This step involves network generation, configuration of the signals, placing detectors inside the network, and loading the traffic into the network. To ascertain the need for calibration, the model is simulated first with the default setting (pre-calibration), and the travel time values are obtained. These values are compared with

field values, and if the error is significant, calibration needs to be done [18]. The unique characteristics of heterogeneous and lane-less traffic need to be addressed in the calibration. The calibration was done in two steps: in the first step, significant parameters were identified and optimal values were calculated by trial and error. In the next stage, most influencing parameters were optimized using GA by minimizing the error between the simulated and field travel time.

3.1 Data Collection

The study site selected is a 2.8 km roadway section. It starts from First Foot Over Bridge (FFOB) near Madhya Kailash (MK) and ends with the SRP Tools intersection in Rajiv Gandhi Salai in Chennai, India.

The study section is a six-lane road with three lanes in each direction. It consists of three signalized intersections: the Tidel Park (TP) intersection, the CSIR intersection, and the SRP Tools intersection. The traffic flow data, which includes the traffic inflows, the proportion of the turning traffic at the intersections, traffic composition, and signal timing and phasing were collected using video recorders for all the approaches of the intersections in the network. Data were recorded for the peak 1 h period in the evening. Travel time data for the model validation was collected using Wi-Fi sensors placed at three different locations within the network, namely FFOB, TP intersection, and SRP tools intersection. The data collected by these sensors included the location ID (FFOB, TP or SRP), Media Access Control (MAC) address of the detected devices, Received Signal Strength Indicator (RSSI), and the Date and Time of detection [26]. The data was collected for 24 min.

3.2 Model Development in SUMO

Steps involved in the implementation of the network in SUMO include road network generation, loading the traffic on the network, and selecting appropriate longitudinal and lateral movement models.

Network generation: The roadway network is developed with its geometric characteristics, such as the number and width of lanes, intersection geometry, etc. The selected roadway network and its geometrical features are imported from OpenStreetMap, a website providing free editable geographical maps, using OSM WebWizard, a Python script in the SUMO package that allows extraction of the roadway network into the simulation.

Vehicular traffic is defined in the developed model by generating routes using Jtrrouter, a Python script that takes vehicle distributions, turning ratios, and the roadway network as input. The output of Jtrrouter is a route file usable by SUMO, which consists of vehicle definitions, vehicle types, departure times, and calculated

routes. Two of the most important inputs of Jtrrouter are vehicle distribution and turning proportions.

Vehicle distributions are defined for each of the six entry locations. They also include the car following, lane changing, vehicle class, and junction-related parameters, which will be identified and optimized in calibration. SUMO provides default parameters for all vehicle types except three-wheelers. Table 1 shows the proportion of different types of vehicles at each of the entry locations.

Turning proportions for each approach of all three intersections are defined by the data collected from the field. These proportions give the split-up of volume by movement type (left turning, right turning, through) on the approach to the intersection.

The intersections examined in the study are controlled by fixed-time signal controllers. The cycle length was observed to vary from 150 to 325 s on the day of data collection. The average cycle length observed in the field is used in the simulation.

Longitudinal and lateral movement models: The longitudinal movement models describe the movement of an individual vehicle in the direction of traffic flow. Several car-following models and psychophysical models are available in SUMO for describing the longitudinal movement of vehicles. Krauss Model, which is one of the available longitudinal movement models in SUMO, has a lesser number of parameters and is easy to extend to multi-class traffic, and hence more suitable for mixed traffic conditions [28]. Hence, this model is used in the present study.

On the other hand, lateral movement models describe the movement of an individual vehicle in the direction lateral to the direction of flow. The lane-changing model is a lateral movement model, which describes the lane-changing maneuver of an individual vehicle. Lane changing is a complex phenomenon as the decision to change lanes depends on several objectives, and at times, some of these result in conflict. Lane changing is even more complex in traffic conditions without lane discipline. The default lane-changing model in SUMO is LC2013. However, the basic assumption in LC2013 is that lane discipline is followed. This model does not allow the lateral movement within a lane and parallel movements of two vehicles in a lane.

Table 1 List of vehicle distributions

Entry location	Proportion of vehicle class			
	2W	PC	3W	HMV
1	0.439	0.499	0.048	0.015
2	0.058	0.923	0.019	–
3	0.39	0.475	0.081	0.054
4	0.332	0.597	0.066	0.005
5	0.458	0.420	0.062	0.059
6	0.383	0.499	0.07	0.047

In addition, using this model, overtaking is not possible within a lane. SL2015 is another lane-changing model available in SUMO, with the following properties:

1. Multiple vehicles (depending on their dimensions) can drive in parallel in the same lane.
2. Vehicles can overtake another vehicle within a single lane.
3. Formation of virtual sub-lanes in dense traffic is possible.

Due to the above properties, SL2015 is more suitable for heterogeneous and lane-less traffic conditions and hence is adopted in this study. The simulation step length must be greater than or equal to the minimum desired time headways of the driver for the simulation to be stable. In the default model, the time step is 1 s and the same was used in this study.

4 Parameter Calibration and Results

To start with, the need for calibration was checked by evaluating the performance of the simulated model using default parameters. For this, the travel time values obtained from the simulation with the default setting (pre-calibration) for three selected segments, namely, FFOB to TP, TP to SRP, and FFOB to SRP were compared with the actual travel time values obtained using Wi-Fi sensors. Mean absolute percentage error (MAPE) was used to quantify the errors, which is calculated as given below

$$MAPE = \frac{1}{N} \times \sum_{i=1}^{N} \frac{|(TT_D)_i - (TT_A)_i|}{(TT_A)_i} \times 100 \quad (1)$$

where

$(TT_D)_i$ = estimated travel times in the ith minute.

$(TT_A)_i$ = actual travel times in the ith minute.

N = number of observations, and.

i = 1, 2, 3…N.

Figure 1 depicts the MAPE obtained for the three streches. From Fig. 1, it can be seen that the MAPE values are very high [14] reinforcing the need for calibrating the parameters for developing an accurate model.

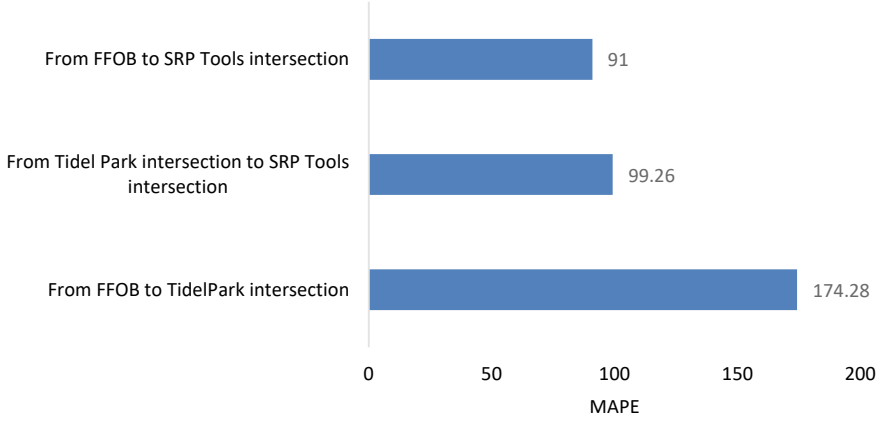

Fig. 1 MAPE of travel time using default parameter values

4.1 Identification of Significant Parameters

A total of 30 parameters of SUMO, which can be grouped as car-following parameters, lane-changing parameters, vehicle characteristics, and junction-related parameters have been investigated in this study. The parameters that have a significant impact on the output of the simulation are identified and calibrated in the next step. The significance of a parameter is ascertained by changing its value from the default value and checking its impact. For every parameter, two simulations are performed with the value of the parameter equal to 0.5 times its default value and 1.5 times its default value. The MAPE for travel times was calculated for both simulations. The average of the change in the MAPE for each case from the MAPE of the default model is then compared to identify significant parameters. Figure 2 shows the plot of the average change in MAPE for different parameters.

The parameters for which the average change in MAPE is greater than 15% are selected as significant parameters. Table 2 lists the significant parameters identified with a description.

The values of the significant parameters can be different for each vehicle class. In the present study, four different vehicle classes are considered, namely, two-wheeler (2W), three-wheeler (3W), passenger car (PC), and bus (HMV).

4.2 Preliminary Calibration

Optimal values of some parameters are adopted directly from previous studies for similar traffic conditions [18, 19, 28, 29]. The remaining parameters are calibrated in the first level by trial and error. In calibration, the value of each of the significant parameters was changed from its lower range to its upper range, one at a time,

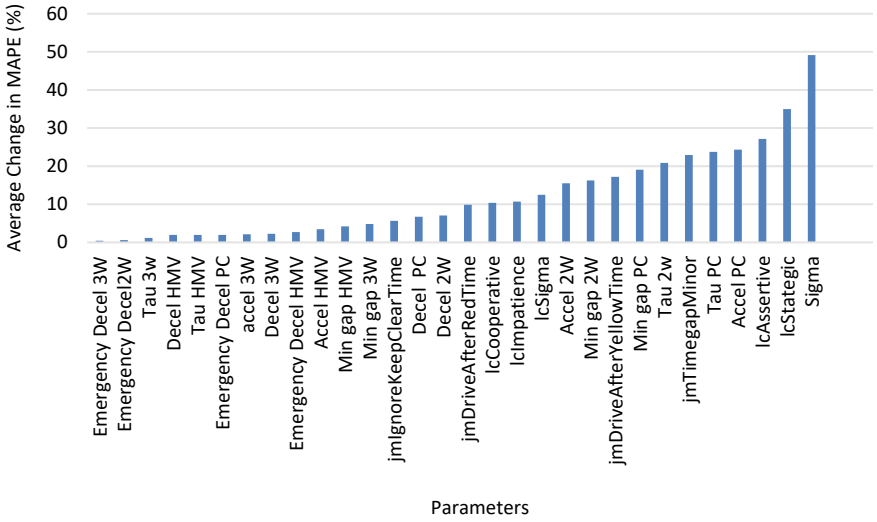

Fig. 2 Average change in MAPE for different parameters

Table 2 List of significant parameters

Parameter type	Parameter name	Description
Car Following Model Parameters	Accel PC	Acceleration capacity of Passenger car (m/s^2)
	Accel 2W	Acceleration capacity of 2-wheeler (m/s^2)
	Tau PC	The driver's desired minimum time headway (seconds)
	Tau 2W	The driver's desired minimum time headway (seconds)
	Sigma	The driver's imperfection (0 for perfect)
	MinGap PC	Minimum gap between vehicles in a stationary state (m) for Passenger car
	Min Gap 2W	Minimum gap between vehicles in a stationary state (m) for 2 wheelers
Lane Changing Model Parameters	lcStrategic	The eagerness of performing strategic lane changing. Higher values will result in earlier lane changing
	lcAssertive	Willingness to accept lower front and rear gaps on the target lane
Junction Related Parameters	jmDriveAfterYellowTime(sec)	This value causes drivers to violate the yellow light if the duration of the yellow phase is lower than the given threshold
	jmTimegapMinor	The minimum time gap when passing ahead of the prioritized vehicle

by 10% of its default value, and the impact on travel time is checked. This was done successively until a change in the parameter's value did not result in travel time improvement. This process was repeated for all the significant parameters. The values of parameters obtained from this process are shown in Table 3.

Using the above-identified values, travel times for the three selected segments are calculated. Travel times of all the vehicles obtained from the simulation are averaged by the minute of their arrival. The actual travel times for the three journeys were obtained from Wi-Fi data. Figure 3 shows a sample comparison of default model travel times, calibrated model travel times, and actual travel time. It can be seen that the calibrated travel time is much closer to the field travel time. Similar trends were observed for the other two sections too.

MAPE is calculated for the simulation models before and after calibration to quantify the errors. Figure 4 depicts the errors observed after the preliminary calibration of parameters. There is a significant reduction in error with the calibration.

Though the errors were significantly reduced with the calibration of the parameters by trial and error, the MAPE values are still high for some cases. This may be because of the large number of parameters being optimized one at a time without varying them together. Hence, simultaneous optimization of multiple parameters was implemented. Genetic Algorithm (GA) was identified to be the best tool for this

Table 3 Parameters along with their default and calibrated/adopted values

Sr. no	Parameter	Adopted/ Calibrated		2W	3W	PC	HMV
1	MinGap(m)	Adopted	Default	2.5	–*	2.5	–*
			Calibrated	0.3	–*	0.91	–*
2	Tau(sec)	Adopted	Default	1	–*	1	–*
			Calibrated	0.3	–*	1.1	–*
3	Sigma	Calibrated	Default	0.5	0.5	0.5	0.5
			Calibrated	0.2	0.2	0.2	0.2
4	Accel (m/s^2)	Calibrated	Default	6	–*	2.9	–*
			Calibrated	6.0	–*	2.9	–*
5	jmDriveAfterYellowTime(sec)	Calibrated	Default	−1	−1	−1	−1
			Calibrated	4	4	4	4
6	jmTimegapMinor (sec)	Calibrated	Default	1	1	1	1
			Calibrated	0.5	0.5	0.5	0.5
7	lcStrategic	Calibrated	Default	1	1	1	1
			Calibrated	1.5	1.5	1.5	1.5
8	lcAssertive	Calibrated	Default	1	1	1	1
			Calibrated	2.5	2.5	2.5	2.5

* Parameter not significant

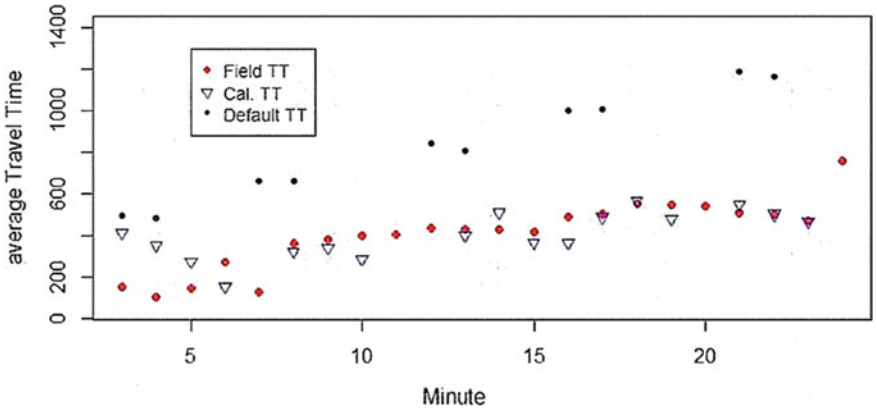

Fig. 3 Comparison of average travel time from FFOB to Tidel Park intersection

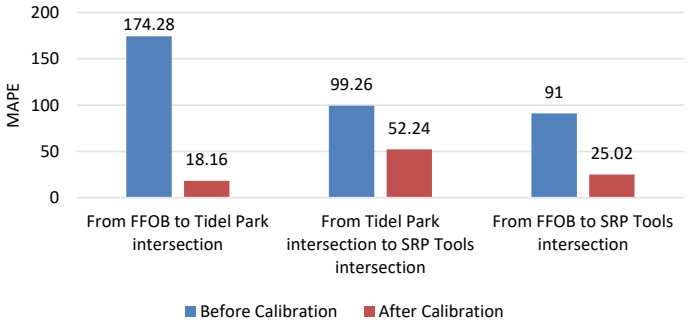

Fig. 4 MAPE for travel time of default and calibrated model

exercise. However, GA is a computationally intense process, and hence only the most influential parameters are optimized using GA.

4.3 Identification of the Most Influential Parameters

The most influential parameters are identified from the list of parameters given in Tables 3 and 4. A total of 11 parameters were identified. Then, 11 different simulations were conducted, each with 1 significant parameter having optimal value found using heuristic approach, and the others having default value. Travel times obtained from these simulations were compared with the default simulation travel times. MAPE with respect to actual travel time was used to find the improvement in travel time. Table 4 lists all 11 significant parameters and corresponding improvements observed for the study segments.

Table 4 **a**. Improvements in MAPE of travel time for FFOB to TIDEL PARK. **b**. Improvements in MAPE of travel time for TIDEL PARK to SRP. **c**. Improvements in MAPE of travel time for FFOB to SRP

Rank	Changed parameter	Improvement in MAPE (%)
(**a**)		
1	Sigma	15.61
2	Accel (PC)	15.2
3	Tau (2W)	13.24
4	Min Gap (PC)	11.96
5	Tau (PC)	1.89
6	Min Gap (2W)	1.69
7	lcStrategic	0.67
8	jmDriveAfterYellowTime	−2.77
9	Accel (2W)	−5.05
10	jmTimegapMinor	−8.83
11	lcAssertive	−12
(**b**)		
1	Min Gap (2W)	109.5
2	jmTimegapMinor	103.58
3	lcAssertive	94.63
4	Accel (2W)	91.98
5	Accel (PC)	91.88
6	Min Gap (PC)	90
7	Tau (2W)	89.52
8	lcStrategic	83.68
9	Sigma	63.96
10	Tau (PC)	38.69
11	jmDriveAfterYellowTime	18.72
(**c**)		
1	Accel (PC)	21.29
2	Tau (2W)	18.53
3	Sigma	15.87
4	Min Gap (PC)	14.18
5	Min Gap (2W)	13.7
6	lcStrategic	12.78
7	jmTimegapMinor	10.68
8	Accel (2W)	9.9
9	lcAssertive	4.36
10	Tau (PC)	4.13
11	jmDrive After Yellow Time	0.39

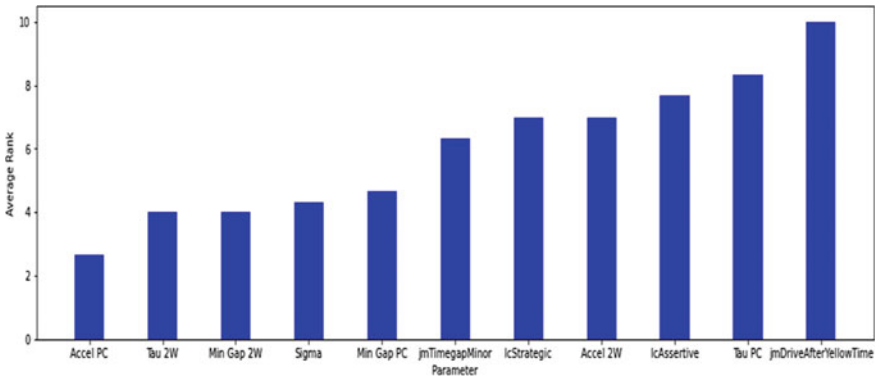

Fig. 5 Average rank of the parameters

To identify the most significant ones, each parameter is given a rank based on the improvements for all three sections. Parameters with the most significant improvement have the smallest rank. The average rank of the parameters obtained for the three sections is plotted in Fig. 5.

From Fig. 5, the acceleration (PC), minimum desired time headway (2W), driver's imperfection, the minimum desired gap by the driver (2W), and the minimum desired gap by the driver (PC) are identified as the five most influential parameters. These five parameters are selected for the GA-based calibration.

4.4 Calibration Using Genetic Algorithm

Since the MAPE values were still high for some cases as the parameters were calibrated by trial and error one at a time, simultaneous optimization could be utilized to improve the performance. GA was found to be the ideal tool for simultaneous optimization as it can handle multiple parameters at a time. As the process is computationally expensive, the optimum parameter values for only the most influential parameters are found out using GA. The optimum parameter values are found by integrating GA with SUMO.

In GA, a set of values are selected randomly from an initial population as 'parent' values and are then assigned a fitness value determined out of the fitness function. The 'child' values are arrived at once the 'parent' values undergo 'mutation' and 'crossover' operations. The fitness value of the 'child' and 'parent' is then compared. The 'child' becomes the next 'parent' if it's found to have a better fitness value than the 'parent'. Else, the 'parent' undergoes mutation again until it arrives at a fitness value lesser than that of the 'child' [32].

The mean absolute percentage error (MAPE) between the simulated and field travel time, as shown in the equation below, was considered the fitness function for the

calibration

$$MAPE = \frac{1}{N}\sum_{i=1}^{N}\frac{\left|\left(TT_{field}\right)_i - (TT)_i\right|}{\left(TT_{field}\right)_i} \times 100, \quad (2)$$

i = 1, 2, 3, …,N.

where $(TT_{field})_i$ is the actual average travel time observed in i^{th} minute for the journey. $(TT)_i$ is the average travel time calculated from the simulation in i^{th} minute from the start of the simulation for the journey.

This MAPE between the actual travel times and travel times calculated from the simulated model was considered as the fitness function. The algorithm was given the number of generations as input. The algorithm terminated after the fixed number of generations. A SUMO software specific strategy is implemented so that the GA package and the SUMO software could work in tandem. For that, a Python program was created using the GA package. GA gives a set of trial parameters after every iteration, and the Python program invokes the simulation model with those parameters. The model then simulates the traffic with these parameters and returns the output files containing the detector data. The Python script calculates the travel time and the value of the fitness function using this data. After calculating the fitness value of all individuals in the population, the GA carries out the selection, crossover, mutation, and replacement. This process is performed until the termination condition is reached. The Jtrrouter tool takes the significant parameters as input and gives the route file usable by SUMO as output. The program was implemented four times, changing the values of the GA parameters. Figure 6 shows the flow chart for the working of the Python program generated.

The Python program takes population size (Np), number of generations (Ng), mutation probability, crossover probability, bounds of the variables, and crossover type as input. The GA parameters used in this study are the Number of Generations (Ng) as 20, the Population size (Np) as 5, the Mutation probability as 0.5, and the crossover probability as 0.5 for uniform crossover. The bounds were selected based on the results of the previous iterations and engineering judgment. Table 5 lists the optimal values found for the parameters and their bounds (Table 3).

The value of the fitness function (MAPE) for the best solution is found to be 9.36%. It is known that as the number of generations and population size increases, the MAPE reduces. However, computational time will be a constraint and hence the best solution out of four implementations is taken as the optimal solution.

Figure 7 compares calibrated model travel time, actual travel time, default model travel time, and the travel time calibrated by trial and error for the selected stretch from the FFOB to SRP tools intersection.

As expected, the average travel time calculated from the default model is significantly higher than the actual travel time. The travel time is much closer to the actual travel time after calibration. To quantify the errors, MAPE was calculated for the above cases before and after calibration. The MAPE was reduced from 91% for the default values to 25.02% with heuristic calibration, and to 9.36% with the

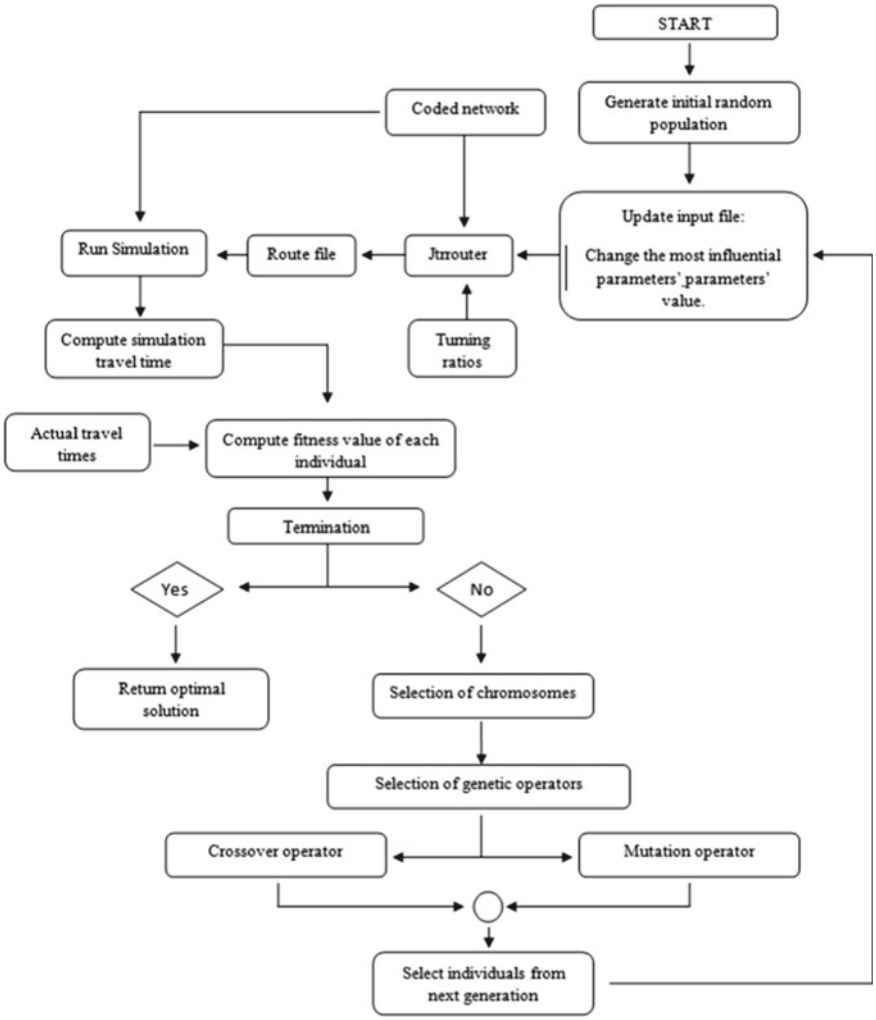

Fig. 6 Flow chart for implementation of GA in calibration

Table 5 Best solution obtained

Variable	Bounds	Best solution found (Using GA)	Best solution found (By trial and error)
Accel (4W)	[3, 5.5]	3.28	2.9
Min gap (2W)	[0.05, 0.5]	0.24	0.3
Tau (2W)	[0.05, 0.3]	0.18	0.3
Min gap (4W)	[0.3, 2]	0.38	0.91
sigma	[0, 0.3]	0.11	0.2

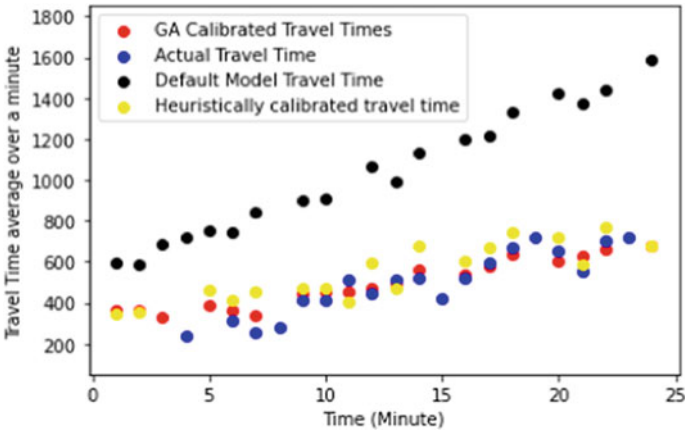

Fig. 7 Comparison of average travel time from FFOB to SRP tools intersection

calibration using GA. This clearly demonstrates that the adapted methodology is suitable in utilizing SUMO, which is primarily developed for homogeneous lane-based traffic, for heterogeneous and lane-less traffic.

5 Conclusions

This study aims at calibrating the microsimulation software SUMO for signalized intersections under heterogeneous and lane-less traffic circumstances. The necessity for calibration is ascertained by the comparison between the simulated and actual travel times. MAPE is used to define the error and a sensitivity analysis is carried out initially to determine the significance of a parameter. This was done by changing each parameter's value to 0.5 and 1.5 times its default value. For both simulations, the MAPE for travel times was determined. A comparison of the average deviation of each case's MAPE from the default model's MAPE is then carried out. The significance of the parameters for which the average MAPE change was higher than 15%, was checked using trial and error. Results revealed an improvement in performance with a MAPE from 91 to 25.02% using this heuristic calibration. As the parameters were calibrated by trial and error, one at a time without altering them together, the MAPE values were still high in some circumstances. GA, which can manage numerous parameters simultaneously, was employed next for simultaneous optimization. As GA is computationally expensive, the study determined the variables that had the greatest influence and were calibrated using GA. The GA-based calibration method combined with SUMO successfully reduced MAPE from 25.02 to 9.36%. According to the findings, the GA is particularly efficient in calibrating the sensitive parameters of the SUMO traffic microsimulation model. This study is one of the first studies that systematically calibrated SUMO parameters for a signalized

intersection under Indian traffic conditions. The calibrated network can be applied to several tasks, such as signal design and analysis. By including more parameters in the sensitivity analysis and modeling various traffic scenarios, this work could be further developed.

Acknowledgements Authors acknowledge the 'Connected Intelligent Urban Transportation Lab', funded by the Ministry of Human Resource Development, Government of India, through project number CEMHRD008432.

References

1. Anand A, Ramadurai G, Vanajakshi L (2014) Data fusion-based traffic density estimation and prediction. J Intell Transp Syst 18(4):367–378
2. Asamer J, Zuylen HG, Heilmann B (2011) Calibrating VISSIM to Adverse Weather Conditions. 2nd International Conference on Models and Technologies for Intelligent Transportation Systems:22–24
3. Balakrishna R, Antoniou C, Ben-Akiva M, Koutsopoulos HN, Wen Y (1999) Calibration of microscopic traffic simulation models: Methods and application. Transp Res Record J Transp Res Board, No. 2007:198–207
4. Bartin B, Ozbay K, Gao J, Kurkcu A (2018) Calibration and validation of large-scale traffic simulation networks: A case study. Procedia Computer Science 130(130): 844–849
5. Behrisch M, Bieker L, Erdmann J, Krajzewicz D (2011) SUMO - Simulation of Urban Mobility: An Overview. In: The Third International Conference on Advances in System Simulation
6. Cameron GDB, Duncan GID (1996) PARAMICS, parallel microscopic simulation of road traffic. Journal of supercomputing. 10(1):25–53
7. Casas J, Ferrer JL, Garcia D, Perarnau J, Torday A (2010) Traffic Simulation with Aimsun. Internat Ser Oper Res Management Sci 145:173–232. https://doi.org/10.1007/978-1-4419-6142-6_8
8. Halati, A., H. Lieu, S. Walker. CORSIM - Corridor Traffic Simulation Model. Presented at Traffic Congestion and Traffic Safety in the 21st Century: Challenges, Innovations, and Opportunities, Chicago, Illinois. 1997. https://trid.trb.org/view/576076
9. Horni A, Nagel K, Axhausen KW (2016) The Multi-Agent Transport Simulation MATSim
10. Hourdakis J, Michalopoulos PG, Kottommannil J (1852) A Practical Procedure for Calibrating Microscopic Traffic Simulation Models. Transportation Research Record. No. 2003:130–139
11. Husch, D. and J. Albeck, SYNCHRO 5.0 User Guide for Windows, Trafficware Corporation, Albany, CA. 2000.
12. Jha M, Moore K, Pashaie B (2004) Emergency Evacuation Planning with Microscopic Traffic Simulation. Transportation Research Record. No.1886 (1), pp 40–48
13. Kim J, Kim JH, Lee G, Shin HJ, Park JH (2020) Microscopic Traffic Simulation Calibration Level for Reliable Estimation of Vehicle Emissions. J Advanc Transp
14. Lawrence KD, Klimberg RK (2018) Advances in Business and Management Forecasting, 1st edn. Emerald Publishing Limited, Bingley, UK
15. Manjunatha P, Vortisch P, Mathew TV (2013) Methodology for the calibration of VISSIM in mixed traffic. Transportation Research Board 92nd Annual Meeting, Washington DC
16. Mathew TV, Bajpai A (2012) SiMTraM – Simulation of Mixed Traffic MObility - User Documentation, pp 1–50. https://www.civil.iitb.ac.in/simtram/docs/SiMTraM_USER.pdf
18. Mathew TV, Radhakrishnan P (2010) Calibration of Microsimulation Models for Nonlane-Based Heterogeneous Traffic at Signalized Intersection. J Urban Planning and Development 136, No. 1, pp 59–66.

19. Mehar A, Satish C, Velmurugan S (2014) Highway Capacity through VISSIM Calibrated for Mixed Traffic Conditions. KSCE Journal of Civil Engineering. No. 18:639–645
20. Park B, Qi H (1934) Development and Evaluation of a Procedure for the Calibration of Simulation Models. Transportation Research Record, No. 2005:208–217
21. Patel V, Chaturvedi M, Srivastava S (2016) Comparison of SUMO and SiMTraM for Indian Traffic Scenario Representation. Transportation Research Procedia, No. 17:400–407
22. PTV, PTV VISSIM 10 User Manual, pp 265–297
23. Punzo V, Ciuffo B (2009) How Parameters of Microscopic Traffic Flow Models Relate to Traffic Dynamics in Simulation. Transportation Research Record: Journal of the Transportation Research Board, No. 2124:249–256
24. Ratrout NT, Rahman SM (2009) A comparative analysis of currently used microscopic and macroscopic simulation software. Arabian J Sci Eng 34, No. 1B, pp 121–133
25. Saidallah M, Fergougui AE, Elalaoui A (2016) comparative study of urban road traffic simulators," MATEC Web of Conferences, vol 81
26. Satya S, Muthurajan PB, Chilukuri BR, Vanajakshi L (2019) Development and Evaluation of a low-cost WiFi Media Access Control Scanner as Traffic Sensor, COMSNETS, Intelligent Transportation Systems Workshop, Bangalore
27. Sha D, Ozbay K, Ding Y (2020) Applying Bayesian Optimization for Calibration of Transportation Simulation Models. Transportation Research Record: Journal of the Transportation Research Board. No. 2674(10): 215–228
28. Shashank Y, Nitin N, Arjuna B, Anilkumar B, Vanajakshi L (2020) Calibration of SUMO for Indian Heterogeneous Traffic Conditions. Recent Advanc Traffic Engineering, pp 199–214
29. Siddharth SMP, Ramadurai G (2013) Calibration of VISSIM for Indian Heterogeneous Traffic Conditions. Procedia Soc Behav Sci 104, pp 380–389
30. Smith L, Beckman R, Baggerly K (1995) TRANSIMS: transportation analysis and simulation system. Publication LA-UR-95–1641 United States. https://www.osti.gov/servlets/purl/88648
31. TransModeler Manual https://www.caliper.com/transmodeler/default.htm
32. Whitley D (1994) A genetic algorithm tutorial. Statistics and Computing, 4(2), pp 65–85
33. Yang Q, Koutsopoulos HN, Ben-Akiva ME (2000) Simulation laboratory for evaluating dynamic traffic management systems. Transport Res Record, No. 1710:122–130. https://doi.org/10.3141/1710-14
34. Zhizhou W, Jian S, Xiaoguang Y (2005) Calibration of VISSIM for Shanghai Expressway Using Genetic Algorithm. Proceedings of the 2005 winter simulation conference, pp 2645–2648

Design Optimization and Statistical Analysis of Parking Characteristics in a Commercial Area of Chandigarh

Kshitij Jassal, Kartick Kumar, and Umesh Sharma

Abstract The spectacular growth of vehicles has brought with it problems of congestion, accidents, parking delays, and environmental degradation. In today's automobile-oriented communities, the issue of parking is critical. The efficient operation of an automobile not only necessitates a well-designed system of roads, but also suitable parking facilities to park at destinations. In the absence of any restrictions, long-time parkers have decreased the parking turnover, increasing the accumulation and congestion, with an average parking index of 166.5%. The accumulation data is obtained by counting the number of vehicles coming in and going out on weekdays with the timing of the study kept between 09:00 am to 09:00 pm. The study focuses on the parking service duration. Linear regression is done to predict the peak hour traffic with respect to four-wheelers. As a result, an optimization formula based on the revenue generation model is used for designing parking lots that consider arrival rate as a function of parking charge and the number of filled spaces designed to optimize. The analysis reveals how to improve On-street parking discipline in terms of the availability of parking spaces and the level of their use if it were paid parking. The model summary provides a high degree of coefficient of variation, with R^2 values of 0.994 and 0.735 for non-peak hour and peak hour, respectively, hence establishing a high goodness of fit.

Keywords Parking accumulation · Traffic · Regression · Optimization

1 Introduction

Every country, within its capabilities, has its own approach to tackle the problems of transportation, according to its needs and solution. Increasing prosperity, change in land-use patterns, and changes in the traffic-generating behaviour of various social groups have aided in the substantial growth of road traffic which ultimately leads to the parking problem in urban areas. Growth of population and motor vehicles coupled

K. Jassal (✉) · K. Kumar · U. Sharma
Punjab Engineering College (Deemed to Be University), Chandigarh 160012, India
e-mail: jassalkj13@gmail.com

A. Dhamaniya et al. (eds.), *Recent Advances in Traffic Engineering*, Lecture Notes in Civil Engineering 377, https://doi.org/10.1007/978-981-99-4464-4_23

with socio-economic development are resulting in quite a steep surge in the transport demand leading to considerable traffic problems. In the past few years, traffic density on roads, especially in the urban areas has grown by leaps and bounds with every vehicle demanding a parking space at the end of a trip or after reaching the designated terminus. Basic statistics pertaining to the availability of parking spaces, the level of their use, and parking demand are required before any method for improving the parking circumstances of any congested regions are established. Then a decision can be made on how to effectively utilize the current parking facilities and when and where they should be used. The transportation system in Chandigarh city has increased manifolds due to various estimates which include, but are not limited to the increase in vehicular population, rise in economic activities, and population explosion. UT Chandigarh has been reported to over a total road length of 3149 km, with about 50,991 registered vehicles, even in the year of a pandemic [6]. The demographic numbers from the last decade provide a brief idea about the total registered vehicles to date, which saw growth from a little over 8 lakhs in 2011 to about 12 lakhs in the year 2021 [6]. In the absence of any restrictions, long-time parkers have decreased the parking turnover, increasing accumulation and congestion. Wrongly parked vehicles on the roadside further interfere with the smooth flow of traffic and may lead to accidents. Parking inventory and net accumulation data of the vehicles form the preliminary study. The analysis suggests that peak hour is overloaded and on-street parking is the major cause of concern in terms of congestion. The area under study, Sector 15, is divided into four parking areas, where the study is conducted by parking lot inventory and parking usage studies which further contain accumulation studies and duration studies.

Wong et al. constructed a simple parking demand model in Hong Kong in the year 2000 to calculate the research area's future parking demand [20]. The model was built with an additive and linear relationship between off-street parking demand and land use as a variable. David A. et al. studied the influence of parking pricing and supply in forecasting parking demand in the Sydney CBD area in 2001 [19]. The parking demand was represented using a nested logic model. According to the finding, the parking fee has a greater influence on a car owner's decision to park in a specific parking lot than the parking supply. In the year 2004, in Hong Kong, parking availability and cost were also discovered to be critical parameters in estimating parking demand [20]. The number of automobiles in the parking lot was established utilizing a snapshot survey method, which took less time and was also less expensive. Zhang, X. et al. investigated vehicle parking behaviour based on the number of parking spaces available, the attractiveness of the destination, the parking scale, and the management measure relationship in 2005 [21]. To analyse the parking accumulation, they incorporated the building's desirable property, as well as the number of parking spaces and price. In 2010, Chakrabarti S. and Mazumder T. developed a relationship that took into account practically all of the key elements that determine parking demand [7]. Age, income, family size, distance travelled, travel time, search time, ease of time, and cost were all the factors that were evaluated. In the research, the level of influence of each parameter on parking was also described. The model analysis revealed that, as expected, parking costs have the greatest influence on

the choice of parking options. Furthermore, all other variables that have a substantial impact on parking decisions are related to time. The majority of drivers make their final parking selection dynamically in proximity to their destination, according to the study results, indicating that the recommended technique is feasible. Kolhar P. went on to recommend particular parking management techniques (short, medium, and long-term) as well as how to apply them [16]. The expenses of proposed parking facilities, as well as potential savings and benefits from better management, are calculated. The SPSS software is used to create parking demand models. Short-term solutions, such as congestion pricing, are recommended to alleviate parking problems quickly since on-street parking management has lower operation and maintenance costs than off-street parking management, and on-street parking management has a higher internal rate of return. However, a long-term management plan (supply of multilevel parking) is chosen based on projected parking demand in the studied locations. On-street and off-street parking fees were assigned, and a financial analysis was conducted. The parking price has been intentionally kept high in comparison to multi-park to prevent people from parking on the street. According to Rathi, M. K., and Patel, D. V., India's rising population has caused a slew of issues. One of the most difficult is car parking, which we deal with daily. Aside from the issue of space for moving automobiles on the road, there is also the issue of space for parking vehicles, which is exacerbated by the fact that most private vehicles are parked for the majority of their time. While residential projects continue to have dedicated parking, the major issue is often with commercial spaces, which is solved by using more open parking spots [19].

The literature provides an insight into different models that have been developed with the use of various variables providing respective reliable relations. But specifically, the variables which estimate the parking demand, i.e., the parking fee, have been of significant importance. Parking behaviour is also driven by the space available, age, demography, travel time, parking cost, etc. The choice of parking depends substantially on these parameters, further helping to reduce congestion. A limited study has been done on the parking discipline of non-paid on-street parking. The revenue generation model provided in the study is an efficient way to determine the same. The results and recommendations will help in evolving a better parking system.

2 Study Area

Sector 15, Chandigarh is one of the busiest sectors in the U.T. Given the demography, the work distribution in and around the sector portrays a large number of trips. Different types of roads in the city (Fig. 1) generate different amounts of traffic volume.

The sector has been further divided into four areas of study. Area I is the off- and on-street parking at Gopal's block, and Area II is the off- and on-street parking at

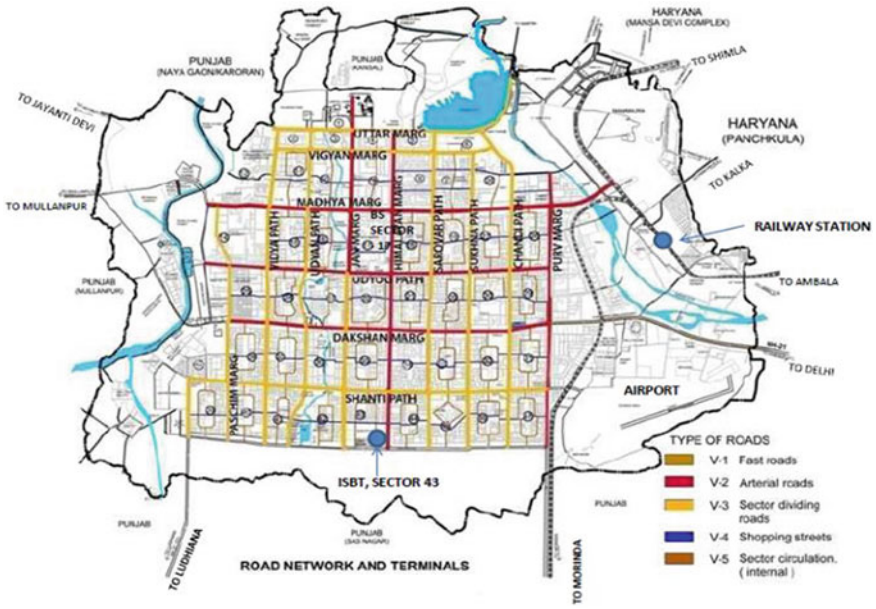

Fig. 1 Original circulation network and transportation nodes (Chandigarh Master Plan, 2031)

Patel Market. Area III is the off- and on-street parking adjacent to the Police Beat Box, and lastly, Area IV is the off-street parking in front of the Dominos (Fig. 2).

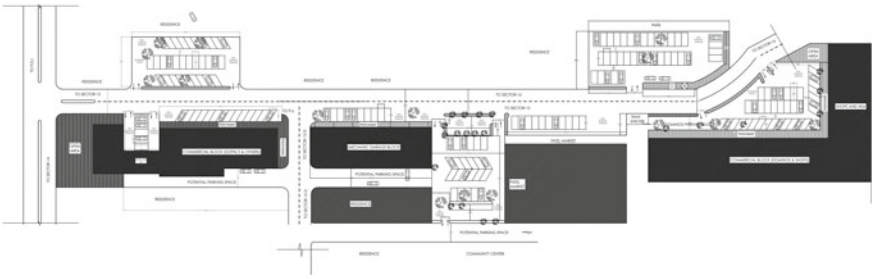

Fig. 2 AutoCAD drawing of the study area, sector 15, Chandigarh

3 Methodology

3.1 Phase I

The first phase introduces data collection by Cordon count and Patrol method for parking survey. The accumulation data was obtained by counting the number of vehicles (cars and two-wheelers) coming IN and going OUT by standing at the entrance and exit for normal weekdays in the sector with the timing of the study kept between 09:00 am to 09:00 pm. The various categories of vehicular traffic were as Two-Wheelers (scooters, motorcycles, and mopeds) and Four-Wheelers (cars, vans, and jeeps). The parking usage survey was performed for off- and on-street parking in all the defined study areas. A frequency of 1 h is considered to be satisfactory for on-street, as well as off-street parking. The parking duration ranges from about half an hour to 9 h because of the land use and location of a variety of human activities in the sector. The accumulation data were recorded for each category on the accumulation form and respective graphs were provided. Further, parking inventory was drawn using AutoCAD software, of the area under consideration.

3.2 Phase II

In the second phase, License Plate Method was used which provides information on the length of time that a certain car occupied the parking spot. As the fee is approximated according to the length of time the car was parked, this will be helpful in determining the fare. If the time gap between parking spots is cut down, then there will be less chances of long-term parkers being overlooked. However, this procedure requires a lot of manual effort. Now, to propose an optimization formulation that minimizes the total revenue lost from a parking lot for a given total capacity, finding an expression for revenue lost per unit time is the first step in distributing the entire given capacity also with the objective of minimizing revenue lost per unit time. By calculating the number of such vehicles returned back (rejected) per unit time by the expected revenue from such vehicles, revenue loss per unit time from each ith vehicle type and jth service class may be computed. The complete formulation to determine the distribution of the total given capacity to minimize/maximize the total revenue lost from the parking lot is as follows:

$$Minimize \sum_{i=1}^{i=I} \sum_{j=i}^{j=J} \lambda_{i,j} \times P_{i,j} \times \beta_{i,j} \times 1/\mathrm{i,j}$$

Subject to

$$B1 \equiv P_{c_{i,j}} \leq \tau \mathrm{p} \quad \forall i \in \{1, 2, 3 \ldots I\}, \forall j \in \{1, 2, 3 \ldots J\}$$

$$B2 \equiv \sum_{i=1}^{i=I_i} \times \sum_{j=i}^{i=j} C_{i,j} \leq C \quad \forall \mathrm{i} \in \{1, 2, 3 \ldots I\}, \forall j \in \{1, 2, 3 \ldots J\}$$

$$B3 \equiv C_{i,j} \geq 0 \quad \forall \mathrm{i} \in \{1, 2, 3 \ldots I\}, \forall j \in \{1, 2, 3 \ldots J\}$$

$$B4 \equiv C_{i,j} \text{ are all integers} \quad \forall i \in \{1, 2, 3 \ldots I\}, \forall j \in \{1, 2, 3 \ldots J\}$$

$$\text{Maximize} \sum_{i=1}^{i=I} \sum_{j=i}^{j=J} \beta_{i,j} \sum_{n_{i,j}=0}^{n_{i,j}=c_{i,j}} n_{i,j} \times P_{n_{i,j}}$$

Subject to

$$C1 \equiv \sum_{i=1}^{i=I} K_i \times \sum_{j=i}^{i=j} C_{i,j} \leq C \quad \forall \mathrm{i} \in \{1, 2, 3 \ldots I\}, \forall j \in \{1, 2, 3 \ldots J\}$$

$$C2 \equiv C_{i,j} \geq 0 \quad \forall i \in \{1, 2, 3 \ldots I\}, \forall j \in \{1, 2, 3 \ldots J\}$$

$$C3 \equiv C_{i,j} \text{ are allintegers} \quad \forall i \in \{1, 2, 3 \ldots I\}, \forall j \in \{1, 2, 3 \ldots J\}$$

$$C4 \equiv \beta_{i,j \text{ are allintegers}} \quad \forall i \in \{1, 2, 3 \ldots I\}, \forall j \in \{1, 2, 3 \ldots J\}$$

For determining the parking fee and for optimum distribution of total given capacity so the objective is to maximize the expected revenue generated per unit time is to be notified. Hence from understanding, it's clearly observed that the parking fee mainly depends upon the arrival rate, and therefore, the arrival rate is the function of the parking fee; mathematically, it can be expressed as $\lambda_{ß\mathrm{i,j}}$. For optimization formulation, the function opted to maximize the expected revenue generated per unit time from ith vehicle type and jth service class is obtained by multiplying the parking fee for a particular vehicle per unit time and the assumed number of vehicles present in the parking lot at any time; mathematically, it can be represented as:

$$\beta_{\mathrm{i,j}} = \sum n_{i,j} = C_{i,j_n} \times Pn_{\mathrm{i,j}}$$

$\beta_{\mathrm{i,j}}$ = Parking fee per vehicle per unit time for ith vehicle type and jth service class; $C_{\mathrm{I,j}}$ = Capacity allotted to ith vehicle type and jth service class; $Pn_{\mathrm{i,j}}$ = Probability that $\mathrm{n_{i,j}}$ spaces out of $\mathrm{C_{i,j}}$ spaces are filled in the parking lot.

4 Results and Statistical Analysis

4.1 Inventory

The parking inventory shows the existing pattern of parking is at both 90º and 60º angles. Within the area of study, i.e., the main market area of Sector 15, there are a total of 217 car spaces available (175 and 42 car spaces are for off-Street and on-street parking areas, respectively). Area wise division shows Area I, with 42 spaces in the off-street parking area and 15 in the on-street area, where, on Saturday and Sunday the accumulation of the off-street parking is maximum as compared to the other days, i.e., 43 four-wheelers with existing capacity of only 36. The peak parking demand is 11.9% higher than the theoretical capacity (36) of the parking sub-area. The accumulation efficiency comes out to be 104.1667 which is over-efficient. For Area II, with 35 spaces available in the off-street parking area and 12 in the on-street area, it is seen that on weekends, especially Fridays, the accumulation of off-street parking is maximum as compared to the other days. The peak parking demand of vehicles is 52, which is 11% higher than the theoretical capacity (46) of the parking sub-area and accumulation efficiency of 101.5%. In case of Area III, where 50 and 15 bays are available in the off-street and on-street parking areas, respectively, on weekends, especially Saturdays, the accumulation of the off-street parking is maximum as compared to the other day, with 92.210% as the accumulation efficiency. A total of 48 parking spaces are available in the off-street parking area of area IV, which has 80.729% accumulation efficiency. The peak parking demand of vehicles is 55, which is 11.4% higher than the theoretical capacity (48) of the parking sub-area. The parking in Sector 15, Chandigarh is overloaded in the time period of 3:00 pm to 9:00 pm but the peak hour is 5:00 pm to 8:00 pm. Table 1 shows the parking inventory in detail for the respective study areas of Sector 15.

The corresponding curves (Figs. 3 and 4) from the accumulation sheet data give us an idea about the existing parking spaces and the average net accumulation of vehicles on all the days of the week. The net accumulation at the off-street parking of Sector 15 adds up to a value of 469, and the same for on-street parking is 238. The average parking index concludes at about 166.5%.

4.2 Statistical Analysis

Statistical investigation of the data was performed on SPSS. Through the use of linear regression analysis, one can investigate the nature of the connection that exists between a single dependent variable, i.e., peak hour/non-peak hour, and an independent variable, i.e., four-wheeler. The Model Summary for this test can be found in Tables 2 and 3. As summary measurements of the model's accuracy, the adjusted version of this coefficient and the multiple correlation coefficient R are also included

Table 1 Parking Inventory, Sector 15, Chandigarh

Sr. no	Type of observation	Possibility	Observation				Comment
			Area I	Area II	Area III	Area IV	
1	Parking Charges	Paid/Free	Free	Free	Free	Free	–
2	Parking Bay Markings	Present/ Absent	Present	Present	Present	Present	Avoid random parking
3	Entry and Exit Gates	Open/ Controlled	Open	Open	Open	Open	Should be controlled
4	Space for Two-wheelers	Present/ Absent	Absent	Absent	Absent	Absent	Cause disturbance
5	Space for Bicycles	Present/ Absent	Absent	Absent	Absent	Absent	Occupies space
6	Parking angle	Parallel, Degree	60 degrees	60 degrees	60 degrees	60 degrees	Limited area
7	Stall length	m/ft	5 m	5 m	5 m	5 m	–
8	Stall Width	m/ft	2.5 m	2.5 m	2.5 m	2.5 m	–
9	Aisle Width	m/ft	2.5 m	2.5 m	2.5 m	2.5 m	–
10	Sign Boards	Present/ Absent	Absent	Absent	Absent	Absent	Must
11	Local Jurisdiction	Govt/Pvt	Open Source	Open Source	Open Source	Open Source	–

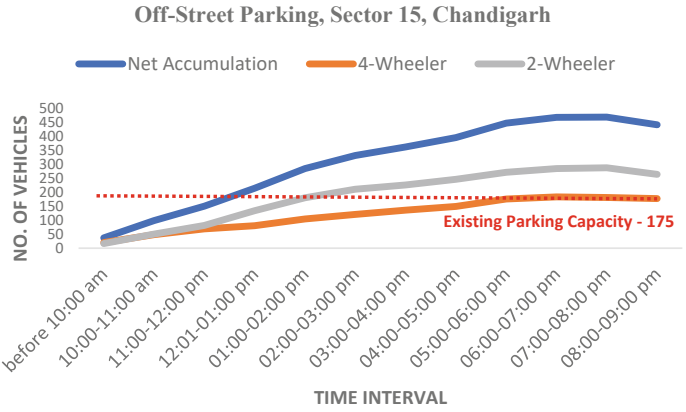

Fig. 3 Net Accumulation of Off-Street Parking, Sector 15, Chandigarh

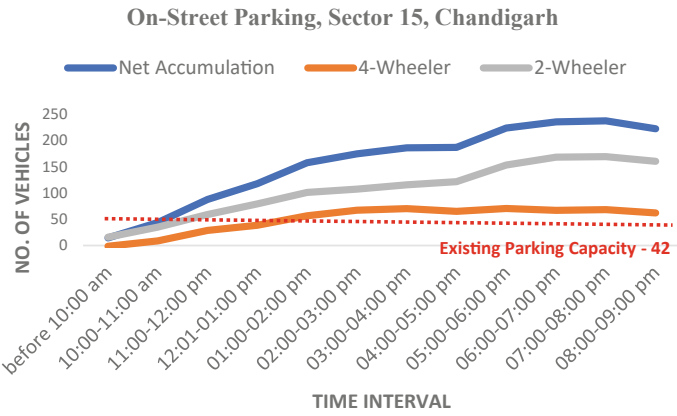

Fig. 4 Net Accumulation of On-Street Parking, Sector 15, Chandigarh

in the Model Summary. As can be observed, for non-peak hours, the Linear Regression Coefficient R equals 0.997 and regarding the amount of variation, the value of R^2 equals 0.994, which suggests that there is a high connection between the factors being studied (the dependent variable) and the variables being studied (the independent variable) (a closer figure to 1.000 means a strong correlation). Similarly, for peak hour, the Linear Regression Coefficient R equals 0.857. The value of R^2 equals 0.735.

The results of the ANOVA test, which are presented in Tables 4 and 5, offer an F-test value for the null hypothesis, which states that not one of the independent variables is connected with a four-wheeler. The confidence interval was set at 95 percent. On the other hand, according to the results of the study, we are able to refute the null hypothesis in the case when $F = 682.361$ and $p = 0.001$.

Table 2 Model summary for non-peak Hour

Model summary				
Model	R	R square	Adjusted R square	Std. error of the estimate
1	0.997[a]	0.994	0.993	0.15968

[a] Predictors: (Constant), four wheelers

Table 3 Model summary for peak hour

Model summary[b]				
Model	R	R square	Adjusted R square	Std. error of the estimate
1	0.857[a]	0.735	0.668	1.07756

[a] Predictors: (Constant), four wheelers
[b] Dependent variable: peak hour

Table 4 Anova for Non-peak hour

ANOVA[a]						
Model		Sum of squares	df	Mean square	F	Sig.
	Regression	17.398	1	17.398	682.361	0.001[b]
	Residual	0.102	4	0.025		
	Total	17.500	5			

[a] Dependent Variable: NON-PEAK HOUR
[b] Predictors: (Constant), FOUR WHEELERS

Table 5 Coefficients for non-peak hour

Coefficients[a]						
Model		Unstandardized coefficients		Standardized coefficients	t	Sig.
		B	Std. Err	Beta		
1	(Constant)	3.885	0.310		12.536	0.000
	Four wheelers	0.071	0.003	0.997	26.122	0.000

[a] Dependent Variable: Non-peak hour

Whereas, the results of the ANOVA test, which are presented in the Table 6 and Table 7 offer an F-test value for the null hypothesis at 95 percent confidence interval too. According to the results of the study, we are able to refute the null hypothesis in the case of peak hour, when $F = 11.071$ and $p = 0.001$ (P 0.01).

The regression model was generated to predict the peak hour traffic with respect to four-wheelers. The coefficients generated suggest a negative relation during peak hour with accumulation of four-wheelers and a positive relation during non-peak hour. Thus, the accumulation could justify the happening of peak hours at any given time. Further, the equation may be determined with the assistance of the coefficient table. Meanwhile, the duration of parking to be provided will also affect the parking space in numbers. Hence, for short-term parking, if high demand is required, i.e., just parked for one hour, it is not economical to provide more parking spaces. So, the regression coefficients can be found in the column labelled "Unstandardized

Table 6 ANOVA for peak hour

ANOVA[a]						
Model		Sum of Sq	df	Mean square	F	Sig.
1	Regression	12.855	1	12.855	11.071	0.001[b]
	Residual	4.645	4	1.161		
	Total	17.500	5			

[a] Dependent Variable: PEAK HOUR
[b] Predictors: (Constant), FOUR WHEELERS

Table 7 Coefficients for Peak Hour

Coefficients[a]						
Model		Unstandardized coefficients		Standardized coefficients	t	Sig.
		B	Std. Err	Beta		
1	(Constant)	−1.030	5.676		−0.181	0.865
	Four Wh	0.107	0.032	0.857	3.327	0.029

[a] Dependent Variable: peak hour

Coefficients" and the sub column labelled "B" of that column. The first is known as the constant or the y-intercept, and the second is the (Y) regression coefficient based on independent (X). The equation for regression (non-peak hour) using the coefficient table is.

$$Y = 3.885 + 0.071X \tag{1}$$

Subjected to constraints; X should be such that $X \geq 70$ *and* $X \leq 150$ (*For the validation of this model*) And the equation for regression (peak hour) using the coefficient table is.

$$Y = -1.030 + 0.107X \tag{2}$$

Subjected to constraints; X should be such that $X \geq 150$ *and* $X \leq 185$ (*For the validation of this model*).

4.3 Validation of Model

For the result and validation of the above equations, that is, (1) and (2), an example which must be within the constraints, such that X ≥ 70 and X ≤ 150, $X \geq 150$ *and* $X \leq 185$, respectively, for the validation of this model, is shown in Tables 8 and 9.

Table 8 Variables

X	Y
79	9.494
88	10.133
103	11.198
116	12.121
133	13.328
147	14.322

Table 9 Variables

X	Y
155	15.555
161	16.197
180	18.231
185	18.765
192	19.514
193	19.621

In Table 8, as we put the respective values in Eq. (1) the values 9.494, 10.133…so on, represent the time of the day, i.e., 9.494 means, it lies between 9:00–10:00 time interval. Similarly, in Table 9, the Y ordinate with respect to the traffic number represents the time interval of the day in 2400 h format.

4.4 Optimisation (Based on Expected Revenue Generated)

From an analysis point of view, off-street parking at a Central Business District, Sector 17, Chandigarh, was taken into consideration, as it relies on the revenue generated through the different parkers throughout the day. The time span was bifurcated as less than 3 h and more than 3 h. The full-day charge for four-wheelers has been kept constant at INR 14/-. On analysis of about four hours, it seemed that about 36 four-wheelers vehicles stay in the parking bays for beyond 3 h. As the analysis is based upon the revenue generation which is to be done by the equation of maximizing, i.e.

$$\text{Maximize} \quad \sum_{i=1}^{i=I} \sum_{j=i}^{j=J} \beta_{i,j} \times \sum_{n_{i,j}=0}^{n_{i,j}=C_{i,j}} n_{i,j} \times P_{n_{i,j}}$$

From the above equation we can compute the revenue generation of the parking, presented as follows:

- Parking fee for a single vehicle = 14 rupees.
- No. of Vehicles in the parking whose stay is more than 3 h = 36 Nos.
- Revenue for these 36 vehicles = 14*36 = 504 rupees.
- Now, suppose the parking capacity is going full, i.e., 20 new vehicles arrive in the parking and occupy the bays that are already covered by cars as pointed out above. So, revenue accordingly, for new arrival vehicles = 36*14 + 20*14 = 784 rupees (profit of 280 rupees.)
- After applying bifurcated parking fees = 14*36 + 36*2 = 576 rupees (incremental charge beyond 2 h parking duration).

Table 10 Expected revenue for parking: Sector 15, Chandigarh

Sr. no	Parking fees (INR)	Units	Expected Revenue (INR)				Comments
			Area I	Area II	Area III	Area IV	
1	8	Rupee/ Hour	280	352	352	376	Area I (if all 35 bays filled); Area II and Area III (if all 44 bays each are filled); Area IV (if all 47 bays filled)
2	9	Rupee/ Hour	315	396	396	423	
3	10	Rupee/ Hour	350	440	440	470	
4	11	Rupee/ Hour	385	484	484	517	
5	12	Rupee/ Hour	420	528	528	564	
6	13	Rupee/ Hour	455	572	572	611	
7	14	Rupee/ Hour	490	616	616	658	

Based on the case study of Sector 17, Chandigarh, the expected revenue generated is calculated for Sector 15 with different sub areas (refer Table 10). The basic optimization formula is used which explains that the expected revenue is generated as the multiplication of parking fee per vehicle per unit time × expected number of vehicles at the parking lot at any time.

5 Conclusion

Demand studies suggest that the parking area of Sector 15, Chandigarh is fully packed to its capacity and is in fact overloaded. As there is no special parking for two-wheelers, they tend to park in the areas provided for cars. Hence, the vehicles are more likely to get crowded in every area and lead to congestion. Accumulation study suggests that due to limited spaces at on-street parking, the four-wheelers tend to go beyond the existing capacity post noon, and far increase at the peak hour, whereas for off-street parking, only at the peak hour the space tends to fall short. But, due to the majority of two-wheeler users in the area, the parking space needs to be segregated. The traffic peak attains a maximum value in the evening session (occurring between 5 to 7 pm). The general parking composition states 65 percent two-wheelers and 35 percent four-wheelers. The parking index clearly shows the overloading of vehicles.

The parking supply will be impacted by the parking time. More parking places should be available if parking is expected to be needed for an extended period of time. If parking is typically only used for a brief period of time, perhaps fewer parking spaces should be offered for economic reasons. More commuters will park and ride

if parking is available for free, but if parking fees are charged, it is certain that this will deter commuters from doing so. The parking time limits with a nominal fee are the need of the hour. Further, the problem of obtaining parking space for the growing number of vehicles, a multilevel parking system at a strategic location, and a reasonable parking price is unavoidable. It offers easy and cost-effective operation, as well as effective maintenance and reliability. The study shows the need to bifurcate parking fees according to the hours, i.e., for 2 h, 14 rupees, and an increment of 2 rupees per hour. It is also recommended that there is a need to instal sensors with cameras and a surcharge should be levied (according to the duration of bay used) when the vehicle is exiting the parking. The study provides a constructive future scope for the administration to work on the problems related to parking discipline in the city. The limitation of the study is the data collection procedure, which is done manually. The videography technique could prove more reliable in order to have the exact vehicle count. Further, the data collection and analysis could vary according to weather conditions, festivity, opening of popular stores in the study area with time, etc.

References

1. Albagul A, Alsharef K, Saad M, Abujeela Y (2013) Design and Fabrication of an Automated Multi-level Car Parking System. Manufacturing Engineering, Automatic Control and Robotics, 173–178
2. Baglane SB, Kulkarni MS, Raut SS, Khatavkar TS (2014) Parking Management System. International Journal of Modern Engineering Research 4(2):72–77
3. Bansal A, Goyal T, Sharma U (2020) Role of Socio-demographic Characteristics in Evaluation of Signalized Crosswalks. J. Inst. Eng. India Ser. A 101:353–360
4. Barter PA (2010) Off-street parking policy without parking requirements: a need for market fostering and regulation. Transp Rev 30(5):571–588
5. Bingle R, Meindertsma D, Oostendorp W, Klaasen G (1987) Designing the optimal placement of spaces in a parking lot. Mathematical Modelling 9(10):765–776
6. Chandigarh Master Plan, 2031.
7. Chakrabarti, S., & Mazumder, T. Behavioral characteristics of car parking demand: a case study of Kolkata. Institute of Town Planners, India Journal, 7–4 (2010)
8. Chen CS, Schonfeld P (1988) Optimum stall angle for large parking lots. J Transp Eng 114(5):574–658
9. Comprehensive Mobility Plan for Chandigarh Urban Complex, 2009
10. Ellis, R. H., Rassam, P. R., and Bennett, J. C. Development and implementation of a parking allocation model. Highway Research Record, (395) (1972)
11. Golias J, Yannis G, Harvatis M (2002) Off-street parking choice sensitivity. Transp Plan Technol 25(4):333–348
12. Hensher DA, King J (2001) Parking demand and responsiveness to supply, pricing and location in the Sydney central business district. Transportation Research Part A: Policy and Practice 35(3):177–196
13. Hilvert O, Toledo T, Bekhor S (2012) Framework and model for parking decisions. Transp Res Rec 2319(1):30–38
14. Indian Road Congress 35–2015
15. Kadiyali, L. R. Traffic engineering and transport planning. Khanna publishers (2013)

16. Kolhar, P. On street parking management plan and cost-benefit analysis for Dharwad City, Karnataka, India. International Journal of Engineering Research and Applications (IJERA) ISSN, 2248–9622 (2012)
17. Mehta, C., Soni, J., & Patel, C. Microcontroller based multi-storey parking. Nirma University International Conference on Engineering (pp. 1–4). IEEE (2011)
18. Rastogi R, Bhatia HC (1998) Parking Analysis of Central Business Area In Chandigarh City-A Tsm (Traffic System Management) Approach. Indian Highways, 26(2)
19. Rathi MK, Patel DV (2012) Different types of Parking Spaces and Multiple Level Car Parking
20. Tong CO, Wong SC, Lau WWT (2004) A demand-supply equilibrium model for parking services in Hong Kong. HKIE Transactions 11(1):48–53
21. Zhang X, Huang HJ, Zhang HM (2008) Integrated daily commuting patterns and optimal road tolls and parking fees in a linear city. Transportation Research Part B: Methodological 42(1):38–56

Distance-Based Speed Prediction Models Using Naturalistic Driving Data on Two-Lane Roads in Mountainous Regions

Mikshu Bhatt, Rushiraj Gohil, Apoorva Gupta, Jaydip Goyani, and Shriniwas Arkatkar

Abstract With the advent of transportation, highway crashes are a major problem affecting human health and the environment. In which, a driver's behavior is the most significant factor affecting highway crashes. Because the speed the driver selects depends on their perception of the curve geometry, it is necessary to identify the effects of curve geometry factors on the driver's speed choice behavior. The present study attempts to develop a distance-based speed prediction model with varying curve radius and grade. For that, 64 curves were selected with the variable curve geometry, especially curve radius. The speed data were collected using the performance box (P-Box) for cars and heavy commercial vehicles (HCVs). A total of 24 P-Box runs were carried out for the subject vehicles. After that, eight different machine learning regression techniques were used to develop the distance-based speed prediction model. Out of them, the AdaBoost regression was found to be more accurate than the other machine learning regression technique. Further, the model results revealed that for similar curve geometry, the drivers' speed choice behavior and other vehicle characteristics significantly influence car and HCVs' speed. Based on the study outcome, highway authorities can provide some proactive measures to reduce the percentage of curve negotiation and increase the operational efficiency of the highway alignments.

Keywords Two-lane highways · GPS · Trip data · Operating speed · Machine learning

M. Bhatt (✉) · R. Gohil · A. Gupta · J. Goyani · S. Arkatkar
Department of Civil Engineering, Under Graduate Scholar, Sardar Vallabhbhai National Institute of Technology, Surat, India
e-mail: mikshubhatt@gmail.com

R. Gohil
e-mail: rushirajgohil93@gmail.com

A. Dhamaniya et al. (eds.), *Recent Advances in Traffic Engineering*, Lecture Notes in Civil Engineering 377, https://doi.org/10.1007/978-981-99-4464-4_24

1 Background

The existing highway geometric design is based on the deterministic design approach. Because the adopted deterministic design approach lacks a measurable safety evaluation of the design. For example, a horizontal curve design is based on the driver comfort criterion. It considered the correlation between the vehicle operating speed, curve radius, friction, and superelevation [1]. In addition, highway alignments, vehicles, and human factors are the three key factors contributing to highway crashes [2]. Out of them, highway infrastructure elements such as horizontal curves, vertical curves, steep grade, potholes, bridges, and under construction/ongoing highways are accountable for a total of 21,40,000 highway crashes in India in the years 2019 and 10,50,000 highway crashes in the year 2020 itself as per the Ministry of Road Transport and Highways [3]. Therefore, the safety of highways is a great matter of concern for the development of highway infrastructure. In addition, the rapid growth in transportation facilities, growing vehicle technology, variety in driver behavior, and conventional design guidelines of the highways are the key factors responsible for making driving on Indian roads unsafe. Toward this, the main aim of transportation engineers is to warrant the safe and well-organized movement of people and goods.

Driver's speed depends upon their perception of the highway in preference to the design speed set by the highway designer. The recommended design speed ignores the effect of geometric design features of the highway on the drivers' operating speed. The evolution of transportation has helped humankind's rapid development and growth throughout the centuries, but it has significantly impacted human health and the environment. In that connection, driver behavior has been recognized as a key contributing factor in most highway crashes [4]. Singh and Kathuria (2021) revealed that human error is the main cause of highway crashes and is responsible for 90% of crashes. Therefore, minimizing human error and enhancing driver decision-making processes might increase highway users' safety and health [5].

Many studies have used technological advancements to obtain more specific and richer data to increase the understanding of driver behavior. As a result, driver behavior datasets have grown substantially larger and more complicated, needing the use of new approaches, such as driver behavior profiles, to analyze them. Mantouka et al. classified the drivers into six categories based on their driving habits: aggressive/risky, aggressive, safe, risky, distracted, and aggressive/distracted [6]. Chen and Chen used the partition around medoids (PAM) algorithm to classify drivers into different profiles depending on their driving behavior. The PAM cluster analysis identified three distinct driving styles and four variables: speed, lateral acceleration, longitudinal acceleration, and braking [7]. Castignani et al. used smartphone device scores to evaluate driving behavior on a scale of 0 to 100 [8]. Liu et al. used the entropy weight analytical hierarchy process to assign weights to analyze the drivers' behavior on steep grades under various traffic stream conditions [9]. Cafiso and Cava carried out a naturalistic driving experiment. They found that the differences between maximum and minimum speeds (V_{max} and V_{mean}) along a highway are good

indicators to correlate design inconsistency with crashes [10]. Ellison et al. used a global positioning system to study the driver profile regarding aggressive acceleration, speeding, and braking. Each trip was allocated its unique temporal and spatial indicator to be subjected to the time of day, day of the month, speed limit, type of intersection, and weather conditions [11].

Dhakal and Marsani found that trucks were the most common vehicles involved in crashes (27%), followed by two-wheelers (25%), which is mainly caused by human behavior, vehicle condition, weather condition, and highway alignments (vertical and horizontal curves), and other factors [12]. Dhahir and Hassan developed driver-level models (DLM) and panel models (PM) to estimate curve speed and comfort threshold distributions. The results revealed that both model types could be used to establish the distributions of modeled variables for reliability analysis and highway design [13]. To this end, the ability to predict the operating speed on horizontal curves plays a critical role in assessing highway design consistency, which refers to the degree to which roadway design aligns with drivers' expectations [14, 15]. Under ideal conditions, the speed limits at horizontal curves should be nearly equal to the 85th percentile of vehicle speeds. Therefore, transportation organizations/engineers and policy-makers greatly understand the crash causation factors and develop suitable safety interventions. Such interventions not only avoid potential crash possibilities but also help in reducing post-crash damages.

1.1 Objectives of the Study

Based on the complete literature review and recognized research gap, following are the research objectives formulated as follows:

1. To study the variation in driver profiles as a function of vehicle speed, curve radius, and grade.
2. To study the suitability of different models for speed prediction on selected mountainous highways with varying curve characteristics.
3. To develop a distance-based speed prediction model to consider highway geometry variables using machine learning models.

2 Study Methodology and Data Collection

The present study selected National Highway 953 (NH-953), 32 km long, connecting two towns, Netrang to Rajpipla in Gujarat, India, as a study area, as shown in Fig. 1. The study section is a two-lane undivided rural highway passing through mountainous terrain. There is a total of 73 curves, from which 64 curves were used for the present study, which comprises the variation in the curve geometric like curve radius, deflection angle, curve length, tangent length, and grade throughout the section. The study methodology adopted for the study is shown in Fig. 2.

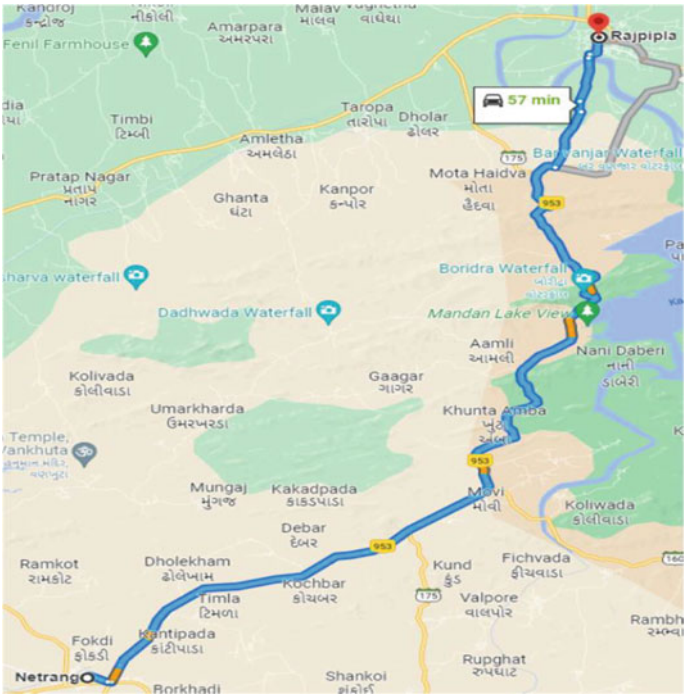

Fig. 1 Google map of the study site (Netrang to Rajpipla)

A brief explanation of each step used for the present research explained as follows:

1. The research gap was identified based on the comprehensive literature review, and the corresponding study objectives were formulated.
2. National Highway 953 (NH-953) was selected as a study area containing the 64 curves having variable geometry.
3. For the selected study area, vehicle trip data were collected using the performance box (P-Box) for the cars and heavy commercial vehicles (HCVs).
4. Afterward, based on the study objectives and curve characteristics, the total nine combinations were clustered, containing the variation in the curve radius and grade of the horizontal curve.
5. For the modeling, the given dataset was divided into two different parts. 80% of the dataset was used for the model calibration purpose, and the remaining 20% of the dataset was used for the training or validation of the model.
6. Various goodness-of-fit measures, such as mean absolute percentage error (MAPE), mean absolute deviation (MAD), and root-mean-square error (RMSE), were used to check the accuracy of the developed model.

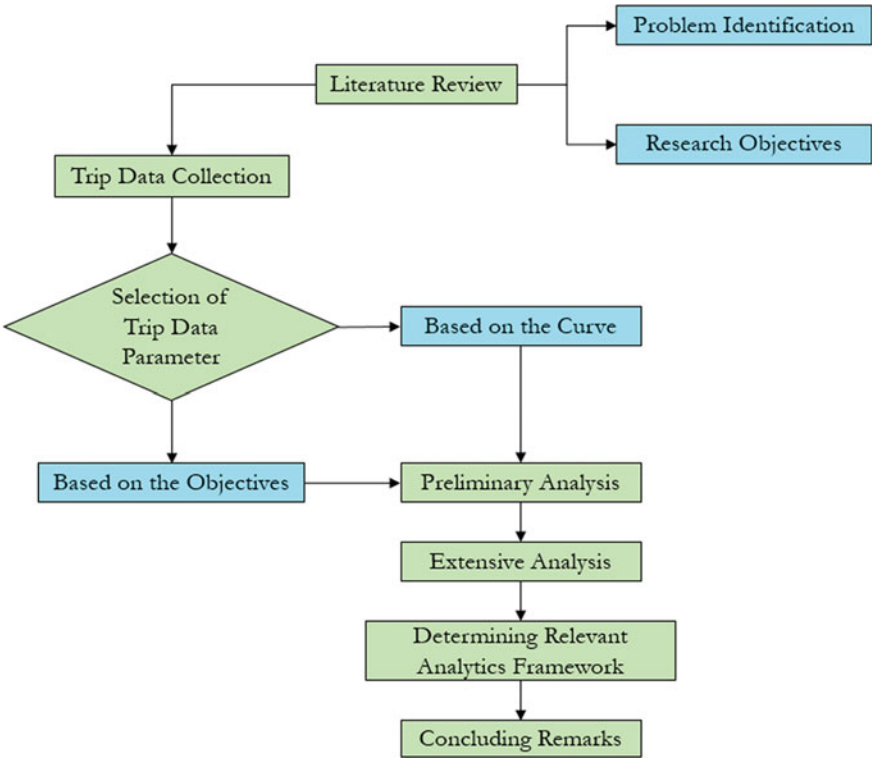

Fig. 2 Study methodology

2.1 Data Collection Process

Trip data were collected for the two dominant vehicle types, cars and heavy commercial vehicles (HCVs), using the global positioning system (GPS) or performance box (P-Box). The P-Box dataset includes various parameters such as time, latitude, longitude, speed, vertical speed, distance, lateral acceleration, longitudinal acceleration, etc. A total of 24 (15 for cars and 9 for HCVs) P-Box runs were collected for the study analysis. During the speed data collection, a research student traveled in the instrumented vehicles and controlled the experiment by mounting and unmounting the device at the beginning and end of each trip, respectively. The participant drivers were informed that the data would be utilized for the university's research work and not for legal enforcement. In addition, P-Box devices and other in-vehicle sensors reduced the problems related to conventional data collection methods such as radar guns, video graphic techniques, etc. Despite its inherent limits, it can provide a more thorough and continuous record of day-to-day driving. In this way, the drivers were encouraged to continue their natural driving style as they usually do. The present study is limited to latitude, longitude, speed, and distance. Further, the two geometric

variables, curve radius and grade, were used to develop a distance-based operating speed prediction model.

2.2 Machine Learning-Based Modeling Approach

Eight different machine learning techniques were used to model the distance-based speed prediction model. These models take in the design parameter such as curve radius and geographical parameters such as grade as input parameters.

A brief explanation regarding each technique is as follows:

1. **Linear Regression**: The linear regression algorithm shows a linear relationship between one or more independent (x) variables and a dependent (y) variable.
4. **Random Forest**: A random forest is an ensemble technique that solves regression and classification tasks by employing many decision trees using a bootstrap procedure. The fundamental idea is to aggregate several decision trees to decide the outcome rather than relying on individual decision trees.
5. **XGBoost**: It is an optimized gradient boosting algorithm through parallel processing, tree pruning, and handling missing values regularization to avoid bias.
6. **AdaBoost Regression**: The most common AdaBoost algorithm is one-level decision trees, or decision trees with only one split. This method creates a model by assigning equal weights to each data point.
7. **Support Vector Regression**: The straight line required to match the data is referred to as a hyperplane in support vector regression. A support vector machine algorithm aims to find a hyperplane in an n-dimensional space that categorizes data points. The data points nearest to the hyperplane on either side of the hyperplane are called Support Vectors.
8. **LightGBM**: It's a gradient boosting framework based on decision trees for enhancing model efficiency and minimizing memory usage. Two unique techniques used are gradient-subjected-to-side sampling and exclusive feature bundling.
9. **Lasso Regression**: Least absolute shrinkage and selection operator (LASSO) is a regression analysis technique used in statistics and machine learning that combines variable selection with regularization to improve the predictivity and interpretability of the statistical model.
10. **Poisson Regression**: The target variable distribution is assumed to have a Poisson distribution in Poisson regression. As a result, the independent variable's variance should equal its mean. This method is utilized when working with discrete, count-based data, where the independent values are non-negative integers and events are assumed to be independent of one another.

3 Results and Discussion

3.1 Preliminary Analysis

Preliminary analysis is carried out on a sample of the whole dataset in which nine different curves are identified for the analysis purpose: seven cars and Five HCVs drivers' data. These curves are classified into clusters based on horizontal curve radius and grade as to how drivers safely negotiate the difficulty curve, as shown in Table 1. It is observed that the curve having a lesser curve radius and passing through the plain terrain are difficult to negotiate. But, with the curve radius increasing due to the reduction in the curve sharpness, drivers can easily negotiate the curve.

Based on Table 1, it is observed that there are nine different combinations of curve radius and grade that are possible. In that connection, Table 2 indicates that for the same characteristics of the grade, there are three possibilities of the curve radius: easy, moderate, and difficult. Accordingly, in this classification, total of nine curves are identified. As the curve radius increases for different grade conditions, the drivers' maneuverability increases or curve negotiation behavior decreases.

After that, a line diagram of the distance versus speed for the one sample curve number 69 (C-69) was plotted, having the plain grade and moderate curve radius as shown in Fig. 3. Seven P-Box runs for the car, and five for HCVs were taken. The results revealed that curve characteristics affect the drivers' speed choice behavior. Therefore, all the drivers have the same speed profile. Moreover, the change in the

Table 1 Clustering criteria for safe negotiation of the curve

Curve radius and negotiation difficulty	Grade
Difficult: less than 50 m	Plain: less than 2%
Moderate: 50 m to 140 m	Moderate steep: 2% to 4%
Easy: more than 140 m	High steep: more than 4%

Table 2 Curve-related characteristics

Grade cluster	Curve radius cluster	Curve number	Curve radius (m)	Grade (%)
Plain	Difficult	C-17	35	−1.37
	Moderate	C-69	75	−1.81
	Easy	C-66	165	−1.21
Moderate steep	Difficult	C-49	50	3.33
	Easy	C-50	145	−2.39
	Moderate	C-71	90	2.52
High steep	Difficult	C-38	45	−4.6
	Moderate	C-34	80	−4.81
	Easy	C-47	145	8.39

driver significantly affects the vehicle's speed. Therefore, there is some deviation in the line of the distance-speed profile, as shown in Fig. 3. Also, almost all the drivers have the same trend, like moving toward the curve center; they decelerate their vehicles and decrease their speed. Further, cars have a higher speed at all three curve points than HCVs. Because the HCVs are affected by their dimension, loading condition, acceleration and deceleration characteristics, etc.

Similar results are shown in Table 3. Table 3 indicates the descriptive statistics of the speed for cars and HCVs based on the curve radius at the three locations. It

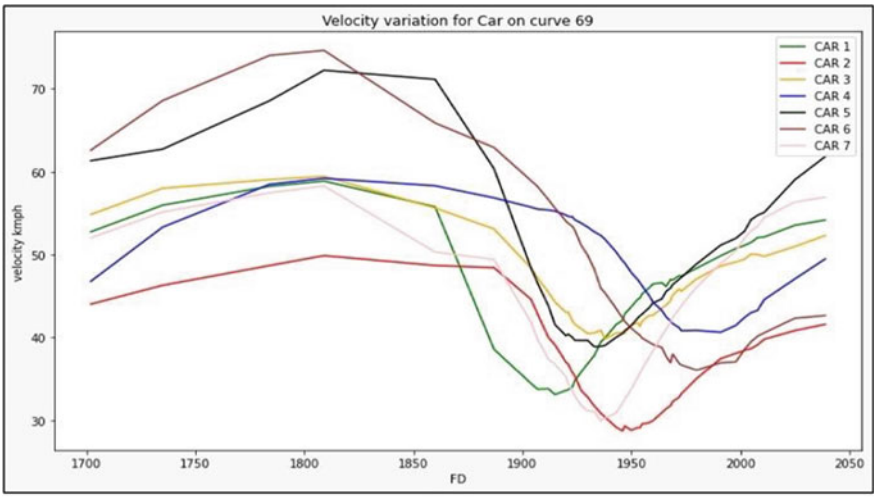

(a) Distance versus speed plot for the cars

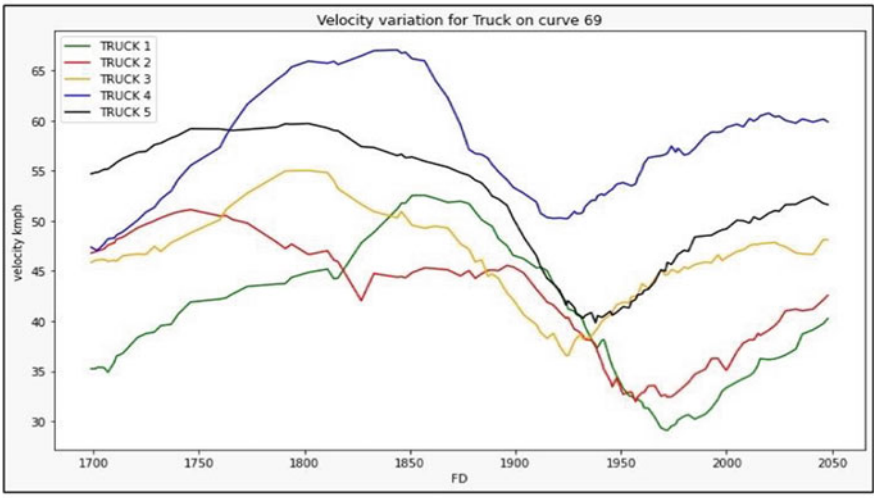

(b) Distance versus speed plot for the HCVs

Fig. 3 Line diagram of distance versus speed for plan grade and moderate curve radius

Table 3 Descriptive statistics of car and HCVs speed

Cluster classification	Curve locations	Mean	Variance	Coefficient of variance
Curve radius < 90 m	Entry Point	44 (35)	149.76 (200.47)	0.273 (0.406)
	Center Point	43 (34)	128.58 (184.17)	0.266 (0.398)
	Exit Point	44 (34)	147.67 (186.13)	0.276 (0.407)
Curve radius 90 to 180 m	Entry Point	52 (44)	145.64 (175.303)	0.235 (0.301)
	Center Point	50 (43)	144.97 (154.15)	0.239 (0.289)
	Exit Point	51 (43)	170.84 (165.404)	0.255 (0.299)
Curve radius 180 to 250 m	Entry Point	49 (38)	105.94 (382.212)	0.209 (0.520)
	Center Point	44 (36)	44.85 (239.24)	0.157 (0.404)
	Exit Point	45 (39)	63.97 (185.97)	0.177 (0.356)

Note Parenthesis () value indicates the HVCs speed results

indicates the cars and higher speed as compared to the HCVs. Further, at the center of the curve, vehicles have minimum speed.

In addition, Fig. 4 shows the variation of acceleration or deceleration for different curve radii. It is noted that as the curve radius increases, drivers tend to move on the curve with uniform speed without accelerating or decelerating much. As the curve radius decreases, drivers tend to change their speed on the curve from their initial speed. It shows that it is easy for drivers to negotiate a curve with a high curve radius with uniform speed rather than significantly changing the speed on a smaller curve radius.

3.2 Model Calibration and Validation

The curve radius and grade were taken as independent variables for the distance-based speed prediction modeling, whereas the speed at every 10 m was considered a dependent variable. Because curve radius and grade are the only independent variables that change with distance. After that, eight machine learning techniques were used for the model calibration and validation purposes, such as linear regression, random forest, XGBoost, AdaBoost regression, support vector regression, lightGBM, and lasso Poisson regression. Before calibrating the model frequency distribution, the speed, curve radius, and grade were plotted, as shown in Fig. 5. It is noted that all three variables are normally distributed. Further, almost 95% of the data lies between two standard deviations in the normal distribution; the speeding limits of the drivers can be estimated on different curves. This can further help in designing the curves and putting proper traffic signs.

The first step followed is to remove the outliers of the data with the help of box plots of two independent variables, which are the curve radius and grade of the

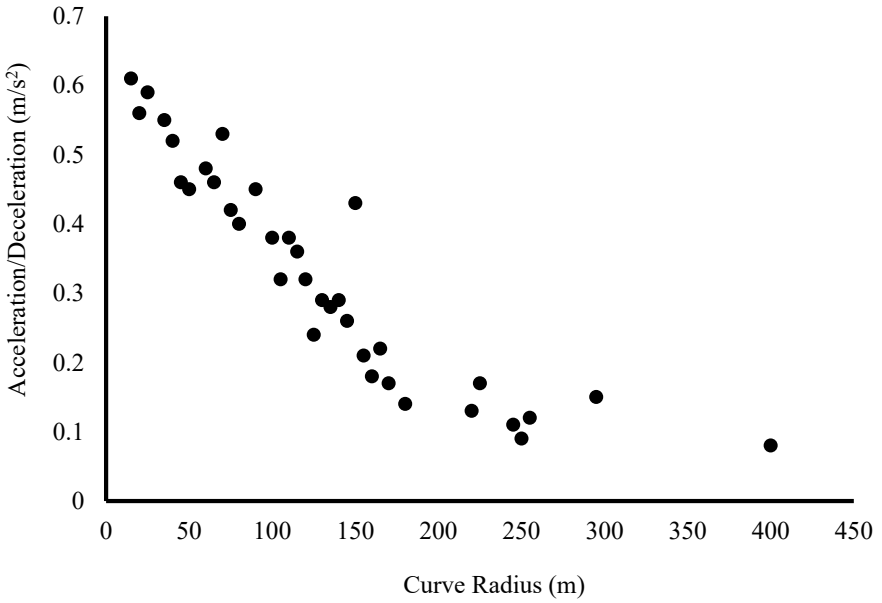

Fig. 4 Comparison of acceleration and deceleration for various curve radius

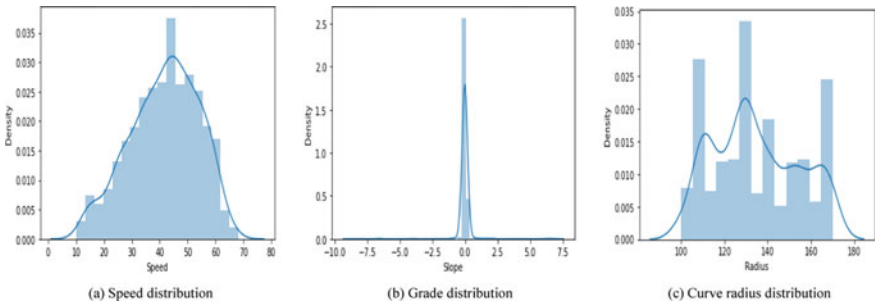

Fig. 5 Frequency distribution of the selected variables

point at every 10 m. The algorithm behind the determination of outliers is subjected to percentile values of the particular variable. The lower bound outliers follow the following equations:

$$\text{Lower Bound} = 25\% \text{ percentile of the variable} + 1.5 * \text{IQR} \quad (1)$$

$$\text{Upper Bound} = 75\% \text{ percentile of the variable} + 1.5 * \text{IQR} \quad (2)$$

IQR is defined as the spread of the middle half of the distribution, which is 25 to 75 percentile of the distribution. The data points above the upper and below the lower bound are considered outliers.

The given dataset is divided into two parts: one is for training the model, and the other is for testing the trained model. Training of models is done on 20% of the total dataset, and testing is done on the rest of the dataset. This dataset is divided into four parts: X_train, Y_train, X_test, and Y_test. X_train and Y_train represent the train dataset's dependent and independent variables, and X_test and Y_test represent the test dataset's dependent and independent variables. After testing different models, a prediction is made with the help of independent variables of the test dataset. These predicted values are then compared with the original values of the dataset, and various analyses are carried out. Various goodness-of-fit measures, viz., mean absolute percentage error (MAPE), mean absolute deviation (MAD), and root-mean-square error (RMSE), were calculated through the following formulas, and the results are shown in Table 4. The MAPE (%) is given by.

$$MAPE = \frac{100}{n}\sum\nolimits_{t=1}^{n}\left|\frac{A_t - P_t}{A_t}\right| \tag{3}$$

$$MAD = \sum_{i=1}^{n}\frac{|A_t - \overline{a}|}{n} \tag{4}$$

$$RMSE = \sqrt{\frac{\sum_{i=1}^{n}(A_t - P_t)^2}{N}} \tag{5}$$

where, A_t = actual value, P_t = predicted value, and $\overline{a}$ = mean of the sample data.

From Table 4, it is observed AdaBoost regression model has lower goodness-of-fit measures compared to the other machine learning modeling technique. This indicates that AdaBoost regression has better predictivity than the other model and is the most suitable technique for the distance-based speed prediction model. Afterward, the line diagram was plotted for the observed versus predicted speed to check the deviation in the speed value, as shown in Fig. 6.

Table 4 Goodness-of-fit measures for the different machine learning model

	LR	RF	XGB	ABR	SVR	LGBM	LAR	PR
MAPE	10.13	8.53	7.69	8.04	9.13	7.03	10.16	7.03
MAD	155.69	108.1	85.1	45.96	127.2	75.45	156.4	75.45
RMSE	12.4	10.4	9.22	6.78	11.28	8.68	12.5	8.68

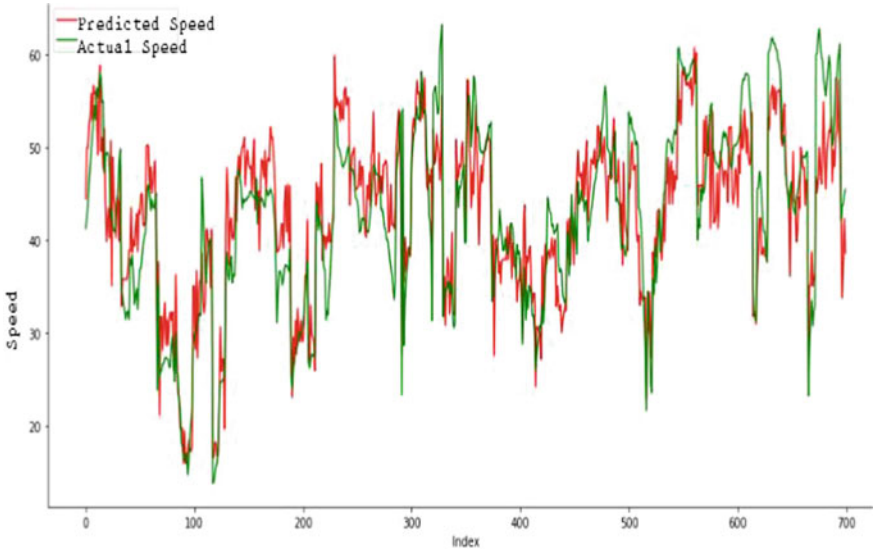

Fig. 6 Line diagram for the predicted speed versus actual speed

4 Conclusions

The present study mainly focuses on developing a distance-based speed prediction model for two-lane roads in mountainous areas. Toward this, 64 curves were selected with varying curve geometric characteristics. From that, nine combinations were identified using the K-means clustering techniques as a curve radius and grade function. The results revealed that the curve having a lower curve radius is more discomforting to negotiate than the curve having a higher curve radius. After that, eight different machine learning regression techniques were used for the model calibration and validation. The AdaBoost regression was found to be more accurate than the other machine learning regression technique. The model results revealed that similar curve characteristics significantly influence the HCVs more than the cars. This is due to the driver's speed choice behavior and other vehicle characteristics. The study results would be useful for the highway authorities to identify the curve with higher percentages of curve negotiation in terms of curve radius and grade. Based on that, they can provide some proactive measures to reduce the percentage of curve negotiation and increase the operational efficiency of the highway alignments. Besides, driver assistance systems are new tools supporting vehicle intelligence, allowing for safer and more effective driving practices.

References

1. Dhahir B (2018) Reliability-Based, Safety-Explicit Horizontal Curve Design using Naturalistic Driving Study, PhD thesis
2. Camacho-Torregrosa FJ, Pérez-Zuriaga AM, Campoy-Ungría JM, García-García A (2013) New geometric design consistency model based on operating speed profiles for road safety evaluation. Accid Anal Prev 61:33–42. https://doi.org/10.1016/j.aap.2012.10.001
3. Ministry of Road Transport and Highways (MoRTH): Road Accidents in India (2020)
4. Choudhary P, Velaga NR (2017) Mobile phone use during driving: Effects on speed and effectiveness of driver compensatory behaviour. Accid Anal Prev 106:370–378
5. Singh H, Kathuria A (2021) Profiling drivers to assess safe and eco-driving behavior – A systematic review of naturalistic driving studies. Accid Anal Prev 161:106349
6. Mantouka EG, Barmpounakis EN, Vlahogianni EI (2019) Identification of driving safety profiles from smartphone data using machine learning techniques. Saf Sci 119:84–90
7. Chen KT, Chen HYW (2019) Driving Style Clustering using Naturalistic Driving Data. Transp. Res. Rec. J. Transp. Res. Board. 2673:176–188
8. Castignani G, Frank R, Engel T (2013) Driver behavior profiling using smartphones. IEEE
9. Liu Z, He J, Zhang C, Xing L, Zhou B (2020) The impact of road alignment characteristics on different types of traffic accidents. J. Transp. Saf. Secur. 12:697–726. https://doi.org/10.1080/19439962.2018.1538173
10. Cafiso S, Cava GL (2009) Driving performance, alignment consistency, and road safety: real-world experiment. Transp. Res. Rec. J. Transp. Res. Board. 2102:1–8
11. Ellison AB, Greaves SP, Bliemer MCJ (2015) Driver behaviour profiles for road safety analysis. Accid Anal Prev 76:118–132
12. Dhakal R, Marsani A (2019) V85th Speed Prediction Model on Horizontal Curve of Two-Lane Highway: A Case Study of Naubise – Naghdunga Road. Int. J. Res. Eng. Sci. Manag. 2:201–209
13. Dhahir B, Hassan Y (2019) Using horizontal curve speed reduction extracted from the naturalistic driving study to predict curve collision frequency. Accid Anal Prev 123:190–199. https://doi.org/10.1016/j.aap.2018.11.020
14. Goyani J, Chaudhari P, Arkatkar S, Joshi G, Easa SM (2022) Operating Speed Prediction Models by Vehicle Type on Two-Lane Rural Highways in Indian Hilly Terrains. J. Transp. Eng. Part A Syst. 148:04022001. https://doi.org/10.1061/jtepbs.0000644
15. Goyan J, Arkatkar S, Joshi G, Easa S (2022) Speed-Based Reliability Analysis of 3D Highway Alignments Passing through Two-Lane Mountainous Terrain. ASCE-ASME J Risk Uncertain Eng Syst Part A Civ Eng. 8, 04022049. https://doi.org/10.1061/ajrua6.0001271

An Integrated Approach to Assess Pavement Condition by Integrated Survey Vehicle as Replacement of Manual Assessment

Smit A. Savaliya, Avinash P. Satasiya, and Shivangkumar N. Dabhi

Abstract The infrastructure of the Country plays a vital role when it's subject to developing stages. Most of the countries are continuously making efforts to maintain their pavement conditions. Pavement or road is one of the continuously used infrastructures for transporting goods and people. It is very important to assess roads by means of any method. Integrated Survey Vehicle and manual methods are used for each parameter to check the overall quality of pavement condition. Data were gathered by both methods and variations were also checked to understand the results of best effective approach. This paper mainly focuses on the methods used to assess pavement conditions mainly by ISV. One stretch of the pavement was assessed by both the manual method and the ISV method. Data regarding pavement quality was gathered to identify methods and pavement quality too. A T-test of gathered data was analyzed to check the significance of the data. Methods and Procedures of determining/evaluations of pavement by both methods are compare and describe in the research.

Keywords Assessment · Inventory of road · Integrated survey vehicle · Pavement condition

1 Introduction

Developed and underdeveloped countries always put tremendous effort into developing their pavement infrastructure. Road Infrastructure always plays a crucial role in the economic development of the Nation. High-quality condition of roads and proper maintenance of road infrastructure are essential for the smooth operation of traffic. India has 2nd largest road network in the entire world in the terms of

S. A. Savaliya (✉) · A. P. Satasiya
Swami Atmanand Saraswati Institute of Technology, Surat, Gujarat 395006, India
e-mail: smitsavaliya76980@gmail.com

S. N. Dabhi
Technical Managers at PTH Consultancy Services LLP, Surat, Gujarat 395006, India

A. Dhamaniya et al. (eds.), *Recent Advances in Traffic Engineering*, Lecture Notes in Civil Engineering 377, https://doi.org/10.1007/978-981-99-4464-4_25

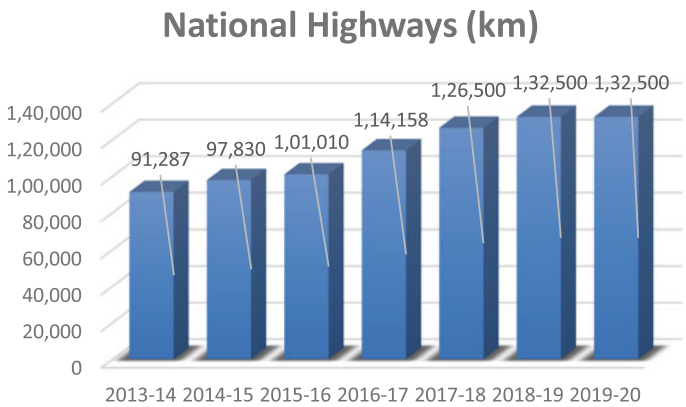

Fig. 1 National highways in km [1]

Distance (Km) [8]. National Highways covers 1,32,500 km, which serve as the arterial Integrated of the India and State highway covers 1,56,694 km of road network. Ministry of Road Transport and Highways, Government of India, is also responsible for the further construction of 27,794 km and maintenance of National Highways (India, 2021). Pavement condition has mainly two categories, namely Inventory of road and Condition of road. Inventory that includes GPS Coordinates, Pavement type and its width, shoulder type and its width, terrain, and wayside amenities. Cracking pattern, Visual Condition, Potholes, Distress, Rutting, Roughness, Raveling, and Failure in transverse Joints are some of the important parameters for the evaluation of road conditions. Parameters need to be identified periodically to maintain their quality. Manual assessment of individual parameters is a time time-consuming process (Fig. 1).

1.1 Road Condition

World Economic Forum published the quality of road scale in 2019. India is on 16th position among 37 countries with having 3.70 scale in which scale of 1 indication of low and 7 is of high in 2019. National Highways Authority of India has decided to undertake a performance assessment and ranking approach of the highways in the country (India, 2021). Objectives of the audit and ranking of National Highway are to take corrective recourse wherever required, and also to improve the quality and provide a higher level of services. The rating system is categorized into three main criteria made up of a total of 39 parameters. The main Criteria are Highway Efficiency (45 marks), Highway Safety (35 Marks), and User Services (20 marks) evaluated on a total of 100 marks [2]. A total of 39 Parameters are under three criteria which helps to understand the proper rating of highways. It is very difficult and time-consuming to identify the proper value of all parameters. Different techniques were used to determine the quality of the parameters of the pavement.

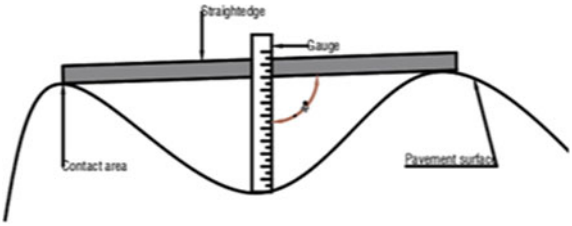

Fig. 2 Straight edge method used for rutting calculation

2 Manual Method for Pavement Assessment

2.1 Manual Rut Depth Measurements

This method involves placing a straight wooden or metal beam across the lane and measuring the distance between the pavement surface and the beam at regular intervals. The beam should be somewhat longer than the lane width and should typically have adjustable legs at each end to level the beam [3]. Measurements are typically taken at 1-ft intervals, but other intervals can be used. Commercially available devices based on this method take and record continuous measurements or profiles along a straight edge. The straight edge method is an acceptable method for obtaining transverse profile and rut depth (Fig. 2).

2.2 Manual Crack and Raveling Measurement

The thickness of the crack is measured by a crack thickness gauge. Gauge having the standard thickness of 0.10 to 3 mm helps to compare crack thickness of pavement. Raveling shows the separation of material that is disintegrated from the pavement. It may be measured by using a linear measuring instrument.

3 Introduction of ISV

An Integrated Survey Vehicle is itself a moving vehicle with the inclusion of an installed GPS system, Laser Crack 000Measurement System (LCMS) [8], Video processing tools and many more tools are also integrated to determine such parameters of pavement rapidly. ISV is used to assess and monitor the pavement conditions within a short period of time with more efficiency and accuracy. The Vehicle and integrated systems are used to collect data for road inventory as well as pavement condition.

Fig. 3 Components of Integrated Survey Vehicle [3]

3.1 Type of Surface Defects Measured and Reported

Vehicle integrated with system like Laser which is based on automatic crack detection system which is known as Laser Crack Measurement System. Camera with high resolution, Integrated DGPS with high accuracy, and In-vehicle data processing software Road Measurement Data System software developed by Data Collection Ltd. (DCL), New Zealand was used for the collection of pavement surface properties and defects [3] (Fig. 3).

3.2 Different Modules of ISV

See Fig. 4.

3.3 Laser Crack Measurement System (LCMS Module) [4]

- Acquires full 4 m width profiles of a highway lane at normal traffic speed
- Capture in both full daylight and nighttime conditions
- Automatic detection of a number of pavement defects.

Fig. 4 LCMS real time survey display during survey (each section is of 10 m length) and LCMS principle of operation [3]

3.4 Laser Profilometer Module

The Laser Profilometer is of 2 lasers as shown in Fig. 3. Profilometer can measure pavement Surface roughness. Laser along with an accelerometer is used to determine the longitudinal profile of the road which is located in the wheel path. The accelerometer is situated 750 mm on the wheel side of the centreline of the vehicle. Post survey, any spikes in the roughness outputs will be excluded that may arise from rumble strips, speed breakers, expansion joints, cattle grids, railway crossings, bridge abutments, etc. Automated checks in the data processing software are already incorporated to exclude any contribution to roughness from collected data below the minimum survey speed which is typically set at 5–30 kmph (user definable) [4] (5 and 6).

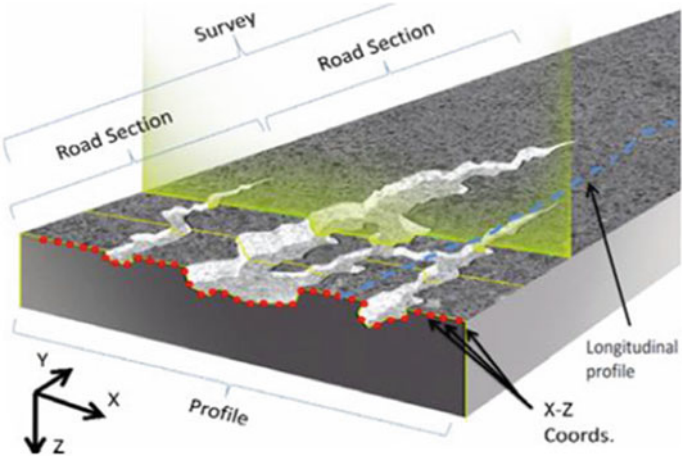

Fig. 5 LCMS data and Image Processed into road sections of 10 m Length

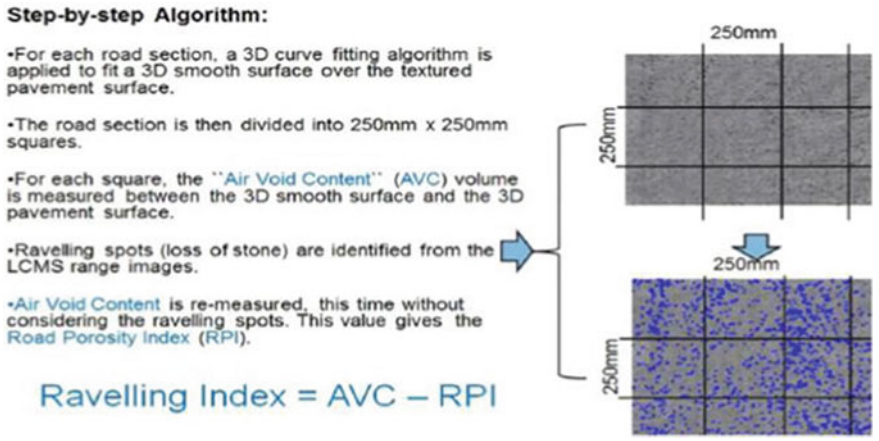

Fig. 6 Raveling Index (RI) calculation steps (2015)

3.5 Surface Defects and Roughness Data from Laser Profilometer

Defects of Road pavement such as Crack pattern, potholes, rupture of the road edge and depressions.

3.6 Surface Defects Data from ISV

The LCMS data types are all summarized over the Road Section lengths (default 10 m). The particular Road section of Recorded data has a separate file and filenames, namely in the form RoadID, SectionID.fis where RoadID is the Romdas Survey ID and SectionID is the sequential Section ID starting from 0 in a six-digit number 000001 (giving max survey length of 10,000 km) [3], e.g., /LCMS_SH14/SH14_000001.fis [5].

LCMS splits the lane into the five bands defined by AASHTO as shown below in Fig. 9.

- The central band (default 1 m wide)
- The two-wheel path bands (default 0.75 m wide)
- And the two outside bands.

3.6.1 Cracking Data

- Chainage of Crack
- Length, Width, and Depth of Crack (in mm)

3.6.2 Severity of Crack

- Very Weak < 3 mm wide
- Weak < 6 mm wide
- Medium < 20 mm wide
- Major > 20 mm wide (Indian road congress, 2019)

3.7 Raveling Data

Raveling is "wearing away of the pavement surface caused by dislodging of aggregates particles and loss of asphalt binder. Raveling ranges from loss of fines to loss of some coarse aggregate and ultimately to a very rough and pitted surface with obvious loss of aggregate" (source: Distress Identification Guide, US Dept. of Transportation, Federal Highway Administration). ISV is also capable of recording the chainage of raveling, determining raveling Index value, evaluating the percentage of raveling, area of raveling (in m^2), and severity of raveling.

3.7.1 Potholes Data

A minimum Diameter of 150 mm of area is considerable as potholes in ISV which is adjustable per system. Value is set according to the "Distress Identification Manual for the Long-Term Pavement Performance Program" published by FHWA (Federal Highway Administration) in 2003.

- Chainage of Pothole
- Area of Pothole (in m^2)
- Maximum and Average Depth (in mm)
- Severity of Crack: Pothole Severity is defined according to IRC:82–2015 as below:
  - Small: Less than 25 mm deep.
  - Medium: 25 mm to 50 mm deep.
  - Large: More than 50 mm deep.

3.7.2 Rutting Data

Pavement having rutting on surface which is maximum vertical displacement in transverse profile. Both traffic loading and environmental influences can cause or contribute to rutting. Traffic loading causes rutting when the passage of loaded wheels, particularly heavy trucks, results in a longitudinal depression in a road surface along a wheel path, due to deformation or abrasion, or a combination of both. Moisture leads to deformation of the road pavement or shoulder which leads to longitudinal depression which is rutting [6].

- Chainage of Road
- Left and Right Wheel Path Rut Depth and Width (in mm)
- Average Lane Rut Depth (in mm)
- Severity of Rut: Rut Severity is defined according to IRC:82–2015 as below:
  - No rutting: Less than 4 mm depth.
  - Low: 4 mm to 10 mm depth.
  - High: More than 10 mm depth.

3.8 Roughness Data from Laser Profilometer

Roughness parameters are presented in Table 2.1 of Annexure-I of the corresponding project for all four lanes (L1, L2, R1, and R2) of the Main Carriageway using LCMS raw data Processing software namely ROMDAS and post processing software, namely DATAVIEW.

- Left and Right Wheel Path IRI in m/km for each lane (Indian road congress, 2019)
- Lane IRI (Average of both wheels IRI) in m/km for each lane
- Roughness Index in mm/km for each lane
- Condition of Road as per IRC: SP:16–2019

3.9 Image Overlay Color Codes Used for Surface Defects [3]

See Figs. 7 and 8.

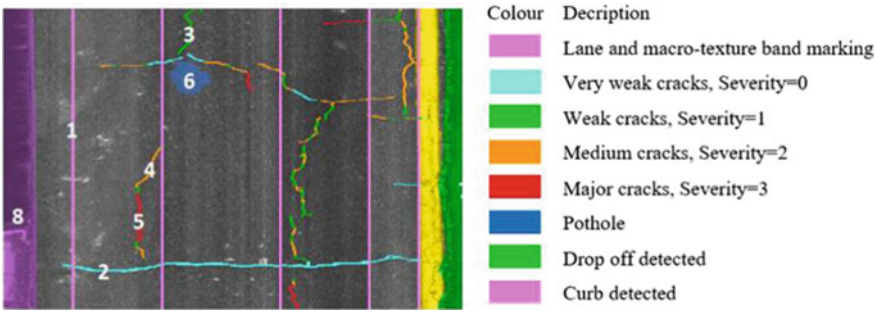

Fig. 7 Image overlay color coding for surface defects

Fig. 8 Location of study area (Puna Canal BRTS Road Surat) [7]

3.10 Pros and Cons

- Cannot be used on wet road surface
- Survey speed shall be within 30 to 80 kmph. Data accuracy will decrease under 20 kmph.
- Survey vehicle shall only be driven by a "trained driver" for safety and accuracy purposes.
- Survey shall be conducted under good daylight conditions for high-quality video data.
- The system shall not be used for extremely bad road conditions.
- Data will be collected rapidly so it is time saving process to use ISV.

4 Study Area

BRTS road of Puna-canal BRTS road of Surat city is inspected by manual and ISV method. Single lane road of 500 mt. of length is inspected. Parameters such as International Roughness index (IRI), Rutting depth, Cracking, and area of Raveling.

5 Data Collection and Interpretation

5.1 Manual Checking, Potholes, Raveling, and Rutting

Photographs of the road were taken for inventory parameters and to check the condition of the road. Manual images were taken to analyze the crack and its patterns on the pavement. Similarly, potholes were also captured manually (Tables 1 and 2).

Table 1 Specification and accuracy of various components

Parameters	Specifications and accuracy
ISV operating speed	80 km/h
GPS Coordinates	longitude, latitude, and altitude using DGPS
Profile depth accuracy	0.5 mm
Measure at least	3.5 m width of highway lane
Minimum images resolution	1600 × 1200
Distance resolution	< 1 mm
All data outputs are in a non-proprietary format	MDB, Excel
Invisible laser fires at the surface up to	28,800 Hz
Rut depth convertible	1.8 m to 3.5 m Straight edge length
Roughness outputs	Both raw longitudinal profiles and IRI
Potholes detection minimum diameter	150 mm (adjustable)
File output	/LCMS-SH14/SH14-000,001.fis
LCMS data types are all summarized over the road section length	10 m (Default)

Table 2 Collected data from manual and ISV methods

Sr nO	Chainage	Lane width	ISV inspection			Manual inspection		
			IRI (m/km)	Rutting depth (mm)	Raveling (m^2)	IRI (m/km)	Rutting depth (mm)	Raveling (m^2)
1	0 + 010	3.90	3.53	2.4	0.053	2.78	4.4	0.013
2	10 + 020	3.90	2.89	2.3	0.032	2.46	4.2	0.018
3	20 + 030	3.90	2.39	1.8	0.039	2.13	0.9	0.007
4	30 + 040	3.90	2.59	2.3	0.022	2.02	2.5	0.014
5	40 + 050	3.90	2.82	7.7	0.001	2.13	11.8	0.026
6	50 + 060	3.90	2.24	1.7	0.003	2.2	5.1	0.001
7	60 + 070	3.90	2.91	2.4	0.077	2.89	5.9	0.017
8	70 + 080	3.90	4	0.4	0.052	3	3.6	0.012
9	80 + 090	3.90	5.4	2.3	0.027	5.99	9.1	0.003
10	90 + 100	3.90	3.33	1.8	0.012	3.6	8.7	0.009
11	100 + 10	3.90	3.84	2.1	0.001	4.46	4.8	0.015
12	110 + 120	3.90	5.92	2.7	0.017	6.05	4.7	0.001
13	120 + 130	3.90	5.68	1.6	0.01	611	4.9	0.004
14	130 + 140	3.90	3.89	2.4	0.008	4.03	4.4	0.004
15	140 + 150	3.90	4.73	6.1	0.03	4.59	3.4	0.01
16	150 + 160	3.90	3.74	4	0.003	3.86	3	0.002
17	160 + 170	3.90	8.48	1.3	0.001	7.1	1.6	0.014
18	170 + 180	3.90	5.82	7.8	0.005	6	4.8	0.001
19	180 + 190	3.90	6.35	3.1	0.008	6.33	1.6	0.004
20	190 + 200	3.90	6.06	2.1	0.028	5.31	1.9	0.002
21	200 + 210	3.90	4.65	1.4	0.001	3.76	2.9	0.012
22	210 + 220	3.90	3.93	3.9	0.016	3.3	0.9	0.004
23	220 + 230	3.90	3.94	3.4	0.011	4.2	1.1	0.017
24	230 + 240	3.90	3.3	2.3	0.016	3.63	3.8	0.011

(continued)

Table 2 (continued)

Sr nO	Chainage	Lane width	ISV inspection			Manual inspection		
			IRI (m/km)	Rutting depth (mm)	Raveling (m^2)	IRI (m/km)	Rutting depth (mm)	Raveling (m^2)
25	240 + 250	3.90	3.4	2.9	0.01	2.52	4	0.012
26	250 + 260	3.90	4.16	4.2	0.001	4.09	3.2	0.002
27	260 + 270	3.90	3.73	0.5	0.004	3.02	2.1	0.009
28	270 + 280	3.90	4.23	4.4	0.007	3.41	2.5	0.001
29	280 + 290	3.90	3.44	2.4	0.009	2.72	2.4	0.009
30	290 + 300	3.90	3.72	1.1	0.001	3.36	2.6	0.019
31	300 + 310	3.90	4.32	1.8	0.008	3.61	2	0.002
32	310 + 320	3.90	5.36	2.3	0.015	4.95	5.5	0.009
33	320 + 330	3.90	4	3.3	0.001	3.95	3.7	0.003
34	330 + 340	3.90	5.5	1.7	0.018	5.08	1.3	0.01
35	340 + 350	3.90	5.61	1.7	0.012	5.97	2.3	0.001
36	350 + 360	3.90	4.07	2.3	0.009	4.66	4.8	0.014
37	360 + 370	3.90	4.53	1.5	0.001	4.89	0.9	0.001
38	370 + 380	3.90	3.37	1.7	0.015	3.81	1.3	0.012
39	380 + 390	3.90	3.51	2	0.001	3.47	2	0.001
40	390 + 400	3.90	5.34	1.8	0.003	5.48	2	0.02
41	400 + 410	3.90	3.99	3.8	0.011	4.26	6.4	0.007
42	410 + 420	3.90	5.21	1.1	0.004	4.83	3.5	0.002
43	420 + 430	3.90	3.42	1.1	0.02	2.88	2.4	0.01

(continued)

Table 2 (continued)

Sr nO	Chainage	Lane width	ISV inspection			Manual inspection		
			IRI (m/km)	Rutting depth (mm)	Raveling (m^2)	IRI (m/km)	Rutting depth (mm)	Raveling (m^2)
44	430 + 440	3.90	2.86	2.3	0.002	2.6	1.1	0.001
45	440 + 450	3.90	6.03	2.1	0.022	5.94	4.1	0.007
46	450 + 460	3.90	3.87	1.5	0.021	4.28	4.5	0.006
47	460 + 470	3.90	3.06	1.9	0.002	2.87	3.7	0.018
48	470 + 480	3.90	5.08	0.9	0.005	6.32	1.9	0.006
49	480 + 490	3.90	3.44	1.2	0.018	3.36	2.2	0.005
50	490 + 500	3.90	2.95	6	0.006	2.63	5	0.002

5.2 Road Assessed by ISV Method

The road was assessed by an Integrated Survey vehicle and the data for interpretation was recorded. Crack patterns and its type was also analyzed by ISV. As shown in Fig. 9 where 1 is indicated Strip, 2 is weak crack, 3 is Medium Crack, 4 is Major Crack and 5 is Pothole [3, 8, 9] (Fig. 10).

6 T-Test

Determination of countable differences between any two types of data which may be relevant to particular features. T-test is one of the testing method which is used to determine hypothesis in data when it's about to statistical comparison. T-test is applied to the collected data from both methods [6] (Tables 3 and 4).

SPSS Software is used to analyze and compare the data with the help of a t-test. With the 99% confidence interval, the significant value of the International Roughness Index (IRI), Rutting, and Raveling have the values of 0.039, 0.002, and 0.011, respectively. The result of the t-test indicates that the hypothesis of collected data from both methods has not been rejected as the value of significance (2 tailed) is less than 0.05 which is the indication of no rejection of hypothesis [10].

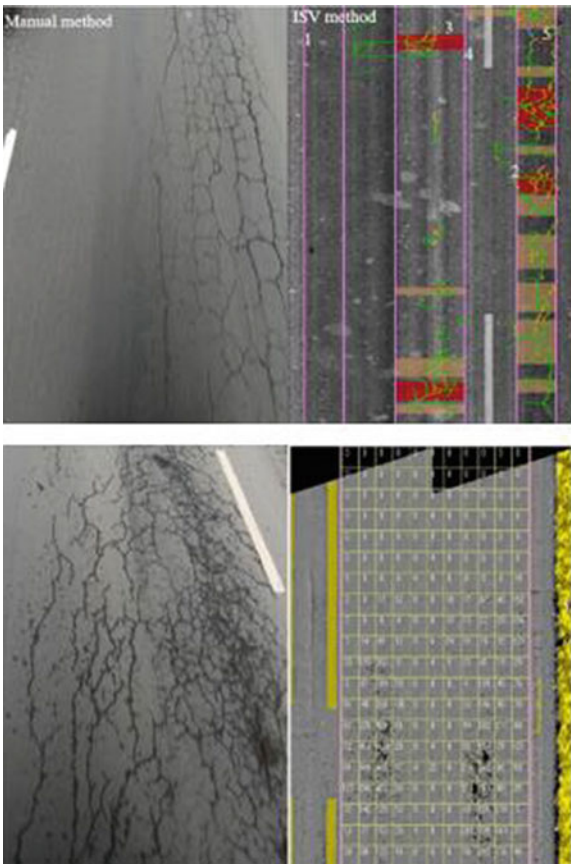

Fig. 9 Road Collection data from Manual method and ISV method

7 Conclusion

Methods and data collection of both data are comparable and show that the Integrated Survey Vehicle gave more classification of crack with clear pictorial representation. ISV inspection has more impact than manual inspection as Fig. 10 shows a comparison of other parameters such as cracks and potholes. ISV is not much more accurate

Fig. 10 Site photographs of manual method

on the very rough surface of the road, therefore, in such cases, manual methods are adopted for the worst condition of pavement quality. One of the disadvantages of ISV is to maintain the speed of the vehicle during the data collection which is why it is very difficult to acquire accurate data on a very rough surface. Strip, weak cracks, medium cracks, major cracks, and potholes all were seen clearly in ISV inspection as compared to manual assessment. ISV will generate the classification of cracks automatically while the manual method has to analyze deeply for the classification of cracks. ISV inspection also helps to represent all cracks and potholes with pictorial representation and enhance to vision either for further process of maintenance work or reliability of pavement or road. Rutting may also be identified quickly in ISV with various components. Technology in one platform makes the assessment process rapid. All the data may be compared over a long period of time for evaluation of quality.

Table 3 T-test results with 95% confidence interval of the difference

Pair sample	Parameters	Mean	Standard deviation	95% confidence interval of the difference		T-test result	Degree of freedom	Significant(2tailed)
				Lower	Upper			
1	IRI by ISV–IRI manual	0.15480	0.516227	0.008090	0.301510	2.120	49	0.039
2	Rutting ISV –Rutting Manual	−1.0120	2.166031	−1.627579	0.396421	3.304	49	0.002
3	Raveling ISV –Raveling Manual	0.00578	0.15467	0.001384	0.010176	2.642	49	0.011

Table 4 T-test results with 99% confidence interval of the difference

Pair sample	Parameters	Mean	Standard deviation	95% confidence interval of the difference		T-test result	Degree of freedom	Significant(2tailed)
				Lower	Upper			
1	IRI by ISV–IRI manual	0.15480	0.516227	−0.40851	0.350451	2.120	49	0.039
2	Rutting ISV–Rutting Manual	−1.0120	2.166031	1.832931	−0.191069	3.304	49	0.002
3	Raveling ISV –Raveling Manual	0.00578	0.15467	0.000082	0.011642	2.642	49	0.011

References

1. Annual Report 2019–2020 Ministry of Road Transport & Highway
2. Tawalare A, Vasudev R (2016) Pavement performance index for indian rural road. Elsevier
3. Romdas (2015) *Romdas* - Providers of Innovative Technology for Measuring and Managing Pavements. Retrieved March 2015, from https://romdas.com/
4. Indian road congress (2019) IRC:Sp:-16 Guidelines On Measuring Road Roughness And Norms. Indian Road Congress, India
5. Banerjee P, Thorat P (2099) Evaluation of performance of GPS receiver in CRRI network survey vehicle. Springer
6. Huang Y, Xu B (2006) Automatic inspection of pavement cracking distress. Journal of electronic imaging
7. https://www.google.co.in/maps
8. Delhi MR (2020) Bharatmala Road to Prosperity Annual Report 2019–2020. New Delhi: Government of India
9. Samsuri S, Surbakti M, Tarigan A (n.d.). A study on the road conditions assessment obtained from international roughness index (IRI):roughometer vs hawkeye. Talenta
10. ASTME1926 (2015) Standard Practice For Computing International Roughness Index Of Roads From Longitudinal Profile Measurements
11. ASTME950 (2001) Standard Test Method For Measuring The Longitudinal Profile Of Traveled Surfaces With An Accelerometer Established Inertial Profiling Reference
12. India NH (2021) National Highway Authority of India. Retrieved July 01, 2021, from www.nhai.gov.in: http://www.nhai.gov.in
13. Singh D, Gundaliya P (2018) Flexible pavment evaluation using profilometer for unevenness. Surat: IRJET

Pavement Design and Cost Analysis of Mine Waste Stabilized Low Volume Roads

Shravan A. Kanalli, Sureka Naagesh, and K. Ganesh

Abstract The extraction of minerals from the earth through mining has been one of the human activities since prehistoric times. These mining activities conducted through surface or sub-surface method leads to the generation of mine waste during the processing and extraction of minerals. The lack of storage space for mine waste and the environmental impact caused due to its storage has also been a major issue for the mining agencies. Black cotton soil (BC soil), on the other hand, is considered problematic due to its swell–shrink behavior during seasonal changes. The subgrade constructed on Black Cotton soil undergoes settlement and causes the pavement structure to fail. In the current study, efforts were made to resolve the issue of storage space of Mine Waste generated from mining activity to strengthen the weak subgrade soil such as BC soil. The engineering properties of Mine Waste stabilized soil samples were carried out and the optimum BC soil–Mine Waste mix was determined. Further, Granulated Blast Furnace Slag (GBFS) was blended with optimum BC soil–Mine Waste to enhance the engineering property. Pavement design was carried out using IITPAVE software. Cost Analysis was performed for the pavement section using the latest schedule of rates of the Dharwad region. Results indicated that 60% BC soil: 40% Mine Waste mix improved CBR strength from 2.3% to 5.6% and hence was considered as an optimum mix. The addition of 30% of GBFS to the optimum BC soil–Mine Waste mix further improved CBR strength to 10%. The same mix resulted in total cost savings of 41%.

Keywords Mine waste · Black cotton soil · Granulated blast furnace slag · IITPAVE · Soil Stabilization

S. A. Kanalli (✉)
SDM College of Engineering and Technology, Dharwad 580002, India
e-mail: shravankanalli@gmail.com; shravankanalli@sdmcet.ac.in

S. Naagesh · K. Ganesh
BMS College of Engineering, Bengaluru 560019, India

A. Dhamaniya et al. (eds.), *Recent Advances in Traffic Engineering*, Lecture Notes in Civil Engineering 377, https://doi.org/10.1007/978-981-99-4464-4_26

1 Introduction

The subgrade is the bottom-most structure of the pavement which is constructed using natural or borrowed materials. This supports the granular layer, viz., subbase, base, and surface course. The performance, life span, and serviceability of the pavement primarily depend on the quality and strength of the subgrade layer. The northern part of Karnataka, India, is largely covered by Black Cotton soil. The presence of Kaolin and Montmorillonite particles leads to the exhibition of high plasticity, compressibility, high swelling, low durability, and reduction in strength. The expansive behavior is possessed by soil due to fluctuations in moisture and the clay minerals existing in the soil. It thus undergoes volume changes on seasonal moisture variation. The road constructed on this soil leads to pavement failure which necessitates frequent maintenance leading to an increase in maintenance cost.

Karnataka is one of the largest producers of Iron Ore mines in India. The mineral assessment done by the mining results in the formation of waste materials due to the removal of overburden. The waste produced is the largest waste generated in excess of the core minerals. The stripping ratio (waste to ore ratio) ranges from 2:1 to 6:1 which means for every one part of minerals produced, there is 2 to 6 times the waste generated [1]. The significant increase in open-cut mining has increased the production of Mine Waste at a higher rate than the minerals extracted. The wastes generated from mining activities in various forms have caused a serious impact on the lives of surrounding areas hampering the environment and resulting in deaths and serious injuries.

Past research has indicated that Iron Ore Mine Waste has found useful applications in the construction industries. As per research conducted by Mohan et al. [2], the use of Mine Waste in the form of coarse aggregate for manufacturing bricks improved the UCS results by 10% on 28 days of curing in comparison with natural aggregates. The studies in Western Australia [1] have found the utilization of Mining Waste for railway and road embankments as an ideal option. The engineering properties of Mine Waste were found to be similar to natural soil. The Mine Waste comprised 33% of clay particles, 17% of silt, and 50% of sand particles. The specific gravity was found to be 2.75. The use of wastes further reduced the need for large excavation of natural soil for the construction of embankments. The requirement of land for Mine Waste storage got reduced. Bastos et al. [3] evaluated the possibility of using Iron Ore Mine Waste in road construction. The microstructure of these wastes was tested by SEM. The compaction characteristics, CBR test, Unconfined Compression test, water absorption, and durability test were conducted to find the suitability of the materials for road construction. The samples were collected from the Iron Quadrangle region in Minas Gerais, Brazil. The results from chemical analysis concluded that the material is class II A, which states the material as nondangerous and noninert material; free from hazardous characteristics like toxicity, corrosivity, etc. It was proven that the Mine Waste was technically feasible when stabilized with 5% cement or 10% of lime.

However, there is a lacuna in the research on the usage of Mine Waste in Black Cotton soil stabilization for subgrade construction. The stress–strain analysis of the Mine Waste stabilized pavement structure is important to determine pavement performance. The cost analysis of roads constructed using Mine Waste needs to be carried out from economic considerations. The present study thus focuses on determining the optimum BC soil–Mine Waste mix for subgrade. Further using GBFS as additives if required to improve the properties and form a substantial mix for the subgrade construction.

2 Materials and Methodology

2.1 Black Cotton Soil (BC Soil)

The soil was collected from Yarikoppa village, Dharwad district, Karnataka, India. The particle size distribution, index properties, compaction characteristics, physio-chemical properties, and strength parameters of BC soil were determined as per Indian Standard (IS) codes. Table 2 represents the properties of BC soil. The soil consists of 14% sand, 42% silt, and 44% clay particles. It is classified as highly compressible clay CH as per IS classification. Liquid Limit and Plasticity Index were found to be 57 and 21.1%, respectively. The UCS and soaked CBR values were found to be 166 kPa and 2.3%, respectively. These results indicate the unsuitability of BC soil for subgrade layer as per MORT&H specification [4].

2.2 Mine Waste

The Iron ore waste in the form of overburden produced from mining was procured at Iron Ore Mining at Venkatagiri Iron Ore Mines, Bellary district, Karnataka, India. The particle size distribution, specific gravity and consistency limits, and mineralogical characteristics of the waste material were determined. The particle size analysis indicated that the Mine Waste consists of 37.72% of sand, 38.78% of silt, and 23.52% of clay particles as per IS classification of soil. The consistency limit of Mine Waste indicated that the material is non-plastic. The specific gravity of Mine Waste was 3.08 due to the higher Iron content in the material. Table 2 indicates the engineering properties of Mine Waste (Table 1).

Table 1 Mineralogical characteristics of materials

Oxides (%^)	BC soil	Mine waste	GBFS
SiO_2	65.54	33.23	13.28
Al_2O_3	20.44	19.67	5.37
Fe_2O_3	–	41.50	24.88
CaO	4.10	2.21	44.8
MgO	3.89	1.22	6.52
K_2O	0.78	0.55	1.63
Na_2O	0	0.19	0.79
TiO_2	0.39	0.19	2.30

Table 2 Engineering properties of materials

Sl. no	Property	BC soil	Mine waste	GBFS	Code
1	Grain size distribution % Gravel Sand Silt Clay	– 14 42 44	– 37.72 38.76 23.52	0.3 83.9 15.8 0	IS:2720-Part IV [5]
2	Soil classification	HRB: A-7-C IS: CH			IS:1498–1970 [6]
3	Specific gravity	2.62	3.08	2.82	IS:2720-Part III [7]
4	Consistency limits (^%) Liquid limit Plastic limit Plasticity index	57 35.9 21.1	NP*	NP*	IS:2720-Part V [8] IS:2720-Part VI
5	California bearing ratio (%)	2.3	–	–	IS:2720-Part XVI [9]
6	Unconfined compression strength (kPa)	166	–	–	IS:2720-Part X [10]
7	Free swell index (%)	55	0	0	IS:2720-Part XL [11]
8	Swell pressure (kPa)	268.70	‘122.58	27.45	IS 2720 Part XLI [12]

2.3 Granulated Blast Furnace Slag (GBFS)

The material was procured from Jindal Steel Work, Toranagallu, Bellary District, Karnataka, India. The specific gravity, particle size distribution, and mineralogical characteristics of the material were determined. The particle size distribution indicates that the GBFS consists of 0.3% of gravel, 83.8% sand, 15.8% silt, and no clay particles. The specific gravity of GBFS was found to be 2.82. The test was carried out as per Indian Standards. The engineering properties of Mine Waste have been shown in Table 2 (Fig. 1).

Fig. 1 Materials used for BC soil stabilization

3 Sample Preparations

Various tests such as Compaction characteristics, Consistency limits, CBR, and UCS were carried out as per standard procedures of IS 2720 and Durability tests as per ASTM D559.

Samples were prepared by mixing BC soil with various Mine Waste content (replacing 10, 20, 30, and 40% of soil) and tested for various parameters. GBFS was further added to the optimum soil–Mine Waste mix that exhibited maximum dry density.

The BC soil–Mine Waste mixes and BC soil–Mine Waste-GBFS mixes were tested after a curing period of 1, 7, and 28 days in order to study the effect of curing. Samples were prepared and cured in a desiccator at 23 °C temperature and 100% relative humidity. The UCS and CBR test samples were prepared for MDD and OMC. CBR test was carried out on samples soaked for 4 days and one hour of drying before testing.

4 Design of Pavement

The analysis of pavement was done using IITPAVE software. The linear elastic multi-layer analysis was performed through software to obtain stress, strain, and deflection. It can be applied to layered systems for different wheel load configurations (single, dual) with different layer behavior. The design life can be evaluated based on the fatigue crack and permanent deformation caused in each period over all load groups. The input parameters for the pavement analysis have been given in Table 3.

Table 3 Input parameters for IITPAVE analysis

Input Parameters	Value
The number of periods in a year	1
The number of load group Single Dual	1 2
No of layers	2–3
No of Z coordinates	Varies among no of interfaces and intermediate points
No of response	9
Unit	SI
Type of loading	Single Axle Single Wheel (SASW) Single Axle Dual Wheel (SADW)
Contact radius of circular loaded area	15.08 cm (SASW) 10.66 cm (SADW, Tandem, Tridem)
Contact pressure on circular loaded area	560 kPa
Radial distance	155 mm

4.1 Input Parameters

The elastic modulus and Poisson's ratio were the prime input embedded in the software. The Poisson's ratio for all the layers was considered as 0.35 as per IRC:37:2018 [13]. The elastic modulus of the material is dependent on the CBR value of the sample. The elastic modulus was determined from equations given in IRC: 37:2018. Equations 1 and 2 gives the elastic modulus value of subgrade. The elastic modulus for granular and surface layer is given in Eq. 3.

$$E = 10 \times CBR \ (CBR < 5\%) \tag{1}$$

$$E = 17.6 \times (CBR)^{0.64} (CBR > 5\%) \tag{2}$$

$$E = EB \times 0.2 \times h^{0.45} \tag{3}$$

where E_B = Modulus of elasticity of supporting layer (MPa); h = layer thickness (mm).

4.2 Rutting Performance Model

The standard rutting performance model, at different reliability levels, was used for the determination of critical strain at the top of the subgrade layer. The pavement layer system was considered efficient when the actual vertical strain is less than the

critical strain obtained from the below equation. Equations 4 and 5 represent the rutting performance model at 80% and 90% reliability, respectively.

$$N_R = 4.1656 * 10^{-8} [1/€_v]^{4.5337} \quad (4)$$

$$N_R = 1.4100 * 10^{-8} [1/€_v]^{4.5337} \quad (5)$$

where N_R = Number of Cumulative ESAL to produce rutting up to 20 mm.

$€_v$ = vertical compressive strain at the top of the subgrade.

5 Results and Discussions

5.1 Effect of Mine Waste on Black Cotton Soil

The Mine Waste was stabilized with BC soil in the form of partial replacement at a rate of 10, 20, 30, 40, and 50% on a trial-and-error basis. The use of Mine Waste indicated a reduction in the Liquid Limit and Plasticity Index from 57 and 21.1%, respectively, to 42.5 and 8% for the partial replacement of 40% of Mine Waste. This was due to the reduction in the repulsive force that acts as particles come in contact with each other. The reduction in surface area and water affinity also contributed to the reduction of liquid limit and plastic limit values.

The 60% BC soil–40% Mine Waste mix also witnessed an improvement in the compaction characteristics due to the higher specific gravity of Mine Waste. MDD and OMC values were 18.96 kN/m^3 and 11.8%, respectively, and are higher than the minimum required MDD as per MORT&H. The compaction of soil at the lower water content is influenced by the flocculation of particles which ultimately reduces OMC values. The repulsion in the clay particles also leads to higher density [14]. The UCS value for untreated BC soil samples was found to be 166 kPa. The value increased gradually up to 197.1 kPa for 40% replacement of Mine Waste and got reduced to 187.58 kPa on further addition of Mine Waste. The UCS achieved after 7 days, and 28 days of curing was 350.15 and 475.52 kPa, respectively. There was also a significant increase in the CBR value on BC soil–Mine Waste samples. The optimum BC soil–Mine Waste mix achieved a CBR of 5.6% in comparison with the untreated BC soil sample of 2.3%.

5.2 Effect of GBFS on BC Soil–Mine Waste Mix

The GBFS was mixed with the soil–Mine Waste mix as an additive at various proportions of 10, 20, 30, and 40% to study its effect on CBR and UCS. It was observed

that for mix 60:40:30, the soaked CBR value was 10% and UCS increased to 233.4 kPa from 197.1 kPa for 1 day curing. The UCS results achieved after 7 days and 28 days of curing was 414.82 and 677.93 kPa respectively. The 10% CBR is classified as the highest quality rating 'S5' as per IRC: SP: 72. GBFS being a cementitious binder material undergoes hydration to form new cementitious compounds like C–A–S–H and C–S–H which increases the strength of treated soil. However, beyond the optimum binder content, the material does not undergo a pozzolanic reaction and behaves like unbounded materials, thus decreasing the strength of the soil sample. The 60:40:30 (BC soil: Mine Waste: GBFS) was considered as the substantial mix.

5.3 Scanning Electron Microscopy (SEM)

The microstructure and morphology of materials were studied using Scanning Electron Microscope. The image produces information on the composition of the sample and its surface topography due to the interaction of electrons with atoms present in the sample. Figure 2a shows untreated BC soil filled with large void spaces. The image indicates the sample as an amorphous material. It lacks the regularity in atomic structure and hence, does not possess a strong mechanical property. Figure 2b indicates the SEM of BC soil–Mine Waste mix. The mix is an amorphous material embedded with metals that gives the charging effect. The mix behaves like an agglomerated material. This was mainly due to the presence of Iron-oxide in Mine Waste. This leads to a slight enhancement in the engineering properties of BC soil. Figure 2c indicates substantial BC soil–Mine Waste-GBFS (60:40:30). It can be clearly seen that the fabric transforms from the particle-based form into a more integrated composition. Figure 2c clearly shows the flocculated material and patches of cementitious products. The soil mixes change from amorphous to crystalline with the addition of GBFS. This is primarily due to the presence of calcium and iron oxide that enhances the engineering properties of the mixes. This phenomenon is predominantly observed in substantial BC soil–Mine Waste-GBFS mix which certainly exhibits its greater effect on micro-structural effect on treated BC soil mix. The crystalline nature of the materials has certainly led to an increase in strength and durability and eventually lead to the reduction in pavement thickness requirement.

5.4 Durability Test

The durability test proves to be a vital parameter in determining the ability of the material in attaining stability and retaining its bond with soil consistently over a long period under the application of destructive weathering agents. The durability studies were carried out on untreated BC soil and substantially treated soil mixes as per ASTM D559 [15]. The test samples were prepared in a similar line with UCS test samples for obtained MDD as per standard proctor test. The test samples of 38 mm

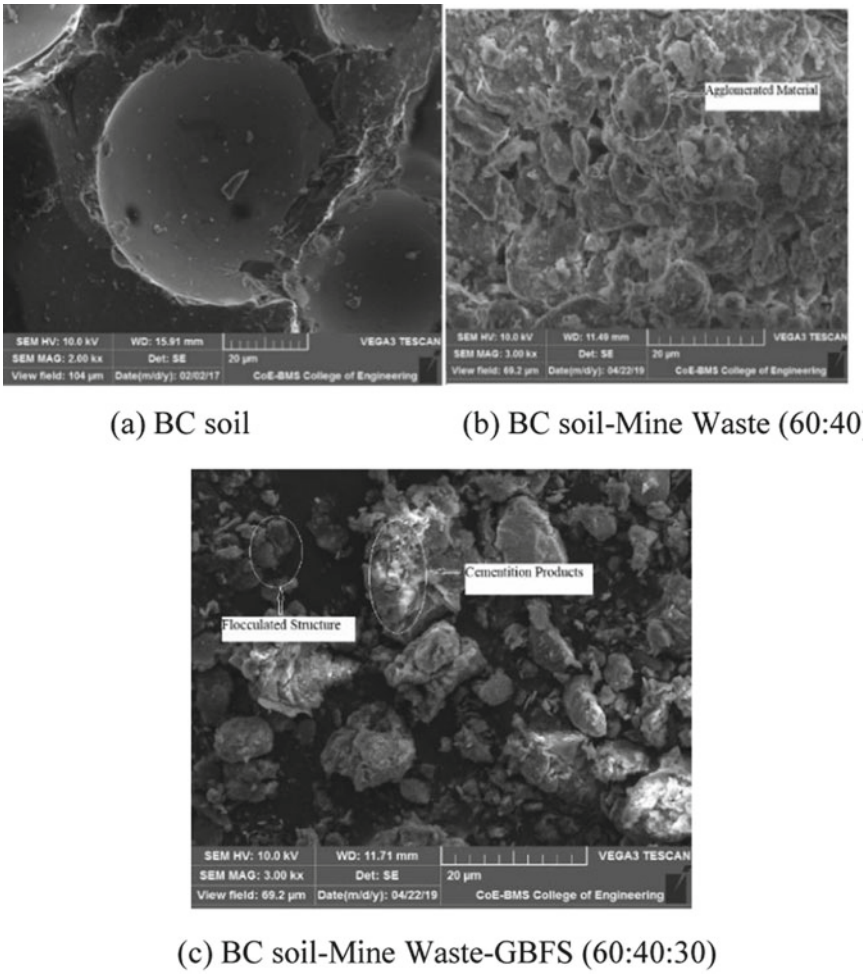

Fig. 2 SEM of untreated and stabilized BC soil

diameter and 76 mm height were prepared as per standard proctor condition. The samples were cured in a desiccator for 7 days. After curing, samples were soaked for a period of 5 h and oven dried for 42 h at a temperature of 71 °C. This 5 h of soaking and 42 h of oven drying constitute one cycle [15]. The results indicated that the untreated BC soil immediately collapsed during the first cycle. The BC soil–Mine Waste (60:40) too couldn't hold the stability and collapsed after two cycles. The soil mixes treated with GBFS withstood 12 cycles of wetting–drying cycles. The percentage loss in weight for substantial BC soil–Mine Waste: GBFS was 9.98%.

5.5 Pavement Design Using IITPAVE

The pavement structure is adopted from IRC SP:72–2015 [16]. The pavement structure consists of WMM granular surfacing laid on a granular base course resting on the subgrade. The input parameters are based on IRC: SP:72–2015 prepared by the Indian Road Congress for the pavement analysis of low volume roads. The pavement analysis for unpaved road is performed for cumulative ESAL of 10,000 to 30,000, 30,000 to 60,000, and 60,000 to 1,00,000. The CBR value of untreated BC soil was 2.3%. As per IRC: SP:72–2015, the subgrade falls in the S1 category which states that the subgrade strength is not suitable for ESAL greater than 30,000. The optimum combination of BC soil: Mine Waste (SM), optimum BC soil: Mine Waste: GBFS (SMG) in subgrade category S3 and S5 respectively. The modified subgrade was analyzed for cumulative ESAL application 10,000–30,000, 30,000–60,000, and 60,000–1,00,000. An unpaved road is not suitable for cumulative ESAL greater than 1,00,000. Table 4 indicates the subgrade and traffic category used in the design. The total pavement thickness of the respective subgrade category and cumulative ESAL applications as per IRC: SP:72–2015 are given in Table 5.

Excess vertical deflection is a major concern in pavement performance. Hence, this is one of the major criteria used for the design of pavement. The results indicate that the modification in the subgrade in the form of partial replacement of materials contributes to the reduction of deflection value. The stabilization also resulted in the reduction of vertical compressive strain at the top surface of the subgrade layer. Table 6 indicates the compressive strain for various cumulative ESAL. The actual strain values were compared with the allowable strain value to check the

Table 4 Category of traffic and subgrade

Materials	Category of subgrade	CBR (%)	Category of traffic	Cumulative ESAL applications
Untreated BC soil	S1	2.3	T1	10,000–30,000
BC soil: Mine Waste (60:40)	S3	5.6	T1	10,000–30,000
BC Soil: Mine Waste: GBFS (60:40:30)	S5	10	T2 T3	30,000–60,000 60,000–1,00,000

Table 5 Total pavement thickness as per IRC SP:72–2015

Subgrade category	Cumulative ESAL applications		
	10,000–30,000	30,000–60,000	60,000–1,00,000
S1 (2%)	300 mm	–	–
S3 (5–8%)	175 mm	250 mm	275 mm
S5 (10–15%)	125 mm	150 mm	175 mm

Table 6 Actual vertical compressive strain of untreated and treated bc soil layer for different axle wheel configurations and various Cumulative ESAL

Materials	Wheel configuration	Vertical compressive strain (Micro strain) Cumulative ESAL		
		10,000–30,000	30,000–60,000	60,000–1,00,000
Untreated BC soil	SASW	4460		
	SADW	3130		
SM mix	SASW	3630	2430	2010
	SADW	2440	2310	1400
SMG mix	SASW	3430	2930	1840
	SADW	2390	1990	1250

Table 7 Critical vertical compressive strain for various cumulative ESAL

Cumulative ESAL	Allowable vertical strain (Micro strain)
10,000–30,000	2420
30,000–60,000	2080
60,000–1,00,000	1850

efficiency of the design. The allowable strain on top of the subgrade layer was determined using the Rutting performance equation (Eq. 4). The actual strain values for different axle wheel configurations were observed. The vertical strain was found to be higher on the Single Axle Single Wheel (SASW) configuration for all the material combinations. Table 7 shows the critical strain for various cumulative strains (Fig. 3).

5.6 Pavement Structure

The ideal pavement structure was determined in consideration with displacement, vertical stresses, and vertical compressive strain on the top of the subgrade layer. The actual vertical strain on the BC soil subgrade layer was higher than the critical strain for all the axle wheel configurations. The actual vertical strain on the pavement structure supported by the modified subgrade provided better results. The compressive strain on the top surface of the subgrade made of modified BC soil was less than the allowable vertical strain for gravel base thickness of 325 mm constructed on optimum BC soil–Mine Waste mix and 225 mm for substantial BC soil–Mine Waste-GBFS mix.

The gravel surfacing of 50 mm supported by a gravel base of 225 mm and resting on the subgrade was considered an ideal pavement structure (Fig. 4).

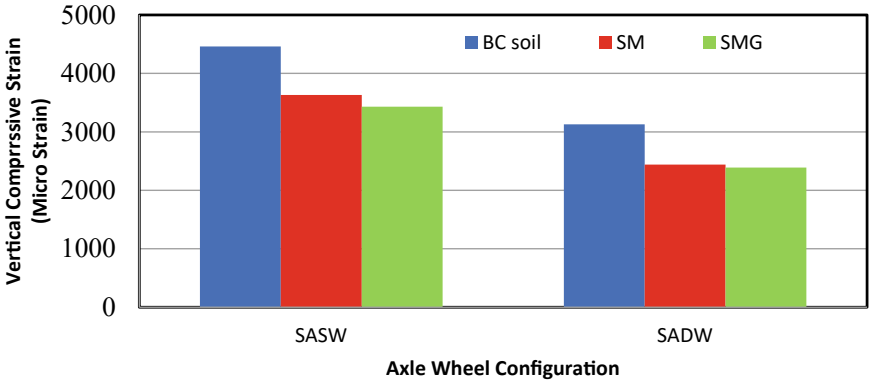

(a) ESAL 10,000-30,000

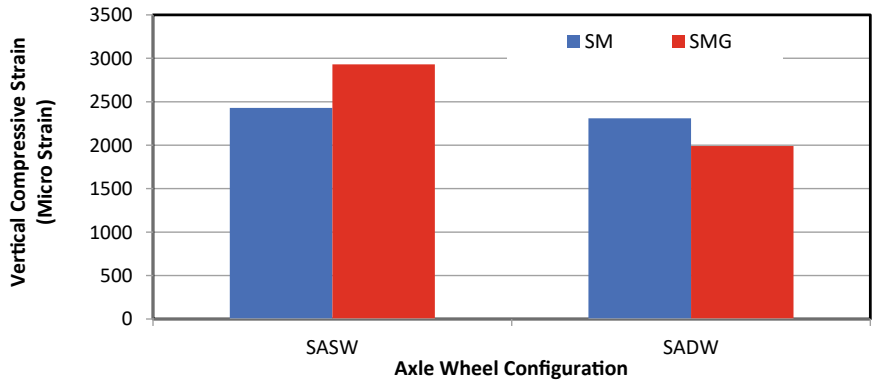

(b) ESAL 30,000-60,000

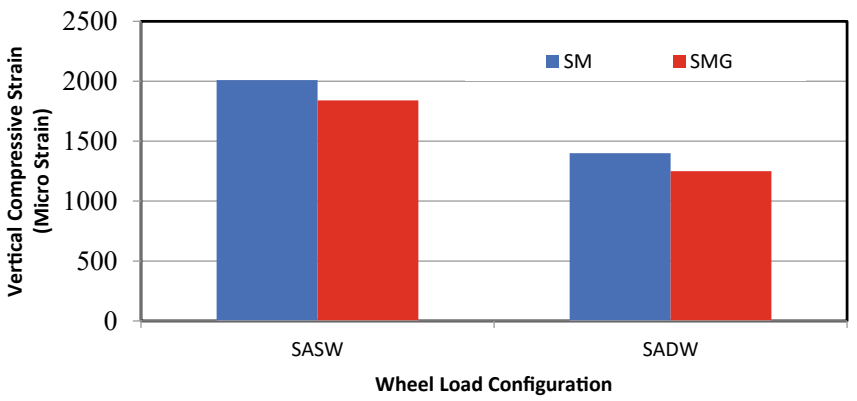

(c) ESAL 60,000-1,00,000

Fig. 3 Compressive strain values of untreated and modified BC soil at various cumulative ESAL

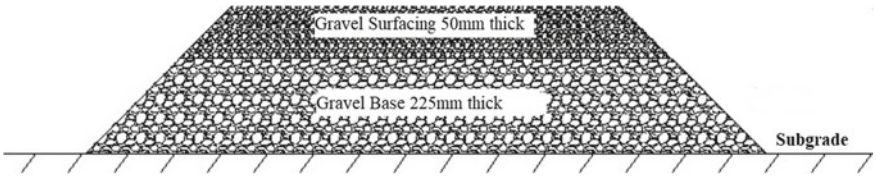

Fig. 4 Pavement structure on SMG mix

Table 8 Cost comparison for low volume roads on untreated and stabilized BC soil subgrade

Material	h (mm)	Total cost/cum (Rs)	Material	h (mm)	Total cost/cum	Savings in cost (%)
Untreated BC soil	500	809.89	SM	325	578.6	28.55
Untreated BC soil	500	809.89	SMG	275	469.98	41

h = Total thickness of pavement

5.7 Cost Evaluation

The alternate design has been developed as per IRC: SP:72–2015 for the BC soil subgrade layer, subgrade layer with modified BC soil, and substantial BC soil–Mine Waste-GBFS mix. The cost analysis was carried out as per the Schedule of Rates 2019, Public Works Department (PWD), Dharwad. Cost analysis consists of construction cost, cost of materials, labor, and transportation cost. All the subgrade materials were obtained free of cost. The transportation cost depended on the location of the material site from Dharwad, Karnataka.

The gravel base layer thickness for untreated BC soil and unsubstantial stabilized BC soil layer has been increased to achieve the actual vertical strain less than the allowable vertical strain. The theoretical pavement structure of untreated BC soil and unsubstantial modified BC soil subgrade layer was compared with the pavement structure of the substantial BC soil–Mine Waste-GBFS mix for cost analysis. A pavement section of 1 m × 1 m was considered for the analysis. The percentage of cost savings was determined for a different combination of materials in comparison with the pavement structure laid on an untreated BC soil layer. Table 8 illustrates the cost comparison for unpaved roads constructed on various types of subgrade layers.

6 Conclusions

1. The soil sample considered for testing is classified as CH Inorganic high compressible clay having a plasticity index of 26%, Unconfined Compressive Strength (UCS) of 166 kPa, and CBR of 2.3%. The laboratory results of various

properties of the soil confirmed that it is highly plastic in nature. Mine waste with a specific gravity of 3.08 was non-plastic with an iron oxide content of 42%. The soil and mine waste mixed in a 60:40 proportion exhibited maximum soaked CBR strength of 5.6% and was considered an optimum Mix. The UCS of 28 days cured optimum mix was found to be 475 kPa.

2. The optimum mix of soil and mine waste was further strengthened by the addition of Granulated Blast Furnace Slag independently in various proportions. The calcium oxide in GBFS was 23%. The maximum soaked CBR was 10% for the optimum mix with 30% GBFS. The improvement in strength upon curing is due to the pozzolanic reaction between soil particles and calcium-rich additives. The formation of CAH and CASH, CSH cementitious compounds is seen in SEM. The crystallization and hardening of these compounds eventually led to the development of strength.
3. The compressive strain was reduced due to the modification of the subgrade layer in comparison with the untreated BC soil subgrade. The requirement of the thickness of the gravel base layer got reduced from 350 to 300 mm for optimum SM mix and 225 mm for optimum SMG mix for cumulative ESAL of 60,000–1,00,000.
4. The reduction in compressive strain for a reduced thickness of gravel base layer of treated soil mixes was mainly due to the higher resilient modulus and CBR values. The vertical compressive strain achieved for all the treated soil mixes was lower than the allowable strain as per the rutting equation.
5. The cost analysis indicated a percentage savings in the cost of 27.33% for the SM mix. However, the maximum percentage cost savings achieved was 41% for the SMG mix. Hence, SMG mix was considered as the substantial mix for unpaved roads. The reduction in cost was mainly due to higher CBR and resilient modulus value that eventually led to the reduction in gravel base thickness for stabilized mixes. The Mine Waste and GBFS were available free of cost from the source.

References

1. Francis Atta Kuranchie et al (2013) Mine Wastes in Western Australia and Their suitability for embankment construction. In: Geo-Congress, pp 1450–1459
2. Yellishetty M et al (2008) Reuse of iron ore mineral wastes in civil engineering constructions: A case study. Resour Conserv Recycl 52:1283–1289. https://doi.org/10.1016/j.resconrec.2008.07.007
3. Bastos LADC et al (2016) Using iron ore tailings from tailing dams as road material. J Mater Civil Eng 28. https://doi.org/10.1061/%28ASCE%29MT.1943-5533.0001613
4. Ministry of Road Transport and Highways, Specifications for Roads, and Bridges, 5th edn. Indian Roads Congress, New Delhi (2013)
5. IS: 2720 PART IV (1986) Methods of Test for Soil, Bureau of Indian Standard, New Delhi
6. IS: 1498 (1970) Indian Standard Code of Practice for Soil Classification, 3rd edn. Bureau of Indian Standards, New Delhi
7. IS: 2720 PART III (2002) Determination of Specific Gravity, Indian Standard Institute, New Delhi

8. IS: 2720 PART V (1985) Determination of liquid Limit and Plastic Limit, Indian Standard Institute, New Delhi
9. IS: 2720 PART XVI (1987). Laboratory Determination of CBR, Indian Standard Institute, New Delhi
10. IS: 2720 PART X (1991) Determination of Unconfined Compressive Strength, Indian Standard Institute, New Delhi
11. IS: 2720 PART XL (1977) Determination of Free Swell Index, Indian Standard Institute, New Delhi
12. IS: 2720 PART Xl (1977) Determination of Swell Pressure, Indian Standard Institute, New Delhi
13. IRC: 37–2018 (2018) Guidelines for the design of Flexible Pavements, Indian Roads Congress, New Delhi, India
14. Lekha BM, Goutham S, Shankar AUR (2014) Evaluation of lateritic soil stabilized with arecanut coir for low volume pavements. Transp GeoTech 2:20–29. https://doi.org/10.1016/j.trgeo.2014.09.00
15. ASTM D 559–03 (2003) Standard test methods for wetting and drying compacted soil-cement mixtures. https://doi.org/10.1520/D0559-03
16. IRC: SP:72 (2015) Guidelines for the Design of Flexible Pavements for Low Volume Rural Roads, The Indian Roads Congress, New Delhi

Driver Perception of Superimposed Horizontal and Vertical Road Curves for Bi-Directional Roads

Lekha Kosuri and Anuj Kishor Budhkar

Abstract With additional dimensional elements, the road appearance gets complicated and hence there is a possibility of erroneous reactions from drivers, which can cause a safety hazard. This paper assesses the perception abilities of the drivers for different roads with superimposition of horizontal and vertical curves. The questionnaire of the survey has been designed as a set of slides, each containing two 3D images of simulated roads having different values of vertical and horizontal curve parameters at various staggering levels arranged successively. The renderings during the design are made with a camera set in congruence with the eye level of the driver on the road. Sixty drivers have been interviewed with this questionnaire, and their ability to distinguish between the curves is recorded as a categorical variable (Yes or No). The responses are modeled using logistic regression wherein the curve parameters and driver demographics are explanatory variables. From the model, it has been observed that the ability to differentiate between the curves decreases with higher radius of the horizontal curve, and higher staggering of the superimposed horizontal and vertical curves. Furthermore, drivers can perceive differences in vertical geometry better than in horizontal geometry. The drivers can distinguish two successive similar curves if the geometric parameter difference is higher, as evident from the model. With the lack of field models, results from this experimental study can be a cue for transportation planners for designing overlapping geometry.

Keywords Driver perception · Horizontal curves · Vertical curves · Superimposed horizontal and vertical curves

1 Introduction

The geometric design is a primary factor that determines the overall safety and effectiveness of road designs. Traditional design standards are established considering different parameters in relative isolation. However, in road systems consisting of more

L. Kosuri (✉) · A. K. Budhkar
Department of Civil Engineering, IIEST, Shibpur, Howrah, West Bengal, India
e-mail: kosuri.lekha@gmail.com

A. Dhamaniya et al. (eds.), *Recent Advances in Traffic Engineering*, Lecture Notes in Civil Engineering 377, https://doi.org/10.1007/978-981-99-4464-4_27

complex designs with multiple geometric parameters overlapping and interacting with each other, it becomes imperative to perform empirical studies that evaluate their safety.

Current manuals like IRC:38–1988 'Guidelines for Design of Horizontal Curves for Highways and Design Tables' [11] and IRC SP 23 (1993) [10] 'Vertical Curves for Highways' have various guidelines for designing horizontal and vertical road curves respectively, but have little information for road designs which have both these parameters overlapping at once.

In such cases, driver perception of the curve becomes a critical determining factor. Several studies [7, 8], etc. have proved that the ability of drivers to perceive the characteristics of the road and hence opt for appropriate speed and direction controls of the vehicle is limited. Erroneous perception can lead to compromised safety. For example, if a driver cannot perceive the difference while driving on various roads, we cannot safely assume that he would be able to adopt the appropriate driving operations like speed. Hence, implementing perception-based geometric designs is vital to ensure design consistency and efficacy.

The objective of this study is to examine the accuracy of drivers of distinct age groups and driving experiences to differentiate between computer-generated renderings of roads having varied and overlapping horizontal and vertical curve parameters. Further, the paper tries to establish a relationship between perception accuracy and the various parameters horizontal and vertical curve radius, angle of deflection of vertical road, driver demographics, etc.

2 Literature Review

2.1 Literature Related to Driver Perception

Junjie et al. [23] studied the role of driver's perception errors for vehicle motion state information in affecting traffic flow oscillations. A real vehicle test and an extended full velocity difference (EFVD) model were used to investigate the effects of the driver's perception errors of the preceding vehicle's velocity and headway changes on a road without lane changing. Results from numerical experiments illustrated that the increase of the interval of the confidence levels is not conducive to smooth traffic flow in those cases. Yang et al. [14] combined a field operational test and numerical simulations of a typical rear-end crash model to estimate the probability of crash occurrence. Time-to-collision (TTC) and driver braking response to impending collision risk were used in an instrumented vehicle to evaluate a decrease in crash probability. Peter et al. [9] explored the detrimental effect of vertical eye-movement carryover from one driving task to another for hazard identification accuracy. It was observed that scanning accuracy was higher for experienced drivers and horizontal scanning movement. Johan et al. [21] explored which curve cues and other variables influence drivers' speed choice in curves through specifically designed surveys. Geometric

road characteristics such as curve radius and deflection angle were identified by the respondents as influencing variables but only shown to affect speed selection when these are visible to the driver and not obscured by trees or other elements. Hassan and Easa [8] studied driver perception of computer-animated 3D representations of horizontal roads with and without overlapping vertical curves and found that driver behavior on horizontal curves depended on the overlapping vertical curve. Similarly, Hanno [7] analyzed driver perception with respect to the 3D effect of combined road alignment and found that many parameters like horizontal curve radius, the algebraic difference in vertical gradients, the percentage of overlap between the vertical and horizontal curves, etc., significantly affected driver perception in various ways.

2.2 Literature Related to Horizontal and Vertical Curves

Mohsen et al. [2] evaluated the effect of overlapping longitudinal slope and vertical curves on the horizontal curve radius by exerting different forces on a vehicle and modeling the direction of their effect. The results demonstrated that the equations for the overlap of a horizontal curve with a crest vertical curve indicate a need for increasing the horizontal curve radius in some cases. Sil et al. [18] developed a speed prediction model for horizontal curves under mixed traffic conditions in a four-lane divided highway. It was observed that some drivers use the full width of pavement to traverse a horizontal curve in a free-flowing condition. Hence, the speeds of these vehicles were relatively higher and did not demonstrate significant speed reduction while entering from a tangent section. Wang et al. [22] studied the speed change behavior of various combined curves. An analysis of the marginal effects of different parameters of combined curves on speed change showed that the type of combined curve affected the speed change behavior of the driver. Nama et al. [16] evaluated the performance characteristics of vehicles for hilly roads using indirect measures such as stability of the vehicle, velocity, and stress on the driver on various hilly road sites. The observations suggested that operating speeds are higher than design speeds. Cheng [5] predicted the probability of roadside accidents for curved sections on highways. The results showed that after vehicle speed, horizontal curve radius was the most significant risk factor.

2.3 Literature Related to Curves in Mixed Traffic Conditions

Munigety et al. (2016) studied and formed a comprehensive review of studies that consider modeling integrated driving phenomena like tailgating, multiple-leader following, swerving, and filtering in mixed traffic conditions of developing countries. Neena et al. (2021) quantified the influence of geometric characteristics of the preceding curve on crashes and developed models for the evaluation of the safety performance of multiple horizontal curves on two-lane non-urban roads. Sil et al. [20]

quantified the perceived speed behavior at the starting and center of horizontal curves on a National Highway in India and proposed operating speed prediction models for them. Choudhari et al. [6] investigated the effect of Horizontal Curves on vehicle speed reduction and road safety on two lanes on an Indian Highway using a fixed-base driving simulator to obtain the speed profile of the drivers in various geometric configurations. The maximum speed reduction (MSR) values for a fair level of safety were calculated which can be used to design horizontal curves. Shallam et al. [17] carried out Operating Speed Models on horizontal curves for two-lane highways to evaluate the 85th percentile operating speed and predict the speed that can match the acceptable design speed. This was used to develop curve-speed prediction equations using data collected at horizontal curves of the highway.

From the above-presented studies, it can be concluded that several studies have shown the importance of driver perception in the safety consideration of a road design. Studies conducted on horizontal and vertical curves in roads have shown that such roads are relatively more prone to accidents and hazard risks and hence need to be critically evaluated with respect to their safety and efficacy, especially in the context of Indian drivers who drive in mixed traffic conditions which is significantly more complex when compared to roads of developed countries.

3 Data Collection Methodology

Studying driver perception of roads with systematically varying geometric parameters in the field can be difficult, considering the fact that even if we find such roads there could be multiple external factors affecting the driver, which we cannot control. Hence, we have conducted a limited study, based on the purposive sampling method of the driver population, on their perception of three-dimensional images providing a realistic view of roads as mentioned in [19]. If the drivers are able to perceive the difference between images containing two different curves, they may perceive these curves differently, and react differently to these curves. However, in case they cannot perceive the difference, it emphasizes the inadequacy in perception, which has the potential to impede the driver's ability to drive safely. Therefore, the study involves providing a series of sets containing two curves, with varied geometric (horizontal and vertical) parameters to be perceived by the driver.

The study is conducted in three stages, (i) Developing 3D renderings of road curves with various parameters, (ii) data collection from drivers, and (iii) modeling the driver responses and analysis (Fig. 1).

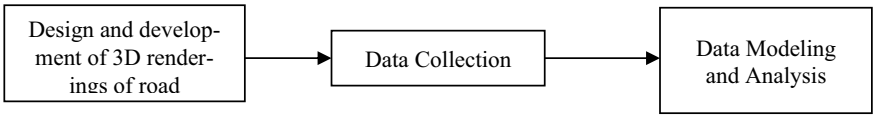

Fig. 1 Flowchart of adopted methodology

3.1 Identification of the Parameters

Since the study involves both horizontal and vertical elements, therefore two-lane rural highways with superimposed horizontal and vertical curves are chosen for this study. For this purpose, a variety of parameters that are used in IRC 66–1976 [12] and IRC SP 23–1993 [10] for the design of horizontal and vertical curves respectively, are considered. Would describe the geometric design elements of the road are considered. As it is practically impossible to design curves for all possible combinations, specific values are considered for each parameter as follows:

1. Design speed: The target speed at which the drivers are intended to travel on the road. The values considered are (in km/h) 65, 70, 80, 100 and 120.
2. Radius of Horizontal Curve (R): The radius is considered to be around the minimum horizontal radius as suggested by IRC 038, taking superelevation e = 0.07 and friction factor f = 0.15. The values are 155, 180, 230, 360 and 520 m.
3. Angle of Deviation of Vertical Curve (N): It is the difference between the grades of the vertical curve. It is considered in an arithmetic progression starting from 4% with a common difference of 2% up to 10%. The scope of the study is restricted to valley curves.
4. Parameter Q: It is a parameter considered which determines the staggering of the superimposed horizontal and vertical curves. It determines what position of the point (in percentage) in the horizontal and vertical curve that is coinciding in the three-dimensional space. Three Q values are considered, which are 0 (when the initial points of both the curves coincide), 0.25 (when the first quarter point of the curves coincide), and 0.5 (when the middle points of the curves coincide).

Reaction time t is considered as 2.5 s in accordance with IRC:66–1976 [12].

The basic parameters are chosen in such a way that other necessary dependent parameters are required to design the curve like the length of the vertical curve (L_v) can be calculated from them.

The horizontal curve is fixed at 45 degrees, and a long tangent follows it. The ratio of the length of the horizontal curve (L_h) to that of the vertical curve is between 0.5 and 2.

3.2 Development of Curve Image Sets

Different software is currently available for rendering 3D models. A 3D design software is needed for this study, which can replicate the real world as close as possible with options to incorporate natural lighting, road, roadside geometry, and texture. Some commercially available software for this purpose are Maya [15], 3DS Max [1], AutoCAD [4], etc. For this study, 3DS Max was adopted, as it is able to give near-perfect renderings of superimposed horizontal and vertical curves with ease.

Suitable road material is chosen to give a texture to the road. The width of the road is considered as 7.5 m, with the crown at the center. The shoulder width is kept

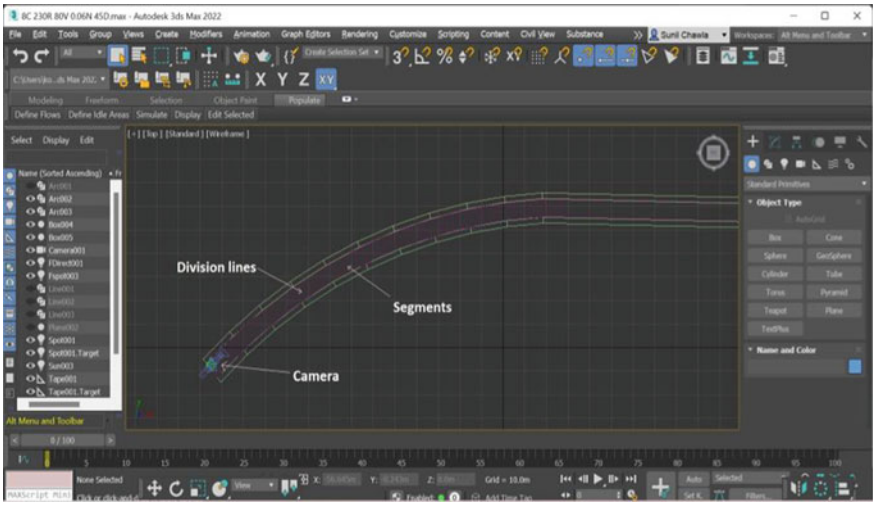

Fig. 2 View of the road in X–Y plane in the 3D modeling software

at 2.5 m. To avoid direction bias, the curves made are right turning only. The terrain is chosen to be flat terrain, with the atmosphere and lighting of the render adjusted to mimic as close to ideal field conditions as possible.

The vertical curve is assumed to be a cubic parabola in accordance with IRC SP 23 [10]. To add smoothness to the road, the horizontal curve is divided into many segments in the X–Y plane as shown in Fig. 2. The Z-coordinates of the vertical curve are then calculated and then the alignment is raised accordingly in each division line of the curve. In cases where the length of the vertical curve is greater than the horizontal curve, the segments are extended into the tangent.

A camera is used to set the position and orientation of the view of the rendering to correspond to the driver's perspective on the road. It is set at a height of 1m from the road surface to mimic the average height of the eye level of a driver. The camera is always placed at the beginning of the horizontal curve as shown in Fig. 2.

Curve Sets. The pairing of the curves is conducted in a sequential manner, i.e., the base curve (Curve A) remains the same, and the comparison curve (Curve B) changes its parameters in an increasing trend. This is done to analyze different comparisons with a fixed base image. On this basis, two sets consisting of 35 pairs each are formed. (see Appendix Table 3 for details of all the pairings).

3.3 Driver Interview Process

Three slideshows are prepared, two of them contain the two sets of curve pairs, and the third one contains a drivers' familiarization set to be used before the actual survey. Each slide consists of one pair of curves (as represented in Fig. 3.) and is

followed by a blank slide to record the response of the driver. The slide with the curves is displayed for a fixed interval, which corresponds to the reaction time of drivers as provided in IRC:66–1976 [12], i.e., 2.5 s, after which the curves disappear. The drivers' responses after perceiving each pair are expected to be in binary: Yes or No, which indicates whether they were able to differentiate between the two curves or not.

A total of 60 drivers with various age groups, gender, driving experiences, and knowledge of driving in a variety of four-wheeled automobiles are interviewed. 25% of the total drivers were female. The mean age of the drivers is 34.2 years. All drivers had a minimum driving experience of 1 year. Figure 4a, b show the statistical distribution of the drivers.

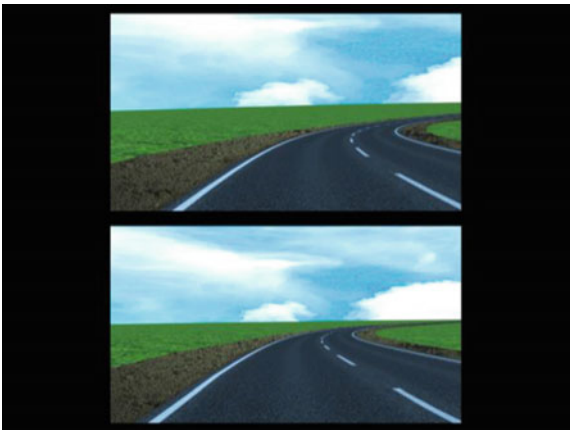

Fig. 3 Sample of curve pairs in survey questionnaire

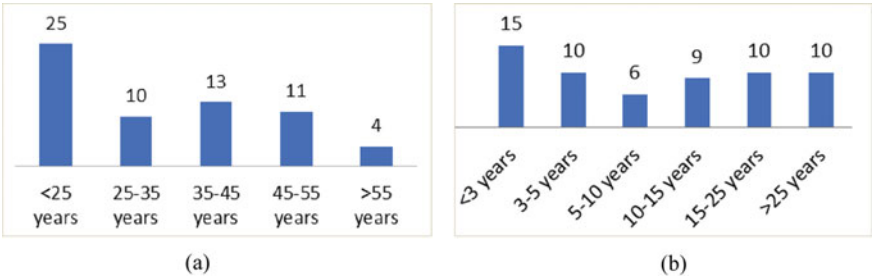

Fig. 4 Number of drivers with respect to (a) age (b) driving experience

Table 1 Evaluation using all variables

	Coefficient	Std. Err	Z	p > |z|
R	−0.0011	<0.001	−2.875	0.004
Change in R	0.0058	0.001	8.761	<0.001
N	0.0307	0.019	1.621	0.105
Change in N	0.3182	0.032	9.873	<0.001
Q	−0.0079	0.003	−2.659	0.008
Change in Q	0.0085	0.004	2.167	0.030
Age	−0.0102	0.006	−1.859	0.063
Gender[1]	0.3775	0.128	2.952	0.003
Experience	−0.0028	0.008	−0.342	0.732
Frequency	0.0141	0.039	0.359	0.720

4 Analysis and Results

Overall, the data set consists of 2100 data points (60 drivers × 35 responses per driver). Here, the dependent variable is the response of the driver (binary: 0 for no difference or 1 for the difference observed), whereas the independent variables are shown in the first column of Table 1.

To model the variation of driver perception (binary) with the independent variables, logistic regression modeling technique is adopted. Firstly, the entire dataset is divided randomly into test data (80% dataset) and validation data (20% dataset). The evaluation of the test data using all the variables is given in Table 2. It was found that the variables: angle of deviation of base curve, experience and frequency are not affecting the drivers' decision significantly (their p-statistic value is greater than 0.05) so they are not considered for further modeling. A new logistic regression model is prepared using the remaining variables. For the driver responses, log-odds (z) expresses the natural algorithm of the ratio between the probability that the driver will not perceive the difference to the probability that he will. The predicted probability (p) of the driver perceiving the difference can be calculated by

$$p = 1 - \left[\frac{1}{1 + e^{-z}}\right] \tag{1}$$

where,

$$z = \ln\left(\frac{\text{probability to not perceive difference}}{\text{probability to perceive difference}}\right) \tag{2}$$

[1] Gender response is in binary format: 1 for Female and 0 for Male.

Table 2 Evaluation using only significant variables

Variable	Coefficient	Std. error	z	p > |z|
Intercept	0.6214	0.199	3.115	0.002
R	−0.0016	<0.001	−3.918	<0.001
ΔR	0.0054	0.001	7.918	<0.001
ΔN	0.3133	0.032	9.807	<0.001
Q	−0.0063	0.002	−2.530	0.011
ΔQ	0.0096	0.004	2.674	0.008
A	−0.0189	0.004	−4.657	<0.001
G	0.2959	0.119	2.492	0.013

β_0 is the constant term, given by the intercept, which indicates overall probability without the influence of any predictor variables, while β_1, β_2, β_3, β_4, β_5, β_6, and β_7,are coefficients of the variables. The model (i.e., values and standard error of β_0, β_1, β_2, β_3, β_4, β_5, β_6, and β_7) is provided in Table 2. R, ΔR, ΔN, Q, ΔQ, A and G are used to represent the horizontal radius of base curve, difference in horizontal radius of the curves, difference in angle of deviation of the curves, staggering of base curve, difference in staggering of the curves, age of the driver and gender of the driver respectively.

4.1 Model Interpretation

- The vertical angle of deviation of base curve (N), driver experience, and driving frequency is found to have no significant effect on the driver perception of the difference in curves. This result is counter-intuitive to many studies Alfonsi et al. [3].
- Drivers are able to distinguish between the curves effectively, if the radius of the base curve (R) is less (as evident from negative β_1 value).
- Greater the difference between the radius of the two images (ΔR), the easier it is for the drivers to perceive the difference between them (as evident from positive β_2 value). This result is in line with the finding of Sil et al. [19].
- The difference in the vertical angle of deviation (ΔN) as well as the staggering value (ΔQ) of the curves has a positive impact on the driver's perception. However, ΔN is seen to have a comparatively greater effect (as evident from positive β_3 and β_5 values respectively).
- The staggering value of the base curve (Q) also had an impact on perception ability. Lesser staggering could be perceived better by the drivers. (as evident from negative β_4 value).

- Female drivers are more likely to perceive the difference than male, while older drivers have lesser perceiving ability in general (as evident from positive β_7 and negative β_6 value respectively).
- Drivers can perceive differences in vertical geometry better than the difference in horizontal geometry.

4.2 Validation

The validation is performed on the validation dataset using confusion matrix. The values of true positive, true negative, false positive and false negative are 109, 94, 66 and 151 respectively, thereby indicating 62% accuracy of logistic regression classifier on the test dataset.

5 Conclusion

The paper presented a methodology to model driver perception, based upon the binary driver response of perceiving the difference between road images consisting of varying horizontal and vertical parameters. It is important to note that although driver response while actual driving is dynamic in nature, the aim of this study was to conduct an initiation into evaluating such perception using limited resources. Logistic regression is used to predict the perception response made by the drivers. Odds to perceive the difference increases with decrease in radius (R); increase in the difference between all geometric parameters of the curves (ΔR, ΔN and ΔQ); and decrease in staggering of the curve (Q). Vertical angle of deviation (N) has little or no impact on perception ability. Age and gender also affect the ability to perceive the difference as noticed from the coefficients, while frequency and experience did not show any noticeable difference in perception. The results are intuitive, with respect to the difference between various parameters of two curves, where the indication is that as the amount of difference increases, the ability to notice it also increases. However, some counter-intuitive findings were also found such as driver experience and frequency not having much impact on such ability of the drivers. This type of study can be adopted as a low-cost alternative in the absence of simulators, which are mostly inaccessible. It can be regarded as a preliminary study to contribute to the field of perception-based geometric design.

5.1 Application and Future Scope

Erroneous perception can lead to compromised safety and hence implementing perception-based geometric designs is vital to ensure design consistency and efficacy.

This information is important while designing the curve combination of horizontal and vertical curves. The outcomes of the study will help the planners to design and construct safer superimposed curves, and assist guiding agencies to formulate thresholds of vertical curves for given horizontal curve geometry, whenever superimposed road geometry is planned, by highlighting the aspects of the geometric design which need to be focused on to ensure the safety of drivers. As concluded from the paper, the engineers may not plan for larger horizontal curves, and use a lesser amount of staggering while designing such combination curves. Building upon this preliminary study, further investigation can be done on such curves using simulators or field studies.

Acknowledgements We sincerely thank Mr. Santosh Kumar and Mr. Ambuj Mishra, who are alumni students of IIEST, Shibpur, for their help in the survey process.

Appendix

See Table 3.

Table 3 List of curves and their parameters

Curve number	Deviation angle (N)	Q	Velocity (v)	Reaction time	f	Lv	Minimum radius (e = 0.07; f = 0.15)	Radius considered
1	0.04	0	65	2.5	0.35	66.79	151.255	155
2	0.04	0	70	2.5	0.35	79.24	175.42	180
3	0.04	0	80	2.5	0.35	106.04	229.12	230
4	0.04	0	100	2.5	0.35	167.23	358	360
5	0.04	0	120	2.5	0.35	238.55	515.52	520
6	0.06	0	65	2.5	0.35	108.67	151.255	155
7	0.06	0	70	2.5	0.35	125.89	175.42	180
8	0.06	0	80	2.5	0.35	163.73	229.12	230
9	0.06	0	100	2.5	0.35	252.51	358	360
10	0.06	0	120	2.5	0.35	358.11	515.52	520
11	0.08	0	65	2.5	0.35	144.90	151.255	155
12	0.08	0	70	2.5	0.35	167.86	175.42	180
13	0.08	0	80	2.5	0.35	218.31	229.12	230
14	0.08	0	100	2.5	0.35	336.68	358	360
15	0.08	0	120	2.5	0.35	477.47	515.52	520
16	0.1	0	65	2.5	0.35	181.12	151.255	155
17	0.1	0	70	2.5	0.35	209.82	175.42	180
18	0.1	0	80	2.5	0.35	272.89	229.12	230
19	0.1	0	100	2.5	0.35	420.85	358	360
20	0.1	0	120	2.5	0.35	596.84	515.52	520
21	0.04	0.25	65	2.5	0.35	66.79	151.255	155
22	0.04	0.25	70	2.5	0.35	79.24	175.42	180
23	0.04	0.25	80	2.5	0.35	106.04	229.12	230
24	0.04	0.25	100	2.5	0.35	167.23	358	360
25	0.04	0.25	120	2.5	0.35	238.55	515.52	520
26	0.06	0.25	65	2.5	0.35	108.67	151.255	155
27	0.06	0.25	70	2.5	0.35	125.89	175.42	180
28	0.06	0.25	80	2.5	0.35	163.73	229.12	230
29	0.06	0.25	100	2.5	0.35	252.51	358	360
30	0.06	0.25	120	2.5	0.35	358.11	515.52	520
31	0.08	0.25	65	2.5	0.35	144.90	151.255	155
32	0.08	0.25	70	2.5	0.35	167.86	175.42	180
33	0.08	0.25	80	2.5	0.35	218.31	229.12	230
34	0.08	0.25	100	2.5	0.35	336.68	358	360
35	0.08	0.25	120	2.5	0.35	477.47	515.52	520

(continued)

Table 3 (continued)

Curve number	Deviation angle (N)	Q	Velocity (v)	Reaction time	f	Lv	Minimum radius (e = 0.07; f = 0.15)	Radius considered
36	0.1	0.25	65	2.5	0.35	181.12	151.255	155
37	0.1	0.25	70	2.5	0.35	209.82	175.42	180
38	0.1	0.25	80	2.5	0.35	272.89	229.12	230
39	0.1	0.25	100	2.5	0.35	420.85	358	360
40	0.1	0.25	120	2.5	0.35	596.84	515.52	520
41	0.04	0.5	65	2.5	0.35	66.79	151.255	155
42	0.04	0.5	70	2.5	0.35	79.24	175.42	180
43	0.04	0.5	80	2.5	0.35	106.04	229.12	230
44	0.04	0.5	100	2.5	0.35	167.23	358	360
45	0.04	0.5	120	2.5	0.35	238.55	515.52	520
46	0.06	0.5	65	2.5	0.35	108.67	151.255	155
47	0.06	0.5	70	2.5	0.35	125.89	175.42	180
48	0.06	0.5	80	2.5	0.35	163.73	229.12	230
49	0.06	0.5	100	2.5	0.35	252.51	358	360
50	0.06	0.5	120	2.5	0.35	358.11	515.52	520
51	0.08	0.5	65	2.5	0.35	144.90	151.255	155
52	0.08	0.5	70	2.5	0.35	167.86	175.42	180
53	0.08	0.5	80	2.5	0.35	218.31	229.12	230
54	0.08	0.5	100	2.5	0.35	336.68	358	360
55	0.08	0.5	120	2.5	0.35	477.47	515.52	520
56	0.1	0.5	65	2.5	0.35	181.12	151.255	155
57	0.1	0.5	70	2.5	0.35	209.82	175.42	180
58	0.1	0.5	80	2.5	0.35	272.89	229.12	230
59	0.1	0.5	100	2.5	0.35	420.85	358	360
60	0.1	0.5	120	2.5	0.35	596.84	515.52	520
61	0	–	65	2.5	0.35	–	151.255	155
62	0	–	70	2.5	0.35	–	175.42	180
63	0	–	80	2.5	0.35	–	229.12	230
64	0	–	100	2.5	0.35	–	358	360
65	0	–	120	2.5	0.35	–	515.52	520

References

1. 3DS Max Homepage, https://www.autodesk.com/products/3ds-max/overview. Last accessed 19 Oct 2022
2. Aboutalebi EM, Hojjati SMF (2021) Evaluation of horizontal curve radius in overlap with longitudinal slope and vertical curve. Transp Lett 13(4):263–272
3. Alfonsi R, Ammari A, Usami DS (2018) Lack of driving experience developed by the H2020 project SafetyCube. In: European road safety decision support system. Accessed from www.roadsafety-dss.eu
4. AutoCAD Homepage, https://www.autodesk.in/products/autocad/overview. Last accessed 19 Oct 2022
5. Cheng G, Cheng R, Pei Y, Xu L (2020) Probability of roadside accidents for curved sections on highways. Math Probl Eng
6. Choudhari T, Maji A (2019) Socio-demographic and experience factors affecting drivers' runoff risk along horizontal curves of two-lane rural highway. J Saf Res 71:1–11
7. Hanno D (2004) Effect of the combination of horizontal and vertical alignments on road safety, Doctoral dissertation, University of British Columbia
8. Hassan Y, Easa SM (2003) Effect of vertical alignment on driver perception of horizontal curves. J Transp Eng 129(4):399–407
9. Hills PJ, Thompson C, Pake JM (2018) Detrimental effects of carryover of eye movement behaviour on hazard perception accuracy: effects of driver experience, difficulty of task, and hazardousness of road. Transp Res Part F: Traffic Psychol Behav 58:906–916
10. Indian Roads Congress Special Publication No. 23 Indian Roads Congress, New Delhi (1993)
11. IRC:38–1988 Guidelines for Design of Horizontal Curves for Highways and Design Tables. Indian Roads Congress, New Delhi (1988)
12. IRC:66–1976 Recommended Practice for Sight Distance on Rural Highways. Indian Roads Congress, New Delhi (1976)
13. Joseph NM, Harikrishna M, Anjaneyulu MVLR (2021) Safety evaluation of multiple horizontal curves using statistical models. Int J Veh Saf 12(1):81–97
14. Li Y, Zheng Y, Wang J, Kodaka K, Li K (2018) Crash probability estimation via quantifying driver hazard perception. Accid Anal Prev 116:116–125
15. Maya Homepage, https://www.autodesk.com/products/maya/overview. Last accessed 19 Oct 2022
16. Nama S, Maurya AK, Maji A, Edara P, Sahu PK (2016) Vehicle speed characteristics and alignment design consistency for mountainous roads. Transp Dev Econ 2(2):1–1
17. Shallam RDK, Ahmed MA (2016) Operating speed models on horizontal curves for two-lane highways. Transp Res Procedia 17:445–451
18. Sil G, Maji A (2017) Development of speed prediction model for curve in mixed traffic conditions. In: International conference on advances in highway engineering and transportation systems (ICAHETS-2017), pp 21–22
19. Sil G, Maji A, Majumdar MM, Maurya AK (2022) Drivers' ability to distinguish consecutive horizontal curves. Can J Civ Eng 49(9):1518–1531
20. Sil G, Nama S, Maji A, Maurya AK (2020) Modeling 85th percentile speed using spatially evaluated free-flow vehicles for consistency-based geometric design. J Transp Eng Part A: Syst 146(2):04019060
21. Vos J, Farah H, Hagenzieker M (2021) How do Dutch drivers perceive horizontal curves on freeway interchanges and which cues influence their speed choice? IATSS Res 45(2):258–266
22. Wang X, Wang X (2018) Speed change behavior on combined horizontal and vertical curves: driving simulator-based analysis. Accid Anal Prev 119:215–224
23. Zhang J, Sun Z, Yu H, Liu M, Yang C (2021) Modeling and simulation of traffic flow considering driver perception error effect. J Transp Eng, Part A: Syst 147(4):04021009

Evolving Feasible Transportation Route from Cement Plant to the Proposed Mines: A Case Study

Nataraju Jakkula and Velmurugan Senathipathi

Abstract It is a mandatory requirement for any envisaged roadway capacity augmentation connecting the facilities like mining plant to obtain environmental clearance from the concerned authority coupled with the assessment of its impact on the traffic plying on the adjoining road network. In addition to the above, the best route to the cement plant has been examined and proposed in this study. In this context, the traffic study was carried out by considering the proposed mining plant at Nandgaon and Ekodi villages as well as exploring the need *(if any)* for capacity augmentation of the connecting roads from plant to mines. Based on the above assessment, the best route for transportation between the proposed mining area and the cement plant has been suggested as the plant will handle a maximum capacity of 2.0 Million Tonne per Annum *(MTPA)* of goods movement in the foreseeable future. To address the above, the relevant traffic surveys were conducted on the study corridor to understand the need for the roadway capacity augmentation *(if any)* which comprised of three routes having varying lengths. Keeping in view the requirement of providing safe commuting passage for various types of vulnerable road users *(VRUs)* like motorised two wheelers as well as bicyclists and pedestrians, it is recommended to provide paved shoulders of 1.5 m wide plus 1.0 m earthen shoulder on two lane bidirectional roads. The existing four lane divided road having two staggered intersections of Gadchandur and Manikgarh needs immediate geometric improvement which would help in achieving smoother radii for turning traffic considering the proportion of multi axle trucks would increase after the opening of the proposed mines. Further, it was recommended towards implementation of strict enforcement in terms of prohibition of on street parking and removal of encroachments. It was also recommended to supplement with the immediate repair and rehabilitation measures of the existing road from Gadchandur to Nandgaon and Ekodi in the form of pothole repair and overlay. Further, the ill designed roundabout at Manikgarh intersection was not designed conforming to IRC:65 (2017) and hence it was necessary to redesign the roundabout conforming to standards and provide adequate diameter of around 15 m as well as improve the staggered intersections coupled with the posting of necessary road signs markings and street lighting. Overall, it is inferred that Gadchandur to

N. Jakkula (✉) · V. Senathipathi
CSIR – CRRI, New Delhi, India
e-mail: jakkula.nataraju@gmail.com

A. Dhamaniya et al. (eds.), *Recent Advances in Traffic Engineering*, Lecture Notes in Civil Engineering 377, https://doi.org/10.1007/978-981-99-4464-4_28

ACL via the proposed road from State Highway to ACL joining behind ACL plant is the best route amongst three routes due to its advantages like shortest distance, devoid of any interaction with local traffic and environment friendly. Incidentally, the proposed improvements were implemented on the ground recently by M/s. ACL at their own cost after the approval by Environmental Impact Assessment committee.

Keywords Mines · Shortest route · Capacity augmentation

1 Introduction

The crushed limestone collected from the proposed mines will be transported from Nandgaon Ekodi mining lease to the main Ambuja Cement Limited plant. The connectivity between ore extracted from the mining area and the cement plant is only accessible by road, which is proposed to be transported through tip trailers i.e. typical multi axle trailers having a registered laden weight of 52 tonnes. Thus, the Gross Vehicle Weight (GVW) of typical multi axle tip trailer proposed to be employed by ACL (as per the information furnished by ACL) is 52 tonnes per truck considering empty laden weight (ELW) of each vehicle deployed is 22 tonnes. The number of tippers operated on daily basis will be 37 spreads over two shifts. However, considering the possibility of availability of only 80% of the estimated fleet on any given day due to logistic issues like maintenance and driver availability, the total number of required tippers is 47. The proposed capacity of limestone production of the proposed mines is 2.0 million tonnes per annum *(MTPA)*. As such, development works and limestone extraction is planned by M/s. ACL from 3rd year onwards with an incremental increase of the production ranging from 0.10, 0.20 and 2.00 million tonnes respectively during 3rd, 4th and 5th year of the mining period. Further, it is proposed by M/s ACL to undertake exploratory drilling during the first three years of the mining period. This proposal is also in line with the existing plant where further capacity expansion is planned. In accordance with the EIA, which is amended time to time, Environmental Clearance is mandatory for the operation of mining area. The essential aspects covered in the environmental clearance report encompass the following:

- The proponent to implement the proposal in an environmentally and socially responsible way; The responsible authority to make an informed decision on the proposal, including the terms and conditions that must be attached to an approval or authorization; and
- Public to understand the proposal and its likely impacts on people and the environment.
- More importantly, to understand and establish the need for the capacity augmentation of link road (which is the sole arterial road connecting from Gadchandur to Nandgaon/Ekodi with M/s Ambuja Cements Limited) spanning a length of about 23 km and developing alternate feasible routes.

Considering the above, it was felt prudent by M/s. Ambuja Cements Limited (ACL) to carry out a comprehensive traffic study of the link roads connecting with the proposed mining plant and thus evolve a feasible route connecting the proposed Ekodi Mines with the ACL crusher area, which is accomplished by CSIR-CRRI based on traffic and safety assessment.

2 Objectives of the Study

- To understand the impact on the roadway capacity assessment due to the new proposed mining plant at Nandgaon and Ekodi Mines, Nandgaon and Ekodi of Chandrapur district in Maharashtra
- To understand the base year traffic characteristics based on the primary traffic data *(collected by CSIR-CRRI)* and secondary source data in terms of road crash scenario on the study area road network and other associated stakeholders.
- To devise appropriate capacity augmentation measures for meeting the projected traffic demands due to the proposed mining plant conforming to the relevant Indian Roads Congress (IRC) standards and Indian Highway Capacity Manual (2018).
- To evolve the best route from Nandgaon Ekodi to ACL for carrying the proposed mines bound traffic.

3 Methodology

Classified Traffic Volume Count (CVC) was conducted using videography between 7:00 AM to 8:00 PM aimed at ascertaining the traffic volumes and composition of traffic on the study stretch. This encompassed the conduct of relevant traffic volume studies on three intersections located on Gadchandur road so as to deduce the classified turning traffic volumes as well as midblock traffic volume on Gadchandur road *(which is a State Highway)*, Penganga road (Bhoyegaon), road destined to Manikgarh as well as road destined to ACL from Gadchandur road. In addition, speed surveys were conducted in the form of spot speed study at selected locations leading to the proposed mining road coupled with Speed and Delay studies starting from the gate of ACL factory main gate up to the start of the Nandgaon Ekodi mines. Efforts were made to collect First Information Report *(FIR)* data on road crashes that occurred on the above roads by seeking the help of M/s. ACL officials who have basically collected the above data from respective police stations due to their local acquaintance. The above data was primarily collected to take a stock of road safety of road users and its consideration in the report. Further, the study team also held discussions with ACL officials. A typical illustration of the existing connectivity to the cement plant and selected traffic survey locations is given in Fig. 1.

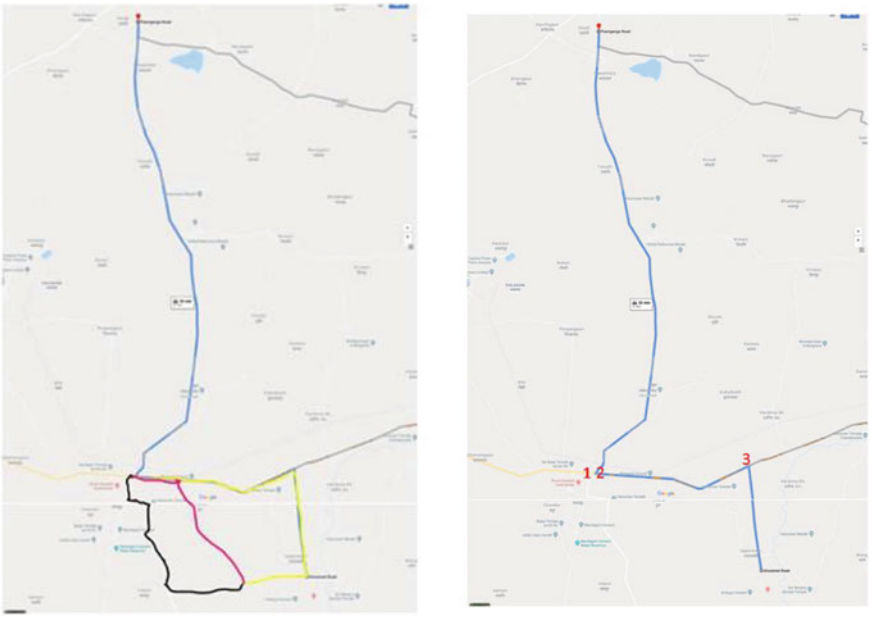

Fig. 1 Map showing the three routes and the selected locations for traffic surveys

4 Data Collection and Analysis

4.1 Midblock Volume Counts

The midblock counts on various road links in the study area were deduced from the intersection volume counts. Thus, the midblock locations covered in the CVC study include Bhoyegaon, Gadchandur state highway, Manikgarh Plant road, Korpana, Balasore and road leading to ACL plant. The PCU factors *[as per CSIR-CRRI (2018)]* given in Table 1 are used for the conversion of CVC into overall PCUs whereas the deduced peak hour flows at the referred locations are presented in Table 2. It can be noted that the peak hour periods are obtained individually for the midblock unlike for the intersection peak period and hence intersection and midblock peak periods may vary a bit.

4.2 Spot Speed Studies

The speed surveys are conducted in such a way that it should serve as representative for speed profile of the entire study section. The location chosen is a straight one, which did not have any influence due to merging of any local traffic. The results of the

Table 1 PCU factors (Indo–HCM: 2018)

PCU factors	SCars	Bcar	Tractors	Tractor and trailors	Cycles	Others	Two wheelers	Auto rickshaws	Auto LCV	LCV	Bus	Mini buses	2-Axle trucks	3-Axle	Multi axle trucks
	1	1.6	7	7	0.4	11.5	0.3	1.2	2	3	4.5	3	5	5	6

Table 2 Peak hour flows on different midblock

Interssection	Mid block	Peak time	SCars	Bcar	Tractors	Tractor and trailors	Cycles	Others	Two wheelers	Auto rickshaws	Auto LCV	LCV	Bus	Mini buses	2-Axle trucks	3-Axle	Multi axle trucks	Total vehicles
Transport nagar	ACL	18.45	19	5	0	0	7	0	270	2	0	5	3	1	3	3	12	330
	Gharchandur	13	61	16	0	4	4	1	431	17	58	30	20	1	7	15	25	690
	Balsore	17	49	52	0	5	0	0	402	22	26	25	18	0	0	3	25	627
Ghadcha ndur	Koripana	10.15	54	72	0	8	37	4	912	31	0	75	13	9	57	22	3	1297
	Bhoygaon	9.15	5	16	0	5	8	3	254	7	0	17	2	1	13	17	20	368
	Balsore	9.3	52	53	0	6	12	4	705	12	0	78	8	7	58	26	9	1030
Manikghar	Manikgar	11.45	48	53	0	2	6	0	478	31	19	9	12	0	6	50	30	744
	Koripana	13.45	62	75	0	8	10	0	883	58	61	65	19	7	13	55	36	1352
	Railway line	15	11	6	0	2	19	0	102	51	24	2	0	0	6	13	2	208
	Gharchandur	13.45	76	61	0	15	11	0	1034	63	68	69	17	8	23	26	41	1542

Table 3 Spot speed survey results on nandgaon midblock

Parameters	All	Car	2W	LCV	2 axle truck	MAV
Sample size	316	23	192	6	33	74
Minimum speed (Km/h)	6	31	16	32	18	6
Maximum speed (Km/h)	65	65	61	49	31	49
Mean speed (Km/h)	37.1	45.4	39.5	42.5	28.3	33.1
Average (Km/h)	35.0	43.7	37.6	40.3	25.3	31.0
15th percentile speed (Km/h)	23.1	31.8	25.9	29.8	14.8	21.2
50th percentile speed (Km/h)	32.5	38.8	34.3	39.2	25.0	27.3
85th percentile speed (Km/h)	41.5	47.2	42.1	43.0	36.3	35.8
95th percentile speed (Km/h)	47.1	59.6	48.7	46.0	31.8	39.8

survey are given in Table 3. The overall 85th percentile speed considering all vehicle types is around 41.5 Kmph whereas 85th percentile speed of two wheelers, cars, LCVs and MAVs are 47.2, 42.1, 43.0 and 35.8 Kmph respectively. This phenomenon may be attributed to the fact that the road section being Intermediate Lane Road and speeds are almost the same across various categories of fast moving vehicles except MAVs.

5 Estimation of Horizon Year Traffic on Link Roads

As mentioned above, ACL has proposed three routes for transportation of mining material from Nandgaon/Ekodi to ACL plant. One link is common for the above three routes which is from Gadchandur to Nandgaon/Ekodi mines. The three possible routes from Gadchandur to ACL plant with distances based on Google map are given below:

- **Route 1**: Gadchandur to ACL via existing SH through Transport Nagar intersection (21 km) *(Yellow line in Fig. 1).*
- **Route 2**: Gadchandur to ACL via Manikgarh plant joining behind ACL (18 km) *(Black line in Fig. 1).*
- **Route 3**: Gadchandur to ACL via **proposed road from State Highway to ACL joining behind ACL** plant *(17.4* km*) (Pink line in Fig. 1).*

Annual growth factors for various vehicle types were assumed between 1 and 3% depending on its observed proportion. As mentioned earlier, ACL has proposed 2.0 MTPA of mines material transport, which amounts to each tipper carrying 30 tonnes coupled with 300 days of working days and hence totaling 6700 tonnes per day which implies that the total truck-load trips required per day are estimated to be 223. In this context, the empty/dead trips back to crusher also added to the road traffic yielding an additional 223 additional trips per day and thus the total trucks

would be 446 per day. ACL has considered 12 h working in a day which yielded 37.2 vehicles *(rounded to 38 vehicles)* through uniform distribution. This traffic due to mines is added to all links of three route options to understand its effect Level of Service *(LoS)* of all links. The estimated year-wise ramp up of the Lime Stone Transportation as per ACL is given in Table 4. As per the Indo-HCM *(2018)* and IRC: 64 [2], Design Service Volume *(DSV)* at LoS-B i.e. *Volume by Capacity ratio (V/C)* of 0.3 at LoS-B that can be handled by intermediate lane is 645 PCUs whereas in the case of two lanes, it is 930 PCUs at V/C of 0.45.

V/C ratio and LoS for base year and horizon year traffic with and without Nandgaon Ekodi Mines are presented in Table 5.

Table 4 Estimated year-wise ramp up of the lime stone transportation as per ACL

Year	Production (in MTPA)	Trips/Hour	Trips per day
Year-III (Feb 2022)	0.1	2	23 (considering 30 t per truck)
Year-IV (Feb 2023)	0.0.2	4	45 (considering 30 t per truck)
Year-V (Feb 2024)	2.0	38	447 (considering 30 t per truck)

Table 5 V/C ratio and LoS for Base Case and Horizon Period Traffic with and Without Mines (CRRI, 2019)

Interssection	Mid block	Peak time	Base year (Feb 2019)			With annual growth (Feb 2024)			Both growth and full mines capacity (Feb 2024)		
			Total PCUs	V/C ratio	LoS	Total PCUs	V/C ratio	LoS	Total PCUs	V/C ratio	LoS
Transport nagar	ACL	18.45	247	0.08	A	288	0.09	A	478	0.15	A
	Gharchandur	13	836	0.27	B	969	0.31	B	1159	0.37	B
	Balsore	17	687	0.22	A	791	0.26	B	981	0.32	B
Ghadcha ndur	Koripana	10.15	1320	0.37	C	1517	0.42	C	1707	0.47	C
	Bhoygaon	9.15	521	0.24	A	590	0.27	B	780	0.36	B
	Balsore	9.3	1221	0.39	B	1395	0.45	B	1585	0.51	C
Manikghar	Manikgar	11.45	909	0.29	B	1036	0.33	B	1226	0.40	B
	Koripana	13.45	1556	0.43	C	1793	0.50	C	1983	0.55	D
	Railway line	15	259	0.12	A	300	0.14	A	490	0.23	A
	Gharchandur	13.45	1753	0.57	C	2019	0.65	D	2209	0.71	D

Under the column, peak time/Peak hour 18.45 means 18:45 to 19:45. 13 means 13:30 to 14:00, 17 means 17:00 to 18:00

6 Conclusions

- The maximum peak hour traffic handled at present on Bhoyegaon road *(which is a common link for three routes)* is 521 PCUs. The estimated V/C ratio by 2024 based on natural annual growth factors and coupled with the assumption of full functioning of Ekodi mines is 0.36 *i.e. Los B*. This implies that LoS is expected to change from LoS A to LoS-B after the opening of Ekodi mines which means *that the opening of mines has a mild i*mpact on the capacity of this link and is expected to operate well within good operating conditions.
- The maximum peak hour traffic handled at present on Gadchandur road towards transport Nagar is 836 PCUs. The estimated V/C ratio by 2024 based on natural annual growth factors and coupled with the assumption of full functioning of Ekodi mines is 0.37 *i.e. Los B*. This implies that LoS would remain virtually the same before and after the opening of Ekodi mines meaning thereby Ekodi mines would have insignificant impact on the capacity of this link.
- The maximum peak hour traffic handled on Manikgarh road is 909 PCUs. The estimated V/C ratio by 2024 based on natural annual growth factors and coupled with the assumption of full functioning of Ekodi mines is 0.40 *i.e., Los B*. This again implies that LoS would remain virtually the same before and after the opening of Ekodi mines meaning thereby Ekodi mines would have insignificant impact on the capacity of this link.
- The maximum peak hour traffic handled at presented on the four lane divided road section near the intersection of Manikgarh and Gadchandur is 1753 PCUs. Further, the traffic expected *(in PCUs)* to be handled after 5 years by considering natural annual growth factors coupled with the assumption of full functioning of Ekodi mines would be 2209 PCUs.

7 Proposed Improvements

The observed traffic flow and composition of traffic in the base year *i.e. February 2019* and projected horizon year traffic due to natural growth coupled with the proposed mine after 5 years; there is a need for the expansion after 2024. As such, State Highway passing through Transport Nagar, Gadchandur and Korpana is in good condition. Another link starting from Manikgarh intersection and joining behind ACL plant via Sona road is a newly built road except for the part of the road from the Manikgarh intersection plant needing attention and removal of encroachments, maintenance of shoulders and repair of pot holes and strict enforcement towards prohibition of on street parking which is a hindrance to smooth traffic flow. Similarly, the link road connecting Nandgaon Ekodi mines to Gadchandur is also in good condition except at few places needing removal of encroachments, proper upkeep of earthen shoulders and repair of potholes and strict enforcement of on street parking. Considering the above estimated traffic scenario in the horizon period of 2024 *(vide*

Tables 4 and 5), it is concluded that there is no need for any road expansion of any of the above four link roads except for their proper upkeep.

The existing four lane divided road having two staggered intersections of Gadchandur and Manikgarh needs immediate geometric improvement which would help in achieving smoother radii for turning traffic considering the proportion of multi axle trucks would increase after the opening of the proposed mines. Further, it is recommended towards implementation of strict enforcement in terms of prohibition of on street parking and removal of encroachments. These measures should be supplemented with the immediate repair and rehabilitation measures of the existing road from Gadchandur to Nandgaon and Ekodi in the form of pothole repair and overlay. In summary, it is recommended that needful measures shall be done on the above intersections and existing road sections, which would help to enhance the safer commuting environment for the mixed mode traffic witnessed on the above Project Corridor.

The ill designed roundabout at Manikgarh intersection is not designed conforming to IRC: 65 [5] titled, "Guidelines for Roundabout Design". Due to its poor design, multi axle trucks find it difficult to make a safe negotiation. It was noted during the field studies that due to in sufficient radii of the above roundabout, negotiating traffic are in direct conflict with straight/other turning traffic. Though the peak hour flows handled at these intersections are in the order of about 2000 PCUs per day in the future, the movement of multi axle trucks has to be managed properly. Hence it is necessary to redesign the roundabout conforming to IRC: 65 [5] by providing adequate diameter of around 15 m as well as improve the staggered intersections coupled with posting of necessary road signs, road markings [conforming to IRC:67 (2022) and IRC:35 (2015)] and street lighting.

Conforming to IRC: 64 [2], IRC: SP-73 (2019) and CSIR–CRRI (2018), it is recommended to provide paved shoulders of 1.5 m wide plus 1.0 m earthen shoulder to facilitate the safe passage for bicyclists and pedestrians so that they can use the shoulder portion. As such, the crossing of pedestrians is negligible and hence there is no need for the provision of grade separated pedestrian facilities at any location on the Project Corridor. Though the existing speed humps in village portions are acting as safe environs for VRUs to cross the road, but their non-standard erections not conforming to IRC: 35 [4] and IRC: 67 (2022) poses serious safety hazardous for the motorists which need to be rectified.

In summary, the route from Gadchandur to ACL via the proposed road from State Highway to ACL joining behind ACL plant is the best route amongst the three routes due to its advantages like shortest distance, devoid of any interaction with local traffic and environment friendly. Incidentally, the proposed improvements were implemented on the ground by M/s. ACL at their own cost after the approval by Environmental Impact Assessment committee, which is presented in Fig. 2.

Fig. 2 Present road condition after capacity augmentation (Road Marking yet to be completed)

Reviewer 1		
1	Grammar mistakes and typos are present in the Manuscript	Corrected
2	Introduction is poorly written	Complete rewrite made
3	What problem do authors need to be addressed through this study?	Capacity augmentation of a mining plant and assess its impact on the traffic plying on the adjoining road network coupled with fixing best route from mining area to the cement plant
4	What is the reference for PCU factors?	Reference mentioned in the revised paper
5	Poor representation of Figure and Table	Table and figures refined
6	Font is not uniform throughout the study	Corrected in the revised paper
7	Section 7 should be well organised	Major rewrite made to address the comments
Reviewer 2		
1	The author did not refer or cite any past study regarding the given topic. No single reference has been found in the introduction or methodology part. The relevance of the study with the progress of the given topic in terms of research is unclear	Project report reference added. Capacity augmentation of a mining plant and assess its impact on the traffic plying on the adjoining road network coupled with fixing best route from mining area to the cement plant
2	Figure 3.1 was drawn by hand and was not clear, not visible and very poor. It should be expected to place a line diagram created with the help of simple MS-paint software	Replaced
3	The Source of Table 4.1 is not mentioned	Corrected and Mentioned

(continued)

(continued)

Reviewer 1		
1	Grammar mistakes and typos are present in the Manuscript	Corrected
4	Table 4.2 has a title peak hour traffic in different midblock, but the last column of the table shows the total number of vehicles, not the PCU calculated. The time shown in Table 4.2 is 18.45, 13, 17, etc.; what does it mean???	Rectified. It is traffic flows in the peak hour. Peak hour 18.45 means 18:45 to 19:45. 13 means 13:30 to 14:00, 17 means 17:00 to 18:00. Made changes in the text
5	What is the significance of spot speed analysis? The authors have made no inferences	Based on the inference drawn, appropriate speed limit has been proposed
6	Please justify vehicular annual growth rate value	Time series and vehicle registration data was not available to estimate growth rates as per IRC. Hence suitably assumed
7	Table 5.1, for year IV, the production value is zero. Even after having zero production, four trips per hour are required. How is this possible???	Some mistake in format; it is now 0.2 which is corrected
8	The comparison in Table 5.2 indicates no such effect will be experienced after having these new vehicles from mines. What is the outcome of the study??	Augmentation study was done to see impact of proposed mining trips and found within Level of Service operating conditions. Only few links LoS is dropping below LoS B and recommended for improvements
9	The proposed improvements suggested at the end of the study are more focussed on the intersection and geometric improvement strategies. The present analysis does not show any evidence regarding that. The study carried out traffic forecasting and capacity estimation analysis. How does this analysis justify the safety and design aspect of any intersection of midblock?	Intersection survey was done to see arrive traffic flows on different approaches of mid blocks to check LoS. The geometric improvements of intersections suggested based on field observations with regard to safety and delays

References

1. CSIR - CRRI (2017) “Indian Highway Capacity Manual” A report submitted to Council of Scientific and Industrial Research *(CSIR)*, New Delhi.
2. IRC: 64 (1990) “Guidelines for Capacity of Road in Rural Areas”, Indian Roads Congress, New Delhi.
3. IRC: SP-73 (2015) “Manual of Specifications and Standards for Two Laning of Highways with Paved Shoulders *(First Revision)*, Indian Roads Congress, New Delhi.
4. IRC: 35 (2015) “Code of Practice for Road Markings (*First Revision)*”, Indian Roads Congress, New Delhi.

5. IRC: 65 (2017) titled, "Guidelines for Roundabout Design", *(First Revision)*", Indian Roads Congress, New Delhi.
6. CRRI Report (2019), Evolving Feasible Transportation Route from Ambuja Cement Limited (ACL) Plant to the proposed Nandgaon Ekodi Mines in Chandrapur District of Maharashtra", A report submitted to M/S Ambuja Cement Ltd.

Effect of Lateral Shift of a Vehicle on Following Vehicles

Heikham Pritam Singh, Ashutosh Kasoundhan, Shubham Thapliyal, and R. B. Sharmila

Abstract Developing countries generally have mixed traffic conditions with non-lane discipline, which causes lateral interaction of multiple vehicles within a single lane. The lateral movement of vehicles affects traffic flow and few studies have been done on vehicle lateral behavior in mixed traffic conditions. Only a small portion of these studies have examined how the lateral movement of a vehicle affects the vehicle that follows it. This research aims to understand and analyze the behavior of the following vehicles due to the lateral shift of their leader vehicles. Trajectory data of vehicles procured from an urban arterial road in Guwahati was used for the study. Two cases of a lateral shift are considered and studied separately. Additionally, a model is developed to forecast how lateral shifts would affect the driving behavior of following vehicles in terms of the top speed attained by those vehicles. Different explanatory variables such as the space gap between vehicles and the speed of vehicles are considered. Finally, it is found that a vehicle's lateral shift has a considerable impact on its following vehicle.

Keywords Trajectory data set · Modeling · Following behavior · Lateral shift · Mixed traffic · Lateral movement

H. P. Singh (✉) · A. Kasoundhan · S. Thapliyal
Civil Engineering Department, Transportation Systems Engineering, Indian Institute of Technology Guwahati, Guwahati 781039, India
e-mail: heikham.pritam@iitg.ac.in

A. Kasoundhan
e-mail: ashutoshkasoundhan@iitg.ac.in

S. Thapliyal
e-mail: shubham.thapliyal@iitg.ac.in

R. B. Sharmila
Civil Engineering Department, Indian Institute of Technology Guwahati, Guwahati 781039, India
e-mail: rb.sharmila@iitg.ac.in

A. Dhamaniya et al. (eds.), *Recent Advances in Traffic Engineering*, Lecture Notes in Civil Engineering 377, https://doi.org/10.1007/978-981-99-4464-4_29

1 Introduction

In developing countries like India, the traffic is composed of a much larger variety of vehicles. In contrast to affluent nations, where cars predominate the traffic composition, developing nations have considerable amounts of practically all vehicle kinds. These different types of vehicles vary in size and maneuverability leading to the different behavior of the vehicles. The use of lane division is also not much followed in case of mixed traffic. So, in heterogeneous traffic conditions, more diversified lateral behavior of vehicles is seen.

The lateral behavior of vehicles is mostly studied in the form of lane-changing behavior. The process of changing lanes is often divided into two categories. In the first category, it is mandatory for the vehicle to change lanes in order to move toward its desired path. The other category is discretionary lane change where the driver changes lanes only to achieve a desired speed or driving condition and is not mandatory to reach the desired destination.

There has been some research on the direction of lane change where deterministic rules were adopted along with random utility models [14]. Gap acceptance models have also been employed for modeling the execution of lane change where the available gap is checked for the feasibility of lane change [3, 5, 11]. Moreover, Lateral dynamics models have been used for modeling the lane change execution process [7]. The majority of vehicles chose the center of the road for driving in undivided mixed traffic conditions [6]. Duration of lateral shift [1] has also been used to research drivers' lateral behavior.

Little research has been conducted on how drivers behave laterally in mixed traffic. The definition of lane change is inappropriate in case of mixed traffic. As the width of a lane may not be acceptable for different sizes of vehicles. Smaller vehicles like bikes can make sufficient lateral movement for overtaking within a single lane. The lateral shift will be a better parameter to analyze the lateral behavior of vehicles in this case. Different authors have adopted different definitions of lateral shift based on the requirements of their study. The lateral movement of a vehicle that is at least equivalent to its width is known as a lateral shift [9]. If a vehicle shifts about its centerline along the width of a road, then it is considered a lateral shift [10]. In this study, lateral shift is defined for two different cases, one for initiation and another for completion.

Vehicles' lateral behavior in mixed traffic circumstances is influenced by the lateral behavior of the vehicles in front of them [12]. The effect of lane changing on minimum spacing and response time of the following driver [16] is one of the very few studies that have been done regarding the microscopic effects of a lateral shift on the surrounding vehicles.

Therefore, there is a need to research how neighboring vehicles behave when their front vehicles make a lateral movement. The present study aims at identifying the behavior of the following vehicle when its leader makes a lateral shift with the following objectives:

- Understanding the interactions among the surrounding vehicles of laterally shifting vehicles.
- Analyze the effect of lateral shift on the maximum speed of the following vehicles.
- Identify the significant factors affecting the following vehicles' behavior due to the lateral shift of a vehicle.
- Develop a model to predict the maximum speed made by the following vehicles due to the lateral shift of their leading vehicles.

A detailed literature review is done in the next section. In Sect. 3, the methodology of data collection, extraction, and identification of lateral shifting vehicles is described. The Sect. 4 discusses the data analysis of lateral shifting vehicles and following vehicles. The Sect. 5 presents the modeling of maximum velocity along with a discussion of the explanatory variables. The conclusion of the study is given in the Sect. 6. In the end, the scope for further research is discussed in Sect. 7.

2 Literature Review

Different studies have been done in the field of lateral behavior of vehicles. Most of these studies were however done for homogenous traffic conditions. To understand the behavior of following vehicles when their leader vehicle (LV) makes a lateral movement, the lateral behavior of the vehicles should be understood first. Different parameters have been used to understand the lateral behavior of vehicles.

One of the most often utilized characteristics to study the lateral behavior of vehicles is the time span of the lane change. Tijerina et al. [13] used the definition of lane change as a vehicle's purposeful lateral movement to cross the lane line and into the neighboring lane. In the study, the authors found out that the duration of lane change varies across city streets and highways. Similarly, Hanowski [4] also considered lane change to be the action of crossing the lane boundary and entering the adjacent lane. It was discovered that the duration of the lane transition was significant, ranging from 1.1s to 16.s. Toledo and Zohar [15] modeled the time it took for a lane shift assuming that a vehicle changes lane once it moves from one lane to the one right next to it. Vehicles were regarded as making several lane changes when they crossed two or more lanes in a row.

Moridpour et al. [8] used a non-linear GM model to analyze the longitudinal behavior of cars and heavy vehicles. In the study, it was found that while changing lanes, the drivers of trucks kept practically constant speeds and did not accelerate or decelerate to modify their speeds in accordance with the speed of vehicles in the target lane. Drivers of cars, however, often speed up prior to the start of the lane-changing move until it is complete, matching their speed to the vehicles moving in the target lane. The findings show that heavy truck and passenger car drivers behave differently when executing lane changes. Cao et al. [2] considered lane change to be a gradual process while modeling the duration of the lane change and discovered that lane change execution is influenced by traffic conflict during lane change events.

Lateral placement of vehicles has also been used to investigate how drivers behave laterally on the road. Kotagi et al. [6] found that the majority of the vehicles chose the middle of the road to move along in undivided mixed traffic conditions. In the study, it was also found that lateral separation of vehicles depends on the subject vehicle's size and the speed of the opposing vehicle. Gap acceptance models have also been used for modeling the execution of lane change where the available gap is checked for the feasibility of lane change [3, 5, 11]. In addition to the gap acceptance model, Lateral dynamics models are also used for modeling the lane change execution process Mathew et al. [7].

Most of these researches, however, were done for homogenous traffic and very few of them are based on mixed traffic. For the condition of mixed traffic, the term "lane change" becomes inappropriate as in mixed traffic conditions various sizes of vehicles are there and the definition of a lane will not apply to all the vehicles. So, the term "lateral shift" is generally used for mixed traffic conditions. Over time, different definitions of the lateral shift have been used. Munigety et al. [9] defined lateral shift as the movement of a vehicle laterally at least equal to its width. Pal et al. [10] considered a vehicle to be laterally shifted if the vehicle shifts about its centerline along the width of a road. Raju et al. [12] found out that the lateral behavior of vehicles can have a significant impact on their following behavior in heterogeneous traffic. The authors studied vehicle behavior in mixed traffic.

By reviewing different studies, it is seen that all these studies focus mostly on the behavior of laterally shifting vehicles. There arises a need to study the effect of the lateral movement of a vehicle on its surrounding vehicles. Zheng et al. [16] did a study to analyze the minimum spacing and response time of following drivers due to lane change of a vehicle. Hence, the current study focuses on analyzing and modeling changes in the velocity of following vehicles when their leader vehicle (LV) makes a lateral shift.

3 Dataset

3.1 Data Collection

Four-hour video data was recorded on a stretch of G.S. Road, Guwahati city, India. It is an urban arterial road with two lanes in each direction. The selected stretch is straight with a width of 6.9 m and a length of 250 m. The camera was placed on a foot-over bridge located at that road stretch. A screenshot of the video recording is shown in Fig. 1a. The plan of the study section is shown in Fig. 1b.

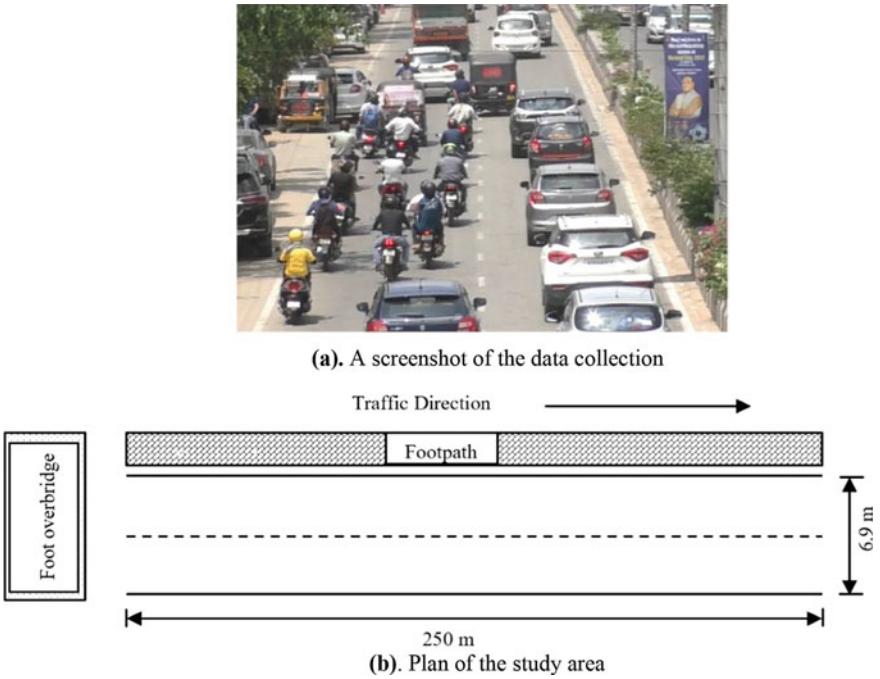

Fig. 1 **a** A screenshot of the data collection. **b** Plan of the study area

3.2 Data Extraction

For data extraction, the video data first was visually monitored to select a time slot giving maximum lateral shift. A time slot of 30 min between 11:00 a.m. and 11:30 a.m. was selected for the extraction. IIT Bombay Traffic Data extractor was used for the extraction of trajectory data of the vehicles along with the vehicle type. A rectangle of length 46.3 m and width 6.9 m was marked on the road and used for calibration on the software. 75,765 observations were extracted which is composed of 1425 vehicle trajectories. The extracted data consist of vehicle id, time, frame no., longitudinal coordinate, and lateral coordinate. By the use of the 3-point moving average approach, the retrieved data was smoothed. From this data, the instantaneous speed along with the acceleration of the vehicles was calculated. Python code was used to determine the leading and trailing vehicles of each vehicle at each time frame, as well as their corresponding speeds, accelerations, and vehicle types.

Cars (37.26%) and two-wheelers (51.79%) were found to be the predominant vehicle on the road. The traffic flow on the road stretch is 1312 PCU/h as per the passenger car unit given by IRC 106–1990. A Summary of traffic flow characteristics is given in Table 1.

Table 1 Summary of traffic flow characteristics

Vehicle type	Average speed (m/s)	Composition (%)
Auto	7.5	5.47
Bus	7	1.68
Car	7.66	37.26
Heavy vehicles	6.9	0.42
LCV	7.42	3.37
Two-wheeler	8.25	51.79

3.3 Search Area

Not all the vehicles moving behind another vehicle shows the following behavior. The leader vehicle (LV) should be within a certain range of distance both laterally and longitudinally to affect the behavior of the following vehicle. So, it is necessary to find out the maximum space headway up to which a vehicle shows the following behavior of the leader vehicle (LV). Search area has been used to depict this maximum headway along with its width and has been defined as the area in front of a vehicle within which the leader vehicle (LV) must be present so that the vehicle is motivated to show the following behavior [1].

In this study, the search area has been defined as the prismatic projected area of vehicles along the direction of traffic where the presence of any other vehicle can affect the movement of the vehicles longitudinally as shown in Fig. 2. Here, vehicle B is in the search area of vehicle A, which will affect in longitudinal movement of vehicle A. Whereas vehicle C is out of the search area so, it will not have any effect on the longitudinal movement of vehicle A. The search area's breadth is considered to be equal to the width of the vehicle. Sensitivity analysis, which compares the average relative speeds of two subsequent vehicles with their space headways, is employed to determine the search area's effective length. It gives an idea of up to what maximum space headway, a vehicle tries to follow its leading vehicle. As seen in Fig. 3, the maximum relative speed is seen at a space headway of 70 m. So, it is concluded that the leading vehicle affects the following vehicle up to only 70 m effectively, and hence the effective search area's length is adopted as 70 m.

3.4 Definition of Lateral Shift

Two different cases of lateral shift are considered in this study as given below.

Case 1. When the subject vehicle (SV) makes a lateral shift and moves away from the following vehicle laterally, leaving more space in front of the following vehicle (FV) as shown in Figs. 4. and 5.

Here the behavior of FV due to shifting away of SV laterally is studied. It is believed that the following vehicle will accelerate to cover up the space in its front.

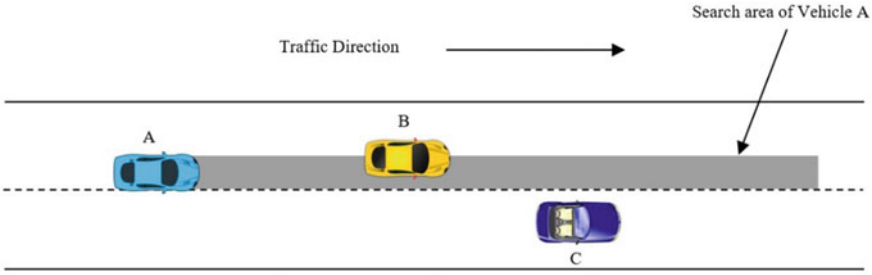

Fig. 2 Search area of a vehicle

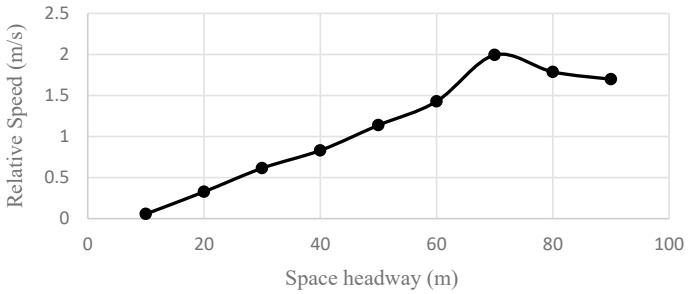

Fig. 3 Sensitivity analysis to determine the search area's length

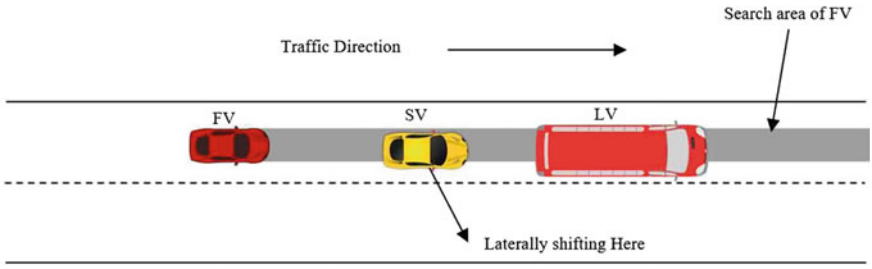

Fig. 4 Case 1—Before lateral shift

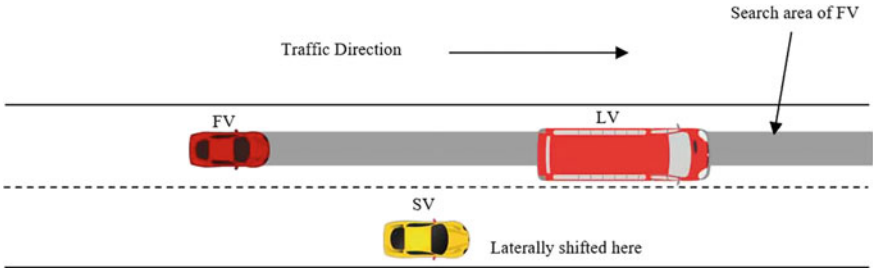

Fig. 5 Case 1—After lateral shift

So, in this case, the maximum speed up to which the following vehicle reaches is analyzed. The starting time of a lateral shift is of main importance in this case and is taken at the instant when the subject Vehicle (SV) moves out of the search area of the current following vehicle. In this case, there is no requirement for the completion time of the lateral shift, and is not considered. To identify the subject vehicles which have shifted away, the following conditions should be satisfied:

(a) Subject vehicle (SV) should be within the search area of FV just before the lateral shift, initially.
(b) Subject vehicle (SV) moves laterally at least equal to its width [9].
(c) Subject vehicle (SV) moves completely out of the search area of their following vehicle, finally.

Case 2. When the subject vehicle (SV) makes a lateral shift and moves toward the target following vehicle (FV) laterally, occupying the space in front of the following vehicle (FV) as shown in Figs. 6. and 7.

Here the behavior of FV due to laterally shifting into SV is studied. In this case, it is believed that the following vehicle (FV) will decelerate as soon as a new subject Vehicle (SV) is introduced to increase its spacing. So, the maximum speed maintained by the following vehicle (FV) is of the main importance here. In this case, the instance of the introduction of a subject vehicle (SV) in the search area of the following vehicle (FV) is considered as the completion time of the lateral shift. The initiation time of

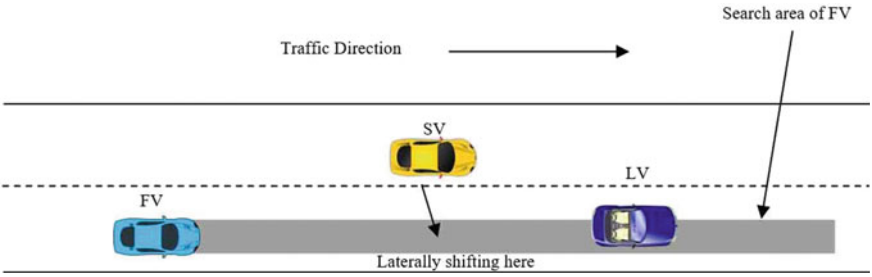

Fig. 6 Case 2—Before lateral shift

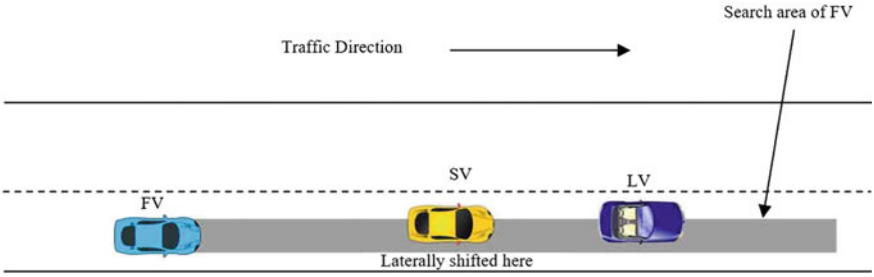

Fig. 7 Case 2—After lateral shift

Table 2 Descriptive statistics of maximum speed adopted by the following vehicles within 5 s after lateral shift

	Case 1 (Max. velocity, m/s)	Case 2 (Max. velocity, m/s)
Mean	11.31	10.48
Mode	6.56	10.2
Median	10.52	9.91
Standard deviation	4.63	3.83

the lateral shift is not required and hence is not considered in this case. The following conditions should be satisfied to identify laterally shifted vehicles.

(a) The Following vehicle (FV) moves laterally at most equal to its width
(b) Subject vehicle is introduced into the search area of the following vehicle (FV).

4 Data Analysis

4.1 Case 1

A total of 2700 lateral shifts were identified. The instant SV gets out of the search area of FV is considered the starting point of lateral shift and there is no requirement of finding out the finishing time of lateral shift in this case. Here the maximum speed of the following vehicles due to lateral shift within 5 s from starting of the lateral shift was analyzed. Out of the 2700 lateral shifts, only 1370 (50.7%) following vehicles increased their speed within 5 s from starting of the lateral shift. The descriptive statistics of the maximum speed adopted by the vehicle are given in Table 2.

4.2 Case 2

A total of 8333 lateral shifts were identified. In this case, the moment a subject vehicle (SV) enters the search area of the following vehicle (FV) is taken as the finishing time of the lateral shift. There is no requirement for starting time of the lateral shift in this case. Here the maximum speed of the following vehicles due to the lateral shift of SV within 5 s from the completion of the lateral shift is analyzed. 6601 following vehicles (79.21%) decreased their speed within 5 s from completion of lateral shift. The descriptive statistics of the maximum speed adopted by the vehicle are given in Table 2.

5 Model for Maximum Velocity

The maximum velocity of the following vehicles within 5 s can depend on many variables like initial speed, acceleration, and space headway of FV, SV, and LV. A multiple linear regression model is developed to forecast the maximum velocity for both cases as in Eq. 1. The variables used in the model however may differ for two different cases.

$$V_{max} = a_o + a_i X_i + \varepsilon \tag{1}$$

where V_{max} = maximum velocity of FV; a_o is the intercept; X_i is the vector of explanatory variables and a_i is its corresponding coefficients; ε is the error term.

5.1 Case 1

The algorithm for extraction of required variables used in modeling is given below:

Algorithm 1. Extraction of data required for modeling in case 1.

Here all the vehicles are considered to be the subject vehicle (SV) and they are checked for the lateral shift.

- ***Start***
- For all vehicles, for all time frames, get leading and following vehicles if present within the search area along with their speed, acceleration, and vehicle types.
- For all vehicles, get the cumulative lateral shift.
- If cumulative shift >= width of vehicle & previous following vehicle != current following vehicle; return lateral shift = yes.
- For all laterally shifted vehicles, get the maximum speed of the following vehicle (FV) within 5 s after lateral shift, space headway between laterally shifting vehicle and its following vehicle (FV), space headway between the following vehicle (FV) and leader vehicle (LV) of laterally shifting vehicle.
- ***End***

The variables used in this case are given in Table 3. Here the values of independent variables are taken at the instant of starting of the lateral shift whereas the value of the dependent variable is taken within 5 s from starting of the lateral shift.

The summary statistics of independent variables with their best-fitted distribution are given in Table 4.

By multiple linear regression of data of vehicles increasing their speed after the lateral shift of subject vehicles, the significant independent variables are identified and shown in Table 5. At a 95% confidence level, all the variables are discovered to be significant. The effect of different variables on the models is explained below with illustrations in Fig. 8.

Table 3 Statistical summary of variables considered in the model for case 1

	Variable	Mean	Std deviation
Independent variables	SV speed (m/s)	8.753	3.494
	LV speed (m/s)	8.842150	3.948
	FV speed (m/s)	6.291	2.705
	FV acceleration (m/s^2)	−0.442	3.742
Dependent variable	Max velocity of FV	11.363	4.066

Table 4 Summary of the statistical parameters of the best-fitted distribution for variables used in case 1

Variable	Type of distribution	Parameters
SV speed	Gen. extreme value	$K = -0.08311\ \sigma = 2.8837\ \mu = 7.2587$
LV speed	Gen. extreme value	$K = 0.01639\ \sigma = 2.707\ \mu = 7.0079$
FV speed	Logistic	$\sigma = 1.4325\ \mu = 6.1543$
FV acceleration	Gen. extreme value	$K = 0.40717\ \sigma = 2.1802\ \mu = -1.1523$

Table 5 Estimation result of max. velocity of FV in case 1

Term	Coefficient	Std error	t-ratio	p-value
Intercept	3.6968923	0.31159	11.86	0.0001
SV speed	0.1933751	0.030118	6.42	0.0001
FV speed	0.6854141	0.0351	19.53	0.0001
FV acceleration	−0.061696	0.023719	−2.60	0.0094
LV speed	0.230806	0.028035	8.23	0.0001

Note Number of observations = 1370; R-Square = 0.39; adjusted R-Square = 0.39

Effect of significant variables: The effect of all the significant factors on the maximum speed of the following vehicles is discussed below:

Subject Vehicle (SV) speed: The following vehicles try to mimic the behavior of their leader vehicles. If the speed of the leader vehicle (LV) is high, the speed of the following vehicle (FV) is also generally high. So, high SV speed before lateral shift leads to a high initial speed of following vehicles after which they generally accelerate more to occupy the space left by the subject vehicles.

Leader Vehicle (LV) speed: If the speed of the leader vehicle (LV) is high then it gives more liberty to the following vehicles to increase their speed just after the SV has shifted away. However, if the LV speed is very low then it gives more constraints to the increase in speed of the following vehicle (FV).

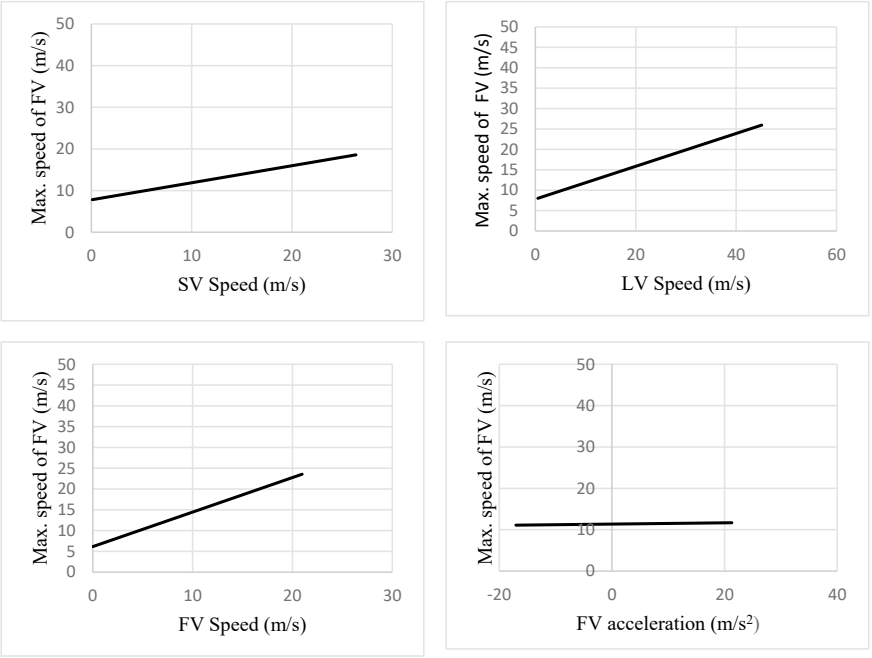

Fig. 8 Effect of significant variables on the maximum speed of FV in case 1

Following Vehicle (FV) speed: If the initial speed of the subject vehicle (SV) is very high, then it is easier to gain a higher speed just after the lateral shift of the subject vehicle (SV).

Following Vehicle (FV) acceleration: The following vehicle's acceleration at the start of the lateral shift has very little effect on the maximum speed of the following vehicle (FV).

5.2 Case 2

The algorithm for extraction of required variables used in modeling is given below:

Algorithm 2. Extraction of data required for modeling in case 2.

Here all the vehicles are considered as a following vehicle (FV) and their leader vehicles are checked for the lateral shift. If a new leader vehicle is introduced in front of FV then that new leader vehicle is taken as subject vehicle (SV) and the former leader vehicle remain as leader vehicle only (LV).

- ***Start***

- For all vehicles, for all time frames, get leading and following vehicles if present within the search area along with their speed, acceleration, and vehicle types.
- For all vehicles, get the cumulative lateral shift
- If cumulative lateral shift of vehicle <= width of vehicle & previous leading vehicle != current leading vehicle; return leader vehicle lateral shift = yes.
- For all laterally shifted leader vehicles, get the maximum speed of the following vehicle (FV) within 5 s after lateral shift, space headway between laterally shifting leader vehicle and its following vehicle (FV), space headway between the following vehicle (FV) and former leader vehicle (LV) of following vehicle (FV).
- ***End***

The variables used in this case are given in Table 6. Here the values of independent variables are taken at the instant of completion of the lateral shift whereas the value of the dependent variable is taken within 5 s from starting of the lateral shift.

The summary statistics of independent variables with their best-fitted distribution are given in Table 7.

By multiple linear regression, the significant independent variables are identified and shown in Table 8. At a 95% confidence level, all the variables are discovered to be significant except for FV acceleration and Space headway between LV and FV. The effect of different variables on the models is explained below with illustrations in Fig. 9.

Effect of significant variables: The effect of all the significant factors on the maximum speed of the following vehicles is discussed below:

Subject Vehicle (SV) speed: The following vehicles try to mimic the behavior of their leader vehicles. If the speed of the leader vehicle (LV) is high, the speed of the following vehicle (FV) is also generally high. So, if a laterally shifting vehicle with high velocity is introduced then the following vehicle (FV) increases its speed to follow that vehicle.

Table 6 Statistical summary of variables considered in the model for case 2

	Variable	Mean	Std deviation
Independent variables	FV speed (m/s)	7.524	3.481
	FV acceleration (m/s^2)	0.565	4.466
	SV speed (m/s)	8.153	3.468
	SV acceleration (m/s^2)	0.247	4.346
	Space headway between SV and FV (m)	19.440	21.544
	Space headway between LV and FV (m)	20.470	22.637
Dependent variable	Max velocity of FV	11.036572	4.167537

Table 7 Summary of the statistical parameters of the best-fitted distribution for variables used in case 2

Variable	Type of distribution	Parameters
SV speed	Lognormal (3P)	$\sigma = 0.17221$ $\mu = 2.7867$ $\gamma = -8.8868$
Space headway between SV and FV	Gen. pareto	K = 0.08019 $\sigma = 16.891$ $\mu = -0..56499$
FV speed	Gen. extreme value	K = −0.22435 $\sigma = 2.2785$ $\mu = 6.0341$
SV acceleration	Gen. extreme value	k = −0..39609 $\sigma = 2.497$ $\mu = -1..0248$
Space headway between LV and FV	Gen. extreme value	k = 0.24995 $\sigma = 10.192$ $\mu = 11.2$
FV acceleration	Gen. extreme value	k = −0.35509 σ = 2.2226 $\mu = -1.1054$

Table 8 Estimation result of max. velocity of FV in case 2

Term	Coefficient	Std. error	t-ratio	p-value
Intercept	4.261	0.130	32.64	0.0001
FV speed (m/s)	0.674	0.013	50.72	0.0001
FV acceleration (m/s^2)	−0.007	0.009	−0.72	0.4687
SV speed (m/s)	0.224	0.013	16.70	0.0001
SV acceleration (m/s)	−0.053	0.010	−5.27	0.0001
Space headway between SV and FV (m)	−0.008	0.002	−3.91	0.0001
Space headway between LV and FV (m)	0.0028	0.002	1.11	0.2687

Note Number of observations = 6601; R-Square = 0.4; adjusted R-Square = 0.4

Following Vehicle (FV) speed: If the initial speed of the following vehicle (FV) is very high, then it is easier to gain higher speed just after the lateral shift of the subject vehicle.

Subject Vehicle (SV) acceleration: If the subject vehicle (SV) accelerates, then it gives a greater opportunity for the following vehicles to gain higher speed just after the lateral shift of the subject vehicle (SV).

Following Vehicle (FV) acceleration: The following vehicle's acceleration at the start of the lateral shift is not affecting the following vehicle (FV) significantly in terms of its maximum attained speed.

Space headway between SV and FV: This variable has very less effect on the maximum speed of the following vehicle (FV). However, with an increase in headway, the maximum speed is also increased slightly to cover up in front.

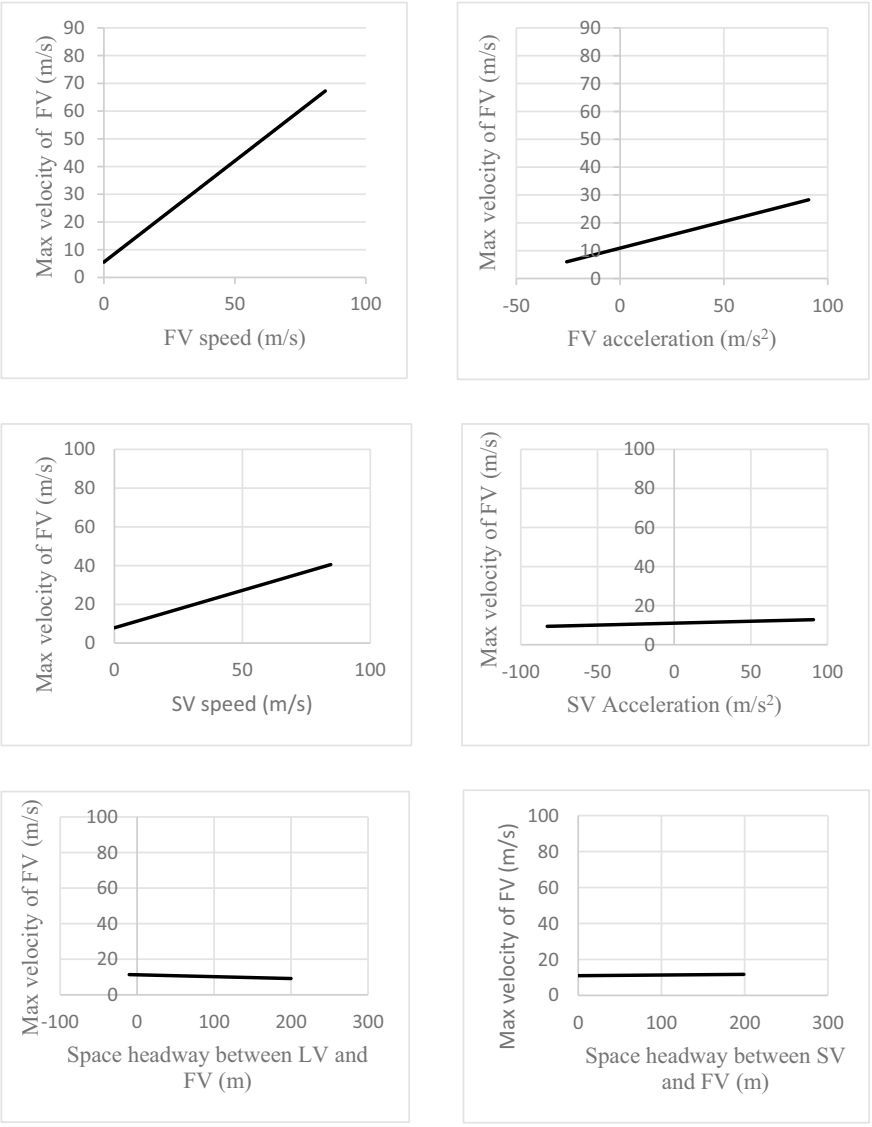

Fig. 9 Effect of significant variables on the maximum speed of FV in case 2

Space headway between LV and FV: This headway is insignificant in explaining the maximum speed of the following vehicle (FV). The reason can be due to the blockage of view due to the introduction of a new subject vehicle between them.

6 Conclusion

Lateral shift is one of the essential components of vehicular movement and it has a significant effect on traffic characteristics both macroscopically and microscopically. Most of the previous studies on lateral behavior have focused on the behavior of laterally shifting vehicles only. In this study, the effect of these laterally shifting vehicles on their surrounding vehicles especially the following has been studied.

The study was done for an urban arterial road in Guwahati city India. The data was collected using a video camera from a foot-over bridge and the trajectory of all the vehicles was extracted using IIT Bombay TDE software. An algorithm was developed to identify the vehicle, which does lateral shift. The results were statistically analyzed and plotted. The behavior of the vehicles was analyzed for two cases separately.

In case 1, the mean of maximum velocity attained by the following vehicle (11.36 m/s) is more than the mean velocity with which the subject vehicle (SV) was initially traveling before the lateral shift. This may be due to the reason that there remains a space as soon as the subject vehicle (SV) leaves the lane hence to fill the space the following vehicle (FV) accelerates and it increases its velocity. A total of 2700 lateral shifts were identified. Out of these 2700 lateral shifts, only 1370 (50.7%) following vehicles increased their speed within 5 s from starting of the lateral shift. Here the low percentage of vehicle accelerating may be due to the reason that there are no safety concerns even if the vehicles don't accelerate.

In case 2 it was found that 79.2% of the following vehicles decelerate within 5 s on the introduction of the subject vehicle (SV) on their front which is significantly higher than that in case 1. This significant proportion of vehicle decelerating may be due to the reason that in this case there arises a risk of collision if the FV doesn't decelerate due to a decrease in headway. So, it is concluded that the lateral shift of a vehicle has a significant effect on the following vehicles.

Additionally, an effort was made to independently forecast the highest speed reached by the FV by the pursuing vehicle during five seconds of the start and end of the lateral shift separately for the two cases. It was found that the speed of FV, SV, and LV were more significant factors affecting the behavior of the following vehicles. Space headway doesn't seem to be having a significant effect on the behavior of the following vehicle.

7 Future Scope

- In this study, a time duration of 5 s was taken for analysis of max. speed after lateral shift. For better accuracy, the time taken for adaptation of following vehicles with new leading vehicles can be analyzed and used instead.
- The effect of lateral shift on macroscopic traffic parameters like flow can be studied.

Only the straight section of the road is considered in this study due to the constraint of data collection. The effect of the geometry of the road on driver behavior can also be studied.

References

1. Asaithambi G, Joseph J (2018) Modeling duration of lateral shifts in mixed traffic conditions. J Transp Eng Part A: Syst 144(9). https://doi.org/10.1061/jtepbs.0000170
2. Cao X, Young W, Sarvi M (2013) Exploring duration of lane change execution. In: Proceedings of Australasian transport research forum. Brisbane, Australia, pp 1–17
3. Choudhury CF, Ramanujam V, Ben-Akiva ME (2009) Modeling acceleration decisions for freeway merges. Transp Res Rec 2124:45–57. https://doi.org/10.3141/2124-05
4. Hanowski RJ (2000) The impact of local/short haul operations on driver fatigue. Ph.D. Dissertation, Dept. of Industrial and Systems Engineering, Virginia Polytechnic Institute and State University
5. Kanagaraj V, Srinivasan KK, Sivanandan R, Asaithambi G (2015) Study of unique merging behavior under mixed traffic conditions. Transp Res F: Traffic Psychol Behav 29:98–112. https://doi.org/10.1016/j.trf.2015.01.013
6. Kotagi PB, Raj P, Asaithambi G (2020) Modeling lateral placement and movement of vehicles on urban undivided roads in mixed traffic: a case study of India. J Traffic Transp Eng (English Edition) 7(6):860–873. https://doi.org/10.1016/j.jtte.2018.06.008
7. Mathew TV, Munigety CR, Bajpai A (2015) Strip-based approach for the simulation of mixed traffic conditions. J Comput Civil Eng 29(5). https://doi.org/10.1061/(asce)cp.1943-5487.0000378
8. Moridpour S, Sarvi M, Rose G (2010) Modeling the lane-changing execution of multiclass vehicles under heavy traffic conditions. Transp Res Rec 2161:11–19. https://doi.org/10.3141/2161-02
9. Munigety CR, Mantri S, Mathew TV, Rao KV (2014) Analysis and modelling of tactical decisions of vehicular lateral movement in mixed traffic environment. In: Proceedings of 93rd transportation research board annual meeting. Transportation Research Board, Washington, DC
10. Pal D, Venthuruthiyil SP, Chunchu M (2020) Characteristics of vehicular lateral shifts in non-lane-disciplined traffic stream. Transp Res Procedia 48:3245–3253. https://doi.org/10.1016/j.trpro.2020.08.153
11. Patil GR, Pawar DS (2014) Temporal and spatial gap acceptance for minor road at uncontrolled intersections in India. Transp Res Record 2461:129–136. National Research Council. https://doi.org/10.3141/2461-16
12. Raju N, Kumar P, Jain A, Arkatkar SS, Joshi G (2018) Application of trajectory data for investigating vehicle behavior in mixed traffic environment. Transp Res Rec 2672(43):122–133. https://doi.org/10.1177/0361198118787364
13. Tijerina L, Garrott WR, Stoltzfus D, Parmer E, Tijerina L, Stoltzfus D, Parmer E (2005) Eye glance behavior of van and passenger car drivers during lane change decision phase. Transp Res Rec: J Transp Res Board
14. Toledo T (2003) Integrated driving behavior modelling. Ph.D. thesis, Dept. of Civil and Environmental Engineering, Massachusetts Institute of Technology
15. Toledo T, Zohar D (2007) Modeling duration of lane changes. Transp Res Rec 1999:71–78. https://doi.org/10.3141/1999-08
16. Zheng Z, Ahn S, Chen D, Laval J (2013) The effects of lane-changing on the immediate follower: anticipation, relaxation, and change in driver characteristics. Transp Res Part C: Emerg Technol 26. https://doi.org/10.1016/j.trc.2012.10.007

Number of Aggregate Sizes and Aggregate Gradation Area: A Correlational Study

Ramu Penki, Subrat Kumar Rout, and Aditya Kumar Das

Abstract Blending aggregates is a procedure of mixing the accessible aggregates for blending to meet the gradation specifications and achieve maximum density. The maximum density of the mix is estimated by considering several aggregate sizes and aggregate gradation areas. Here the research was carried out to find the optimum number of aggregate sizes that are to be adopted in the mix followed by considering the economic factor, it is known that if the no. of aggregate sizes is increased the gradation area decreases and vice versa, due to the presence of more aggregate's size voids can be easily filled. But if there are a greater number of aggregate sizes are adopted the mechanized cost increases so the economy also should be in view while choosing the optimum number of aggregate sizes. An optimum number of aggregate sizes is estimated by evaluating how many aggregate sizes influence the gradation area of the mix. To study the influence of two variables on each other sample data containing combined gradation percentage passing along with sieve size and no. of aggregates used in the mix was collected. Later, graphs were developed for each mix to evaluate the gradation area by integrating the limits. A correlation was conducted between aggregate sizes in the mix and obtained gradation area. Similarly, Regression analysis is performed. The outcome of the correlation relation is a weak negative correlation with a value of −0.1486. Through regression analysis, linear equations are developed for the same and the P-Value of sample data is obtained to be 0.318754. Through this correlation and regression analysis, it is concluded that generated model can't be accepted globally based on P-value. In order to make the model to be accepted globally more influence parameters must be added to the model in evaluating the gradation area, which can improve model performance.

R. Penki (✉) · A. K. Das
Civil Engineering Department, Siksha 'O' Anusandhan University, Bhubaneswar, India
e-mail: ramu.p@gmrit.edu.in

R. Penki
Civil Engineering, GMRIT, Rajam, Srikakulam, A.P, India

S. K. Rout
Department of Civil Engineering, National Institute of Technology Rourkela, Rourkela, India

A. Dhamaniya et al. (eds.), *Recent Advances in Traffic Engineering*, Lecture Notes in Civil Engineering 377, https://doi.org/10.1007/978-981-99-4464-4_30

Keywords Number of aggregate sizes · Gradation area · Job mix · Correlation · Regression

1 Introduction

Bituminous mix/concrete and asphalt concrete are terms that can be used interchangeably [1]. Bituminous concrete is a composite material (sandwich or monolithic) that combines the elements of asphalt and various types of aggregates in predetermined quantities and most widely used pavement among all other types of pavement due to its ease of construction and maintenance [2]. The constituent materials of bituminous concrete are aggregates, filler and binder (bitumen) [3]. In general, aggregates account for 92–96% of bituminous concrete [4]. So, Aggregates play a major role and alter the weight transfer mechanism of pavements to a large amount [5]. As a result, they must be properly evaluated before being used in construction. Aggregates must be not only strong and durable but also of suitable shape, size (nominal and maximum size), texture, angularity, polished stone value, contact point, binder adhesiveness, excellent mechanical properties and free from deleterious material to make the pavement act monolithically [6–9]. The pavement is laid by mixing the constituent material as per the design requirements and specifications provided by MoRTH. Numerous bituminous mix designs were proposed (i.e., gradation methods) in defining the material proportion to meet certain target mixture volumetrics (i.e., density and void content) and it was done in a sequential process of selecting aggregates, gradation (sieving), blending of aggregates. Worldwide it is an accepted practice to follow the guidelines provided by various transportation agencies regarding aggregate gradation and the type of mix to be adopted for laying asphalt concrete mixture. In general, the specifications provided were based on past experiences and an understanding of local circumstances [10]. Gradation exhibits a huge impact on mix performance and it is believed that the best gradation is one that yields maximum density [11]. The maximum density of the mix is obtained when it possesses different-sized aggregates [12], due to this particle arrangement takes place where the smaller-sized particles will occupy the void spaces in between the large-sized aggregates which creates a large contact area which creates a smaller number of void spaces, as a result, the obtained mix will be of high density and it will possess better stability and performance under the action of loads. Usually, aggregate gradation is done by using the Fuller-Thomson gradation test [13]. The determination of aggregate proportion strongly depended on some aggregate sizes to be blended (mixed) and the limits of each grade (aggregates retained on each sieve size) [9].

The words aggregate gradation and aggregate blending are the most widely used in the concept of mix design. Aggregate gradation is the segregation of aggregates according to size through sieve analysis and it is classified namely, viz., well-graded, gap graded, open-graded, etc., and their proportioning is known as aggregate blending. Aggregate blending is a process of calculating the quantities of aggregates

of various sizes to make a final blend (referred to as job mix) that can fulfill the pre-defined each sieve's specified limitations that is to be blended (mixed) together to meet the gradation limitations [14]. Gradation limits are often specified in terms of range by the proportion of aggregates passing through each sieve, and MORTH criteria are used [15]. The preparation of the aggregates' overall gradation for a mix is regarded as an important phase in the designing of a bituminous concrete mixture. The choice of aggregates involves aggregate gradation, cost, design requirements and the number of sizes required in the mix. To meet the precise gradation requirement, aggregates for asphalt mix must be picked from diverse stocks [16]. To have a perfect mix of bituminous concrete the gradation alone can't be taken into consideration, aggregates should have seamless characteristics as mentioned above with decent material properties, and other influence parameters of aggregates are briefly discussed as follows:

Size of Aggregates. The size of aggregates greatly influences the selection of material to be incorporated into the mix. The large-sized aggregates exhibit higher stability, skid resistance and compatibility of a mix. The type and degree of compaction also depend on the size of aggregates, if the maximum size of aggregates is too small then compaction will be difficult as small-sized aggregates can be easily distorted under heavy load/compaction [17].

Nominal size of aggregates. The nominal aggregate size (NMAS) and aggregate gradation type influence the "surface frictional characteristics of mixes". Because of expanding the NMAS in the blend, the top surface shows better macrotextures and diminished miniature surfaces for both fine and coarse total degrees. The frictional qualities of the bottom surfaces, on the other hand, are only affected by the kind of aggregate gradation. Because fine material migrates to the bottom surface after compaction, the bottom layers are essentially identical to each other [18].

The shape of Aggregates. The mechanical behavior of aggregates depends upon the shape of aggregates. The properties of aggregate that rely on shape are durability, workability, shear resistance, tensile strength, binder content, etc. The shape of aggregates is likely to be angular, rounded, flaky, elongated, etc. The mix should have complied with all the types of aggregates while angular aggregates should be more in proportion when compared to other aggregate shapes. It is because angular aggregates provide a good locking effect between the aggregates and take/transfer the load efficiently without breaking of aggregates while other aggregates will fail easily under load due to one of the mean dimensions being very less hence the aggregates are weak in taking the load [19].

Texture. Generally, the texture of aggregates is observed either as rough or smooth texture. Smooth-textured aggregates are favorable for workability while rough-textured aggregates play a vital role in establishing the bond strength [20].

Angularity. It is used to determine the form or shape of aggregate (round or angular) and the higher temperature resistance of bituminous mixes relying on this parameter [21].

Contact point. At high and low temperatures, aggregates having a greater number of contact sites between two aggregate particles have a significant influence on bituminous mixture performance properties, all samples demonstrated strong mechanical performance at all temperatures [22].

Noise. Noise production from the pavement is subject to the percentage of void content in the mix. The relation between void content and the production of noise is inversely proportional to each other. If the air void content is more the noise produced by the pavement when the vehicle moves noise produced will be less or vice versa [23].

The mix that is produced, should be sound without any flaws and it must perform well in any harsh condition without failing [24–27]. So, it is important to find the feasible job mix formula by appropriate gradation. The most preferred gradation is well-graded, as it produces maximum density [28].

Job Mix Formula. The job mix formula is used to determine the necessary proportions of various aggregates to make the composite. It is the curve that is close to the maximum density lane when the curve is plotted between sieve sizes and percentage passing and this curve is used as a reference in a mixing [29, 30].

Aggregates gradation curve and area. Aggregate gradation is done to determine the size of aggregates in the mix to obtain a dense bituminous mix by particle size distribution i.e., by sieve analysis. The different sizes of aggregates ("coarse, fine and filler") are mixed in certain proportions to get the job mix to obtain the desired mix as per the specification. For example, if needed to mix a certain number of sizes the blending is done through various methods such as "trial and error" method, "graphical and analytical" methods where one should plot the graph by using the values of upper limits (UL) and lower limits (LL) as per the specifications of MORTH. The proportion of each sieve should be in between the UL and LL and it must be as close as possible to the maximum density line (MDL). MDL is determined by (d/D)0.45. The gradation area is the area enclosed between the maximum density line and the combined gradation (job mix) curve [29, 30].

2 Problem Statement

The earlier research was carried out on the influence of size, shape, texture, angularity, gradation, etc. in the design mix. The research on gradation was limited to determining the percentage of each size of aggregates to get maximum density. The research gap in the area of aggregate blending is to choose how many aggregate sizes to be employed in the mix to have a minimum area between the MDL and job mix formula. It is necessary to know how many aggregate sizes to be employed in the mix because the number of aggregate sizes vastly influences the density and air voids content in the mix. If the mix is present with a greater number of different-sized aggregates, then obtain mix will be denser with less number of voids when compared to the mix of less number of different-sized aggregates and vice versa. But the choice of the number of aggregate sizes depends upon various factors such

as economy, availability, source, etc., Here the term economy of aggregates includes the cost of extraction, cutting, dressing, transportation, placing, etc.,

Objectives

To estimate what should be the optimum number of aggregate sizes (aggregates retained on different-sized sieves) that should be adopted to have minimum gradation area in the mix.

To explore the correlation between the number of aggregate sizes and the gradation area.

To examine whether the variation in aggregate gradation area in some aggregate sizes by simple regression analysis.

To check the feasibility of AI-based forecasting methods.

3 Methodology

This project's technique is based on a collection of mix configurations that are employed to create a bituminous concrete mixture in different research papers obtained from open-source articles, research papers, journals, etc. A total of 49 different samples were collected, these samples are a combination of different aggregate composition that is comprised of 3, 4, 5, 6, or 7 gradations in the mix. The gradation area for each of the forty-nine samples is calculated by using Excel. Where the data sets are collected from various primary and secondary data sources like research papers, thesis, etc. The data set includes information on sieve sizes and the combined percentage of passing that is used in the mix. Then a graph is plotted for each individual set that is collected from different sources. A graph is plotted between the combined gradation percentage of passing against the sieve size that is raised to the power of 0.45 for angular aggregate, this plot gives the job mix curve and it is smoothened by using the curve fitting method of higher order polynomial function. The other plot is the maximum density line (MDL). MDL is plotted between the sieve size that is raised to the power of 0.45 and the value calculated from the following equation i.e.,

$$\left(\frac{d}{D}\right)^{0.45} * 100 \tag{1}$$

where d = respective sieve size; D = largest sieve size that is employed.

Now the area enclosed between the MDL and Job mix curve is calculated by integrating the trendline equation with the upper and lower limits. These higher and lower limits correspond to the sieve size raised to 0.45. Obtained areas are subtracted to get the enclosed area in between the MDL and Job mix curve. Similarly, the gradation area is calculated for each sample and a correlation relation is found between the aggregate size and combined gradation area. The correlation relation gives an idea of

how the number of aggregate sizes influences the combined gradation area. To find the compatibility of the obtained correlation relation result the relation is estimated through various methods such as the scatter diagram method, person's correlation (r), Kendall Rank, Spearman's Rank correlation and Point-Biserial Correlation. Later to know the level of confidence and existence of the relationship are evaluated by t-static and p-value tests. The relation between gradation area and aggregate size is a general observation that with the increase in several gradation sizes, the gradation area will decrease. This is due to the void spaces in between particles will be occupied by smaller-sized aggregates when we have different sizes in the mix it is easy to fill the void spaces and ultimately the mix will be dense.

3.1 Correlation Methods

Scatter Diagram Method. A scatter diagram is used to investigate the relationship between parameters and how one variable relates to another. If the variables on the graph are interrelated, the points will be close to a curve or line. A scatter diagram or scatter plot depicts the nature of a connection. If all of the data points in this scatter plot stretch down the line, the correlation is considered to be perfect and corresponds to unity. However, if the points are scattered throughout the space on either side of the line, then the correlation between the plotted parameters is low. The correlation is considered to be linear if the scatter points are close to or on a line. These plots gave the idea of a relation between two parameters based on the trend line direction i.e., positive, negative and neutral. These types of plots are mainly used to find whether a relationship persists between the two variables or not.

Pearson's Product Moment Coefficient of Correlation (r). Pearson correlation (r) coefficient is heavily influenced by extreme values, which can exaggerate or diminish the strength of the association, and is thus inappropriate when one or both variables are not normally distributed. To find the correlation between variables x and y, the given formula to calculate Pearson's correlation coefficient is

$$r = \frac{\sum_{i=1}^{n} (x_i - x)(y_i - y)}{\sqrt{\left[\sum_{i=1}^{n} (x_i - \overline{x})^2\right]\left[\sum_{i=1}^{n} (y_i - \overline{y})^2\right]}} \tag{2}$$

where xi and yi are the ith individual's x and y values.

Kendall Rank. When one or more of the test assumptions are violated by the data, Kendall rank correlation (non-parametric) is an alternative to Pearson's correlation (parametric). When your sample size is small and there are many tied ranks, this is the best non-parametric alternative to Spearman correlation.

$$\tau = \frac{(\text{number of concordant pairs}) - (\text{number of doscordant pairs})}{\binom{n}{2}}$$

where

$\binom{n}{2} = \frac{n(n-1)}{2}$ is the binomial coefficient for the number of ways to select two things from a set of n options.

Kendell's coefficient has different modifiers such as Tau-a, Tau-b and Tau-c. Tau-b is majorly used to adjust when rank is tied.

Tau-b. When the ranks are tied, the Tau-b statistic is utilized to make modifications.

Tau-b values vary from 1 to +1. A value of zero indicates the absence of association. The Kendall Tau-b coefficient is calculated as.

$$\tau_B = \frac{n_c - n_d}{\sqrt{(n_0 - n_1)(n_0 - n_2)}} \tag{3}$$

where, $n_0 = n(n\text{-}1)/2$; $n_1 = \sum_i t_i(t_i - 1)/2$; $n_2 = \sum_j u_j\left(u_j - 1\right)/2$; n_c = Number of concordant pairs; n_d = Number of discordant pairs; t_i = Number of tied values in the ith group; u_j = number of tied values in the jth group.

Spearman's Rank Correlation Coefficient. It is appropriate when one or both variables are skewed or ordinal, and it is resilient in the presence of extreme values.

The formula for computing the sample spearman's correlation coefficient for a correlation between variables x and y is provided by

$$r_s = 1 - \frac{\sum_{i=1}^{n} d_i^2}{n\left(n^2 - 1\right)} \tag{4}$$

where di is the difference in ranks for x and y.

Point-Biserial Correlation. A point-biserial correlation measures the degree and direction of the association between one continuous variable and one dichotomous variable. It is a subset of Pearson's product-moment correlation, which is employed when two continuous variables are assessed on a dichotomous (binary) scale.

$$r_b = \frac{\overline{x}_1 - \overline{x}_0}{S_x}\sqrt{\frac{n_0 n_1}{n(n-1)}} \tag{5}$$

where, $Sx = \sqrt{\frac{1}{n}\sum_{i=1}^{n}(x_i - \overline{x})^2}$

4 Results and Discussion

4.1 Effect of No. of Aggregates on Aggregate Gradation Area

Generally, the gradation area is dependent on the no. of aggregate sizes in the mix. The gradation area can be affected by the nominal size of aggregates. To examine the effect of the no. of aggregates a graph is developed between the no. of aggregates and the gradation area as shown in fig. Through the fig, it is observed that when 7

no. of aggregate sizes are present the gradation area is 6.94. Similarly, three peaks are observed one peak value at 4 and two peak values at 3 no. of aggregates with gradation areas of 111.2, 123.75 and 106.41. The reason for the large variation in gradation area compared to other samples is the maximum size of the aggregate considered by the authors. Peak 1 corresponds to 4 different-sized aggregate mixes possessing high gradation area this is due to the size of aggregates considered by the author. Here the author considered the aggregate size of 13.2 mm as the highest size as a result the gradation area is large. Usually, the size of aggregates that are considered for BM mix is medium-sized aggregates such as 26.5 and 19 mm. Peak 2 corresponds to the 3 different-sized aggregates with a gradation area of 123.75 because the author considered 75 mm aggregate as the highest size and other sizes were 53 and 26.5 mm so the presence of voids will be very high. Due to the absence of smaller-sized aggregates, the voids in the large aggregates cannot be filled properly due to this the pavement can fail easily under the action of loads. The gradation area at peak 3 is 106.41 here author considered 40 mm as the maximum size along with 20 and 6.3 mm aggregates. The variation in gradation is due to choosing the large-sized aggregates which result in the creation of voids, when large-sized aggregates are used one should consider a greater number of different-sized aggregate (i.e., more than 4 sizes depending on the need) which reduces the void and to minimize the gradation area. Through this, it is concluded that the choice of aggregate size also plays a key role in the gradation area (Fig. 1).

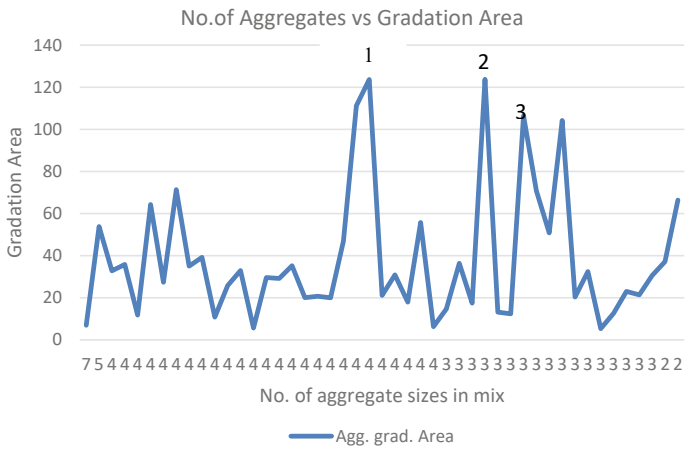

Fig. 1 No. of aggregates sizes in the mix and aggregate gradation area

4.2 Correlation and Regression Analysis

Then correlation relation is found between the two variables to estimate the influence of one parameter over the other. Correlation is estimated among the number of aggregate sizes and gradation area. The correlation was found to be negative which is very obvious but it is a weak negative correlation as the obtained value of Pearson's correlation (r) is −0.1486. It is satisfying the condition that if the number of aggregate sizes is increased in the mix the gradation area is decreased this occurs due to the filling of voids that are present in between large-sized particles and the mix will be dense enough. Other than finding a correlation relation, regression analysis can be performed.

Regression analysis is the process of estimating the relation between a dependent variable and a supporting equation that can be developed in the form of a linear equation or multiple linear regression. When the dependent variable is reliant on numerous independent factors, multiple linear regression is established. Through regression analysis one can comment on the relation between the variables (R^2), significance, variable of data, etc. by estimating multiple R, R^2, ANOVA and p-value tests. In this study regression analysis is performed on the collected data and outcomes of multiple R, R^2 and adjusted R^2, the variability of data is 0.148623, 0.022089, 0.00357 and 2.208875 respectively.

The correlation between real Y and expected Y is defined by multiple R. (Y is the dependent variable) and signifies how strong the relationship is. If the value of multiple R corresponds to 1 then there is a perfect positive relation, if it is 0 then there is no relationship between the dependent and independent variables. The obtained value is 0.15 and the relationship is typical. R^2 is a statistical measure of fit those measures how much variance in a dependent variable in a regression model is explained by the independent variable(s). If the R^2 value is 1, then perfect positive linear association exists, if the value is 0, then there is no association. Here the obtained R^2 value is 0.022, which is possessing a very small negative association. The variability of data is estimated from the ANOVA table, by calculating the ratio of values of regression SS to that of a total of ANOVA, through which the percentage of variability is estimated. The value of variability is 2.208875 [0.637284(SS)/28.85106 (Total)]. The significance of the model is given by p-value. The P-value shows how confident is your model and it doesn't vary much with any sort of data to show that created model is confident the p-value should be minimum. The variability of study data is 0.024864 i.e., 2.4864%. Through this, we can conclude that the variability of data is very low and the model is confident enough and P- value is 0.284458 i.e., 28.44%. The regression equations obtained from regression analysis are

$$\text{No. of aggregate sizes} = 3.783991 + \text{Aggregate gradation area} * (-0.00376) \tag{6}$$

$$\text{Aggregate Gradation Area} = 60.10736 + \text{No. of aggregate sizes} * (-5.87324) \tag{7}$$

The equations are developed by interchanging the dependent variable i.e., changing the variables X and Y. Here in Eq. (6) No. of aggregates made as dependent variable similarly in Eq. (7) aggregate gradation area as the dependent variable and regression equations are developed.

By using Eq. 1 one can determine the no. of aggregate sizes to be employed, that are to be mixed. So, the maximum density of the mix can be achieved with a minimum gradation area. To estimate the optimum no. of aggregates assuming gradation area as zero in Eq. 1. And no. of aggregates obtained is 3.78 which is equal to 4 different-sized aggregates are to employed in the mix as per the study data. Using Eq. (7) gradation area is determined by substituting the value obtained from Eq. (6). To reduce the gradation area number of aggregate sizes can be increased. But, with the increase in aggregate sizes, the voids get filled and the mix will be equal to MDL. Usually, the bitumen mixes should contain 4–5% to accommodate secondary compaction after laying. So, several aggregate sizes should be adopted wisely to make a mix consisting of 4–5% of voids as per the specifications of MORTH. The developed equations possess a p-value above 10% so, they can't be accepted globally. To make a model to be accepted globally efforts must be made in developing an efficient model and it can be accepted when the regression and p-value are 1 or nearly and less than 10% respectively.

From the result, it is observed that the model is experiencing weak correlation, regression and p-value this is due to the limited data sets and most of the mixes that are collected consisting of three different-sized aggregates and very few data sets consisting of 4 or more aggregate sizes. Based on the obtained correlation it is very complex to predict the optimum number of sizes to be incorporated in the mix design. Several other factors influence choosing aggregate sizes. The factors include strength, source, availability, size of aggregates, etc., as these parameters cannot be included in the correlation relationship. So, to have a better interpretation of data adoption of advanced technology or methods of computer operations such as Random-forest, SVM, etc. these techniques use the hidden layers and help to link several unlinked factors to give better results in predicting the optimum number of aggregate sizes to be selected. And estimation of correlation through various methods wasn't possible because the dependent variable was dependent on one single independent variable. So, the estimation of Kendall's Rank and Spearman's correlation wasn't possible. For the presented data, only Pearson's correlation and regression analysis were performed to make the concluding remarks.

5 Conclusion

The following are the key outcomes for the data:

1. It is very difficult to model (using ml) the behavior of aggregate gradation area solely based on one parameter i.e., no aggregate sizes. To model the AI model the dependable parameters must be two or more, by this, the model creation will be

feasible and have better reliability over the generated model. The other parameters that can be considered for AI Model creation can be the angularity of aggregates, texture, stone polishing value, proportioning of aggregates (aggregate blending), nominal size of aggregate, source (industrial by-product, natural & hybrid), cost, etc. With the addition of these parameters, there could be a better model to predict the gradation area.

2. For a given no of aggregates for example (4), the gradation area is changing from 6 to 60 approximately, which is almost a 1000% difference between the minimum and maximum values. This indicates that either there is no correlation between the aggregates and area, or there are other variables that are affecting the relationship. If it is because of the other variables, including their information, can improve the model.
3. The data available is largely skewed, i.e., 80–90% of the data of the proportions are related to no = 4, and no = 3 only. For others it is very less i.e., for 5 or more aggregate sizes, this can have an impact while developing ML-based models.
4. Because of the less variability in the no of aggregates and the absence of other predictor variables models such as random forest, the decision tree generally tends to provide the mean value of the given observations at a particular number of aggregate sizes. Hence, the reliability is questionable.
5. Probably it would be better to use linear regression only compared to ML models at the moment. The ML models have the almost same performance and their explanation ability is less compared to the linear regression model.

6 Future Scope

A mathematical relation can be established between theoretical voids obtained from aggregate gradation area and the practical percentage of air voids obtained from the Marshall Mix design. Statistical analysis or AI-based model development for aggregate gradation area can be done by the inclusion of additional parameters mentioned in the study.

References

1. Widyatmoko I (2016) Sustainability of bituminous materials. Sustain Constr Mater 343–370. https://doi.org/10.1016/b978-0-08-100370-1.00014-7
2. Khan AB, Jain SS (2020) Assessment of strength characteristics of bituminous concrete modified using HDPE. Transp Res Procedia 48:3734–3755. https://doi.org/10.1016/j.trpro.2020.08.045
3. Mohammad Harun-Or-Rashid G, Mohayminul Islam M (2020) A review paper on: effect of different types of filler materials on marshall characteristics of bitumen hot mix. Int J Mater Sci Appl 9(3):40. https://doi.org/10.11648/j.ijmsa.20200903.11

4. Hegab OA, El-Badawy SM, Hashish EY (2017) Geological and geotechnical assessment of gabal ataqa dolostones, for pavement construction in Egypt. Int J Sci: Basic Appl Res 36(4):56–73
5. Maitra SR, Reddy KS, Ramachandra LS (2010) Load transfer characteristics of aggregate interlocking in concrete pavement. J Transp Eng 136(3):190–195. https://doi.org/10.1061/(asce)te.1943-5436.114
6. Bessa IS, Branco VTFC, Soares JB, Neto JAN (2015) Aggregate shape properties and their influence on the behavior of hot-mix asphalt. J Mater Civ Eng 27(7):04014212. https://doi.org/10.1061/(asce)mt.1943-5533.0001181
7. Topal A, Sengoz B (2005) Determination of fine aggregate angularity in relation with the resistance to rutting of hot-mix asphalt. Constr Build Mater 19(2):155–163. https://doi.org/10.1016/j.conbuildmat.2004.05.004
8. Petersen D, Fletcher T, Chandan C, Masad E, Sivakumar K (2002) Measurement of aggregate texture and its influence on hot mix asphalt (HMA) permanent deformation. J Test Eval 30(6):10856. https://doi.org/10.1520/jte12340j
9. Stakston AD, Bahia HU (2003) The effect of fine aggregate angularity, asphalt content and performance graded asphalts on hot mix asphalt performance. Wis Highw Res Program 92:45–98
10. Swamy AK, Sandhu KK, Foxlow J (2018) Improving quality control through chance constrained programming: a case study using Bailey method. Int J Pavement Res Technol 11(2):128–137. https://doi.org/10.1016/j.ijprt.2017.11.004
11. Afaf AH (2014) Effect of aggregate gradation and type on hot asphalt concrete mix properties. JES J Eng Sci 42(3):567–574. https://doi.org/10.21608/jesaun.2014.115005
12. Cai X, Wu KH, Huang WK, Wan C (2018) Study on the correlation between aggregate skeleton characteristics and rutting performance of asphalt mixture. Constr Build Mater 179:294–301. https://doi.org/10.1016/j.conbuildmat.2018.05.153
13. Thushara VT, Murali Krishnan J (2020) permanent deformation characterisation of gap-graded and continuous graded aggregate blends for bituminous mixtures. In Proceedings of the 9th international conference on maintenance and rehabilitation of pavements. Mairepav9. pp 493–505
14. Vavrik WR, Pine WJ, Carpenter SH (2002) Aggregate blending for asphalt mix design: bailey method. Transp Res Rec 1789(1):146–153
15. Alshamsi KS (2006) Development of a mix design methodology for asphalt mixtures with analytically formulated aggregate structures. Louisiana State University and Agricultural & Mechanical College
16. Singh P, Walia GS (2014) Review of optimization methods for aggregate blending. Int J Adv Res Civ, Struct, Environ Infrastruct Eng Dev 1(3):1–8
17. Liu W, Gao Y, Huang X (2017) Effects of aggregate size and specimen scale on asphalt mixture cracking using a micromechanical simulation approach. J Wuhan Univ Technol-Mater Sci 32(6):1503–1510
18. Khasawneh MA, Alsheyab MA (2020) Effect of nominal maximum aggregate size and aggregate gradation on the surface frictional properties of hot mix asphalt mixtures. Constr Build Mater 244:118355
19. Khairandish MI, Chopra A, Singh S, Chohan JS, Kumar R (2022) Effect of gradation and morphological characteristics of aggregates on mechanical properties of bituminous concrete and dense bituminous macadam. Iran J Sci Technol, Trans Civ Eng 46(1):293–307
20. Raposeiras AC, Vega-Zamanillo Á, Calzada-Pérez MÁ, Castro-Fresno D (2012) Influence of surface macro-texture and binder dosage on the adhesion between bituminous pavement layers. Constr Build Mater 28(1):187–192
21. Wang H, Bu Y, Wang Y, Yang X, You Z (2016) The effect of morphological characteristic of coarse aggregates measured with fractal dimension on asphalt mixture's high-temperature performance. Adv Mater Sci Eng
22. Busang S, Maina J (2022) Influence of aggregates properties on microstructural properties and mechanical performance of asphalt mixtures. Constr Build Mater 318:126002

23. Sun J, Zhang H, Yu T, Wu G, Jia M (2022) Influence of void content on noise reduction characteristics of different asphalt mixtures using meso-structural analysis. Constr Build Mater 325:126806
24. Sandeep RG, Ramesh A, Vijayapuri VR, Ramu P (2021) Laboratory evaluation of hard grade bitumen produced with PPA addition. Int J Pavement Res Technol 14:505–512. https://doi.org/10.1007/s42947-020-0068-2
25. Akhil N, Ramu P, kalyan shetty S, (2019) Experimental investigations on the rut resistant surface layer with inclusion of marble dust and sisal fibers. Mater Today Proc 18:3233–3246. https://doi.org/10.1016/j.matpr.2019.07.199
26. Gottam SR, Adepu R, Penki R (2020) Evaluation of bituminous mix characteristics prepared with laboratory developed high modulus asphalt binder. J Inst Eng Ser A 101:701–712. https://doi.org/10.1007/s40030-020-00462-4
27. Reddy GS, Ramu P (2019) Design of bituminous mixes for heavily trafficked roads–a boon to indian roads. Int J Tech Res Sci 4:34–38. https://doi.org/10.30780/IJTRS.V04.I06.005
28. Kumar KK, Penki R (2022) A scientometric analysis on aggregate blending, pp 621–634
29. Soujanya C, Akhila Priya G, Ramu P, Naveen Kumar C (2019) A novel technique to design optimum bituminous mix designs based on R studio and autograph with integration. Mater Today Proc 18:4566–4579. https://doi.org/10.1016/j.matpr.2019.07.431
30. Ramu P, Sarika P, Kumar VP, Sravana P (2016) Analytical method for asphalt concrete job mix formula design. Int Res J Eng Technol 03:7

Simulation Approach for Analysis of Signalized Intersection Capacity Under the Influence of Access Point: A Case Study

J. Athira, K. T. Arshida, Yogeshwar V. Navandar, and K. Krishnamurthy

Abstract The interaction between surrounding activities and regular traffic at signalized intersections leads to a reduction in their performance. Such activities include flow from an access point, on-street parking, etc. The effect of access traffic near signalized intersections is not much explored. Manuals like HCM (2010) and Indo HCM (2017) do not address the potential change in capacity due to this factor. This research is an assessment of the influence of access flow on the capacity of nearby signalized intersections under mixed traffic environment. The videographic data from the field is collected during peak hours. Indo HCM method is followed to analyze the capacity at signalized intersections. The outcome of this study shows there is a significant effect on the capacity of the signalized intersection if there is an access point in proximity. The maximum capacity reduction observed was in the range of 19 to 24%. A microsimulation model was developed using VISSIM to study the effect of varying access flow (zero to 285 PCU/hour) and distance of access point from stop line (10 m to 120 m) on the capacity of the intersection. It was observed that an increase in access flow causes more reduction in capacity. Position of access point also plays a crucial role as it is observed that beyond 100 m from the stop line of the approach considered, the access flow has less effect on the capacity and beyond 120 m, the effect diminishes. Hence while designing a signalized intersection, planners should ensure there is no access point within 100 m of the intersection. The result of this study will be useful for planners and academicians for capacity evaluation of signalized intersections.

Keywords Signalized intersection · Capacity · Access point · Simulation

J. Athira (✉) · K. T. Arshida · Y. V. Navandar · K. Krishnamurthy
Department of Civil Engineering, NIT, Calicut, Kerala, India
e-mail: athirajp94@gmail.com

K. T. Arshida
e-mail: arshida_m200352ce@nitc.ac.in

Y. V. Navandar
e-mail: navandar@nitc.ac.in

K. Krishnamurthy
e-mail: kk@nitc.ac.in

A. Dhamaniya et al. (eds.), *Recent Advances in Traffic Engineering*, Lecture Notes in Civil Engineering 377, https://doi.org/10.1007/978-981-99-4464-4_31

1 Introduction

In a road network, the capacity of intersections is a constraint and vital for measuring its performance. Signalized intersections are vulnerable to complex vehicular movements. So, it is indispensable to plan them carefully to maintain performance efficiency. Saturation flow and capacity are significant parameters considered for performance evaluation of signalized intersections. Highway Capacity Manual (HCM) was the first extensive effort to estimate capacity at signalized intersections. In HCM [1], the adjustment factors to capacity include average lane width, right turn on red, percent of heavy vehicles, bus stops, pedestrian activities, bicycle activities, and parking activities. Indo Highway Capacity Manual (Indo HCM) is an indigenous manual used in Indian traffic conditions. Indo-HCM, [2] considers the width of approach, bus stops, right-turning vehicles, and initial surge of vehicles for the calculation of saturation flow. Canadian Capacity Guide for Signalized Intersections considers factors such as lane width, grade, transit stops, parking, and pedestrians for capacity estimation. Some situations are not addressed in these manuals. The effect of access points is one such factor. Access points create more conflicting areas and thus traffic blocks and more delays. The vehicles from access can cause a temporary bottleneck which can lead to additional delay. Access traffic causes lane and speed changes in the approaches, leading to queuing and green time loss. The traffic that drives from and to the accesses negatively impacts the downstream intersection as well as the smoothness of main road traffic. Hence, access management is crucial to the efficient and safe operation of the intersections. Unsignalized T- intersections or neighborhood openings near the signalized intersection can be considered access points.

Flow from the access point hinders traffic movement on the intersection approaches. Three types of traffic flow will be present due to the access traffic. They are merging flow—flow that merges to the main road from access, separation flow—separates from the main road to the access point, and passing through flow—flow that has to pass through the straight flow while they get in or out of the access point. These are shown in Fig. 1. In the present study, the selected sites have two-lane, two-way approaches with medians. The passing through flow is nil since there are no median openings near the access point.

Microsimulation models can be used to represent real-world traffic systems. They are very helpful in representing the dynamic nature of these traffic systems. PTV VISSIM is a microscopic, time-step- and behavior-based simulation model. Any type of geometric configuration and unique driver or operational behaviors can be modeled in PTV VISSIM. The VISSIM models can be used to analyze the traffic characteristics, which will otherwise be difficult to measure from the field.

This paper highlights the field capacity estimation in the presence of access flow near signalized intersections. A realistic microsimulation model of the signalized intersection is modeled using VISSIM to estimate the effect of access points.

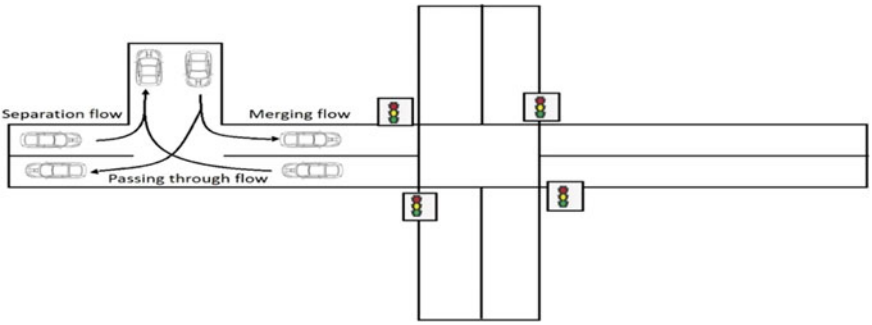

Fig. 1 Types of Access traffic flows

2 Literature Review

A systematic literature review of the existing research reveals that for signalized intersections, literature on capacity affected by nearby access points is sparser. Li et al. [3] developed a capacity model for signalized intersections that considers both arrival traffic on the main road and access traffic using merging time. Zhao et al. [4] presented a theoretical model to estimate the capacity of lane group by considering access point impact at signalized intersections with two positions of access points (upstream or downstream) and six types of access traffic flows. They found that access point impact on capacity is significant at signalized intersections. Zhang and Lu [5] studied arterial roads with unsignalized access points using Traffic Software Integrated System (TSIS), a microscopic traffic simulation model. The average delay time of the minor road is analyzed in many situations and given standards for intersection approaches concerning traffic volume. They found that when the traffic volumes are high, there should be higher control on access flow. Cao and Menendez, [6] studied the changes in the service rate of signalized intersections due to parking maneuvers. The analytical model built by them relates reduction in service rate to the distance of parking maneuvers from the intersection. Rao et al. [7] computed the impact of on-street parking and both curb side and bus bay bus stops on the capacity of mid blocks in Delhi, India.

In transportation operations and management analysis, microscopic simulations are widely used since it is less expensive, safer, and quicker than making it a practical reality and testing [8]. Proposed improvements and alternatives can be effectively analyzed and evaluated using microsimulation. VISSIM is one of the microsimulation techniques which is easy to use [9]. Moen et al. [10] compared to different traffic simulation and traffic analysis programs. They found that in VISSIM, interaction between different modes of transit with other motorized traffic can be modeled. VISSIM can also be used to model complex geometries and generate vehicles randomly and flexibly.

Most of the available literature on the calibration of micro simulators for signalized intersections is primarily limited to homogeneous traffic conditions. Manjunatha

et al. [11] suggested a methodology for automating the calibration of the VISSIM microsimulation model for signalized intersections in mixed traffic with different traffic characteristics. They have observed driver behavior in mixed traffic to make adjustments in the simulation. From multi-parameter sensitivity analysis, they identified calibration parameters and obtained the optimum values by reducing the error between field delay and simulated delay. Siddharth and Ramadurai [12] have used data from an intersection in Chennai with heavy flow and presented a method and results on sensitivity analysis and automatic calibration of the VISSIM model.

The studies discussed above state that the presence of access points creates a greater number of conflict points, and thus, it becomes a threat to road users. But manuals like HCM, [1] and Indo-HCM [2] to which most academicians and planners resort, did not address this effect on the capacity calculation of signalized intersections. Furthermore, the effect of access points in mixed traffic conditions is less studied. Hence, more research should be done in this field, and better management measures to avoid a reduction in capacity and safety should be proposed.

3 Research Methodology

The Indo-HCM, [2] manual provides a procedure to assess field saturation flow at signalized intersection in which it is the average flow of all the intervals for an unobstructed flow [Eq. (1)] [2]. At fixed short time intervals during the green number of vehicles passing the stop line is counted.

$$\boldsymbol{S} = \boldsymbol{n_i} \times \boldsymbol{P_i} \times \frac{3600}{\boldsymbol{CI}} \tag{1}$$

where, $\boldsymbol{S}$= Flow that is crossing the stop line in PCU per hour, $\boldsymbol{n_i}$= Number of vehicles of type 'i' crossing the stop line during count interval, $\boldsymbol{P_i}$= PCU value of vehicle type 'i' and $\boldsymbol{CI}$ represent Count Interval in seconds.

The flow under prevailing conditions is given by Eq. (2) [2]. If any obstructions are reported within a cycle, those observations should be discarded.

$$\boldsymbol{SF} = \frac{\sum \boldsymbol{S}}{\boldsymbol{N_e}} \tag{2}$$

where, $\boldsymbol{SF}$= Field measured saturation flow under prevailing conditions in PCU per hour, $\sum \boldsymbol{S}$= Sum of all values of flows excluding the values where obstructions were found but including the start-up values if initial surge is reported, $\boldsymbol{N_e}$= Number of count intervals excluding ones during obstructions were reported.

Three hour classified traffic volume data and control data were collected at two signalized intersections in India. The data were used to estimate the saturation flow values and then capacity values. For capacity estimation Indo-HCM, 2017 provides

a relation relating capacity and saturation flow [Eq. (3)] [2].

$$C_i = SF_i\left(\frac{g_i}{C}\right) \tag{3}$$

where, C_i = Capacity of movement group 'i' (in PCU/hour), SF_i = Saturation flow of movement group 'i' under prevailing conditions (in PCU/hour), g_i = Effective green time for movement group 'i' (in seconds), and C = Overall cycle time (in seconds).

The values of saturation flow and capacity were estimated for various access flows and a good fit model is obtained relating percent reduction in capacity and access flow. VISSIM microsimulation modeling is also developed for the study area and carried out the analysis of capacity by changing the access flow and position of the access point. An exponential model gives a good relation between percent reduction in capacity and distance of access point from stop line.

The research methodology adopted for the study is shown in Fig. 2. After a comprehensive literature review suitable study sites were selected. Videographic data collected were extracted to get the capacity of signalized intersection in the presence of access point and for VISSIM modeling. VISSIM model is calibrated by trial and error method and is validated with a new set of data. The influence of access traffic and distance of access point from stop line is analyzed using VISSIM microsimulation.

4 Data Collection

The data are collected from two signalized intersections located within the city of Calicut in Kerala, India, namely Stadium Junction and Malaparamba Junction. The traffic, geometric, and control data were collected from the selected sites. Traffic data were collected on weekdays using videography, and classified traffic volumes were extracted manually from the collected data. The data were collected in dry weather during peak hours in the morning and evening. The survey details are given in Table 1.

The selected intersections are four-legged, and the longitudinal gradient is almost zero. The access flow considered in the present study is the flow to and from the off-street parking lots near the intersections. Figure 3 shows the google earth images of Stadium Junction and Malaparamba Junction, and the access points of the corresponding intersections are highlighted.

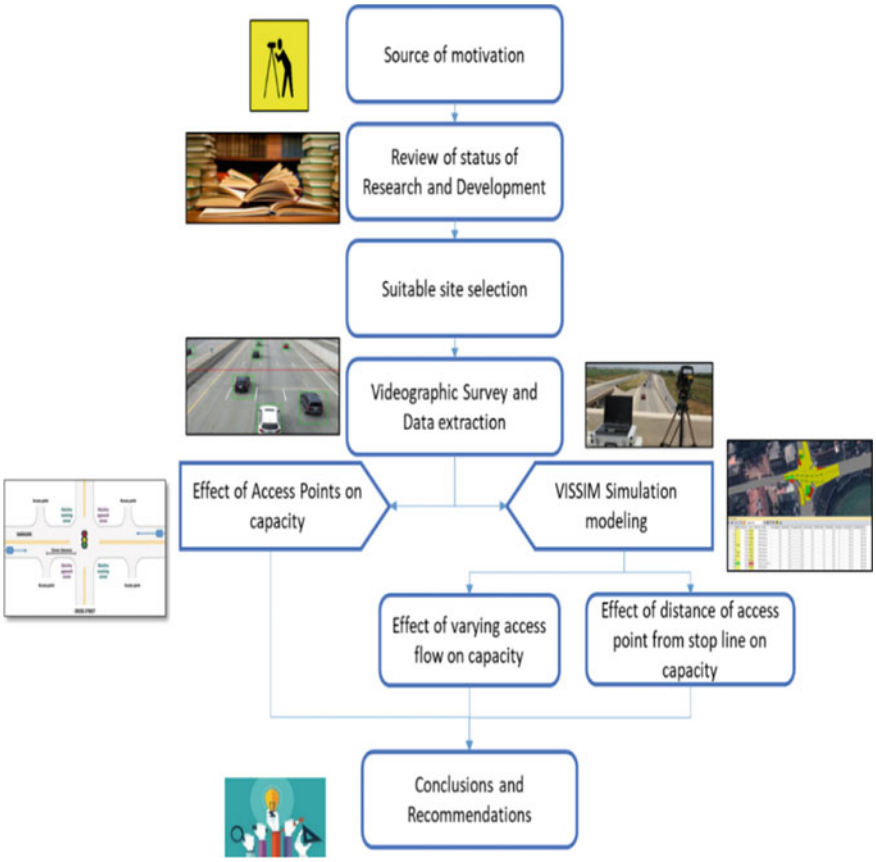

Fig. 2 Research methodology

Table 1 Data collection details

Sl No	Intersection	City	State	Date and day	Timing
1	Stadium junction	Calicut	Kerala	18 January 2022, Tuesday	9.30 a.m. to 11.30 a.m and 3.30 p.m. to 5.30 p.m
2	Malaparamba junction	Calicut	Kerala	19 January 2022, Wednesday	9.30 a.m. to 11.30 a.m and 3.30 p.m. to 5.30 p.m

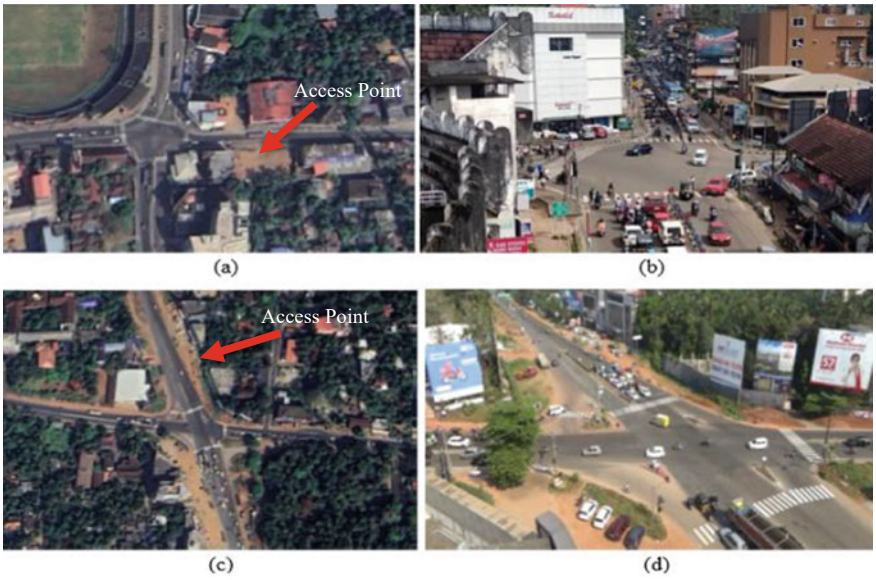

Fig. 3 **a** Google Earth image of Stadium Junction. **b** Field of view of the camera at Stadium Junction. **c** Google Earth image of Malaparamba Junction. **d** Field of view of the camera at Malaparamba Junction

4.1 Geometric and Control Data

The phase diagrams of two intersections are shown in Fig. 4. The approaches considered for the study are the Puthiyara Road approach (phase 4 of Stadium Junction) and the Kannur Road approach (phase 1 of Malaparamba Junction).

The width of approach, the width of access points, and signal details of the Stadium junction and the Malaparamba junction are given in Table 2.

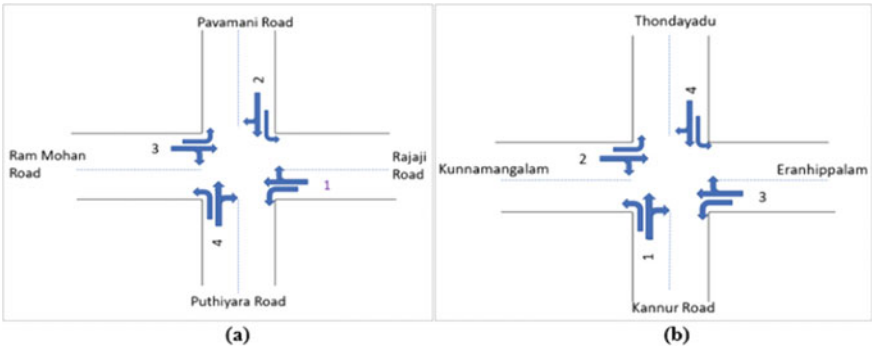

Fig. 4 **a** Phase diagram of Stadium Junction. **b** Phase diagram of Malaparamba Junction

Table 2 Geometric details and control data of desired approaches

Details	Stadium junction	Malaparamba junction
Width of approach (m)	3.75	7.5
Width of the access point (m)	4	4
Distance of access point from stop line (m)	40	80
Green time (Sec)	23	24
Amber time (Sec)	2	3
Cycle time (Sec)	157	133

4.2 Classified Traffic Volume

The vehicles were classified into six types, namely Two Wheelers (TW), Three Wheelers (auto), Cars, Buses, Light Commercial Vehicles (LCV), and Heavy Commercial Vehicles (HCV). To regard the variations in their static and dynamic characteristics, they are converted into equivalent Passenger Car Units (PCU) [13]. The PCU values used throughout the study are adopted from Indo-HCM [2]. The proportions of vehicles of approaches (with the presence of access points) to the intersections and corresponding access points are shown in Table 3.

The major portion of traffic consists of TWs and cars in both intersections, followed by three-wheelers (Auto). The access traffic mainly consists of mainly TWs, cars, three-wheelers, and a few LCVs. However, there were no buses or HCVs present in the access traffic.

Table 3 Proportion of vehicles

Vehicle type	Vehicle proportion (%)			
	Stadium junction		Malaparamba junction	
	Puthiyara road	Access point	Kannur road	Access point
TW	70.53	51.61	41.39	15.15
Auto (3W)	11.2	3.23	7.11	18.18
Car	15.47	43.55	40.19	66.66
Bus	1.47	0	0.14	0
LCV	1.33	1.61	6.69	3.03
HCV	0	0	4.48	0

5 Field Capacity Analysis

Field saturation flow is measured using Indo HCM [2] method. Capacity is estimated by the multiplication of saturation flow rate and split ratio. The values of field saturation flow and capacity were estimated for varying access flows and in the absence of access flow for the two intersections, and it is presented in Table 4.

Maximum capacity is obtained when there is no access flow present. Even though the capacity reduction observed in both the intersections is comparable when the flow from access point is the same, the reduction observed is slightly higher in the case of the Stadium junction. This may be because access point at Stadium junction (at 40 m from stop line) is closer to the intersection compared to the access point at Malaparamba junction (at 80 m from stop line). The variation of percent reductions in capacity for different access flows is shown in Fig. 5.

The percent reduction in capacity has a linear variation with increasing access flow for both the selected intersections. Hence, access flow impacts the capacity of the intersection considerably.

Table 4 Saturation flow and capacity values for varying access flow

Access flow (PCU/hour)			Saturation flow (PCU/hour)		Capacity (PCU/hour)		Percent reduction in capacity (%)	
Inflow (to access)	Outflow (From access)	Total	Stadium junction	Malaparamba junction	Stadium junction	Malaparamba junction	Stadium junction	Malaparamba junction
0	0	0	2808	6020	447	1222	0	0
0	58	58	2616	5717	417	1161	7	5
72	0	72	NA	5587	NA	1134	NA	7
0	144	144	2534	5501	404	1117	10	9
158	0	158	NA	5299	NA	1076	NA	12
58	144	202	2394	5184	381	1052	15	14
72	144	216	2290	5026	365	1020	19	17
202	58	259	NA	4950	NA	1005	NA	18
0	288	288	2250	NA	358	NA	20	NA
144	158	302	NA	4723	NA	959	NA	22
130	202	331	NA	4651	NA	944	NA	23
144	202	346	NA	4622	NA	938	NA	23

(NA—Not Applicable)

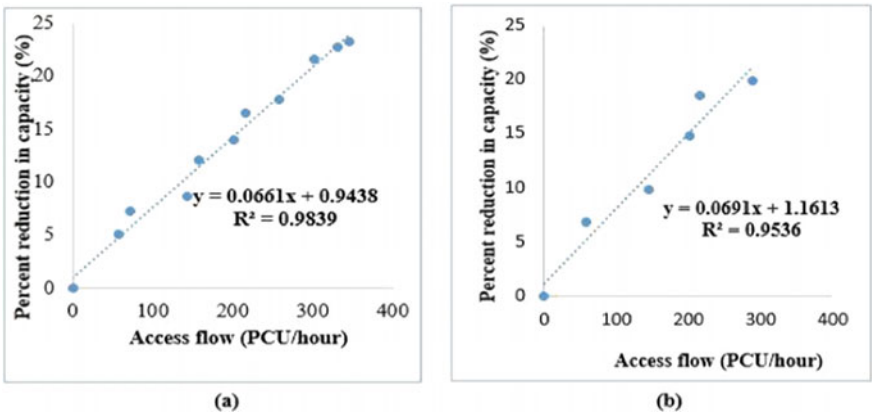

Fig. 5 **a** Percent reduction in capacity versus Access flow at Stadium Junction. **b** Percent reduction in capacity versus Access flow at Malaparamba Junction

6 Development of Simulation Model

A base model which accurately represents the geometrical and control attributes of the study area was developed for Stadium Junction. A calibrated and validated model can then be used for capacity analysis of the intersection. The following steps were involved for base model development in PTV VISSIM: (i) development of link network, (ii) defining model parameters, (iii) model calibration, and (iv) validating the model.

6.1 Link Network Development

The most crucial aspect of VISSIM modeling is accurately representing the intersection geometry. The width of the approaches, number of approaches, number of lanes, turning area, access point, etc., are represented using links and connectors. Figure 6 shows links and connectors drawn for VISSIM modeling.

6.2 Defining Model Parameters

Vehicle Types: The next step in VISSIM simulation is to define both static characteristics and dynamic characteristics of each vehicle type traversing the intersection. The previous versions of the VISSIM simulation model came with a set of the standard type of vehicles such as motorcycles, cars, buses, and trucks. It did not have non-standard vehicles such as motorized three-wheelers which is very common in

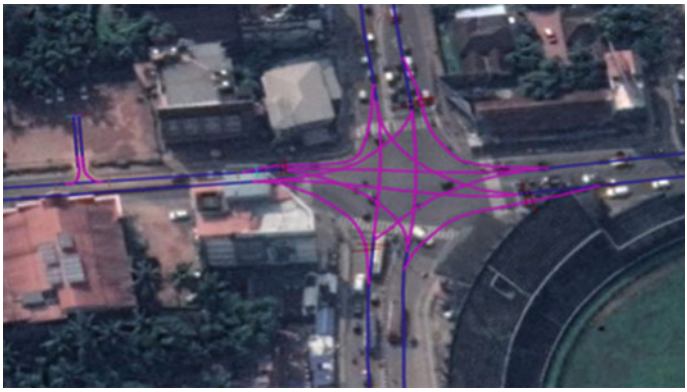

Fig. 6 Geometric representation of site in PTV VISSIM

mixed traffic, but the new versions have the model for motorized three-wheelers. The dimensions and desired speeds of the vehicle categories were coded for each vehicle type. Vehicular characteristics used as input to VISSIM are shown in Table 5.

Vehicle Inputs and Traffic movements: Each turning movement and its proportion needs to be represented properly so that the simulation model is comparable with reality. For all approaches, three movements—that is, left, through, and right movements- and for access flow, two movements—merging and separation flow—are observed in the field. Movement-wise vehicular proportions of each approach and access flow are given in Table 6.

To represent the heterogeneous traffic movements, the option 'driver behavior' is set to 'any', the vehicles are allowed to overtake along either side by setting 'overtaking' to 'all', and by admitting diamond queuing by setting 'diamond queuing' to 'yes'. The possible conflicting areas are to be identified, and priority rules should be given according to the field conditions.

Signal Phasing: The proper representation of signal control system is very important. The cycle time, phasing sequence, green time, amber time, and red time should be represented accurately. A fixed signal program was created with a cycle time of 157 s to replicate cycle time observed in the field. Four signal groups were created

Table 5 Vehicular characteristics

Vehicle type	Length (m)	Breadth (m)	Desired speed (kmph)	Traffic composition (%)
TW	1.870	0.640	35	52.66
Auto	3.200	1.400	30	23.28
Car	4.150	1.605	40	17.48
Bus	10.100	2.430	35	5.30
LCV	6.100	2.100	30	1.28

Table 6 Details of vehicles at Stadium Junction

Approaches	Traffic volume (Vehicles/hour)	Movement	Percent of vehicles for each movement (%)
Rajaji road	1462	Through	34.82
		Right	37.96
		Left	27.22
Pavamani road	1701	Through	36.45
		Right	13.05
		Left	50.50
Ram Moham road	1469	Through	33.90
		Right	52.96
		Left	13.14
Puthiyara road	750	Through	56.67
		Right	20.53
		Left	22.80
Access flow	142	Merging	43.66
		Separating	46.33

to represent signal details of the right and through movements of 4 approaches. A fifth signal group was given to the left turning movements of all approaches, which has to stop for 7s during the pedestrian green.

Driver Behavior Parameters: Three features are included primarily in driving behavior characteristics, namely, car-following behavior, lane-changing behavior, and lateral distance. PTV VISSIM implements two variants of car-following models they are, Wiedemann-74 and Wiedemann-99. Wiedemann's car-following model makes an assumption that there are four different driving states they are free driving, approaching, following, and braking (PTV 2010).

The values for distinct calibration parameters were considered by reviewing previous studies and also by observing videos taken from the field.

6.3 Calibration and Validation of the VISSIM Simulation Model

Calibration of the model is a repetitive process involving comparison of the model to the field and making necessary adjustments to the model. During calibration, the parameters which affect the behavior of the network created in VISSIM are modified so that the model replicates field conditions. Wiedemann-99 car-following model was adopted for the work since its results showed the least variation with field values when compared with Widemann-74. The parameters sensitive for the present study were found by changing the value of each parameter by 10% at a time and

keeping all others as default values. The parameters that give a significant change in simulated delay and delay obtained using default parameters are considered to be sensitive. Parameter optimization was done by lessening the absolute error in field delay and simulated delay. The optimized values of sensitive parameters are presented in Table 7.

The calibrated model is then validated with an additional set of untried field data, among which the input volume, traffic composition, and other data are compared. The mean absolute percentage (MAPE) error between the classified traffic volume and delay from field and simulation is computed. The error in validation is 7.49%, as shown in Table 8.

Table 7 Calibrated parameter set

Serial no	Parameters	Default value	Optimized value				
			TW	Auto	Car	Bus	LCV
1	CC0	1.5	0.37	0.7	1	1.5	1.2
2	CC1	0.9	0.43	1.2	0.81	0.94	0.81
3	CC8	3.5	3	3	3	3	3
4	Number of interaction objects	4	3	3	3	3	3
5	Lateral minimum distance at 0 km/hour	0.2	0.15	0.15	0.15	0.15	0.15
6	Lateral minimum distance at 50 km/hour	1	0.70	0.70	0.70	0.70	0.70

Table 8 Calibration errors and validation errors of the model

	Calibration of model			Validation of model		
	Field value	Simulated	Error (%)	Field value	Simulated	Error (%)
TW	529	517	2.27	515	509	1.17
Auto	84	78	7.14	80	73	8.75
Car	116	118	1.72	147	140	4.76
Bus	11	12	9.09	10	11	10.00
LCV	10	12	20.00	9	10	11.11
Delay (s)	44.03	46.40	5.38	53.15	58.01	9.14
	MAPE		7.60	MAPE		7.49

7 Analysis Using VISSIM Simulation Model

With the calibrated and validated simulation model, two scenarios are considered to estimate the effect on the capacity. In the first scenario, capacity values are estimated by changing the access flows and in the second scenario capacity values are assessed by changing the positions of access points.

7.1 Scenario 1. Variation in Capacity with Access Flow

The capacity in the field is observed to reduce with an increase in the access flow. To find the exact variation in capacity with increase in access flow VISSIM simulation was carried out. The observed access point volume in the field data was 95 PCU/hour. The simulation was run by increasing the access flow by 50% each time. Figure 7 shows simulated percent capacity reduction values with respect to access flow and comparison of percent capacity values obtained from field and simulation. The simulated values of capacity reduction also show a quadratic variation with access flow. A similar trend was observed in the field. The access flow and corresponding percentage reduction in capacity are given in Table 9.

A paired t-test is executed to check if there is a crucial difference between the simulated values and field observed values of percentage reduction in capacity. At 5% level of significance, the tcritical value is 2.57 for 5° of freedom. The t-statistical value of 1.33 is less than tcritical value, which indicates there is no significant disparity in simulated values and field values of percentage reduction in capacity.

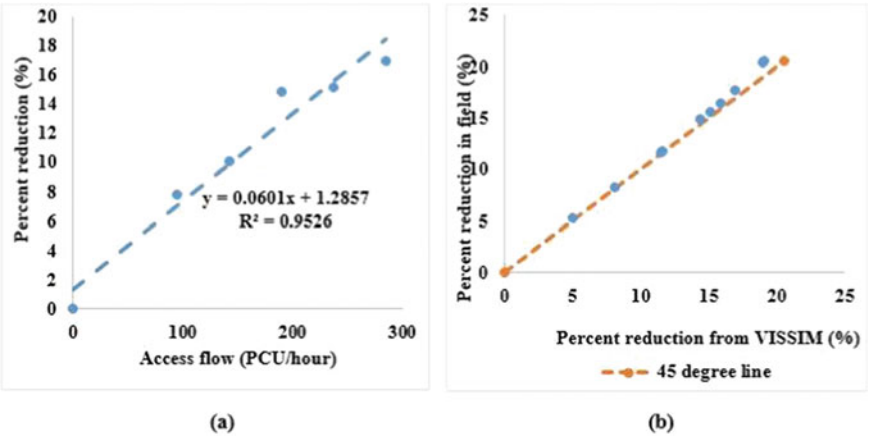

Fig. 7 **a** Percent reduction in capacity versus Access flow from VISSIM. **b** Comparison of field values and simulated values for percent reduction in capacity with respect to access flow

Table 9 Percent reduction in capacity for varying access flow

Sl No	Access flow (PCU/hour)	Capacity (PCU/hour)	Percent reduction in capacity (%)
1	0	496	0
2	95	460	7.36
3	143	445	10.40
4	190	428	13.74
5	238	418	15.76
6	285	407	17.89

7.2 Scenario 2. Variation in Capacity with the Distance of Access Point from Intersection

The effect of position of access point from the stop line of the intersection can be studied by varying the positions of access points in the simulation model. The effect is observed by changing the distance of access point from stop line by a definite amount (10 m). The location was changed until the capacity value observed was the same as capacity in the absence of access flow. Values of the percent reduction in capacity for distinct positions of access point on the approach are listed in Table 10.

A logarithmical relation gives a good fit model between the capacity values and the distance of access point from stop line. The variation of capacity with a change in position of access point is shown in Fig. 8a. Percent capacity reduction varies logarithmically with distance of access point from the stop line. Figure 8b shows the relation between position of access point and percent reduction in capacity.

Table 10 Percent reduction in capacity for varying position of access point

Serial no	Distance from stop line (m)	Capacity (PCU/hour)	Percent reduction in capacity (%)
1	10	175	64.68
2	20	306	38.28
3	30	391	21.29
4	40	428	13.75
5	50	443	10.66
6	60	459	7.50
7	70	463	6.71
8	80	466	6.01
9	90	469	5.40
10	100	478	3.65
11	110	488	1.63
12	120	495	0.32

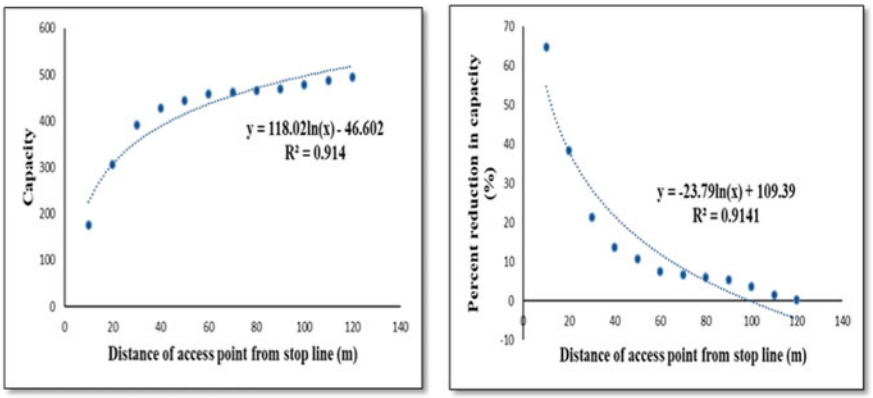

Fig. 8 **a** Capacity versus Distance of access point. **b** Percent reduction in capacity versus Distance of access point

The reductions in capacity values are very significant if the access point is within 50 m from the stop line of approach. After 100 m the reduction is not in a considerable amount and beyond 120 m the effect of access point diminishes.

8 Conclusions

Present study analyzed the effect of access point on the capacity of signalized intersection under heterogeneous non-lane based traffic conditions. Referring to the methodology of Indo HCM [2] capacity was estimated on the basis of collected field data. The presence of access flow near signalized intersection leads to reduction of the capacity of the approach. The results reveal that with an increase in access flow, there will be more capacity reduction. A quadratic relation is the best fit between capacity reduction and access flow.

The results from VISSIM microsimulation show a similar trend on signalized intersection capacity under the effect of varying access flow. The variation in capacity with the distance of access point from stop line is also analyzed. As the distance between access point and stop line of corresponding approach increases it was observed that, capacity of the approach is increasing logarithmically. When the cycle length is 157 s and green time ratio is 0.15, up to 100 m from stop line, access point significantly affects the capacity and beyond 120 m, its effect can be nullified. This result is in-line with the previous study [4] that with a cycle length of 120 s and green time ratio of 0.27, the access point located more than 100 m upstream of the signalized intersection has no effect on the capacity. Thus, there should not be any access point in 100 m vicinity of signalized intersection. Hence, it is recommended

that while planning signalized intersections, access point should be given due importance and placed accordingly so that its impact does not affect the capacity to a higher level.

The present research work did not consider the effect of access point in the downstream side of intersection and other side friction factors (factors like on-street parking, bus stops etc.).

Moreover, the present study was limited to two signalized intersections located in the southern part of India. It is recommended that in future researchers may target other locations in India and other countries, considering local and geographical effects.

References

1. HCM, Highway Capacity Manual 2010, vol. 2. Transportation research board (2010)
2. Indo-HCM, Indian Highway Capacity Manual (Indo-HCM). (2017)
3. Li W, Bai Y, Li S, Huo G (2014) Study on the effect of access on the capacity of signalized intersection. In: Access management theory and the practice – proceedings 2nd international conference. Access management AM 2014, pp 316–324
4. Zhao J, Ma W, Yang X (2013) Effect of access point on signalized intersection capacity. In: Transportation research board 92nd annual meeting
5. Zhang G, Lu J (2010) Study on unsignalized access points using microscopic traffic simulation. Proc Conf Traffic Transp Stud ICTTS 383:990–998
6. Cao J, Menendez M (2015) Generalized effects of on-street parking maneuvers on the performance of nearby signalized intersections. Transp Res Rec 2483(1):30–38
7. Rao AM, Velmurugan S, Lakshmi KMVN (2017) Evaluation of influence of roadside frictions on the capacity of roads in Delhi, India. Transp Res Procedia 25:4771–4782
8. Park BB, Schneeberger JD (1856) Calibration and validation case study of VISSIM simulation model for a coordinated actuated signal system, vol 3, pp 185–192
9. Ratrout NT, Rahman SM (2009) A comparative analysis of currently used microscopic and macroscopic traffic. Arab J Sci Eng 34(1):121–133
10. Moen B, Fitts JW, Carter D, Ouyang Y (2000) A comparison of The VISSIM model to other widely used traffic simulation and analysis programs. In: Institute of transportation engineers 2000 annual meeting and exhibit, Nashville, TN
11. Manjunatha P, Vortisch P, Mathew T (2013) Methodology for the calibration of VISSIM in mixed traffic. In: Transportation research board (TRB) 92nd annual meeting, p 11
12. Siddharth SMP, Ramadurai G (2013) Calibration of VISSIM for Indian heterogeneous traffic conditions. Procedia - Soc Behav Sci 104:380–389
13. Dhamaniya A, Chandra S (2016) Conceptual approach for estimating dynamic passenger car units on urban arterial roads by using simultaneous equations. Transp Res Rec J Transp Res Board 2553(1):108–116

Area Based Cross Classification Measure of Social Vulnerability with Accessibility to Health Services and a Heterogeneous Customer Satisfaction Index for IPT Services in Imphal

S. Padma, S. Velmurugan, Ravindra Kumar, and Yendrembam Arunkumar Singh

Abstract Mobility and accessibility enhance the quality of life of an individual and act as a measure towards a developed economy. Often times it is noted that the accessibility/mobility needs are modeled based on disparity between demand and supply to identify areas of potential transport weakness. In the present paper, a case is made to highlight the health care based transport needs of Imphal through development of a social vulnerability based index and distance based accessibility measure. The development of an area based social vulnerability index is done through indicators signifying personal socio economic factors of disadvantage. The indicators chosen shall be limited to those that are available on Census of India website; disaggregated to individual wards (census boundaries). The index shall measure the demand, and the supply gap is assessed through a distance based accessibility measure. The second segment of the paper shall discuss the development of heterogeneous customer satisfaction index for the daily IPT (Auto/Shared Auto) commuters of Imphal.

Keywords Index for social vulnerability · Principal component analysis · Heterogeneous customer satisfaction index · Accessibility measure

S. Padma (✉) · S. Velmurugan · R. Kumar
CSIR-Central Road Research Institute, Delhi Mathura Road, New Delhi, India
e-mail: padma.crri@nic.in

Y. A. Singh
Manipur Institute of Technology, Imphal, India

A. Dhamaniya et al. (eds.), *Recent Advances in Traffic Engineering*, Lecture Notes in Civil Engineering 377, https://doi.org/10.1007/978-981-99-4464-4_32

1 Introduction

Limited mobility and accessibility can lead to lower quality of life and well being, as well as social exclusion. Traditional approaches to transport modeling assess and identify the disparity amongst persons of transport needs and supply through conventional four stage modeling approaches. Literature specifies that the quantitative approaches to measure the geographical dispersion of people with transport needs can be a socio economic measure, population measure, measure of transport supply, and measure of distance, cost and accessibility [1–3]. In the current paper, the need for transport is measured through the identification of social vulnerability based indicators from the Census of India website. The indicators reflect the economic profile of households/wards/areas and thereby act as a proxy to households/wards/areas of transport needs to services such as hospitals. Socio economic transport needs based indices are often used to identify the gaps between needs and supply [4–6]. Indices based spatial identification of transport needs give the flexibility of using existing census based secondary data to arrive at spatial indices that enable clustering of regions into areas of low/high transport needs [7].

The choice of indicators identified to be included in the index development of transport needs should be reflective of one/several of the various forms of social exclusion, namely, physical exclusion, economic exclusion and fear-based exclusion [8]. Based on the surmise that social exclusion is reflective of the socio economic status of the individual, an area based evaluation of social exclusion would entail indicators chosen to reflect the economic status of the people living in the area. The indicators for the current study were thus finalized.

While several methods are available to model indices, the current paper shall make use of Principal Components Analysis method (PCA) based factor analysis algorithm used in SPSS. PCA is a popular method towards reducing the dimensionality of large number of interrelated indicators while retaining as much as possible the variance in the data [9]. Development of indices using PCA is prevalent in healthcare related services [10–13] with off-late importance in transportation planning as well. PCA is utilized to arrive at the weights for each indicator. In several instances only the weights of the first principal component are used for generating the scores [6, 12, 14] however it has been argued that only the usage of first principal components which usually explains a very low variance would be erroneous [12].

The second aspect of study in the current paper is the heterogeneous customer satisfaction index [15] for the IPT services plying in Imphal. The questionnaire was designed to include various forms of IPT services, namely, auto, share auto, taxi, e-rickshaw, cycle-rickshaw, and Tata Magic (Van) however, the survey results indicated that the questionnaire had been filled incompletely without the mention of the IPT type in more than 90% of the sample collected. Hence, the arrival of the heterogeneous customer satisfaction index was based on the fare paid for the service as a proxy for identification of the type of service used by the commuter.

The paper has been segmented such that Sect. 2 describes the study area, Sect. 3 describes the developed indices and Sect. 4 provides the derivation of accessibility

measure for health services in Imphal, Sect. 5 gives the cross classification of accessibility measures with the developed vulnerability index, Sect. 6 gives the developed heterogeneous customer satisfaction index and Sect. 7 gives the conclusion of the paper.

2 Study Area

As indicated in the previous section, an attempt is made towards developing the area based index for social vulnerability based on socio economic status based indicators along with heterogeneous customer satisfaction index. The following segment shall describe the study area.

2.1 Imphal

Imphal forms the capital city of Manipur and the administrative set up is such that the city falls within the jurisdiction of two districts namely, Imphal East and Imphal West.

'Imphal West district was created in 1997 out of the erstwhile Imphal district by transferring all the villages and towns of Imphal West I and Imphal West II subdivisions vide Government of Manipur (Secretariate) Revenue Department Order No. 6/1/ 73-R(Pt-VIII) dated 17th June 1997 under the Manipur Land Revenue and Land Reforms Act of 1960. Imphal East district came into existence as a result of the bifurcation of the earlier Imphal District into two districts known as (I) Imphal West (II) Imphal East under the Govt. of Manipur order No.6/ 1/73-(Pt-VII), dated 17th June 1997. The district lies between latitudes 240 39′ 49.09" N and 250 4′ 5.45" N and longitudes 930 55′ 30" E and 940 8′ 42" E approximately' [16].

'The main artery of communication for the city is the 325 kms of National Highway No.2 connecting Imphal with Dimapur in the neighboring state of Nagaland. From Imphal, it runs in the south-east for another 110 kms to the International border town of Moreh on the Indo-Myanmar border. Another road of considerable economic importance is the 225 kms National Highway No. 37 viz. New Cachar Road, connecting Imphal with Silchar in Assam via Jiribam on the western fringe of the Manipur valley. The surface road length of National Highways, State Highways, PWD Roads, Rural Road, Urban Road and Project Road was 1,746 km, 715 km, 4,884 km, 4,906 km, 127 km and 972 km respectively, during the year 2015' [17].

2.2 Intermediate Public Transport Services in Imphal

Intermediate Public Transport is used to fill the gap between formal public transport and the private vehicles. Intermediate public transport are normally not used for regular commute such as to work or to schools; however in cities like Imphal wherein no formal share of public transport exists for within city commute, Intermediate Public transport attain the role of main mode of transportation. The various forms of IPT services available in Imphal are share autos, autos, taxis, cycle-rickshaw, e-rickshaw, Tata Magic, and Maruti van. These IPT services act as means of transport between the districts as well as within the city. Kunhikrishnan and Srinivasan [18] investigated the choice of distinct intermediate public transport modes for work trips in Chennai and indicated that aggregating the IPT modes to a single mode would result in biased coefficients and suggests keeping disaggregate modes. IPT in Imphal operates in both fixed routes and flexible schedules. It also acts as a demand responsive transport on a hire/prebooked basis. Hansen [19] defines IPT as services which act in deficiency of formal public transport system, similar to the current transport system prevalent in Imphal.

3 Area Based Index for Social Vulnerability (ABISV)

Indices development using PCA has been quite prevalent in the field of health sciences, urban quality of life and business climate indicator. The current paper utilizes the steps highlighted in [10, 14] which encompass broadly the methodology of formulating indices based on PCA algorithm based factor analysis [10]. Highlights the application of PCA based factor analysis in developing a socio economic composite index with indicators foreseen to impact early childhood development. The paper discusses the statistical requirements of chosen indicators in order for it to be used in development of index. A similar approach adopted in [14] highlights the indicators that can be used to assess the areas with transport deficiency.

The area based index for social vulnerability is formulated using personal socio economic status based indicators. Since the measure is on social vulnerability the developed index indicates advantaged areas through low index score whereas disadvantaged areas are indicated through high index score [1, 14]. The index has been calculated for the 37 Traffic Analysis Zones (TAZs) within Greater Imphal Region (Fig. 1).

The ABISV is calculated as followed in two different ways from the literature:

It is calculated as the weighted sum of the factor score coefficients/components scores [10]

$$\mathrm{ABISV_j} = \sum_{k=1}^{K} \omega_k \mathrm{FSC}_k \tag{1}$$

Fig. 1 Study area Traffic Analysis Zones (TAZs) for Imphal encompassing Greater Imphal area

K—total number of factors/components determined to be extracted for maximum explanation of variance within the data

$$\omega_k = \frac{\text{percentage variance explained by component/factor k}}{\text{total variance explained uptill K}}$$

FSC_k—factor score coefficient of component/factor k corresponding to each ward j.

It is calculated as the weighted sum of the indicators [14] of social vulnerability for different indicators within the wards. The formulation of the index is as follows:

$$\text{ABISV}_j = \sum_{i=1}^{n} \text{TI}_{ij} \text{P}_{ik} \tag{2}$$

TI_{ij}—the standardized personal socio economic indicator for transport needs i of ward j; and P_{ik} is the weighting of the personal socio economic Indicator for transport needs i under component/factor k where k is assumed to be 1 (component/factor 1).

The indicators of transport disadvantage are standardized so that they take values between 0 and 1, using the following equation:

$$T_{ij} = \frac{I_{ij} - I_i^{min}}{I_i^{max} - I_i^{min}} 100$$

And the weights for the indicators are assessed as follows [20–22]:

$$\mathrm{P_{ik}} = \frac{(\mathrm{FL_{ik}})^2}{\lambda_{\mathrm{k}}}$$

FL_{ik}—is the factor loading of indicators i for component/factor $k = 1$.

λ_k—eigenvalue for component/factor $k = 1$.

The indicators chosen for development of index were proportion of female, proportion below 6, proportion of female kids below 6, proportion of illiterates, proportion of female illiterates, proportion of marginal workers, proportion of female marginal workers, proportion of non workers, proportion of female non workers, proportion of female main workers, proportion of main other worker, proportion of female main other worker, proportion of marginal other worker, proportion of marginal other worker female, proportion of main workers from agriculture, industrial and cultivation, proportion of main workers from household industries and cultivation female, proportion of marginal workers from household industries and cultivation female, proportion of marginal workers from industries and cultivation. Some of the indicators mentioned above form the subset of other indicators for e.g., proportion of main workers essentially encompasses proportion of main 'other' workers and proportion of main agriculture laborers, industrial and cultivation workers. The above mentioned indicators were initially processed to carry out the necessary descriptive analysis and from these, a set of indicators were finally chosen as they confirmed to the requisite condition for carrying out PCA based factor analysis in SPSS. Table 1 shows the final set of indicators chosen such that the KMO statistics obtained was 0.665 and the Bartlett's test is significant (Table 2).

3.1 Interpretation of Results from PCA

The indicators as shown in Table 1 were included in the factor analysis. Since the indicators were not standardized the correlation matrix was used to extract the principal components. The individual indicator's measure of sampling adequacy was ascertained from the anti-image correlation table. The components with eigenvalues above 1 were used as the criteria to extract the components and accordingly, 3 components were extracted. The factor loading obtained is as shown in Table 3.

Table 1 Area based personal socio economic Indicators considered for area based index for Social Vulnerability for the study area of Imphal

Indicator	Mean	5% Trimmed mean	Skewness	Kurtosis	Range
Prop of population less than 6 years of age$	0.1077	0.1081	−0.307	0.018	0.05
			0.388		
Prop of illiterate female population*$	0.3383	0.3374	0.548	−0.250	0.11
			0.388		
Prop of households with no Assets*$	0.1493	0.1490	0.223	0.709	0.16
			0.388		
Prop of households not availing bank facilities$	0.4251	0.4278	−0.228	−0.004	0.64
			0.388		
Prop of households without latrine facility within the premises*	0.1598	0.1596	0.140	−0.771	0.23
			0.388		
Prop of households not having treated tap water as main source of drinking water*$	0.4754	0.4707	0.272	0.013	0.85
			0.388		
Prop of households with single and no exclusive dwelling room*$	0.3810	0.3796	0.424	0.284	0.27
			0.388		
Prop of household with drinking water far away from premises*	0.4923	0.4914	−0.093	−0.686	0.71
			0.388		

*Square root transformation: new indicator value = sqrt (old indicator value)

Table 2 KMO and Bartlett's test

Kaiser–Meyer–Olkin measure of sampling adequacy		0.665
Bartlett's test of sphericity	Approx. Chi-Square	124.812
	df	28
	Sig.	0.000

Table 3 shows the correlation of the indicators with the components it is to be noted that a positive loading indicates negative association with the component. The first component explains 41.24% of the variance and includes indicators namely, proportion of illiterate female population, proportion of population less than 6 years of age, proportion of households not availing bank facilities and proportion of households not having treated tap water as main source of drinking. Component 1 can be described to indicate the 'Literacy based economic wellbeing'. It means that a better 'literacy based economic wellbeing' is associated with lower proportion of illiterate

Table 3 Result of PCA: varimax rotation factor matrix

Indicators	Component		
	1	2	3
Prop of households with no assets*			0.805
Prop of households not availing bank facilities	0.565		0.545
Prop of households without latrine facility within the premises*			0.821
Prop of households not having treated tap water as main source of drinking water*	0.442	0.774	
Prop of households with single and no exclusive dwelling room		−0.739	
Prop of households with drinking water far away from premises*		0.813	
Prop of illiterate female population*	0.911		
Prop of population less than 6 years of age	0.888		
Percent of variance	41.24	19.817	13.823

females and lower proportion of children less than 6 year, low proportion of household not availing bank facilities and low proportion of households not having treated water.

Component 2 explains 19.817% of the variance and is indicative of the 'Basic amenities service level' implying a better 'basic amenities service level' through low proportion of households with drinking water far away from premises and low proportion of households not having treated tap water as main source of drinking water and a high proportion of households with single and no exclusive dwelling room. Essentially the negative loading on proportion of households with single and no exclusive dwelling room is indicative of the fact that certain characteristics are lacking in the latent variable associated with the principal component.

Component 3 which explains 13.823% of the variance can be described as indicative of 'economic wellbeing' implying that a better 'economic wellbeing' of the area is indicated through low proportion of households with no assets, low proportion of households without latrine facilities within the premises and low proportion of households not availing banking facilities.

As seen in Table 3, there are indicators which give a negative relationship with the component hence Table 4 without suppressing the coefficients is produced. Herein it is seen that component 1 loadings are all in positive and as determined by several studies [12, 21, 23] the component 1 loadings are often used as weights for development of index.

From the above, it is seen that the components successfully capture the social vulnerability of areas. These social vulnerability indicators position the wards relative to each other and are able to help the policy makers to identify the study areas in need of essential services. Figure 2 shows the indices developed based on Eq. (1). Similarly, Fig. 3 shows the relative ABISV of the wards using Eq. 2 standardized using min–max normalization. The component loadings using Eq. 2 are shown in Table 5.

Table 4 Result of PCA: varimax rotation factor matrix without suppressing the smaller coefficients

Indicators	Component		
	1	2	3
Prop of population less than 6 years of age	0.888	0.252	0.221
Prop of illiterate female population*	0.911	0.096	0.147
Prop of households with no assets*	0.196	−0.057	0.805
Prop of households not availing bank facilities	0.565	−0.068	0.545
Prop of households without latrine facility within the premises*	0.081	0.280	0.821
Prop of households not having treated tap water as main source of drinking water*	0.442	0.774	−0.136
Prop of households with drinking water far away from premises*	0.276	0.813	0.104
Prop of households with single and no exclusive dwelling room	0.180	−0.739	−0.142

Table 5 Result of PCA: Varimax rotation factor matrix using Eq. 2

Indicators	Component		
	1	2	3
Prop of households with no assets*	0.172	−0.024	0.832
Prop of households not availing bank facilities	0.551	0.240	0.638
Prop of households without latrine facility within the premises*	0.057	0.204	0.830
Prop of households not having treated tap water as main source of drinking water*	0.459	0.776	-0.056
Prop of households with single and no exclusive dwelling room	0.203	−0.717	-0.164
Prop of households with drinking water far away from premises*	0.232	0.831	0.162
Prop of illiterate female population*	0.910	−0.025	0.088
Prop of population less than 6 years of age	0.824	0.256	0.337

Extraction method: principal component analysis. Rotation method: varimax with Kaiser Normalization

Figures 2 and 3 shows the relative positioning of the wards based on ABISV categorized into 4 groups using jenks natural break (QGIS).

4 Accessibility Measure to Various Hospitals in Imphal

Accessibility measure (Acc_i) forward i is given as [24]

$$Acc_i = \sum_{j=1}^{N} S_j d_{ij}^{-x} \tag{3}$$

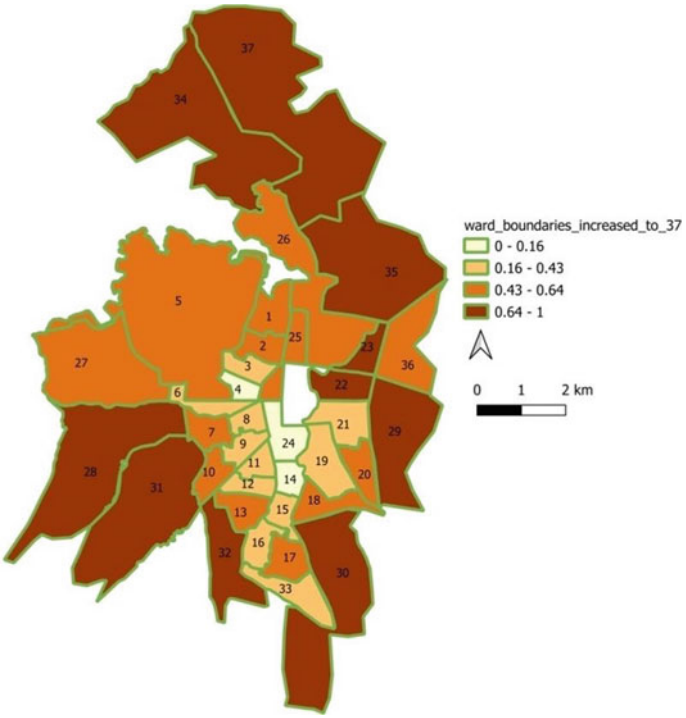

Fig. 2 The segregation of the wards into relative ABISV using Eq. 1

where S_j is opportunities in ward j; d_{ij} is the distance/ time between zone *i* and *j* and *x* is the exponent describing travel time/ distance and N is the total number of wards considered in the study area. In the current study, the following form of friction factor associated with distance is adopted

$$f(U_{ij}) = aU_{ij}{}^{b}e^{cU_{ij}} \tag{4}$$

where

U_{ij} Value of the utility (for example distance or travel time) between zone i and zone j a, b, c Parameters to be estimated;

The current study makes use of the accessibility measure as in [6]

$$Acc_i = \sum_{k=1}^{K} \alpha^s{}_{i.k} + \sum_{j=1, j\neq i}^{N} \left(\sum_{k=1}^{K} \alpha^s_{j,k} \right) f(U_{ij}) \tag{5}$$

In [6] the services are segregated into hospitals, Maternity care services, Municipal dispensaries and health posts. In Imphal only 2 hospitals are present within the defined study area hence the segregation into services is avoided and combined accessibility

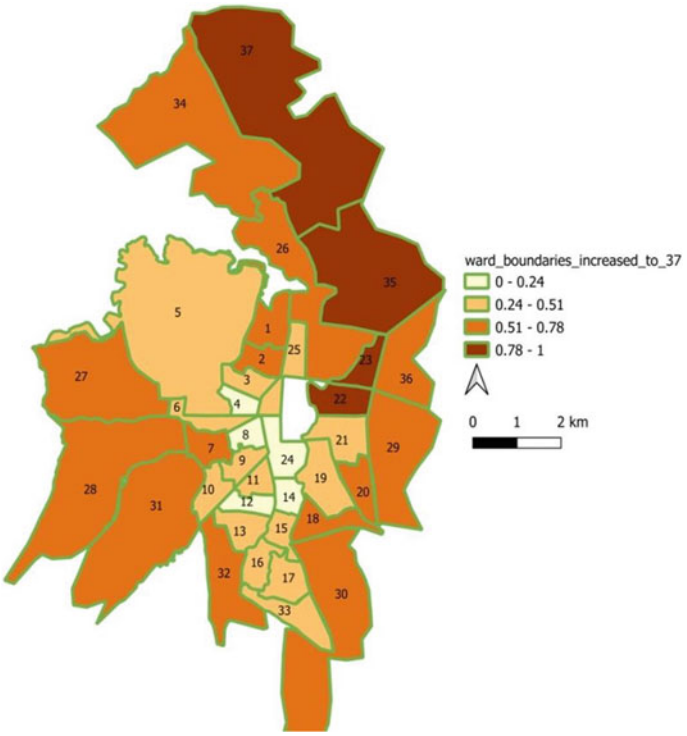

Fig. 3 The segregation of wards into relative ABISV using Eq. 2

of hospitals, primary health care facilities, community health centers, urban primary health centers and urban health center is assessed (Fig. 4). The value of a = 0.269; b = 0.097; c = −0.213 has been adopted from the CMP study for Ahmedabad [25].

5 Spatial Cross Classifications of Accessibility Level and ABISV

In order to assess the gap between the accessibility measure and social vulnerability index a cross classification mapping is done. The cross classification mapping is based on 'above' for accessibility measures higher than the average of all the wards implying good accessibility to health facilities and 'below' implying poor accessibility to health facilities. Similarly, the ABISV derived is categorized as 'above' implying High vulnerability and 'below' as Low Vulnerability. The first value in the legend (Figs. 5 and 6) indicates the ABISV values whereas the second value indicates accessibility measure.

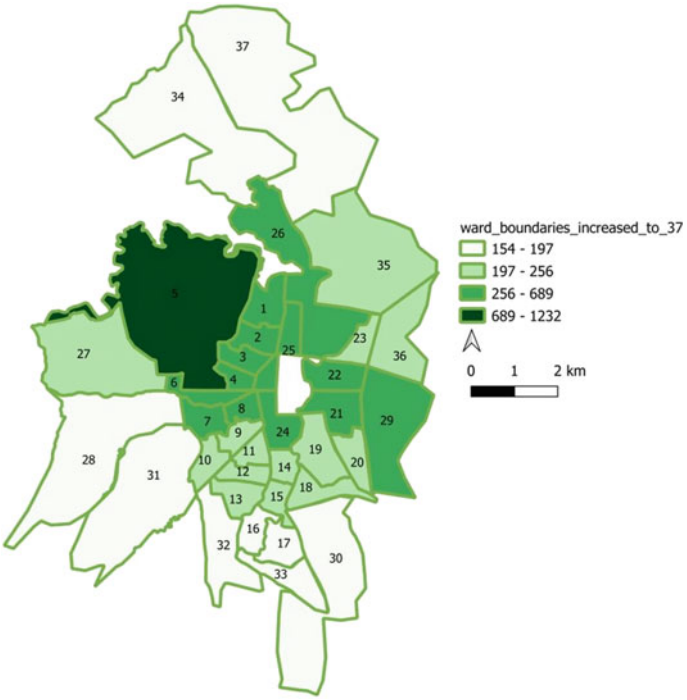

Fig. 4 The segregation of wards into accessibility measure for various health services using Eq. 5

From Figs. 5 and 6 one can deduce that the criteria wherein policy intervention would be required would be when ABISV is high (Above) and Accessibility is low (Below). Therefore wards 27,28, 31 32 30,18,20,22,23,36,25,26,34 and 37 would require policy interventions for provision of health services.

6 Heterogeneous Customer Satisfaction Index

Imphal is characterized by the prevalence of IPT services as the major mode of commute. Amongst the IPT services fixed route share autos are predominantly used for daily commute. An attempt was made to assess the customer satisfaction index for evaluating the transit service quality based on Heterogeneous customer satisfaction which takes into account the heterogeneity amongst user's judgments about the different service aspects [15].

The questionnaire was distributed amongst the IPT commuters of various wards and the scoring of importance ranged from 1 to 10 (1—unimportant, 5—neutral and 10—very important). Similarly, the scoring of satisfaction ranged from 1 to 10 (1—unsatisfied, 5—neutral and 10—very satisfied) and a total of 1500 was ascertained

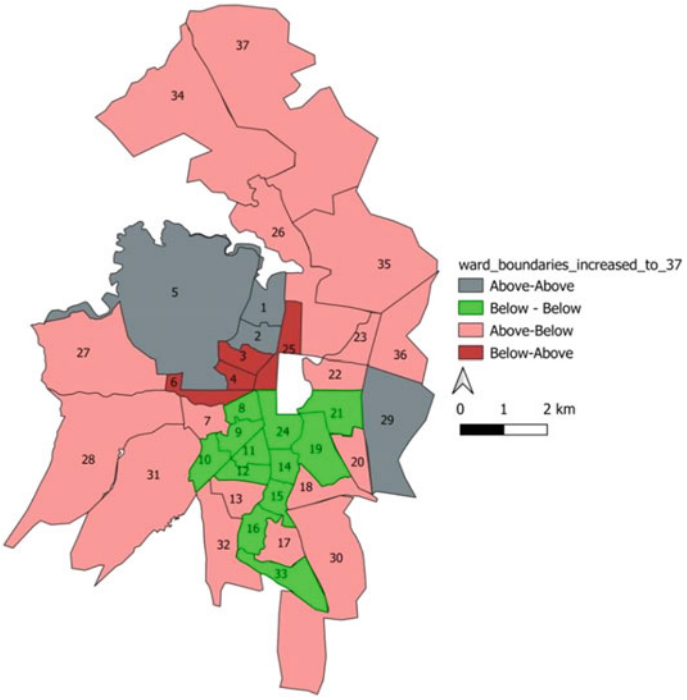

Fig. 5 Cross classification based on ABISV (Eq. 1) and accessibility measure

as the required sample size, however the surveyor was not able to complete several questionnaires and in several questionnaires the IPT mode chosen for commute was not marked. The collected sample was segregated based on daily commute and the current analysis pertains to IPT commuters who commute daily using the service. Since many questionnaires were not filled with chosen IPT, fare paid was used to ascertain the probable mode of travel. Accordingly, the assessment was done for 151 collected auto/share auto daily commute samples. Table 5 provides a descriptive analysis of the importance and satisfaction scores as reported for various service attributes.

The customer satisfaction index and heterogeneous satisfaction index were evaluated based on the following equations [15]:

$$CSI = \sum_{x=1}^{X} \overline{ST_x}.W_x \tag{6}$$

CSI—Customer Satisfaction Index.

$\overline{ST_x}$—mean of satisfaction scores expressed by users on service quality x attribute.

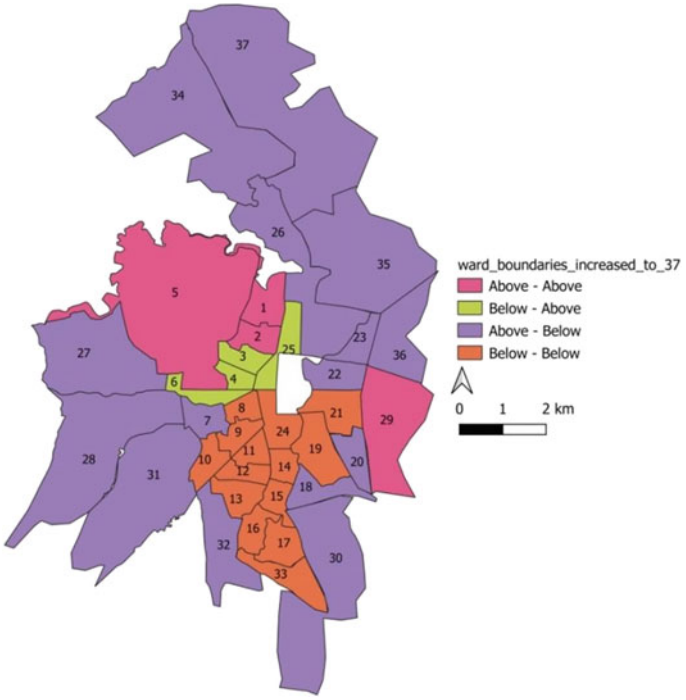

Fig. 6 Cross classification based on ABISV (Eq. 2) and accessibility measure

W_x—Importance weight is the weight of x attribute calculated on the basis of the importance scores expressed by users. It is specifically the ratio between the mean of the importance scores expressed by users on attribute x and the sum of the average importance scores of all the service quality attributes

$$W_x = \frac{\overline{I}_x}{\sum_{x=1}^{X} \overline{I_x}} \tag{7}$$

$$HCSI = \sum_{x=1}^{X} \overline{ST_x}^c . {W_x}^c \tag{8}$$

HCSI—Heterogeneous Customer Satisfaction Index.

$\overline{ST_x}^c$—mean satisfaction scores expressed by users on x attribute corrected according to the dispersion of the scores from the average value (Fig. 7 and Table 7).

$W_x{}^c$—is the weight of the x attribute, calculated on the basis of the importance scores expressed by users, corrected according to the dispersion of the scores from the average value.

Table 6 Importance and satisfaction statistics

Attribute	Attribute number	Importance				Satisfaction			
		Mean	Var	Conf Int		Mean	Var	Conf Int	
The distance of the IPT stop from your origin (access distance) in terms of your usage of the IPT service	1	5.43	1.95	5.21	5.66	3.68	1.45	3.49	3.87
The distance of the IPT stop from your destination (egress distance) in terms of your usage of the IPT service	2	5.298	2.81	5.03	5.57	3.53	1.46	3.33	3.72
Number of routes of IPT between your origin and destination in terms of your usage of the IPT service	3	4.89	1.97	4.66	5.11	3.85	1.84	3.63	4.07
The frequency of IPT services between your origin and destination in terms of your usage of the IPT service	4	4.85	2.33	4.61	5.1	3.8	1.63	3.63	4.04
The arrival of IPT services at the designated time (reliability) between your origin and destination in terms of your usage of the IPT service	5	5.046	2.03	4.82	5.28	4.19	1.7	3.98	4.4

(continued)

Table 6 (continued)

Attribute	Attribute number	Importance				Satisfaction			
		Mean	Var	Conf Int		Mean	Var	Conf Int	
The distance of the IPT stop from your origin (access distance) in terms of your usage of the IPT service	1	5.43	1.95	5.21	5.66	3.68	1.45	3.49	3.87
The seat availability within an IPT service while traveling between your origin and destination in terms of your usage of the IPT service	6	5.52	1.75	5.3	5.73	4.59	2.14	4.35	4.8
The cleanliness within an IPT service while traveling between your origin and destination in terms of your usage of the IPT service	7	5.76	2.57	5.50	6.02	4.75	2.67	4.48	5.01
The safe driving practices of an IPT driver while traveling between your origin and destination in terms of your usage of the IPT service	8	6.18	2.64	5.92	6.44	4.51	2.6	4.25	4.77
The safety within an IPT service in terms of property theft/eve teasing while traveling between your origin and destination in terms of your usage of the IPT service	9	7.44	3.022	7.16	7.72	4.17	2.89	3.9	4.45

(continued)

Table 6 (continued)

Attribute	Attribute number	Importance				Satisfaction			
		Mean	Var	Conf Int		Mean	Var	Conf Int	
The distance of the IPT stop from your origin (access distance) in terms of your usage of the IPT service	1	5.43	1.95	5.21	5.66	3.68	1.45	3.49	3.87
The safety at the IPT stop in terms of property theft/eve teasing while waiting for the service at the IPT stop in terms of your usage of the IPT service	10	7.44	3.88	7.13	7.76	3.82	2.99	3.54	4.1
The total travel time between an Origin and Destination while using an IPT service in terms of your usage of the IPT service	11	6.16	3.32	5.87	6.45	3.85	2.3	3.6	4.09
IPT stop ambiance (lighting, seating availability, shelter) in terms of determining your usage of the IPT service	12	5.32	3.14	5.03	5.60	4.01	1.54	3.81	4.21
The maintenance of IPT service in terms of number of breakdowns for determining your usage of the IPT service	13	4.85	3.9	4.53	5.17	4.1	2.42	3.88	4.38

(continued)

Table 6 (continued)

Attribute	Attribute number	Importance				Satisfaction			
		Mean	Var	Conf Int		Mean	Var	Conf Int	
The distance of the IPT stop from your origin (access distance) in terms of your usage of the IPT service	1	5.43	1.95	5.21	5.66	3.68	1.45	3.49	3.87
Ticket cost for determining your usage of the IPT service	14	5.03	2.57	4.77	5.28	4.51	2.18	4.27	4.75
Ecological vehicle such as E-rickshaw or E-Auto or E-bus for your choice to commute	15	4.85	2.32	4.6	5.09	4.71	1.77	4.49	4.92
The space required for accommodating the goods that you are carrying within the service in determining your usage of the IPT service	16	4.92	1.87	4.7	5.14	4.53	1.92	4.31	4.76
The comfort of seats within an IPT service while traveling between your origin and destination in terms of your usage of the IPT service	17	4.94	2.46	4.69	5.19	4.19	2.17	3.95	4.4

(continued)

Table 6 (continued)

Attribute	Attribute number	Importance				Satisfaction			
		Mean	Var	Conf Int		Mean	Var	Conf Int	
The distance of the IPT stop from your origin (access distance) in terms of your usage of the IPT service	1	5.43	1.95	5.21	5.66	3.68	1.45	3.49	3.87
The number of transfers of IPT service while traveling between your origin and destination in terms of your usage of the IPT service	18	4.96	2.24	4.72	5.2	4.11	2.42	3.86	4.36
The presence of a designated IPT stop in terms of usage of the IPT service	19	5.14	2.77	4.87	5.41	4.19	2.56	3.94	4.45
The total monthly expenditure spent traveling from your origin in terms of usage of the IPT service	20	4.88	2.97	4.6	5.16	4.33	2.62	4.1	4.59
The waiting time to assess an IPT service between your origin and destination	21	5.03	2.84	4.76	5.3	4.53	2.80	4.26	4.8

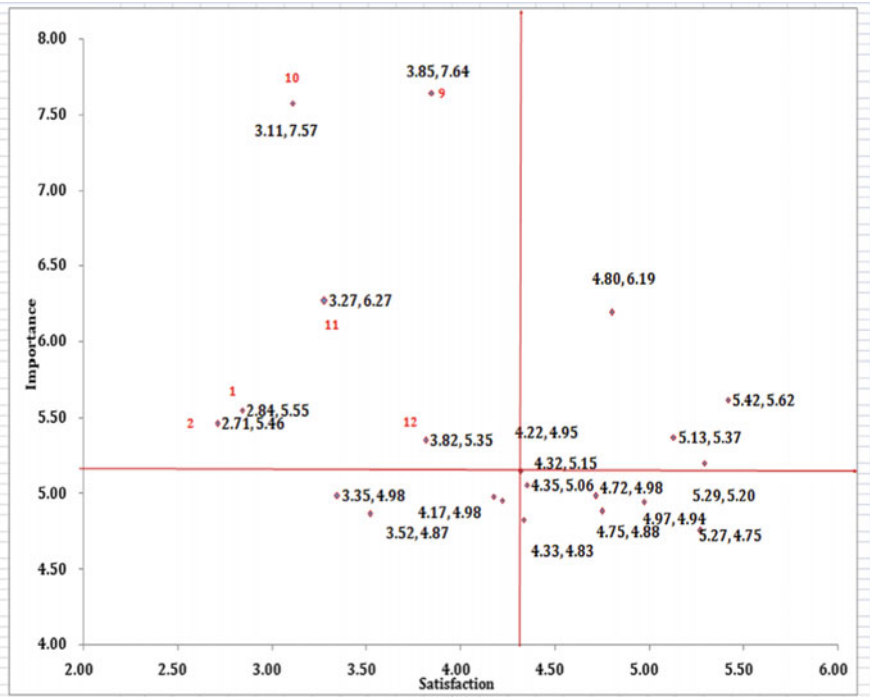

Fig. 7 The importance satisfaction diagram

$$\overline{ST_x}^{c} = \overline{ST}_x \frac{\frac{\overline{ST_x}}{var(ST_x)}}{\sum_{x=1}^{X} \frac{\overline{ST_x}}{var(ST_x)}} X \tag{9}$$

$$W_x{}^{c} = \frac{\frac{\overline{I_x}}{var(I_x)}}{\sum_{x=1}^{X} \frac{\overline{I_x}}{var(I_x)}} \tag{10}$$

Table 7 Calculating CSI and HCSI

Attribute number	Importance weights	Weighted score	Corrected importance weight	Corrected satisfaction	
1	0.048	0.166	0.048	2.839	0.137
2	0.048	0.160	0.048	2.710	0.129
3	0.043	0.162	0.043	3.345	0.146
4	0.042	0.162	0.042	3.518	0.149
5	0.044	0.188	0.044	4.351	0.192
6	0.047	0.217	0.047	5.130	0.241
7	0.049	0.233	0.049	5.416	0.266
8	0.054	0.241	0.054	4.800	0.259
9	0.067	0.267	0.067	3.847	0.257
10	0.066	0.238	0.066	3.108	0.205
11	0.055	0.202	0.055	3.275	0.179
12	0.047	0.186	0.047	3.817	0.178
13	0.042	0.179	0.042	4.335	0.183
14	0.043	0.196	0.043	4.972	0.215
15	0.041	0.194	0.041	5.272	0.219
16	0.043	0.189	0.043	4.749	0.202
17	0.043	0.181	0.043	4.222	0.182
18	0.043	0.181	0.043	4.174	0.181
19	0.045	0.190	0.045	4.319	0.194
20	0.043	0.193	0.043	4.715	0.205
21	0.045	0.213	0.045	5.290	0.240
	CSI	4.14		HCSI	4.16

7 Conclusion

The paper has attempted to provide a framework for assessing the accessibility measure for public health care facilities based on travel distance based impedance function and also assess the social vulnerability index based on two different evaluation methods provided in the literature. The paper also highlights the satisfaction index as perceived by daily commuters of IPT services in Imphal. From the analysis, it can be deduced that certain policy interventions in terms of provision of healthcare facilities need to be formulated especially in wards with high social vulnerability. Similarly, the overall customer satisfaction index indicates that daily commuters are not very satisfied with the current IPT services. The analysis indicates that the importance given to the service attributes by the commuters is also lesser than 5 (unimportant) which could be an indication that perhaps the daily commuters

are unaware of the better service attributes and thereby are unable to associate the required importance to the attributes.

8 Discussion

The paper has highlighted the accessibility measure for various health care facilities as well as the social vulnerability index for the study area. The cross mapping of the accessibility measure with the social vulnerability index helps in the identification of traffic analysis zones which need infrastructural interventions in the development of health care facilities. Such an intervention greatly improves the accessibility of regions with higher socially vulnerable group to health care facilities.

The customer satisfaction index developed is a measure of how the commuters perceive the quality of IPT services provided to them. The maximum importance given by the commuters is to the safety associated with property as well as individuals (eve teasing) both while waiting for the service as well as within the service. The variance corrected satisfaction level of the corresponding safety attribute is also low. This is an indication for the implementation agencies to better improve the safety by ensuring property theft reporting policy with increased penalization of the route/vehicle owners in the event of frequent property theft in their vehicle. Sensitization of drivers towards women's safety and handling of untoward situations resulting in eve teasing of women should be taught to the drivers through various training programs. The safe driving practices which also feature in the current commuter's high importance list should also be addressed through adequate driver training programs on safe driving practices. The reliability as well as seat availability of services needs to be addressed through increasing the fleet sizes. Similar policy implementations can be brought about through a comparative assessment of the importance and the satisfaction scores provided by individuals for the IPT services.

Acknowledgement The authors gratefully acknowledge the financial support extended by National Mission on Himalayan Studies for the project 'Trip Patterns and its implications on Intermediate Public Transport Services in Imphal, India' vide grant number NMHS_SP_SG_68 NMHS/2019-20/SG68/68.

References

1. Currie G (2004) Measuring spatial distribution of public transport needs and identifying gaps in the quality of public transport provision. Transp Res Rec: J Transp Res Board 1895:137–214
2. World Development Report (2012) Gender equality and development background paper, gender and mobility in the developing world
3. A Gendered Perspective of the Shelter–Transport–Livelihood Link: The Case of Poor Women in Delhi

4. Boisjoly G, El-Geneidy A (2016) Daily fluctuations in transit and job availability: a comparative assessment of time-sensitive accessibility measures. J Transp Geogr 52:73–81. https://doi.org/10.1016/j.jtrangeo.2016.03.004
5. Boisjoly G, Moreno-Monroy AI, El-Geneidy A (2017) Informality and accessibility to jobs by public transit: evidence from the Saõ Paulo metropolitan region. J Transp Geogr 64:89–96. https://doi.org/10.1016/j.jtrangeo.2017.08.005
6. Sharma G, Patil GR (2021) Public transit accessibility approach to understand the equity for public healthcare services: a case study of Greater Mumbai. J Transp Geogr
7. Nutley S (2003) Indicators of transport and accessibility problems in rural Australia. J Transp Geogr 11(1):55–71
8. Church M, Frost K (2000) Sullivan 'transport and social exclusion in London.' Transp Policy 7:195–205
9. Jolliffe IT Principal component analysis, 2 edn. Springer publications
10. Krishnan V (2013) Constructing an area-based socioeconomic index: a principal components analysis approach
11. Vyas S, Kumaranayake L (2006) Constructing socio-economic status indices: how to use principal components analysis. Health Policy Plan 21(6):459–468. https://doi.org/10.1093/heapol/czl029
12. Howe LD, Hargreaves JR, Huttly SR (2008) Issues in the construction of wealth indices for the measurement of socio-economic position in low-income countries. Emerg Themes Epidemiol 5:3. https://doi.org/10.1186/1742-7622-5-3
13. Jackson EF, Siddiqui A, Gutierrez H et al (2015) Estimation of indices of health service readiness with a principal component analysis of the Tanzania Service Provision Assessment Survey. BMC Health Serv Res 15:536. https://doi.org/10.1186/s12913-015-1203-7
14. Jaramillo C, Lizárraga C, Grindlay AL (2012) Spatial disparity in transport social needs and public transport provision in Santiago de Cali (Colombia). J Transp Geogr 24:340–357
15. Eboli L, Mazzulla G (2009) A new customer satisfaction index for evaluating transit service quality. J Public Transp 12(3):2009
16. Census Handbook East Imphal and West Imphal (2011). https://censusindia.gov.in/census.website/. Accessed 10 Sept 2021
17. Economic Survey Manipur 2020–21. http://desmanipur.gov.in/files/NewsFiles/15Feb2021011944Economic%20Survey%20Manipur,%202020-21.pdf. Accessed 12 Sept 2022
18. Kunhikrishnan P, Srinivasan KK (2018) Investigating behavioural differences in the choice of distinct Intermediate Public Transport (IPT) modes for work trips in Chennai city. Transp Policy 61
19. Soegijoko BTS (1982) Intermediate public transportation for developing countries case study: Bandung, Indonesia, 1982, Ph.D. thesis. Massachusetts Institute of Technology
20. Kotzee I, Reyers B (2016) Piloting a social-ecological index for measuring flood resilience: a composite index approach. Ecol Ind 60:45–53. https://doi.org/10.1016/j.ecolind.2015.06.018
21. Principal Component Analysis. https://www.statstutor.ac.uk/resources/uploaded/principle-components-analysis.pdf
22. McKenzie DJ (2003) Measure inequality with asset indicators. BREAD Working Paper No. 042. Cambridge, MA: Bureau for Research and Economic Analysis of Development, Center for International Development, Harvard University
23. Houweling TAJ, Kunst AE, Mackenbach JP (2003) Measuring health inequality among children in developing countries: does the choice of the indicator of economic status matter? Int J Equity Health 2:8
24. Hansen WG (1959) How accessibility shapes land use. J Am Plan Assoc 25(2):73–76. https://doi.org/10.1080/01944365908978307
25. Comprehensive Mobility Plan—Ahmedabad ; CRRI report (2021)

Evaluation of Air Quality for Various Demand Management Scenario (Work from Home and Switch to Electric) for a Region in Delhi NCR

U. Gupta, S. Padma, R. Singh, A. Shukla, N. Dogra, and S. Ram

Abstract The transport sector contributes towards 28% and 24% of total pollution for PM2.5 and PM10 respectively in the Winter season in the region of Delhi according to a source apportionment study 2016 carried out by The Energy and Resource Institute (TERI). In order to control the air pollution in the atmosphere, Electric vehicles are being promoted via various schemes to lure the public to make a switch from petrol or diesel run vehicles to electricity run vehicles (EV). This paper aims to study the effectiveness of implementing such schemes. In addition to this, the effects of initiatives such as Work from Home (WFH) on pollutant concentration reduction are also studied. This is achieved by creating an air dispersion model using UK based ADMS-Urban software for three scenarios namely Original Scenario, Switch to Electric (STE) scenario and WFH Scenario and comparing the output concentration for each scenario. To better understand the contribution of traffic on pollutants, three different intensities of traffic volume have been incorporated in this paper, namely High Traffic Road, Medium Traffic and Low Traffic. Since the major air pollutants emerging from the transport sector constitutes NO_x and CO, a lot of research has been done in the past to understand these pollutants but little research has been done on the minor pollutants of the transport sector that is PM10 and PM2.5. Till date, all the research evaluated the particulate matter concentration collectively, combining all sizes of PM. This research focuses on drawing a line between PM10 and PM2.5 and therefore the effect on these pollutants due to the implementation of the demand management scenario has been done separately for PM10 and PM2.5. It is found that a reduction of up to 4.19% for STE scenario and 2.32% for WFH is

U. Gupta (✉) · S. Ram
Department of Civil Engineering Gautam, Buddha University, Greater Noida, U.P. 201312, India
e-mail: uditagupta99@gmail.com

S. Padma · R. Singh · A. Shukla
Transport Planning and Environment Division, CSIR-Central Road Research Institute, New Delhi 110025, India
e-mail: padma.crri@nic.in

N. Dogra
Environment and Health, The Energy and Resources Institute (TERI), New Delhi 110003, India

A. Dhamaniya et al. (eds.), *Recent Advances in Traffic Engineering*, Lecture Notes in Civil Engineering 377, https://doi.org/10.1007/978-981-99-4464-4_33

possible for high traffic roads for PM10. For PM2.5, the reduction observed is 1.13% and 2.23% for WFH and STE scenarios respectively.

Keywords ADMS-Urban · PM2.5 · PM10 · Work-from-home · Switch-to-electric · Traffic volume

1 Introduction

According to World Air Quality Report 2021, New Delhi emerged as the most polluted capital city in the world. Government organizations have started various pilot projects to combat air pollution in the capital city such as building smog towers, convincing farmers to opt for alternatives of stubble burning, sprinkling water at major road junctions, promoting electric vehicles (EV) and many more. But the air quality of Delhi is far from "Good" or "Satisfactory" levels of AQI. During COVID-19 pandemic, improvement in air quality was reported and few months later, work from home (WFH) became a convenient and essential part of our lives. Moreover, the Switch to Electric (STE) vehicle initiative is gaining pace in the capital city. This paper assesses the effect on air pollution levels if scenarios such as Switch to Electric and work from home are implemented to the possible extent.

ADMS-Urban: ADMS-Urban is an air dispersion modeling software developed by UK based research facility, CERC. It is based on the Gaussian dispersion model and Monnin-Obukhov length: two important factors in air modeling [1]. For Indian areas, software ADMS is relatively new therefore in the recent past, various researchers have focused on the performance of ADMS-Urban for Indian regions. Mohan et al. [2] compared the performance of AERMOD (an existing air dispersion model) and ADMS for Total Suspended Particulate Matter (TSPM) concentration in Delhi and concluded that both models have a tendency to underpredict. It used statistical parameters such as correlation coefficient, index of agreement, IA, fractional bias, FB, Normalized root mean square error, NMSE (0.05–0.29), Geometric Mean Bias, GMB, Geometric Variance, GV, root mean square error, RMSE (50.47–192.83) and scatter plots between model results and observed results to establish the validity of the model.

Vijay et al. [3] evaluated the performance of ADMS-Urban model for PM10 concentrations at the roadside of two cities, one in Chennai and two, in Newcastle in UK. It has used statistical parameters like IA, FB, VG and NMSE (0.19 for Chennai) and concluded that ADMS-Urban works with reasonable accuracy for PM in both cities but shows better results for European cities.

Source apportionment studies for Delhi NCR: Over the past decade, few source apportionment studies have been carried out to trace the pollutant concentration. Air Quality Monitoring Emission Inventory and Source Apportionment Studies for Delhi, NEERI, 2007 carried out at various locations in DELHI including Ashram chowk (inside our study area). According to this report in winter season, vehicles contribute about 11% of total PM10. A newer similar study conducted by TERI and ARAI

called Source Apportionment of PM2.5 and PM10 of Delhi NCR for Identification of Major Sources suggests that the transport sector contributes towards 28 and 24% of total pollution for PM2.5 and PM10 respectively in the winter season in Delhi NCR [4].

Various policy measures or Traffic management strategies (TMS) and their effect on air quality have been studied extensively over several years. Bigazzi and Rouleau [5] comprehensively reviewed the effect of TMS on air quality by categorizing them into Travel Demand Management (TDM), Transportation Control Measures (TCM), and Congestion Mitigation and Air Quality Improvement programs. It was inferred from the above studies that the impact of TMS on Vehicle Kilometers Traveled (VKT) and the corresponding average emission rates (mass per VKT) brought about positive changes in ambient air quality [6]. Sharma et al. [7] suggests that shifting to EV vehicle will reduce PM2.5 concentration levels generated from road sources by 25% (contribution of transport sector in PM2.5 concentration).

Righi et al. [8] used a method given by European Environment Agency to calculate emission rate based on volume of traffic, emission factors and road length [5]. Similar methodology is used by Gulia et al. [9] based on emission factors for different vehicle types, age profiles and fuel types and traffic flow [10]. Different methods are used to assign background concentration for modeling requirements. Gulia et al. [9] chose the background concentration as the lowest concentration of PM2.5 and CO of monitored data. Bell et al. [10] used the Panchkula Station located in Northern Haryana for measuring background concentrations for the same size of study area as used in this study. Biggart et al. [11] explained that the location of background concentration should be chosen such that the location lies in the upwind direction of the study area.

For Indian vehicles, ARAI formulated emission factors for pollutants such as CO, NO_x, PM and others for each vehicle type in 2007 under the funding of the Central pollution control board (CPCB). But the emission factors booklet does not differentiate between PM10 and PM2.5. As per our literature research, till now these emission factors are being used to carry out research work on PM with no specification of the pollutant being PM10 or PM2.5. Therefore, in this study, emission factors for PM10 and PM2.5 for different vehicle type are adopted from the latest literature to use updated emission factors [12, 13].

The objective of this study is to evaluate the reduction in air pollutant concentration if STE and WFH scenarios/policies are implemented and to understand the effect on air pollutant concentration of different traffic intensities.

2 Methodology

This paper studies three scenarios: Original (O), Switch-To-Electric (STE) and Work-From-Home (WFH). For each scenario, traffic fleet is measured/calculated using necessary assumptions, and the effect on the concentration of PM10 and PM2.5 is evaluated. The methodology used is explained below:

2.1 Model Preparation Using ADMS-Urban Software

In order to create an air dispersion model, ADMS-software requires the following input data in order to create the required model: Time varying emission rates, meteorology data and the background concentration of pollutants.

Time varying emission factors are software calculated values obtained by using the emission rates of road sources and time varying factors (variation in vehicle flow with change in hours of a day). This study has adopted distance-based emission factors from secondary sources [12, 13] for different vehicle types (differentiated further based on age and fuel type). The emission factors used in this study are summarized in Table 1. These emission factors are used to calculate emission rates using the following formula used by Gulia et al. [9]. Emission rates are assigned to each road source.

$$P(i) = \sum \sum N(j,\ k) * EF(i,\ j,\ k) j\, k$$

where,

P(i) = Emission rate of pollutant 'i' (i = PM10, PM2.5)

N(j,k) = Number of vehicles of a particular type 'j' and age of vehicle 'k',

EF(i,j,k) = Emission factor for pollutant 'i' in the vehicle type 'j' and age 'k' (gm/km), j = Type of vehicle (Cars-Petrol, Diesel, CNG driven, bus, HCV, LCV, 2W).

Traffic flow count studies were carried out at eight road sections using video cameras for estimating the traffic time varying factors. It is the ratio of the number of vehicles traveling in an hour to the daily average number of vehicles. Hourly emission rates or time varying emission rates are taken into account to address variations in traffic flow during peak hours and non-peak hours. Figure 1 shows the hourly variation of emission rates.

Table 1 Emission factors of PM10 and PM2.5 in gm/km. *Source* Mishra and Goyal [13], Habib et al. [12]

Vehicle type	PM10[a] [13]			PM2.5[b] [12]		
Age (years)	<5	5–10	>10	<5	5–10	>10
2 Wheelers	0.018	0.25	0.035	0.018	0.018	0.018
Bus	0.014	0.014	0.014	0.018	0.018	0.018
LCV	0.5	0.8	0.8	0.5	0.5	0.5
HCV	0.6	0.7	0.9	1	1	1
3 Wheelers	0.014	0.014	0.014	0.023	0.023	0.023
Cars (Petrol)	0.005	0.005	0.005	0.062	0.206	0.033

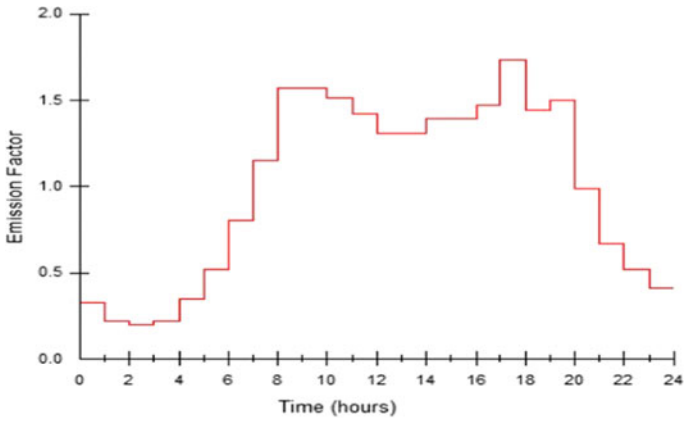

Fig. 1 ADMS-Urban generated plot showing hourly emission factors

The traffic flow is categorized in different vehicle types such as Cars, Buses, Cycle, Two Wheelers, Light Commercial Vehicle (LCV), 6Axle-3Axle, Multi-Axle Vehicle, CNG Autos, E-Rickshaws, 3–4 Wheelers Goods, Cycle Rickshaws and others was observed. To take account of the vehicle age, the age distribution of vehicles is adopted from a study done by IIT Delhi. The percentage of vehicle are divided into categories of less than 5 years old vehicles, 6–10 years of age, 11–15 years of age and vehicles that are older than 15 years. The proportion of vehicles being older than 15 years is very low due to the fact that it is not allowed in Delhi to run vehicles older than 15 years of age. The percentages are tabulated below in Table 2 and to take account of various fuel types being used for driving vehicles, fuel-based segregation is adopted from a study done by CRRI in 2016 and the values used are tabulated in Table 3.

Meteorology factors were jointly obtained from Central Pollution Control Board (CPCB) run Continuous Station Status Portal and from Integrated surface dataset (Global) provided by National Centers for environmental information, and National Oceanic and atmospheric administration (NOAA). This study also takes similar

Table 2 Vehicle distribution in various age groups

Vehicle type	<5	6–10 yrs	11–15 yrs	>15 yrs
Two wheelers	73	23	3	1
Cars	68	26	6	1
LCV (CNG)	84	13	3	0
Tempo	54	31	15	0
Truck	49	35	17	0
Buses	22	70	8	0
Auto (CNG)	39	56	5	0

Table 3 Vehicle distribution based on fuel type

Two wheelers		Cars				Autos			Buses		HCVs
4 stroke	2 stroke	CNG	LPG	Diesel	Petrol	LPG	Petrol	CNG	CNG	Diesel	Diesel
83	17	9	1	27	63	1	2	97	71	29	100

assumptions as Biggart et al. [11] that mixing height is assumed to be equal to the model calculated Planetary Boundary layer (PBL).

For background concentration, a source apportionment study is used. It suggests that the transport sector contributes towards 28 and 24% of total pollution for PM2.5 and PM10 respectively in winter season in Delhi NCR [4]. The background concentration of air pollutants is measured at upwind direction of the study area and 72 and 76% (excluding road transport contribution) of the measured data is opted as background concentration. Please NOTE this method of calculating background concentration can be used only for PM10 and PM2.5 as these pollutants are built into the software and considered as a special case [USER Manual].

{ADMS-Urban calculates the pollution from road sources (transport sector) of particulate matter for both exhaust and non-exhaust (wear and tear of tires, brake applying) emissions. ADMS Urban considers particulate matter pollution as a special case. It has divided the PM into three categories: Coarse particulates, Secondary particulates and Primary particulates. Coarse particulate includes emissions from non-combustion sources such as suspended soils and dusts, particles from construction work. Secondary particulate includes particulate which forms in the atmosphere, following the release of emissions in the gaseous phase. It also includes emissions from combustion sources outside the study area. The primary particulates include sources of emission within the study area. ADMS -Urban models primary particulates only. The background concentration should include the total sum of coarse particulates and secondary particulates.}

Because the concentration of pollutants varies with time therefore hourly background concentration has to be entered. Since there is no mechanism to measure the pollution generated from all sources but transportation for our study area, therefore this method has been adopted.

Study period: As in National Capital Territory of Delhi, Air quality worsens during winter season, therefore the focus of the study has been chosen as winter season. The contribution percentage for evaluating background concentration is therefore chosen for the winter season. The pollutant concentration data used for validating the model is also measured in the month of February 2021. The hourly values of background concentration are measured at the upwind direction of the study area near Ashram Chowk in February 2021 [11].

2.2 Validation of Model

The concentration of PM10 and PM2.5 were recorded at six different locations; Sarita Vihar (SV), Tekhand (TK), Shaheen Bagh (SB), C V Raman Marg (CV), Madanpur Khadar (MK) and Noor Nagar (NK). These locations are chosen such that two of these lies in different intensity of traffic volume: High Traffic, Medium Traffic and Low Traffic. The traffic flow at a rate of around 10,000 veh/hr is observed at high traffic locations, 4000 veh/hr at medium traffic locations (CV, SB) and 500 veh/hr at Low Traffic conditions (MK, NN). Diurnal variation of PM 10 and PM 2.5 measured at receptor locations are shown in Fig. 2. The hourly values of concentration of PMs obtained from the ADMS-Urban are validated with the observed data measured at six receptor sites. The model is validated using normalized root mean square error (NMSE), root mean square error (RMSE) and R^2 values. The acceptable range of NRMSE value is −0.5–0.5 [14]. NMSE and RMSE values are calculated for six locations as tabulated in Table 4. As shown in the table below the NMSE values for all locations are within the allowable range except for Noor Nagar area. The reason behind this is the generation of dust pollution very near to the receptor location due to heavy construction work in Noor Nagar area. This dust pollution couldn't be added to the common background concentration of the entire area.

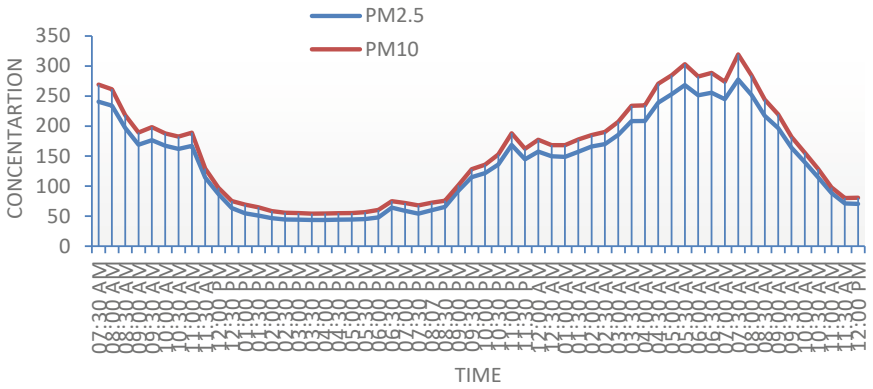

Fig. 2 Diurnal variation of PM 10 and PM 2.5 in study area

Table 4 Validation result of model developed

		High traffic		Medium		Low traffic	
		SV	TK	SB	CV	MK	NN
NMSE	PM2.5	0.152	0.355	0.282	0.367	0.344	0.485
	PM10	0.261	0.418	0.46	0.36	0.35	0.7
RMSE	PM2.5	14.456	14.25	15.345	32.58	37.58	62.476
	PM10	29.731	35.36	22.96	34.07	28.74	263.7

Scatter plots of ADMS-urban generated pollutant concentration versus measured concentration were prepared. Due to the word limit, only scatter plots of only one location i.e., Sarita Vihar is presented here, though for PM2.5, R^2 value equals 0.9027 and for PM10, R^2 value equals 0.7808 is obtained. The results showed good validation of the model developed. After validating the model, we came to the conclusion that model is working perfectly fine, therefore this model can be used in different scenarios, which is described in the next section.

2.3 Estimating Predicted Pollution for WFH and STE Scenario

To calculate the pollutant concentration in the scenario of WFH and STE, updated/reduced traffic volumes are desired. The methodology opted for the same is explained below (Fig. 3).

2.3.1 Work from Home

While assessing the possible number of trips that can be converted to 'work from home' one looks at the economic profile of the commuters. It is a well-known fact that developing country like India has less of the salaried workers, self-employed workers and more of hire workers and casual workers. The hire workers and casual workers seldom have a job that can entail them to sit at home and complete it. Such sectors mostly need the physical presence of the workforce and therefore cannot be accounted in the 'work from home' policies. A study conducted by IIT Delhi indicates that 77% of the bus commuters have less than Rs. 30,000 as the annual income thereby making only 23% of the bus commuters to be candidates for 'work from home'. Advani et al. [15] based on various employment sectors and the number

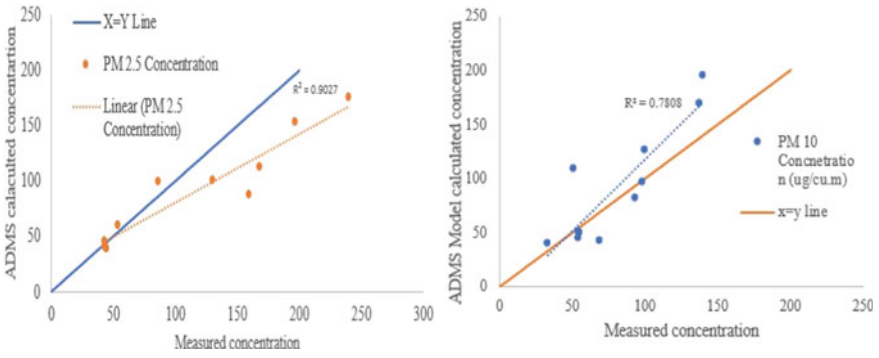

Fig. 3 Scatter plot of measured vs modeled values for PM2.5 and PM10 at Sarita Vihar Locations

Table 5 Elasticity value and growth rate

Vehicle type	Elasticity value	Growth rate
Cars	0.078616	2.737679
Bus	0.737674	25.68827
Autos	−0.27738	1.401954
2 Wheelers	0.319015	11.10915

of trips carried out using various modes by these employment sectors, the proportion of employment sector considered for WFH for various modes of travel is evaluated as 38% of 2-Wheelers, 38% of cars, 53% of metro and 58% bus. Removing these proportions from traffic flow, we get traffic flow for WFH scenario.

2.4 Switch to Electric

Delhi EV policy 2020 aims to convert 25% of newly registered vehicles to electric by 2025. Assuming this objective is achieved, modified traffic volume is evaluated using the following method.

This study uses the economic method of projection. Electric vehicle penetration is evaluated by co-relating growth in per capita income with newly registered private vehicles such as cars and 2 wheelers and Net State Development product per capita is co-related with growth in buses and autorickshaws (considering 2011 as base year). Net State Development Product (NSDP) and per capita income from 2011 to 2021 is taken from Annual Economic survey of Delhi and a number of newly vehicles registered is taken from Road Transport Year Book published by Ministry of Road Transport and Highways (MORTH). From the regression, the Coefficient of x variable is taken as elasticity value. Growth rate is taken as the product of elasticity value and an average of growth of NSDP/per capita income. The number of vehicles obtained is reduced to 75% as per Electric vehicle policy 2020, Delhi. Rest of the vehicle types are assumed to be running at existing fuel type proportionally.

As there is no tail–pipe emissions in electricity run vehicles, therefore, emission factors for these are taken as ZERO (Table 5).

3 Results

A comparison of the daily average concentration of PM10 and PM2.5 for the original scenario and for demand management scenarios (WFH, STE) is analyzed. The reduction in pollutant concentration is evaluated and is capsulated in the table. Highest percentage of reduction in concentration in WFH and STE scenarios is observed to be 2.32% and 4.196% for High traffic roads for PM10 (Table 6).

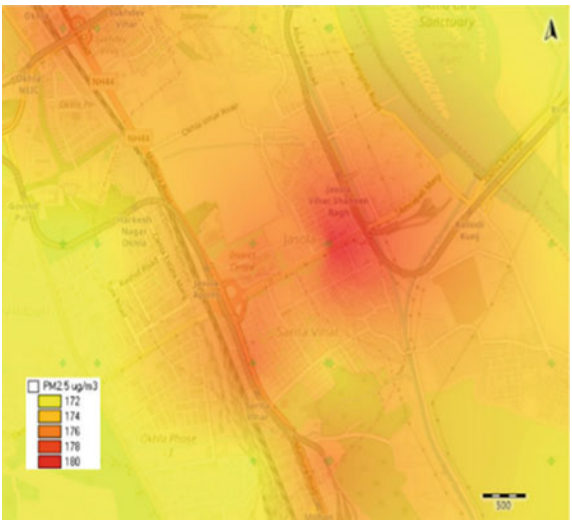

Fig. 4 Shows contour plot for PM2.5 for entire study area (ug/m^3)

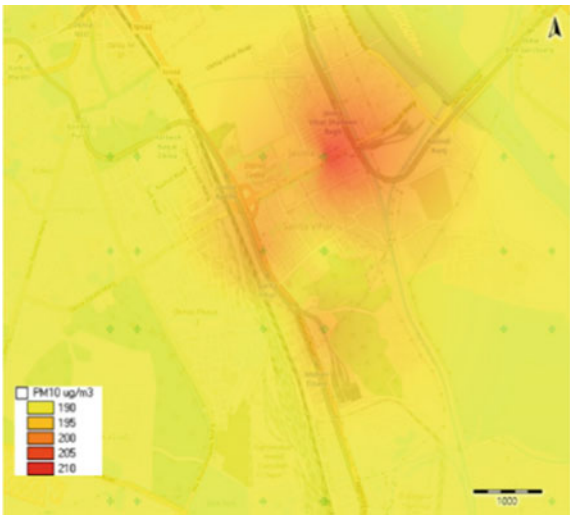

Fig. 5 Shows contour plot for Pm10 for entire study area (ug/m^3)

Table 6 Percentage reduction for STE and WFH scenarios

Receptor	Traffic flow type	Scenario	PM10	PM2.5
Sarita Vihar (SV)	High	WFH	2.32	1.13
C V Raman Marg (CV)	Medium		1.99	0.826
Madanpur Khadar (MK)	Low		0.51	0.253
Sarita Vihar (SV)	High	STE	4.196	2.23
C V Raman Marg (CV)	Medium		4.19	2.23
Madanpur Khadar (MK)	Low		0.89	0.494

4 Discussion of Results and Conclusion

Pollution Reduction in WFH Scenarios

As stated earlier, the Source apportionment study, 2016 underlines that the transport sector contributes towards 28% and 24% of total pollution for PM2.5 and PM10 respectively in the winter season in the region of Delhi. In this study, percentage reduction is evaluated. For high traffic road section, percentage reduction is observed at 2.32% and 1.13% for PM10 and PM2.5 respectively. For medium traffic roads, the reduction percentage stands at 1.99% and 0.826% for PM10 and PM2.5 respectively. And the percentage reduction further decreases for low traffic flow roads and is equal to 0.51% for PM10 and 0.253% for PM2.5. Among the three different types of road traffic volumes viz, High Traffic, Medium Traffic and Low traffic, not only the traffic flow is varying but also the traffic composition is different. For e.g., on low traffic sections; two wheelers, e-rickshaws, cycles and CNG autos, the least polluting vehicles (in terms of tail pipe emissions) form the majority portion. Hence removing number of possible trips to the office in order to implement WFH does not bring much change in the concentration of PM10 and PM2.5 at low traffic sections. On the other hand, high traffic road sections' traffic composition is majorly made of passenger Cars, Buses and Two wheelers, therefore removing a number of trips resulted in a significant percentage reduction in pollutant concentration. (Road transport sector). It looks promising if this study is extended to the entire NCT region, the transport sector's contribution towards total pollution can be brought down in pollutant concentration.

Pollution Reduction STE Scenario

In this scenario, the percentage reduction found is greater than the percentage reduction in WFH scenario, even though applying STE scenario only removes/ lesser percentage of vehicles (on cars, buses, two wheelers and auto-rickshaw) than it is removed by WFH. But the modified composition for STE scenario is such that the percentage reduction is greater than found for WFH scenario. Possible reason is, in STE CNG run autos are also replaced by electric Autos, therefore more reduction in pollutant concentration for STE is observed, as CNG autos produce a significant quantity of PM pollutants due to incomplete combustion of fuel and lubricating oil. For PM10 and PM2.5 percentage reduction is same for high and medium traffic flow conditions i.e., 4.19% and 2.23% respectively. In low traffic conditions, the percentage reduction comes down to 0.89% and 0.49% for PM10 and PM2.5.

Contour Plots

Contour plots for original scenario are created in this study. Contour plots are made for the study area considering all sources of pollution and not just only the transport sector. In other words, contour plots are plotted using background concentration plus road source contribution (model generated) (Figs. 4 and 5).

Diurnal Variation of PM10 and PM2.5 Concentration as Measured

Diurnal concentration plots of either observed or modeled data show a trend where pollutant concentration starts to decrease from around 11:30 am and continues to remain in safe limits till late afternoon. The concentration starts to gradually increase from around 7:00 pm to 9:00 pm and further the concentration exponentially increases till around 5:00 am in the morning. This trend observed is similar for all locations. This trend is independent of source of pollutant and is dependent on factors affecting stability of atmosphere (such as solar radiation, and wind speed). Source of pollution determines the quantity of pollutants but suspension and existence of pollutants are determined by atmospheric factors (explained further in the next paragraph). Policy makers can use this trend and can shift the working hours (offices, schools and others) timings starting from morning (8:00 am to 10:00 am) to later timings (11:30 am to 12:00 pm).

Performance of Model

ADMS-Urban is a software designed primarily for European countries. Efforts have been made by the developer in the software so that it can be used worldwide. But while using the software following observations came to light.

Effect of Solar Radiation on Pollutant Concentration

Stability of atmosphere plays a crucial role in determining the pollutant's concentration. During evening and nighttime, when the ambient temperature starts to fall, an inversion layer is formed near the surface in which all the pollutants are trapped near the ground surface. When the sun rises the next day (as solar radiation increases), as ambient temperature rises, the inversion layer formed previous night rises above the ground surface and the pollutants trapped near ground surface gets dispersed. Because of this in the morning, pollutant concentration is higher, during the afternoon when solar radiation is maximum, pollutant concentration is minimum, by the time of evening, pollutant concentration is higher due to the inversion layer again.

While transitioning from forenoon to afternoon, drastic reduction in concentration is observed (measuring pollutant concertation) but ADMS- Urban generated model lags this reduction in concentration by an hour, which affects the statistical parameters to some extent causing damage to the validation of model.

Acknowledgements The authors of this paper acknowledge the contribution of CPCB and National Oceanic and atmospheric administration (NOAA) in providing necessary meteorology data.

References

1. Jänicke B, Milošević D, Manavvi S (2021) Review of user-friendly models to improve the urban micro-climate. Atmosphere 12(10):1291

2. Mohan M, Bhati S, Sreenivas A, Marrapu P (2011) Performance evaluation of AERMOD and ADMS-urban for total suspended particulate matter concentrations in megacity Delhi. Aerosol Air Qual Res 11(7):883–894
3. Vijay P, Shiva Nagendra SM, Gulia S, Khare M, Bell M, Namdeo A (2021) Performance evaluation of UK ADMS-urban model and AERMOD model to predict the PM_{10} concentration for different scenarios at Urban Roads in Chennai, India and Newcastle City, UK. In: Shiva Nagendra SM, Schlink U, Müller A, Khare M (eds) Urban air quality monitoring, modelling and human exposure assessment. Springer transactions in civil and environmental engineering. Springer, Singapore. https://doi.org/10.1007/978-981-15-5511-4_12
4. Source Apportionment of PM2.5 & PM10 of Delhi NCR for Identification of Major Sources, 2018, TERI
5. Bigazzi AY, Rouleau M (2017) Can traffic management strategies improve urban air quality? A review of the evidence. J Transp Health 7:111–124. https://doi.org/10.1016/j.jth.2017.08.001
6. Air Quality Monitoring Emission Inventory and Source apportionment Studies for Delhi, NEERI, 2007
7. Sharma I, Chandel MK (2020) Will electric vehicles (EVs) be less polluting than conventional automobiles under Indian city conditions? Case Stud Transp Policy 8(4):1489–1503
8. Righi S, Lucialli P, Pollini E (2009) Statistical and diagnostic evaluation of the ADMS-Urban model compared with an urban air quality monitoring network. Atmos Environ 43(25):3850–3857
9. Gulia S, Nagendra SS, Khare M (2014) Performance evaluation of ISCST3, ADMS-Urban and AERMOD for urban air quality management in a mega city of India. Int J Sustain Dev Plan 9(6):778–793
10. Bell M, Williams H, Goodman P (2021) Bottom—up modelling air quality in Delhi and potential air quality interventions. In: Indian international conference on air quality management
11. Biggart M, Stocker J, Doherty RM, Wild O, Hollaway M, Carruthers D, Shi Z (2016) Street-scale air quality modelling for Beijing during a winter 2016 measurement campaign. Atmos Chem Phys 20(5):2755–2780
12. Habib G (2017) Chemical and optical properties of PM2. 5 from on-road operation of light duty vehicles in Delhi city. Sci Total Environ 586:900–916
13. Mishra D, Goyal P (2014) Estimation of vehicular emissions using dynamic emission factors: a case study of Delhi, India. Atmos Environ 98:1–7
14. Dėdelė A, Miškinytė A (2015) The statistical evaluation and comparison of ADMS-Urban model for the prediction of nitrogen dioxide with air quality monitoring network. Environ Monit Assess 187:578. https://doi.org/10.1007/s10661-015-4810-1
15. Advani M, Velmurugan S, Padma S (2020) Impact of COVID-19 on the demand of road based public transport and the potential improvement through infrastructure and service changes in Delhi. In: A paper presented at the-international e-conference on pandemics and transport policy (ICPT2020), 7th December 2020

Study of Driver Behavior in Overtaking Maneuvers on Undivided Road in Indian Context

Indrajeet Kumar and Amit Kumar Yadav

Abstract The most difficult and important maneuvers on undivided road is overtaking maneuvre. Fast moving vehicles overtake slow moving vehicles with facing incoming traffic from the opposite direction. Lateral movements of vehicle are influenced by various parameters like driver behavior, vehicle type and vehicle speed. Drivers of small vehicles like motorcycles have the flexibility to maintain closer safe distances from the vehicles in front, and tolerate smaller lateral clearances while making lateral movements inside the lane as well as across the lanes. While heavy vehicle drivers have less freedom when it comes to increasing/decreasing speed and operating lateral movements. The main objective of this study is to evaluate lateral features of drivers on two-lane two-way undivided roadways. And develop model for lateral features of vehicles. For this, video graphic techniques were used to collect traffic data on urban undivided road segment in Aurangabad, Bihar, India. For various types of subjects and opposing pair, lateral separation was analyzed by multiple linear regression models. The findings demonstrate that as vehicle sizes increase, lateral separation decreases and the ability of the present and opposing vehicles to maneuver laterally reduces. Most of the vehicle (71.2%) travels in the center of the highway, with lateral placing of 2-5 m. Multinomial logistic regression was used to model how vehicles on urban undivided roadways chose their lateral shifts. The result of this study can be used for developing road safety features during overtaking maneuvers in Aurangabad (Bihar). This study would also be helpful in implementing education regularity about road safety education.

Keywords Undivided road · Mixed traffic · Lateral clearance · Overtaking behavior · Lateral movement · Regression technique · Lateral shift

I. Kumar (✉) · A. K. Yadav
Central University of Jharkhand Ranchi, Ranchi 835205, India
e-mail: indrajeetkumar0294@gmail.com

A. K. Yadav
e-mail: amit.yadav@cuj.ac.in

A. Dhamaniya et al. (eds.), *Recent Advances in Traffic Engineering*, Lecture Notes in Civil Engineering 377, https://doi.org/10.1007/978-981-99-4464-4_34

1 Introduction

The type of traffic on Indian roadways is largely heterogeneous. Heterogeneous behaviors of individuals on Indian roadways find difficulties in overtaking maneuvers. On undivided roads, overtaking is one of the most complex and vital maneuvers, when traffic passes slower moving vehicles in the opposite lane while incoming traffic comes from the other direction. Overtaking maneuvers in various traffic conditions have been studied. In-depth research has been done on overtaking distance, overtaking time, the impact of opposing traffic, traffic volume, and acceleration-deceleration behavior while overtaking. In order to perform a safe overtaking maneuver, it is vital to consider the longitudinal following distance, lateral gap, relative speed, and speed of the interacting vehicles. In reality, the kind of vehicle frequently determines the driver's behavior. The features of an engine and a vehicle's weight can affect how quickly a driver accelerates. A vehicle's size determines how much room it requires and how easily it can turn, which influences a driver's lateral movement behavior. A big vehicle, such as a truck, for example, provides less freedom to its driver when maneuvering through a traffic stream. In describing driver behavior in mixed traffic situations, there are several flaws. A small vehicle, such as a Bike, on the other hand, gives its driver more flexibility in moving within and across lanes, which commonly results in lane discipline violations. Poor lane discipline and the presence of different vehicle types have a range of physical and psychological effects on the nearby cars and drivers, which can raise or reduce the capacity of the road. Vehicle diversity and a lack of lane discipline are particularly apparent in traffic situations in developing nations like Bangladesh, China, Indonesia, and India. To describe driving conditions in mixed traffic networks, this research offers complete driver behavioral models. This paper presents a quick evaluation of existing driver behavioral models in order to highlight their strengths and flaws in understanding driver behavior in mixed traffic situations. Several factors prompted this investigation. There aren't as many researches on the overtaking behavior of vehicles in mixed traffic as there are on homogenous traffic in emerging nations. On undivided highways with mixed traffic, vehicle overtaking behavior has regrettably not been well studied.

1.1 Objectives of the Study

i. To evaluate lateral features of vehicle-based driver on two-lane two-way undivided roadways (urban).
ii. To develop model for lateral movement of driver (vehicle-based).

2 Methodology

Overtaking maneuver is a challenging maneuver that needs exact awareness about speed, volume, time and space gaps. Vehicle kind and lane discipline are key factors in predicting driver behavior in mixed traffic situations. Based on the information from various literature reviews regarding overtaking behavior of drivers, a reference model has been proposed that shows how the vehicle lateral movement can be used for model formation. Road stretches of NH-139(Aurangabad to Patna) are used for this study. In this paper, data is collected by video graphic technique and data accumulation has been done. With the help of "regression analysis" data analysis has been done using traffic data extractor software. The behavior of drivers during lateral movement of various types of vehicles is analyzed. The impact of features of surrounding vehicles on driver lateral movement is also investigated. Find the effect of surrounding traffic environment on driver's lateral movement behaviors. Vehicle based driver's immediate front, left, and right routes are also analyzed. Variables that are used to examine the driver motivation and decision making during lateral movement behavior of drivers are surrounding (ongoing and opposing) vehicles. Lateral placement and speed of currently driving vehicle, and lateral placement and opposing driving vehicle for various kinds of vehicle graph is plotted in this paper to find the result, t-test (MS Excel) is done for validation. This test is based on mean and standard deviation. 75% of total data is used for model formation for lateral positioning (lateral feature) of vehicle-based driver on urban two-lanes undivided road and 25% of total data is used for validation of the model.

3 Data Collection and Analysis

In the Indian city of Aurangabad, data was collected for this study on a 7 m wide, urban undivided road segment (two-lane) during morning peak hours (8:30–9:30 a.m.) and evening peak hours (4:30–5:30 p.m.) for two weekdays (PB Kotagi, 2020) utilizing video graphic techniques. A 100-m road stretch of NH-139 was selected for this study. This road stretch is considered for accurate trajectory of vehicle. Traffic data extract precise trajectory data for 300m road stretch (Caleb Ronald Munigety, 2014). Traffic data extractor (TDE) software was used to extract the data from the video footage. In this paper, two days (4 h) video footage are used for vehicle count. Vehicle count has been done by traffic data extractor software. A total of 5125 vehicles were extracted for this paper that was taken across a 100-m section of the National Highway (NH-139), Aurangabad Bihar. Mark on the road at every 10m interval. Accuracy of trajectory interval is set in TDE software, click the four points of the identified rectangle in L, B ordered pair format and give the length and breadth in the input box in. (L-100m, B-7m). Now, to extract vehicle lateral placement, select the vehicle type and click a fixed tire of each vehicle. At each click, the video will automatically move to the next frame, according to the accuracy value set (1 s).

Significance of pedestrian movement on highways is very less that's why pedestrians are not considered in this paper.

Figure 1a, b depicts the study section's vehicle count. About 1304 motorized vehicles pass through the part of the road per hour, including bikes (B) making up the majority (52.9%) and buses having the smallest proportion (2.4%). Around 2517 motorized vehicles travel in the opposite way via this portion of the road per hour, including bikes (B) making up the majority (51.7%) and buses representing the minority (2.8%).

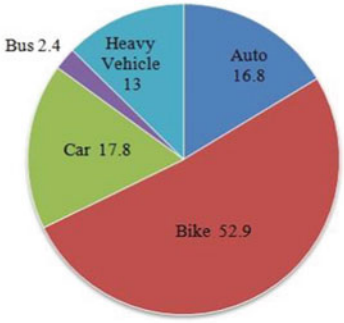

(a)

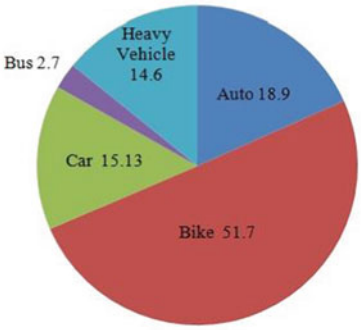

(b)

(c)

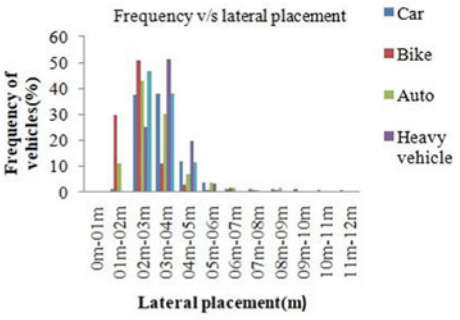

(d)

Fig. 1 Composition of the vehicles in the research area. **a** Current direction (Towards Obra). **b** Opposing direction (In the direction of Jasoiya more). **c** Vehicle frequency count by TDE software. **d** Graph between Frequency distribution and lateral placement of several vehicle categories

3.1 Longitudinal Movement Behavior

Several driver and vehicle-related variables, including speed, acceleration capacity, vehicle size, and traffic composition, were extracted from the trajectory data, with assistance from TDE output. Average speed, acceleration and standard deviation, are given in Table 1.

$$\text{Mean value of speed (Mv)} = \frac{\text{Sum of speed of all vehicles}}{\text{Total number of vehicle}} \tag{1}$$

where M_v = Mean value of speed

$$\text{Standard deviation } (\sigma) = \sqrt{\frac{\sum(xi - m)^2}{N}} \tag{2}$$

where σ = Standard deviation

M = mean value of speed

N = the size of sample

xi = Each value of speed and acceleration.

According to the above table, the speed of various types of vehicles ranges from 5.61 m/s to 16.025 m/s. Car has shown maximum velocity and bus shows minimum velocity range. Acceleration of the vehicle is also varying from 1.52 m/s^2 to 2.31 m/s^2. Bike having maximum acceleration value and for Bus the value of acceleration is minimum. To better understand driver behavior, space headways were measured for several leader–follower vehicle types. A total of 498 datasets were utilized in the study. The mean and standard deviation of the speeds of the leading and following vehicles are quite similar, indicating the presence of the following behavior. The average following-headway varies by vehicle type. When one of the leading or following vehicles had a bike, the average following headway was significantly reduced.

Table 1 Vehicles characteristic that travel on an Aurangabad highway

	Samples taken	Speed of vehicles (m/s)		Acceleration of vehicles (m/s^2)		Width of vehicles (m)
		m_v	σ_v	m_v	σ_v	
Car	863 (16.2%)	16.025	2.53	1.89	1.25	1.50–2.00
Heavy vehicle	708 (13.29%)	6.32	2.25	1.89	0.83	2.50–3.00
Bike	2682 (50.36%)	14.58	3.56	2.31	1.23	0.50–0.75
Auto	937 (17.59%)	10.98	1.89	1.62	1.11	1.20–1.50
Bus	135 (2.5%)	5.61	1.48	1.52	0.93	2.50–3.00

3.2 *Lateral Positioning of Vehicles*

Frequency distribution with lateral placement for different types of vehicles is shown in Fig. 2c. Due to their smaller size and greater mobility, Auto and bikes cover almost the whole stretch of highway since they have a propensity to cover every transverse separation present on the highway. A large percentage of the vehicles (71.2%) preferred to move in the Center of the highway, with a lateral placing of 2–3 m. In order to maintain greater speeds, 88.8% of vehicles, as opposed to Bikes (63.08%) and autos, prefer to travel near the Central part of the highway (77.52%). Further, I observed that number of lateral movements made by each type of vehicle is different. For example, for a given time frame an auto makes one lateral movement, a bike can make two or three lateral movements in same time frame. Hence lateral movement duration for different types of vehicles can vary considerably. Analyze this significance with linear regression to determine whether it is acceptable or not. It was noted that bikers virtually never made lateral movements when operating their small vehicles. However, a visual examination of the camera pictures showed that small-sized vehicle drivers regularly conducted lateral lane changes and lane crossings. Table 2 shows descriptive statistics for each vehicle type's lateral positioning and speed. Both two-wheelers (14.58 m/s) and cars (16.03 m/s) go quicker on average than heavier vehicles, which move at a slower mean speed (6.32 m/s) due to their higher mass and less maneuverability.

Graphs were created to compare the lateral positioning and speed of the subject vehicles traveling in the same direction, as shown in Fig. 2a–e. The correlation coefficient's value was used to evaluate the effectiveness of the regression analysis. The remaining 25% of the data was used to validate the model after it had been created using 75% of the data. These graphs show that all five different vehicle types followed a second-degree polynomial connection. Due to their propensity for overtaking and greater maneuverability, most Bike go at higher speeds towards the center of the road. They are also less affected by other vehicles. Auto and cars continue at relatively constant speeds until they reach the middle of the road, where they begin to slow down as they approach the opposing lane under the effect of oncoming traffic. Heavy vehicles often move at slower rates, and other vehicles do not obstruct their motion.

Because it was believed that the opposing vehicles' speeds would potentially have an impact on the ongoing vehicle's lateral position, their speed was also extracted. The graph between an oncoming vehicle's lateral positioning and the speed of an opposing vehicle is depicted in Fig. 2f–j. The findings show that the opposing vehicle's speed will not significantly affect the lateral positions of the current vehicles when they are moving in their respective lanes. The speeds of oncoming traffic are decreased when the current traffic (especially Bikes and cars) shifts into the opposing lane. A comparison has been done between the expected speed value and speed value actually seen in the field for various lateral poisoning. Average absolute error for every transverse placement was determined and it is less than 15% including all types of vehicles, which satisfied the 15% limit [11]. Hence, model closely satisfied field conditions. Heavy vehicle placements on the lateral do not change considerably

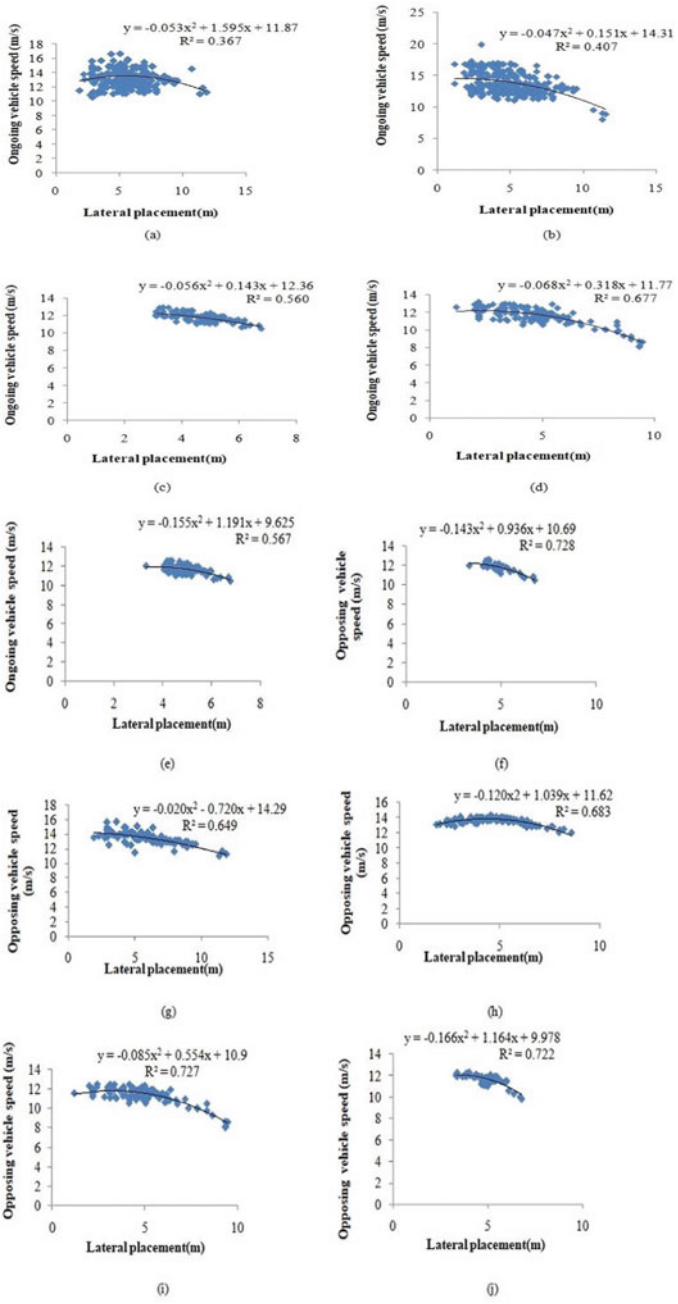

Fig. 2 Relationship between ongoing vehicle's speed and lateral placement. **a** Bikes. **b** Car. **c** Auto. **d** Heavy vehicle. **e** Buses. Relationship between opposing vehicle's speed and lateral placement. **f** Bikes. **g** Car. **h** Auto. **i** Heavy vehicle. **j** Buses

Table 2 Descriptive data on vehicle's speed and lateral positioning

Types of vehicles	Sample taken	Lateral positioning (m)				Speed (m/s)			
		Mean	SD	Minimum	Maximum	Mean	SD	Minimum	Maximum
Car	863	2.85	1.17	1.18	6.8	16.03	2.53	9.32	19.84
Bike	2682	2.86	1.07	1.15	6.5	14.58	3.56	3.53	16.48
Auto	937	2.35	1.03	1.2	5.6	10.98	1.89	5.5	16.2
Heavy vehicle	708	2.53	1.08	2.18	4.1	6.32	2.25	2.32	13.53
Bus	135	2.24	0.59	2.28	4.3	5.61	1.48	3.34	14.55

when they are opposed to when they are not. It demonstrates that opposing vehicles have little effect on large vehicles. It is due to its larger size and less maneuverability.

Figure 3 illustrates distributions of frequency for the lateral positioning of all five types of vehicles when they are unopposed and opposed. Due to their smaller proportions and superior maneuverability, two-wheelers can also be seen to be lateral spread virtually across the full road width. They attempt to squeeze between the cars since they are not particularly affected by opposing traffic.

Even when heavy vehicles are opposed by other types of vehicles, they move with a transverse positioning of 2–5 m. Regression analysis was used to create a model that forecasts where the subject vehicles would be driven on undivided highways. Vehicle placement is uncertain and subject to a variety of variables. As a result, a model for estimating vehicle lateral placement is developed. The presence of buses, heavy vehicles, Bikes, cars, and autos, as well as the speed of each category of vehicle, are factors taken into consideration when developing the model (both as ongoing vehicle and opposing vehicle). To choose the variables that would have the greatest influence and to get rid of the ones that wouldn't, a correlation analysis was done. 75% of the total data were utilized to create the model, while the remaining 25% were used for model validation. The created model that is used for forecasting where the ongoing vehicle (Y) will be positioned laterally is given in Eq. (3) [7].

$$Y = \beta_0 + \beta_1 X_1 + \beta_2 X_2 + \beta_3 X_3 + \beta_4 X_4 + \beta_5 X_5 + \beta_6 X_6 + \beta_7 X_7 + \beta_8 X_8 + \varepsilon \quad (3)$$

Above equation β_0 is the intercept(constant), β_1 β_2 β_3…… β_8 are the regression coefficient of independent variable X_1 X_2 X_3……X_8. In the above equation, X_1 represents the absence/presence of bikes, X_2 and X_3 represent the absence/presence of Auto and Cars in ongoing direction. The opposite vehicle categories, Bikes, Cars, and Autos, are represented by X_5 X_6 X_7. X_4 denotes the current vehicle's speed. X_8 denotes the opposing vehicle's speed. It is found that the model's R^2 value is calculated to be 0.61. Observed value of F is 16.42 and critical value of F is 2.42. The truth that the model's F-observed quantity is greater than the critical quantity suggests that it is statistically meaningful. To find the significant variables in the

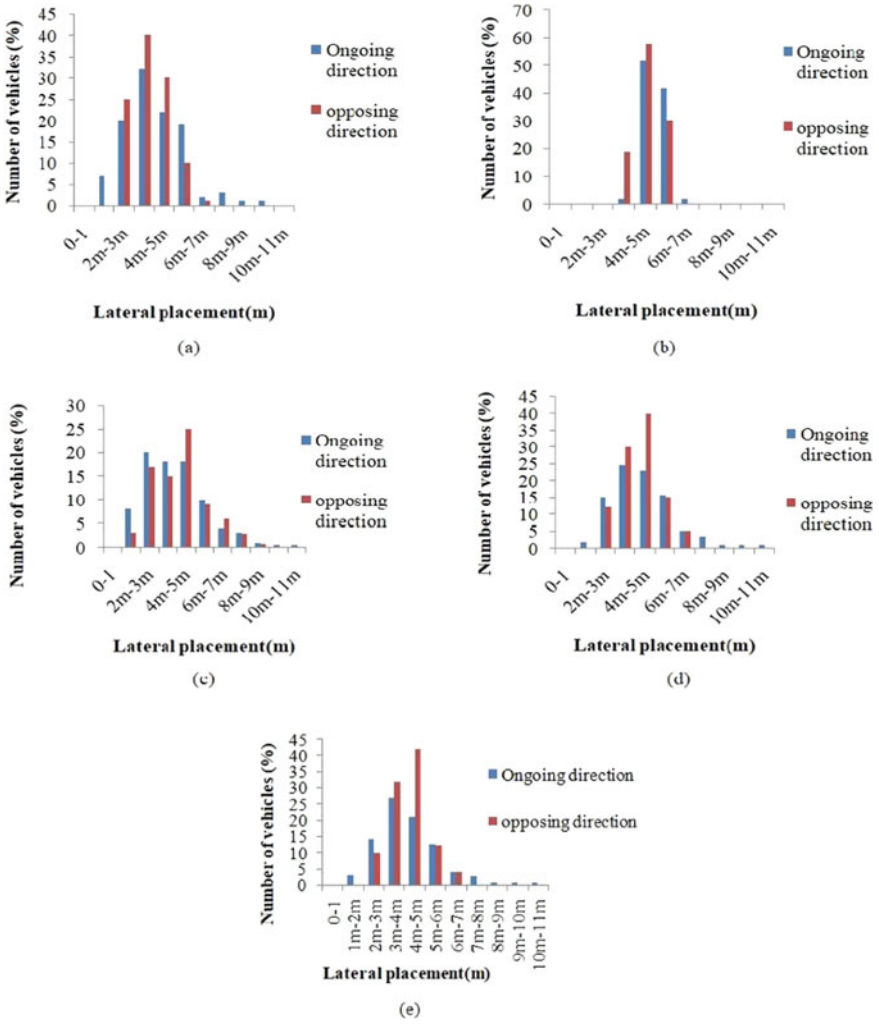

Fig. 3 Frequency distributions of various vehicle's lateral placement when they are in opposition and when they are not. **a** Bike. **b** Auto. **c** Car. **d** Heavy vehicle. **e** Buses

created model, the values of the coefficients, t-statistics (t_{stat}), and p value were evaluated. Regression analysis was performed again utilizing the significant variables after significance testing, and the model coefficients were computed for the updated model as shown in Table 3. If there is no other vehicle in the opposite lane, the subject vehicle will move to the Center of the road as its speed increases, primarily with the intention of overtaking. When the speed of the opposing vehicle rises, the subject vehicle moves to the left side of the road to prevent a collision. Bikes and autos have a considerable impact on lateral placement as continuing vehicles. They take up nearly the full road width. The Mean Absolute Percentage Error values, which

were determined by comparing predicted and observed values and found to be less than 15%, show that the model reasonably reflects the field conditions.

$$\begin{aligned} Y &= 15.61 + 3.94X_1 + 2.94X_2 + 2.62X_3 \\ &+ 0.43X_4 - 2.74X_5 + 2.02X_6 - 2.22X_7 \\ &- 1.21X_8 + 0.15 \end{aligned}$$

3.3 Lateral Separation of Vehicles

Out of 5325 total numbers of vehicles, 2682 vehicles are considered for lateral separation consideration of each category of vehicles. Out of the total number of vehicles considered for study, Bikes have greater number with larger lateral separation and Buses have least number with small lateral separation. It is due to smaller in size and greater in maneuverability for bikes and larger in size and lesser in maneuverability for Buses and Heavy Vehicles. The descriptive statistics regarding the lateral separation of various vehicle types are shown in Table 4. It has been found that faster moving vehicles, like Bikes, maintain a greater mean lateral spacing (5.01 m) while slower moving vehicles have lesser lateral spacing (2.53 m).

In order to understand the drivers' subsequent activity, the spacing headways kept by various leader–follower vehicle type configurations were measured. A total of 876 datasets in all were chosen for the investigation. The lateral separation values for various opposing and ongoing vehicle pairs as well as standard deviation and mean of ongoing and opposing vehicle lateral separation for various vehicle type configurations are displayed in Table 5.

For all five types of vehicles, Lateral separation is depending on various factors. Observed value of F is 80.08 and while critical value of F is 2.65. The headway changes depending on the combinations of vehicle types. When a bike was among the leading or trailing vehicles, the mean following headway was noticeably smaller. To determine whether there is a discernible change in the lateral separation of vehicles,

Table 4 Analytical data for lateral gap of all five types of vehicles

Different types of vehicles	Sample taken	Lateral separation (m)			
		Mean	SD	Minimum	Maximum
Total	2682	3.85	1.7	0.6	8.7
Buses	67	2.65	1.68	1.4	6.3
Bike	1117	5.01	1.97	0.8	8.4
Auto	684	4.35	1.34	0.8	8.0
Heavy vehicle	168	2.53	1.68	1.5	6.4
Car	646	2.85	1.6	0.7	8.2

Table 5 Summary data for continuing and opposing vehicle pairs' lateral separation

Pair of moving and opposing vehicles	Sample taken	Lateral separation of vehicles (m)			
		Mean	Standard deviation	Maximum	Minimum
Bike and bus	15	3.8	1.1	4.9	0.5
Auto and bike	38	4.9	1.1	7.6	2.1
Bike and car	209	3.9	1.5	7.3	0.8
Bike and auto	79	4.7	1.4	7.3	3.1
Bikes and bikes	197	5.7	1.8	8.9	1.8
Car and bike	166	4.0	1.2	6.4	1.5
Car and car	65	3.1	1.2	4.8	0.6
Car and auto	65	3.0	1.3	5.0	0.4
Auto and car	42	3.1	1.2	5.6	1.1

Regression analysis was used. For this, total of 1005 sample size has been considered and applied to the different-different cases for seeing the variation of lateral gap with the velocity. Out of these sample sizes, 508 cases have opposing vehicle speed greater than subject vehicle speed. While 345 cases have opposing vehicle speed is less than subject vehicle speed. For 152 cases, speed of both types of vehicles is the same. Lateral separation is maximum with maximum mean value.

3.4 Vehicle Lateral Movement Analysis

In homogenous and lane-disciplined traffic situations, lateral movement is symbolized by the lane-changing procedure. The form of lateral movement known as a lateral shift occurs when, while being influenced by the leader vehicle, the ongoing vehicle shifts lateral position by an amount equal to vehicle width. A lateral shift to the left or right might occur based on how the leading vehicle acts. A total of 494 lateral movements were documented in this investigation, involving left shifts (22.32%) and right shifts (77.68%). Bikes performed 78% of the lateral moves [9]. The decision to change one's existing route, the choice of an alternative course, and the execution of the lateral shift can all be divided into three parts. The impact of opposing vehicles on lateral shift incentive and path choice was also researched because, on undivided roads, opposing traffic strongly influences the flow of current traffic.

Figure 4 illustrates the interaction between the subject vehicle's speed and the front vehicle's speed in the current track. When compared to leader vehicles, the subject vehicle's higher speed values may tempt the drivers to make a lateral shift. t-test with unequal variances was performed, to determine whether the subject vehicle speeds varied significantly from leader vehicle speeds. In the case of all vehicles, it is discovered that the mean speed of the subject vehicle (14.27 m/s) is higher than

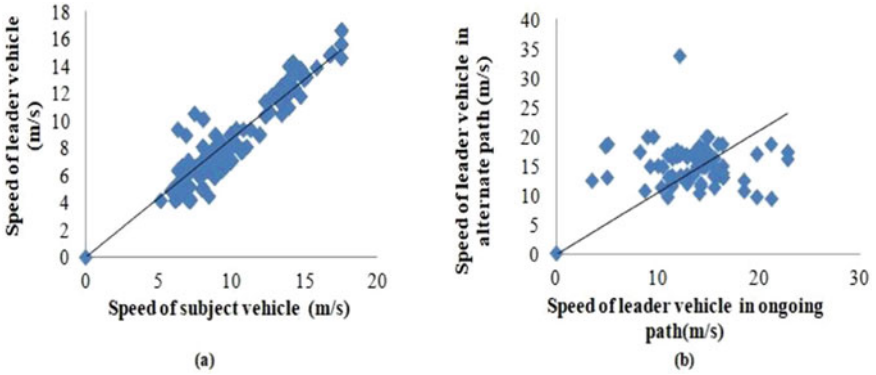

Fig. 4 **a** A comparison of the subject vehicle's and the leader vehicle's speeds along the current path. **b** Relationship between leader's Vehicles Speed in ongoing and alternate paths

the mean speed of the leader vehicle (13.19 m/s), indicating that the null hypothesis is rejected. Calculated value of t test is greater than critical value of t test. ($T_{stat} = 5.96 > t_{crit} = 1.96$).

3.5 Leader Vehicles Speeds in Current Path, Target Path and Alternate Path

When subject vehicles decide for lateral shift, the leader vehicle's speed in the target path is a key factor. A driver can always choose to target either the left or the right path when performing a lateral maneuver. Traffic characteristics on both nearby paths are examined in order to identify the variables that might affect the decision to choose this target path. A statistical t-test was carried out to verify these behaviors under the null hypothesis. t-test, findings show that mean speed in the present path (12.34 m/s) is considerably lower than the mean speed in the target path (13.31 m/s) for leader vehicle. The mean speed of alternate path is observed to be 13.47 m/s. t stat value is obtained in target path is 2.99 while for alternate path it found to be 2.33. Critical value of t test is 1.98. t-test, findings show that mean speed in the present path (15.47 m/s) is considerably higher than the mean speed in the alternate path (13.81 m/s) for leader vehicle, shown by t-test[t-stat is greater than $t_{critical}$ {$t_{stat}(2.99) > t_{crit}(1.98)$}]. However, according to the findings of the t-test, the leading vehicle's speed in the present path is considerably higher than the speed in the alternate way. This experiment supports the fact, that path selection is influenced by speed.

3.6 *Longitudinal and Lateral Gaps in Target and Alternate Paths*

Only 34.1% of cases including all vehicles show longitudinal gaps being larger in the target path than in the alternate path, as shown in Fig. 5a. As a result, the findings demonstrate that the longitudinal space gap is not a crucial consideration when deciding on paths. Results of t-test demonstrate that the longitudinal distance in the target path (20.1 m) is considerably smaller than the longitudinal gap in the alternate way for all vehicles (23.4 m). A statistical t-test was carried out to verify these behaviors from test result it observed that t stat is equal to 2.66 while critical value of t-test is 1.61 $\{t_{stat}\ (2.66) > t_{crit}\ (1.61)\}$. From graph it is observed that mean value of lateral separation for target path is 6.25 while in alternate path is 3.50, t stat value is observed to be 10.35 and critical value of t test is 1.98. For 84.29% of aggregate cases, demonstrating that lateral gap is a significant path selection parameter is shown in Fig. 5b. As a result, the subject vehicle tends to select the right goal path. Lateral gaps in the target and alternate pathways were compared using a t-test to see if they differed considerably. The null hypothesis is thus rejected $\{t_{stat}\ (10.35) > t_{crit}\ (1.98)\}$, as it is discovered that the alternate path has a smaller mean lateral gap than the target path, in the case of all vehicles. Investigations were also done into how opposing vehicles affected a subject vehicle's lateral movement.

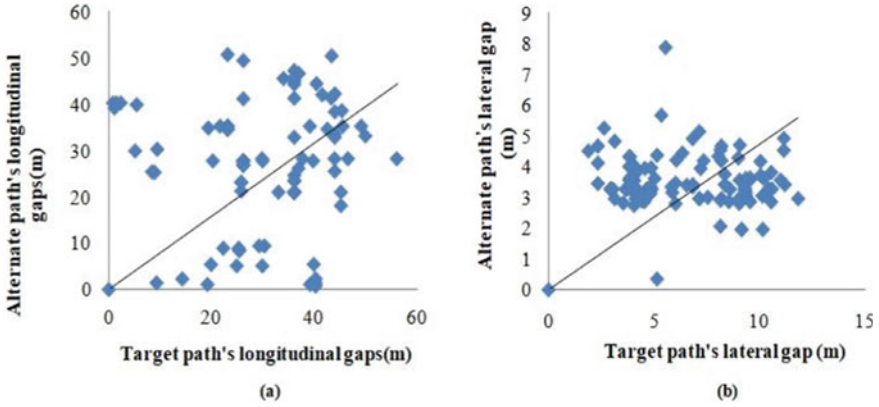

Fig. 5 **a** Relationship between the target path's longitudinal gaps and the alternate path's longitudinal gaps. **b** Relationship between the target path's lateral gaps and the alternate path's lateral gaps

3.7 Multinomial Logistic Regression Model

Model the lateral shift path decisions made by all vehicles using multinomial logistic regression. These regression models presuppose that each path's log-odd followed a linear model as specified in Eq. (4) [7].

$$\eta \mathrm{iq} = ln \frac{\pi i q}{\pi i Q} = \alpha \mathrm{q} + \mathrm{Xi}\beta \mathrm{q} \tag{4}$$

where η is the chosen lateral shift's log-odd, π=lateral shift choice. α_q = Regression constant and β_q = vector of regression coefficient, q = 1,2,3……, (Q-1). As a reference, a suitable category Q is fixed. The estimations can be interpreted similarly to the linear regression model in Eq. (3). Choice of lateral shift is represented by dependent variable, and independent variables are X1- size of subject vehicle and X2- size of leader vehicle, X3-Leading vehicle's lateral separation from the right neighboring leading vehicle, X4-Leading vehicle's lateral separation from the right neighboring leading vehicle, X5-Subject vehicle's relative speed with respect to leader vehicle, X6-Following vehicle's (right move to the leader vehicle) relative speed with respect to leader vehicle, X7-Following vehicle's (left move to the leader vehicle) relative speed with respect to leader vehicle, and X8 lateral separation between the leading and opposing vehicles.

The deciding factors for the path selection were found out to be the leader vehicle speeds and lateral gaps between the target and other paths. 75% of the data was utilized for model construction, with the remaining 25% used for verification. The statistical significance of the entire model was assessed using chi-square test. At a 5% level of significance, the results show that the model as a whole is statistically significant [p value = 0.000 [7]]. To assess the significance of each independent variable, the standard error value and significance value are utilized. Calculation of model parameter which is based on choice of target path is demonstrated in Table 6.

According to the model's findings, a subject vehicle is more likely to choose a left or right shift than to continue on its current course when its size is smaller and that of the leader vehicle is larger. Drivers typically favor the right-side way as a result. According to other studies, drivers are also more eager to change into the right shift than the left shift [9]. The same was seen in the actual traffic data that was collected in Aurangabad, India. There were 394 lateral shifts in total, 65 of which were left shifts and the other 329 were right shifts. As a result, right shifts have a higher forecast success rate (84.2%) than left shifts (59.1%). The created and validated model's coefficients were compared after the models were validated using 25% of the collected data. The findings indicate that the typical absolute percentage error is less than 4%.

Table 6 Model parameter estimations

Lateral shift of vehicle	Model's variable	Regression coefficient (β)	Standard error	Wald	p value
Shift to the left	Intercept at X = 0	0.412	1.355	0.101	0.71
	Dimension of subject vehicle	−3.016	0.691	18.680	0.00
	Size of the leader's vehicle	1.701	0.427	12.560	0.00
	Leading vehicle's lateral separation from the right neighboring leading vehicle	−0.072	0.135	2.451	0.00
	Leading vehicle's lateral separation from the left neighboring leading vehicle	0.759	0.181	12.870	0.00
	Subject vehicle's relative speed with respect to leader vehicle	−0.228	0.111	3.525	0.049
	Following vehicle's (right move to the leader vehicle) relative speed with respect to leader vehicle	−0.185	0.081	8.577	0.00
	Following vehicle's (left move to the leader vehicle) relative speed with respect to leader vehicle	0.274	0.097	8.208	0.00
	Lateral separation between the leading and opposing vehicles	−0.083	0.162	3.828	0.00
Shift to the right	Intercept at X = 0	−1.745	1.638	1.355	0.30
	Dimension of the subject vehicle	−1.914	0.632	14.740	0.00
	Size of the leader's vehicle	0.020	0.405	2.802	0.01

(continued)

Table 6 (continued)

Lateral shift of vehicle	Model's variable	Regression coefficient (β)	Standard error	Wald	p value
	Leading vehicle's lateral separation from the right neighboring leading vehicle	0.632	0.192	6.617	0.01
	Leading vehicle's lateral separation from the left neighboring leading vehicle	−0.891	0.171	22.140	0.00
	Subject vehicle's relative speed with respect to leader vehicle	−0.206	0.109	3.962	0.05
	Following vehicle's (right move to the leader vehicle) relative speed with respect to leader vehicle	0.089	0.076	2.212	0.03
	Following vehicle's (left move to the leader vehicle) relative speed with respect to leader vehicle	−0.507	0.091	25.620	0.00
	Lateral separation between the leading and opposing vehicles	0.617	0.220	7.092	0.00

4 Summary and Conclusion

Analyze and model how drivers are positioned and move laterally on urban undivided roadways when there is mixed traffic. A multiple linear regression model was created to forecast the subject vehicle's lateral placement, and it was discovered that speed and types of vehicles have a greater influence in lateral placement of the subject vehicle. The many driving forces behind vehicles' lateral shifting were examined. From a variety of driver behavior studies that have been done and from the behavioral models that are presented in this study, the following are the main findings (Conclusion) of this study.

1. 71.2% of the total vehicle prefers Center part of the highway for traveling, with an average lateral placing of 2–5 m.

2. As compared to other vehicles, Bikes, Cars and Autos manage their lateral shift when overtaking leader vehicles. Due to their bigger proportions, heavy vehicles are less affected by opposing vehicles, and as a result, their lateral placements do not differ considerably when they are in opposition to one another.
3. With increasing size of ongoing vehicle and increasing opposing vehicle speed, lateral separation of vehicles reduces and increases, respectively.
4. Tendency of the driver that they choose either right lateral shift or left lateral shift is affected by subject and leader vehicle size, right shift increases by size of leader vehicle while left shift increases by decreasing in size of subject vehicle.
5. By the increasing of lateral separation between opposing direction vehicle and leader vehicle during movement of vehicles driver in ongoing direction, a subject vehicle is more likely to shift to the right and less likely to move to the left.
6. The following headways that drivers maintain are determined by the types of leader and follower vehicles. The lengths of lateral movement range noticeably across different vehicle kinds.

The results of this study may be applied to vehicle placement logic to determine the lateral positions of vehicles at the simulation road stretch's beginning point.

The developed Model can be used in the microscopic analysis of vehicles. By creating a class-wise model, the model for lateral placement and movement may be further enhanced. The study's results can be broadly interpreted by accumulating and studying a lot of data.

Reviewer Comments

Sl. No	Comments	Revised paper (Remark)
1	Abstract, the practical implication of study's findings is not clear	Result of this study can be used for developing road safety in Aurangabad (Bihar) which can enhance the understanding of road users about road feature during overtaking maneuvers Finding of this study would also be helpful in implementing education regularity about road safety education. Traffic jam due to wrong overtaking maneuvers can also be reduces. This finding is included in abstract
2	Introduction, first line does not seem correct. Please check the statement	The type of traffic on Indian roadways is largely heterogeneous. Heterogeneous behaviors of individual on Indian roadways find difficulties in overtaking maneuvers
3	Second objective of this study is not clear	To develop model for lateral movement of driver (vehicle-based)

(continued)

(continued)

Sl. No	Comments	Revised paper (Remark)
4	Methodology section should be re-written. It has serious writing issues	Overtaking maneuver is challenging maneuver that need exact awareness about speed, volume, time and space gaps. Vehicle kind and lane discipline are key factor in predicting driver behavior in mixed traffic situation. Based on the information from various literature reviews regarding overtaking behavior of driver a reference model has been proposed that shows how the vehicle lateral movement can be used for model formation. Road stretches of NH-139(Aurangabad to Patna) is used for this study. In this paper data is collected by video graphic technique and data accumulation has been done. With the help of "regression analysis" data analysis has been done using traffic data extractor software. Behavior of drivers during lateral movement of various types of vehicle is analyzed. The impact of features of surrounding vehicle on driver lateral movement is also investigated. Find effect of surrounding traffic environment on driver's lateral movement behaviors. Vehicle based driver's immediate front, left, and right routes are also analyzed. Variables that are used for examine the driver motivation and decision making during lateral movement behavior of drivers is surrounding (ongoing and opposing) vehicles. Lateral placement and speed of currently driving vehicle, and lateral placement and opposing driving vehicle for various kind of vehicle graph is plotted in this paper to find the result, t-test (MS excel) is done for validation. This test is based on mean and standard deviation. 75% of total data is used for model formation for lateral positioning (lateral feature) of vehicle-based driver on urban two-lane undivided road and 25% of total data is used for validation of model
5	Methodology chart should be revised	Revised
6	Section 3, It should be evening peak hours. Please correct it	Evening peak hours (4:30–5:30 p.m.) for two weekdays (Punith B. Kotagi, 2019)
7	Why did you select 100 m stretch? On what basis stretch was selected?	This road stretch is considered for accurate trajectory of vehicle. Traffic data extract precise trajectory data for 300 m road stretch (Munigety et al. 2014)
8	How did you select the two days? Which days were selected?	In this paper two days (4 h) video footage are used for vehicle count
9	How did you count vehicle? Was it done by manual counting?	Vehicle count has been done by traffic data extractor software

(continued)

(continued)

Sl. No	Comments	Revised paper (Remark)
10	What point was selected for calculating lateral placement? And how did you select a point on vehicle to measure its trajectory?	Mark on road at every 10m interval. Accuracy of trajectory interval is set in TDE software, click the four points of the identified rectangle in L, B ordered pair format and give the length and breadth in the input box in. (L-100m, B-7m). Now, to extract vehicle lateral placement, select the vehicle type and click a fixed tire of each vehicle. At each click, the video will automatically move to the next frame, according to the accuracy value set (1 s)
11	Why did you not count pedestrians? And what about the other categories of vehicles like LCVs?	Significance of pedestrian movement on highway is very less that's why pedestrians are not considering in this paper
12	Figure 2 shows that there is a vehicle (truck) parked on the road? Does it not create friction to moving vehicles?	It creates friction to moving vehicles, but vehicle (truck) stay there only for few minutes to fill air in vehicle (truck) tire Not parked on the road
13	Author extracted 5125 vehicles' trajectories; then why only 498 data sets were used in this study?	A total of 5125 vehicle were extracted for this paper. Out of 5125 vehicle 498 vehicles are used lateral trajectory
14	Table 2, if the road width is 7 m, how the lateral positioning can be more than that? Please explain	Revised
15	There is mismatch between caption of Fig. 3 and text. Even your axis titles were not match with caption of figure	Figure 3 Relationship between ongoing vehicle's speed and lateral placement. (a) Bikes. (b) Car. (c)Auto. (d) Heavy vehicle. (e) Buses. Relationship between opposing vehicle's speed and lateral placement. (f) Bikes. (g) Car. (h) Auto. (i) Heavy vehicle. (j) Buses
16	How did you test the significance for your statement "The findings show that opposing vehicle's speed will not significantly affect the lateral positions of the current vehicles when they are moving in their respective lanes"?	The speeds of oncoming traffic are decreased when the current traffic (especially Bikes and cars) shifts into the opposing lane. A comparison has been done between expected speed value and speed value actually seen in the field for various lateral poisoning. Average absolute error for every transverse placement was determined and it is less than 15% including all types of vehicle, which satisfied the 15% limit (Mathew and Radhakrishnan 2010)

(continued)

(continued)

Sl. No	Comments	Revised paper (Remark)
17	Table 3, reviewer could not understand, why does the coefficient of availability increase lateral positioning of subject vehicle? Similarly, what is the probable reason for positive sign of presence of car in opposite direction on lateral position of subject vehicle?	Revised
18	It would be better if author explain all the terms with the help of figure like lateral separation, lateral displacement, alternate path, etc. It can help readers to identify the reference points	Add figure and revised
19	Section 3.1.5, I could not understand why was the speed in current path more than target path?	t-test, findings show that mean speed in present path (12.34 m/s) is considerably lower than the mean speed in the target path (13.31 m/s) for leader vehicle t-test, findings show that mean speed in the present path (15.47 m/s) is considerably higher than the mean speed in the alternate path (13.81 m/s) for leader vehicle
20	Section 3.1.6, How did you decide the critical value of t-test? Why is it changing?	In this section analysis has been done using t test for two path one is for target path and another for alternate path that's why it changing
21	Section 3.1.7., P value cannot be zero. It should be greater than 0	[p value = 0.000 {Punith B. kotagi et al. (2019)}]
22	For developing MNL model, how many samples were selected? How did you mark samples based on their lane shift? What was the criterion to call a movement a lateral shift? The video was recorded for 100 m stretch only, how did you decide regarding all these movements?	Total 394 samples were selected. According to other studies, drivers are also more eager to change into the right shift than the left shift (Mathew et al. 2014). The same was seen in the actual traffic data that was collect in Aurangabad, India. A lateral shift to the left or right might occur based on how the leading vehicle acts. The form of lateral movement known as a lateral shift occurs when ongoing vehicle shifts lateral position by an amount equal to vehicle width. Mark on road at every 10m interval. Accuracy of trajectory interval is set in TDE software, click the four points of the identified rectangle in L, B ordered pair format and give the length and breadth in the input box in. (L-100m, B-7m).Now, to extract vehicle lateral placement, select the vehicle type and click a fixed tire of each vehicle. At each click, the video will automatically move to the next frame, according to the accuracy value set (1 s)

(continued)

(continued)

Sl. No	Comments	Revised paper (Remark)
23	Section 3.1.7., Why the equations were written separately for each independent variable? Can we not write a utility equation?	Revised
24	Discussion part is missing in this paper which will strengthen your work	The results of this study may be applied to vehicle placement logic to determine the lateral positions of vehicles at the simulation road stretch's beginning point Developed Model can be used in microscopic analysis of vehicles
25	Limitations and future scope should also be discussed in paper	By creating a class-wise model, the model for lateral placement and movement may be further enhanced. The study's results can be broadly interpreted by accumulating and studying a lot of data

References

1. Chunchu M, Kalaga RR, Seethepalli NVSK (2010) Analysis of microscopic data under heterogeneous traffic conditions. Transport 25(3):262–268. https://doi.org/10.3846/transport.2010.32
2. Dutta B, Vasudevan V (2020) Insight into driver behavior during overtaking maneuvers in disorderly traffic: an instrumented vehicle study. Transp Res Procedia 48:719–733. https://doi.org/10.1016/j.trpro.2020.08.074
3. Dey PP, Chandra S, Gangopadhaya S (2006) Lateral distribution of mixed traffic on two-Lane roads. J Transp Eng 132(7):597–600. https://doi.org/10.1061/(asce)0733-947x(2006)132:7(597)
4. Gowri A, Sivanandan R (2015) Evaluation of right-turn lanes at signalized intersection in non-lane-based heterogeneous traffic using microscopic simulation model. Transp Lett 7(2):61–72. https://doi.org/10.1179/1942787514y.0000000034
5. Gray R, Regan DM (2005) Perceptual processes used by drivers during overtaking in a driving simulator. Hum Factors 47(2):394–417. https://doi.org/10.1518/0018720054679443
6. Hassan SA et al (2014) Factors affecting overtaking behaviour on single carriageway road: Case study at Jalan kluang-kulai. Jurnal teknologi 71(3). https://doi.org/10.11113/jt.v71.3765
7. Kotagi PB, Raj P, Asaithambi G (2020) Modeling lateral placement and movement of vehicles on urban undivided roads in mixed traffic: a case study of India. J Traffic Transp Eng (English Edition) 7(6):860–873. https://doi.org/10.1016/j.jtte.2018.06.008
8. Kanagaraj V et al (2015) Trajectory data and flow characteristics of mixed traffic. Transp Res Rec 2491(1):1–11. https://doi.org/10.3141/2491-01
9. Munigety CR, Vicraman V, Mathew TV (2014) Semiautomated tool for extraction of microlevel traffic data from videographic survey. Transp Res Rec 2443(1):88–95. https://doi.org/10.3141/2443-10
10. Mahapatra G, Maurya AK (2013) Study of vehicles lateral movement in non-lane discipline traffic stream on a straight road. Procedia Soc Behav Sci 104:352–359. https://doi.org/10.1016/j.sbspro.2013.11.128

11. Mathew TV, Radhakrishnan P (2010) Calibration of microsimulation models for nonlane-based heterogeneous traffic at signalized intersections. J Urban Plan Dev 136(1):59–66. https://doi.org/10.1061/(asce)0733-9488(2010)136:1(59)
12. Mocsári T (2013) Analysis of the overtaking behaviour of motor vehicle drivers. Acta Tech Jaurinensis 2(1):97–106. https://acta.sze.hu/index.php/acta/article/view/209
13. Polus A, Livneh M, Frischer B (2000) Evaluation of the passing process on two-Lane rural highways. Transp Res Rec 1701(1):53–60. https://doi.org/10.3141/1701-07
14. Tang TQ et al (2007) A new overtaking model and numerical tests. Phys A 376:649–657. https://doi.org/10.1016/j.physa.2006.10.044

Identification of Crash Severity Level of Unsignalized Intersection Blackspots in Mixed Traffic Scenario

Arpita Saha and Pratik Deshmukh

Abstract A blackspot is where accidents are most likely to happen as it has a history of a significant number of accidents in recent years. Amid different types of blackspot locations, unsignalized intersections are the critical ones as vehicular movement at these locations is dependent on driver behaviour. Hence, the present study seeks to predict the chances of accidents at unsignalized intersection blackspots by proposing crash severity levels using estimated surrogate safety parameters i.e., PET, and MTTC values. In that context, data for four unsignalized intersection blackspots with different intersection geometry were gathered from Nagpur, India, along with crash data from the previous three years. PET and MTTC of the through and right-turning vehicles from major and minor roads were estimated. Threshold values of PET and MTTC were proposed using clustering analysis and depending on those values, the crash severity levels were divided into four levels for unsignalized intersection blackspots. The proposed crash severity levels will be useful to rank the unsignalized intersection blackspots considering the severity of possible crashes.

Keywords Blackspot · Crash severity level · Surrogate safety parameters · Unsignalized intersection · Mixed traffic scenario

1 Introduction

In emerging nations like India, road safety is gaining concern and attention, which has a large population and inadequate infrastructure to accommodate the growing demand for vehicles. Road traffic accidents are the ninth leading cause of death for

A. Saha (✉)
Assistant Professor, Department of Civil Engineering, Visvesvaraya National Institute of Technology Nagpur, Maharashtra 440010, India
e-mail: arpitasaha@civ.vnit.ac.in

P. Deshmukh
Post Graduate Student, Department of Civil Engineering, Visvesvaraya National Institute of Technology Nagpur, Maharashtra 440010, India
e-mail: pratikd098@gmail.com

A. Dhamaniya et al. (eds.), *Recent Advances in Traffic Engineering*, Lecture Notes in Civil Engineering 377, https://doi.org/10.1007/978-981-99-4464-4_35

people of all ages. The number of fatalities on the world's roads, which currently stands at 1.35 million each year, is intolerably high. Developing nations have substantially higher fatality rates than industrialized nations. The combination of fast motorization, poor infrastructure, and ineffective legislation and enforcement is blamed for the high number of road fatalities.

In India, traffic-related incidents continue to be the leading cause of fatalities, disabling conditions, and hospitalizations. According to World Road Statistics (2018), India has the highest number of fatal road accidents among the 199 nations, followed by China and the United States. According to the WHO Global Report on Road Safety (2018), around 11% of all fatal accidents worldwide occur in India. India ranks third in terms of injuries behind the United States of America and Japan. According to World Road Statistics (2018), India ranks 11th in terms of the number of people killed per lakh of the population. According to the Road Accident Report for 2019 released by MORTH (2019), a total of 449,002 accidents occurred in the nation during the calendar year 2019, resulting in 151,113 fatalities and 451,361 injuries. According to the MORTH (2020) report, incidents in India resulted in the deaths of about 1.3 lakh individuals and injured more than 3.4 lakh others.

To assess collision probability, road safety analysis has traditionally relied on collision data. This needs traffic collisions and 5–10-year crash data. Intersection configurations and road usage patterns may have changed dramatically throughout this time. This traditional method of road safety analysis has stated drawbacks i.e., crash data spanning several years, unavailability of crash data, underreporting of crashes and inaccurate information about crash patterns. Therefore, surrogate safety measures have become a popular alternative in recent years for safety analysis. Surrogate safety measures are chosen using a conflict analysis for safety. Traffic crashes are incidents that don't always result in accidents. The traffic conflict technique can detect relatively close accidents in real-time traffic, giving it a quicker and more effective way to predict accident frequency and repercussions. India's road system is complicated. India has a disorderly transportation environment, with many people breaking traffic restrictions. In India, unsignalized junctions are unregulated intersections where vehicles from any direction enter the intersection and attempt to cross and turn on the road, resulting in multiple conflicting points and increasing the likelihood of an accident. Lane indiscipline and lack of traffic rule enforcement also play a significant role in this case. Specifically, in India, 84% of the accidents occurred at unsignalized intersections MoRTH (2019). Therefore, the severity of accidents and the safety of vehicular traffic at unsignalized intersections are really a matter of concern.

As India has heterogeneous traffic conditions, the study aims to propose the severity level of accidents using appropriate surrogate safety measures as per Indian requirements. By recommending severity threshold values for crossing conflicts and rear-end conflicts of the through and right-turning vehicles from major and minor roads, this study ultimately aims to increase intersection safety. The Post Encroachment Time (PET) was used for crossing conflicts and Modified Time to Collision (MTTC) for rear-end conflicts, with them a range of values is proposed considering four levels of severity. In terms of safety, it is possible to identify potentially

dangerous intersections using the proposed severity levels. This will be useful for facility management, intersection reconstruction, and rehabilitation. Finding critical unsignalized intersections in terms of safety is made easier with the aid of the study.

2 Background Research

Recent years have witnessed a number of research focused on assessing the safety of vehicular traffic at intersections utilizing surrogate safety measures. Some of the most widely utilized surrogate safety measures are Post Encroachment Time (PET), Time to Collision (TTC), Modified Time to Collision (MTTC), and Deceleration Rate to Avoid Crash (DRAC). Zheng and Sayed (2019b) evaluated the effectiveness of four generally used indicators: time to collision (TTC), modified time to collision (MTTC), post encroachment time (PET), and deceleration to prevent a crash (DRAC). The findings of the past studies revealed that all four indicators identify traffic conflicts differently, with MTTC producing accurate crash estimates. The crash prediction using both TTC and PET was reasonable, although TTC has the propensity to overestimate and PET has a tendency to underestimate. So, PET was used to determine traffic safety and attempts were made to propose different threshold values. Using micro-simulation modelling of Post Encroachment Time, the level of traffic safety at an uncontrolled intersection with mixed traffic was evaluated by Killi and Vedagiri (2014). The volume and traffic composition were changed during the study, and the impact on the PET values was examined. Additionally, using the clustering technique, Mohanty et al. (2020) developed severity indices for likely traffic crashes at the median opening. The concepts of vital safe ratio and speed to PET ratio have been devised by the authors in order to more effectively examine traffic safety at median openings based on minimum stopping sight distance (SSD). However, Paul and Ghosh [1] and Babu and Vedagiri (2016) observed that PET alone may not provide an accurate reflection of safety in a developing nation like India where traffic interactions are frequent. The higher speed of conflicting vehicles offers a significant risk to drivers and frequently results in severe crashes. As a result, speed is employed in conjunction with PET to detect critical conflicts. For this concept, the braking distance approach was employed to determine the critical speed and found critical conflicts. Paul and Ghosh [1] classified 18.97% to 31.29% of conflicts as critical, with the highest number of right-turning HV's and through PTWs. Whereas, Babu and Vedagiri (2016) classified 20.3% of conflicts as critical, with right-turning LMVs at higher risk. Based on PET threshold values, attempts have been made to discern between critical conflicts. Using a PET threshold value of 1 s, Goyani, Paul, and Gore (2020) observed that the percentage of critical conflicts increased when disputes were involved between 2 and 3Ws. The strongest association was found to be 1 s for 2W and 1.5 s for LMV and HV, resulting in 18.8% to 29.5% significant conflicts. Adding to this, Paul and Ghosh (2019) offered CDF based technique for calculating the PET threshold. For this purpose, numbers from 0 to 3.5 s were employed. The effect of applying several countermeasures, such as higher tables,

rotation, and speed bumps, on PET values was studied by Vedagiri and Killi (2015). It was observed that PET values were affected by modifying the volume, percentage of vehicles, and vehicle speed. Reddy et al. (2019) conducted a similar study and examined the impact of speed bumps on crash severity. They discovered lower values when speed bumps were present and 43% of conflicts to be critical when threshold values of 1.5 s are applied. For severe crash types at unsignalized junctions, Paul and Ghosh [2] developed a conflict severity index (CSI) based on crash risk severity. PET and predicted kinetic energy loss is used to calculate CSI for key crossing conflicts, while Delta t, or the difference between the Modified Time to Collision (MTTC) and the Time-to-Stop (Ts) values, was utilized for rear-end conflicts.

The outcome of the past studies indicates that post encroachment time (PET) and modified time to collision (MTTC) are the most widely adopted and accurate surrogate safety measures to act as proactive safety indicators for unsignalized intersections in India. The analysis of traffic conflicts at an unsignalized intersection utilizing surrogate safety measures like PET and TTC has been the subject of a significant number of research. Critical conflicts were determined using the braking distance concept. Moreover, some studies were focused on the effect of changing traffic volume, and traffic composition on SSM parameters. However, TTC does not consider the change in speed of the vehicle while travelling through the conflict area. In that context, MTTC provides a more accurate prediction of potential crashes. Therefore, it can be concluded that the severity level of potential crashes at unsignalized intersections can be estimated more accurately with the help of PET and MTTC values. Therefore, the present study aims to propose crash severity levels for crossing and rear-end conflicts of unsignalized intersection blackspots using PET and MTTC as surrogate safety parameters.

3 Selecting Site and Data Collection

In the present study, to assess the safety performance using surrogate safety parameters, four unsignalized blackspot intersections of Nagpur city were selected. Out of them, three intersections were three-legged and the remaining one was a four-legged intersection. Nagpur is an emerging metropolis and the third-largest city in the state of Maharashtra. In the year 2021, the urban roads of Nagpur experienced approximately 1000 accidents. The Nagpur Municipal Council has identified 114 blackspots throughout the city. For the study, unsignalized intersection blackspots were identified and grouped into three-legged and four-legged intersections. The locations were selected in such a way that limited influence of pedestrians and cyclists exist, they were away from the bus stops and parking facilities, and are of similar geometry. The geometric details of the study blackspots are shown in Table 1. Figure 1 depicts the four-legged and three-legged unsignalized intersection blackspots selected in Nagpur City.

The crash data for the selected unsignalized intersection blackspots were collected from the Deputy Commissioner of Police Office, Traffic Police Department, Nagpur,

Table 1 Details of the selected blackspot locations of Nagpur city

Blackspot intersection location	Location geometry	Approach width (m)				Latitude of the site (N)	Longitude of the site (E)
		Leg 1	Leg 2	Leg 3	Leg 4		
		Major road		Minor road			
Telephone exchange Chowk	4-legged	19.1	22.5	17.5	22.1	21° 8′55.16"	79° 7′12.02"
Sadar police station	3-legged	10.2	8	11	X	21° 9′42.41"	79° 4′15.03"
Dattawadi Chowk	3-legged	9.25	9.25	11.5	X	21° 9′8.32"	79° 0′2.37"
Maruti Seva Amravati Road	3-legged	18	18	9.5	X	21° 9′9.97"	79° 1′14.37"

Maharashtra. The crash data was collected for the years 2019, 2020, and 2021. The main aim of collecting the crash data was to identify the time period during which the maximum number of accidents occurred. To capture large numbers of potential conflicts as feasible, that specific time period was utilized for traffic data collection. The collected crash data showed the details of variation in the type of accidents such as fatal, grievous injury (GI), minor injury (MI), not injured (NI), and the number of persons killed within the time period. The entire day was divided into intervals of three hours for representing the number of accidents.

Figure 2 was plotted using the collected crash data. The graph in Fig. 2 displays data regarding the number of fatal accidents that occurred throughout the course of the years; 2019, 2020, and 2021 at an interval of three hours. It is observed from the crash data that the variation in the frequency of fatal crashes is quite less between 12 and 9 a.m., while the highest number of fatal accidents occurs between 6 and 9 p.m. Moreover, minimal variation is observed between 12 to 3 p.m. and 3 to 6 p.m. Therefore, it is required to collect data between 6 p.m. and 9 p.m. to capture the maximum number of potential fatal crashes. However, it is not practically possible to capture vehicular traffic movement at night due to limited visibility. So, traffic data was collected for all the study sites from 12 Noon to 6 p.m. on weekdays. The traffic data was collected using the videography technique. The data collection was conducted on a bright sunny day in favourable weather conditions using a high-definition camera during the selected hours. Vehicle movement in all directions can be seen clearly as the camera was positioned in such a way that the whole intersection's conflict zone was visible.

India follows left-hand driving, so, vehicles turning left from major and minor roads do not face difficulty at an intersection. However, right-turning vehicles either from major or minor roads have to stop and wait to cross the road until they find a suitable gap. In case of high traffic, drivers have to wait for a longer period to find a safe gap. Because of waiting for a longer period, drivers lose patience and try to accept minor gaps leading to a risky and unsafe crossing and thereby resulting in a

(a) Dattawadi Chowk (S-1)

(b) Maruti Seva Amravati Road (S-3)

(c) Sadar Police Station (S-2)

(d) Telephone Exchange Chowk (S-4)

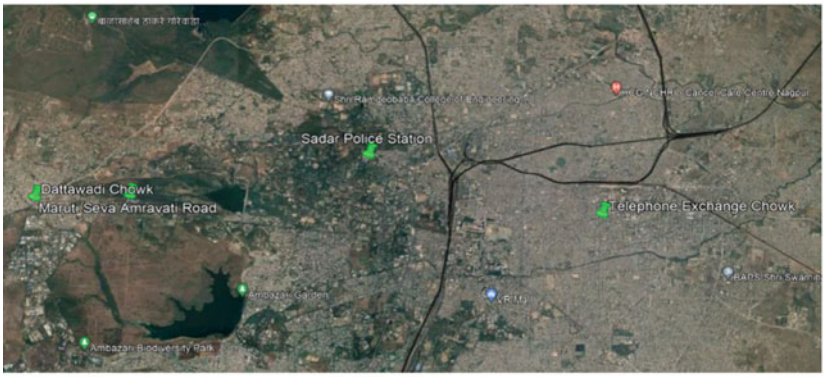

(e) Location of Study Blackspots of Nagpur City

Fig. 1 Unsignalized intersection blackspots of Nagpur City

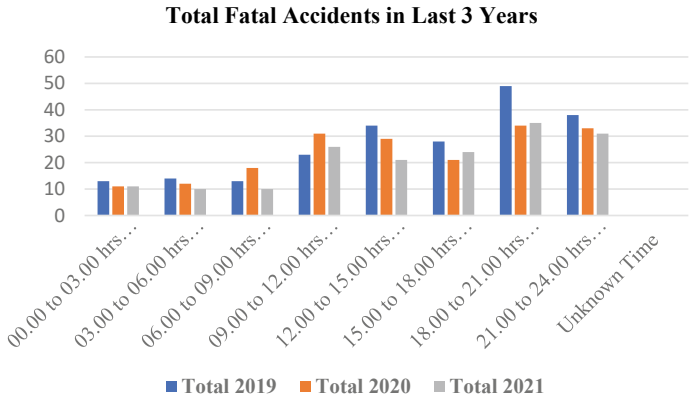

Fig. 2 Fatal accidents data for the years 2019, 2020, and 2021

possible crash. Therefore, in this study, conflicts between right-turning vehicles and through-moving vehicles were taken into consideration. A pictorial representation of the types of conflicts considered in the present study is shown in Fig. 3. Following are the types of conflict that were considered while carrying out the study.

(a) In case of three-legged intersections: (i) Conflict between the right-turning vehicles from the major roads and through-moving vehicles on the major roads. (ii) Conflict between right-turning vehicles from the minor roads and through-moving vehicles on the major roads. (b) In case of four-legged intersection: Conflict between two through-moving vehicles along the minor and major roads.

4 Extraction of Surrogate Safety Parameters

Surrogate safety parameters like PET and MTTC were extracted for different movements. In the present study, the heterogeneous traffic stream was categorized into four categories i.e. motorized 2W, motorized 3W, LMV and HV as per Indo HCM (2017).

Using Autodesk AutoCAD version 2020 software, the whole conflict area of each study intersection was divided into an identical number of square grids of 2.5 m × 2.5 m in order to extract PET and MTTC from the video. The 2.5 m × 2.5 m grid was laid considering the dimensions of the conflict area at the intersection. The grids were then overlaid on the actual videos using Corel Video Studio Pro X6, a video editing software. To estimate the speed of conflicting vehicles, a trap length of 20 m was marked at each site, one at the intersection's entry and another one at a distance of 20 m beyond that. The altered videos were played back using Kinovea software at a frame rate of thirty frames per second in order to derive surrogate safety parameters. The speed and acceleration of the corresponding vehicles were extracted using Data from Sky software and the data obtained was used in the estimation of the modified

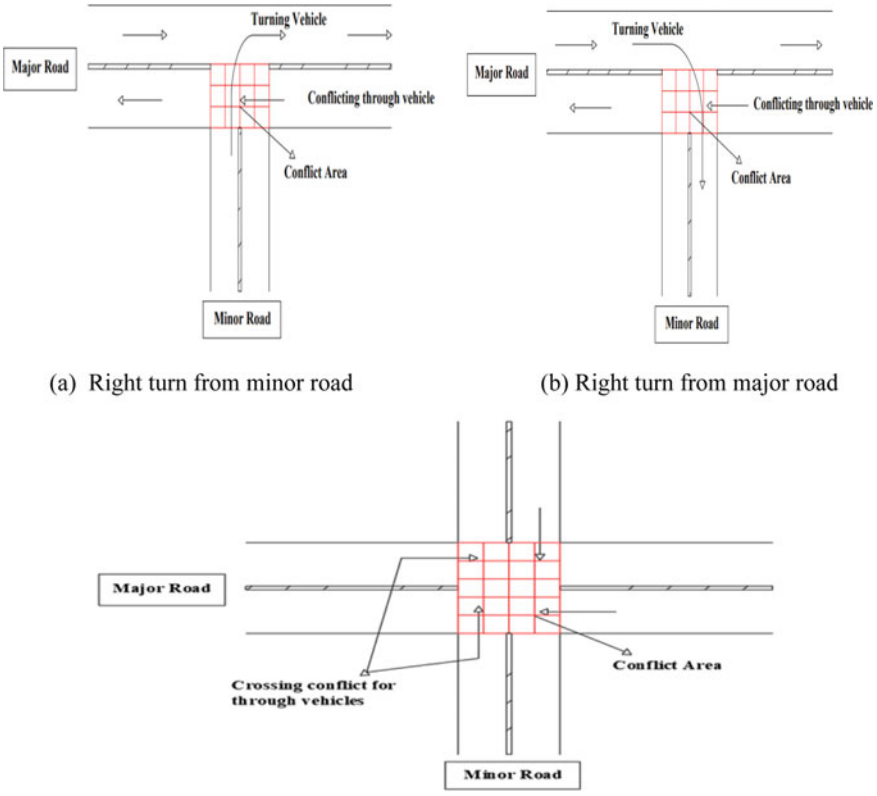

Fig. 3 Types of Crossing conflict at three-legged (**a**, **b**) and four-legged (**c**) intersections

time to collision (MTTC) of rear-end conflicts. Additionally, the traffic volume and vehicle composition of the study intersection blackspots were calculated. Table 2 gives a detailed idea about the same.

It is observed from Table 2 that 2Ws are the highest in proportion in the existing traffic stream of all sites; ranging from 48 to 77%, followed by LMVs (16–41%),

Table 2 Traffic composition at study blackspot locations

Study site	Traffic volume (Veh/hr)	% Composition			
		2W	3W	LMV	HV
S-1	6094	61	6	20	14
S-2	1942	77	2	16	5
S-3	2843	48	3	41	8
S-4	9285	74	3	17	5

HVs (5–14%) and 3Ws (2–6%). Therefore, it is evident that a significant variation is present in the traffic composition of the study intersection blackspots.

4.1 Estimation of Post Encroachment Time (PET) for Crossing Conflicts

The possible crossing conflicts were studied to estimate the post encroachment time (PET) of the conflicting vehicle. PET is the time difference between the right-turning vehicle leaving the conflict area (t_1) and the through-moving vehicle entering the conflict area (t_2).

t_1 = time at which the right-turning vehicle exits the conflict area

t_2 = time at which the through-moving vehicle enters the conflict area.

Figure 4 shows a defined intersection conflict area divided into square grids of 2.5 m × 2.5 m in size and in red colour, the lines in orange colour represent the 20-m trap length to determine the speed of a through-moving vehicle. PET was calculated by considering the particular grid in which a conflict could occur. In Fig. 4 a conflict between right-turning 2W and through-moving 2W can be seen in the grid highlighted with a black circle. The frame number corresponding to the time t_1 and t_2 is obtained and the PET value was determined by the time difference between the two values. The frame number corresponding to when the vehicle's front wheel reaches and leaves the trap was noted for measuring the speed of through-moving vehicles, with this time difference the speed is calculated.

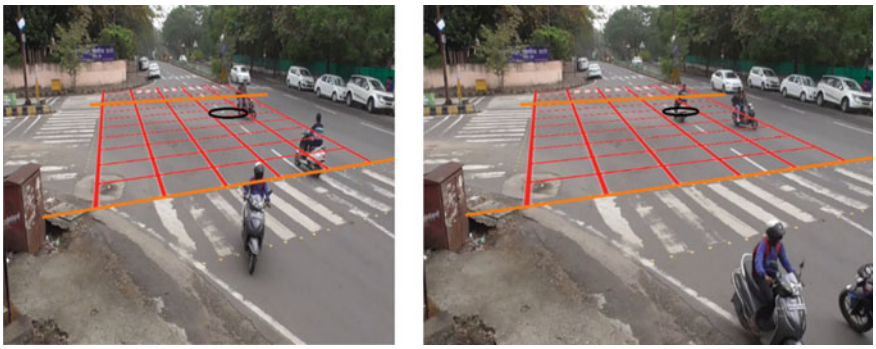

Fig. 4 Movement of vehicles in the intersection conflict area

4.2 *Estimation of Modified Time to Collision (MTTC) for Rear-End Conflicts*

The modified time to collision (MTTC) method was used to estimate any potential rear-end collisions between the two vehicles. The most well-known time-based proximal indication for analyzing rear-end collisions is time to collision. It is the time taken by two vehicles to collide if they remain at their current speeds and on the same path. However, time to collision (TTC) has its own drawbacks: it ignores the relative distance, speed, and acceleration or deceleration of the interacting vehicles, leading to the omission of numerous potential conflict scenarios. Therefore, modified time to collision (MTTC) is used in the present study to analyze rear-end conflict situations.

The rear-end conflicts between the vehicles were considered if the leading and following vehicles were present in the same grid. The video data was processed using Data from Sky software to extract the speed and acceleration of vehicles involved in the rear-end conflicts. Moreover, the distance between two vehicles was calculated using the size of the grid overlaid on the video. It is observed in Fig. 5 that the 2W and LMV have a chance of possible rear-end collision.

To identify rear-end conflicts at unsignalized intersections using a time-based intermediate indicator i.e., MTTC for each conflict scenario, Paul and Ghosh (2021) proposed a method (Eq. 1) to estimate MTTC based on the field observed and extracted data. In the present study, the same process was followed to estimate MTTC values for rear-end conflicts.

$$\text{MTTC} = \frac{-\Delta U \pm \sqrt{\Delta U^2 + 2\Delta a d}}{\Delta a} \tag{1}$$

where, d = distance of separation between two vehicles, Δa = relative acceleration of two vehicles and ΔU = relative velocity of two vehicles.

Fig. 5 Identification of rear end conflicts at unsignalized intersection

4.3 Characterization of PET and MTTC

The parameters properties were examined after determining the PET and MTTC values for crossing and rear-end conflicts. The number of conflicts discovered at each location, as well as the average, lowest, and highest of PET and MTTC, were computed. PET values between each right-turning and through movement were estimated for all study sites from the collected video data. The details of PET values of the study sites are given in Table 3. It is observed that the four-legged intersection, S-4 has the highest number of conflicts followed by S-2, S-1, and S-3 respectively. It is because the traffic volume per hour was highest at S-4. The average PET values range from 1.32 to 2.34 s. It can be concluded from the assessment of Table 3 that nonprioritized vehicles used hazardous right-turning operations in front of vehicles with the right of way rather than yielding to through traffic on the main road.

It is also evident from the MTTC values of Table 3 that the number of conflicts observed for rear-end collision is very less compared to the conflicts observed for PET values. The average value of MTTC is 0.83–1.69 s. It indicates that the time of collision is very less as the drivers have very less time to react. The key conflicts for rear-end collisions at four-legged and three-legged intersections are split based on the leading and trailing vehicle categories. In the case of a four-legged intersection, the maximum number of rear-end collisions is reported for 2W-2W and LMV-2W. In the case of three-legged intersections, rear-end conflicts are found to be the highest for 2W-LMV and LMV-LMV. In the case of three-legged intersections, the highest number of crossing conflicts are observed for 2W-2W followed by LMV-LMV. Whereas, in the case of a four-legged intersection, 2W-2W interactions possess the highest number of crossing conflicts followed by 3W-3W.

Table 3 Characterization of PET and MTTC of the study sites

Parameter	Study sites			
	S-1	S-2	S-3	S-4
No. of identified conflicts	490	508	477	774
Maximum PET (sec)	6.07	9.00	7.70	10.17
Minimum PET (sec)	0.03	0.13	0.03	0.03
Average PET (sec)	1.82	2.34	1.99	1.32
Identified rear-end conflicts	73	45	41	57
Maximum MTTC value (sec)	4.16	8.32	7.97	4.63
Minimum MTTC value (sec)	0.15	0.12	0.08	0.09
Average MTTC value (sec)	1.31	1.69	1.47	0.83

5 Proposal of Crash Severity Level Using Clustering

Cluster analysis was used to classify the conflicts based on their severity levels. In the present study, the k-means clustering approach was used to define threshold values of PET and MTTC for different severity levels. The Elbow method was used to validate the outcome of the clustering analysis. To check the quality of the proposed clusters, a graph was plotted for the Elbow method as shown in Fig. 6. The Elbow approach changed the number of clusters, or k, from 1 to 10. The Within-Cluster Sum of Square, or WCSS, was determined for each value of k. A cluster's WCSS is the total squared distance between each point and the centroid. The elbow-shaped point on the graph where the shape abruptly changes was chosen as the best value for k. Then K-mean clustering was used to the group data and identify the severity levels for crossing and rear-end conflicts.

In the case of K-mean clustering, the value of k was selected by using the Elbow method. While plotting the graphs for crossing as well as rear-end conflicts in the case of three-legged and four-legged intersections, at $K = 4$ the graph became constant. Therefore, to obtain the severity level of conflicts, the conflict values were divided into four levels, with severity level A being the most severe and severity level D being the least severe. Figure 6 shows the graphs for crossing conflicts in the case of three-legged intersections using the Elbow method and clustering analysis. A similar graph was plotted for a four-legged intersection.

A range of PET values was proposed for the different severity levels of crossing conflicts. PET values for three-legged intersections lie in the range of 0.033 to 0.767 s, representing the most severe conflicts, indicating severity Level A. Similarly, a PET value of less than 0.767 s indicates potentially dangerous situations at the time of crossing as the drivers have less time to react. PET values for severity level B range from 0.8 to 1.33 s, which is likewise lower values. On the other hand, the severity

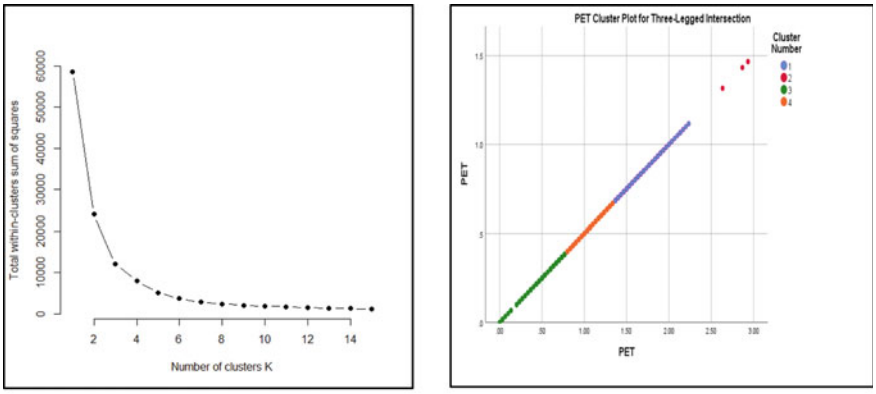

(a) Elbow Method (b) Clustering Analysis

Fig. 6 Graphical representation of clustering analysis

category D represents the least severe condition with PET values ranging from 2.633 to 2.933 s. If the PET values go beyond 2.933 s, it indicates the intersection is safe from a potential crash. However, for a four-legged intersection, the PET values are less and lie between 0.033 and 0.233 s for severity level A.

Table 4 shows that the corresponding PET values for the various severity levels for intersections with four legs are lower than those for intersections with three legs. As a result, it can be said that four-legged intersections are more severe than three-legged intersections in terms of crossing conflicts when intersection severity is defined based on PET values.

A similar analysis was carried out for rear-end conflicts using the MTTC values. It was observed that, in the case of a three-legged intersection, the values for MTTC were observed to be in the range of 0.08 to 0.724 s for the severity level A. The observed values are quite less and indicate a high possibility of dangerous rear-end collision. The MTTC values for severity level B ranges from 0.769 to 1.297 s and range from 1.372 to 2.008 s for level C. On the other hand, the severity level D indicates the lowest severe conflict range where the MTTC values lie in the range of 2.179 to 2.889 s. MTTC values greater than 2.889 s indicate the least chance of a crash. It is observed from Table 4 that the proposed MTTC values for different crash severity levels are lesser in the case of four-legged intersections than in three-legged intersections. Therefore, it can be concluded that four-legged crossings are more vulnerable to rear-end conflicts than three-legged intersections. Furthermore, the lower MTTC levels indicate a larger likelihood of confrontations.

6 Conclusions

The blackspot locations are more susceptible to accidents. In the present study, the safety of vehicular traffic at unsignalized intersection blackspots is studied using surrogate safety measures. The crash severity level was proposed using cluster analysis based on the threshold values for crossing and rear-end conflicts. From the study, the following findings can be formed:

- At the study locations, the average PET values for crossing conflicts vary from 1.32 s to 2.34 s. For MTTC, the average values for rear-end conflicts range from 0.83 s to 1.69 s.
- For crossing conflicts, severity levels A–D range from 0.033 to 2.933 s for three-legged intersections and from 0.033 to 0.967 s for four-legged intersections.
- For rear-end conflicts, severity levels A–D range from 0.08 to 2.889 s for three-legged intersections and from 0.091 to 1.794 s for four-legged intersections.
- It is observed from the estimated values of PET and MTTC that for vehicle combinations 2W-2W is having the highest percentage of conflicts, stating that 2Ws are involved in more serious conflicts.

Table 4 Proposed crash severity levels for crossing and rear end conflict

Type of intersection	Indicator (sec)	Severity levels for crossing and rear-end conflicts			
		A-critical	B-high	C-medium	D-low
Three-legged	PET	$0.033 \leq PET \leq 0.767$	$0.800 \leq PET \leq 1.330$	$1.367 \leq PET \leq 2.233$	$2.633 \leq PET \leq 2.933$
Four-legged	PET	$0.033 \leq PET \leq 0.233$	$0.267 \leq PET \leq 0.433$	$0.467 \leq PET \leq 0.667$	$0.700 \leq PET \leq 0.967$
Three-legged	MTTC	$0.080 \leq MTTC \leq 0.724$	$0.769 \leq MTTC \leq 1.297$	$1.372 \leq MTTC \leq 2.008$	$2.179 \leq MTTC \leq 2.889$
Four-legged	MTTC	$0.091 \leq MTTC \leq 0.478$	$0.507 \leq MTTC \leq 0.885$	$0.964 \leq MTTC \leq 1.425$	$1.720 \leq MTTC \leq 1.794$

6.1 Limitations and Future Scope

- The study is constrained to blackspot locations of Nagpur city only, hence different blackspot locations of other cities can be considered.
- The proposed severity levels need to be validated for other blackspot locations.
- While proposing the severity levels, vehicle-vehicle interaction was not taken into consideration.
- The study's future scope includes the creation of safety-based warrants for unsignalized junctions.

References

1. Paul M, Ghosh I (2018) Speed-based proximal indicator for right-turn crashes at unsignalized intersections in India. J Transp Eng Part A: Syst 144(6):04018024–1- 04018024–9
2. Paul M, Ghosh I (2021) Development of conflict severity index for safety evaluation of severe crash types at unsignalized intersections under mixed traffic. Saf Sci 144(105432):1–14
3. World Health Organization, Global status report on road safety, 1–296 (2018).
4. Paul M, Ghosh I (2020) Post encroachment time threshold identification for right-turn related crashes at unsignalized intersections on intercity highways under mixed traffic. Int J Inj Contr Saf Promot 27(2):121–135
5. Vedagiri P, Killi DV (2015) Traffic safety evaluation of uncontrolled intersections using surrogate safety measures under mixed traffic conditions. Transp Res Rec 2512(1):81–89
6. Kumar A, Paul M, Ghosh I (2019) Analysis of pedestrian conflict with right-turning vehicles at signalized intersections in India. J Transp Eng Part A: Syst 145(6):04019018–1–12
7. Qi W, Wang W, Shen B, Wu J (2020) A modified post encroachment time model of urban road merging area based on lane-change characteristics. IEEE Access 8:72835–72846
8. Peesapati LN, Hunter MP, Rodgers MO (2013) Evaluation of post encroachment time as surrogate for opposing left-turn crashes. Transp Res Rec 2386(1):42–51
9. Shekhar BS, Vedagiri P (2018) Proactive safety evaluation of a multilane unsignalized intersection using surrogate measures. Transp Lett 10(2):104–112
10. Killi DV, Vedagiri P (2014) Proactive evaluation of traffic safety at an unsignalized intersection using micro-simulation. J Traffic Logist Eng 2(2):140–145
11. Gettman D, Head L (2003) Surrogate safety measures from traffic simulation models. Transp Res Rec 1840(1):104–115
12. KA SR, Chepuri A, Arkatkar SS, Joshi G (2020) Developing proximal safety indicators for assessment of un-signalized intersection–a case study in Surat city. Transp Lett 12(5):303–315
13. Pawar NM, Gore N, Arkatkar S (2022) Examining crossing conflicts by vehicle type at unsignalized T-intersections using accepted gaps: a perspective from emerging countries. J Transp Eng Part A: Syst 148(6):05022004–1–17
14. Mohanty M, Panda B, Dey PP (2021) Quantification of surrogate safety measure to predict severity of road crashes at median openings. IATSS Res 45(1):153–159
15. Biswas S, Singh B, Saha A (2016) Assessment of level-of-service on urban arterials: a case study in Kolkata metropolis. Int J Traffic Transp Eng 6:303–312
16. Government of India, Road Accidents in India-2018 (2019) Ministry of road transport and highways. Transp Res Wing 33(1):75–79

17. Government of India, Road Accidents in India-2018 (2020) Ministry of road transport and highways. Transp Res Wing 33(1):75–79
18. Zheng L, Sayed T (2019) Comparison of traffic conflict indicators for crash estimation using peak over threshold approach. Transp Res Rec 2673(5):493–502

Use of Toll Transaction Data for Travel Time Prediction on National Highways Under Mixed Traffic Conditions

Chintaman Santosh Bari, Parth Jhaveri, Satyendra Kumar Sharma, Shubham Gupta, and Ashish Dhamaniya

Abstract Knowledge of accurate travel time is an important aspect for both users and traffic engineers/planners. Hence, the travel time models should predict the travel time more accurately by considering different traffic characteristics. Limited studies are carried out for travel time distribution prediction for different vehicle classes plying on National Highway (NHs), under mixed traffic conditions. Hence, an attempt is madeh in the present study (a) to evaluate the travel time and (b) to develop the vehicle classwise travel time prediction model. For this, a study stretch of 38 km of National Highway (NH)-48 between Karjan Toll Plaza and Narmada Toll Plaza located in the western part of India is considered. Travel time of different vehicle classes obtained from toll transaction data for seven days continuous count has been used for analysis. It is observed that there is a wide variation in the travel time of different vehicle classes and within the same vehicle class. Further, distribution analysis was carried out for the best-fitted distribution, and it was found that the Generalized Extreme Value (GEV) distribution explains the travel time variation well. Using the base of GEV distribution, the GEV parameters, i.e., location, scale, and shape parameter equations are developed based on traffic volume and traffic composition. The results showed that the developed equations predict well for travel time.

Keywords Travel time · Generalized extreme value distribution · Location parameter · Scale parameter · Shape parameter · Prediction

C. S. Bari
Department of Civil Engineering, COEP Technological University, Pune, India

P. Jhaveri · S. K. Sharma · S. Gupta · A. Dhamaniya (✉)
Department of Civil Engineering, Sardar Vallabhbhai National Institute of Technology (SVNIT), Surat, India
e-mail: adhamaniya@gmail.com

A. Dhamaniya et al. (eds.), *Recent Advances in Traffic Engineering*, Lecture Notes in Civil Engineering 377, https://doi.org/10.1007/978-981-99-4464-4_36

1 Background

Developing countries like India face congestion on National Highways (NHs) due to the ever-increasing vehicular population and transport infrastructure constraints. Further, the presence of different vehicular classes with static and dynamic characteristics along with non-lane-based traffic causes the situation to become more critical [1]. Due to these congestion levels on NHs, the travel time vary with the time of the day (TOD) and day of the week (DOW) for the same route. For the commuters and the users plying on NH, the travel time is one of the factors used for the planning of trip. Travel times are a more direct way to evaluate (and for drivers to "feel") the effectiveness of traffic management, particularly from the viewpoint of travelers [2]. Travel time variation and longer travel time not only add to the anxiety and stress of the commuters but also result in a waste of productive time [3]. Further, the service performance of any road link can be well assessed by the travel times of the vehicles. Thus, knowledge of accurate travel time can assist traffic engineers and planners in increasing safety and also for effective traffic operation planning. The modeling of trip time gets difficult given the variety of variables affecting corridor traffic flow. The development of travel time estimation models has been attempted by numerous researchers using a variety of methodologies, including analytical method, time series method, soft computing, and simulation technique.

Chien and Kuchipudi [4] applied the Kalman filtering algorithm to predict dynamic travel time using recent and historical data gathered by Road Side Terminals (RSTs) in New York. They concluded that historic path-based data performs better for travel time prediction in peak hours. Vanajakshi et al. [5] applied the Kalman filtering technique for travel time prediction of Buses operating under heterogeneous traffic conditions. They used the Global Positioning System (GPS) data of Buses from Chennai, India. They concluded that the Kalman filtering performs well with a maximum absolute percentage error of 17.09%.

Yazici et al. [6] studied the travel time reliability of urban roadway links in New York City using the Global Positioning System (GPS) taxi dataset. Three different reliability measures were used, including Coefficient of Variation (COV), skewness, and width of distribution for identifying DOW and TOD periods. They found that the travel time data is always skewed for urban roadway networks. Khoei et al. [7] used Seasonal Auto-Regressive Integrated Moving Average (SARIMA) method for travel time prediction in Brishabe city. The travel time data obtained from Bluetooth sensors were used. They found that the SARIMA with seasonal coefficient increases the prediction accuracy in comparison with the naïve technique. To overcome the bias due to traditional travel time prediction models, Li et al. [8] proposed a temporal-spatial queuing model based on speed and headway. Mendes-Moreira et al. [9] suggested a heterogeneous ensemble approach with dynamic selection employing various algorithms, including support vector machines, random forest, and projection pursuit regression, resulting in travel time predictions with higher accuracy and robustness. The data of loop detectors were used by Davies et al. [10] for travel time

prediction on highways. Local linear regression was used along with traffic flow and density data for prediction.

Wang et al. [11] developed a travel time prediction model for freight vehicles using loop detector data and GPS-based data. They used the cluster analysis along with the speed density relationship for the prediction. They concluded that the developed model performed better than the traditional Bureau of Public Roads (BPR) and Akcelik models. Qiao et al. [12] proposed the nonparametric travel time prediction model with the help of different traffic and weather conditions for freeways. The data consist of the historical and real-time dataset, including data on TOD, precipitation type, and its intensity, visibility, and wind speed. Singh et al. [13] studied travel time reliability and variability on urban arterial roads in India. Wi-fi sensors were used to gather the data at three different locations, and the top capping threshold of 2400 s was used to process the data. Wi-fi sensors were used to calculate travel time values. Peak and off-peak hours of the day, as well as the season of the year, were determined by travel time variability. They found that the Generalized Extreme Value (GEV) distribution well explains the travel time variation. The travel time index (TTI), buffer time index (BTI), and planning time index (PTI) were calculated to examine trip time reliability. K-means clustering technique was used to build a reliability-based LOS threshold. They concluded that the BTI as a reliability measure better explains the variation in travel time.

Taghipour et al. [2] evaluated the performance of different machine learning models for short-term travel time prediction. Data from multiple sources, such as loop detectors, probe vehicles, etc., were used as training and testing datasets. They found that Random Forest (RF) model performed well than Artificial Neural Network (ANN) and K-Nearest Neighbour (KNN). Qiu and Fan [14] developed predicted travel time for freeway corridors by applying four different machine learning algorithms: Decision Trees (DT), Random Forest (RF), Extreme Gradient Boosting (XBoost), and Long Short-Term Memory neural network (LSTM). They found that the RF model was the most promising model and could cover larger variability in datasets. Sihag et al. [1] combinedly predicted travel time for all vehicle classes using the GPS trajectory dataset under heterogeneous disordered traffic conditions. Different data driven models are used such as linear regressions, decision trees, random forests, and gradient boosting regression (GBR). They concluded that the GBR is the best for Indian traffic conditions due to higher performance and computational efficiency.

The above literature review shows that various studies have been carried out for mean travel time prediction for developed countries using various statistical and data-driven methods. Few studies are carried out for Indian traffic conditions, but mostly for urban roadways [1, 13] or for single vehicle classes such as Buses [5, 15]. Limited studies are carried out for travel time prediction for NHs for Indian traffic conditions considering different vehicle classes. Hence, the present study is carried out to develop travel time prediction models for different vehicle classes plying on NH using historical toll transaction data. Apart from mean travel time, an attempt has been made to develop the prediction model for travel time distribution. For this, a distribution analysis of travel time is carried out.

The remainder of the paper is as follows. Section 2 describes the data collection and pre-processing of the data. In this, the detailed description of data from the field and toll authority are described. Afterward, Sect. 3 describes the preliminary analysis of travel time and speed data. In Sect. 4, travel time analysis with respect to TOD and DOW are described. Next to it, the distribution fit analysis for travel time is described in Sect. 5. Lastly, travel time parameter prediction models are developed.

2 Data Collection and Pre-processing of the Data

For the present study, two sources of data are used. The primary traffic data was collected from the field using a videographic survey at the study location, and the secondary data was obtained from the National Highway Authority of India (NHAI) in the form of toll transaction data.

2.1 Toll Transaction Data

NHAI has provided the toll transaction data of two toll-plazas on NH-48, which are Karjan toll plaza (KARTP) and Narmada toll plaza (NATP), with the license plate information. NH-48 is the busiest highway in India, connecting Mumbai and Delhi. Both the toll-plazas are 38 km apart on the same highway. Data from NHAI was obtained in an Excel sheet for a period of a month consisting of Transaction Date and Time, Vehicle Number, and Auditor Class (Fig. 1). Now, considering these two toll-plazas, both direction traffic is noted as (a) KARTP-NATP and (b) NATP-KARTP. For the whole analysis, a total of five vehicle classes are considered viz, Car, Light Commercial Vehicle (LCV), Bus, Heavy Commercial Vehicle (HCV), and Multi Axle Vehicle (MAV). MAV consists of three to six-axle vehicles, while trucks and tractors are considered in HCV.

2.2 Videographic Data Collection

To study the speed characteristics, videographic data was collected from the midblock section between the same stretch in normal weather conditions. A 60-m trap (Fig. 1) was made on the highway to find the speed variation for different vehicle classes.

The data was extracted using AVIDEMUX software to get the speed variation on the study stretches with an accuracy of 0.04 s. The speed of each vehicle class was found by noting down the in and out-time of different vehicles from the trap.

Fig. 1 Data collection

3 Preliminary Analysis

3.1 Deriving Travel Time From Toll Transaction Data

To find out travel time, first, license plate matching must be done so that the same vehicle can be traced at both toll-plazas. For this, the dataset was arranged separately according to their travel direction, i.e., KARTP-NATP and NATP-KARTP direction. The index-match function in the EXCEL spreadsheet was used to capture and match the vehicles. Figure 2 shows the temporal variation of the matched vehicle volume per hour (vph) for a week plying in NATP- 6 KARTP direction. The matching rate was found to be approximately 97%. Figure 2 shows that the period from 4 to 6AM is off-peak time with the least volume plying on the road. In comparison, the peak time varies twice in the daytime (9AM–11AM and 5PM–8PM) and once at night-time (1AM–2AM). The average proportion observed on the highway was Car (43.62%), LCV (8.37%), Bus (16.61%), HCV (2.94%), and MAV (28.46%). Further, it was observed that the proportion of different vehicle classes varies with the TOD. For example, the lowest proportion of Cars was observed as 13.36% at night between 4 and 6AM. On the other hand, the MAV proportion reaches a maximum of 49.30% at 5AM. Thus, one can estimate the variation in travel time by knowing the variability in the traffic volume pattern and variation in traffic composition.

The travel time variation with respect to TOD without capping is shown in Fig. 3. It can be seen that travel time varies from 24.39 s/veh/km to 1384.23 s/veh/km for Cars (Fig. 3a). On the other hand, for MAV, it varies from 30.34 s/veh/km to 1103.39 s/veh/km (Fig. 3b). The same analysis was carried out for different vehicle classes, and it was found that exceptional travel times are obtained from the matching. The

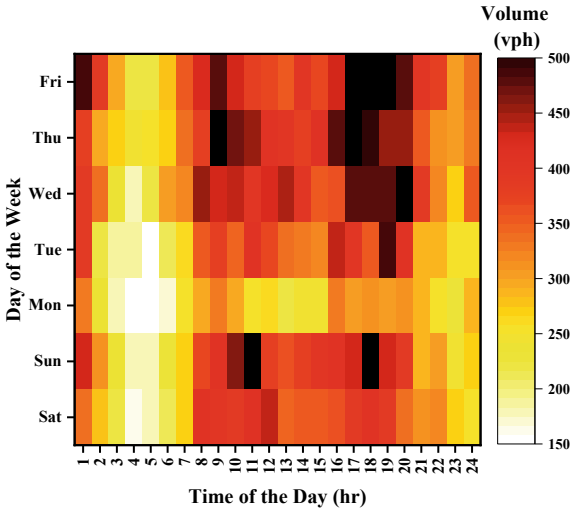

Fig. 2 Temporal variation of the traffic flow for NATP-KARTP in a week

high values of travel times are obtained which may be due to slow-moving vehicles, rejuvenation, and maintenance of vehicles. Hence, there is a need for capping the travel time to remove the outliers for getting the field representative travel times. For capping, the speed thresholds are developed based on the field data, as discussed in the next section.

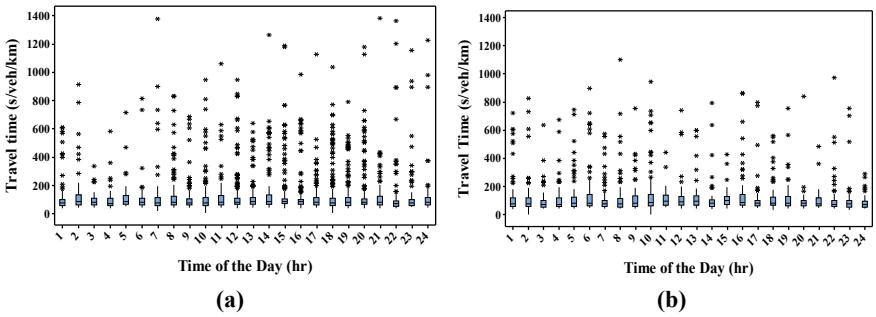

Fig. 3 Travel time variation without capping for 1 Jan data (**a**) Car (**b**) MAV

4 Speed Data Analysis

Speed is a fundamental parameter of traffic flow used for identifying the operational state of the traffic stream. The maximum speed observed among all classes was for Cars (112.50 km/h), and the minimum speed was for MAV (20.15 km/h). These variations in speed can be attributed to the acceleration-deceleration characteristics, power-to-weight ratio of vehicles, etc. [16].

Figure 4 shows the cumulative distribution function (CDF) plot of speed for different vehicle classes. The CDF of the Car is ahead of all other distributions, while that of MAV is behind all. This completely shows the variation in speed between vehicle classes. Considering, 85th percentile speed, the Car speed is about 28.01% higher than LCV and 39.94% higher than MAV. It is observed that a minimum of 85% of drivers of all vehicle classes are driving within the speed limit of 100 km/h. These speed variations directly affect the travel time of the vehicle; hence, these obtained speed values are used for capping the vehicle classwise travel time values for further analysis.

4.1 Filtering of Travel Time Data

Travel time is useful for understanding the delineation of peak and off-peak hours and the peak of the week [17]. Hence, the obtained travel time should be reliable and represent the actual field travel time. Hence, three-stage filtering was adopted to eliminate outliers from the travel time dataset.

Stage 1—Minimum travel time based on the 85th percentile speed.
Stage 2—Maximum travel time based on the 15th percentile speed.
Stage 3—Filtered data for removing outliers.

Stage 1: Processing Data using Lower Capping Criterion.

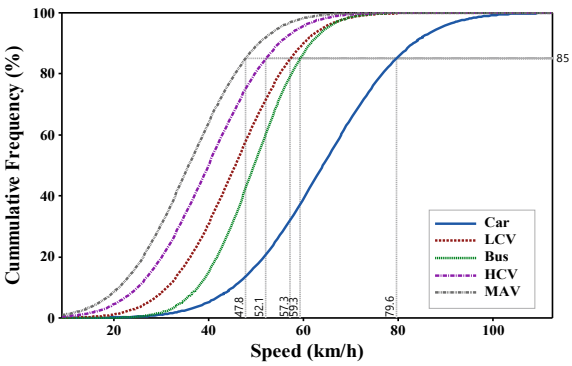

Fig. 4 CDF plots of speed

Outliers were eliminated during the first processing stage by using a lower capping criterion. A lower capping criterion of minimum travel time of each vehicle class was adopted based on the 85th percentile speed. This was done to remove the outliers with very less travel time, which can significantly affect the results.

Stage 2: Processing Data using Upper Capping Criterion.

In the second stage of processing, outliers were eliminated by using an upper capping criterion. Based on the lowest speed possible, taken as the 15th percentile speed, an upper capping level for the maximum travel duration of each vehicle class was adopted. This cut-off was established based on the time it would take for any mode of transportation to complete the segment under maximum congestion.

Stage 3: Processing First Stage Filtered Data for Removing Outliers.

After the second stage filter of matched data, the third stage of processing involves removing outliers using the interquartile range. Using these capping criteria, the lower and upper cap values of travel time were obtained. The lower and upper capped values for different vehicle classes are Car (37.89 s/veh/km and 78.95 s/veh/km), LCV (51.45 s/veh/km and 105.87 s/veh/km), Bus (51.44 s/veh/km and 90 s/veh/km), HCV (56.26 s/veh/km and 133.32 s/veh/km) and MAV (60.00 s/veh/km and 156.58 s/veh/km).

5 Travel Time Analysis

For data analysis, firstly, the travel time range values (according to capping limits) for each vehicle class of 24-h variation are arranged separately. Figure 5a, b shows the box plot of TOD variation of capped travel time data for Car and MAV on 1-Jan 2022, respectively. It can be seen that the means and median of travel time are nearly similar for Car whereas for MAV, the difference between both is observed.

The descriptive statistics of vehicle classwise travel time for all combined data is as shown in Table 1. The travel time of Car varies between 54.41 s/veh/km to 78.94 s/veh/km. For LCV, the traffic flow pattern differs greatly from that of Car. The travel

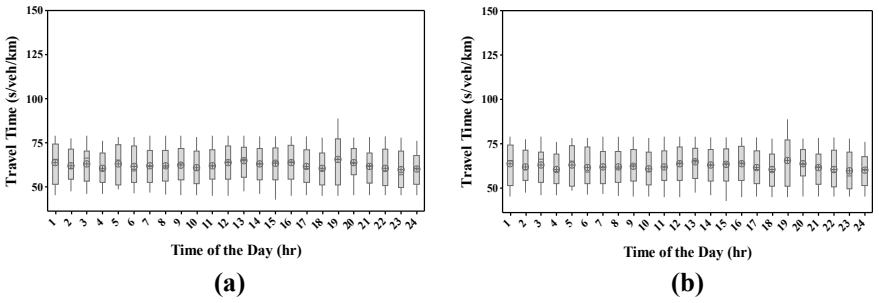

Fig. 5 Temporal variation of capped travel time on 1 Jan **a** Car, **b** MAV

time for LCV is 20.29% more than Car, due to poor acceleration/deceleration characteristics and power-to-weight ratio. The observed travel time for LCV is 51.50 s/veh/km to 97.66 s/veh/km.

Buses take lesser time to cover the entire stretch. The travel time for Buses was found to vary between 63.82 s/veh/km to 85.11 s/veh/km. In comparison, the median travel time of a Bus is 1.14 times that of a Car. Interestingly, the coefficient of variation (COV) of the Buses is lower than that of all. This can be attributed to the characteristics of the Bus as a public transport vehicle. The Buses have fixed schedules, and the drivers always have time pressure to complete the journey within stipulated times. Further, most Bus drivers are accustomed to the routes; hence, the travel time variation was found to be lower for Buses. The median travel time for HCV is 28.59% higher than Car, but COV is the highest among all. This is because of the smaller sample size and higher standard deviation (SD) of travel times. On the other hand, the median travel time of MAV is 41.92% higher than Car with a COV of 0.12. It is lower than HCV, and hence, it can be said that the travel time of MAV is more reliable than HCV.

Understanding the travel time variability for different TOD and days of the week (DOW) is a crucial task before performing further analysis. The peak and off-peak hours of the day, the peak day of the week, and the year's peak season may all be identified using these patterns of travel time variability. Variations in a day's hour and a weekday are considered in this study due to the limited amount of data that is accessible. Heat maps were plotted at one-hour intervals for a typical weekday and weekend to visualize the travel time.

From all the analyses, it is observed that the volume variation is not the same for all days; it differs according to the TOD and DOW, but the pattern shows some consistent results (Fig. 2). Similarly, travel time also varies according to different TOD and DOW.

Table 1 Descriptive statistics of vehicle classwise travel time (s/veh/km) for all combined data

Vehicle class	Mean	Median	SD	COV	Minimum	Maximum	15th percentile	85th percentile	Change in median travel time with respect to Car (in %)
Car	65.77	64.53	6.06	0.09	54.41	78.94	59.42	74.06	–
LCV	77.52	77.62	6.74	0.09	51.50	97.66	71.37	83.13	20.29
Bus	73.63	74.08	3.60	0.05	63.82	85.11	69.98	77.15	14.80
HCV	84.17	82.97	12.88	0.15	57.14	117.74	71.74	97.57	28.59
MAV	90.57	91.58	11.10	0.12	63.37	116.79	76.69	100.76	41.92

The study of travel time with respect to TOD for a whole week is carried out to study the oscillations in the pattern. Figure 6a shows the vehicle classwise average travel time variation for a week. It can be seen that the travel time of Cars is lower between 4 and 6 AM in the morning, which can be attributed to the lower volume of Cars in this period, as discussed earlier. Further, it is evident from Fig. 6a that the travel time is lower for Cars and higher for MAVs for the total period. Further, COV variation is also checked for different vehicle classes, and it was observed that the COV is lowest for Buses, followed by Car and LCVs. The higher COVs are clearly distinguished from Fig. 6b for HCVs. Looking at COV as the reliability measure [6], Buses are more reliable than other classes. Further, for all vehicle classes, the skewness of travel time is also checked. The positive skewness of travel time is observed for Cars, meaning that the larger travel times values are observed less frequently. Further, as seen from Fig. 6c, the skewness of most classes is negative in the early morning except for HCV, depicting the high skewness nature of travel time.

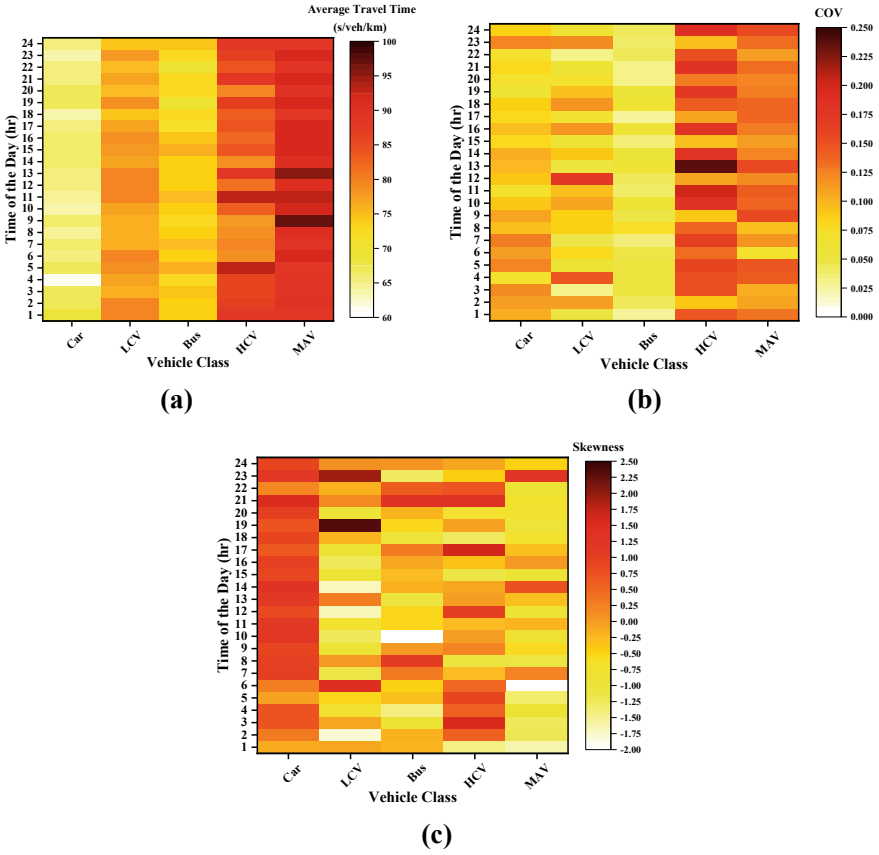

Fig. 6 TOD variation of **a** Average travel time variation, **b** COV, **c** Skewness

The relationship between different statistical measures such as average travel time, SD, and COV is studied using scatter plots. For this, the data of 24-h × 7 days is considered at a one-hour interval. For example, Fig. 7a shows the relationship between SD and average travel time calculated for each hourly period. It can be seen that the SD increases with an increase in average travel time. The same pattern is observed by Yazici et al. [18]. To study the vehicle classwise variation, a plot between COV and average travel time is studied. For Cars, the COV varies between 0.06 and 0.12 with a minimum average travel time (Fig. 7b). On the other hand, the COV of buses is the lowest of all (0.02–0.07). Further, the values of COV of HCVs are more dispersed, showing the less reliable travel time of HCVs.

By visualizing the travel pattern for cars throughout the week, the most congested days are Monday and Friday, while the travel time on Sunday is quite less (Fig. 8a). For LCV, the busiest days were Sunday and Wednesday throughout the week. The lower travel times are seen on Monday for other vehicle classes except for Car. As Monday is the start of the week, most commuters drive to their workplaces from their homes; hence, the travel time for Cars was found to be higher. Keeping in mind these whole analyses, it can be concluded that the travel time varies with TOD and DOW depicting the variation due to traffic characteristics. Hence, there is a need to develop a travel time prediction model that can help to know travel time according to the traffic volume and composition.

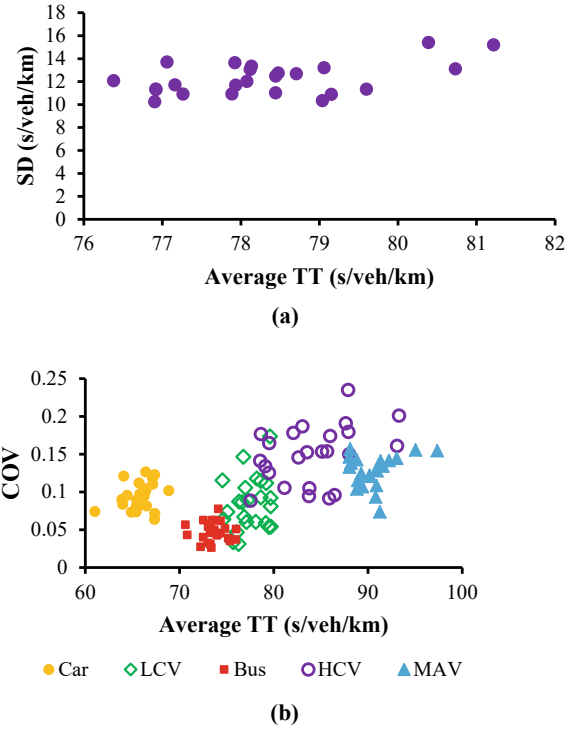

Fig. 7 Relation between **a** SD of travel time and Average travel time, **b** COV and average travel time

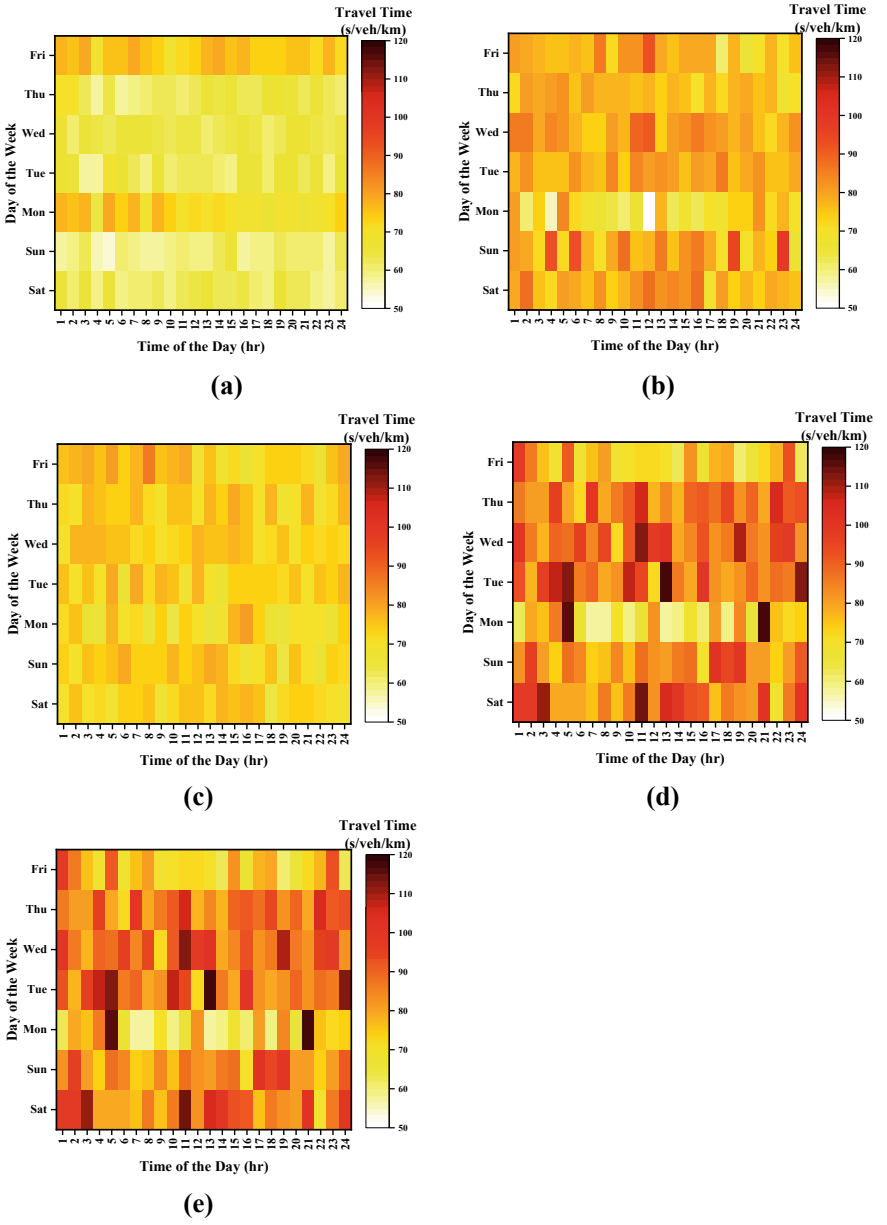

Fig. 8 Travel time variation with respect to DOW **a** Car, **b** LCV, **c** Bus, **d** HCV and **e** MAV

6 Distribution Fit Analysis

Before moving towards the development of the model, the distribution fit analysis of travel time is carried out using Kolmogorov–Smirnov (KS) test. It is a nonparametric test and thus can be applied for any dataset without prior assumption. The KS test is similar to other statistics in which the Dstat and Dcrit values are to be compared, where D is the maximum distance between the empirical and fitted CDF curve. For the present study, the level of significance is taken as 5%. The literature shows that the travel time follows the normal, lognormal, Gamma, and Generalized Extreme Value (GEV) distribution. Hence, all these four candidate distributions are considered for the present study to find the best-fitted distribution for travel time. EASYFIT software was used for calculating the statistical values of each candidate distribution. The procedure of distribution fit analysis is carried out for each vehicle class and DOW, separately. The results of distribution fit along with KS statistics are shown in Table 2.

It can be seen that the KS statistics value of GEV distribution is lower for most cases, illustrating the best-fitted distribution. It was followed by Normal and Lognormal. Gamma was also fitted for all the cases, but it came up as the best-fitted distribution in only a couple of cases. Hence, from the above analysis, the GEV is denoted as the best-fitted distribution for travel time. Figure 9 shows the probability density plots (PDF) and CDF plots for Car and MAV for all candidate distributions. It can be seen that the GEV captures the variability in travel time well.

Considering GEV, the shape factors (κ) are studied for different vehicle classes, as shown in Fig. 10. It can be seen that the median k for Cars, LCVs, and Buses are positive while for HCVs and MAVs are negative. Thus, for heavy commercial vehicles, the travel time follows Type III GEV distribution (Weibull distribution), while others follow Type II GEV (i.e., Frechet) distribution [19]. The physical essence of negative κ leads to the presence of higher values of travel times than the other ones [20]. Thus, considering this theoretical and statistical background, an attempt to predict GEV parameters for travel time prediction is carried out in the next section.

7 Travel Time Prediction Model

Focussing on the objective of the present study, an attempt is made to develop a travel time prediction model for mixed traffic conditions based on traffic volume and traffic composition. As seen from the literature, most of the studies have tried the prediction of mean travel time, but as the travel time is not a constant value and it varies depending on multiple factors such as traffic characteristics, drivers' behavior, etc., there is a need to develop the model that gives the accurate value of the travel time. As can be seen that the travel time follows a GEV distribution; the parameters of GEV, i.e., location parameter (μ), scale parameter (σ), and shape parameter (κ), describes the GEV distribution properly. Hence, the prediction models for GEV parameters are developed in the present study. The core idea is taken from

Table 2 Vehicle classwise best-fitted distribution for travel time

Data considered	Vehicle class	Gamma	Normal	Lognormal	GEV	Best fitted
All combined	CAR	0.1016	0.1133	0.0962	0.0521	GEV
	LCV	0.0938	0.0854	0.1034	0.0704	GEV
	BUS	0.0774	0.0710	0.0805	0.0434	GEV
	HCV	0.0516	0.0706	0.0635	0.0567	Gamma
	MAV	0.0807	0.0671	0.0921	0.0534	GEV
Saturday	CAR	0.0872	0.0874	0.0929	0.0760	GEV
	LCV	0.0935	0.1016	0.0901	0.0773	GEV
	BUS	0.1094	0.1055	0.1118	0.0832	GEV
	HCV	0.1389	0.1557	0.1341	0.0986	GEV
	MAV	0.1045	0.1121	0.1036	0.0803	GEV
Sunday	CAR	0.1225	0.1276	0.1212	0.0999	GEV
	LCV	0.1140	0.1277	0.1079	0.0586	GEV
	BUS	0.0951	0.0930	0.0979	0.1313	Normal
	HCV	0.1109	0.1203	0.1017	0.0960	GEV
	MAV	0.1268	0.1318	0.1284	0.0913	GEV
Monday	CAR	0.1409	0.1473	0.1404	0.1166	GEV
	LCV	0.0760	0.0741	0.0836	0.0960	Normal
	BUS	0.0806	0.0841	0.0847	0.0704	GEV
	HCV	0.1329	0.1446	0.1108	0.1079	GEV
	MAV	0.0915	0.0876	0.0926	0.1149	Normal
Tuesday	CAR	0.1218	0.1173	0.1251	0.0973	GEV
	LCV	0.1510	0.1528	0.1255	0.1313	Lognormal
	BUS	0.0829	0.0843	0.0860	0.0772	GEV
	HCV	0.1487	0.1670	0.1430	0.0760	GEV
	MAV	0.1295	0.1376	0.1242	0.1108	GEV
Wednesday	CAR	0.0763	0.0803	0.0779	0.0775	Gamma
	LCV	0.0856	0.0889	0.0907	0.0746	GEV
	BUS	0.0965	0.0964	0.1012	0.0827	GEV
	HCV	0.1204	0.1324	0.1196	0.0900	GEV
	MAV	0.1044	0.1053	0.1077	0.0949	GEV
Thursday	CAR	0.1078	0.1149	0.1052	0.1030	GEV
	LCV	0.1022	0.1007	0.1058	0.1052	Normal
	BUS	0.1375	0.1396	0.1408	0.1309	GEV
	HCV	0.1117	0.1152	0.1189	0.0972	GEV
	MAV	0.1816	0.1894	0.1879	0.1043	GEV
Friday	CAR	0.0738	0.0796	0.0698	0.0858	Lognormal
	LCV	0.1713	0.1767	0.1613	0.1790	Lognormal

(continued)

Table 2 (continued)

Data considered	Vehicle class	Gamma	Normal	Lognormal	GEV	Best fitted
	BUS	0.0945	0.1017	0.0897	0.0993	Lognormal
	HCV	0.1251	0.1406	0.1230	0.0765	GEV
	MAV	0.1354	0.1420	0.1339	0.1029	GEV

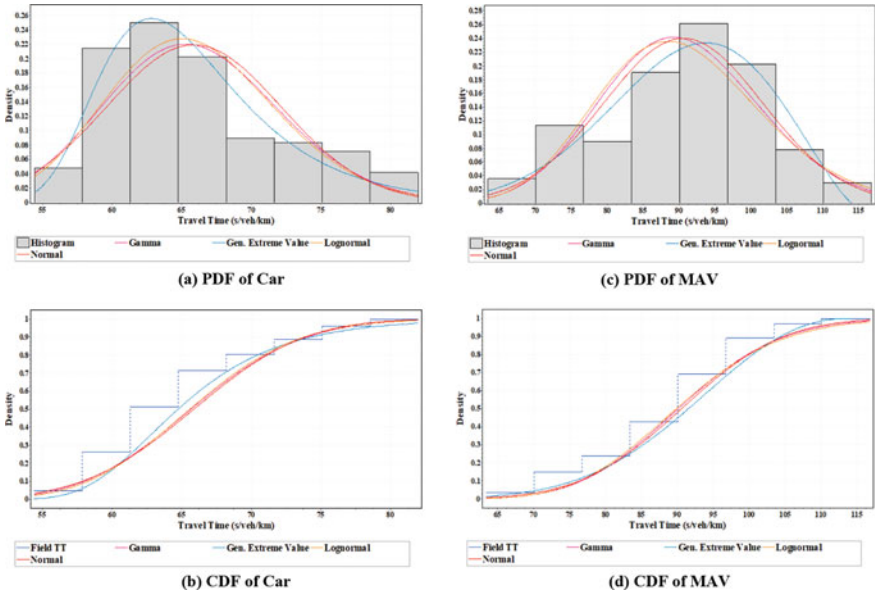

Fig. 9 Distribution fit graphs for different candidate distributions

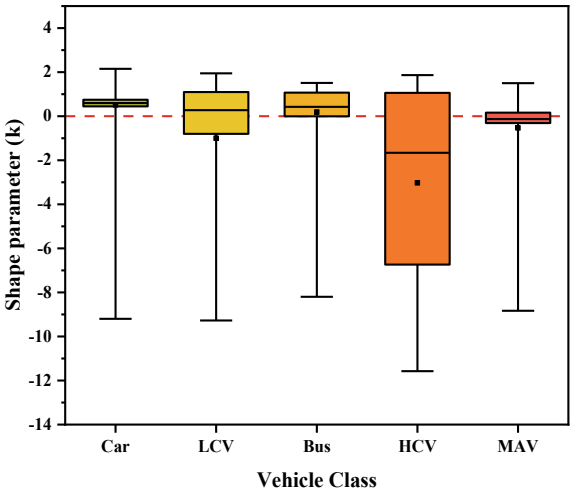

Fig. 10 Vehicle classwise variation in k

the development of spatial and GEV model study from rainfall analysis [21]. Further, such analysis was also carried out for developing parameter functions for headway distributions [22, 23]. A statistical method known as multiple regression is used, which combines many explanatory variables to predict the outcomes of a response variable. The general form of the equation considered is as shown in Eq. 1.

$$(Parameter)_i = \pm a_1{*}V \pm a_2{*}P_{Car} \pm a_3{*}P_{LCV} \pm a_3{*}P_{Bus} \pm a_4{*}P_{HCV} \pm a_5{*}P_{MAV} \quad (1)$$

(Parameter) $i = \mu$ or σ of travel time for vehicle class 'i' (s/veh/km);

V = Traffic Volume (vph).

a_1, a_2, a_3, a_4, a_5, and a_6 = Coefficient.

P_{Car} = Proportion of car; P_{LCV} = Proportion of LCV; P_{Bus} = Proportion of Bus; P_{HCV} = Proportion of HCV; P_{MAV} = Proportion of MAV.

The developed vehicle classwise travel time prediction models, along with the p-values of each coefficient and R^2 value, are shown in Table 3.

From Table 3, it can be seen that for μ, the coefficients of all variables are positive (except for Bus), which shows that the mean travel time increases with an increase in either traffic volume or traffic composition of any vehicle class. For Buses, the coefficient of traffic volume is negative. This can be correlated with the driver's behavior on the Bus. As the Bus is a public transport vehicle, the driver has to follow the schedule of arrival and departure at each origin and departure. Hence, they have time pressure to complete the journey within the stipulated time. Further, most of them are accustomed to the route, and hence, they travel at a faster rate. Hence, as the volume increases, these factors affect causing a negative effect on travel time. The p-values of all the developed coefficients are less than 0.05 (except some, which are significant at 0.10), showing that the coefficients are statistically significant.

For the prediction of κ, the general form of the equation is considered, as shown in Eq. (2). The shape parameter is very sensitive to uncertainties; hence, the general form of Eq. (1) is not used for prediction [24]. Instead, Eq. (2) is used that predicts the shape parameter using the location and scale parameters.

$$(\kappa)_i = \pm a_1 * (\mu)_i \pm a_2 * (\sigma)_i \quad (2)$$

The developed equations for shape parameter (κ) are having R-square of more than 83%, which is satisfactory. The above equations (Tables 3 and 4) were developed by 80% of the total sample data. The remaining 20% of the data is used for validation purposes. The comparison between predicted (from equations) and field observed travel times parameter values are carried out with the mean absolute percentage error (MAPE) (Eq. 3).

Table 3 Parameter equations for different vehicle classes

Vehicle class	Parameter	Volume	P_{Car}	P_{LCV}	P_{Bus}	P_{HCV}	P_{MAV}	R^2
Car	μ (Coeff)	0.00236	66.15	67.81	62.87	66.17	66.76	99.86
	P-Value	0.058*	0.000	0.000	0.000	0.000	0.000	
	σ (Coeff)	0.00450	8.336	6.21	5.28	0.05	7.329	98.08
	P-value	0.100*	0.000	0.001	0.000	0.989	0.000	
LCV	μ (Coeff)	0.0540	66.07	86.00	59.71	54.90	70.36	98.79
	P-Value	0.029	0.000	0.000	0.000	0.043	0.000	
	σ (Coeff)	0.0291	4.56	33.38	2.99	−16.7	−1.78	79.50
	P-value	0.009	0.050	0.000	0.043	0.019	0.094	
Bus	μ (Coeff)	−0.02461	78.38	64.61	73.36	87.50	74.03	99.88
	P-Value	0.002	0.000	0.000	0.000	0.000	0.000	
	σ (Coeff)	0.00318	5.90	−1.89	11.11	4.04	3.88	87.34
	P-value	0.018	0.000	0.005	0.000	0.064*	0.008	
HCV	μ (Coeff)	0.0355	70.91	27.60	94.93	11.40	84.70	99.36
	P-Value	0.084*	0.000	0.024	0.000	0.069*	0.000	
	σ (Coeff)	0.026664	−4.930	9.07	8.78	80.40	−7.76	68.05
	P-value	0.005	0.019	0.102	0.006	0.000	0.000	
MAV	μ (Coeff)	0.0736	72.69	83.84	83.87	54.60	77.03	99.82
	P-Value	0.000	0.000	0.000	0.000	0.000	0.000	
	σ (Coeff)	0.01273	6.28	21.24	6.70	18.56	4.56	95.54
	P-value	0.072*	0.000	0.000	0.005	0.019	0.002	

*Values significant at 10%, Remaining significant at 5%

$$M = \frac{1}{n}\sum_{t=1}^{n}\left|\frac{A_t - F_t}{A_t}\right| * 100 \tag{3}$$

M = mean absolute percentage error.

n = number of times the summation iteration happens.

A_t = Field travel time parameter (s/veh/km).

F_t = Predicted travel time parameter (s/veh/km).

The obtained MAPE values for all developed equations are given in Table 5. It can see that the MAPE value for each vehicle class is <20%, which is good and fairly acceptable. Thus, the developed equations can be used for predicting travel time parameters in the field.

Table 4 Developed equations for the shape parameter

Vehicle class		μ	σ	R^2
Car	Coefficient	−0.00402	0.1116	97.18
	p-value	0.006	0.000	
LCV	Coefficient	0.00868	0.02244	83.87
	p-value	0.026	0.000	
Bus	Coefficient	−0.01014	0.2158	86.70
	p-value	0.000	0.000	
HCV	Coefficient	−0.08872	−0.0524	98.39
	p-value	0.061*	0.000	
MAV	Coefficient	−0.00953	0.0657	79.38
	p-value	0.000	0.000	

*Significant at 0.10, others at 0.05

Table 5 Validation results

Vehicle class	Parameter	MAPE Value (%)
Car	μ	2.70
	σ	9.09
	κ	17.02
LCV	μ	8.82
	σ	19.67
	κ	18.70
Bus	μ	2.99
	σ	13.28
	κ	19.65
HCV	μ	6.84
	σ	16.82
	κ	10.79
MAV	μ	3.49
	σ	19.93
	κ	20.91

8 Conclusions

The present study developed a framework for the distance-based dynamic toll for mixed traffic conditions. For this, a detailed study of the travel time of vehicles on NH is carried out. The travel time is studied with respect to TOD and DOW. It can be seen that the travel time of the Car varies between 54.41 s/veh/km to 78.94 s/veh/km. The travel times of MAVs were found to be 41.92% higher than the mean travel time of Car. Further, the COV of Buses was found to be the lowest, and for HCVs, it was the

highest. Distribution fit analysis shows that the travel time follows GEV distribution. Further, travel time prediction models are developed based on traffic volume and composition. The MAPE values are lower than the prescribed limits, and hence, it can be said that the developed models can be used for travel time prediction in the field.

References

1. Sihag G, Parida M, Kumar P (2022) Travel time prediction for traveler information system in heterogeneous disordered traffic conditions using GPS trajectories. Sustain MDPI 14:1–20
2. Taghipour H, Parsa AB, Mohammadian A (2020) (Kouros): a dynamic approach to predict travel time in real time using data driven techniques and comprehensive data sources. Transp Eng 2:100025. https://doi.org/10.1016/j.treng.2020.100025
3. Ravi Sekhar C, Madhu E, Kanagadurai B, Gangopadhyay S (2013) Analysis of travel time reliability of an urban corridor using micro simulation techniques. Curr Sci 105:319–329
4. Chien SIJ, Kuchipudi CM (2003) Dynamic travel time prediction with real-time and historic data. J Transp Eng 129:608–616. https://doi.org/10.1061/(ASCE)0733-947X(2003)129:6(608)
5. Vanajakshi L, Subramanian SC, Sivanandan R (2009) Travel time prediction under heterogeneous traffic conditions using global positioning system data from buses. IET Intell Transp Syst 3:1–9. https://doi.org/10.1049/iet-its:20080013
6. Yazici M, Kamga C, Mouskos K (2012) Analysis of travel time reliability in New York City based on day-of-week and time-of-day periods. Transp Res Rec 83–95 (2012). https://doi.org/10.3141/2308-09
7. Khoei AM, Bhaskar A, Chung E (2013) Travel time prediction on signalised urban arterials by applying SARIMA modelling on bluetooth data. Australas Transp Res Forum, ATRF 2013—Proceedings
8. Li L, Chen X, Li Z, Zhang L (2013) Freeway travel-time estimation based on temporal-spatial queueing model. IEEE Trans Intell Transp Syst 14:1536–1541. https://doi.org/10.1109/TITS.2013.2256132
9. Mendes-Moreira J, Jorge AM, Freire de Sousa J, Soares C (2015) Improving the accuracy of long-term travel time prediction using heterogeneous ensembles. Neurocomputing 150:428–439 (2015). https://doi.org/10.1016/j.neucom.2014.08.072
10. Davies J, Duke A, Clarke SS, Rupnik J, Fortuna B (2015) Travel time prediction on highways. In: Proceedings—15th IEEE international conference computer and information technology CIT 2015, 14th IEEE international conference on ubiquitous computing and communication IUCC 2015, 13th IEEE international conference dependable, autonomous and secure computing, pp 1435–1442. https://doi.org/10.1109/CIT/IUCC/DASC/PICOM.2015.215
11. Wang Z, Goodchild AV, McCormack E (2016) Freeway truck travel time prediction for freight planning using truck probe GPS data. Eur J Transp Infrastruct Res 16, 76–94. https://doi.org/10.18757/ejtir.2016.16.1.3114
12. Qiao W, Haghani A, Shao CF, Liu J (2016) Freeway path travel time prediction based on heterogeneous traffic data through nonparametric model. J Intell Transp Syst Technol Plann Oper 20:438–448 (2016). https://doi.org/10.1080/15472450.2016.1149700
13. Singh V, Gore N, Chepuri A, Arkatkar S, Joshi G, Pulugurtha S (2019) Examining travel time variability and reliability on an urban arterial road using Wi-Fi detections—A case study. J East. Asia Soc Transp Stud 13:2390–2411
14. Qiu B, Fan W (2021) Machine learning based short-term travel time prediction: numerical results and comparative analyses. Sustainability 13:1–19. https://doi.org/10.3390/su13137454
15. Chepuri A, Joshi S, Arkatkar S, Joshi G, Bhaskar A (2020) Development of new reliability measure for bus routes using trajectory data. Transp Lett 12:363–374. https://doi.org/10.1080/19427867.2019.1595356

16. Bari CS, Navandar YV, Dhamaniya A (2021) Analysis of vehicle specific acceleration and deceleration characteristics at toll plazas in India. Transp Dev Econ 7:1–19. https://doi.org/10.1007/s40890-021-00115-6
17. Mathew S, Pulugurtha SS, Mane AS (2020) Effect of toll roads on travel time reliability within its vicinity: a case study from the state of North Carolina. Transp Lett 12:604–612. https://doi.org/10.1080/19427867.2019.1671043
18. Yazici MA, Kamga C, Ozbay K (2014) Highway versus urban roads: analysis of travel time and variability patterns based on facility type. Transp Res Rec 2442:53–61. https://doi.org/10.3141/2442-07
19. Hossain I, Imteaz M, Khastagir A (2021) Study of various techniques for estimating the generalised extreme value distribution parameters. IOP Conf Ser Mater Sci Eng 1067:012065. https://doi.org/10.1088/1757-899x/1067/1/012065
20. Bari CS, Chandra S, Dhamaniya A (2022) Service headway distribution analysis of FASTag lanes under mixed traffic conditions. Physica A 604:127904. https://doi.org/10.1016/j.physa.2022.127904
21. Yoon S, Kumphon B, Park JS (2015) Spatial modeling of extreme rainfall in northeast Thailand. J Appl Stat 42:1813–1828. https://doi.org/10.1080/02664763.2015.1010492
22. Kong D, Guo X (2016) Analysis of vehicle headway distribution on multi-lane freeway considering car-truck interaction. Adv Mech Eng 8:1–12. https://doi.org/10.1177/1687814016646673
23. Weng J, Meng Q, Fwa TF (2014) Vehicle headway distribution in work zones. Transp A Transp Sci 10:285–303. https://doi.org/10.1080/23249935.2012.762564
24. Friederichs P, Thorarinsdottir TL (2012) Forecast verification for extreme value distributions with an application to probabilistic peak wind prediction. Environmetrics 23:579–594. https://doi.org/10.1002/env.2176

Implementation of Airfield Pavement Management System in India

Pradeep Kumar, Sachin Gowda, and Aakash Gupta

Abstract Airfield pavements need to be maintained regularly to ensure smooth and safer airport operations and to keep pavement conditions long-lasting. The airfield Pavement Management System (APMS) is a systematic tool for this purpose. Depending upon the functional condition of the pavement, APMS tools allow timely detection of pavement surface defects during the preliminary stages of deterioration and prevent serious pavement distresses that will require extensive uneconomical repairs in the future. Without regular maintenance, pavements may not reach their intended structural lifespan. Timely pavement maintenance and repairs are important to ensure adequate load carrying capacity, good pavement friction for the safe operation of aircraft, better riding quality in all weather conditions, and minimal intrusion of foreign object debris (FOD). In this paper, the authors are intended to discuss the international APMS development practices and details of various functional condition indicators such as Pavement Condition Index (PCI), Boeing Bump Index (BBI), FOD Potential Index, etc. currently used to develop APMS in India to assess the existing pavement condition and to arrive at the needs for maintenance & rehabilitation (M&R). This paper discusses the detailed methodology adopted for the APMS including data collection techniques, distress parameters to be considered for airfield pavement evaluation, data analysis and storage tools and adoption of maintenance and rehabilitation strategies for Indian airports.

Keywords Airfield management · Pavement condition index · Boeing bump index

P. Kumar (✉) · S. Gowda · A. Gupta
CSIR-CRRI, New Delhi 110025, India
e-mail: pkumar.crri@nic.in

S. Gowda
e-mail: Sachin08.crri@nic.in

A. Dhamaniya et al. (eds.), *Recent Advances in Traffic Engineering*, Lecture Notes in Civil Engineering 377, https://doi.org/10.1007/978-981-99-4464-4_37

1 Introduction

The most effective way to preserve runways, taxiways, aprons, and other pavement surfaces is to implement a comprehensive maintenance program. A strategic maintenance program includes a coordinated, budgetary and systematic approach to both preventive and corrective maintenance. A systematic approach ensures constant vigilance. A comprehensive maintenance program should be updated annually and should include an inspection schedule and a list of required equipment and products. Airport engineers must ensure systematic repairs and take precautions where necessary.

The prioritization of maintenance strategies is initially done based on functional condition of the pavement. The functional parameters of the pavement surface are Roughness, Pavement Surface Distresses and Frictional Characteristics. In normal practice, if the functional condition exceeds a certain standard limit, then that pavement is considered for immediate maintenance, irrespective of its structural condition.

1.1 Introduction Airfield Pavement Management System (APMS)

The APMS is typically computerized software, which facilitates the storage and analysis of airfield pavement-related data. It is a systematic method of (a) assessing the existing condition of pavements, (b) arriving at M&R needs, and (c) Prioritization of requirements for effective utilization of funding levels.

There are two levels in the Airfield Pavement Management System (APMS) [1]. AC 150/5380-7B [2] namely, the Project level and the network level.

The project level of APMS concerns an identified technical management of every single project or individual pavement section. At a project level, the data regarding identified sections like pavement material characterization, loading pattern, environmental data, and maintenance/construction cost are required.

Unlike the project level, the network level deals with a group of sections (which is also called a network) in prioritizing the specific project to be executed to attain a better quality of the network. Projects selected at network level analysis may not serve as the best project for an individual project/section. However, it'll result in better performance of the whole network identified.

1.2 Evaluation of Airfield Pavements

Systematic monitoring of pavement performance includes functional as well as structural evaluation of airfield pavements by using modern devices, which helps in achieving long-lasting, better performance and efficient management of pavement

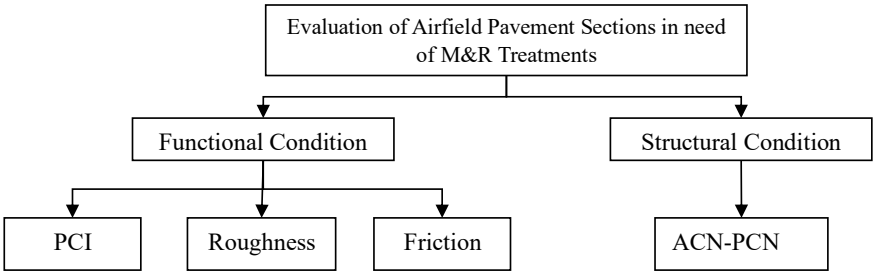

Fig. 1 Preliminary hierarchy structure of the parameters

network within the given budget. A preliminary hierarchy structure based on the functional and structural condition parameters is represented in Fig. 1 [3–5].

1.3 Functional Evaluation

Functional evaluation deals with surface distress such as roughness (measured in terms of the International Roughness Index), pavement surface friction characteristics, and potential for damage due to foreign object debris (FOD) [6, 7]. The PCI is commonly used as a functional evaluation indicator, which is based on pavement surface distresses and will be presented first, followed by pavement roughness, pavement friction, and FOD.

1.4 Pavement Condition Index (PCI)

PCI is a pavement surface condition evaluation methodology which is developed by 'The US Army Corps of Engineers and is described in the FAA Advisory Circular on Guidelines and Procedures for Maintenance of Airport Pavements and in ASTM Standard' [8]. Distresses developed in pavements are an indication of deterioration which may be due to traffic load, climatic conditions, defects in the construction methodology adopted, or a combination of any of these. It is a measure of the existing condition of a pavement surface on visual-based inspection of distresses observed on the surface, which is represented from 0 to 100 (failed and excellent condition respectively). PCI values are arrived at based on distress type, extent, and severity. As per ASTM standards, there are 15 and 16 types of pavement distress are recognized in Plain Cement Concrete (PCC) and Asphaltic Concrete (AC) pavements respectively.

In practice, pavement distress data to arrive at PCI values are quantified based on a visual inspection survey by trained evaluators. However, data can also be acquired by using advanced surveying machinery like pavement imaging by laser scanning

Table 1 PCI rating and recommended pavement treatment

PCI	Rating	Performance description	Recommended treatment
100–86	Good	Only minor distresses	Routine maintenance only
85–71	Satisfactory	Low and medium distresses	Preventive maintenance
70–56	Fair	Some distresses are severe	Preventive maintenance and rehabilitation
55–41	Poor	Severity of some distresses can cause operational problem	Rehabilitation or reconstruction
40–26	Very poor	Severe distresses causing operational problems	Rehabilitation and reconstruction
25–11	Serious	Many severe distresses causing operational restrictions	Immediate repairs and reconstruction

and interpreting them with advanced processing tools. Adoption of mechanized techniques results in measuring distresses on the entire pavement section rather than data collection on a sampling basis, which results in arriving at precise PCI ratings.

Airfield Pavement Distresses and conditions were surveyed as per methods outlined in 'FAA Advisory Circular 150/5380-6C and ASTM D 5340 (2018) [8].' PCI rating & recommended Pavement Treatment are summarized in Table 1.

1.5 Airfield Pavement Roughness

The FAA (2019), [9] defines profile roughness as, 'surface profile deviations over a portion of the runway that may increase fatigue on airplane components, reduce braking action, impair cockpit operations, which may affect the safe operation of aircraft and cause discomfort to passengers'.

1.6 Pavement Roughness Evaluation Using the Boeing Bump Index (BBI)

The BBI is based on zones of roughness; acceptable, excessive, and unacceptable (Fig. 2). If the BBI value is below 1, then the criteria for the Boeing bump is in the acceptable zone. However, if BBI values exceed more than 1, then it falls either in unacceptable or excessive zones in Fig. 2.

FAA [9, 10] recommends measuring the runway surface roughness profile along with the centerline and at a lateral offset (left and right) of 3.05 m (10 feet) for Airplane Design Group (ADG) II and III aircraft, and offset of 5.22 m (17.5 feet) for ADG IV, V, and VI aircraft. If traffic at a given airfield pavement contains all airplane groups then we have to take measurements at all locations [11].

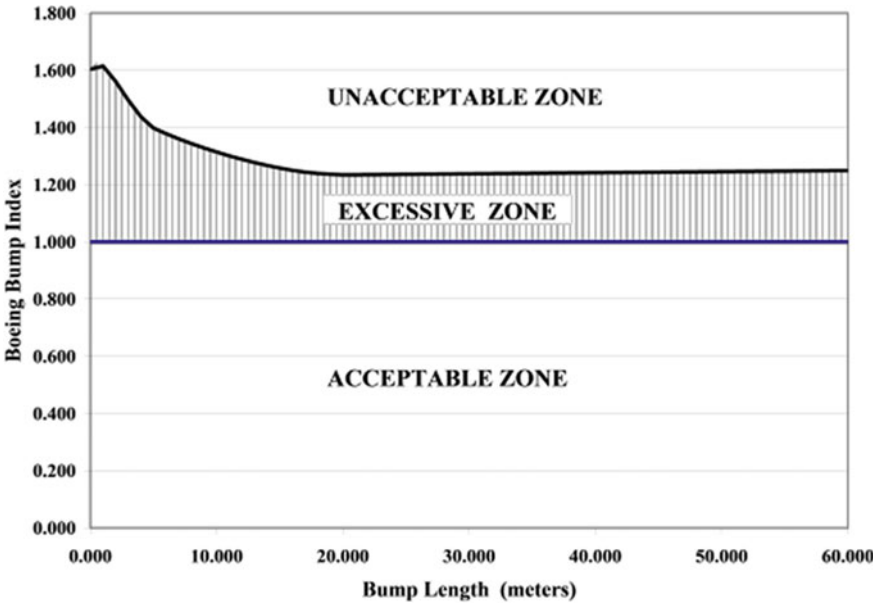

Fig. 2 Boeing bump index—Roughness acceptance criteria [10]

1.7 Pavement Friction

Pavement friction is defined as the resistance offered to the motion of a vehicle tyre by the pavement surface. It is a very important safety concern for an aircraft with heavy weight and high landing speeds, particularly when the pavement is in wet condition. Continuous Friction Measuring Equipment (CFME) is used to determine friction levels on runways.

1.8 Foreign Object Debris (FOD)

Any kind of object, whether it is live or not, which is located in an inappropriate location of airfield pavement and has the potential capacity to injure the airfield or an air carrier personnel leading to damage to the aircraft is called FOD. The presence of FOD is evaluated by FOD Potential Index.

The FOD Index is arrived from calculated PCI by considering only the severity/distress levels which are capable of producing FOD. FOD index is not frequently used at major airports.

2 Methodology for APMS

For the development of APMS, Geographic Information System (GIS) based database has been prepared with the integration of a geo-referenced base map with the Global Positioning System (GPS) tagged distress data collected using Automated Road Survey System. QGIS with Google Maps, Hawkeye Processing Tool Kit, and PAVER software tools have been used for the development work [12, 13]. The flowchart for the Determination of Airfield Pavement Condition Index using PAVER software is shown in Fig. 3.

3 Preparation of Airfield Pavement Network and Determination of Pavement Condition Index (PCI) Using APMS Software

3.1 Development of Base Maps-Digitization and Inventarization

The base map serves as an initial inventory database creation source in the PAVER software. The attributes included in the base map pertain to three levels of the hierarchy of the airfield pavement network. The Network related attributes are Network ID, Network Name; Branch Related attributes included are Branch ID, Branch Name, Use; and Section based attributes included are Section ID, From, To, Surface, Rank, Construction Date, Length, Width, Slab Width, and Slab Length.

3.2 Field Inspections and Preparation of Distress Dataset

The field inspection of the airfield network was done using Network survey Vehicle (NSV). The NSV data collected was decoded in the laboratory using an image processing technique to quantify the distresses identified on airfield pavements in terms of distress type, extent and severity. The distress data collected are geo-tagged to compile in the GIS database [14] as shown in Fig. 4. The database prepared in this way includes the distresses at the sample level in accordance with the ASTM D 5340-18 [8].

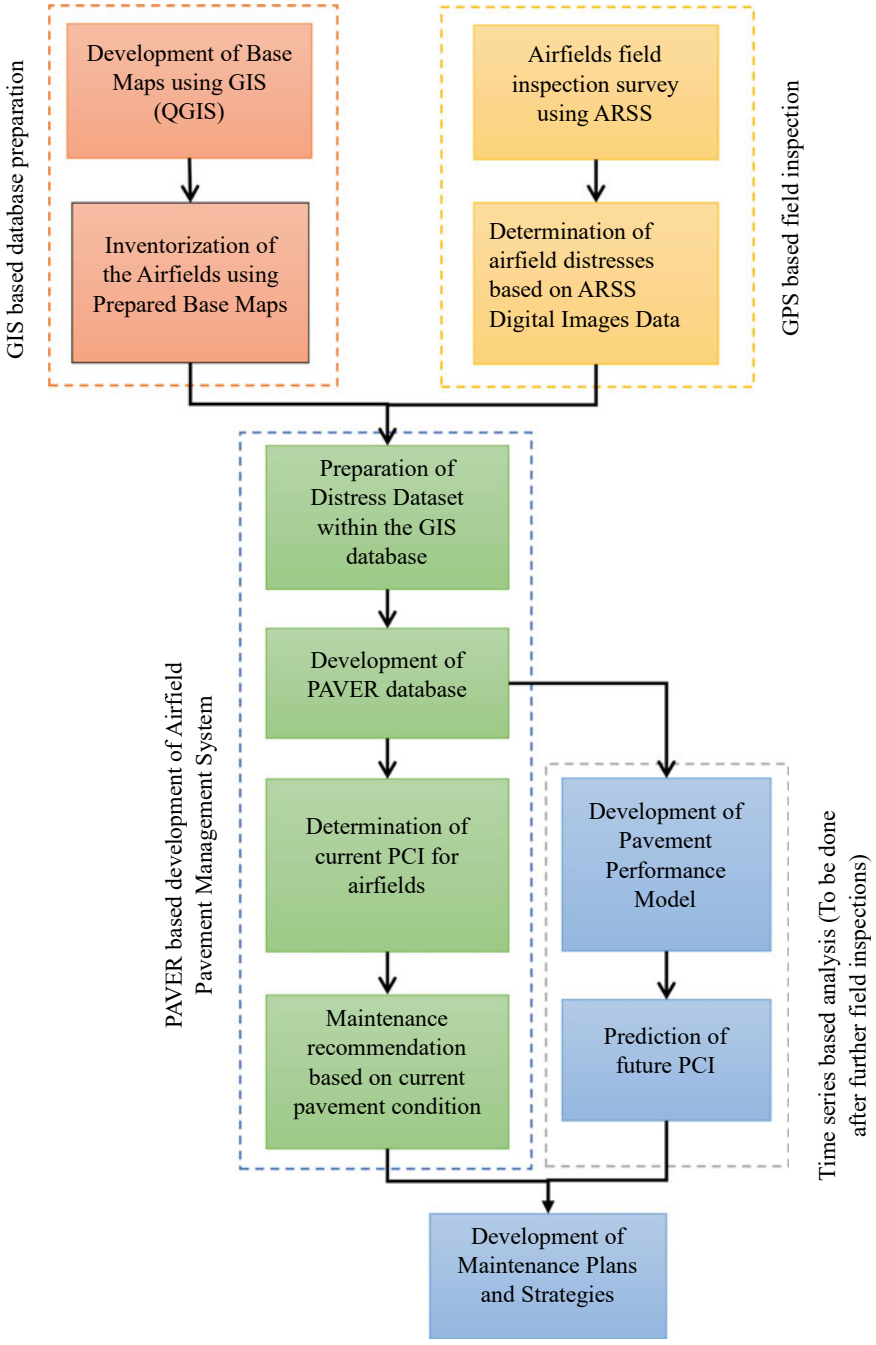

Fig. 3 Determination of airfield pavement condition index using GIS and PAVER software

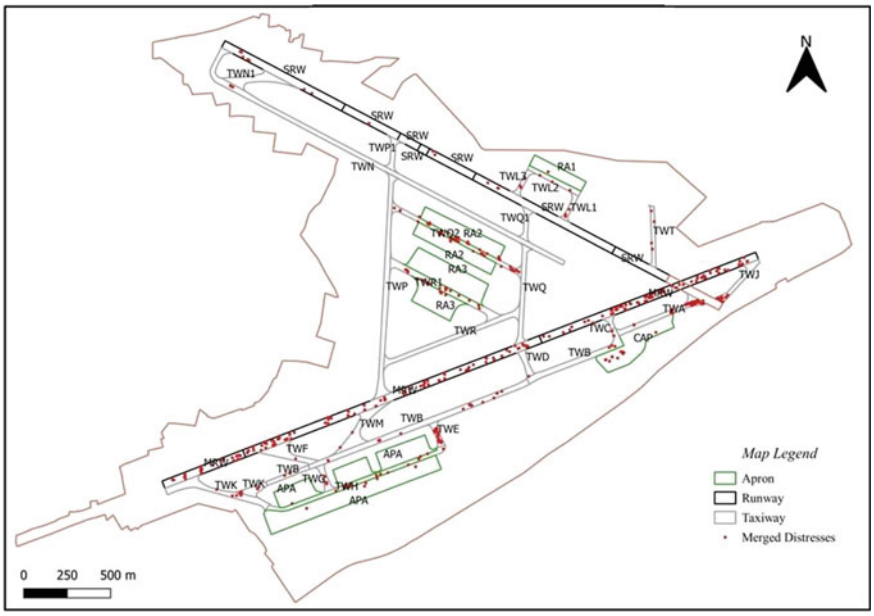

Fig. 4 Merging observed distresses with inventory database

3.3 Preparation of PAVER Database and PCI Determination

For the determination of PCI using PAVER, the first and foremost step is to prepare a database of airfields as per the acquired secondary data. The base map was prepared with the help of secondary data as an initial inventory database, which was imported into the PAVER's database using GIS/Tabular import. Similarly, the samples layer created in the GIS was imported into the PAVER database. The prepared database was ready to serve as the base dataset in the PAVER over which the inspection data was imported after each inspection.

As mentioned, the inspection of airfields was conducted using NSV. The inspection data obtained were imported as new inspection data in the PAVER corresponding to the date of a survey on the airfield pavement. The inspection import procedure is as shown in Figs. 5 and 6 for rigid and flexible surfaces respectively. The PCI representation of the airfield pavement network is shown in Fig. 7.

4 Conclusions

- The result of the pavement condition index presented in Table 2 indicates that PCI values vary from 89 to 100, which indicates a good condition of the pavement and recommends routine maintenance only as per the guidelines.

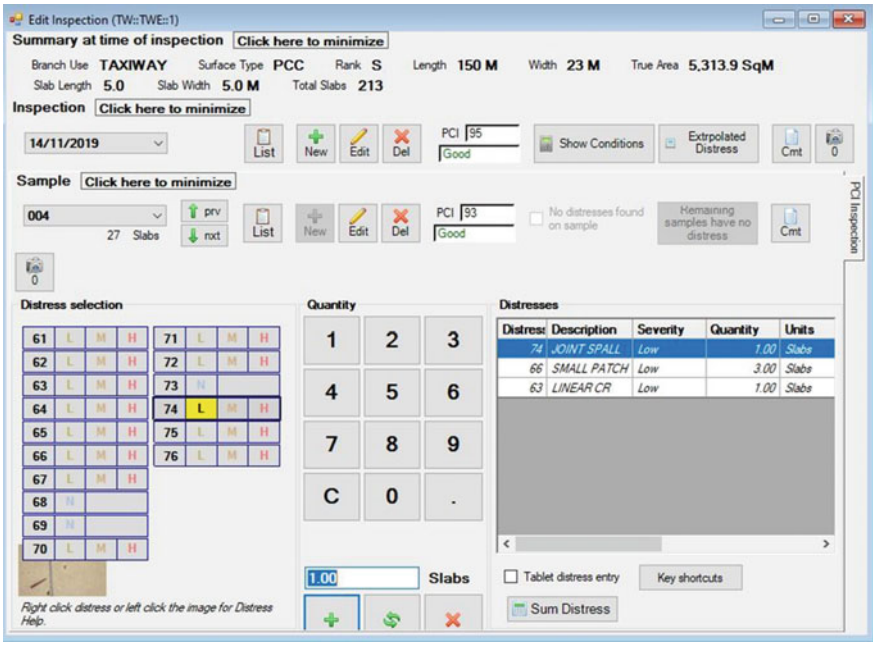

Fig. 5 Rigid pavement surface inspection import wizard

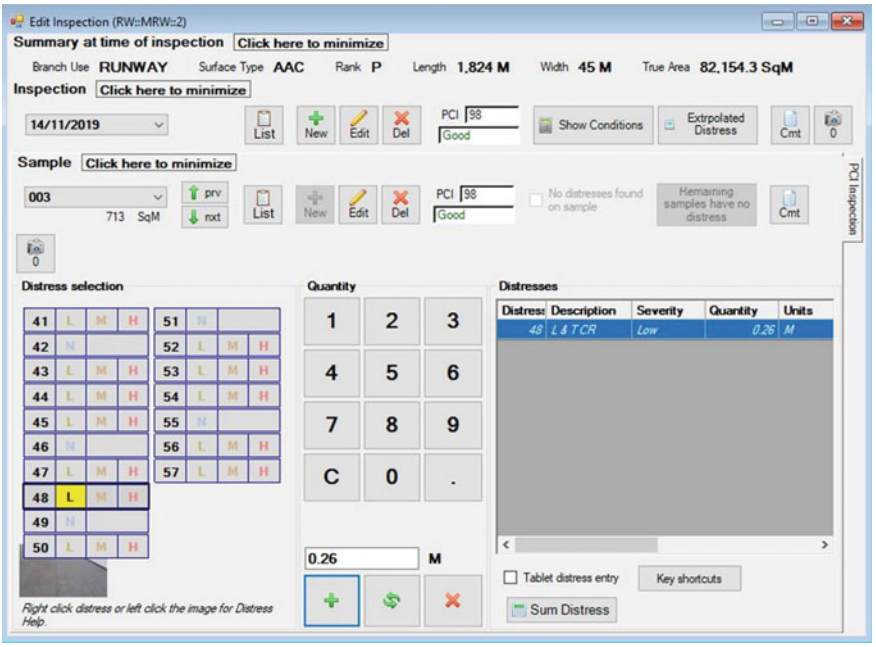

Fig. 6 Flexible pavement surface inspection import wizard

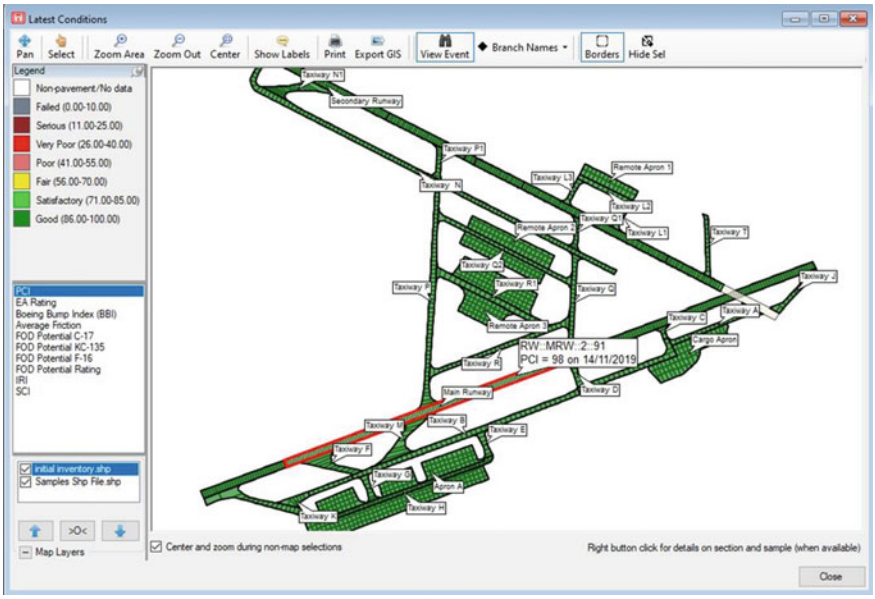

Fig. 7 PCI representation of the airfield pavement network

- FOD potential rating indicates that there is no issue related to FOD on the studied airfield pavement.
- The roughness values (Boeing Bump Index) for the main runway and secondary runways were calculated using the longitudinal profile data collected by the laser profilometer installed in the network survey vehicle. The BBI valves obtained for the main runway and secondary runway, both are within permissible limits.
- NSV-based inspection allows accurate and efficient collection of GPS tagged data in respect of pavement surface profile and distresses for automatic quantification of pavement condition index, Boeing bump index, and FOD potential index.
- Airfield Pavement management system based on functional condition assessment in terms of PCI, BBI, and FOD helps in detecting pavement defects and repairing them at early stages, which is considered an important preventive maintenance protocol.
- Finally, based on PCI data, the maintenance strategies can be easily worked out as per the criteria given in Table 1.
- Delay in implementing routine maintenance at early stages eventually leads to the occurrence of serious pavement distresses which may require uneconomical extensive repairs.

Table 2 Result of various indices

Road ID	Section ID	PCI (Nov 2019)	PCI category	FOD potential rating	FOD potential rating category	BBI
MRW	1	98	Good	11	Good	0.52
MRW	2	97	Good	11	Good	
MRW	3	98	Good	11	Good	
SRW	1	100	Good	0	Good	0.93
SRW	2	100	Good	0	Good	NA
SRW	3	100	Good	0	Good	NA
TWA	1	89	Good	5	Good	NA
TWB	1	99	Good	10	Good	NA
TWC	1	100	Good	0	Good	NA
TWD	1	100	Good	0	Good	NA
TWE	1	90	Good	5	Good	NA
TWF	1	100	Good	0	Good	NA
TWG	1	99	Good	0	Good	NA
TWH	1	100	Good	0	Good	NA
TWJ	1	96	Good	0	Good	NA
TWK	1	100	Good	0	Good	NA
TWK	2	99	Good	0	Good	NA
APA	1	100	Good	0	Good	NA
APA	2	100	Good	0	Good	NA
APA	3	100	Good	0	Good	NA

References

1. FAA (AC 150/5380-7B) (2014) Airport pavement management program (PMP), Federal Aviation Administration, U.S. Department of Transportation
2. Grothaus HJ, Helms TJ, Germolus S, Beaver D, Carlson K, Callister T, Kunkel R, Johnson A (2009) ACRP report 16th guide book for managing small airport
3. Irfan M, Khurshid MB, Iqbal S, Khan A (2015) Framework for airfield pavements management—an approach based on cost-effectiveness analysis. Eur Transp Res Rev 7(2)
4. White G, Kitchen R (2019) Parametric comparison of the whole of life cycle cost of rigid parametric comparison of the whole of life cycle. In: Eighteenth annual international conference on pavement engineering, Asphalt Technology and Infrastructure, Liverpool, England
5. Babashamsi P, Khahro SH, Omar HA, Al-Sabaeei AM, Memon AM, Milad A, Khan MI, Sutanto MH, Yusoff NIM (2022) Perspective of life-cycle cost analysis and risk assessment for airport pavement in delaying preventive maintenance. Sustainability 14(5):2905. https://doi.org/10.3390/su14052905
6. Chai G, Bell P, Mcnabb K, Wardle L, Oh E (2022) Comparison of flexible airfield pavement designs using FAARFIELD v1.42 and APSDS 5.0. In: Lecture Notes in Civil Engineering. Springer International Publishing, pp 359–373. https://doi.org/10.1007/978-3-030-87379-0_26

7. Guo L, Wang H, Gagnon J. Comparison analysis of airfield pavement life estimated from different pavement condition indexes. J Transp Eng, Part B: Pavements 147(2):04021002. https://doi.org/10.1061/jpeodx.0000254
8. FAA (AC 150/5380-6C) (2014) Guidelines and procedures for maintenance of airport pavements, Federal Aviation Administration, U.S. Department of Transportation
9. Loprencipe G, Zoccali P (2019) Comparison of methods for evaluating airport pavement roughness. Int J Pavement Eng 20(7):782–791. https://doi.org/10.1080/10298436.2017.1345554
10. FAA (AC150/5380-9) (2009) Guidelines and procedures for measuring airfield pavement roughness, Federal Aviation Administration, U.S. Department of Transportation
11. ICAO Annex 14, Annex 14—Aerodromes, Volume 1- Aerodrome Design and Operations, International Civil Aviation Organization (2018)
12. Kumar P, Sharma M (2022) Functional condition evaluation of airfield pavements using automated road survey system—A case study of a small sized airport. In: Lecture Notes in Civil Engineering. Springer International Publishing, pp 185–196. https://doi.org/10.1007/978-3-030-87379-0_13
13. Miah MT, Oh E, Chai G, Bell P (2020) An overview of the airport pavement management systems (APMS). Int J Pavement Res Technol 13(6):581–590. https://doi.org/10.1007/s42947-020-6011-8
14. Schwartz CW, Rada GR, Witczak MW, Rabinow SD. GIS applications in airfield pavement management. Transportation Research Record (1311)

Two-Lane Bidirectional Traffic Flow Patterns

Shreya Dey, Suresh Nama, and Akhilesh Kumar Maurya

Abstract The paper aims to study the effects of an individual type of vehicle's volume of both in-line and opposing traffic on the speed of vehicles. A relatively few studies have been conducted in India to observe the effect of opposing traffic volume on the speed of different vehicles and the entire traffic stream, whereas bidirectional traffic condition is the most prevailing condition in India. In this paper, results were obtained for the speed-volume relationship for five classes of vehicles: Car, motorized two-wheeler, motorized three-wheeler, bus/truck, and light commercial vehicle (LCV). The results obtained from this study can be used to calculate speeds for different traffic volumes and compositions, ascertain various traffic improvement measures, and evaluate the level of service for roads with similar traffic situations.

Keywords Heterogeneous traffic · Bidirectional road · Speed-density relationship · Linear regression · Different category of vehicles

1 Introduction

India is a developing country, with most roads comprising two-lane bidirectional traffic. The traffic on these roads is highly heterogeneous, with poor lane discipline. The speeds of the vehicles on these roads also vary widely depending on various parameters related to the driver characteristics, type of vehicle, type of road, and type of traffic. Vehicle speed becomes a crucial safety factor in bidirectional traffic with various vehicle classes. On a bidirectional road, opposing traffic composition and volume plays a significant role in the behavior of the traffic in the opposite direction, especially when various types of vehicles having widely varying dimension and dynamic characteristics like two-wheeler, car, three-wheeler, truck, bus, LCV

S. Dey
Associated Regional and University Pathologists, Inc., Dublin, Ireland

S. Nama (✉) · A. K. Maurya
Indian Institute of Technology Guwahati, Guwahati, Assam 781039, India
e-mail: nsureshce@gmail.com

A. Dhamaniya et al. (eds.), *Recent Advances in Traffic Engineering*, Lecture Notes in Civil Engineering 377, https://doi.org/10.1007/978-981-99-4464-4_38

share the same roadway. Therefore, the present paper attempts to develop the speed-volume relationship for the overall and individual class of vehicles for a two-lane bidirectional road under mixed traffic conditions with poor lane discipline.

2 Literature Review

Only limited studies have been carried out in India to develop speed-density equations, and even few research has been found studying speed-density equations for the two-lane bidirectional roads in India. Research conducted by Porter et al. [1] recommended that ordinary least square regression gives appropriate results in modeling 85th percentile free flow speed. Kubota [2] used a three-stage least square regression to model speed at the tangent section and speed at the entrance of the next unsignalized intersection. Bester [3] developed a model to calculate the speed of trucks assuming speed varies linearly with acceleration. Sun and Zhou [4] used cluster analysis to develop multi-regime speed-density relationships. Banihashemi et al. [5] used a linear regression model for speed modeling. After analyzing speed data, Nama et al. [6] found that the drivers' speeds exceed the design speeds. Al-Ghamdi [7] concluded that the operating speed exceeded the speed limit, that the regression model gives a better estimate for operating speed than the normal model, and that the Bayesian technique could be used to increase the accuracy of 85th percentile speed estimates when small samples are considered. This technique can be advantageous as long as some prior information is available. Donnell et al. [8] also used a regression model for predicting speed. Xie et al. [9] also developed a regression equation to find the relation between speed, density, and lane changing. Hastim and Ramli [10] developed a simulation program based on generating a large set of random numbers on Fortran Power station to know which distribution the speed data will follow. Jun [11] suggested that on certain roadway systems, the Gaussian mixture model using the EM algorithm could properly characterize the severity and variability in speed distribution due to congestion. Abbas et al. [12] explored the 85th percentile speed (which is considered as the operating speed of a road) model on the horizontal curve on two-lane rural highways. This study attempts to develop a model that harmonizes the designer's considerations and the road user's expectations. Multiple regression equations were developed for this purpose using Minitab software. Gong and Stamatiadis [13], Sil et al. [14], and Nama et al. [15] also used a multiple-regression model for speed modeling for four-lane horizontal curves. D'Andrea et al. [16] applied Neuro-Fuzzy techniques to the data set to know the most appropriate data classification and concluded that the method used for analysis is very flexible with respect to the number of variables and number of data. Bonneson and Pratt [17] developed an empirical relationship to a model, operating speed on a horizontal curve. The variables considered in the study are curve radius, rate of superelevation, deflection angle, and tangent speed. Many factors affect the speed at horizontal curve, e.g. tangent speed, vehicle type, curve deflection angle, tangent length, curve length, available stopping sight distance, grade, and vertical curvature [15].

The literature shows that various geometric parameters influence the speed and volume of traffic on two-lane highways. It is also observed that most of the speed models developed are based on the ordinary least square regression (OLSR) technique. Therefore, in the current study, the operating speed models are developed using OLSR in two phases, one independent of the road and the other with the road as a parameter, the details of which are presented in the following sections.

3 Data Collection and Analysis

3.1 Site Details

This study collected data from four two-lane bidirectional road sections in the northeastern region of India, Assam. (Fig. 1). This research is not considering non-motorized vehicles or pedestrians. Therefore, sites were chosen so that the presence of non-motorized vehicles (e.g., pedal cycle, cycle-rickshaw) and pedestrian activity were minimal and thus could be neglected. The traffic stream was of mixed character consisting of different types of vehicles like motorized three-wheeler, Car, motorized two-wheeler, buses, trucks, and LCVs. Sites were selected far away from side friction, like intersections, bus stops, parking lots, curves, and crosswalks. The photographs of the chosen site where speed data were collected are given in Fig. 1a–d.

3.2 Characteristics of the Road

The road surface was smooth enough to neglect its effect on speed reduction. A significant amount of traffic flow was present at all the sites. Roads having two-lane undivided carriageways and four-lane divided carriageways were used for data collection. The width of the two-lane roads used for data collection varies from 7.5 m to 9.6 m. Details of road width and shoulder nature with its width are presented in the following Table 1.

3.3 Data Collection and Extraction

Data were collected by video recording technique. The stretch chosen for placing video cameras was straight, and the camera was placed at a high position to capture both directions of traffic, as shown in Fig. 2. Two sections were marked at a distance of 100 m apart to collect vehicle data as shown in Fig. 3.

Video recording was carried out to extract data to the accuracy of 1/25 s. In-time and out-time of individual vehicles were found, and speeds were obtained by

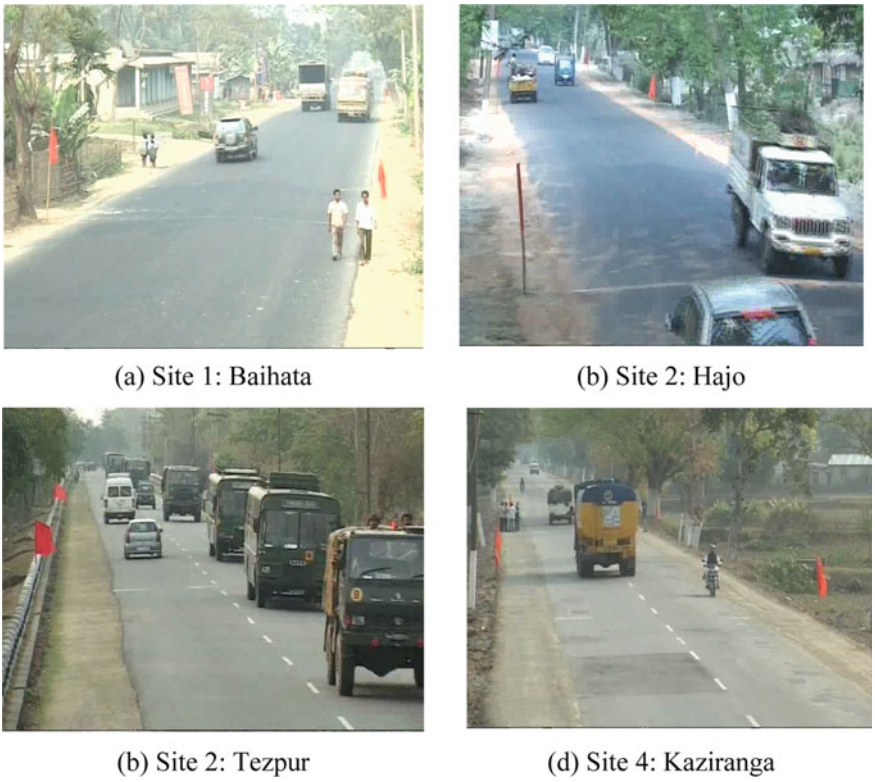

Fig. 1 Data collection sites

Table 1 Two lane data collection site details

Site No.	Site name	Road width (m)	Type of shoulder	Shoulder width (m)	Adjoining land use details	Classification as per HCM
1	Baihata (NH-37)	9.6	Earthen	1	Residential	Class III
2	Hajo (NH-37)	8.5	Earthen	2	Industrial	Class II
3	Tezpur (NH-37)	7.5	Earthen	1.2	Agricultural	Class I
4	Kaziranga (NH-37)	8.6	Earthen	1	Open land	Class I

Fig. 2 Photograph of the instrument set-up for data collection

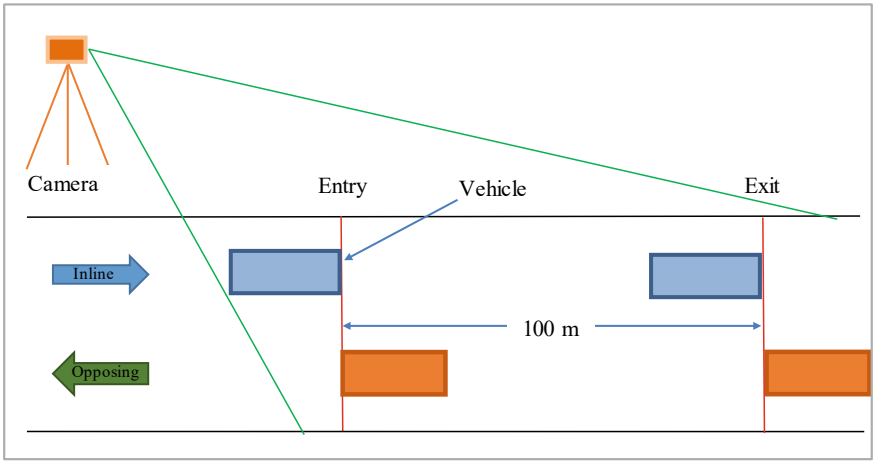

Fig. 3 Line diagram of video recording instrument set-up used in data collection

dividing trap length by travel time between the two sections. In Fig. 4 road section at night time is shown. The volume and speed of overall and classwise vehicles were calculated for each 5 min interval.

The speed and vehicle volume data were extracted manually from the video data collected. As shown in Fig. 3, both the entry and exits are marked at 100 m intervals at the data collection sites. Taking these lines as reference lines separated by 100 m, the speed data of the vehicles are measured using Eq. 1 by noting the vehicle's entry and exit times from the video-recorded data

Fig. 4 Sections during the night period of data collection

$$Speed = \frac{Exit\ Time - Entry\ Time}{Distance} = \frac{Exit\ Time - Entry\ Time}{100} \quad (1)$$

Linear regression equations were developed to determine the speed as a function of classwise vehicle volume. Two cases have been considered, one for the effect of the volume of different vehicles traveling on in-line traffic and the other for the effect of the volume of opposing traffic on the other direction's traffic.

4 Speed-Density Model for a Two-Lane Bidirectional Road

Most of the roads in India comprise bidirectional traffic of mixed characteristics, so it is worth finding out the effect of opposing traffic volume on speed behavior. Apart from speed, another fundamental macroscopic parameter required to explain any traffic behavior is density. It is essential to model speed for better planning and designing any roadway system. Speed models help designers in having some idea about the operating speed on a roadway. Speed models also help in assessing the expected speed changes of individual vehicles traversing the road due to changes in other traffic or geometric parameters included in the model. In bidirectional roads, specifically, when various types of vehicles having widely varying physical dimensions and dynamic characteristics share the same roadway, it is logical to model speed for the individual class of vehicles separately. In this section, speed prediction model has been developed and presented for a two-lane bidirectional road. The results obtained from this study can be calibrated and validated for use in a similar situation. Speed models for mixed traffic conditions are required to predict the changes in the speed of an individual vehicle due to the presence of other vehicles in the traffic stream. A generalized speed model was developed, which can be used for any road width and traffic composition.

4.1 Research Methodology

The variation in speed depends on many factors related to driver behavior, traffic parameters, the road's geometric characteristics, vehicular properties, and environmental conditions. For a given time and site, the other parameters remain the same, and then the crucial governing factor is the traffic properties like flow, density, and composition. The relative interaction between the vehicles depends on the flow and proportion of a particular vehicle type in the traffic stream. An increase in the flow results in an increase in density and, therefore, frequent changes in the speed of the individual vehicle and traffic stream. Different vehicles have different physical sizes, maneuvering abilities, and dynamic properties. So, the speed of different types of vehicles will be influenced to different extents due to changes in the composition of the traffic stream. In a mixed traffic situation, density will vary with the relative proportion of small and large vehicles in the traffic stream as interaction among the vehicles affects speed a lot; thus, composition plays a significant role in the vehicular speed, and the effect again varies with the flow level too. Therefore, it will be logical to consider the density of individual vehicle classes on the road as the traffic stream is composed of various vehicles. The basic model, which is the Green Shield model, has been considered for the modeling.

$$V = V_f(1 - \frac{K}{K_j}) \tag{2}$$

$$V = V_f - V_f \frac{K}{K_j} \tag{3}$$

$$V = a - b * K \tag{4}$$

In heterogeneous traffic situations, various types of vehicles share the same roadway, and the speed behavior depends on the composition and density of different vehicles. So it is essential to consider the density of different classes of vehicles. So the general Greenshield model can be rewritten as below, as also proposed by Dhamaniya and Chandra [18].

$$V_i = a_i - \sum_{j}^{N} b_{ij} * K_j \tag{2}$$

N is the total number of vehicles present in the traffic stream. The first term in the above equation, i.e., a_i represents the free flow speed (FFS) of vehicle type *i*. K_j is the density of the vehicle type *j*.

Many combinations given below were tried based on the above-mentioned linear model.

(a) Total opposite and total in-line direction traffic density (PCU/km):

$$V_i = a_0 - a_1 * K_{opp} - a_2 * K_{inline}$$

(b) Total opposite and total stream density (PCU/km):

$$V_i = a_0 - a_1 * K_{opp} - a_2 * K$$

(c) Classwise opposing traffic density and classwise combined density (veh/km):

$$V_i = a_0 - a_1 * K_{21} - a_2 * K_{22} - a_3 * K_{23} - a_4 * K_{24} - a_5 * K_{25} - a_6 * K_1 - a_7 * K_2 - a_8 * K_3 - a_9 * K_4 - a_{10} * K_5$$

(d) Classwise density (veh/km) of in-line traffic and classwise density (veh/km) of opposing traffic:

$$V_i = a_0 - a_1 * K_{11} - a_{12} * K_{12} - a_3 * K_{13} - a_4 * K_{14} - a_5 * K_{15} - a_6 * K_{21} - a_7 * K_{22} - a_8 * K_{23} - a_9 * K_{24} - a_{10} * K_{25}$$

(e) Total density of opposing traffic (veh/km) and classwise density (veh/km) of in-line traffic:

$$V_i = a_0 - a_1 * K_{opp} - a_2 * K_{car} - a_3 * K_{bus} - a_4 * K_{2w} - a_5 * K_{3w} - a_6 * K_{LCV}$$

(f) Total density of opposing traffic (PCU/km) and classwise density (veh/km) of in-line traffic:

$$V_i = a_0 - a_1 * K_{opp} - a_2 * K_{car} - a_3 * K_{bus} - a_4 * K_{2w} - a_5 * K_{3w} - a_6 * K_{LCV}$$

where V_i is the speed of each vehicle category in kmph, the value of a_0 represents the value of free flow speed in kmph. K is the total density of the traffic stream in PCU/km. K_{inline} and K_{opp} are the total densities of in-line and opposing traffic streams in PCU/km, and K_1, K_2, K_3, K_4, K_5 are the total densities of Car, bus/truck, *2W, 3W,* and *LCV,* respectively, in veh/km. K_{11}, K_{12}, K_{13}, K_{14}, K_{15} are the in-line traffic densities of Car, bus/truck, two-wheeler, three-wheeler, LCV, respectively, in veh/km and K_{21}, K_{22}, K_{23}, K_{24}, K_{25} are opposing traffic densities of Car, bus/truck, two-wheeler, three-wheeler, LCV respectively in veh/km.

4.2 Proposed Speed-Density Model Development

The speed data were extracted for each category of vehicle and classwise volume and speed were calculated at each 5 min interval. Density has been calculated by dividing 5 min traffic volume by 5 min average speed. Simultaneous equations were developed and solved using a program written in MATLAB software. A generalized speed-density model which is flexible for any width of road has been proposed to

represent the speed of bidirectional roads. Speed models have been developed for each of five types of vehicles namely, Car, Bus/Truck, Motorized Two-wheeler (2W), Motorized Three-wheeler (3W) and Light Commercial Vehicle (LCV) using speed and density at each 5 min interval. In the proposed model total density of opposing traffic and vehicle classwise densities of the in-line traffic stream has been included to study the effect of opposing traffic as well as that of classwise vehicle volume on speed of different category of vehicle. Out of all data, 35% of that were separated randomly for validating the model. Various combinations were tried to develop the final model, and among all the models, the one which gave the best results in terms of the least square error has been presented in the following pages. The steps to get the final model are shown in Fig. 5.

Among various models tried as mentioned before, model no. (f) came out to be the best representative model in terms of least square error. It was found that the composition of traffic stream in both the directions were more or less the same, thus

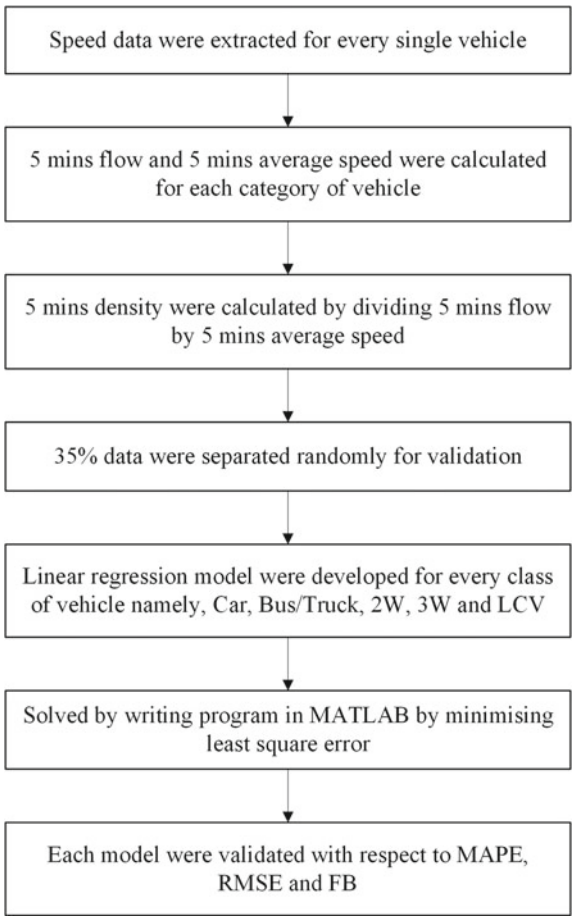

Fig. 5 Flowchart of the steps to develop the final model

all the speed data were combined. Models were developed to represent the speed of any direction and 65% of the total data has been used to develop the classwise models, which are presented below.

$$V_i = a_0 - a_{iopp} * K_{opp} - a_{icar} * K_{car} - a_{ibus/truck} * K_{bus/truck} - ai_{2w} * K_{2w} - a_{i3w} * K_{3w} - a_{iLCV} * K_{LCV}$$

where, i is five categories of vehicles considered for the study. The constants or co-efficients corresponding to opposing traffic density and density of different class of vehicles i.e. a_{iopp}, a_{icar}, $a_{ibus/truck}$, a_{i2w}, a_{i3w}, a_{iLCV} are expected to be different for different class of vehicle and on different models as the density of different vehicles will have a different impact on different types of vehicles.

In order to validate the model, 35% of the overall data were separated. The data consisted of 5 min of average speeds, which are observed speed and 5 min classwise traffic volume, which has been used to calculate predicted/expected speed. Mean absolute percentage error (MAPE), Root mean square error (RMSE) and Fractional Bias (FB) values were calculated to check the consistency of the calculated values with the observed ones.

4.3 Developed Models

In Fig. 6 it shows the percentage composition of vehicles in the traffic stream at four sites. It can be observed that except for Bus/Truck and Two-wheeler, other vehicles percentages are similar. Generalized speed models were developed combining all data. The width of the four sites under study namely, Tezpur (Site-3), Hajo (Site-2), Kaziranga (Site-4), and Baihata (Site-1) are 7.5 m, 8.5 m, 8.6 m, and 9.6 m, respectively. Two cases were considered; in one, the lane width factor is not considered and in the other a_i(W-7.5) term is included to take into account the variation/change in speed due to the change in road width. 7.5 indicates the standard lane width for a two-lane undivided facility. Table 2 lists the sample size of 5 min speed of different types of vehicles.

Case-1: Excluding the width of the road

The following model has been chosen to develop the speed-density equations in which road width has not been considered.

$$\mathbf{V_i} = a_0 - a_1 * K_{opp} - a_2 * K_{car} - a_3 * K_{bus/truck} - a_4 * K_{2w} - a_5 * K_{3w} - a_6 * K_{LCV}$$

The five sets of equations obtained from the above analysis are shown below,

$$V_{car} = 78.94 - 0.203 * K_{opp} - 0.903 * K_{car} - 0.715 * K_{bus/truck}$$

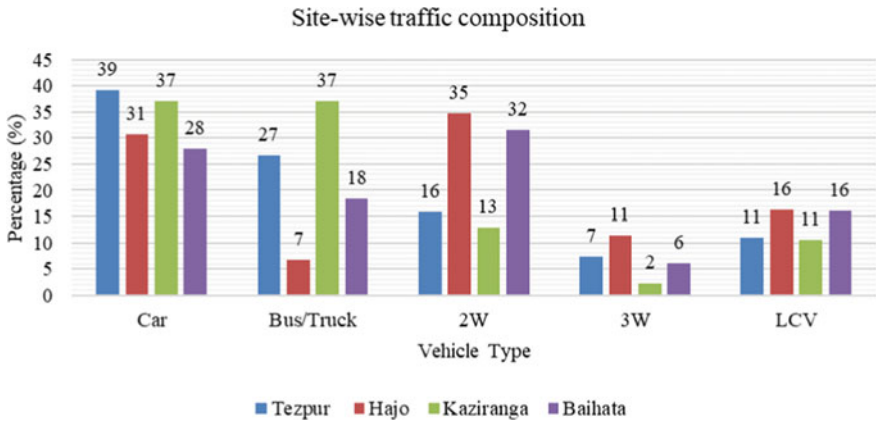

Fig. 6 Traffic composition at four two-lane bidirectional roads

Table 2 Sample size of different categories of vehicle

Vehicle type	Sample size
Car	585
Bus/Truck	533
Two-wheeler	538
Three-wheeler	323
LCV	501

$$-0.198 * K_{2w} - 0.166 * K_{3w} - 0.322 * K_{LCV}$$

$$V_{bus} = 60.57 - 0.20 * K_{opp} - 0.237 * K_{car} - 0.798 * K_{bus/truck} - 0.139 * K_{2w} - 0.084 * K_{3w} - 0.30 * K_{LCV}$$

$$V_{2w} = 57.86 - 0.09 * K_{opp} - 0.975 * K_{car} - 0.688 * K_{bus/truck} - 0.153 * K_{2w} - 0.010 * K_{3w} - 0.107 * K_{LCV}$$

$$V_{3w} = 48.49 - 0.105 * K_{opp} - 0.256 * K_{car} - 0.412 * K_{bus/truck} - 0.040 * K_{2w} - 0.303 * K_{3w} - 0.315 * K_{LCV}$$

$$V_{LCV} = 65.86 - 0.165 * K_{opp} - 0.608 * K_{car} - 0.512 * K_{bus/truck} - 0.113 * K_{2w} - 0.108 * K_{3w} - 0.598 * K_{LCV}$$

Tables 3 and 4 show the FB and RMSE values and t values for the above regression equations.

Table 3 FB and RMSE values for the generalized model excluding width factor

	Car	Bus/Truck	Two-wheeler	Three-wheeler	LCV
FB	0.001	0.053	0.001	−0.001	0.005
RMSE	9.46	10.169	10.60	8.12	10.57

Table 4 Significance values of the independent variables for generalized the model excluding width factor

Vehicle type	Co-efficients					
i	a_{iopp}	a_{icar}	$a_{ibus/truck}$	a_{i2w}	a_{i3w}	a_{iLCV}
Car	8.33	7.80	6.32	2.64	1.06	2.10
Bus/Truck	9.08	2.33	7.65	2.01	0.59	2.19
Two-wheeler	4.14	9.80	6.81	2.22	0.04	1.96
Three-wheeler	4.43	2.47	3.18	0.60	2.02	2.46
LCV	6.49	5.17	4.24	1.97	0.68	3.45

It is observed from the above table that some vehicles are showing insignificance with respect to t values (Fig. 7).

From the generalized speed models, it can be observed that Car's speed is affected most and Two-wheeler's speed is affected least by the opposing traffic. Table 5 shows the values of calculated free flow speed values and predicted free flow speed values.

Table 6 shows that the free flow speed predicted by the models are a good representation of the actual observed free flow speeds. Table 6 demonstrates the name of vehicles affecting the highest and least speed of the various vehicles.

It can be observed from the table that for Bus/Truck and Three-wheeler, speed gets affected most by Bus/Truck and speed of all other categories of vehicles are influenced the highest by Cars in the same direction. This may be due to the presence of high percentage of Car and heavy vehicles in the stream. Due to Car having excellent properties and heavy vehicles having bigger size, desired operating speed of the

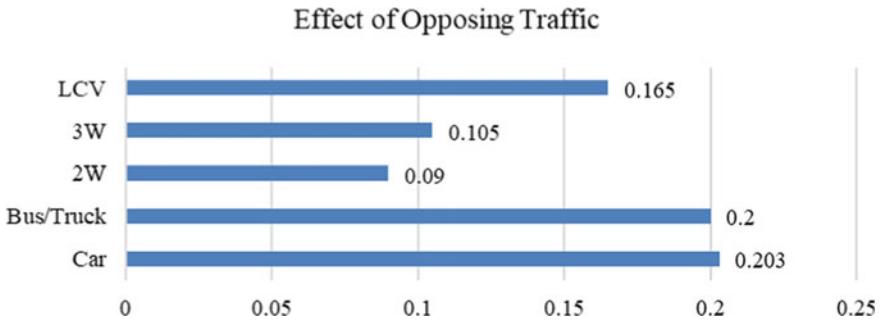

Fig. 7 Effect of opposing traffic on different type of vehicles

Table 5 Comparison between observed and estimated Free Flow Speed (FFS) when width of the road excluded in the model

Vehicle type	85th percentile speed (kmph)	Free flow speed from the model (kmph)
Car	79.47	78.94
Bus/Truck	61.71	60.57
Two-wheeler	59.64	57.86
Three-wheeler	48.19	48.49
LCV	66.30	65.86

Table 6 Effect of in-line traffic stream on different types of vehicles when width of the road excluded in the model

Type of vehicle	Effect of In-line traffic stream	
	Most	Least
Car	Car	Two-wheeler
Bus/Truck	Bus/Truck	Two-wheeler
Two-wheeler	Car	Three-wheeler
Three-wheeler	Bus/Truck	Two-wheeler
LCV	Car	Three-wheeler

other vehicles get interfered. Two-wheeler and Three-wheeler has the least effect on every class of vehicles and this is due to them having good maneuverability.

Case-2: Including width of road

The flowing linear regression equation is the other model which includes the road width in order to examine the effect of differing widths on speed variability.

$$\begin{aligned}\mathbf{V_i} =& a_0 - a_1 * K_{opp} - a_2 * K_{car} - a_3 * K_{bus/truck} \\ & - a_4 * K_{2w} - a_5 * K_{3w} - a_6 * K_{LCV} + a_7 * (W - 7.5)\end{aligned}$$

W = width of observed two-lane road in meter.

In this case of study, road width is considered to develop the models. W is the variable for four different sites and 7.5 m is included to consider the standard width of two-lane road. Therefore, (W-7.5) term indicates the effect of width change on speed.

$$\begin{aligned}V_{car} =& 73.26 - 0.226 * K_{opp} - 0.815 * K_{car} - 0.646 * K_{bus/truck} \\ & - 0.176 * K_{2w} - 0.189 * K_{3w} 0.401 * K_{LCV} + 15 * (W - 7.5)\end{aligned}$$

$$\begin{aligned}V_{bus} =& 61.59 - 0.20 * K_{opp} - 0.601 * K_{car} - 0.617 * K_{bus/truck} - 0.089 * K_{2w} \\ & - 0.011 * K_{3w} - 0.235 * K_{LCV} + 1.01(W - 7.5)\end{aligned}$$

$$V_{2w} = 53.01 - 0.395 * K_{opp} - 0.298 * K_{car} - 0.203 * K_{bus/truck}$$

$$-0.223 * K_{2w} - 0.091 * K_{3w} - 0.212 * K_{LCV} + 1.102(W - 7.5)$$

$$V_{3w} = 47.54 - 0.115 * K_{opp} - 0.356 * K_{car} - 0.311 * K_{bus/truck} - 0.070 * K_{2w} - 0.303 * K_{3w} - 0.315 * K_{LCV} + 1.10(\mathrm{W} - 7.5)$$

$$V_{LCV} = 63.06 - 0.165 * K_{opp} - 0.678 * K_{car} - 0.401 * K_{bus/truck} - 0.203 * K_{2w} - 0.156 * K_{3w} - 0.354 * K_{LCV} + 1.68(W - 7.5)$$

Tables 7 and 8 show the FB and RMSE values and t values for the above regression equations.

As for the previous case, in this case also some variables are indicating their insignificance in influencing speed at 5% significant level. Even though some parameters have no significant impact on speed at 5% significant but still they have been considered just to keep the symmetry across the equations for different vehicle types after verifying their significance at 10% significance level. In Fig. 8, the impact of opposing traffic on different class of vehicles can be compared. It is observed that when width factor is considered, two-wheeler seem to be affected most by the opposing traffic whereas the three-wheeler is least affected.

Table 9 shows the calculated free flow speed and estimated free flow speed from the model and Table 10 shows the list of vehicles which have most and least influence on the vehicles traveling in the same direction.

The results presented in Table 9 show that the observed speed and model predicted speed values are nearly the same which indicates the model's suitability.

Table 7 FB and RMSE values for the generalized model including width factor

	Car	Bus/Truck	Two-wheeler	Three-wheeler	LCV
FB	−0.014	0.021	0.018	−0.035	0.017
RMSE	9.72	10.95	10.91	8.50	10.58

Table 8 Significance values of the independent variables for generalized the model including width factor

Vehicle type	Co-efficients						
i	a_{iopp}	a_{icar}	$a_{ibus/truck}$	a_{i2w}	a_{i3w}	a_{iLCV}	a_{w}
Car	9.03	6.85	5.56	2.28	1.97	2.54	2.52
Bus/Truck	9.00	5.85	5.86	2.27	0.08	1.70	1.98
Two-wheeler	15.50	2.56	1.97	2.76	0.57	1.97	1.87
Three-wheeler	4.64	3.29	2.29	1.00	1.96	2.35	2.19
LCV	6.30	5.59	3.22	2.56	0.96	1.98	2.71

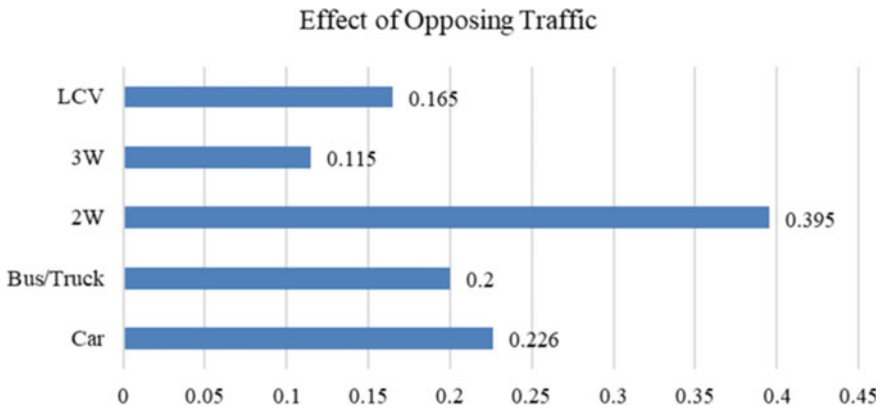

Fig. 8 Effect of opposing traffic on different types of vehicles

Table 9 Comparison between observed and estimated Free Flow Speed (FFS) when width of the road included in the model

Type of vehicle	85th percentile speed (kmph)	Free flow speed from the model (kmph)
Car	79.47	73.26
Bus/Truck	61.71	61.59
Two-wheeler	59.64	53.01
Three-wheeler	48.19	47.54
LCV	66.30	63.06

Table 10 Effect of in-line traffic stream on different types of vehicles when width of the road included in the model

Vehicle type	Effect of In-line traffic stream	
	Most	Least
Car	Car	Two-wheeler
Bus/Truck	Bus/Truck	Two-wheeler
Two-wheeler	Car	Three-wheeler
Three-wheeler	Car	Two-wheeler
LCV	Car	Three-wheeler

Like for the previous cases in this case too it is noticed that Two-wheeler and Three-wheeler has least effect on different vehicles and except for heavy vehicles, Car has maximum effect on all other class of vehicles.

4.4 Validation of the Proposed Model

As mentioned before, three parameters i.e. Mean Absolute Percentage Error (MAPE), Root Means Square Error (RMSE) and Fractional Bias (FB) were chosen for validating the developed models. The Range of fractional bias (FB) varies from −2 to +2 and if the value of FB is zero that indicates perfect agreement between observed value and predicted value. The values of FB came out to be reasonable which also indicates good agreement between actual and calculated values. Table 11 shows the results of the validation in terms of MAPE, RMSE and FB, carried out with the 35% data separated from the main data for validating the model. The MAPE and RMSE values are acceptable and the values of FB also indicate that there lies good agreement between the observed and predicted speed values.

Table 12 displays the root mean square error (RMSE) values of the two cases i.e. models which include the road width and models which don't consider the road width.

It can be observed from Table 12 that the error values are not markedly different meaning that road width does not have a significant effect on the speeds of vehicles. It was found in the previous speed distribution analysis that speed at Site-III which is having the least road width (7.5 m) have vehicles traveling at a higher speed than the other sites which are having higher road width (8.5 m, 8.6 m, and 9.6 m). The reason behind this demeanor may be low flow at most of the time of the day at that

Table 11 MAPE, RMSE and FB values of the generalized model

Case	Type of vehicle	MAPE	RMSE	FB
Excluding road width	Car	14.534	9.474	0.010
	Bus/Truck	15.572	10.254	0.004
	Two-wheeler	18.227	9.848	−0.008
	Three-wheeler	13.095	7.771	−0.009
	LCV	16.998	10.587	0.011
Including road width	Car	14.665	9.613	0.009
	Bus/Truck	16.584	10.257	0.011
	Two-wheeler	17.829	9.922	−0.009
	Three-wheeler	12.694	7.825	0.019
	LCV	17.910	10.850	0.004

Table 12 RMSE values for two cases considered in the model

Width factor	Vehicle type				
	Car	Bus/Truck	Two-wheeler	Three-wheeler	LCV
Excluded	9.46	10.17	10.60	8.12	10.57
Included	9.72	10.95	10.91	8.50	10.58

particular site and very good road quality with barrier on either side at the edge of the shoulder. Whereas, for Site-1 and Site-II flow is high for most of the time of day and open land having lower ground level than the road level is present beyond the shoulder. However, though Site-IV has low flow, it has lower operating speed than Site-III even after having wider road than Site-III. This may be due to inferior road quality in Site-IV. Therefore, it is learned that not only road width, but there are also many factors that are to be studied and included in a model to represent the actual variation in speed due to road width.

5 Conclusions

In this study, linear regression equation has been used to develop the speed-density relationship. Classwise vehicle speeds were modeled to have a better view of the heterogeneity of traffic. The speed models presented in this study can be used for similar kinds of traffic and roadway situations, and it is flexible to any number of vehicle category. Among various cases, the model which uses combined opposing traffic density (PCU/km) and in-line density (vehicle/km) of the individual class of vehicle gives the best results in terms of least square error. It was observed that if the opposing traffic flow is more, the effect of opposing traffic flow on the speed of individual classes of the vehicle is more. Cars face maximum speed reduction due to the presence of opposing traffic. The smaller vehicles like Two-wheeler and Three-wheeler have the least effect on the speed of all classes of vehicles plying in the same direction. It can also be concluded that even though all roads are two-lane with bidirectional traffic, in order to calculate the effect of road width accurately, it is necessary to compare roads with similar road surface conditions, roadside barriers, overall speed distribution patterns, and nearby local features.

In developing nations such as India, the heterogeneity of traffic and the presence of bidirectional roads are prevalent features of roadway traffic. Opposing traffic plays a significant role in controlling overall traffic behavior on bidirectional roads, particularly in areas where lane discipline is lacking. To ensure an efficient transportation system, it is crucial to conduct further research on modeling speed under mixed traffic conditions, considering various scenarios to gain a clearer understanding of speed behavior in these complex traffic situations.

References

1. Porter RJ, Mahoney KM, Mason JM (2007) Estimation of relationships between 85th percentile speed, standard deviation of speed, roadway and roadside geometry and traffic control in freeway work zones. In: Session 309 of the 86th annual meeting of the transportation research board
2. Kubota H (2013) Profile-speed data-based models to estimate operating speeds for urban residential streets with a 30 km/h speed limit. IATSS Res 36(2):115–122

3. Bester CJ (2000) Truck speed profiles. Transp Res Record 1701(1):111–115
4. Sun L, Zhou J (2005) Development of multiregime speed–density relationships by cluster analysis. Transp Res Rec 1934(1):64–71
5. Banihashemi M, Dimaiuta M, Wang H (2011) Operating speed model for low-speed rural two-lane highways: design consistency module for interactive highway safety design model. Transp Res Rec 2223(1):63–71
6. Nama S, Maurya AK, Maji A, Edara P, Sahu PK (2016) Vehicle speed characteristics and alignment design consistency for mountainous roads. Transp Dev Econ 2(2):1–11
7. Al-Ghamdi AS (1998) Spot speed analysis on urban roads in Riyadh. Transp Res Rec 1635(1):162–170
8. Donnell ET, Ni Y, Adolini M, Elefteriadou L (2001) Speed prediction models for trucks on two-lane rural highways. Transp Res Rec 1751(1):44–55
9. Xie H, Jiang Y, Zhang L (2011) Empirical study on relationship among the lane-changing, speed and traffic flow. Syst Eng Procedia 2:287–294
10. Hustim M, Ramli MI (2013) The vehicle speed distribution on heterogeneous traffic: space mean speed analysis of light vehicles and motorcycles in Makassar –Indonesia. Proc Eastern Asia Soc Transp Stud 9
11. Jun J (2010) Understanding the variability of speed distributions under mixed traffic conditions caused by holiday traffic. Transp Res Part C: Emerg Technol 18(4):599–610
12. Abbas SKS, Adnan MA, Endut IR (2011) Exploration of 85th percentile operating speed model on horizontal curve: a case study for two-lane rural highways. Procedia Soc Behav Sci 16:352–363
13. Gong H, Stamatiadis N (2008) Operating speed prediction models for horizontal curves on rural four-lane highways. Transp Res Rec 2075(1):1–7
14. Sil G, Nama S, Maji A, Maurya AK (2018) The 85th percentile speed prediction model for four-lane divided highways in ideal free flow condition (No. 18-02808)
15. Nama S, Sil G, Maurya AK, Maji A (2022) Development of speed distribution model and prediction of geometric parameter influence on driver speed through artificial neural network. J Eastern Asia Soc Transp Stud 14:2004–2014
16. D'Andrea A, Carbone F, Salviera S, Pellegrino O (2012) The most influential variables in the determination of V85 speed. Procedia Soc Behav Sci 53:633–644
17. Bonneson JA, Pratt MP (2009) Model for predicting speed along horizontal curves on two-lane highways. Transp Res Rec 2092(1):19–27
18. Dhamaniya A, Chandra S (2013) Speed prediction models for urban arterials under mixed traffic conditions. Procedia Soc Behav Sci 104:342–351